What is the Prognostic Role of γδ T Cells in Colorectal Cancer?

Hannah-Louise Jessica Hayman

BSc (Hons)

Submitted in fulfilment of the requirements for the degree of PhD

Institute of Cancer Sciences College of Medical, Veterinary and Life Sciences

October 2022

The work presented in this thesis was performed by the author except where acknowledged. This thesis has not been submitted for a degree or diploma at this or any other institution.

Hannah-Louise Jessica Hayman

October 2022

Acknowledgements

Nobody completes a PhD by themselves, so I would like to highlight the varied contributions to which I owe this work. To Professor Joanne Edwards for being a tireless mentor and ever-present source of support and making sure I had a place in the lab even when I retreated to a cave in the mountains. To Dr Seth Coffelt for taking a chance on a lowly undergraduate, out of her depth. To Dr Antonia Roseweir, for welcoming me into the lab as a newbie and not allowing distance to lessen your contribution. Special thanks to my supervisors collectively – thank you for being so understanding through the turmoil. I would also like to thank everybody in the Edwards lab, Coffelt lab and the Glasgow Tissue Research Facility, you are all amazing.

Appreciation for Dr Kathryn Pennel for always one upping my disasters and slowly erasing my level of lab standards, yet still imparting her knowledge gained as a Queen Anne Scholar – absolute role model. To Chrissy Bigley for maintaining all IT systems and providing crucial insights into botanical methodology. Thanks to Dr Jean Quinn for always knowing how to balance kindness and sternness, although I only experienced the former because she thinks I'm delightful – one is awfully grateful isn't one. Many thanks to Dr Anna Kilbey, for showing me the ropes – I still can't believe I was allowed back. To Phungern Khongthong for being a smile that never faded, a calming voice and for regularly calling me a genius. To Dr Marta Campillo, for seeing me over the line. Gratitude to Dr Gerard Lynch for your endless insights. Thank you to all the patients who consent to provide samples for scientific research – you are the reason we search for answers and the key to finding them.

With love to my parents for not giving up on me when all others did, seeing the potential I could not see in myself and forgiving everything it took for me to find my way. Thanks to my Nan for a 30-year supply of half tubes of fruit pastilles, which I don't even like. Many thanks to Sirus Hayman for not complaining when I took him out for walks at 3 am, and just generally being a very good boy, mostly. Also, for listening to me whine almost as much as he does and providing unlimited cuddles and making me whole again – I love you pup. Blessings of Gaea to Wonder Woman for embodying all the values I look for in others and hope to develop in myself. Shout out to the NMC community for being the friends I didn't know I needed. Massive hug for Amy McCoull for being a friend, a guide and a 10/10 source of dog pictures. Love to Kayt Quambro, for all the late-night conversations and emergency sandwiches – good times. Endless gratitude to Lisa Simpson, for picking up a discarded undergraduate mentee and never letting go.

Finally, I would like to dedicate my PhD to Jessica 'Jess' Hayman. You were my best friend, and I miss you always. During every stressful day and every endless night, I was never alone. Sweet dreams xx

Summary

Colorectal cancer (CRC) is the third most common cancer in men and second most common in women worldwide, rising from fourth and third most common in 2002, respectively [1-3]. The Tumour Node Metastasis (TNM) staging system was devised to stratify CRC patients by their disease attributes; the penetration of the tumour into surrounding tissue and spread to lymph nodes and distant organs; but this method warrants significant improvement [4, 5]. Attempts to resolve this issue have produced a genomic and transcriptomic method from bulk tumour sequencing (consensus molecular subtypes) which classifies patients as CMS1 through to CMS4 [6]. Due to its origin from bulk sequencing the CMS is hindered by a lack of tumour specificity, and so the cell intrinsic subtypes were developed to utilise characteristics of the tumour cells only, producing CRIS-A through to CRIS-E [7]. Given the significant contribution that the immune landscape plays in CRC, there is significant interest in utilising the immune landscape to further hone CRC stratification, resulting in the Immunoscore® which utilises counts of $CD3^+$ and $CD8^+$ lymphocytes [8, 9]. However, the immune landscape includes a variety of immune cells with may hold additional information for patient stratification, including specifically unconventional γδ T cells in CRC due to their relative enrichment, and so this thesis seeks to examine the representation of γδ T cells within the primary tumour and adjacent normal tissue and determine their prognostic value, comparing this to the well characterised CD8 T cells.

To accomplish this goal, immunostaining was employed to measure the density of γδ T cells and CD8 T cells within the primary tumour and adjacent normal tissue of patients from three geographically distinct CRC cohorts representing Scotland, Norway, and Thailand. It was found that both lymphocyte populations were reduced in the primary tumour compared to the adjacent normal tissue and in the epithelium compared to the stroma/lamina propria. These data were used to histologically classify cases as low or high for γδ or CD8 T cells and these groups used to conduct survival analysis, determining that patients with a high density of the conventional CD8 T cells had a favourable prognosis, as expected from the literature [8]. However, contrary to previous studies which utilised a flawed transcriptional methodology [10, 11], γδ T cells were found to be an unfavourable prognostic factor. Furthermore, these results were transcriptionally validated by reclassifying cases based on the transcription of genes encoding γδ TCR and CD8 coreceptor chains. This not only validated the histological findings, but also highlighted that supervised analysis using these genes may be an avenue to improving transcriptional methods of lymphocyte deconvolution.

Following on from this, analysis of genomic and transcriptomic sequencing data was conducted to elucidate the genomic and transcriptomic landscapes underlying cases that are histologically classed as low or high for γδ T cells or CD8 T cells. This analysis revealed that cases with a greater density of γδ T cells or CD8 T cells are more likely to carry mutations in genes which are often mutated in the microsatellite regions of MSI cases (*ASTE1, TTK*), and are associated with a greater immune infiltrate. However, MMR deficiency, which is responsible for the development of MSI, was not sufficient to result in the greater immune infiltrate. Thus, this study hypothesises that MMR deficiency and subsequent MSI does not result in greater immune infiltration, but rather lays a foundation for which genetic aberrations can activate a route to immune infiltration. Unfortunately, transcriptional analysis was not informative.

This thesis has demonstrated a clear difference in the prognostic role of γδ T cells and CD8 T cells, highlighting the need to extend our measure of the immune landscape to include less well characterised immune cells. However, doing so may require a multiplex approach to better determine the role of these cells relative to each other, as this analysis produces two singleplex layers of information without details of their relationships. In addition, it not fully understood how these cells are functioning to exert such contrasting prognostic effects, and so further studies to characterise their relative function roles would be valuable. In conclusion, this thesis adds a histological component to the growing data showing that the immune landscape is a prime candidate to improve disease stratification for CRC patients, and ultimately further our ability to give them the best outcome.

Graphical Abstract

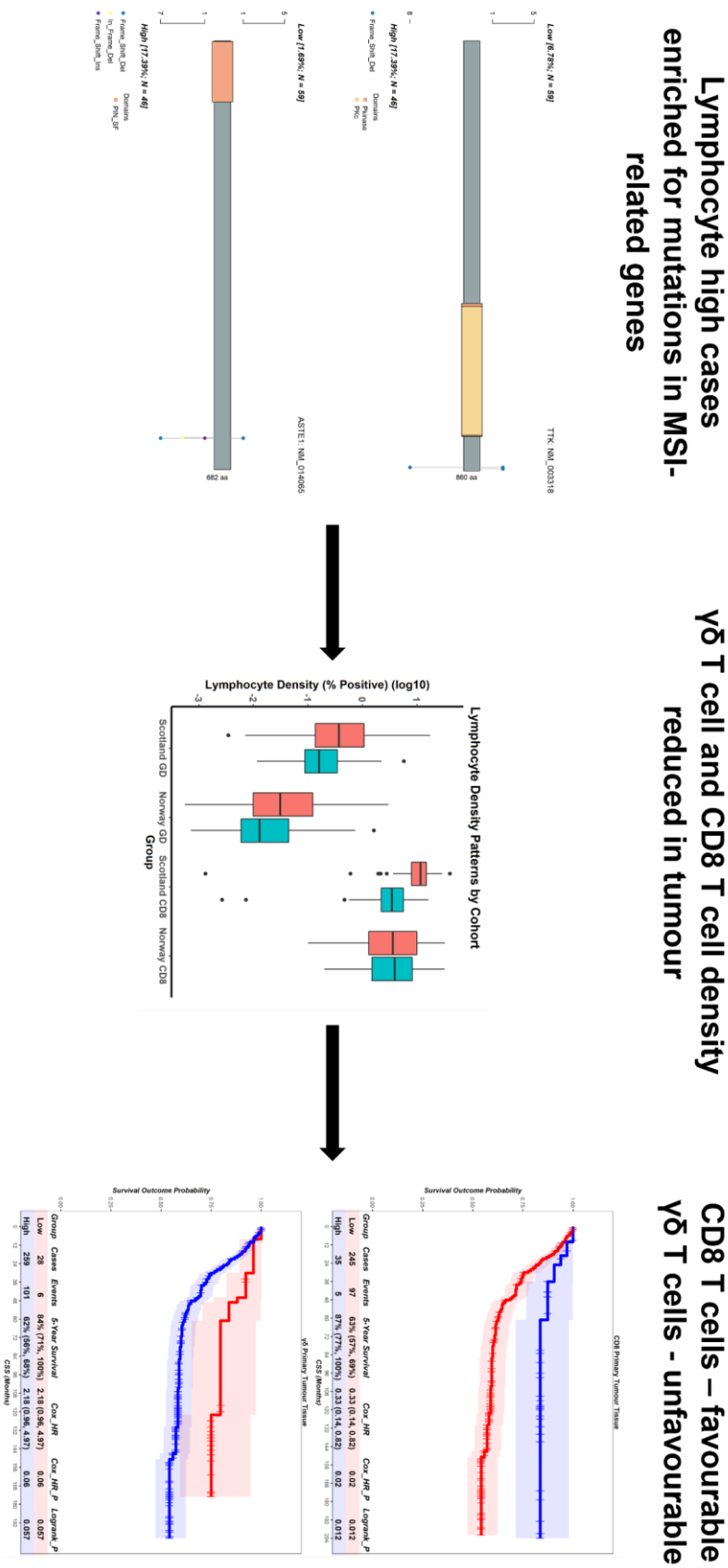

Publications and Presentations

Publications relating to this thesis

Suzuki, T, **Hayman, L**, Kilbey, A, Edwards, J, Coffelt, SB. Gut γδ T cells as guardians, disruptors, and instigators of cancer. Immunol Rev. 2020; 298: 198– 217. https://doi.org/10.1111/imr.12916.

Al-Badran SS, Grant L, Campo MV, Inthagard J, Pennel K, Quinn J, Konanahalli P, **Hayman L,** Horgan PG, McMillan DC, Roxburgh CS, Roseweir A, Park JH, Edwards J. Relationship between immune checkpoint proteins, tumour microenvironment characteristics, and prognosis in primary operable CRC. J Pathol Clin Res. 2021 Mar;7(2):121-134. doi: 10.1002/cjp2.193. Epub 2020 Dec 18. PMID: 33338327; PMCID: PMC7869939.

Toshiyasu Suzuki, Anna Kilbey, Rachel A. Ridgway, **Hannah Hayman**, Ryan Bryne, Nuria Casa Rodríguez, Anastasia Georgakopoulou, Lei Chen, Michael Verzi, David Gay, Ester G. Vázquez, Hayley L. Belnoue-Davis, Kathryn Gilroy, Anne Helene Køstner, Christian Kersten, Chanitra Thuwajit, Ditte Andersen, Robert Wiesheu, Anett Jandke, Natalie Roberts, Karen Blyth, Antonia Roseweir, Simon J. Leedham, Philip D. Dunne, Joanne Edwards, Adrian Hayday, Owen J. Sansom, Seth B. Coffelt. β-catenin obstructs γδ T cell immunosurveillance in colon cancer through loss of BTNL expression. Cancer Immunology Research. 2022. bioRxiv 2022.06.10.495115; doi: https://doi.org/10.1101/2022.06.10.495115.

Poster presentations

The prognostic role of gamma delta T-cells in CRC is dependent on patient population. **L Hayman**, Anne Helene Køstner, Christian Kersten, Donald McMillan, Antonia Roseweir, Seth Coffelt, Joanne Edwards. BSI Congress 2021. Edinburgh, UK.

Regulation of IL-17-producing γδ T cells in breast cancer metastasis. Sarah C. Edwards, Anna Kilbey, Robert Wiesheu, Erin R. Morris, **L Hayman,** Damiano Rami, Seth B. Coffelt. NCRI 2018. Glasgow, UK.

Contents

List of Figures

Figure S27 – Time-to-event (cancer-specific survival) analysis for CD8 T cells in the adjacent normal tissue.

Figure S28 – Time-to-event (cancer-specific survival) analysis for CD8 T cells in the primary tumour epithelium.

Figure S29 – Time-to-event (cancer-specific survival) analysis for CD8 T cells in the primary tumour stroma.

Figure S30 – Time-to-event (cancer-specific survival) analysis for CD8 T cells in the primary tumour tissue.

Figure S31 – Time-to-event (overall survival) analysis for CD8 T cells in the adjacent normal epithelium.

Figure S32 – Time-to-event (overall survival) analysis for CD8 T cells in the adjacent normal stroma.

Figure S33 – Time-to-event (overall survival) analysis for CD8 T cells in the adjacent normal tissue.

Figure S34 – Time-to-event (overall survival) analysis for CD8 T cells in the primary tumour epithelium.

Figure S35 – Time-to-event (overall survival) analysis for CD8 T cells in the primary tumour stroma

Figure S36 – Time-to-event (overall survival) analysis for CD8 T cells in the primary tumour tissue.

Figure S37 – Time-to-event (disease-free survival) analysis for CD8 T cells in the adjacent normal epithelium.

Figure S38 – Time-to-event (disease-free survival) analysis for CD8 T cells in the adjacent normal stroma.

Figure S39 – Time-to-event (disease-free survival) analysis for CD8 T cells in the adjacent normal tissue. Patients

Figure S40 – Time-to-event (disease-free survival) analysis for CD8 T cells in the primary tumour epithelium.

Figure S41 – Time-to-event (disease-free survival) analysis for CD8 T cells in the primary tumour stroma

Figure S42 – Time-to-event (disease-free survival) analysis for CD8 T cells in the primary tumour tissue.

Figure S43 – Time-to-event (recurrence-free survival) analysis for CD8 T cells in the adjacent normal epithelium.

Figure S44 – Time-to-event (recurrence-free survival) analysis for CD8 T cells in the adjacent normal stroma.

Figure S81 – Time-to-event (overall survival) analysis for CD8 T cells in the healthy tissue tissue.

Figure S82 – Time-to-event (overall survival) analysis for CD8 T cells in the primary tumour epithelium.

Figure S83 – Time-to-event (overall survival) analysis for CD8 T cells in the primary tumour stroma.

Figure S84 – Time-to-event (overall survival) analysis for CD8 T cells in the primary tumour tissue.

Figure S85 – Time-to-event (disease-free survival) analysis for CD8 T cells in the normal adjacent epithelium.

Figure S86 – Time-to-event (disease-free survival) analysis for CD8 T cells in the normal adjacent stroma.

Figure S87 – Time-to-event (disease-free survival) analysis for CD8 T cells in the normal adjacent tissue.

Figure S88 – Time-to-event (disease-free survival) analysis for CD8 T cells in the primary tumour epithelium

Figure S89 – Time-to-event (disease-free survival) analysis for CD8 T cells in the primary tumour stroma.

Figure S90 – Time-to-event (disease-free survival) analysis for CD8 T cells in the primary tumour tissue.

Figure S91 – Time-to-event (recurrence-free survival) analysis for CD8 T cells in the normal adjacent epithelium.

Figure S92 – Time-to-event (recurrence-free survival) analysis for CD8 T cells in the normal adjacent stroma.

Figure S94 – Time-to-event (recurrence-free survival) analysis for CD8 T cells in the normal adjacent tissue.

Figure S95 – Time-to-event (recurrence-free survival) analysis for CD8 T cells in the primary tumour epithelium.

Figure S96 – Time-to-event (recurrence-free survival) analysis for CD8 T cells in the primary tumour stroma.

Figure S97 – Time-to-event (recurrence-free survival) analysis for CD8 T cells in the primary tumour tissue.

Figure S98 – Time-to-event (overall survival) analysis for γδ T cells in the normal adjacent epithelium.

Figure S99 – Time-to-event (overall survival) analysis for γδ T cells in the normal adjacent stroma.

Figure S100 – Time-to-event (overall survival) analysis for γδ T cells in the normal adjacent tissue.

List of Tables

Glossary and Abbreviations

Glossary

Cancer-specific survival: Time until cancer-induced death

Closed-source: Software's publisher or another person reserves some licensing rights to use, modify, share modifications, or share the software, restricting user freedom with the software they lease

Disease-free survival: Time to death or recurrence

Durvalumab: A monoclonal antibody which binds and blocks the checkpoint inhibitor ligand PD-L1

Ipilimuab: A monoclonal antibody which binds and blocks the checkpoint inhibitor receptor CTLA-4

Nivolumab: A monoclonal antibody which binds and blocks the checkpoint inhibitor receptor PD-1

Open-source: Copyright holder grants users the rights to use, study, change, and distribute the software and its source code to anyone and for any purpose

Overall survival: Time until death due to any cause

Pembrolizumab: A monoclonal antibody which binds and blocks the checkpoint inhibitor receptor PD-1

QuPath: Cross-platform open-source software for digital pathology and whole slide image analysis

Recurrence-free survival: Time to recurrence

Tremelimumab: A monoclonal antibody which binds and blocks the checkpoint inhibitor receptor CTLA-4

Unconventional T cells: T cells distinct from $CD4^+/CD8^+$, usually not MHC-restricted

VisioPharm: A closed-source software for digital pathology analysis.

Abbreviations

ACT: Adoptive cell transfer

AOM: Azoxymethane

APC: Adenomatous polyposis coli

AREG: Amphiregulin

BRAF: V-raf murine sarcoma viral oncogene homolog B1

BrHPP: Bromohydrin pyrophosphate

BTN: Butyrophilin

BTNL: Butyrophilin-like

CAR: Chimeric antigen receptor

CDR: Complementarity-determining region

CIMP: CpG island methylation phenotype

CIN: Chromosomal instability

CMS: Consensus molecular subtypes

CRC: CRC

CRIS: CRC intrinsic subtypes

CSCs: Cancer-associated stem cells

CSS: Cancer-specific survival

DFS: Disease-free survival

DNA: Deoxyribonucleic acid

DOT: Delta One T cells

DSS: Dextran sodium sulphate

EGFR: Epidermal growth factor receptor

EMT: Epithelial-mesenchymal transition

EPCR: Endothelial protein C receptor

ETBF: Enterotoxigenic Bacteroides fragilis

FFPE: Formalin-fixed paraffin embedded

GvHD: Graft versus host disease

HLA: Human leucocyte antigen

HMG-CoaR: 3-hydroxy-3-methylglutaryl coenzyme A

HR: Hazard ratio

IEL: Intraepithelial T cell

IFN: Interferon

IHC: Immunohistochemistry

IL: Interleukin

IPP: Isopentenyl pyrophosphate

ITAM: Immunoreceptor tyrosine-based activation motif

KRAS: Kirsten rat sarcoma virus

MHC: Major histocompatibility complex

MIC: MHC class I polypeptide–related sequence

MSI: Microsatellite instability

MSS: Microsatellite stable

NKG2D: Natural killer group 2D

OR: Odds ratio

OS: Overall survival

PDX: Patient derived xenograft

PE: Phycoerythrin

RFS: Recurrence-free survival

RNA: Ribonucleic acid

RORγt: RAR-related orphan receptor gamma t

SCNA: Somatic copy number alterations

TCGA: The Cancer Genome Atlas

TCR: T cell receptor

TEGs: Engineered T cells

TGF: Transforming growth factor

TIL: Tumour infiltrating lymphocyte

TLR: Toll-like receptor

TMA: Tissue microarray

TME: Tumour microenvironment

TNM: Tumour node metastasis

TSA: Tumour specific antigen

Chapter 1:
Introduction

Chapter 1 - Introduction

1.1 CRC (CRC)

1.1.1 CRC incidence

CRC is the third most common cancer in men and second most common in women worldwide, rising from fourth and third most common in 2002, respectively [1-3]. CRC is estimated to kill over 881 000 people worldwide [1-3]. Incidence and mortality are likely to increase as life expectancy rises and developing countries become increasingly westernized. Key risk factors for CRC include increased red meat consumption, low fibre intake, and a low level of physical activity [12-14].

1.1.2 CRC development

1.1.2.1 Sporadic CRC

The progression from adenoma to CRC is driven by the acquisition of multiple genetic aberrations. There are two types of adenomas whose genetic mutations differ that correspond with two postulated avenues to CRC. Traditional adenoma conversion to carcinoma follows a procession of mutations termed the chromosomal instability pathway (CIN). In the case of serrated polyps, mutational drivers consist of *BRAF* mutations, CpG island methylator phenotype (CIMP), and microsatellite instability (MSI) [15, 16].

1.1.2.2 Hereditary CRC

Although significant hereditary factors are present in approximately 35% of CRC incidence [17], driver mutations in genes causing established hereditary syndromes account for approximately 5% of CRC incidence [18, 19]. The most prevalent of these hereditary syndromes is Lynch syndrome [20, 21], driven by a mutation in genes that jeopardize DNA mismatch repair (MMR), such as *MLH1*, *MSH2*, *MSH6*, and *PMS2* [22-30]. The remaining hereditary syndromes are associated with severe polyposis and subsequently an increased likelihood of progression from the polyp stage, such as Peutz-Jeghers syndrome [31], familial adenomatous polyposis, and other adenomatous polyposis syndromes [32].

1.1.2.3 Chromosomal instability pathway

The CIN pathway (Figure 1.1) begins with mutations in the tumour suppressor protein, *APC*, the inactivation of which allows for stabilization and translocation of β-catenin to the nucleus where it participates in upregulation of WNT target genes [33, 34]. Further mutations occur in *KRAS*, TGFβ signalling, *PIK3CA*, and *TP53*, leading to progression of the tumour [35-38], and may be influenced by MSI [39]. This seminal work by Fearon and Vogelstein [40] still forms the basis of the genetic modelling of CRC.

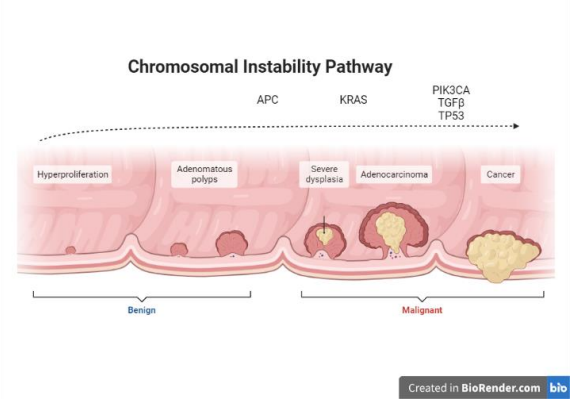

Figure 1.1 – Chromosomal instability pathway. *Representation of the Vogelstein model of progression in CRC. Early adenomas develop because of loss-of-function mutations in APC. The extent of the adenoma is exacerbated due to mutations in KRAS. Further mutations accumulate in PIK3CA, TGFβ and TP53.*

1.1.2.4 Microsatellite instability

MSI is a phenotypic sign of a state of DNA MMR deficiency which describes the impairment of the DNA MMR system, which responds to the incorrect incorporation of bases during DNA replication, because of mutations in key DNA MMR genes including; *MLH1*, *MSH2*, *MSH6*, and *PMS2* [22-30]. In this state of MMR deficiency errors accumulate and greatly extend the length of microsatellites [41]. This state of microsatellite instability is associated with right-sided disease [42, 43] and increased immune infiltration [44-46] which is believed to be a key factor in the favourable prognosis for MSI patients [47-49]. DNA MMR deficiency is histologically tested [50] and is congruous with PCR diagnosis of MSI [51].

1.1.2.5 CpG island methylation

CpG islands are regions of DNA with a high density of cytosine-guanine pairs which are present at many promoters and act as regulators when they undergo methylation to inducing gene silencing and some cancers have a substantial rate of methylation, termed the CpG island methylator phenotype [15, 52-54].

If the silenced genes are tumour-suppressor proteins, then disease progression can occur. CIMP is more common in right-sided disease compared to left sided [55-58].

1.1.3 Colorectal classification

1.1.3.1 Anatomy

The colon is a long (~150cm), tubular organ consisting of a mucosal layer surrounded in muscle and connective tissue which decreases in diameter from ~7cm to ~2.5cm moving from the proximal colon to the distal colon [59, 60]. The proximal colon (right sided) begins with the cecum (which connects the colon to the small intestine) and moves through the ascending colon where it turns at a 90° angle (hepatic flexure) to become the transverse colon [59, 60]. At the end of the transverse colon, it again turns at a 90° angle (splenic flexure) to become the distal colon (left sided) consisting of the descending colon and the sigmoid colon which connects the colon to the rectum and then the anus [59, 60]. The colon functions to absorb water and nutrients from chyme and subsequent formation progression into faeces, and expulsion via the connected rectum [59, 60]. Although often referred to under the umbrella term of CRC, there are three underlying pathologies reflective of the location of tumour development; left sided CRC, right sided CRC, and rectal CRC. These classifications are distinct in their location along the intestinal tract but also in biological traits associated with their development and patient prognosis. Right sided CRC has a greater immune infiltrate [42], be MMR deficient [43] and have *BRAF* mutations [61]. In addition, there is a gradient of immune composition and microbiome along the intestinal tract [62].

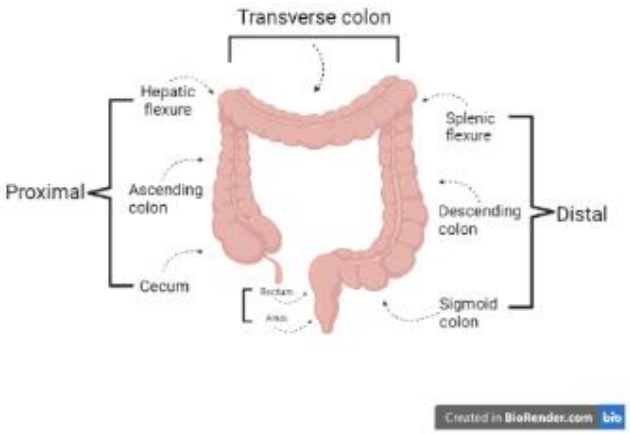

Figure 1.2 – Colorectal anatomy. *Representation of the anatomy of the colon and rectum. The colon begins in at the cecum, progressing as the ascending colon up to the hepatic flexure, turning 90° to become the transverse colon and turning 90° once more to the descending colon, moving through the sigmoid colon and ending in the rectum and anus.*

1.1.3.2 Dukes staging

Dukes staging was developed in the context of rectal cancer in the 1930's and later adapted for classification of cancer within the colon and expanded to feature distant metastasis [63, 64]. Dukes' classification describes cancers as stage A in which the tumour remains confined within the rectal wall, stage B which extend through the rectal wall and stage C defined as those with metastasis to the lymph nodes – stage D was later added to include cases with metastases to distant organs [63, 64]. Although now transcended by the TNM staging system, the key characteristics of Dukes' method are present in TNM staging.

1.1.3.3 TNM staging

The current gold standard method for staging colorectal tumours is the Tumour Node Metastasis (TNM) staging system (Table 1.1), 8th edition [5, 65], which classes cases as TNM 0-IV via coding of individual stages for staging of the penetration of the tumour, spread to lymph nodes and metastasis. The T stage is T0 if no primary tumour is present and proceeds through T1-4 as the tumour invades into the submucosa (1), muscularis propria (2), subserosa (T3) and additional organs or peritoneum (T4). The N stage is N0 if no metastases are found within the lymph nodes and proceeds through N1-2 as the tumour spreads to 1-3 lymph nodes (N1) or ≥ 4 lymph nodes (N2). The M stage is M0 if no metastases are present in distant organs, and this includes distant lymph nodes, proceeding to M1 if distant metastases are detected. These classifications are then used to encode a comprehensive TNM stage. The TNM stage is stage 0 if there is no tumour present or is classed as carcinoma *in situ*. TNM stage is stage I if the tumour is T1N0M0 or T2N0M0. TNM stage is stage II if the tumour is T3N0M0 or T3N0M0. TNM stage is stage III if the tumour is T∀N1M0 or T∀N2M0. TNM stage is stage IV if the tumour is T∀N∀M1. The TNM staging system accurately predicts the best (stage I) and worst (stage IV) prognosis of CRC patients but is not sufficiently accurate in stratifying patients within stage II and stage III [4, 66]. CRC is also highly heterogenous [67] and this is not captured within the TNM staging system.

Table 1.1 – TNM staging. *Summary table of coding process for TNM stage and associated clinical descriptions.*

TNM Staging System – Coding

TNM Stage	T Stage	N Stage	M Stage
0	Carcinoma *in situ*	N0	M0
I	T1-2	N0	M0
IIA	T3	N0	M0
IIB	T4a	N0	M0
IIC	T4b	N0	M0
IIIA	T1-2	N1/N1c	M0
	T1	N2a	M0
IIIB	T3-4a	N1/N1c	M0
	T2-3	N2a	M0
	T1-2	N2b	M0
IIIC	T4a	N2a	M0
	T3-4a	N2b	M0
	T4b	N1-2	M0
IVA	Any	Any	M1a
IVB	Any	Any	M1b
IVC	Any	Any	M1c

TNM Staging System – Clinical Descriptions

TNM Stage	Clinical Description
T0	No primary tumour present
T1	Tumour has invaded into the submucosa
T2	Tumour has invaded into the muscularis propria
T3	Tumour has invaded into the subserosa
T4	Tumour has invaded into additional organs or penetrated the peritoneum
N0	No metastasis detected in lymph nodes
N1	Metastasis detected within 1-3 lymph nodes
N2	Metastasis detected within ≥4 lymph nodes
M0	No metastasis detected in distant organs (including lymph nodes)
M1	Metastasis detected in distant organs (including lymph nodes)

1.1.3.4 CMS subtyping

In 2015, a consortium of CRC scientists agreed on a set of four molecular subtypes derived from gene expression data, termed consensus molecular subtypes (CMS) (Table 1.2) [6]. The authors produced the CMS subtypes from over 3000 patients to determine biological characteristics associated with each CMS subtype. CMS1, the immune-related group, is characterized by MSI and high immune infiltrate, in addition to high CIMP, *BRAF* mutations, activation of the JAK/STAT pathway, and an intermediate overall survival. CMS2, the canonical subtype, is characterized by high DNA somatic copy number alterations (SCNA), low immune infiltrate and stromal invasion, activation of WNT signalling, and the best overall survival. CMS3 is characterized by mutations in KRAS, low immune infiltrate and stromal invasion, activation of metabolic genes, and an intermediate survival. CMS4 is characterized by high SCNA, high stromal invasion, activation of the TGFβ and VEGF pathways, and the worst overall survival.

Table 1.2 – CMS subtypes. *Summary table of the consensus molecular subtypes.*

	CMS1 – Immune	**CMS2 – Canonical**	**CMS3 – Metabolic**	**CMS4 – Mesenchymal**
Subtype features	MSI^+	$SCNA^+$	$SCNA^-$	$SCNA^+$
	$CIMP^+$	WNT/MYC activation	$CIMP^-$	Stromal infiltration
	BRAF mutations		$MSI^{+/-}$	TGF-β activation
	Immune infiltration		Deregulated metabolism	
Prognosis	Good, unless post-relapse	Intermediate	Intermediate	Poor

1.1.3.5 CRIS subtyping

The severity of prognosis in the CMS4 subtype raised the possibility that the stroma is a leading edge factor in the progression of CRC, whilst effects intrinsic to cancer cells may be confounded by the stroma [68]. *Isella et al* took the approach of using patient-derived xenografts (PDXs), transplanting human tumours into mice, which allow for human-specific microarrays to disregard stromal components [7, 69]. The authors developed a classifier which produced five subtypes, termed the CRC intrinsic subtypes (CRIS) (Table 1.3). CRIS-A is mucinous and highly enriched for MSI or *KRAS* mutations. CRIS-B is defined by greater activity of the TGF-β pathway and EMT. CRIS-C consists of increased activity in the EGFR signalling. CRIS-D is defined by activation of the WNT pathway and overexpression of IGF2. CRIS-E reflects a Paneth cell phenotype and mutations in *TP53*. CRIS-B is considered to have the worst prognosis and CRIS-D the best prognosis, with CRIS-A, CRIS-C and CRIS-E having an intermediate prognosis.

Table 1.3 – CRIS subtypes. *Summary table of the CRC intrinsic subtypes.*

	CRIS-A	**CRIS-B**	**CRIS-C**	**CRIS-D**	**CRIS-E**
Subtype features	MSI^+ *BRAF* mutations Mucinous	TGF-β activation EMT	EGFR activation	WNT activation IGF2 overexpression	*TP53* mutations *KRAS* mutations
Prognosis	Intermediate	Poor	Intermediate	Good	Intermediate

1.1.3.6 Histological subtyping

Given the difficulty in translating genomics and transcriptomics into routine pathology as well as the costly nature of generating and analysing gene expression data for every patient with CRC, a phenotypic subtyping method was developed based on the CMS subtypes with the aim of introducing histology-based subtyping into clinical practice [70, 71]. This method incorporates immune cell infiltration using the Klintrup-Mäkinen (KM) grade, proliferation of cancer cells using the KI-67 marker, and stromal invasion using the tumour-stroma percentage [70]. These measures produce four phenotypic subtypes: immune, canonical, latent, and stromal. The phenotypic subtypes are prognostic classifiers in stage I-stage III CRC independent of TNM staging and predict recurrence and chemotherapy response [71].

1.1.3.7 Therapeutic management of CRC

The current approach to therapeutic management of CRC is multi-model and primarily consists of surgery, chemotherapy and radiotherapy [72]. The primary treatment procedure is a colectomy extending 5cm either side of the tumour. Surgery is also prevalent in rectal cancer with a total mesorectal excision for those rectal cancer in the mesorectum. Based on stratification by TNM staging, patients can receive neoadjuvant or adjuvant chemotherapy. Stage III patients receive either FOLFOX (folinic acid, fluorouracil and oxaliplatin) or CAPOX (capecitabine and oxaliplatin), usually over the course of six months but the SCOT trial suggests that a three-month treatment period could be equally effective with lesser side effects [73]. Radiotherapy is used in a neoadjuvant setting to reduce tumour burden in advanced rectal cases in advance of surgical procedures, sometimes in concert with chemotherapy [74], and can improve survival [75]. Radiotherapy can be administered as short-course radiotherapy (SC-RT) consisting of five fractions of 5 Gy one week prior to surgery or long-course chemoradiotherapy (LC-RT) consisting of 28 fractions of 1.8 Gy concurrent with chemotherapy four to eight weeks prior to surgery [76]. Evidence is building to show that radiotherapy also induces, through multiple mechanisms, a change in the TME to be more immunologically active [77]. This is of special interest as cancer treatment continues to lean into the potential of the immune system.

In CRC, the presence of a large immune infiltrate has become a clear favourable prognostic factor [8, 10, 78, 79]. Immune cells can develop a dampened immune response when checkpoint interactions take place, including the PD-1/PD-L1 and CTLA-4/B7-1/B7-2 checkpoints on T cells [80, 81], thus reducing the ability of the immune system to counteract tumour development and growth. Immunotherapies have been developed and approved for use in CRC to target these immune checkpoints, Pembrolizumab and Nivolumab to target PD-1/PD-L1 and Ipilimumab targeting CTLA-4. The goal of these therapies is to reinvigorate the exhausted T cells but they are ineffective in cases without significant immune infiltration and thus their efficacy in CRC is restricted to MSI-H/MMR deficient cases [82], in which they demonstrate substantial efficacy [83, 84]. However, MSS patients with advanced refractory CRC have a better overall survival when treated with the combination of Tremelimumab (CTLA-4) and Durvalumab (PD-1) [85] and Durvalumab is subject to ongoing clinical trials investigating the ability of radiotherapy to enhance the immune environment for effective use of Durvalumab (PRIME-RT, NCT04621370 [86] and DUREC, NCT04293419). If radiotherapy can be harnessed to bolster the immune landscape in CRC patients, then the potential of checkpoint inhibitors may be unlocked for a larger portion of CRC patients.

Another exciting arm of immunotherapy is engineered T cells, including chimeric antigen receptors (CARs) which have demonstrated efficacy in haematological cancers [87] but failed makeprogress in solid tumours such as CRC [88]. One such issue is the lack of availability of tumour specific antigens (TSAs) and there is a large drive to resolve this issue with selected targets including EGFR, MUC1 and CEA [89]. An alternative approach would be to introduce significant numbers of ‘off the shelf’ T cells into the TME, thus allowing any patient to theoretically benefit from an immune infiltration. This approach is likely reliant on γδ T cells, an unconventional subset of T cells, which are active independent of human leukocyte antigen (HLA) restriction and thus limits the risk of graft-versus-host disease (GvHD) [90]. Ultimately, data so far would suggest that a truly impactful immunotherapy will need to not only apply the significant cytotoxic potential of immune cells, but also prime the TME for application of those therapies, requiring a combinational approach.

1.2 γδ T Cells in the Intestine

1.2.1 γδ T cell structure

γδ T cells (Figure 1.3) are an unconventional T cell subset of T cells utilising a T cell receptor (TCR) consisting of a γ chain and a δ chain, in contrast to conventional T cells which use α and β chains. Each chain consists of a constant region and a variable region. The constant region includes a disulfide bond connecting the two chains, the transmembrane region, and the cytoplasmic tail [91]. As γδ T cells mature, they undergo rearrangement of the variable (V), diversity (D) and joining (J) gene segments (VJ in the γ chain and VDJ in the δ chain), resulting in a distinct variable region with three hypervariable complementarity-determining regions (CDRs) which form the TCR's binding site [92]. As in the case of αβ T cells, γδ T cells are bound at the cell surface with a CD3 coreceptor containing immunoreceptor tyrosine-based activation motif (ITAM) domains for signal transduction. In humans, there are six functional γ chains; Vγ2, Vγ3, Vγ4, Vγ5, Vγ8 and Vγ9, and three δ chains; Vδ1, Vδ2 and Vδ3 [93-95]. In the human gut, γδ T cells are predominantly Vγ4Vδ1 [96].

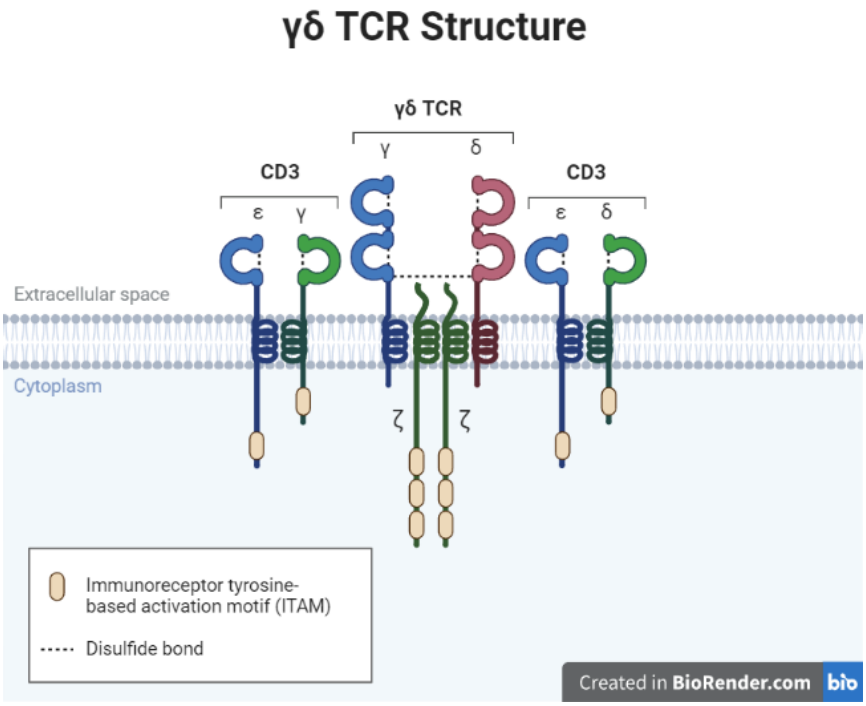

Figure 1.3 – γδ T cell TCR structure. *Graphical representation of the structure of the γδ T cell TCR.*

1.2.2 γδ T cell intestinal compartment formation

γδ T cell generation in humans is highly complex and tightly regulated. γδ T cells emerge from the foetal or adult thymus as naive cells with polyclonal TCRs or imprinted effector cells, some of which express an invariant TCR [97-102]. Interestingly, Vγ9Vδ2 cells generated during foetal development are replaced by Vγ9Vδ2 cells with a different TCR in adults [103, 104], indicating a TCR switch of unknown importance. After birth, Vδ1 cells dominate γδ T cell development, overtaking Vδ2 cell numbers in the thymus, gut, and skin [96, 105-108], although Vγ9Vδ2 do remain and act as antigen presenting cells to induce $CD4^+$ T cell expression of IL-22 [109]. With age, however, Vγ9Vδ2 cells expand to become the most abundant subset in the blood and spleen. The appearance of human gut Vγ4Vδ1 cells may also occur independently of the thymus, but the ontogeny of these human cells is still not well addressed [110]. γδ T cells in the gut are subject to further environmental cues however, with their development and maintenance in the intestine requiring interaction with butyrophilin-like 3 (BTNL3) and butyrophilin-like 8 (BTNL8) [111-113]. In contrast, limited work suggests a negative regulatory role for BTNL2 [114]. These proteins interact with germline encoded regions of the TCR, CDR2 and HV4 loops which contribute to the antigen-binding site, that are not subject to clonality whilst allowing for clonally restricted antigen binding in the CDR3 loops [91, 113]. γδ T cells in the liver, the primary location of metastasis in CRC, are understudied but a population has been found characterized by the expression of Vδ1 as well as established resident markers, such as CD69, CXCR3, and CXCR6 [115]. The original origin of these cells is not clear. The intestinal lumen is covered in a layer of epithelia featuring crypt structures. At the base of these crypts, $LGR5^+$ intestinal stem cells rapidly divide and differentiate to give rise to component cells of the epithelia including enterocytes, tuft cells and goblet cells [116]. Enterocytes form tight junctions to create a strong defensive barrier. Goblet cells synthesise and release mucins to protect the surface later. Tissue resident γδ T cells patrol along the basement membrane contacting epithelial cells [117, 118] and maintaining the integrity of epithelial tissue by detecting signs of bacterial presence [119] or stress signals [120-122].

1.2.3 γδ T cell ligands

γδ T cells are distinct from αβ T cells in that the γδ TCR is not major histocompatibility complex (MHC) restricted [123], and these cells normally lack expression of CD4 and CD8 except for CD8αα-expressing cells which are gut-specific [123-125]. γδ T cells recognise multiple ligands (Table 1.4) including stress molecules such as endothelial protein C receptor (EPCR), MHC class I chain-related A/B (MICA/MICB) [126, 127], and annexin A2 [128, 129], pathogen specific antigens [130] and MHC class I-like molecules [131-138]. However, these ligands are only relevant to a portion of γδ T cells and our understanding of γδ T cell ligands remains limited. In addition, γδ T cells recognise members of the butyrophilin (BTN) and butyrophilin-like (BTNL) family, which are structurally and phylogenetically related to the B7 superfamily of co-stimulatory molecules [139]. This includes the previously discussed BTNL3 and BTNL8 that are integral to the maintenance of the gut-specific γδ T cell compartment [111-113], and the BTN3A1-BTN2A1 heterodimer which acts as a sensor for phosphoantigens such as isopentenyl pyrophosphate (IPP) [140-143] which often accumulates intracellularly in tumours due to dysregulated metabolism [144].

Table 1.4 – Human γδ T cell ligands. *Summary table of the known ligands for human γδ T cells.*

Ligand	Category	T Cell Subset
Phycoerythrin	Pathogen	Vγ2-9Vδ1
IPP	Stress surveillance	Vγ9Vδ2
EPCR	Stress surveillance	Vγ4Vδ5
MICA	Stress surveillance	Vγ2-9Vδ1
Annexin A2	Stress surveillance	Vγ8Vδ3
CD1c	MHC-like	Vγ2-9Vδ5
CD1d	MHC-like	Vγ2-9Vδ5
MR1	MHC-like	Vγ2-9Vδ1-3
BTNL3	Regulatory	Vγ4Vδ1-3
BTNL8	Regulatory	Vγ4Vδ1-3

1.2.4 Anti-tumourigenic role of γδ T cells

Research into the anti-tumourigenic functions of γδ T cells (Figure 1.4) have so far been focused on the Vγ9Vδ2 circulatory population. Whether isolated from the ascites of a metastatic CRC patient, the primary tumour of a CRC patient, or the peripheral blood of a healthy donor, Vγ9Vδ2 cells exhibit cytotoxic ability against various CRC cell lines [145]. Vγ9Vδ2 cells exhibit equivalent cytotoxic capacity whether from cancer patients or healthy donors, suggesting that the anti-tumourigenic capacity of Vγ9Vδ2 cells is not influenced by the tumour. However, after co-culture with supernatant from CRC patient-derived cancer stem cells (CSCs), γδ T cells have reduced proliferation and IFNγ expression and increased IL-17 expression [146]. These observations indicate the ability of γδ T cells to recognize cancer cells is influenced by the tumour microenvironment (TME). Despite these promising results, there is increasing interest in the $V\delta2^-$ subsets, particularly the Vδ1 cells. The dominant population in human colorectal tumours are Vδ1 cells [96], and they display cytolytic reactivity against CRC cell lines both in vitro and in a xenograft model [147-150]. Vδ1 cells conduct cytotoxic action against cancer cell independent of MHC molecule recognition [149]. One study reported that Vδ1 cells from the primary tumour of three CRC patients (one metastatic) exhibited greater cytotoxic activity against epithelial tissue compared to alternative tissue types, as quantified by percentage cell lysis and IFNγ release [147]. This raises the possibility that Vδ1 cells are reacting to a ligand of epithelial origin via receptors such as NKG2D which are constitutively expressed on these cells [120, 122, 126, 151-153].

When Vδ1 cells and Vδ2 cells, isolated from the peripheral blood of CRC patients and healthy donors, are compared, Vδ1 cells exhibit a higher level of expression of markers of cytotoxicity, activation, and differentiation. This phenotype translates to functionality, with Vδ1 cells demonstrating a greater degree of cell lysis against CRC cell lines when compared to Vδ2 cells [149, 150]. A subpopulation of Vγ4Vδ1-expressing IELs expressing $NKp46^+$ were recently characterised [153]. $NKp46^+$ γδ T cells produce more IFNγ, granzyme B, and CD107a than the $NKp46^-$ population after being cocultured with the K562 cell line (myelogenous leukaemia) and kill K562 cells more efficiently. Blocking NKp46 also reduces K562 killing in these cocultures [153]. In summary, a stronger anti-tumorigenic potency was demonstrated by Vδ1 cells compared to Vδ2 cells. It is important to understand how these cells function in the context of metastasis as this is the cause of a large portion of cancer deaths.

In an orthotopic mouse xenograft model, consisting of luciferase-expressing HT29 cells injected into the cecum of immunodeficient mice, primary tumour growth and the formation of spontaneous metastases are reduced with administration of Vδ1 cells [154]. There is also a decrease in HT29 cell growth in the lung after intravenous administration of Vδ1 cells [154]. Together, these data demonstrate that Vδ1 cells are capable of significant anti-tumourigenic and anti-metastatic activity against CRC. Thus, continually growing research into these cells is elucidating how they differ from Vδ2 cells and how best to utilise them.

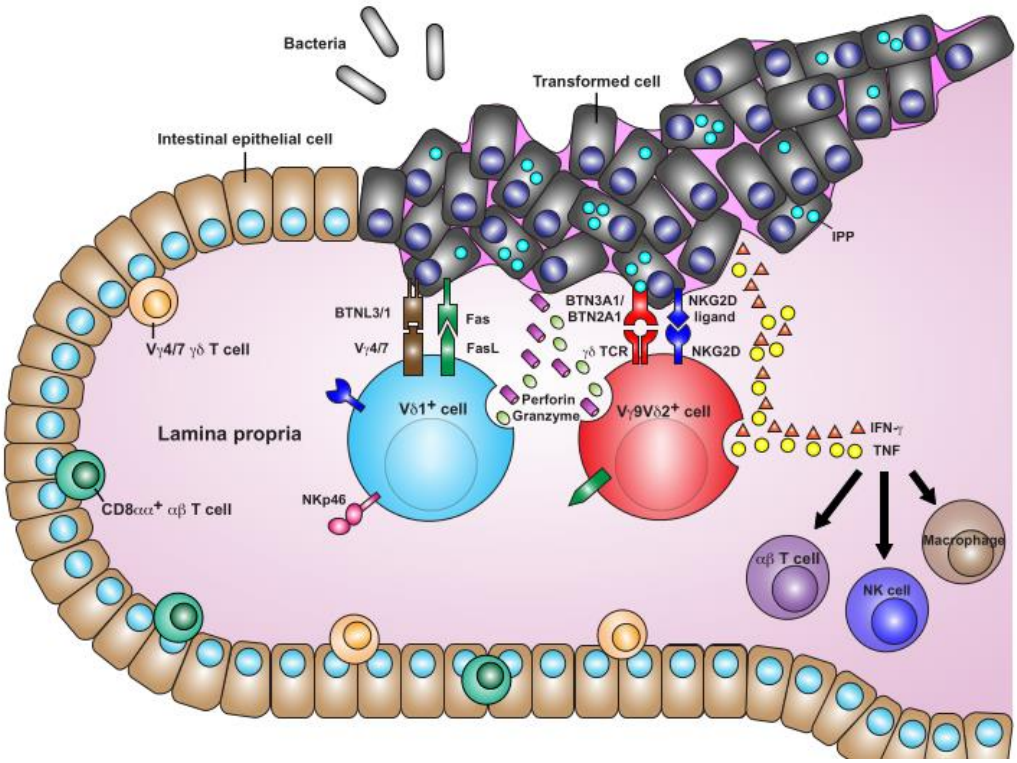

Figure 1.4 - Anti-tumorigenic functions of γδ T cells in CRC – adapted from Suzuki et al [155]. *In humans, two major subsets of γδ T cells can recognize and kill cancer cells: One is the gut resident Vδ1 cell subset and the other is the Vγ9Vδ2 cell subset that enters the gut from the circulation. Both subsets express cytotoxic molecules, such as granzyme, perforin, FasL, IFNγ, and TNF. During immunosurveillance, γδ T cells may sense abnormalities through the NKG2D receptor by stress ligands expressed on cancer cells. Vδ1 cells that express the Vγ4 chain (or Vγ7 chain in mice) and NKp46 may bind cancer cells through BTNL3 (or BTNL1 in mice). By contrast, Vγ9Vδ2 cells recognize cancer cells through BTN3A1/BTN2A1 heterodimers, which bind to the γδ T cell receptor (TCR) after activation by the IPP metabolite, a product of the mevalonate pathway.*

1.2.5 Pro-tumourigenic role of γδ T cells

Our understanding of how γδ T cells promote CRC (Figure 1.5) is still limited but data so far is centred around IL-17-producing γδ T cells subsets. This association between IL-17-producing γδ T cells and pro-tumourigenicity has also been demonstrated in other cancer types [156-160]. It should be noted that these data are from murine models, but they give an insight into how IL-17 might function in human disease. The toll-like receptor (TLR) pathway is a significant factor in tumourigenesis driven by mutant *APC* or loss of *APC* [161, 162]. In these models, deletion of MyD88, an adapter molecule mediating TLR signalling, there is a reduction in pro-inflammatory molecules including COX-2, IL-6, IL-23, and IL-1β, and subsequent tumour formation. These pro-inflammatory molecules are triggered and contribute to cancer progression because of the epithelial barrier being breached and subsequent exposure of microbial products to myeloid cells. The result of these circumstances is increased production of IL-17A by CD4 T cells and γδ T cells. Deletion of *IL17a* or *IL17ra* in APC models phenocopies the reduced tumour development seen in MyD88 studies [162-164]. IL-17A stimulates the proliferation of APC-deficient enterocytes by activating MAPK signal transduction pathways [163]. Whether the source of IL-17A is αβ or γδ T cells, genetic deletion of IL-17A inhibits tumour formation in $APC^{Min/+}$ mice [165]. Together, these data highlight that CRC development can be promoted via inflammation induced by TLR-mediated activation of IL-17-producing CD4 T cells and γδ T cells. As Vγ7 IELs are not capable of making IL-17, these IL-17–producing γδ T cells are likely Vγ4 or Vγ6 cells. Like APC models, enterotoxigenic Bacteroides fragilis (ETBF)–induced mouse models of CRC feature an increased quantity of Th17 cells and IL-17–producing γδ T cells [166-168]. However, in contrast to the $APC^{Min/+}$ model, Th17 cells and IL-17–producing γδ T cells are redundant in this model as γδ T cells also express IL-17A and depletion of STAT3 to inhibit Th17 function does not prevent tmourigenesis. Thus, for tumour formation to be inhibited in the ETBF model, removal of both Th17 cells and γδ T cells would be required [167]. Considering this, and that γδ T cells express higher levels of IL-17A than CD4 T cells, it may be a better approach to target IL-17A instead of Th17 cells or IL-17–producing γδ T cells, although this would require identification and inhibition of shared regulators of IL-17A expression in both cell types. One strategy may be the targeting of RORγt, the master transcriptional regulator of IL-17A, via manipulating its degradation. ITCH-mediated ubiquitination is a regulator of RORγt protein expression and mice with ITCH knockout are more susceptible to AOM/dextran sodium sulphate (DSS)–induced tumorigenesis because of IL-17 production by CD4 T cells and γδ T cells [169].

In autoimmune disorders in humans where Th17 cells and γδ T cells contribute to the pathology, such as multiple sclerosis, psoriasis, and rheumatoid arthritis, small molecule inhibitors exist which are candidates for drug repurposing in the context of cancer therapy [170]. As most data originates from mouse studies, it remains controversial whether the importance of IL-17–producing γδ T cells in cancer is equally relevant in human disease.

Although the production of IL-17A by human circulatory Vγ9Vδ2 can be induced *in vitro* under the conditions of IL-23, IL-1β, TGFβ, and/or IL-7, they do not appear to do so *in vivo* [171-173]. However, IL-17-producing γδ T cells are found in human CRC, particularly in the tumour where they correlate with tumour stage, tumour size, invasion, lymph node metastasis, vascular and lymphatic invasion, and immunosuppressive neutrophils [146, 174-176]. A portion of these cells expressing CD39 also appear to suppress anti-tumourigenic T cells [175]. To resolve a limitation of current data on the role of γδ T cells in CRC, the lack of mouse models reflective of CRC pathologies, more complex mouse models are being developed which may provide a greater perspective [177]. This includes a model to replicate complete progression to metastasis to the liver, allowing for interrogation of a key aspect of CRC. The importance of TGFβ signalling in murine CRC metastasis was emphasised using organoids carrying mutations in *APC*, *KRAS*, *TGFBR2*, and *TP53* [178], in which survival was improved and metastasis reduced when mice underwent therapy with a combination of PD-L1 and TGFβ inhibitors. Potentially, metastasis in this model is partially driven via immunosuppression by TGFβ-producing γδ T cells that suppress cytotoxic CD8 T cells [179]. The ability of IL-17–producing γδ T cells to control immunosuppressive neutrophils, thus promoting tumour progression and metastasis, has been shown in murine breast cancer [159]. Collectively, this suggests that γδ T cells may have significant pro-tumourigenic and pro-metastatic functions in CRC. These models will not only improve our understanding of IL-17, but potentially reveal additional pro-tumourigenic factors. Another recently developed mouse model is driven by mutations in *KRAS*, loss of p53 and overexpression of NOTCH1 and showed that neutrophils are a contributory factor in liver metastasis [180]. In a murine sarcoma model driven by mutations in *KRAS* and *TP53*, γδ T cells supressed anti-tumourigenic T cells via galectin-1 expression [181], and a murine lung cancer model driven by mutations in *KRAS* and *TP53* in which IL-22 and amphiregulin (AREG) exacerbated tumour growth [182]. A significant limitation in our understanding of γδ T cell biology is much of it is of murine origin, but human and murine γδ T cells are distinct. Thus, a key research need is to understand how much of this understanding translates into human disease.

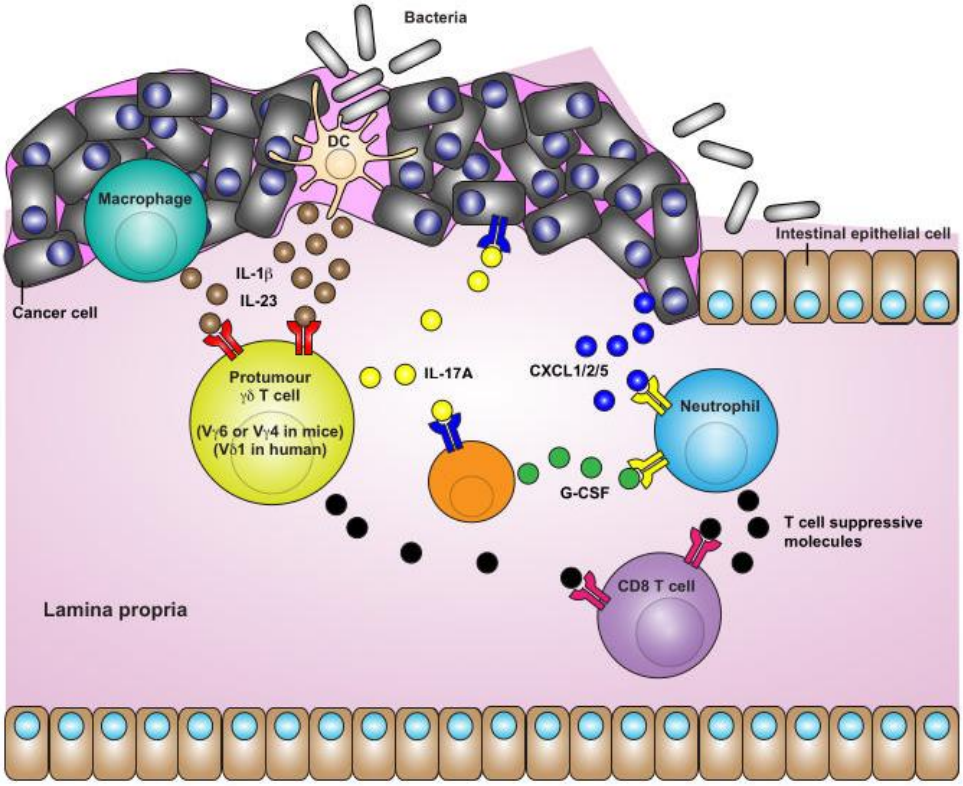

Figure 1.5 - Pro-tumorigenic functions of γδ T cells in CRC - adapted from Suzuki et al [155]*. Breakdown of the epithelial barrier by the disorganization of cancer cells allows bacteria to penetrate gut tissue. These microorganisms activate dendritic cells (DC) and macrophages to secrete the cytokines, IL-1β and IL-23, which are received by γδ T cells expressing Vδ1 cells in humans (Vγ6 or Vγ4 cells in mice). In response to this stimulus, these γδ T cell subsets release IL-17A, and IL-17A can induce proliferation of cancer cells or induce G-CSF expression by other cells. G-CSF mediates neutrophil expansion; neutrophils are drawn into the tumour microenvironment by the chemokines, CXCL1, CXCL2, or CXCL5. Neutrophils and γδ T cells can suppress the anti-tumour activity of CD8 T cells to promote cancer progression.*

1.2.5 The prognostic potential of γδ T cells in CRC

The current gold standard tumour burden/nodal status/metastasis (TNM) staging system suffers from inconsistencies, with crossover between stage II and III patient prognosis and 25% of stage II and stage III patients relapse despite the lack of evidence for residual cancer cells or distant metastasis following surgical resection [4, 183]. Thus, there is a need to develop more stringent prognostic tools in CRC. Additionally, TNM does not predict response to chemotherapy. Attempts have been made to improve on this system by employing the immune landscape, resulting in the Immunoscore [9], which is based on the observation that T cells have a strong, favourable prognostic role in CRC. This data stems from a study of 415 CRC patients, which demonstrated that patients had an improved disease-free survival if their tumour was infiltrated by CD3, CD8, or CD45RO (effector/memory) T cells at the tumour centre or invasive margin [8]. Further to this, of those classified as having a high Immunoscore, only 4.8% suffered relapse within five years [78]. As the Immunoscore utilises CD3 T cells, γδ T cells are included within its measurements, but γδ T cells are only a small proportion of CD3 cells [146, 184], so whether they contribute significantly to the Immunoscore is not clear. As the Immunoscore is associated with a favourable outcome, one can speculate that γδ T cells would likewise be favourable, although this was shown to not be the case in other cancer types [185, 186]. However, a comprehensive histological study of the prognostic role of γδ T cells is yet to be performed.

A large part of the justification for therapeutic use of γδ T cells in CRC emanates from a 2015 study which suggests that γδ T cells are a pan-cancer favourable prognostic factor [10]. This study utilised 18,000 human tumours, including CRC, to perform computational lymphocyte deconvolution using the CIBERTSORT algorithm [11], which uses bulk transcriptomics to derive immune cell populations. The overall outcome of this study was that myeloid cells were unfavourable whilst lymphoid cells were favourable, with γδ T cells being the most favourable subset. Unfortunately, the gene signatures used to delineate lymphocyte subsets using CIBERSORT are flawed and demonstrate significant overlap between those identifying γδ T cells and those identifying other subsets [187]. These gene signatures are derived from peripheral blood immune cells [11]. Vγ9Vδ2 purified from the peripheral blood of 12 healthy donors had CIBERSORT applied and demonstrated significant overlap between CD8 T cells, CD4 T cells, and NK cells [187]. To resolve this, the CIBERSORT gene signature for γδ T cells was refined to 375 genes and resulted in an improved detection of Vγ9Vδ2 T cells. In CRC, TCR signalling, TLR signalling, antigen processing, cytolytic activity, and interferon response pathways all correlated with the abundance of αβ T cells, but not Vγ9Vδ2 T cells. These results aside, a good outcome was observed in CRC patients associated with either αβ T cells or Vγ9Vδ2 T cells [187]. The same methodology was applied to another cohort with equivalent results [146]. However, this methodology is specific to Vγ9Vδ2 T cells, which are only dominant in the circulatory system. Thus, it is vital to understand the prognostic value of gut-resident Vδ1 subset and IL-17–producing subsets. A poor survival outcome in CRC is associate with both IL-17-producing γδ T cells [174, 175] and *IL17A* expression [146, 188]. However, the mere presence of γδ T cells does not contribute to tumourigenesis, but rather their functional capabilities such as cytolytic activity.

Using the transcriptomic expression of granzyme A and perforin, a quantitative measure of immune cell cytolytic activity (CYT) was developed [189]. Based on TCGA datasets, normal colorectal tissue had a higher CYT score then colorectal tumour tissue, especially those which were MSI [189-191]. In the context of both overall and disease-free survival, a high CYT score is associated with a favourable prognosis. γδ T cells, CD4 T cells, NK cells, and anti-tumorigenic macrophages are all present at a higher density in CRC tumours with a high CYT score compared to those with a lower CYT score [190, 191]. However, these γδ T cells were identified using CIBERSORT, so it can be inferred that these are Vγ9Vδ2 cells which is unsurprising given that Vγ9Vδ2 cells, like αβ T cells, are enriched in MSI tumours [146, 192]. It is not clear if γδ T cells specifically contribute to a high CYT score by production of granzyme A and perforin, but it is a valid hypothesis.

γδ T cells have demonstrated an ability to predict checkpoint inhibitory response in some cancer types, but whether this is the case in CRC is not clear. Melanoma patients with a low abundance of Vδ1 cells or high abundance of Vδ2 cells, overall survival is improved [193].

1.2.6 The therapeutic potential of γδ T cells in CRC

As γδ T cells recognise MHC-unrestricted antigens and exhibit potent cytotoxicity, their potential for immunotherapy is substantial. Early data in renal, breast and lung cancers suggest that immunotherapy with Vγ9Vδ2 T cells can have a positive impact on cancer progression and is well tolerated [194-198]. Thus, a great effort is being made to develop therapeutic protocols for preconditioning γδ T cells prior to *ex vivo* adoptive cell transfer (ACT). Primarily, this has focused on Vγ9Vδ2 cells expanded via IL-2 and zoledronate, although this method is time consuming [195, 196, 199, 200]. Post-surgical administration of zoledronate-expanded Vγ9Vδ2 cells in CRC patients combats pulmonary metastases, maintaining their CD107a expression and ability to produce IFNγ [201], although the efficacy of these Vγ9Vδ2 cells in controlling tumour progression was not reported. A potential improvement is to further develop the expansions protocols, such as by adding IL-23 [202, 203]. An alternative is concurrent administration of synthetic phosphoantigens and this has been tried in CRC, such as Bromohydrin pyrophosphate (BrHPP, IPH 1101) [204], which results in an initial increase in the number of Vγ9Vδ2 cells extracted [205]. Furthermore, circulatory Vγ9Vδ2 cells expanded *ex vivo* with BrHPP and IL-2 have a strong cytolytic capacity and effector phenotype, and this cytolytic activity is both TCR and NKG2D-mediated [206]. Other work has found success in boosting cytolytic activity in Vγ9Vδ2 cells by blocking the immune checkpoint B7-H3 [207]. This would suggest that Vγ9Vδ2 cells can be an efficacious and well tolerated immunotherapy in CRC. Another approach to boosting Vγ9Vδ2 cells is to target antigen recognition as Vγ9Vδ2 cells show cytotoxicity against CRC cell lines based on IPP-stimulated activation of BTN3A1 [145, 208-212], thus inducing IPP accumulation will position BTN3A1 and BTN2A1 in the right conformational position for Vγ9Vδ2 cell recognition. Zoledronate, which blocks farnesyl pyrophosphate synthase and prevents conversion of IPP to cholesterol or ubiquinones, induces accumulation of IPP and subsequently sensitises CRC cells to Vγ9Vδ2-mediated killing [209, 213]. To capitalise on these approaches however, it is important to optimise patient selection. p53 suppresses mevalonate pathway enzymes, whilst these enzymes are increased in p53-mutant and p53-deficient cases of breast, liver, and CRC [214-216]. Potentially, p53 mutant tumours may be more susceptible to Vγ9Vδ2 immunotherapy. The mevalonate pathway is also inhibited at the hydroxyl-methylglutaryl coenzyme A reductase (HMG-CoAR) stage by statins upstream of IPP, thus preventing IPP accumulation. Thus, statins can induce apoptosis of p53-deficient CRC cells [214], but also reduce Vγ9Vδ2 cell-mediated recognition of CRC cells. As *TP53* mutations are prevalent in CRC, particularly in distal tumours [217], this adds yet another potential route to improve Vγ9Vδ2 therapy.

Finally, γδ T cells can contribute to immunoptherapy via bispecific antibodies, transduction of the γδ TCR into αβ T cells (TEGs) [218, 219], and chimeric antigen receptors (CARs) [220, 221]. Additionally, *ex vivo* expansion protocols for Vδ1 cells could be favourable (Delta One T [DOT] cells) [222]. Activation of Vγ9Vδ2 cells concurrent with inhibition of EGFR has been demonstrated with bispecific antibodies and demonstrates potential in CRC cell lines [223]. This kind of approach could produce precise therapies for patient subsets such as those with KRAS-mutant tumours resistant to EGFR-targeted antibodies [224].

1.3 Research Aims and Hypotheses

This thesis sought to determine the difference in density of two key lymphocyte populations in the intestine, γδ T cells and CD8 T cells, and how any difference in their density associates with the clinical outcome for patients. In addition, the thesis aimed to elucidate the mutational and transcriptional landscapes of patients classified by their relative density of these lymphocyte populations. To achieve these aims, the following objectives were pursued:

1. Investigate, via IHC, the density of γδ T cells and CD8 T cells in the primary tumour and adjacent normal tissue of in three CRC patient cohorts from distinct geographical, social, and genetic backgrounds.
2. Utilise the literature and associated clinical data of these cohorts to contextualise any differences in lymphocyte density observed in an inter-cohort manner by identifying differences in patients treated in Scotland compared to those treat in Norway or Thailand, and in an intra-cohort manner by identifying differences between the primary tumour and adjacent normal tissue.
3. Determine the differential prognosis, or lack of, between patients grouped by their lymphocyte density, in both the primary tumour and the adjacent normal tissue.
4. Elucidate the mutational landscape underlying any differences in lymphocyte density and determine if the prognosis of patients in the context of this mutational landscape matches that observed by lymphocyte density.
5. Transcriptionally validate the histological classification of patients by lymphocyte density by extracting the transcriptional data for genes that are structurally integral to γδ T cells and CD8 T cells and compare this to histological classification.

6. Transcriptionally investigate the expression of the *BTNL* genes which encode γδ T cell regulatory proteins and determine if this associates with the expected density classification.
7. Transcriptionally investigate the prognostic role of γδ T cells and CD8 T cells by extracting the transcriptional data for genes that are structurally integral to γδ T cells and CD8 T cells, reclassify lymphocyte density groups using this data and apply the same survival methodology previously used with histological data.
8. Elucidate the transcriptional landscape underlying any differences in lymphocyte density.

Chapter 2:
Materials and methods

Chapter 2 - Materials and Methods

2.1 Immunostaining

2.1.1 γδ T Cells

Immunohistochemistry (IHC) was used to examine the presence of γδ T cells in samples using the δ chain (epitope: not mapped) of the γδ T cell's TCR as a marker. The δ chain antibody has been externally validated (1,2) and we have conducted our own internal validation. Samples were dewaxed with Histoclear (National Diagnostics, LOT 14-19-09) and rehydrated using graded alcohols (VWR Chemicals, LOT 19B064008 and 19G314006) (100%, 90%, 70%). Antigen retrieval was induced by heating samples under pressure for five minutes in a citrate (pH 6.0) buffer. Endogenous peroxides were quenched with 3% hydrogen peroxide for 20 minutes at room temperature. Non-specific antibody binding was blocked by treating samples with 1.5% serum (Vector Labs Horse S-2000, LOT ZE1108) diluted in antibody diluent (DAKO, LOT 10151797), for 1 hour at room temperature. Slides were incubated with primary antibody (Santa Cruz, TCR δ Mouse H-41 sc-100289, LOT K1318 or K2618), isotype control (Invitrogen, Mouse IgG1 kappa P3.6.2.8.1, LOT 2031807) or no antibody for 30 minutes at room temperature in antibody diluent (DAKO, LOT 10151797). δ chain expression was detected by incubation with a one-step secondary antibody/enzyme product (Vector Labs ImmPress MP-7500, LOT ZF0514) for 30 minutes at room temperature and visualised by incubation with the chromagen 3,3'-diaminobenzidine (Vector Labs ImmPact SK-4105, LOT ZE1108) for three to five minutes at room temperature. Samples were counterstained with haematoxylin (ThermoScientific 6765001, LOT 446498), dehydrated using graded alcohols (VWR Chemicals, LOT 19B064008 and 19G314006) (70%, 90%, 100%) and mounted using Omnimount (National Diagnostics, Cat# HS-110, Lot# 08-17-19, Cas# 64742-95-6). Slides were scanned at x20 magnification using a Hamamatsu NanoZoomer (Hertfordshire, UK) by Glasgow Tissue Research Facility.

2.1.2 CD8 T Cells

IHC was used to examine the presence of CD8 T cells in samples using the CD8 coreceptor as a marker. Slides were stained using an Epredia™ Lab Vision™ Autostainer 480S-2D. Deparaffinisation and antigen retrieval were conducted with slides in antigen retrieval buffer (Thermofisher, TA-999-DHBH) at 97°C for 30 minutes, followed by sequential rinses with TBST (Thermofisher TA-999-TT) at 65-85°C and room temperature. Peroxidase blocking (Thermofisher, TA-125-H2O2Q) and protein blocking (Thermofisher, TA-125-UB) were carried out for 10 minutes each, with TBST rinses in between. Slides were incubated with primary antibody (DAKO (Agilent), M7103, LOT 20083402), isotype control (Invitrogen, Mouse IgG1 kappa P3.6.2.8.1, LOT 2031807) or no antibody for 30 minutes at room temperature in antibody diluent (Thermofisher, TA-125-ADQ). Antibody amplification (TL-125-QPB) and secondary antibody (TL-125-QHD) incubations were carried out for 10 minutes each with TBST rinses in between. Visualisation lasted for 5 minutes, slides rinsed, and counterstained in the MYR MYREVA SS-30 Slide Stainer using program #3 ICC. Slides were mounted manually (Pertex mounting media, Histolabs, 00801) or using an automated coverslipper (Epredia CTM6 Automated Glass Coverslipper, ClearVue Mountant). Slides were scanned at x20 magnification using a Hamamatsu NanoZoomer (Hertfordshire, UK) by Glasgow Tissue Research Facility.

2.2 Digital Analysis Workflow

Raw images are imported into VisioPharm within a database hierarchy consisting of Cohort > Marker > Images. The first level of tissue compartments (primary tumour, adjacent normal tissue, metastases and liver) is manually annotated as 'regions' (Figure 3.3A/B), with care taken to avoid artefacts such as folded tissue, areas of significant background and haematoxylin debris, which are misidentified as $\gamma\delta$ T cells (Figure 3.3C/D). Blank regions within the annotation (such as in sections cut from a block previously used to create TMAs) are not avoided as the analysis runs on cell numbers, so those regions will not alter the output. From this point, analysis is digital and can be applied *en masse* to the images and allowed to run unattended in a queued format, analysing approximately 30 full sections per day. Analysis is conducted with two apps. The first app is applied to the manual annotations and classifies tissue as epithelium or stroma/lamina propria. The second app is applied to regions created by the first app and counts all positive cells, outputting the metric '% positive', defined as the % of all cells in the region that are positive. The development of this workflow is described in chapter '3.2.3 VisioPharm'.

2.3 Patient Cohorts

2.3.1 Scotland cohort

Cohort consists of 1030 patients who had undergone a potentially curative resection for stage I-IV CRC between 1997 and 2007 at the Glasgow Royal Infirmary, Western Infirmary or Stobhill Hospitals (Glasgow, UK). Resection was considered curative based on pre-operative computed tomography and intra-operative findings. Tumours were staged using the fifth edition of the AJCC/UICC-TNM staging system. Tumour differentiation, graded as well/moderate or poor in accordance with Royal College of Pathologists, and additional data were taken from pathology reports issued following resection. Following surgery, patients with stage III or high-risk stage II disease and without significant co-morbid disease precluding adjuvant treatment were considered for 5-fluorouracil-based chemotherapy. Patients were followed up for at least five years and date and cause of death were crosschecked with the cancer registration system and the Registrar General (Scotland). Cancer-specific survival (CSS) was measured from date of surgery until date of death from CRC. 359 patients were included in a sub-cohort for analysis. Safehaven number: GSH/18/ON007.

2.3.2 Norway Cohort

A parent cohort of 299 patients with stage II-III CRC who have undergone potentially curative surgical resection for CRC at Southern Hospital Trust in Norway. All patients underwent surgery between 2000 and 2020. 293 patients were included in a sub-cohort for analysis. Tumours were staged according to the 5th edition of the AJCC TNM classification from 2000 to 2009, 7th edition of the AJCC TNM classification from 2010 to 2017 and 8th edition of the AJCC TNM classification thereafter.

2.3.3 Thailand Cohort

A parent cohort of 411 patients with stage I-IV CRC who have undergone potentially curative surgical resection for CRC at hospitals in Thailand. All patients underwent surgery between 2009 and 2016. 320 patients were included in a sub-cohort for analysis. Tumours were staged according to the 6^{th} or 7^{th} editions of the AJCC TNM classification.

2.4 Statistical Analysis

2.4.1 Generating Cut Points for Continuous Variables

Cut points for classification by lymphocyte density were determined using the maximally selected rank statistic [225, 226]. This method considers that an unknown cut point (μ) in our continuous variable of interest (X) produces two groups of observations around an outcome (Y). To identify μ, various cut off values along the continuous variable of interest are used to determine a logrank test statistic using a given survival outcome and time. To prevent inappropriate group numbers, cut points are determined within the bounds of quantiles with minimum (ε_1) and maximum (ε_2) proportions of 0.1 and 0.9, where $0<\varepsilon_1<\varepsilon_2<1$ and μ is within ε_1 and ε_2. The test statistics for all cut points are then ranked (high to low) and the cut point corresponding to the highest-ranking test statistic is chosen as the cut point. Cut points were determined using cancer-specific survival. Cut point analysis was conducted using an R (V4.2.1) work flow built on the R packages 'survminer' V0.4.9 and 'maxstat' v0.7.25 [227, 228].

2.4.2 Time-To-Event Analysis

Definition of survival variables

Cancer-specific survival is defined as time until cancer-induced death. Disease-free survival is defined as time to death or recurrence. Overall survival is defined as the time until death due to any cause. Recurrence-free survival is defined as time until recurrence of disease.

Kaplan Meier plots

Kaplan Meier plots were used to determine if there was an association between lymphocyte density and each of the analysed survival outcomes (CSS, DFS, OS, RFS). Hazard ratios were determined via Cox regression. Analysis was conducted using an R (V4.2.1) analysis workflow built on the R packages 'survminer' V0.4.9, 'survival' V3.4.0 and 'survivalanalysis' V0.3.0 [227, 229, 230].

2.4.3 Mutational Analysis

Mutational profiling was performed on a subset of patients (n = 200). DNA was previously extracted from FFPE sections by NHS molecular diagnostics, Dundee and stored at -80°C. DNA quality and concentration were determined using the Qubit assay (ThermoFisher, Massachusetts, USA). Samples with a DNA concentration of >10ng/µL were included in the study. Sequencing was outsourced and performed by Dr Susie Cooke and the Glasgow Precision Oncology Laboratory (GPOL) using a custom in-house designed panel of 151 cancer-associated genes. Mutational analysis was conducted using self-developed R [231, 232] functions (ref appendix) in addition to the MafTools package [233]. Analysis was conducted in R V4.2.1 with mafTools V2.12.0. The tumour epithelium compartment was excluded from mutational analysis due to insufficient data to run the analysis. Oncoplots were produced using MafTools' 'oncoplot' function. Mutational summary dashboards were produced using MafTools' 'plotmafSummary' function.

Single mutated genes associated with cases low or high for a lymphocyte population are determined using the 'clinEnrich' function, which utilises MafTools' 'clinicalEnrichment' function and runs Fisher's test on a contingency table of WT/mutant and lymphocyte low/high, producing an odds ratio (lymphocyte low group as reference) and associated p value for mutations. This analysis is restricted to genes with > 5 cases with mutations in the analysed gene. All genes featured in the results of clinical enrichment are passed to the 'geneCombHR' function which builds cox proportional hazards models and produces a hazard ratio and associated p value for all mutations. The results of clinical enrichment and survival analysis are passed to the 'intSurvLymph' function to produce bubble plots, highlighting genes selected with the criteria of a hazard ratio or odds ratio of > 2 or < 0.5 and a p value < 0.05. All genes from clinical enrichment that are significant at a threshold of < 0.05 and have an OR < 0.5 or > 2 are extracted and passed to somatic interactions analysis. Somatic interactions are analysed using mafTools' 'somaticInteractions' function which applies Fisher's test to a contingency table of mutated and non-mutated samples for each gene to identify mutually exclusive (OR < 1) and co-occurring mutations (OR > 1).

To allow for plot generation, if the genes passed to somatic interaction analysis holds < 5 valid genes for either the low or high groups, the genes list is padded with randomly sampled genes from all intersecting genes from all unique genes in the low and high groups until ≥ 5 valid genes are included. Lollipop plots were generated using MafTools' 'lollipopPlot2' function. Protein structures are derived from the PFAM database [234]. If there are > 1 transcripts, the longest is selected. All p values are unadjusted unless specified otherwise. P values are adjusted using the false discovery rate (FDR), defined as the ratio of the number of false positive results to the number of total positive test results. An FDR of < 0.05 is considered significant, indicating that of results classed as significant by the unadjusted p value, < 5% are null.

2.4.4 Transcriptional Analysis

Analysis was conducted in R V4.2.1 [231]. Transcriptional classification of cases as 'Low' or 'High' for lymphocyte populations was conducted as previously described for histological classification (chapter 2.4.1 Generating Cut Points for Continuous Variables). To compare gene expression by histological classification, the normalised gene expression matrix was extracted from the DESeq object and comparisons were made via Welsch's t-test. Correlations between histological lymphocyte density (raw % positive count prior to classification) and gene expression was determined using Pearson's correlation. Mosaic plots were built on contingency tables with associated Chi^2 test using the R package 'vcd' V1.4.10 [235]. Time-to-event analysis was conducted as previously described (2.4.2 Time-To-Event Analysis). Differential expression was calculated using 'DESeq2' V1.36.0 with γδ primary tumour and CD8 primary tumour being calculated independently, log fold changes were shrunk using the 'apeglm' method and hypothesis testing carried out with a Wald test. Pathway analysis was conducted using the 'fgsea' R package V1.22.0 [236] and associated molecular signature database [237, 238].

Chapter 3:
Assessment of the density of lymphocyte populations across patient cohorts and tissue compartments

Chapter 3: Assessment of the density of lymphocyte populations across patient cohorts and tissue compartments

3.0 Summary

To understand how progression from normal tissue to tumour tissue affects our two lymphocyte populations of interest, the density of lymphocytes was analysed in the primary tumour and adjacent normal tissue using immunohistochemistry and a digital image analysis workflow. The results showed a higher density of lymphocytes in the adjacent normal tissue compared to the primary tumour and this was consistent across the three study cohorts representing Scotland, Norway, and Thailand. The only exception was CD8 T cells in the Norway cohort, which showed no difference. This suggests that some extent of immune exclusion is taking place within the tumour tissue.

The second key finding was that both lymphocyte populations were consistently present at a greater density in the stroma compared to the epithelium. Localisation within the epithelium is a key factor in their immune function. This suggests that in addition to immune exclusion, there is an alteration to the localisation of lymphocytes within the tumour, although there is a potential methodological explanation for this result.

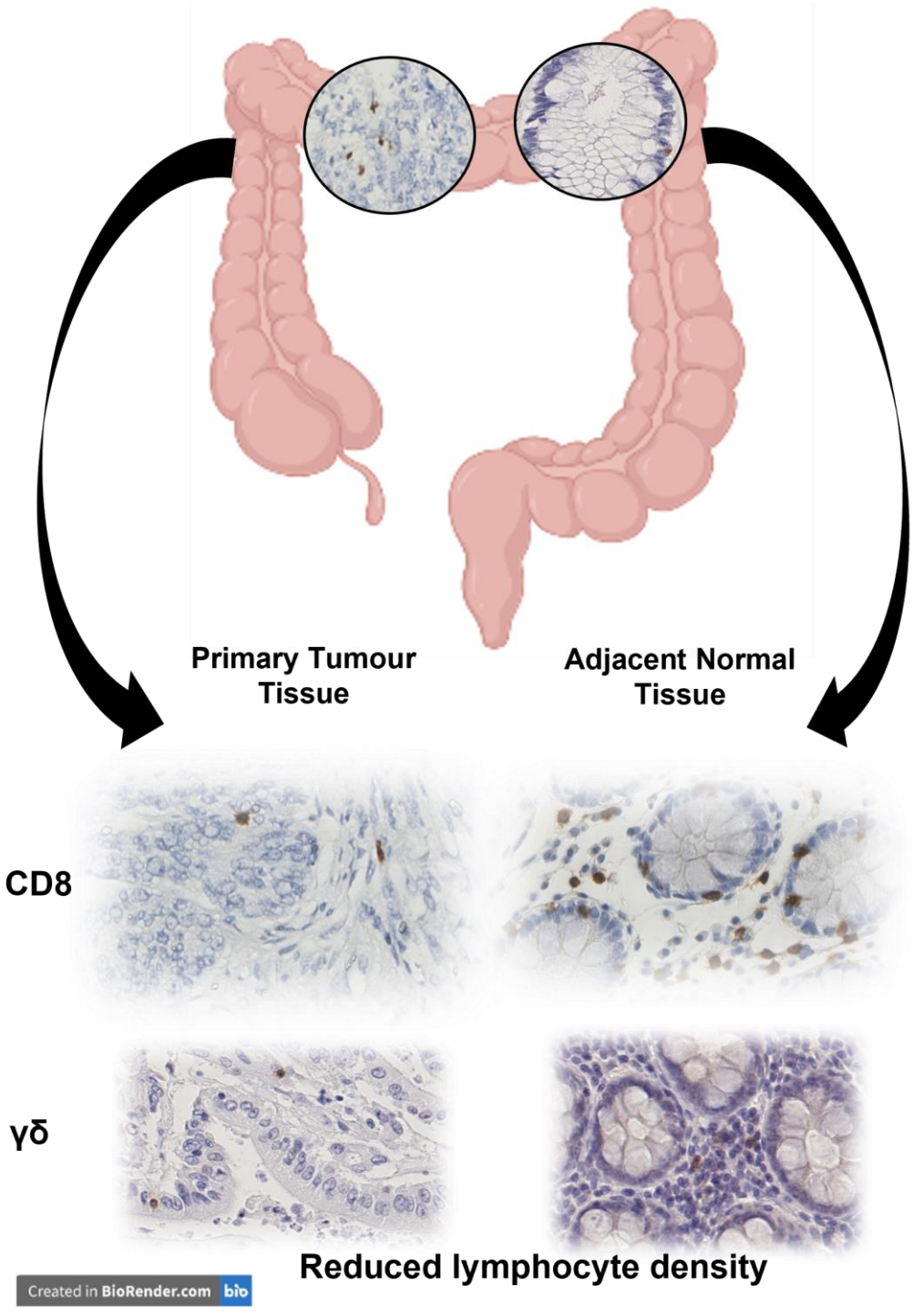
Primary Tumour Tissue
Adjacent Normal Tissue
CD8
γδ
Reduced lymphocyte density
Created in BioRender.com bio

3.1 Introduction

The role of the immune system in cancer progression, as either suppressor or propagator, has emerged as a crucial factor in predicting the course of and treating cancers. Research has demonstrated that this role is dependent on myriad factors, including the localisation and density of immune cells within the tumour, surrounding tissue and systemic environment. This observation is supported by seminal work including a study in 415 CRC patients showing that increased infiltration of CD3, CD8, or CD45RO (effector/memory) T cells at the tumour centre or invasive margin, but particularly when high in both, is associated with greater disease-free survival [8] – this study led to the introduction of the Immunoscore® [9]. Other inflammatory scores further highlight the prognostic power of the immune infiltrate, such as the Klintrup-Mäkinen score [239].

Research to date focuses on conventional T cell and myeloid cell populations. T cell research has explored total T cell count ($CD3^+$) or cytotoxic T cells ($CD8^+$), which are favourable [8], or helper and regulatory T cells ($CD4^+$) which are variably favourable or unfavourable [188, 240]. Unconventional T cell subsets, such as γδ T cells, are not as well studied in this context. Attempts to rectify this have relied heavily on omics data and is primarily studied in mice. γδ T cells are present at a low density in the most tissue compartments [241, 242] but are relatively enriched in the intestinal tract compared to other tissue compartments, where they constitute approximately 40% of T cells [243, 244]. Compared to adjacent normal tissue, γδ T cells are present at a lower density in the primary tumour [244].

There is yet to be a comprehensive histological evaluation of the distribution and role of γδ T cells in human CRC and how this compares to traditional CD8 ‘effector’ T cells. To understand the distribution of γδ T cells, the relative density and localisation of CD8 and γδ T cells was investigated by comparing the distribution of these metrics across three geographical cohorts of patients (Scotland, Norway and Thailand) and across tissue regions (primary tumour and adjacent normal tissue) and compartments (epithelium and stroma).

3.2 Analysis Workflow

3.2.1 Immunohistochemical staining of tissue sections

To investigate γδ and CD8 T cells in these patient cohorts, sections of resected tumours were stained for the δ chain of γδ T cells or the CD8α isoform of CD8 T cells (Figure 3.1) using singleplex immunohistochemistry. The expression observed in the stained samples were then analysed using a digital image analysis workflow.

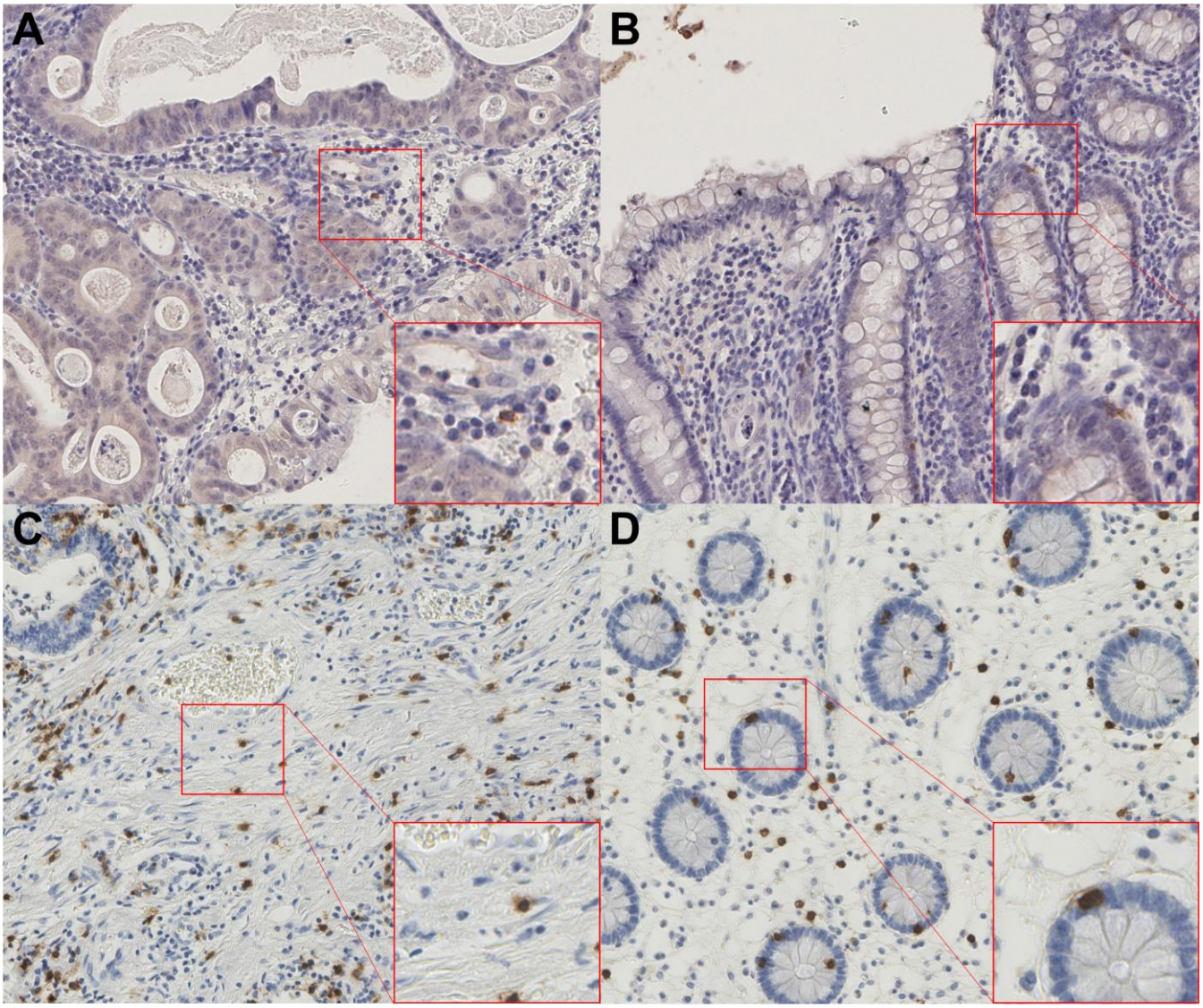

Figure 3.1 – Example staining of γδ T cells. *(A) Example staining of γδ T cells in the primary tumour at 20x magnification, and further magnified to 40x. (B) Example staining of γδ T cells in the adjacent normal tissue at 20x magnification, and further magnified to 40x. (C) Example staining of CD8 T cells in the primary tumour at 20x magnification, and further magnified to 40x. (D) Example staining of CD8 T cells in the adjacent normal tissue at 20x magnification, and further magnified to 40x.*

3.2.2 QuPath

The initial digital image analysis workflow was created using QuPath, an open-source digital pathology software platform for use in image analysis [245], and is widely used within the digital pathology field [246]. Raw images are imported into QuPath as part of a 'Project' folder. The first level of tissue compartments (primary tumour, adjacent normal tissue, metastases and liver) is manually annotated as 'regions' (Figure 3.2A-D). Digital analysis is applied *en masse* to all images in the project using a dual script classification workflow. The classifier was built using QuPath's own cell detection system (Figure 3.2E/F) to detect total cells and positive cells ($\gamma\delta$ T cells) based on mean DAB intensity, which extracts relevant features (Figure 3.2G/H) and smooths those features by updating pixel measurements with a new measurement based on the average of the neighbouring cells - a radius of 50µm was used (Figure 3.2I). This stage of the analysis process is then developed into a script as the first script of the classification workflow. A classifier is then built based on these features. To classify images, the first script is applied to extract the features, as when the classifier was built (Figure 3.2C/D). The second script is then applied to classify the tissue based on those features (Figure 3.2J/K).

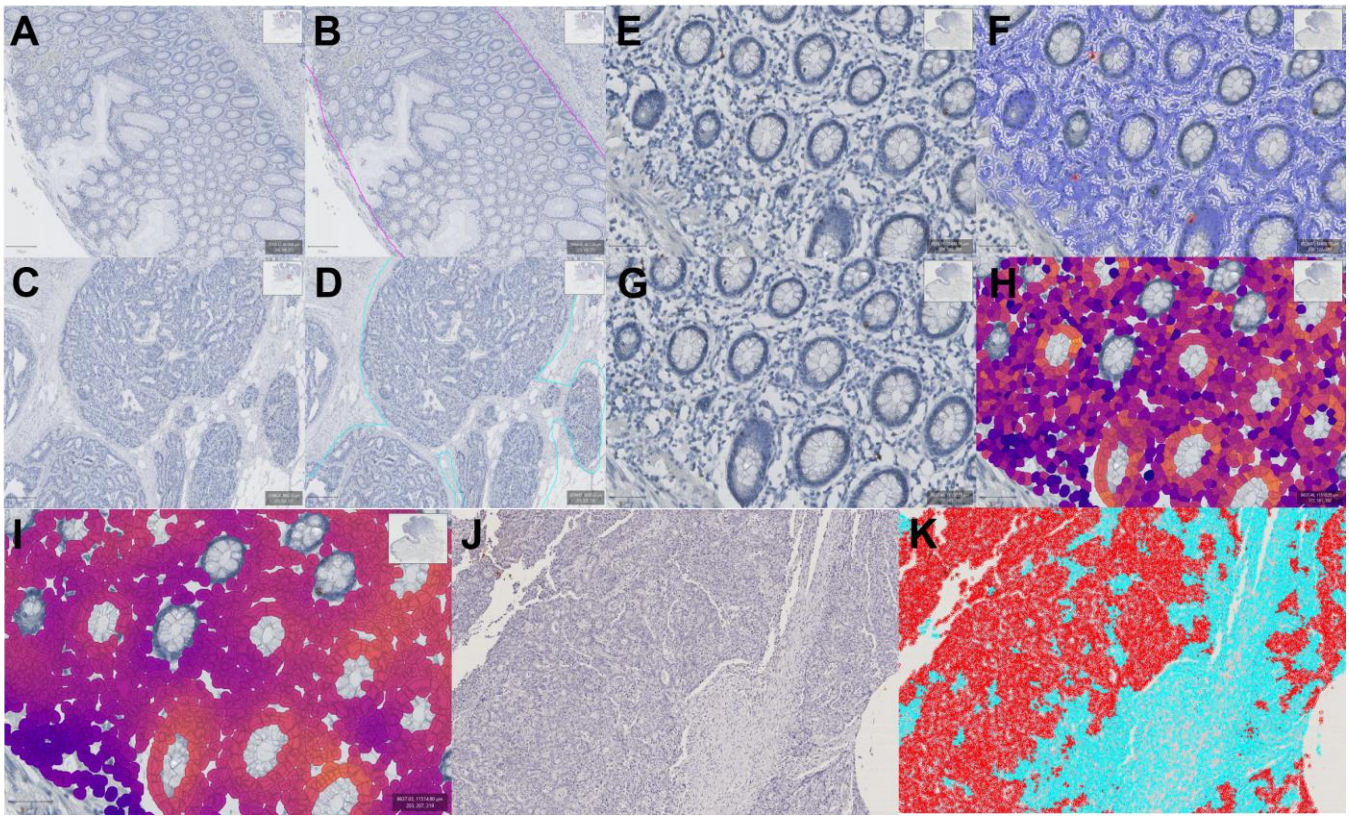

Figure 3.2 – QuPath analysis workflow. *(A-D) Manual identification and annotation of tumour regions (C/D) and adjacent regions of adjacent normal tissue (A/B) (that is untransformed, but often inflamed). (E/F) Detections of cells, including positive cells, and extraction of features. (G/H) Measurement map based on features extracted from cell detection. (I) Measurement map for smoothed variants of features extracted from cell detection. (J/K) Classification of a region of primary CRC tumour tissue. Epithelium is displayed in red. Stroma is displayed in blue.*

3.2.3 VisioPharm

To ensure an optimal workflow, QuPath was assessed alongside a workflow developed with a comparator software, VisioPharm. VisioPharm is a closed source digital pathology platform with a focus on artificial intelligence [247], and is widely used within the digital pathology field [248, 249]. Raw images are imported into VisioPharm within a database hierarchy consisting of Cohort > Marker > Images. The first level of tissue compartments (primary tumour, adjacent normal tissue, metastases and liver) is manually annotated as 'regions' (Figure 3.3A/B), with care taken to avoid artefacts such as folded tissue, areas of significant background and haematoxylin debris, which are misidentified as γδ T cells (Figure 3.3C/D). Blank regions within the annotation (such as in sections cut from a block previously used to create TMAs) are not avoided as the analysis runs on cell numbers, so those regions will not alter the output. From this point, analysis is digital and can be applied *en masse* to the images and allowed to run unattended in a queued format, analysing approximately 30 full sections per day.

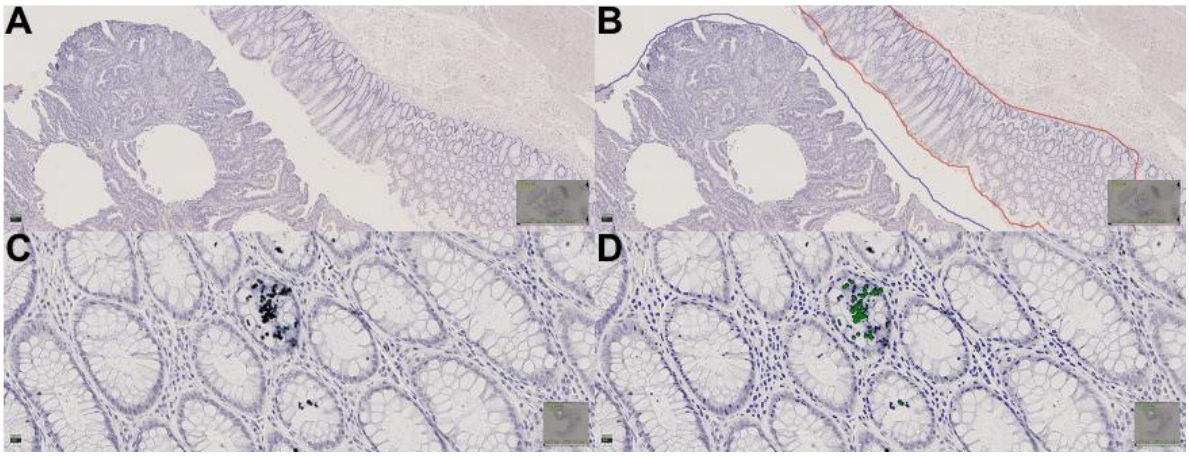

Figure 3.3 – Manual annotations in VisioPharm workflow. *(A/B) Delineation of tumour and adjacent normal y tissue region by manual annotation, tumour in blue and adjacent normal in red. (C/D) Example of an artefact capable of interfering with analysis of γδ T cells - cells identified as positive for the δ chain are highlighted in green.*

App #1 - Classification of Tissue

A set of images were collated, including entries from all colorectal cohorts being used, and used to train a classifier. Tumour and adjacent normal tissue are classified with separate classifiers that are trained on identical images but differentiate in how they use training features. To create training data on an image, a region of interest is drawn, areas of epithelial tissue are labelled as 'Epithelium' and some adjacent stroma is labelled as 'Stroma' (Figure 3.4A).

The classifier is built using a K-means clustering algorithm which partitions all observations into a set number of clusters, in this case two as we are providing two supervisory classes, ‘Epithelium’ and ‘Stroma’. K-means clustering places two centroids in random locations and each data point is placed and assigned to its nearest centroid, becoming a data point within that cluster. The points of each cluster are averaged, and the mean becomes the new centroid for that cluster. The process of determining a data point’s nearest centroid, and thus its cluster, continues iteratively until the value of the centroids no longer changes.

Classification features for both tumour and adjacent normal tissue consist of the generic R, G and B channels and the counter stain haematoxylin. As the staining procedure does not include eosin or multiplex staining with a tissue marker, the level of contrast available to delineate epithelium and stroma is limited. To try and account for this chromaticity blue was added to look at the blue proportion without the inclusion of intensity, as is present in RGB. Additionally, we investigated the relevance of RGB contrasts and found contrast green-blue to have some degree of separation. The tumour classifier makes use of two additional custom features. The first is the application of an 11-pixel median filter to the haematoxylin feature, which takes the haematoxylin value of each pixel and its surrounding pixels (within an 11-pixel range) and changes its value to the median of those values (Figure 3.4B/C). This effectively blurs the image and reduces the amount of noise in the signal. The second divides the haematoxylin value by the chromaticity blue value (the two primary sources of contrast available), with the intention of creating a variable which captures any difference in relative staining (Figure 3.4B/D). The result of classification is the labelled delineation of the epithelium and stroma (Figure 3.4E), which is subsequently converted to corresponding regions for further analysis with app #2 (Figure 3.4F).

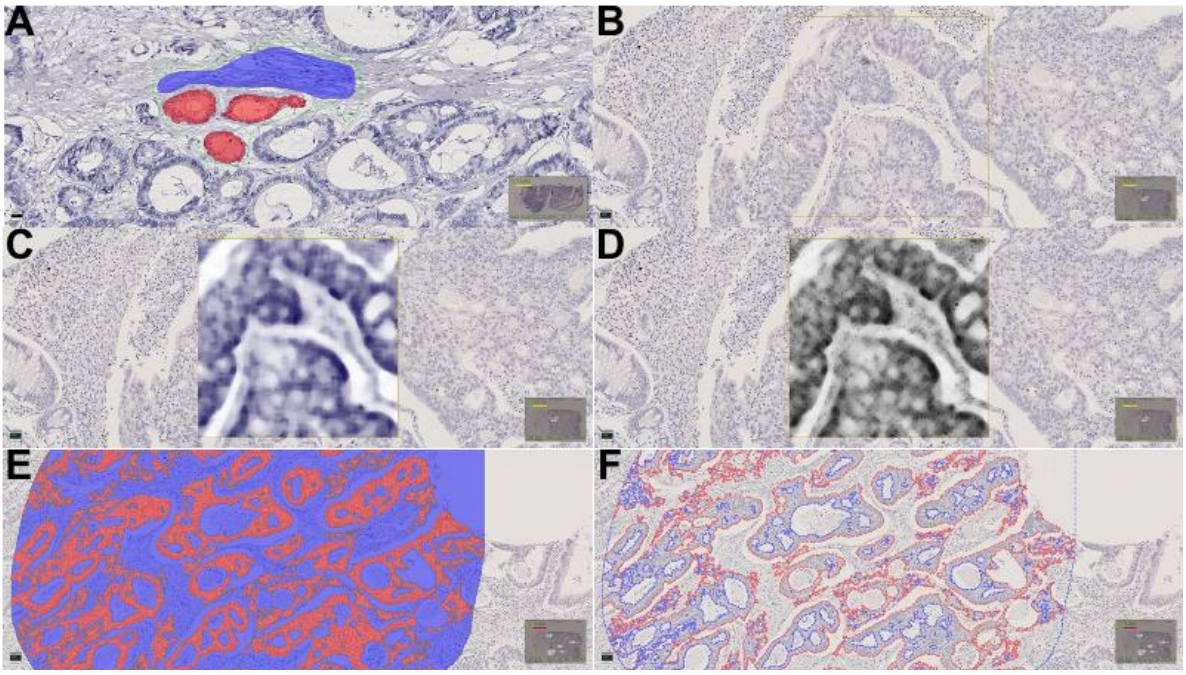

Figure 3.4 – VisioPharm classifier training. *(A) Manual annotation of epithelial and stromal regions for training the tumour classifier. Epithelium is annotated in red. Stroma is annotated in blue (B/C/D) Representation of tissue visualised as the full IHC image, the median haematoxylin feature and the haematoxylin/chromaticity blue merged feature. (E/F) Final stage classification of tumour tissue into epithelium and stroma, and the subsequent conversion to regions for analysis. Epithelium is displayed in red. Stroma is displayed in blue.*

App #2 - Identification of γδ T Cells and Calculations

The analysis of γδ T cells in tissue was applied to all active regions for analysis, as created in app #1. γδ T cells were identified using two features. The first feature is the application of a five-pixel mean filter to the chromogenic DAB feature, which takes the DAB value of each pixel and its surrounding pixels (within a five-pixel range) and changes its value to the mean of those values (Figure 3.5A/B/C). This accounts for variability in the staining intensity of DAB within a given γδ T cell, which may have been a particular issue for γδ T cells which have a weaker and patchier stain than other T cell membranous markers.

The second is a dual component feature which is derived from the haematoxylin stain and acts to smooth out and improve the boundaries of the haematoxylin feature (Figure 3.5A/D/E). The first component is a polynomial smoothing filter, which functions as the previously mentioned mean and median filters but with a greater weighting to the pixels in the centre of the filter field and is applied at a field size of 21 pixels at an order of two, the latter representing the extent of smoothing. The second component uses a polynomial Laplace filter at a field size of 15 pixels at an order of two, which applies a Laplacian matrix to detect rapid changes in intensity, thus better detecting the edges of the features in an image. The efficacy of the second component is reliant on the smoothing provided by the first component, and together they improve the definition of generic cellular shapes at the expense of finer details. These two features improve the identification of $\gamma\delta$ T cells (Figure 3.5F).

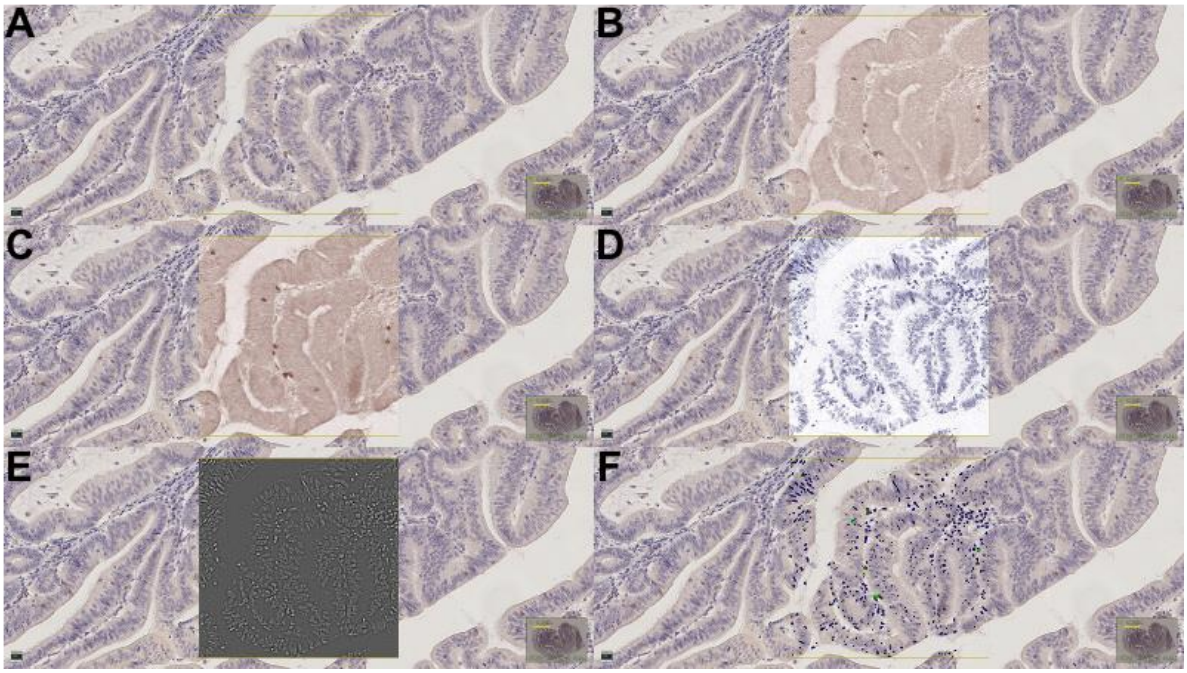

Figure 3.5 – Smoothing of the haematoxylin feature. *(A) Representation of tumour region stained with IHC for $\gamma\delta$ T cells. (B/C) Representation of tumour region with the chromogenic DAB feature and the DAB feature subject to a mean filter. (D/E) Representation of tumour region with the haematoxylin feature and the haematoxylin feature subject to smoothing. (F) Example identification of $\gamma\delta$ T cells within the tumour region. Central boxes display the tissue restricted to only the indicated feature.*

3.2.4 Workflow Comparison

The first component for comparison is the ability of the classifier to accurately classify colorectal tissue (tumour or adjacent normal) as either epithelium or stroma/lamina propria. The default analysis for comparison of two classifiers is intersection over union (or Jaccard index) analysis [250], which lays the predicted region (by classifier) over the true region and computes the ratio of intersection (the area included in both regions) over the union (the total area of the composite region). This comparison was carried out using a partial variant of intersection over union analysis due to technical difficulties in conducting true intersection over union analysis across two platforms. Instead, the reliability of each classifier to accurately differentiate between epithelium and stroma was determined by annotating regions of epithelium within an outer region, of which the area is also known. The classifier was then applied to the outer region and the area of epithelium (as per classifier) directly compared with the known total area of epithelium within that region using scatter plots, Bland-Altman [251] analysis and intra-class correlation coefficients (ICCC) [252, 253] (Two-way mixed, agreement).

Both QuPath and VisioPharm produced acceptable classification of adjacent normal tissue (Figure 3.6A/B and Figure 3.6E/F), with ICCCs of 0.598 and 0.685, respectively. These ICCC values both fall within the ‘moderate’ category, those ICCC values between 0.7 and 0.75. Classification of tumour tissue by QuPath and VisioPharm (Figure 3.6C/D and Figure 3.6G/H) was excellent (between 0.75 and 0.9) and moderate with ICCC values of 0.832 and 0.716, respectively. QuPath produced a much higher ICCC in the tumour tissue than did VisioPharm, whilst the reverse was true in the case of adjacent normal tissue. It was therefore decided that VisioPharm was the optimal workflow at it provided a more balanced accuracy with both measures achieving ICCC values in the top half of the ‘moderate’ category, whereas QuPath showed greater variation between tissue regions.

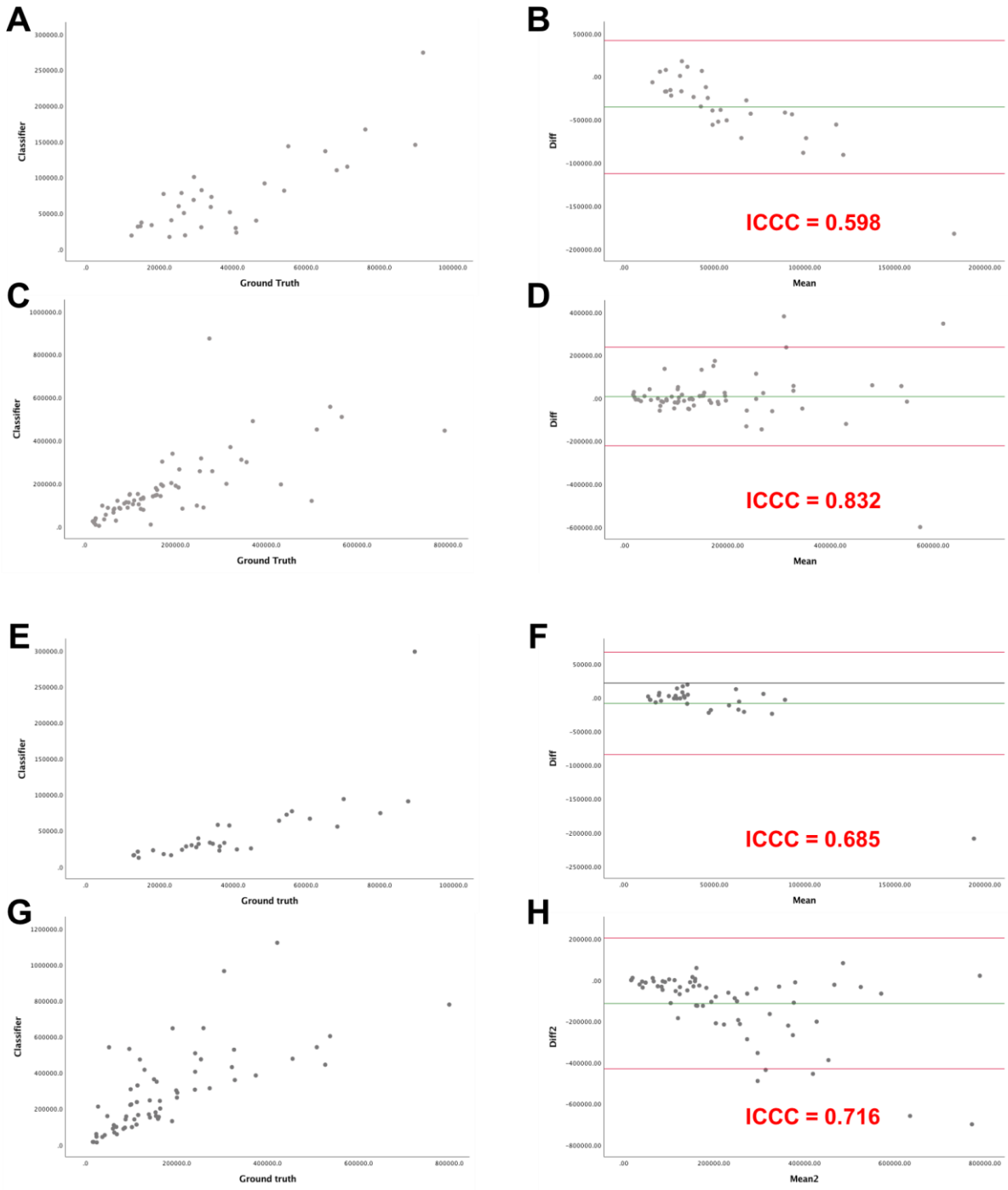

Figure 3.6 – Intersection over union analysis. *(A/B) Partial intersection over union analysis of the QuPath classifier in adjacent normal tissue, presented as a scatter plot of the ground truth measurement (X axis) and the corresponding measurement provided by the classifier (Y axis) (A), and Bland-Altman analysis of agreement with accompanying ICCC (B). (C/D) Partial intersection over union analysis of the QuPath classifier in tumour tissue, presented as a scatter plot of the ground truth measurement (X axis) and the corresponding measurement provided by the classifier (Y axis) (C), and Bland-Altman analysis of agreement with accompanying ICCC (D). (E/F) Partial intersection over union analysis of the VisioPharm classifier in adjacent normal tissue, presented as a scatter plot of the ground truth measurement (X axis) and the corresponding measurement provided by the classifier (Y axis) (E), and Bland-Altman analysis of agreement with accompanying ICCC (F). (G/H) Partial intersection over union analysis of the VisioPharm classifier in tumour tissue, presented as a scatter plot of the ground truth measurement (X axis) and the corresponding measurement provided by the classifier (Y axis) (G), and Bland-Altman analysis of agreement with accompanying ICCC (H).*

The second component for comparison is the ability of the classifier to accurately detect γδ T cells, which was tested using Bland-Altman plots and intraclass correlation coefficient as previously described. Manual scoring of γδ T cells was used as a 'true' score, scored within the regions prior to running analysis. 40 samples, taken from multiple CRC cohorts, were used for comparison of GD T cell identifiers. Scores as determined by QuPath showed no correlation with the true score (Figure 3.7A). QuPath scores achieved an acceptable ICC of 0.774 and a Bland-Altman plot showed that most QuPath scores were mostly within the confidence limits but showed significant proportional bias with the difference in scores increasing as the magnitude increases, suggesting that QuPath struggles to score accurately as the volume of γδ T cells increases (Figure 3.7B). VisioPharm showed correlation although this tailed off slightly as magnitude increased (Figure 3.7C). VisioPharm scores achieved a good ICC of 0.802 and a Bland-Altman plot showed that VisioPharm scores were mostly within the confidence limits but without significant proportional bias (Figure 3.7D). Thus, it was determined that VisioPharm can identify γδ T cells with greater accuracy than QuPath.

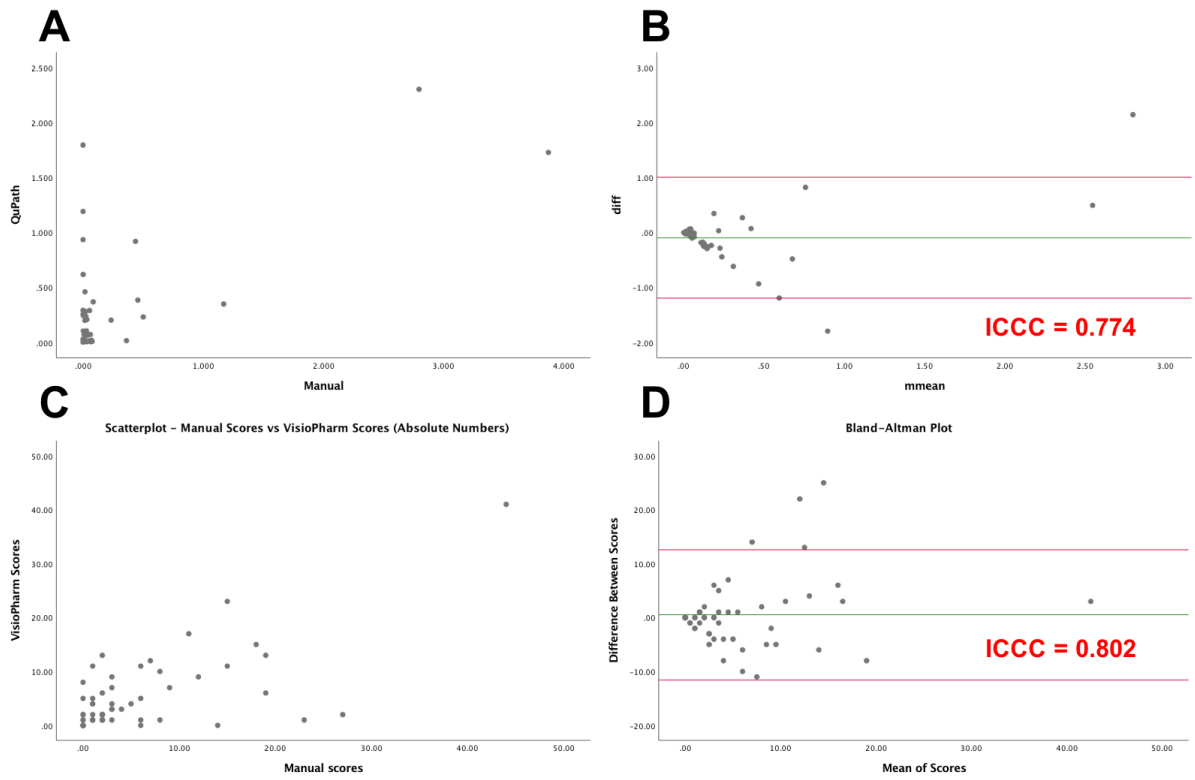

Figure 3.7 – Comparison of manual and digital scoring. *(A) Scatterplot of manual γδ T cell score vs digital scoring with QuPath. (B) Bland Altman of manual γδ T cell score vs digital scoring with QuPath. (C) Scatterplot of manual γδ T cell score vs digital scoring with VisioPharm. (D) Bland Altman of manual γδ T cell score vs digital scoring with VisioPharm.*

3.2.5 Digital image analysis workflow selection

A digital image analysis workflow was selected based on performance in classifying tissue and identifying lymphocytes. QuPath (ICC = 0.832) was superior for classification of tumour tissue compared to VisioPharm (ICC = 0.716), but QuPath (ICC = 0.598) was inferior for classification of adjacent normal tissue compared to VisioPharm (ICC = 0.685) (Figure 3.6). VisoPharm was deemed superior for tissue classification as it provided an appropriate performance for both tissue types, whereas QuPath performed less consistently between the two tissue types. VisioPharm (ICC = 0.802) was superior to QuPath (ICC = 0.774) for identification of lymphocytes (Figure 3.8). The difference in identification was not of great magnitude, but QuPath suffered from proportional bias, further highlighting VisioPharm as the best workflow. Additionally, VisioPharm is aided by additional utilities such as greater usability with regards to the user interface and management of data and files and a greater suite of easily available measures such as spatial analysis.

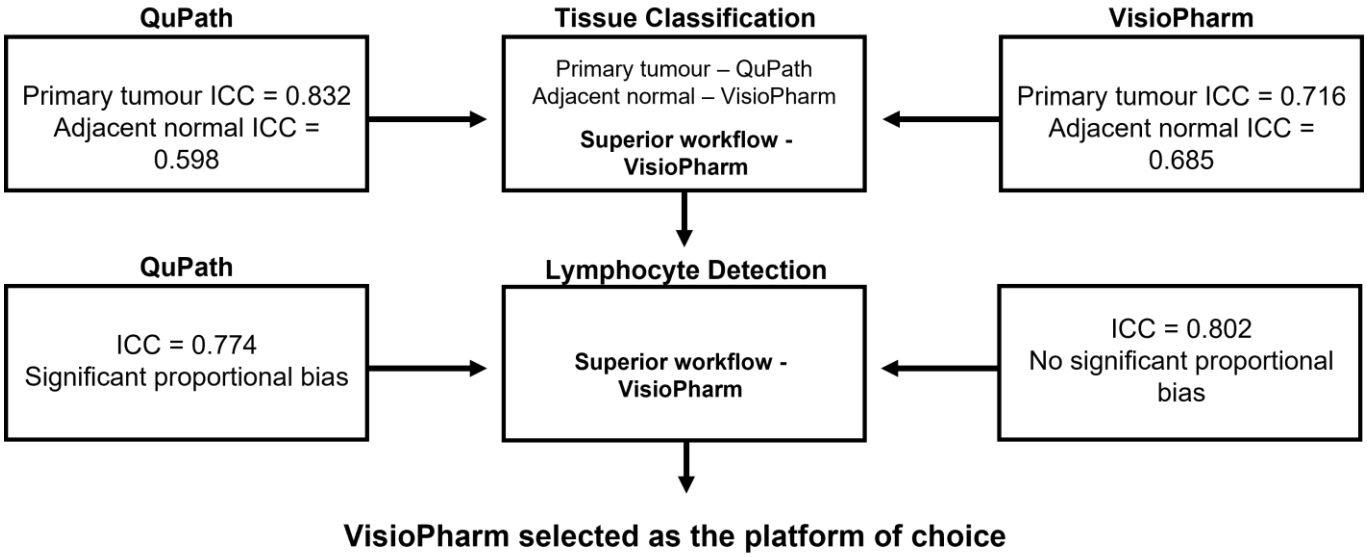

Figure 3.8 – Flow diagram representing the process of digital image analysis workflow selection. *Central column denotes the stage of the analysis process and the digital image analysis workflow deemed to be superior. Left (QuPath) and right (VisioPharm) columns summarise performance of digital image analysis workflows for that stage of the analysis process.*

3.2.6 Generation of lymphocyte density metric

After tissue classification and identification of lymphocytes, a score (% positive) is produced for each combination of tissue region and compartment (primary tumour/adjacent normal tissue and epithelium/stroma/whole tissue), defined as the % of total cells within an analysed region that are positively identified as the target cell type. This metric is taken forward for analysis of lymphocyte density and investigations into their prognostic effects.

3.3 Scotland Cohort

3.3.1 Clinicopathological characteristics of patient cohort

359 patients from the Scotland cohort were included in a sub-cohort for analysis. Patient cohort characteristics of the full cohort and sub-cohort are outlined in Table 3.1. The sub-cohort was comparable to the full cohort except for TNM stage with a slight imbalance towards stage I and stage III, respectively. There was an even split between female (53%) and male (47%) patients. Considerably more patients were equal to or above the age of 65 (69%) than below 65 (31%). Surgeries were primarily elective (75%). The tumour site was imbalanced with more tumours being present in right (47%) sided disease than left sided disease (31%), with rectal disease (22%) being the lowest. Patients were primarily T stage III/IV (55%/34%), N stage 0/I (52%/34%), M stage 0 (96%) and TNM stage II/III (43%/46%). Tumours were predominantly moderately/well differentiated (90%). Most patients did not have vascular invasion (65%). Patients were largely mismatch repair proficient (79%). Patients were mostly graded as Klintrup-Mäkinen weak (69%). Patients primarily had a low tumour stroma percentage (70%). 22% of patients received adjuvant therapy whilst 8% did not, but 70.2% of patients have an unknown status for adjuvant therapy. Neoadjuvant therapy was predominantly absent (97%). Most patients survived beyond 30 days after surgery (94%). Median follow-up (alive cases, n = 104) in the sub-cohort was 136 months. There was a total of 138 cancer deaths and 109 non-cancer deaths in the sub-cohort. Patients were excluded if they had received neoadjuvant therapy (n = 12), died within 30 days of surgery (n = 23) or had stage IV disease (n = 10) (Figure 3.9). Patients were further excluded if they had stage I disease so that analysed cohorts were stage matched (stage II/III) (n = 27) (Figure 3.9).

Table 3.1 – Scotland Cohort. Clinicopathological characteristics of patients in the Scotland cohort. *Table showing the number (and %) of patients exhibiting clinical features and comparison between the full cohort and the sub-cohort included for analyses.*

Patient Characteristics - Scotland Cohort			
	Full Cohort	Sub-cohort	P-Value
Sex			
Female	539 (52 %)	190 (53 %)	0.846
Male	491 (48 %)	169 (47 %)	
Age			
≥65	708 (69 %)	247 (69 %)	0.982
<65	322 (31 %)	112 (31 %)	
Surgery Type			
Elective	801 (78 %)	268 (75 %)	0.216
Emergency	228 (22 %)	91 (25 %)	
Missing	1 (0.1%)	0 (0%)	
Tumour Site			
Right	430 (42 %)	168 (47 %)	0.272
Left	340 (33 %)	110 (31 %)	
Rectum	253 (25 %)	80 (22 %)	
Missing	7 (0.7%)	1 (0.3%)	
T Stage			
I	44 (4 %)	11 (3 %)	0.102
II	122 (12 %)	29 (8 %)	
III	560 (54 %)	197 (55 %)	
IV	304 (30 %)	122 (34 %)	
N Stage			
0	629 (61 %)	186 (52 %)	0.0144
I	273 (27 %)	123 (34 %)	
II	123 (12 %)	48 (13 %)	
III	1 (0 %)	1 (0 %)	
Missing	4 (0.4%)	1 (0.3%)	
M Stage			
0	1004 (97 %)	346 (96 %)	0.164
I	21 (2 %)	12 (3 %)	
Missing	5 (0.5%)	1 (0.3%)	
TNM Stage			
I	138 (13 %)	30 (8 %)	0.00494
II	483 (47 %)	153 (43 %)	
III	388 (38 %)	164 (46 %)	
IV	21 (2 %)	12 (3 %)	
Differentiation			
Moderate/Well	919 (89 %)	322 (90 %)	0.804
Poor	111 (11 %)	37 (10 %)	
Vascular Invasion			
No	681 (66 %)	232 (65 %)	0.608
Yes	349 (34 %)	127 (35 %)	
MMR Status			
Proficient	822 (80 %)	284 (79 %)	0.658
Deficient	178 (17 %)	66 (18 %)	
Missing	30 (2.9%)	9 (2.5%)	
Klintrup-Mäkinen Grade			
Weak	696 (68 %)	248 (69 %)	0.589
Strong	314 (30 %)	104 (29 %)	
Missing	20 (1.9%)	7 (1.9%)	
Tumour Stroma Percentage			
Low	747 (73 %)	251 (70 %)	0.223
High	254 (25 %)	101 (28 %)	
Missing	29 (2.8%)	7 (1.9%)	
Adjuvant Therapy			
No	222 (22 %)	78 (22 %)	0.215
Yes	112 (11 %)	29 (8 %)	
Missing	696 (67.6%)	252 (70.2%)	
Neoadjuvant Therapy			
No	984 (96 %)	347 (97 %)	0.416
Yes	38 (4 %)	10 (3 %)	
Missing	8 (0.8%)	2 (0.6%)	
Mortality Within 30 Days			
No	968 (94 %)	336 (94 %)	0.841
Yes	49 (5 %)	18 (5 %)	
Missing	13 (1.3%)	5 (1.4%)	

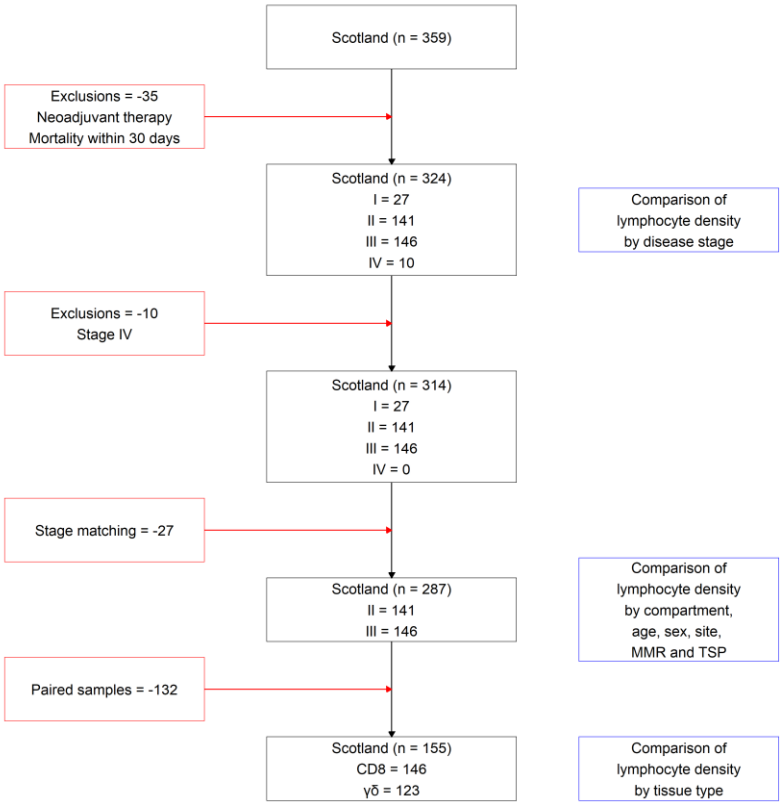

Figure 3.9 – Scotland Cohort. Consort diagram for lymphocyte density analysis in the Scotland cohort. *Red boxes denote removal of cases. Blue boxes denote analyses that use cases present at that level of the consort diagram.*

3.3.2 γδ T cell density by tissue region

To understand whether lymphocyte density is altered in diseased tissue compared to the normal tissue environment, the density of γδ T cells was investigated in the primary tumour and the adjacent normal tissue. To prevent any bias created by cases with exceptionally low or high lymphocyte density having only primary tumour tissue or only adjacent normal tissue available, standard exclusions were expanded to restrict cases to those with data available for both the primary tumour and the adjacent normal tissue. In the whole tissue, γδ T cells were present at a greater density in the adjacent normal tissue than in the primary tumour (p = <0.001) (Figure 3.10A) and adjacent normal tissue had a greater variance in γδ T cell density (Figure 3.10B). In the stroma, γδ T cells were present at a greater density in the adjacent normal tissue than in the primary tumour (p = 0.0069) (Figure 3.10A) and adjacent normal tissue had a greater variance in γδ T cell density (Figure 3.10B). In the epithelium, γδ T cells were present at a greater density in the adjacent normal tissue than in the primary tumour, although not statistically significant (p = 0.131) (Figure 3.10A) and adjacent normal tissue had a greater variance in γδ T cell density (Figure 3.10B).

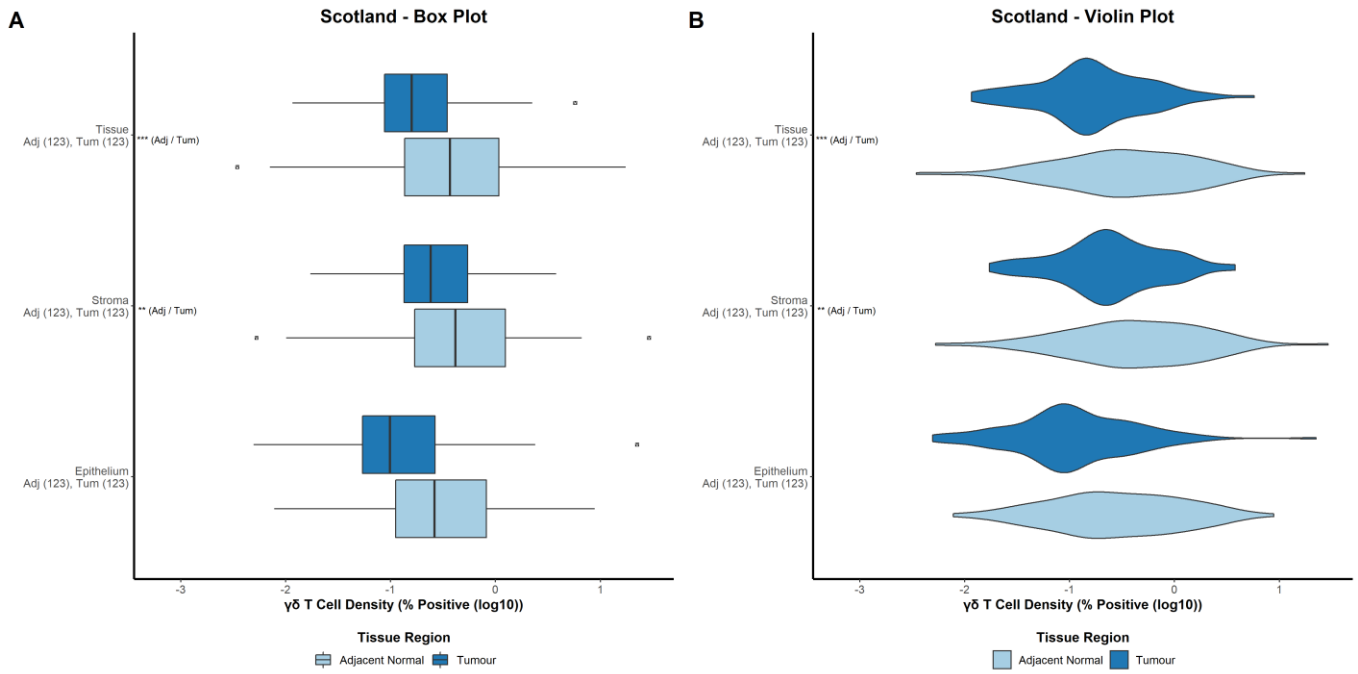

Figure 3.10 - Scotland Cohort. Assessment of γδ T cell density in the primary tumour and adjacent normal tissue. *Box plot presentation of γδ T cell density in the primary tumour (dark blue) and adjacent normal tissue (light blue). The box is representative of the interquartile range (middle 50% of data points), the vertical line denotes the median and the minimum and maximum are denoted by whiskers. Outliers are represented by an open triangle within an open square (A). Violin plot presentation of γδ T cell density in the primary tumour (dark blue) and adjacent normal tissue (light blue). The shape of the data reflects the distribution of the data points, which is not discernible in box plots (B). Y axis labels state the tissue compartment (epithelium, stroma and whole tissue) and below, the test groups with number of cases in brackets. X axis is log10 of the % of total cells within a region positive for the marker of interest. Inline labels denote the lowest standard statistical significance threshold reached (non-significant not shown) using a paired t-test, <0.05 (*), <0.01 (**) or <0.001 (***), with test groups in brackets.*

3.3.3 γδ T cell density by tissue compartment

Lymphocyte localisation is vital to function [254], particularly γδ T cells which patrol the epithelium to maintain intestinal homeostasis [117]. Thus, lymphocytes were scored for the whole tissue (primary tumour or adjacent normal) and for the epithelium and stroma separately and these latter regions compared. In the primary tumour, γδ T cells were present at a greater density in the stroma than the epithelium, although not statistically significant (p = 0.199) (Figure 3.11A). In the adjacent normal tissue, γδ T cells were present at a greater density in the stroma than the epithelium at a lesser magnitude than in the primary tumour (p = 0.045) (Figure 3.11A). γδ density showed greater variance in the adjacent normal tissue than in the primary tumour (Figure 3.11B).

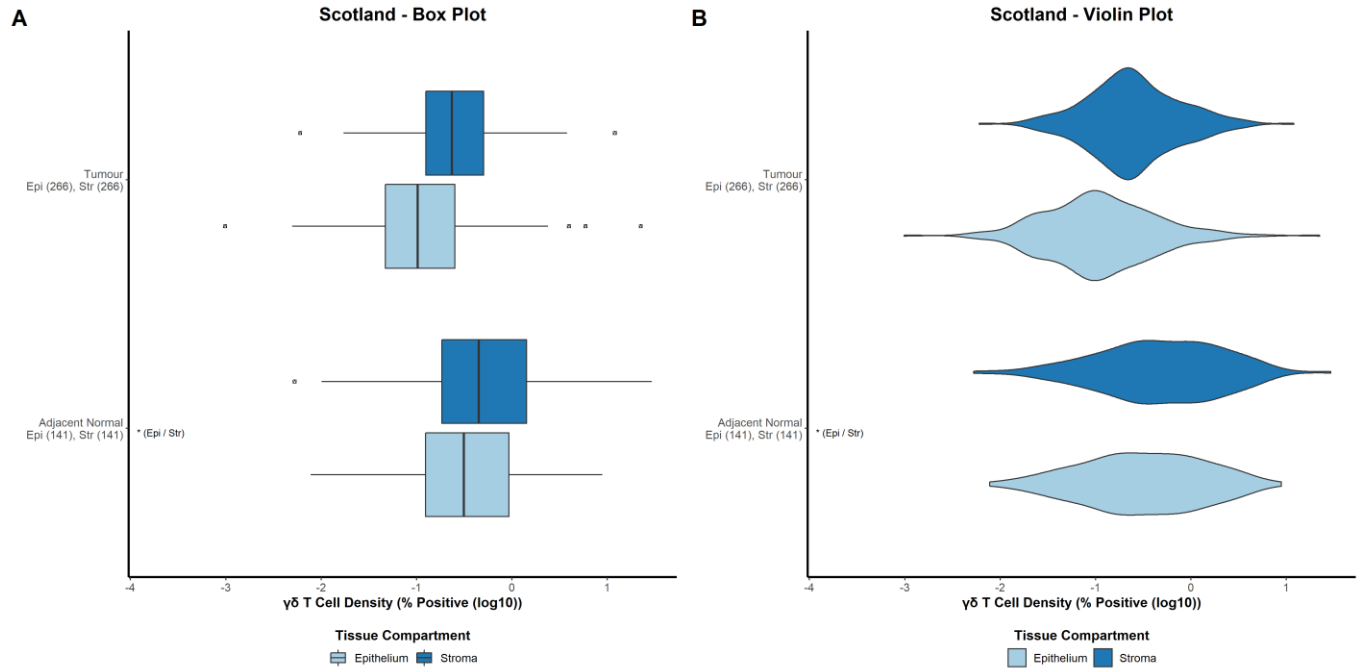

Figure 3.11 - Scotland Cohort. Assessment of γδ T cell density in the stroma and epithelium. *Box plot presentation of γδ T cell density in the stroma (dark blue) and epithelium (light blue). The box is representative of the interquartile range (middle 50% of data points), the vertical line denotes the median and the minimum and maximum are denoted by whiskers. Outliers are represented by an open triangle within an open square (A). Violin plot presentation of γδ T cell density in the stroma (dark blue) and epithelium (light blue). The shape of the data reflects the distribution of the data points, which is not discernible in box plots (B). Y axis labels state the tissue compartment (primary tumour and adjacent normal tissue) and below, the test groups with number of cases in brackets. X axis is log10 of the % of total cells within a region positive for the marker of interest. Inline labels denote the lowest standard statistical significance threshold reached (non-significant not shown) using a Welch two sample t-test, <0.05 (*), <0.01 (**) or <0.001 (***), with test groups in brackets.*

3.3.4 γδ T cell density by TNM stage

The primary tumour data consists of tumours at various stages of disease progression, stratified using the TNM staging system, which have variable tumour microenvironments and clinical outcomes. Thus, to understand whether data for the primary tumour is representative of all cases or stage-dependent, γδ T cell density was investigated across the four TNM stages. To conduct this analysis the standard exclusions were altered to include stage I and stage IV patients. In the adjacent normal stroma, there was no difference in γδ T cell density between stage I-IV patients (p = 0.801) (Figure 3.12A). In the primary tumour stroma, there was no difference in γδ T cell density between stage I-IV patients (p = 0.509) (Figure 3.12A). In the adjacent normal epithelium, there was no difference in γδ T cell density between stage I-IV patients (p = 0.531) (Figure 3.12A). In the primary tumour epithelium, there was no difference in γδ T cell density between stage I-IV patients (p = 0.662) (Figure 3.12A). In the adjacent normal tissue, there was no difference in γδ T cell density between stage I-IV patients (p = 0.768) (Figure 3.12A). In the primary tumour tissue, there was no difference in γδ T cell density between stage I-IV patients (p = 0.696) (Figure 3.12A). There was a lesser variance in γδ T cell density in stage IV patients compared to stage I-III patients (Figure 3.12B), but this is likely due to the very low numbers of stage IV patients.

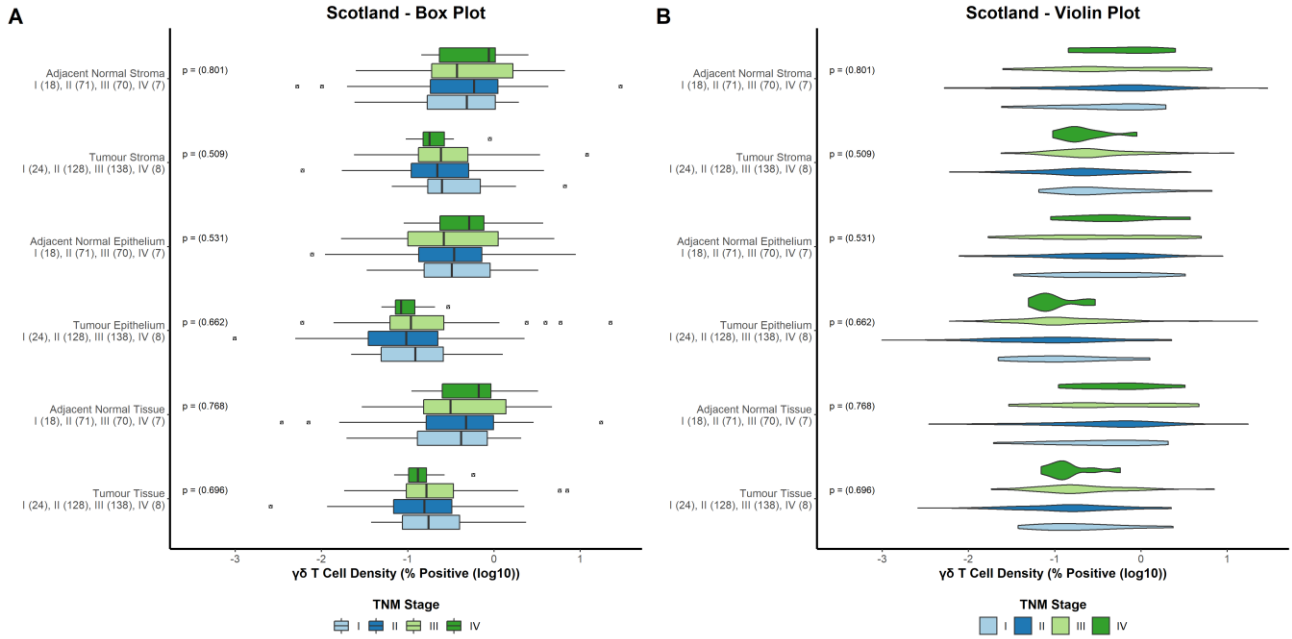

Figure 3.12 - Scotland Cohort. Assessment of γδ T cell density across TNM stages. *Box plot presentation of γδ T cell density in stage I (light blue), stage II (dark blue), stage III (light green) and stage IV (dark green) patients. The box is representative of the interquartile range (middle 50% of data points), the vertical line denotes the median and the minimum and maximum are denoted by whiskers. Outliers are represented by an open triangle within an open square (A). Violin plot presentation of γδ T cell density in stage I (light blue), stage II (dark blue), stage III (light green) and stage IV (dark green) patients. The shape of the data reflects the distribution of the data points, which is not discernible in box plots. Outliers are represented by an open triangle within an open square (B). Y axis labels state the tissue compartment (primary tumour or adjacent normal tissue and epithelium, stroma or whole tissue) and below, the test groups with number of cases in brackets. X axis is log10 of the % of total cells within a region positive for the marker of interest. Inline labels denote the lowest standard statistical significance threshold reached (non-significant not shown) using a one-way ANOVA, <0.05 (*), <0.01 (**) or <0.001 (***), with statistically significant (<0.05) group comparisons noted below as determined by Tukey's post-hoc test.*

3.3.5 γδ T cell density by age

Incidence of CRC increases with aged populations, although cases in younger populations are increasing [255], and so the density of γδ T cells was investigated in patients aged < 65 years of age or ≥ 65 years of age. In the adjacent normal stroma, patients < 65 years of age had γδ T cell density no different than those ≥65 years of age (p = 0.879) (Figure 3.13A). In the primary tumour stroma, there was no difference in γδ T cell density between patients < 65 years of age and those ≥65 years of age (p = 0.489) (Figure 3.13A). In the adjacent normal epithelium, patients < 65 years of age had a mildly greater γδ T cell density than those ≥65 years of age, although not statistically significant (p = 0.236) (Figure 3.13A). In the primary tumour epithelium, there was no difference in γδ T cell density between patients < 65 years of age and those ≥65 years of age (p = 0.234) (Figure 3.13A). In the adjacent normal tissue, patients < 65 years of age had a mildly greater γδ T cell density than those ≥65 years of age, although not statistically significant (p = 0.574) (Figure 3.13A). In the primary tumour tissue, there was no difference in γδ T cell density between patients < 65 years of age and those ≥65 years of age (p = 0.349) (Figure 3.13A). The primary tumour compartments had a mildly lesser variance in γδ T cell density than adjacent normal tissue compartments.

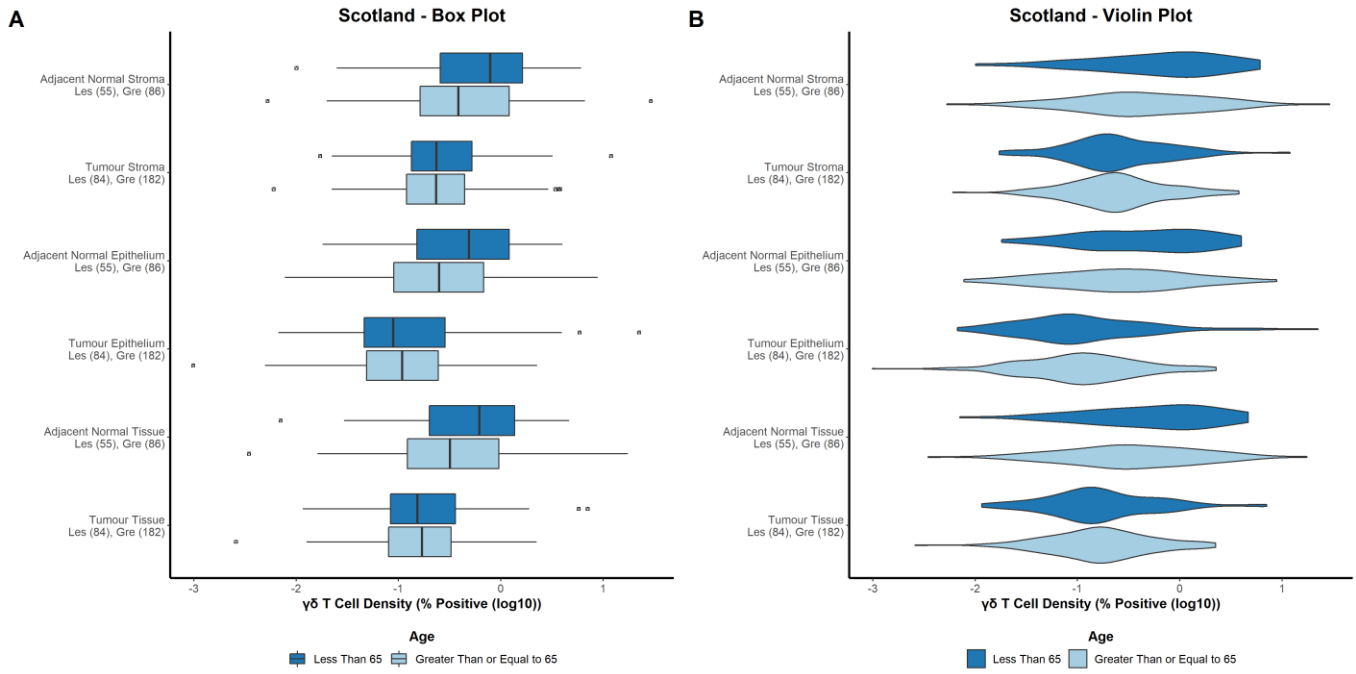

Figure 3.13 - Scotland Cohort. Assessment of γδ T cell density in patients aged <65 or ≥65. *Box plot presentation of γδ T cell density in patients aged <65 (dark blue) or ≥65 (light blue). The box is representative of the interquartile range (middle 50% of data points), the vertical line denotes the median and the minimum and maximum are denoted by whiskers. Outliers are represented by an open triangle within an open square (A). Violin plot presentation of γδ T cell density in patients aged <65 (dark blue) or ≥65 (light blue). The shape of the data reflects the distribution of the data points, which is not discernible in box plots. Outliers are represented by an open triangle within an open square (B). Y axis labels state the tissue compartment (primary tumour or adjacent normal tissue and epithelium, stroma or whole tissue) and below, the test groups with number of cases in brackets. X axis is log10 of the % of total cells within a region positive for the marker of interest. Inline labels denote the lowest standard statistical significance threshold reached (non-significant not shown) using a Welch two sample t-test, <0.05 (*), <0.01 (**) or <0.001 (***), with test groups in brackets.*

3.3.6 γδ T cell density by sex

Sex is a prominent factor in CRC incidence, with males having a greater incidence rate than females [256, 257], thus, the difference in γδ T cell density between male and female patients was investigated. In the adjacent normal stroma, there was a slightly greater density of γδ T cells in male patients compared to female patients (p = 0.058) (Figure 3.14A). In the primary tumour stroma, there was no difference in the density of γδ T cells in male patients compared to female patients (p = 0.401) (Figure 3.14A). In the adjacent normal epithelium, there was a slightly greater density of γδ T cells in male patients compared to female patients (p = 0.0088) (Figure 3.14A). In the primary tumour epithelium, there was no difference in the density of γδ T cells in male patients compared to female patients (p = 0.580) (Figure 3.14A). In the adjacent normal tissue, there was a slightly greater density of γδ T cells in male patients compared to female patients (p = 0.022) (Figure 3.14A). In the primary tumour tissue, there was no difference in the density of γδ T cells in male patients compared to female patients (p = 0.793) (Figure 3.14A). Compartments in the primary tumour had a lesser variance in the density of γδ T cells compared to compartments in the adjacent normal tissue (Figure 3.14B).

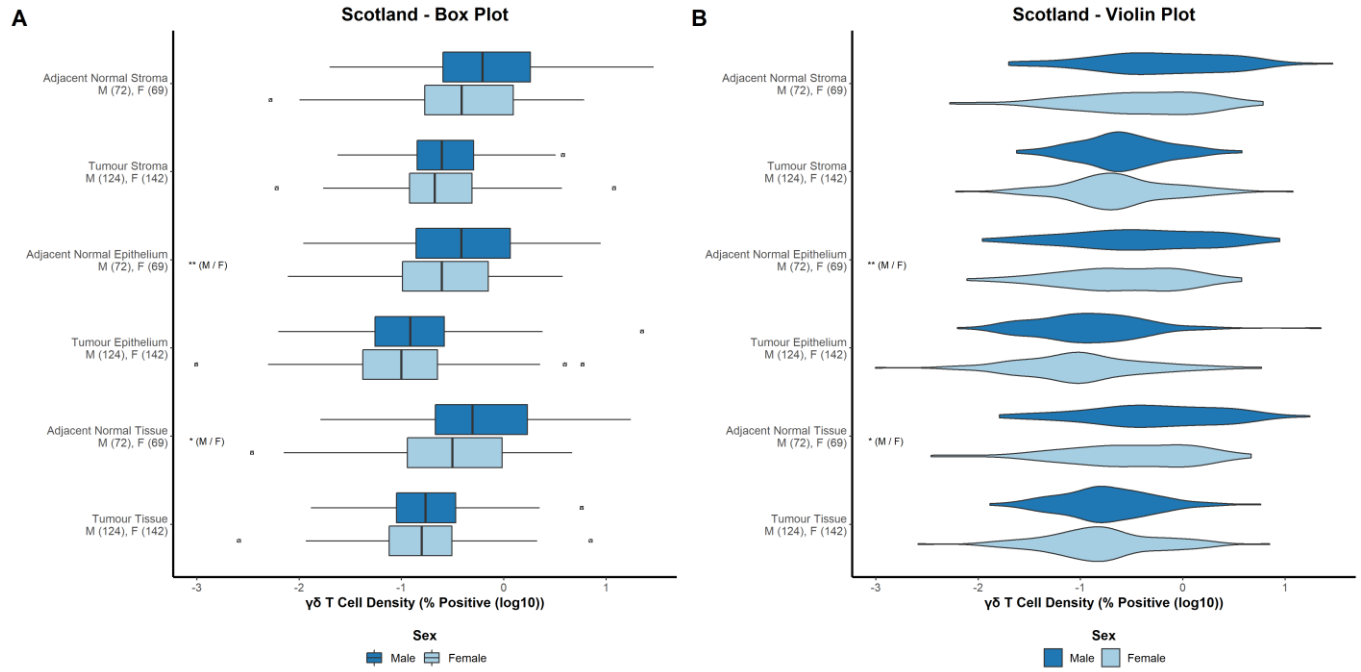

Figure 3.14 - Scotland Cohort. Assessment of γδ T cell density in male and female patients. *Box plot presentation of γδ T cell density in male patients (dark blue) or female patients (light blue). The box is representative of the interquartile range (middle 50% of data points), the vertical line denotes the median and the minimum and maximum are denoted by whiskers. Outliers are represented by an open triangle within an open square (A). Violin plot presentation of γδ T cell density in male patients (dark blue) or female patients (light blue). The shape of the data reflects the distribution of the data points, which is not discernible in box plots. Outliers are represented by an open triangle within an open square (B). Y axis labels state the tissue compartment (primary tumour or adjacent normal tissue and epithelium, stroma or whole tissue) and below, the test groups with number of cases in brackets. X axis is log10 of the % of total cells within a region positive for the marker of interest. Inline labels denote the lowest standard statistical significance threshold reached (non-significant not shown) using a Welch two sample t-test, <0.05 (*), <0.01 (**) or <0.001 (***), with test groups in brackets.*

3.3.7 γδ T cell density by site

There are molecular, histological, and prognostic differences associated with CRC tumours located in the proximal side of the splenic flexure (right-sided), distal side of the splenic flexure (left-sided) and the rectum. Thus, the density of γδ T cells was investigated in the context of these tumour sites. In the adjacent normal stroma, there was a mildly greater density of γδ T cells in the right-sided cases compared to the left-sided and rectal cases (p = 0.086) (Figure 3.15A). In the primary tumour stroma, there was no difference in the density of γδ T cells in the right-sided, left-sided, and rectal cases (p = 0.519) (Figure 3.15A). In the adjacent normal epithelium, there was no difference in the density of γδ T cells in the right-sided, left-sided, and rectal cases (p = 0.120) (Figure 3.15A). In the primary tumour epithelium, there was no difference in the density of γδ T cells in the right-sided, left-sided, and rectal cases (p = 0.166) (Figure 3.15A). In the adjacent normal tissue, there was a mildly greater density of γδ T cells in the right-sided cases compared to the left-sided and rectal cases (p = 0.059) (Figure 3.15A). In the primary tumour tissue, there was no difference in the density of γδ T cells in the right-sided, left-sided, and rectal cases (p = 0.501) (Figure 3.15A). There was no difference in the variance of γδ T cell density between tissue compartments (Figure 3.15B).

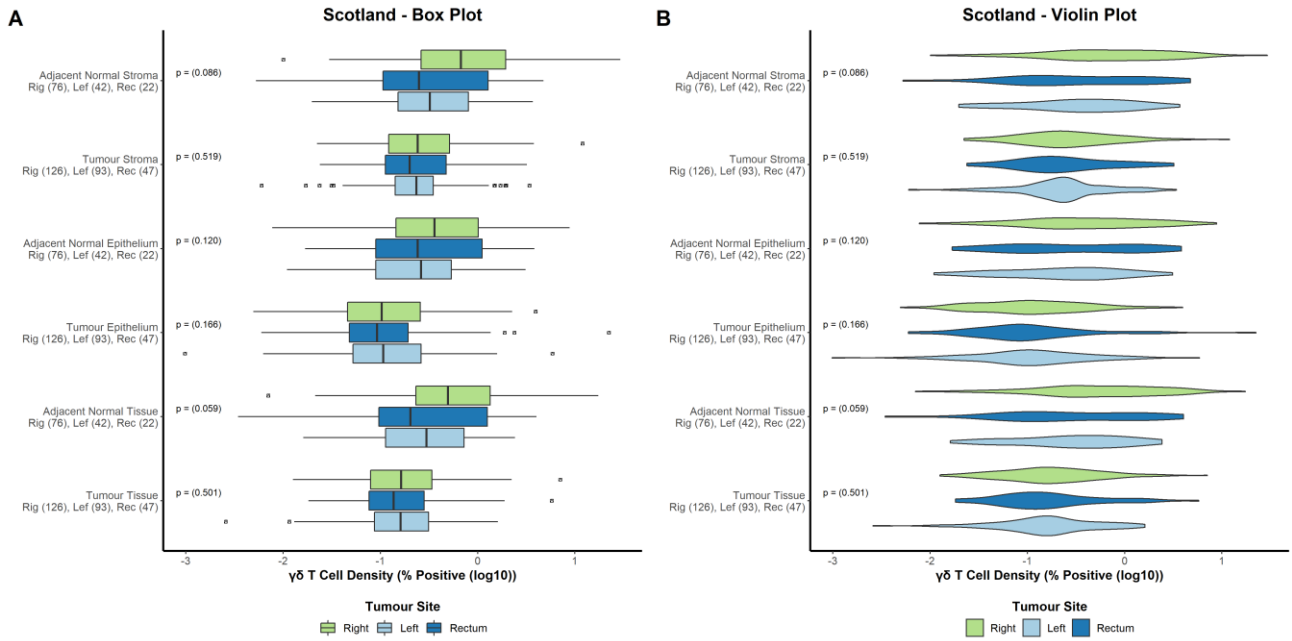

Figure 3.15 - Scotland Cohort. Assessment of γδ T cell density in tumour sites. *Box plot presentation of γδ T cell density in right-sided (light green), left-sided (light blue) and rectal disease (dark blue). The box is representative of the interquartile range (middle 50% of data points), the vertical line denotes the median and the minimum and maximum are denoted by whiskers. Outliers are represented by an open triangle within an open square (A). Violin plot presentation of γδ T cell density in right-sided (light green), left-sided (light blue) and rectal disease (dark blue). The shape of the data reflects the distribution of the data points, which is not discernible in box plots. Outliers are represented by an open triangle within an open square (B). Y axis labels state the tissue compartment (primary tumour or adjacent normal tissue and epithelium, stroma or whole tissue) and below, the test groups with number of cases in brackets. X axis is log10 of the % of total cells within a region positive for the marker of interest. Inline labels denote the lowest standard statistical significance threshold reached (non-significant not shown) using a one-way ANOVA, <0.05 (*), <0.01 (**) or <0.001 (***), with statistically significant (<0.05) group comparisons noted below as determined by Tukey's post-hoc test.*

3.3.8 γδ T cell density by MMR

Deficiency in the DNA mismatch repair system results in microsatellite instability which is associated with an increased immune infiltration into the tumour and a favourable outcome [41, 48, 258]. Thus, γδ T cells were investigated in patients determined to be proficient or deficient for DNA mismatch repair. In the adjacent normal stroma, there was no difference in the density of γδ T cells between DNA mismatch repair proficient and deficient patients (p = 0.165) (Figure 3.16A). In the primary tumour stroma, there was no difference in the density of γδ T cells between DNA mismatch repair proficient and deficient patients (p = 0.315) (Figure 3.16A). In the adjacent normal epithelium, there was no difference in the density of γδ T cells between DNA mismatch repair proficient and deficient patients (p = 0.289) (Figure 3.16A). In the primary tumour epithelium, there was no difference in the density of γδ T cells between DNA mismatch repair proficient and deficient patients (p = 0.194) (Figure 3.16A). In the adjacent normal tissue, there was no difference in the density of γδ T cells between DNA mismatch repair proficient and deficient patients (p = 0.214) (Figure 3.16A). In the primary tumour tissue, there was no difference in the density of γδ T cells between DNA mismatch repair proficient and deficient patients (p = 0.193) (Figure 3.16A). There was a mildly lesser amount of variance in γδ T cell density in primary tumour compartments compared to adjacent normal tissue compartments (Figure 3.16B).

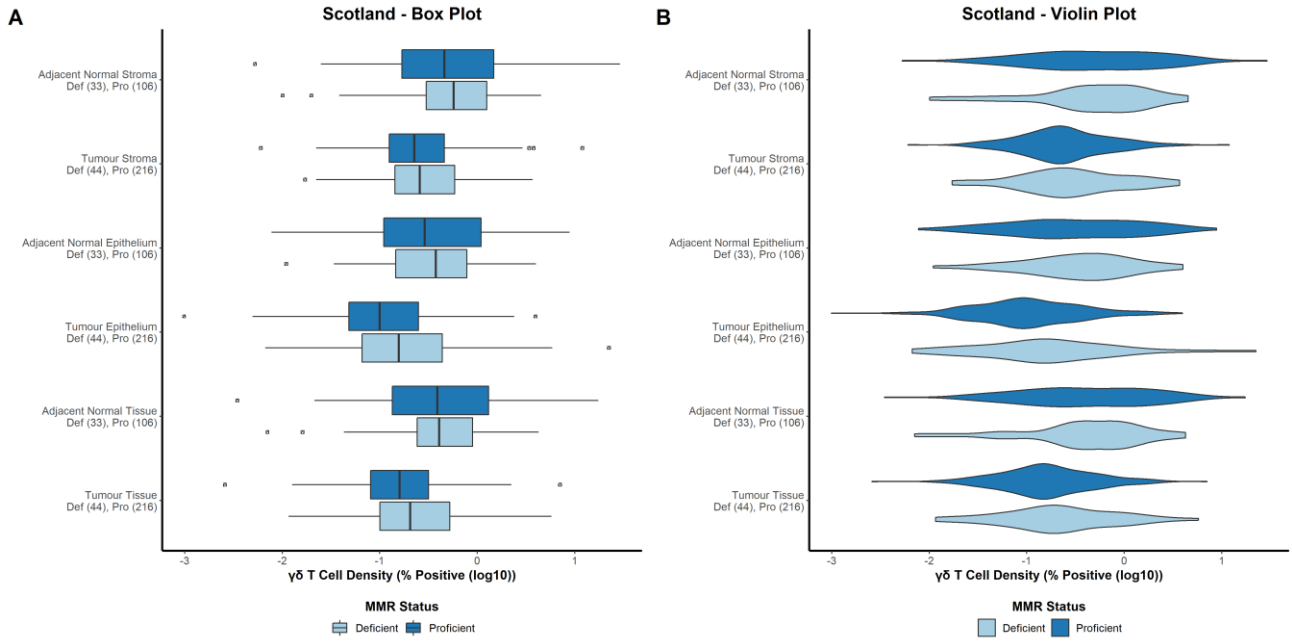

Figure 3.16 - Scotland Cohort. Assessment of γδ T cell density by mismatch repair status. *Box plot presentation of γδ T cell density in MMR deficient (light blue) and MMR proficient (dark blue) patients. The box is representative of the interquartile range (middle 50% of data points), the vertical line denotes the median and the minimum and maximum are denoted by whiskers. Outliers are represented by an open triangle within an open square (A). Violin plot presentation γδ T cell density in MMR deficient (light blue) and MMR proficient (dark blue) patients. The shape of the data reflects the distribution of the data points, which is not discernible in box plots. Outliers are represented by an open triangle within an open square (B). Y axis labels state the tissue compartment (primary tumour or adjacent normal tissue and epithelium, stroma or whole tissue) and below, the test groups with number of cases in brackets. X axis is log10 of the % of total cells within a region positive for the marker of interest. Inline labels denote the lowest standard statistical significance threshold reached (non-significant not shown) using a Welch two sample t-test, <0.05 (*), <0.01 (**) or <0.001 (***), with test groups in brackets.*

3.3.9 CD8 T cell density by tissue region

To understand whether lymphocyte density is altered in diseased tissue compared to the normal tissue environment, the density of CD8 T cells was investigated in the primary tumour and the adjacent normal tissue. To prevent any bias created by cases with exceptionally low or high lymphocyte density having only primary tumour tissue or only adjacent normal tissue available, standard exclusions were expanded to restrict cases to those with data available for both the primary tumour and the adjacent normal tissue. In the whole tissue, CD8 T cells were present at a greater density in the adjacent normal tissue than in the primary tumour (p = <0.001) (Figure 3.17A). In the stroma, CD8 T cells were present at a greater density in the adjacent normal tissue than in the primary tumour (p = <0.001) (Figure 3.17A). In the epithelium, CD8 T cells were present at a greater density in the adjacent normal tissue than in the primary tumour (p = <0.001) (Figure 3.17A). There was no difference in the variance of CD8 T cell density between the primary tumour and adjacent normal tissue compartments (Figure 3.17B).

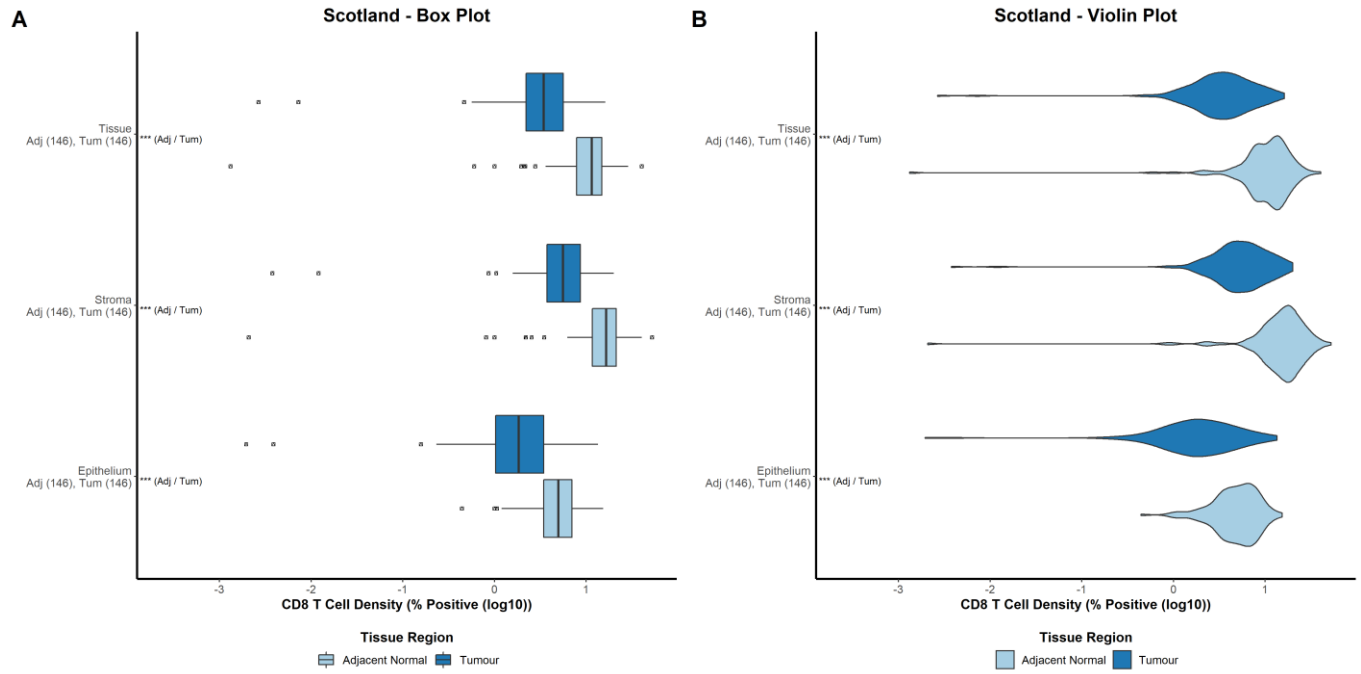

Figure 3.17 - Scotland Cohort. Assessment of CD8 T cell density in the primary tumour and adjacent normal tissue. *Box plot presentation of CD8 T cell density in the primary tumour (dark blue) and adjacent normal tissue (light blue). The box is representative of the interquartile range (middle 50% of data points), the vertical line denotes the median and the minimum and maximum are denoted by whiskers. Outliers are represented by an open triangle within an open square (A). Violin plot presentation of CD8 T cell density in the primary tumour (dark blue) and adjacent normal tissue (light blue). The shape of the data reflects the distribution of the data points, which is not discernible in box plots (B). Y axis labels state the tissue compartment (epithelium, stroma and whole tissue) and below, the test groups with number of cases in brackets. X axis is log10 of the % of total cells within a region positive for the marker of interest. Inline labels denote the lowest standard statistical significance threshold reached (non-significant not shown) using a paired t-test, <0.05 (*), <0.01 (**) or <0.001 (***), with test groups in brackets.*

3.3.10 CD8 T cell density by tissue compartment

Lymphocyte localisation is vital to function [254]; thus, lymphocytes were scored for the whole tissue (primary tumour or adjacent normal) and for the epithelium and stroma separately and these latter regions compared. In the primary tumour, CD8 T cells were present at a greater density in the stroma than the epithelium (p = <0.001) (Figure 3.18A). In the adjacent normal tissue, CD8 T cells were present at a greater density in the stroma than the epithelium (p = <0.001) (Figure 3.18A). There was no difference in the variance of CD8 T cell density between compartments in the primary tumour and adjacent normal tissue (Figure 3.18B).

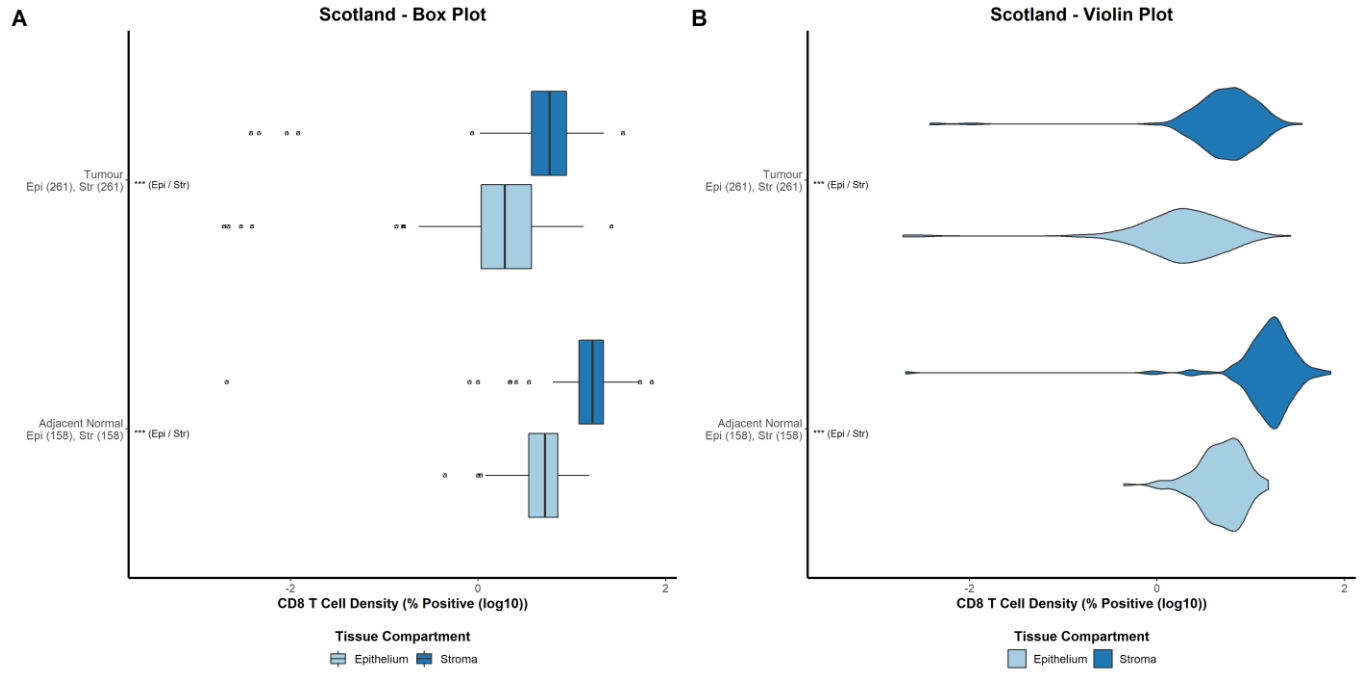

Figure 3.18 - Scotland Cohort. Assessment of CD8 T cell density in the stroma and epithelium. *Box plot presentation of CD8 T cell density in the stroma (dark blue) and epithelium (light blue). The box is representative of the interquartile range (middle 50% of data points), the vertical line denotes the median and the minimum and maximum are denoted by whiskers. Outliers are represented by an open triangle within an open square (A). Violin plot presentation of CD8 T cell density in the stroma (dark blue) and epithelium (light blue). The shape of the data reflects the distribution of the data points, which is not discernible in box plots (B). Y axis labels state the tissue compartment (primary tumour and adjacent normal tissue) and below, the test groups with number of cases in brackets. X axis is log10 of the % of total cells within a region positive for the marker of interest. Inline labels denote the lowest standard statistical significance threshold reached (non-significant not shown) using a Welch two sample t-test, <0.05 (*), <0.01 (**) or <0.001 (***), with test groups in brackets.*

3.3.11 CD8 T cell density by TNM stage

The primary tumour data consists of tumours at various stages of disease progression, stratified using the TNM staging system, which have variable tumour microenvironments and clinical outcomes. Thus, to understand whether data for the primary tumour is representative of all cases or stage dependent, CD8 T cell density was investigated across the four TNM stages. To conduct this analysis the standard exclusions were altered to include stage I and stage IV patients, although no stage IV patients had CD8 data available. In the adjacent normal stroma, there was no difference in CD8 T cell density between stage I-III patients (p = 0.476) (Figure 3.19A). In the primary tumour stroma, there was no difference in CD8 T cell density between stage I- III patients (p = 0.209) (Figure 3.19A). In the adjacent normal epithelium, there was no difference in CD8 T cell density between stage I- III patients (p = 0.549) (Figure 3.19A). In the primary tumour epithelium, there was no difference in CD8 T cell density between stage I-III patients (p = 0.104) (Figure 3.19A). In the adjacent normal tissue, there was no difference in CD8 T cell density between stage I- III patients (p = 0.391) (Figure 3.19A). In the primary tumour tissue, there was no difference in CD8 T cell density between stage I- III patients (p = 0.322) (Figure 3.19A). There was a lesser variance in CD8 T cell density in adjacent normal tissue compartments compared to the primary tumour compartments (Figure 3.19B).

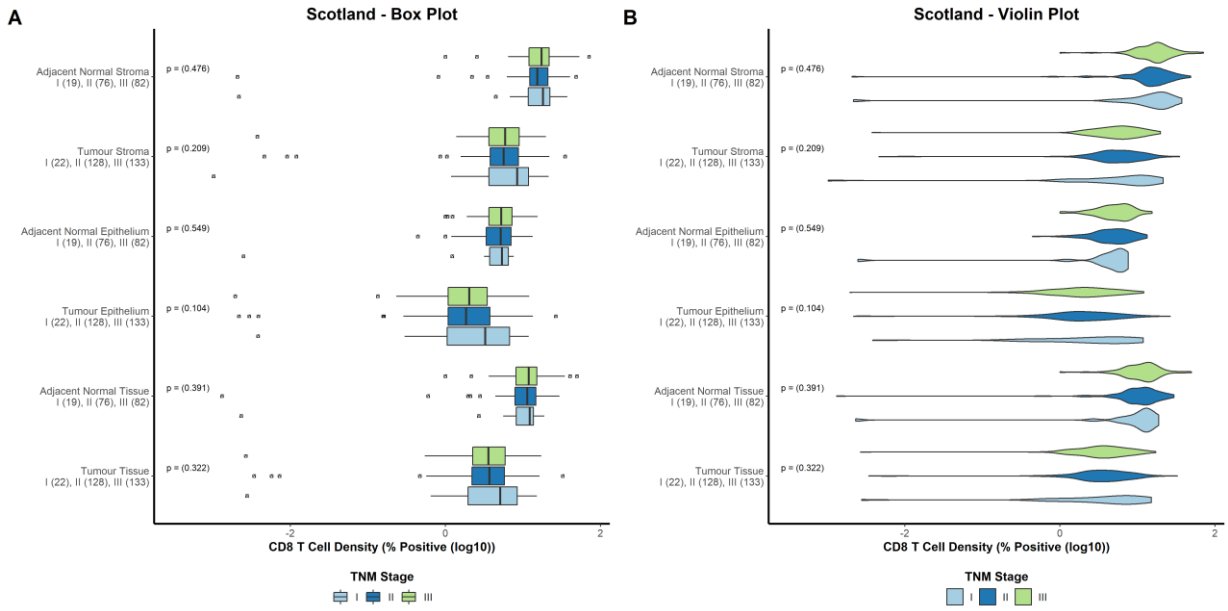

Figure 3.19 - Scotland Cohort. Assessment of CD8 T cell density across TNM stages. *Box plot presentation of CD8 T cell density in stage I (light blue), stage II (dark blue), stage III (light green) and stage IV (dark green) patients. The box is representative of the interquartile range (middle 50% of data points), the vertical line denotes the median and the minimum and maximum are denoted by whiskers. Outliers are represented by an open triangle within an open square (A). Violin plot presentation of CD8 T cell density in stage I (light blue), stage II (dark blue), stage III (light green) and stage IV (dark green) patients. The shape of the data reflects the distribution of the data points, which is not discernible in box plots (B). Y axis labels state the tissue compartment (primary tumour or adjacent normal tissue and epithelium, stroma or whole tissue) and below, the test groups with number of cases in brackets. X axis is log10 of the % of total cells within a region positive for the marker of interest. Inline labels denote the lowest standard statistical significance threshold reached (non-significant not shown) using a one-way ANOVA, <0.05 (*), <0.01 (**) or <0.001 (***), with statistically significant (<0.05) group comparisons noted below as determined by Tukey's post-hoc test.*

3.3.12 CD8 T cell density by age

Incidence of CRC increases with aged populations, although cases in younger populations are increasing, and so the density of CD8 T cells was investigated in patients aged < 65 years of age or ≥ 65 years of age [255]. In the adjacent normal stroma, there was no difference in CD8 T cell density between patients < 65 years of age and those ≥65 years of age (p = 0.063) (Figure 3.20A). In the primary tumour stroma, there was no difference in CD8 T cell density between patients < 65 years of age and those ≥65 years of age (p = 0.0025) (Figure 3.20A). In the adjacent normal epithelium, there was no difference in CD8 T cell density between patients < 65 years of age and those ≥65 years of age (p = 0.095) (Figure 3.20A). In the primary tumour epithelium, there was no difference in CD8 T cell density between patients < 65 years of age and those ≥65 years of age (p = 0.0024) (Figure 3.20A). In the adjacent normal tissue, there was no difference in CD8 T cell density between patients < 65 years of age and those ≥65 years of age (p = 0.077) (Figure 3.20A). In the primary tumour tissue, there was no difference in CD8 T cell density between patients < 65 years of age and those ≥65 years of age (p = 0.0033) (Figure 3.20A). The primary tumour compartments had a mildly greater variance in CD8 T cell density than adjacent normal tissue compartments (Figure 3.20B).

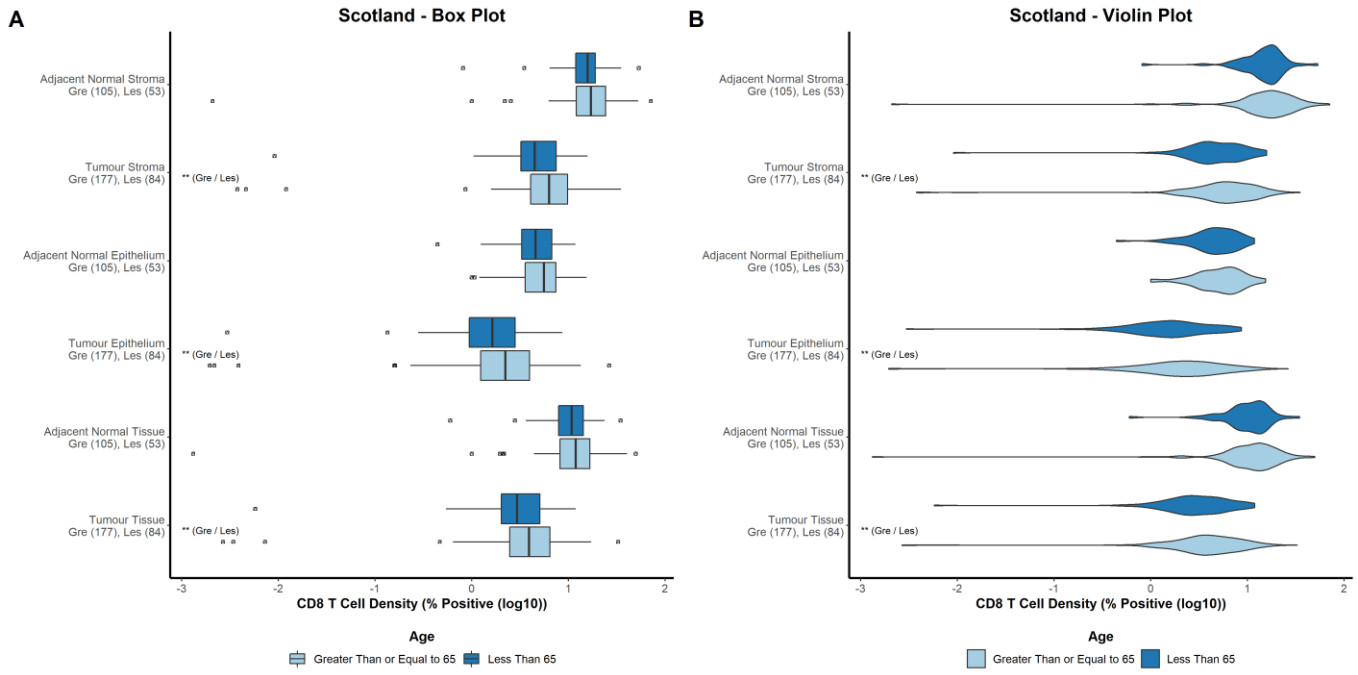

Figure 3.20 - Scotland Cohort. Assessment of CD8 T cell density in patients aged <65 or ≥65. *Box plot presentation of CD8 T cell density in patients aged <65 (dark blue) or ≥65 (light blue). The box is representative of the interquartile range (middle 50% of data points), the vertical line denotes the median and the minimum and maximum are denoted by whiskers. Outliers are represented by an open triangle within an open square (A). Violin plot presentation of CD8 T cell density in patients aged <65 (dark blue) or ≥65 (light blue). The shape of the data reflects the distribution of the data points, which is not discernible in box plots. Outliers are represented by an open triangle within an open square (B). Y axis labels state the tissue compartment (primary tumour or adjacent normal tissue and epithelium, stroma or whole tissue) and below, the test groups with number of cases in brackets. X axis is log10 of the % of total cells within a region positive for the marker of interest. Inline labels denote the lowest standard statistical significance threshold reached (non-significant not shown) using a Welch two sample t-test, <0.05 (*), <0.01 (**) or <0.001 (***), with test groups in brackets.*

3.3.13 CD8 T cell density by sex

Sex is a prominent factor in CRC incidence, with males having a greater incidence rate than females [256, 257], thus, the difference in CD8 T cell density between male and female patients was investigated. In the adjacent normal stroma, there was no difference in the density of CD8 T cells in male patients compared to female patients (p = 0.558) (Figure 3.21A). In the primary tumour stroma, there was no difference in the density of CD8 T cells in male patients compared to female patients (p = 0.151) (Figure 3.21A). In the adjacent normal epithelium, there was no difference in the density of CD8 T cells in male patients compared to female patients (p = 0.793) (Figure 3.21A). In the primary tumour epithelium, there was no difference in the density of CD8 T cells in male patients compared to female patients (p = 0.133) (Figure 3.21A). In the adjacent normal tissue, there was no difference in the density of CD8 T cells in male patients compared to female patients (p = 0.661) (Figure 3.21A). In the primary tumour tissue, there was no difference in the density of CD8 T cells in male patients compared to female patients (p = 0.127) (Figure 3.21A). Compartments in the adjacent normal tissue had a lesser variance in the density of CD8 T cells compared to compartments in the primary tumour (Figure 3.21B).

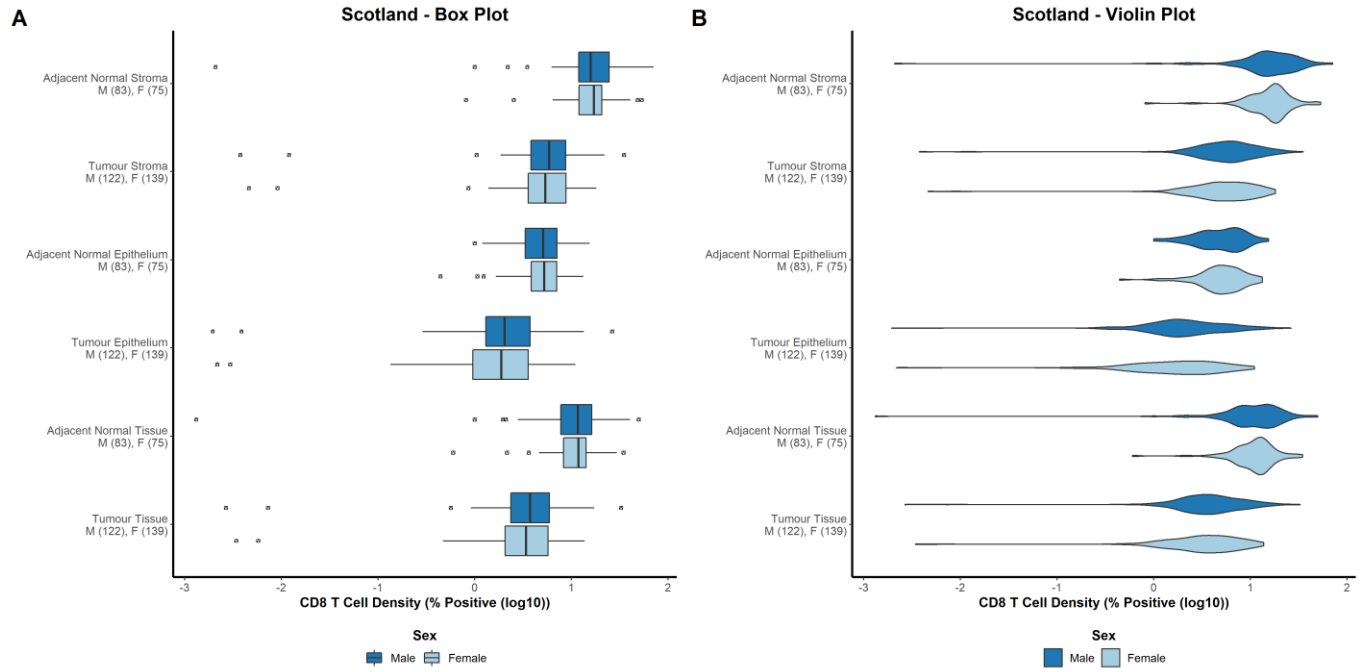

Figure 3.21 - Scotland Cohort. Assessment of CD8 T cell density in male and female patients. *Box plot presentation of CD8 T cell density in male patients (dark blue) or female patients (light blue). The box is representative of the interquartile range (middle 50% of data points), the vertical line denotes the median and the minimum and maximum are denoted by whiskers. Outliers are represented by an open triangle within an open square (A). Violin plot presentation of CD8 T cell density in male patients (dark blue) or female patients (light blue). The shape of the data reflects the distribution of the data points, which is not discernible in box plots. Outliers are represented by an open triangle within an open square (B). Y axis labels state the tissue compartment (primary tumour or adjacent normal tissue and epithelium, stroma or whole tissue) and below, the test groups with number of cases in brackets. X axis is log10 of the % of total cells within a region positive for the marker of interest. Inline labels denote the lowest standard statistical significance threshold reached (non-significant not shown) using a Welch two sample t-test, <0.05 (*), <0.01 (**) or <0.001 (***), with test groups in brackets.*

3.3.14 CD8 T cell density by site

There are molecular, histological, and prognostic differences associated with CRC tumours located in the proximal side of the splenic flexure (right-sided), distal side of the splenic flexure (left-sided) and the rectum. Thus, the density of CD8 T cells was investigated in the context of these tumour sites. In the adjacent normal stroma, there was a mildly greater density of CD8 T cells in the right-sided cases compared to the left-sided, and this was statistically significant (p = <0.001) (Figure 3.22A). In the primary tumour stroma, there was no difference in the density of CD8 T cells in the right-sided, left-sided, and rectal cases, and this was statistically significant (p = <0.001) (Figure 3.22A). In the adjacent normal epithelium, there was a mildly greater density of CD8 T cells in the right-sided cases compared to the left-sided, and this was statistically significant (p = <0.001) (Figure 3.22A). In the primary tumour epithelium, there was no difference in the density of CD8 T cells in the right-sided, left-sided and rectal cases, and this was statistically significant (p = 0.0014) (Figure 3.22A). In the adjacent normal tissue, there was a mildly greater density of CD8 T cells in the right-sided cases compared to the left-sided, and this was statistically significant (p = <0.001) (Figure 3.22A). In the primary tumour tissue, there was no difference in the density of CD8 T cells in the right-sided, left-sided, and rectal cases, and this was statistically significant (p = 0.001) (Figure 3.22A). There was no difference in the variance of CD8 T cell density between tissue compartments (Figure 3.22B).

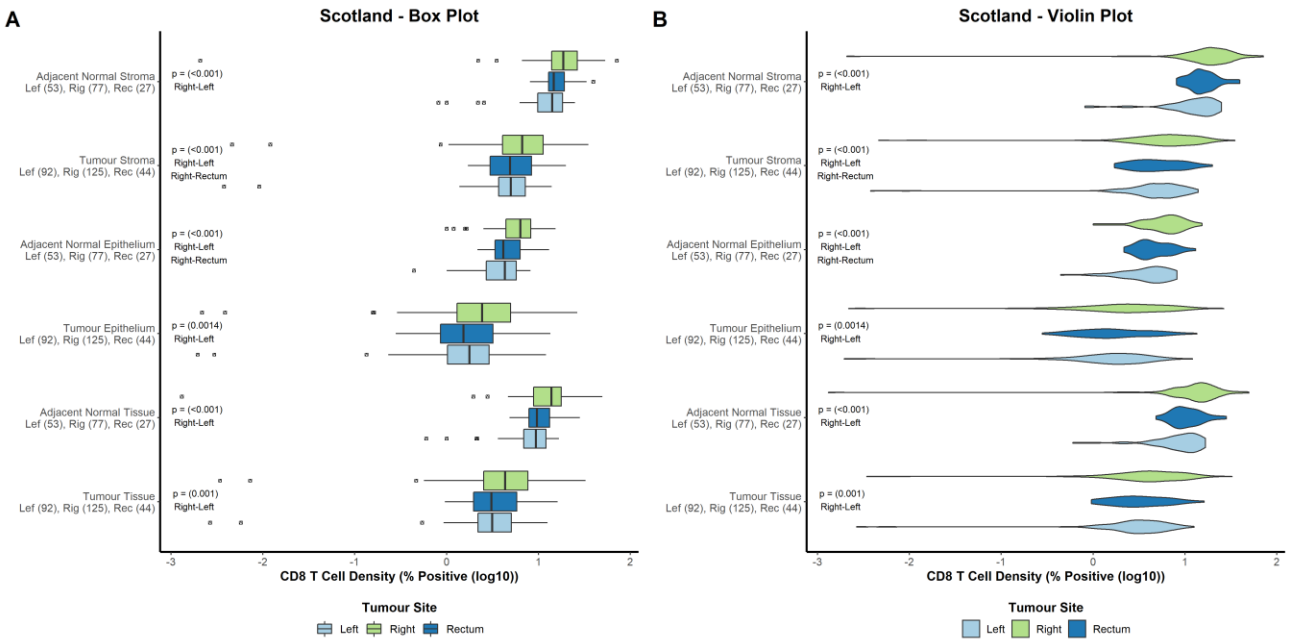

Figure 3.22 - Scotland Cohort. Assessment of CD8 T cell density in tumour sites. *Box plot presentation of CD8 T cell density in right-sided (light green), left-sided (light blue) and rectal disease (dark blue). The box is representative of the interquartile range (middle 50% of data points), the vertical line denotes the median and the minimum and maximum are denoted by whiskers. Outliers are represented by an open triangle within an open square (A). Violin plot presentation of CD8 T cell density in right-sided (light green), left-sided (light blue) and rectal disease (dark blue). The shape of the data reflects the distribution of the data points, which is not discernible in box plots. Outliers are represented by an open triangle within an open square (B). Y axis labels state the tissue compartment (primary tumour or adjacent normal tissue and epithelium, stroma or whole tissue) and below, the test groups with number of cases in brackets. X axis is log10 of the % of total cells within a region positive for the marker of interest. Inline labels denote the lowest standard statistical significance threshold reached (non-significant not shown) using a one-way ANOVA, <0.05 (*), <0.01 (**) or <0.001 (***), with statistically significant (<0.05) group comparisons noted below as determined by Tukey's post-hoc test.*

3.3.15 CD8 T cell density by MMR

Deficiency in the DNA mismatch repair system results in microsatellite instability which is associated with increased immune infiltration in the tumour and a favourable outcome [41, 258]. Thus, CD8 T cells were investigated in patients determined to be proficient or deficient for DNA mismatch repair. In the adjacent normal stroma, there was no difference in the density of CD8 T cells between DNA mismatch repair proficient and deficient patients ($p = 0.161$) (Figure 3.23A). In the primary tumour stroma, there was a statistically significant difference in the density of CD8 T cells between DNA mismatch repair proficient and deficient patients ($p = 0.014$) (Figure 3.23A). In the adjacent normal epithelium, there was a statistically significant difference in the density of CD8 T cells between DNA mismatch repair proficient and deficient patients ($p = 0.026$) (Figure 3.23A). In the primary tumour epithelium, there was a statistically significant difference in the density of CD8 T cells between DNA mismatch repair proficient and deficient patients ($p = 0.049$) (Figure 3.23A). In the adjacent normal tissue, there was no difference in the density of CD8 T cells between DNA mismatch repair proficient and deficient patients ($p = 0.077$) (Figure 3.23A). In the primary tumour tissue, there was a statistically significant difference in the density of CD8 T cells between DNA mismatch repair proficient and deficient patients ($p = 0.031$) (Figure 3.23A). There was a mildly lesser amount of variance in CD8 T cell density in adjacent normal compartments compared to primary tumour tissue compartments (Figure 3.23B).

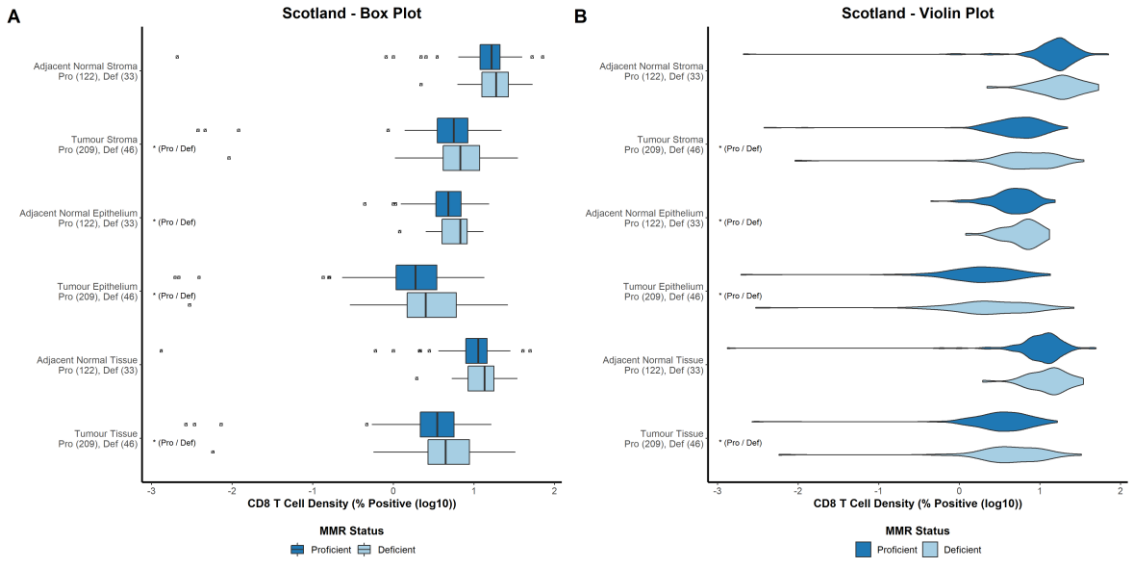

Figure 3.23 - Scotland Cohort. Assessment of CD8 T cell density by mismatch repair status. *Box plot presentation of CD8 T cell density in MMR deficient (light blue) and MMR proficient (dark blue) patients. The box is representative of the interquartile range (middle 50% of data points), the vertical line denotes the median and the minimum and maximum are denoted by whiskers. Outliers are represented by an open triangle within an open square (A). Violin plot presentation CD8 T cell density in MMR deficient (light blue) and MMR proficient (dark blue) patients. The shape of the data reflects the distribution of the data points, which is not discernible in box plots. Outliers are represented by an open triangle within an open square (B). Y axis labels state the tissue compartment (primary tumour or adjacent normal tissue and epithelium, stroma or whole tissue) and below, the test groups with number of cases in brackets. X axis is log10 of the % of total cells within a region positive for the marker of interest. Inline labels denote the lowest standard statistical significance threshold reached (non-significant not shown) using a Welch two sample t-test, <0.05 (*), <0.01 (**) or <0.001 (***), with test groups in brackets.*

3.3.16 Comparison of γδ and CD8 T cell density

Compared to the expected density of CD8 T cells in tissue, the expected density of γδ T cells is hypothesised to be much less. In addition, the functional role of these lymphocyte populations is different and their comparative roles not clear [155]. Thus, the comparative density of γδ and CD8 T cells was investigated.

In the adjacent normal stroma, CD8 T cells were present at a vastly greater density than γδ T cells (p = <0.001) (Figure 3.24A). In the primary tumour stroma, CD8 T cells were present at a vastly greater density than γδ T cells (p = <0.001) (Figure 3.24A). In the adjacent normal epithelium, CD8 T cells were present at a vastly greater density than γδ T cells (p = <0.001) (Figure 3.24A). In the primary tumour epithelium, CD8 T cells were present at a vastly greater density than γδ T cells (p = <0.001) (Figure 3.24A). In the adjacent normal tissue, CD8 T cells were present at a vastly greater density than γδ T cells (p = <0.001) (Figure 3.24A). In the primary tumour tissue, CD8 T cells were present at a vastly greater density than γδ T cells (p = <0.001) (Figure 3.24A). The density of CD8 T cells was subject to greater variance than the density of γδ T cells (Figure 3.24B).

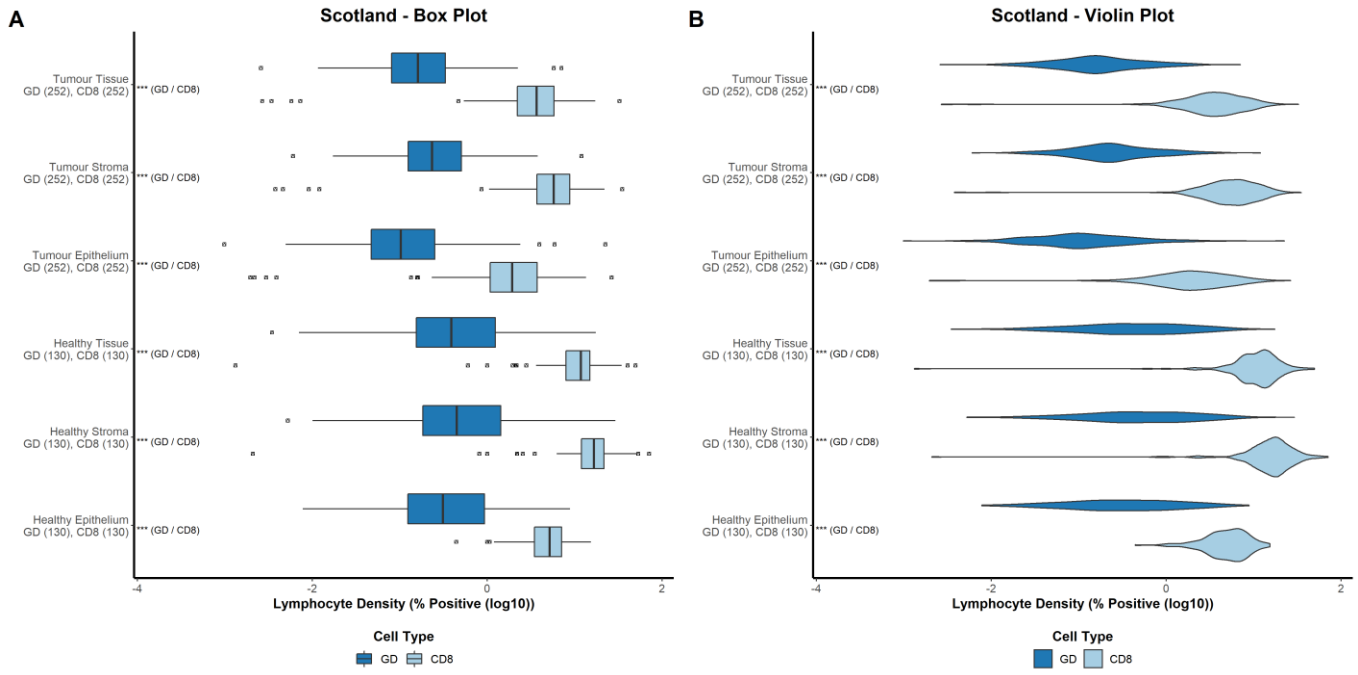

Figure 3.24 - Scotland Cohort. Assessment of comparative γδ and CD8 T cell density. *Box plot presentation of γδ T cell density (dark blue) and CD8 T cell density (light blue). The box is representative of the interquartile range (middle 50% of data points), the vertical line denotes the median and the minimum and maximum are denoted by whiskers. Outliers are represented by an open triangle within an open square (A). Violin plot presentation of γδ T cell density (dark blue) and CD8 T cell density (light blue). The shape of the data reflects the distribution of the data points, which is not discernible in box plots. Outliers are represented by an open triangle within an open square (B). Y axis labels state the tissue compartment (primary tumour or adjacent normal tissue and epithelium, stroma or whole tissue) and below, the test groups with number of cases in brackets. X axis is log10 of the % of total cells within a region positive for the marker of interest. Inline labels denote the lowest standard statistical significance threshold reached (non-significant not shown) using a paired t-test, <0.05 (*), <0.01 (**) or <0.001 (***), with test groups in brackets.*

3.4 Norway Cohort

3.4.1 Clinicopathological characteristics of patient cohort

293 patients from the Norway cohort were included in a sub-cohort for analysis. Patient cohort characteristics of the full cohort and sub-cohort are outlined in Table 3.2. The sub-cohort was comparable to the full cohort. There was an even split between female (52%) and male (48%) patients. Considerably more patients were equal to or above the age of 65 (79%) than below 65 (21%). Surgeries were all elective (100%). The tumour site was imbalanced with more tumours being present in right (59%) sided disease than left sided disease (41%). Patients were primarily T stage III (91%), N stage 0/I (63%/28%), M stage 0 (100%) and exclusively TNM stage II/III (63%/37%). Tumours were predominantly moderately/well differentiated (77%). Most patients did not have vascular invasion (80%). Patients were mostly graded as Klintrup-Mäkinen weak (87%). Patients had a close balance of tumour stroma percentage low (55%) and high (45%). The majority of patient did not receive adjuvant therapy (80%). Almost all patients survived beyond 30 days after surgery (99%). Median follow-up (alive cases, n = 183) in the sub-cohort was 77 months. There was a total of 35 cancer deaths and 75 non-cancer deaths in the sub-cohort. Patients were excluded if they had died within 30 days of surgery (n = 3) (Figure 3.25).

Table 3.2 - Clinicopathological characteristics of patients in the Norway cohort. *Table showing the number (and %) of patients exhibiting clinical features and comparison between the full cohort and the sub-cohort included for analyses.*

Patient Characteristics - Norway Cohort			
	Full cohort (N=299)	**Sub-cohort (N=293)**	**P-Value**
Sex			
Female	157 (53 %)	152 (52 %)	0.878
Male	142 (47 %)	141 (48 %)	
Age			
≥65	237 (79 %)	231 (79 %)	0.899
<65	62 (21 %)	62 (21 %)	
Surgery Type			
Elective	299 (100 %)	293 (100 %)	0.805
Tumour Site			
Right sided	179 (60 %)	174 (59 %)	0.905
Left sided	120 (40 %)	119 (41 %)	
T Stage			
I	2 (1 %)	2 (1 %)	1
II	10 (3 %)	10 (3 %)	
III	273 (91 %)	267 (91 %)	
IV	14 (5 %)	14 (5 %)	
N Stage			
0	189 (63 %)	186 (63 %)	0.997
I	83 (28 %)	81 (28 %)	
II	27 (9 %)	26 (9 %)	
M Stage			
0	298 (100 %)	292 (100 %)	0.805
Missing	1 (0.3%)	1 (0.3%)	
TNM Stage			
II	189 (63 %)	186 (63 %)	0.946
III	110 (37 %)	107 (37 %)	
Differentiation			
Moderate/Well	228 (76 %)	227 (77 %)	0.815
Poor	57 (19 %)	54 (18 %)	
Missing	14 (4.7%)	12 (4.1%)	
Vascular Invasion			
No	240 (80 %)	234 (80 %)	0.933
Yes	24 (8 %)	24 (8 %)	
Missing	35 (11.7%)	35 (11.9%)	
Klintrup-Mäkinen Grade			
Weak	261 (87 %)	255 (87 %)	0.926
Strong	36 (12 %)	36 (12 %)	
Missing	2 (0.7%)	2 (0.7%)	
Tumour Stroma Percentage			
Low	163 (55 %)	162 (55 %)	0.85
High	136 (45 %)	131 (45 %)	
Adjuvant Therapy			
No	237 (79 %)	234 (80 %)	0.857
Yes	62 (21 %)	59 (20 %)	
Mortality Within 30 Days			
No	296 (99 %)	290 (99 %)	0.98
Yes	3 (1 %)	3 (1 %)	

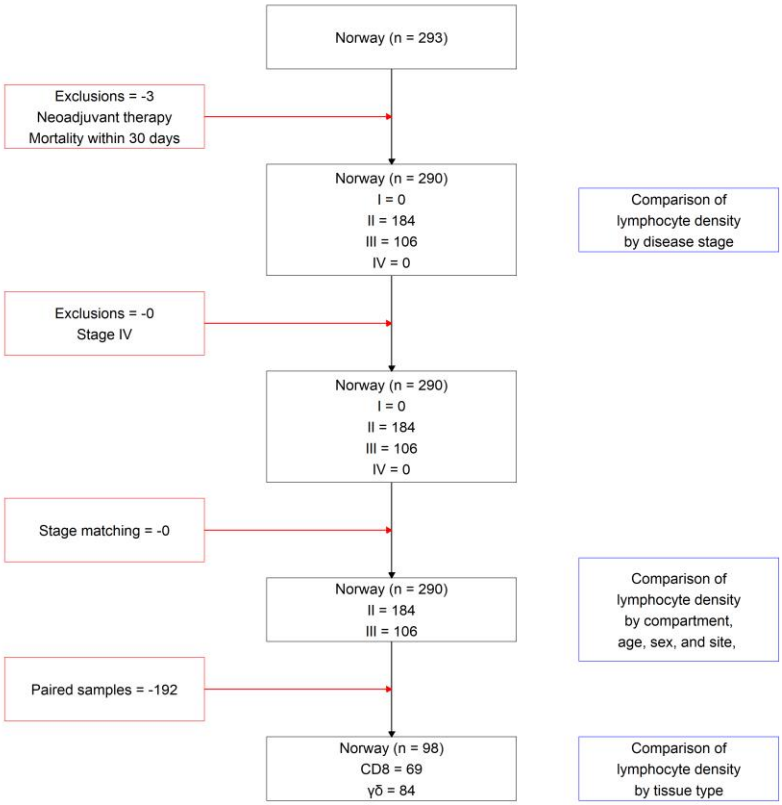

Figure 3.25 – Consort diagram for lymphocyte density analysis in the Norway cohort. *Red boxes denote removal of cases. Blue boxes denote analyses that use cases present at that level of the consort diagram.*

3.4.2 γδ T cell density by tissue region

To understand whether lymphocyte density is altered in diseased tissue compared to the normal tissue environment, the density of γδ was investigated in the primary tumour and the adjacent normal tissue. To prevent any bias created by cases with exceptionally low or high lymphocyte density having only primary tumour tissue or only adjacent normal tissue available, standard exclusions were expanded to restrict cases to those with data available for both the primary tumour and the adjacent normal tissue. In the whole tissue, γδ T cells were present at a greater density in the adjacent normal tissue than in the primary tumour (p = 0.0091) (Figure 3.26A) and adjacent normal tissue had a greater variance in γδ T cell density (Figure 3.26B). In the stroma, γδ T cells were present at a greater density in the adjacent normal tissue than in the primary tumour (p = 0.020) (Figure 3.26A) and adjacent normal tissue had a greater variance in γδ T cell density (Figure 3.26B). In the epithelium, γδ T cells were present at a greater density in the adjacent normal tissue than in the primary tumour (p = 0.0068) (Figure 3.26A) and adjacent normal tissue had a greater variance in γδ T cell density (Figure 3.26B).

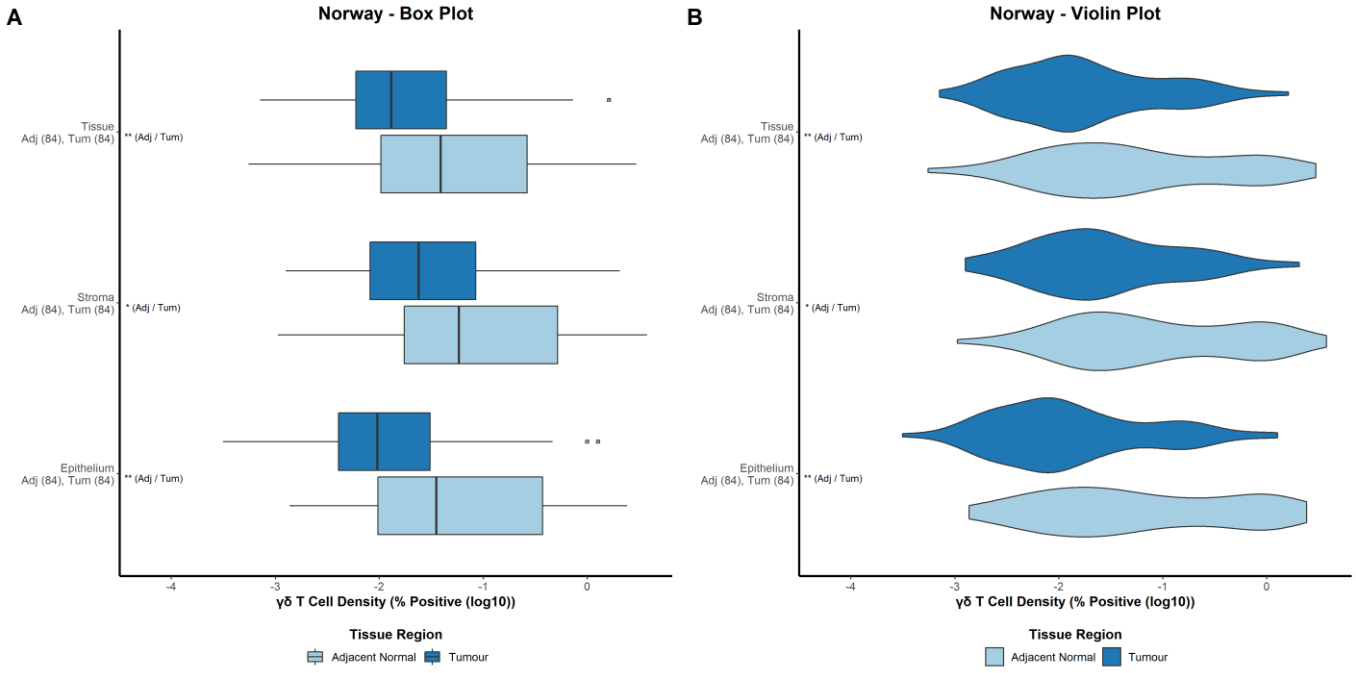

Figure 3.26 - Norway Cohort. Assessment of γδ T cell density in the primary tumour and adjacent normal tissue. *Box plot presentation of γδ T cell density in the primary tumour (dark blue) and adjacent normal tissue (light blue). The box is representative of the interquartile range (middle 50% of data points), the vertical line denotes the median and the minimum and maximum are denoted by whiskers. Outliers are represented by an open triangle within an open square (A). Violin plot presentation of γδ T cell density in the primary tumour (dark blue) and adjacent normal tissue (light blue). The shape of the data reflects the distribution of the data points, which is not discernible in box plots (B). Y axis labels state the tissue compartment (epithelium, stroma and whole tissue) and below, the test groups with number of cases in brackets. X axis is log10 of the % of total cells within a region positive for the marker of interest. Inline labels denote the lowest standard statistical significance threshold reached (non-significant not shown) using a paired t-test, <0.05 (*), <0.01 (**) or <0.001 (***), with test groups in brackets.*

3.4.3 γδ T cell density by tissue compartment

Lymphocyte localisation is vital to function [254], particularly γδ T cells which patrol the epithelium to maintain intestinal homeostasis [117]. Thus, lymphocytes were scored for the whole tissue (primary tumour or adjacent normal) and for the epithelium and stroma separately and these latter regions compared. In the primary tumour, γδ T cells were present at a greater density in the stroma than the epithelium (p = 0.047) (Figure 3.27A). In the adjacent normal tissue, there was no difference in the density of γδ T cells between the stroma and the epithelium (p = 0.384) (Figure 3.27A). γδ density showed no difference in variance between the adjacent normal tissue and the primary tumour (Figure 3.27B).

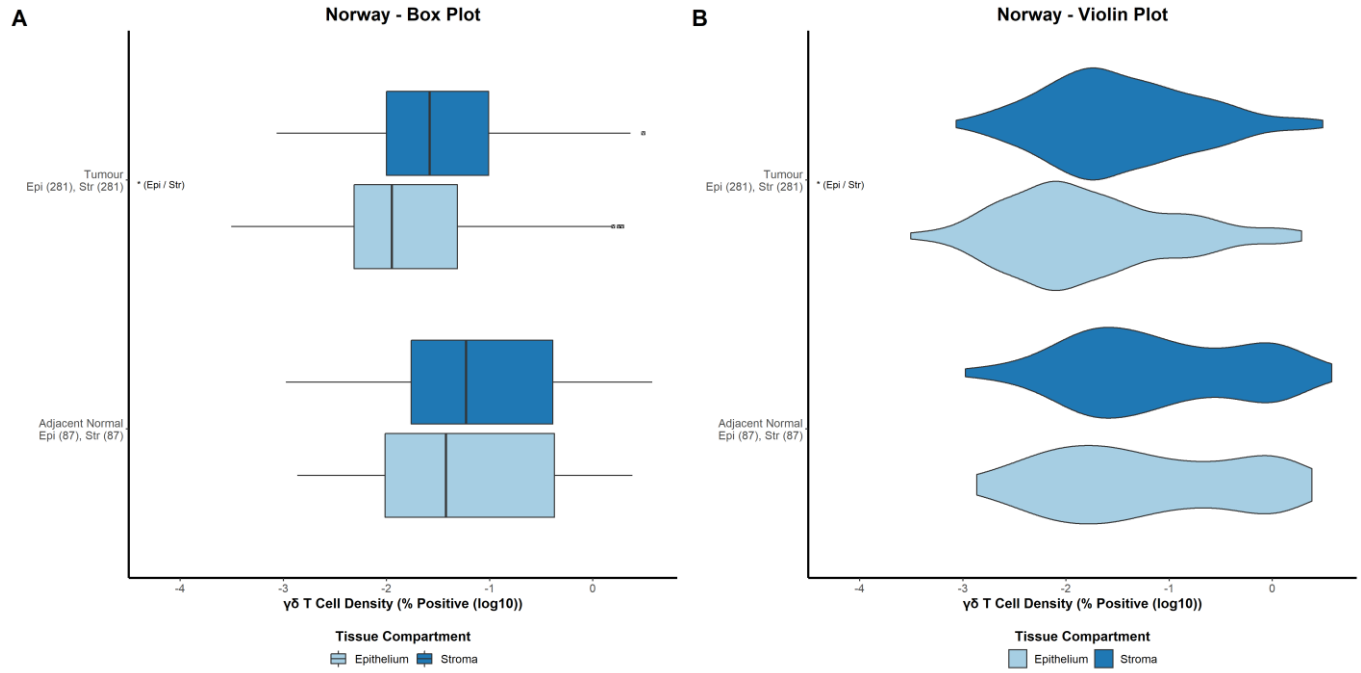

Figure 3.27 - Norway Cohort. Assessment of γδ T cell density in the stroma and epithelium. *Box plot presentation of γδ T cell density in the stroma (dark blue) and epithelium (light blue). The box is representative of the interquartile range (middle 50% of data points), the vertical line denotes the median and the minimum and maximum are denoted by whiskers. Outliers are represented by an open triangle within an open square (A). Violin plot presentation of γδ T cell density in the stroma (dark blue) and epithelium (light blue). The shape of the data reflects the distribution of the data points, which is not discernible in box plots (B). Y axis labels state the tissue compartment (primary tumour and adjacent normal tissue) and below, the test groups with number of cases in brackets. X axis is log10 of the % of total cells within a region positive for the marker of interest. Inline labels denote the lowest standard statistical significance threshold reached (non-significant not shown) using a Welch two sample t-test, <0.05 (*), <0.01 (**) or <0.001 (***), with test groups in brackets.*

3.4.4 γδ T cell density by TNM stage

The primary tumour data consists of tumours at various stages of disease progression, stratified using the TNM staging system, which have variable tumour microenvironments and clinical outcomes. Thus, to understand whether data for the primary tumour is representative of all cases or stage-dependent, γδ T cell density was investigated across the four TNM stages. To conduct this analysis the standard exclusions were altered to include stage I and stage IV patients. In the adjacent normal stroma, there was no difference in γδ T cell density between stage II-III patients, although this result was statistically significant (p = 0.049) (Figure 3.28A). In the primary tumour stroma, there was no difference in γδ T cell density between stage II-III patients (p = 0.840) (Figure 3.28A). In the adjacent normal epithelium, there was no difference in γδ T cell density between stage II-III patients (p = 0.079) (Figure 3.28A). In the primary tumour epithelium, there was no difference in γδ T cell density between stage II-III patients (p = 0.657) (Figure 3.28A). In the adjacent normal tissue, there was no difference in γδ T cell density between stage II-III patients (p = 0.054) (Figure 3.28A). In the primary tumour tissue, there was no difference in γδ T cell density between stage II-III patients (p = 0.910) (Figure 3.28A). There was no difference in variance in γδ T cell density between stage II and stage III patients (Figure 3.28B).

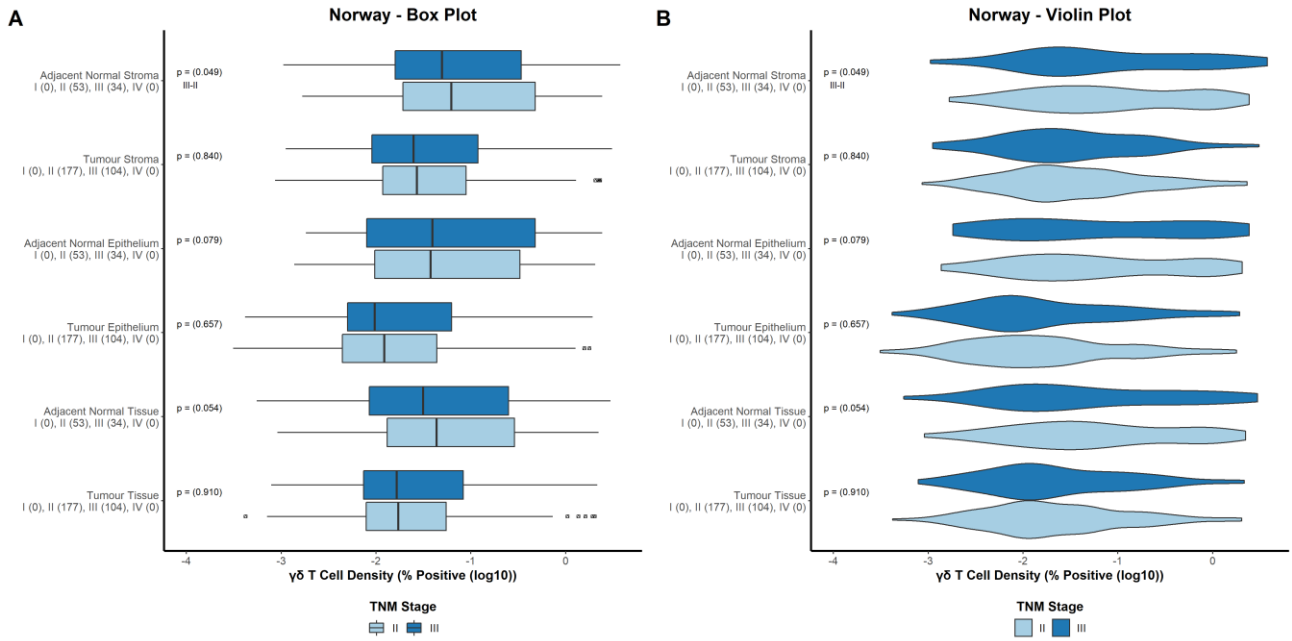

Figure 3.28 - Norway Cohort. Assessment of γδ T cell density across TNM stages. *Box plot presentation of γδ T cell density in stage I (light blue), stage II (dark blue), stage III (light green) and stage IV (dark green) patients. The box is representative of the interquartile range (middle 50% of data points), the vertical line denotes the median and the minimum and maximum are denoted by whiskers. Outliers are represented by an open triangle within an open square (A). Violin plot presentation of γδ T cell density in stage I (light blue), stage II (dark blue), stage III (light green) and stage IV (dark green) patients. The shape of the data reflects the distribution of the data points, which is not discernible in box plots. Outliers are represented by an open triangle within an open square (B). Y axis labels state the tissue compartment (primary tumour or adjacent normal tissue and epithelium, stroma or whole tissue) and below, the test groups with number of cases in brackets. X axis is log10 of the % of total cells within a region positive for the marker of interest. Inline labels denote the lowest standard statistical significance threshold reached (non-significant not shown) using a one-way ANOVA, <0.05 (*), <0.01 (**) or <0.001 (***), with statistically significant (<0.05) group comparisons noted below as determined by Tukey's post-hoc test.*

3.4.5 γδ T cell density by age

Incidence of CRC increases with aged populations, although cases in younger populations are increasing, and so the density of γδ T cells was investigated in patients aged < 65 years of age or ≥ 65 years of age [255]. In the adjacent normal stroma, patients < 65 years of age had a γδ T cell density no greater than than those ≥65 years of age (p = 0.316) (Figure 3.29A). In the primary tumour stroma, there was no difference in γδ T cell density between patients < 65 years of age and those ≥65 years of age (p = 0.618) (Figure 3.29A). In the adjacent normal epithelium, patients < 65 years of age had a mildly greater γδ T cell density than those ≥65 years of age (p = 0.333) (Figure 3.29A). In the primary tumour epithelium, there was no difference in γδ T cell density between patients < 65 years of age and those ≥65 years of age (p = 0.432) (Figure 3.29A). In the adjacent normal tissue, patients < 65 years of age had a mildly greater γδ T cell density than those ≥65 years of age (p = 0.314) (Figure 3.29A). In the primary tumour tissue, there was no difference in γδ T cell density between patients < 65 years of age and those ≥65 years of age (p = 0.547) (Figure 3.29A). The primary tumour compartments had a mildly greater variance in γδ T cell density than adjacent normal tissue compartments.

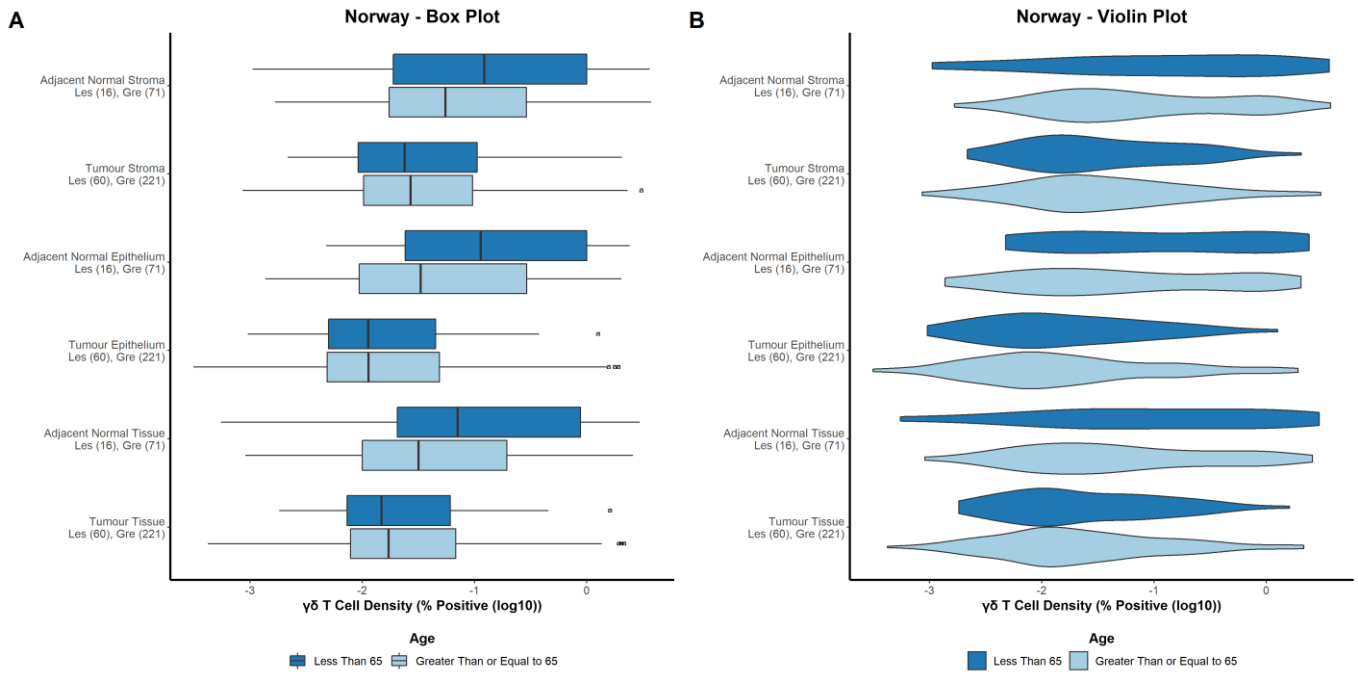

Figure 3.29 – Norway cohort. Assessment of γδ T cell density in patients aged <65 or ≥65. *Box plot presentation of γδ T cell density in patients aged <65 (dark blue) or ≥65 (light blue). The box is representative of the interquartile range (middle 50% of data points), the vertical line denotes the median and the minimum and maximum are denoted by whiskers. Outliers are represented by an open triangle within an open square (A). Violin plot presentation of γδ T cell density in patients aged <65 (dark blue) or ≥65 (light blue). The shape of the data reflects the distribution of the data points, which is not discernible in box plots. Outliers are represented by an open triangle within an open square (B). Y axis labels state the tissue compartment (primary tumour or adjacent normal tissue and epithelium, stroma or whole tissue) and below, the test groups with number of cases in brackets. X axis is log10 of the % of total cells within a region positive for the marker of interest. Inline labels denote the lowest standard statistical significance threshold reached (non-significant not shown) using a Welch two sample t-test, <0.05 (*), <0.01 (**) or <0.001 (***), with test groups in brackets.*

3.4.6 γδ T cell density by sex

Sex is a prominent factor in CRC incidence, with males having a greater incidence rate than females [256, 257], thus, the difference in γδ T cell density between male and female patients was investigated. In the adjacent normal stroma, there was a slightly greater density of γδ T cells in male patients compared to female patients (p = 0.191) (Figure 3.30A). In the primary tumour stroma, there was no difference in the density of γδ T cells in male patients compared to female patients (p = 0.593) (Figure 3.30A). In the adjacent normal epithelium, there was no difference in the density of γδ T cells in male patients compared to female patients (p = 0.319) (Figure 3.30A). In the primary tumour epithelium, there was no difference in the density of γδ T cells in male patients compared to female patients (p = 0.658) (Figure 3.30A). In the adjacent normal tissue, there was a slightly greater density of γδ T cells in male patients compared to female patients, although this was not statistically significant (p = 0.235) (Figure 3.30A). In the primary tumour tissue, there was no difference in the density of γδ T cells in male patients compared to female patients (p = 0.667) (Figure 3.30A). Compartments in the primary tumour had a slightly greater variance in the density of γδ T cells compared to compartments in the adjacent normal tissue (Figure 3.30B).

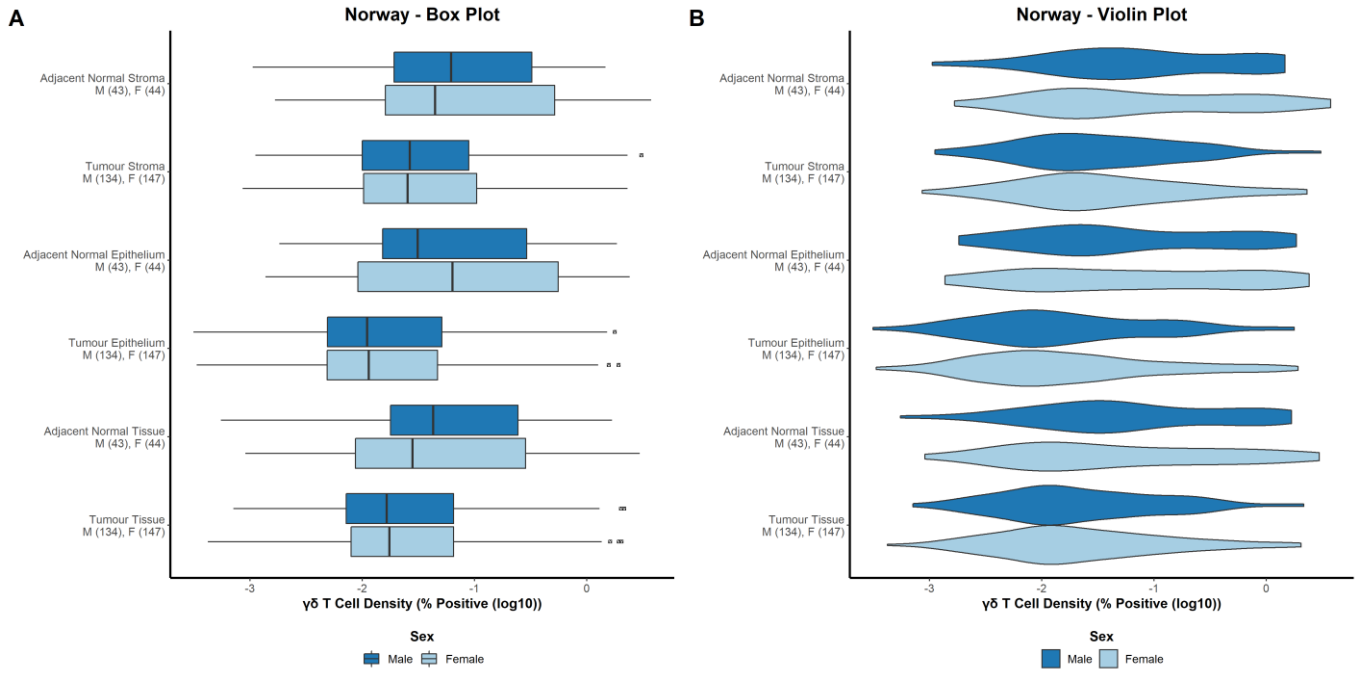

Figure 3.30 – Norway cohort. Assessment of γδ T cell density in male and female patients. *Box plot presentation of γδ T cell density in male patients (dark blue) or female patients (light blue). The box is representative of the interquartile range (middle 50% of data points), the vertical line denotes the median and the minimum and maximum are denoted by whiskers. Outliers are represented by an open triangle within an open square (A). Violin plot presentation of γδ T cell density in male patients (dark blue) or female patients (light blue). The shape of the data reflects the distribution of the data points, which is not discernible in box plots. Outliers are represented by an open triangle within an open square (B). Y axis labels state the tissue compartment (primary tumour or adjacent normal tissue and epithelium, stroma or whole tissue) and below, the test groups with number of cases in brackets. X axis is log10 of the % of total cells within a region positive for the marker of interest. Inline labels denote the lowest standard statistical significance threshold reached (non-significant not shown) using a Welch two sample t-test, <0.05 (*), <0.01 (**) or <0.001 (***), with test groups in brackets.*

3.4.7 γδ T cell density by site

There are molecular, histological, and prognostic differences associated with CRC tumours located in the proximal side of the splenic flexure (right-sided), distal side of the splenic flexure (left-sided) and the rectum. Thus, the density of γδ T cells was investigated in the context of these tumour sites. In the adjacent normal stroma, there was no difference in the density of γδ T cells in the right-sided cases compared to the left-sided (p = 0.687) (Figure 3.31A). In the primary tumour stroma, there was no difference in the density of γδ T cells in the right-sided and left-sided (p = 0.453) cases (Figure 3.31A). In the adjacent normal epithelium, there was no difference in the density of γδ T cells in the right-sided cases compared to the left-sided cases (p = 0.428) (Figure 3.31A). In the primary tumour epithelium, there was no difference in the density of γδ T cells in the right-sided and left-sided cases (p = 0.866) (Figure 3.31A). In the adjacent normal tissue, there was no difference in the density of γδ T cells in the right-sided cases compared to the left-sided cases (p = 0.560) (Figure 3.31A). In the primary tumour tissue, there was no difference in the density of γδ T cells in the right-sided and left-sided cases (p = 0.594) (Figure 3.31A). There was no difference in the variance of γδ T cell density between tissue compartments (Figure 3.31B).

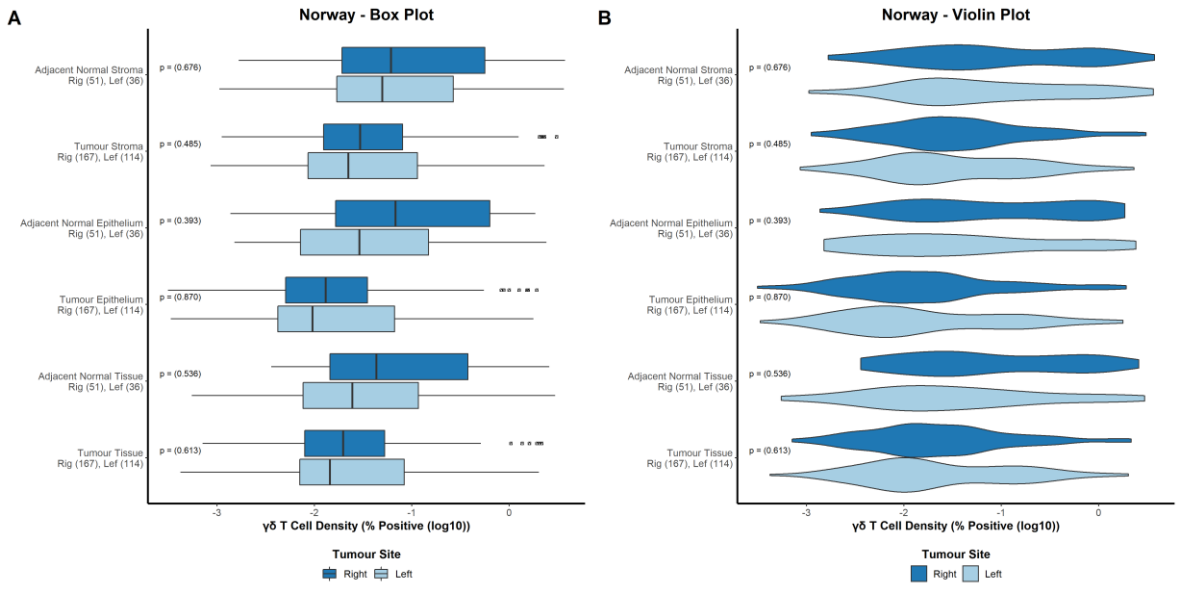

Figure 3.31 – Norway cohort. Assessment of γδ T cell density in tumour sites. *Box plot presentation of γδ T cell density in right-sided (dark blue) and left-sided (light blue)). The box is representative of the interquartile range (middle 50% of data points), the vertical line denotes the median and the minimum and maximum are denoted by whiskers. Outliers are represented by an open triangle within an open square (A). Violin plot presentation of γδ T cell density in right-sided (dark blue) and left-sided (light blue)). The shape of the data reflects the distribution of the data points, which is not discernible in box plots. Outliers are represented by an open triangle within an open square (B). Y axis labels state the tissue compartment (primary tumour or adjacent normal tissue and epithelium, stroma or whole tissue) and below, the test groups with number of cases in brackets. X axis is log10 of the % of total cells within a region positive for the marker of interest. Inline labels denote the lowest standard statistical significance threshold reached (non-significant not shown) using a one-way ANOVA, <0.05 (*), <0.01 (**) or <0.001 (***), with statistically significant (<0.05) group comparisons noted below as determined by Tukey's post-hoc test.*

3.4.8 CD8 T cell density by tissue region

To understand whether lymphocyte density is altered in diseased tissue compared to the normal tissue environment, the density of CD8 T cells was investigated in the primary tumour and the adjacent normal tissue. To prevent any bias created by cases with exceptionally low or high lymphocyte density having only primary tumour tissue or only adjacent normal tissue available, standard exclusions were expanded to restrict cases to those with data available for both the primary tumour and the adjacent normal tissue. In the whole tissue, there was no difference in CD8 T cell density between the adjacent normal tissue and the primary tumour (p = 0.235) (Figure 3.32A). In the stroma, there was no difference in CD8 T cell density between the adjacent normal tissue and the primary tumour (p = 0.010) (Figure 3.32A). In the epithelium, there was no difference in CD8 T cell density between the adjacent normal tissue and the primary tumour (p = 0.132) (Figure 3.32A). There was no difference in the variance of CD8 T cell density between the primary tumour and adjacent normal tissue compartments (Figure 3.32B).

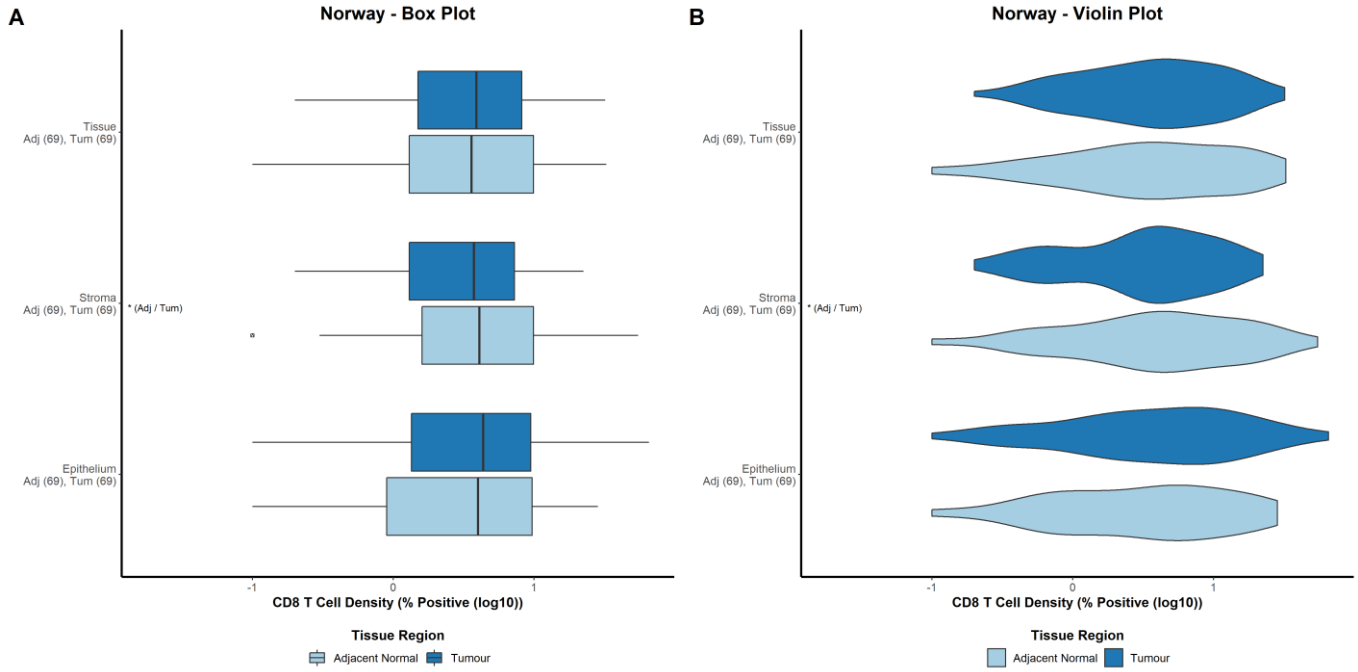

Figure 3.32 – Norway cohort. Assessment of CD8 T cell density in the primary tumour and adjacent normal tissue. *Box plot presentation of CD8 T cell density in the primary tumour (dark blue) and adjacent normal tissue (light blue). The box is representative of the interquartile range (middle 50% of data points), the vertical line denotes the median and the minimum and maximum are denoted by whiskers. Outliers are represented by an open triangle within an open square (A). Violin plot presentation of CD8 T cell density in the primary tumour (dark blue) and adjacent normal tissue (light blue). The shape of the data reflects the distribution of the data points, which is not discernible in box plots (B). Y axis labels state the tissue compartment (epithelium, stroma and whole tissue) and below, the test groups with number of cases in brackets. X axis is log10 of the % of total cells within a region positive for the marker of interest. Inline labels denote the lowest standard statistical significance threshold reached (non-significant not shown) using a paired t-test, <0.05 (*), <0.01 (**) or <0.001 (***), with test groups in brackets.*

3.4.9 CD8 T cell density by tissue compartment

Lymphocyte localisation is vital to function [254]; thus, lymphocytes were scored for the whole tissue (primary tumour or adjacent normal) and for the epithelium and stroma separately and these latter regions compared. In the primary tumour, there was no difference in the density of CD8 T cells between the stroma and epithelium, and this result was statistically significant (p = <0.0016) (Figure 3.33A). In the adjacent normal tissue, there was no difference in the density of CD8 T cells between the stroma and epithelium (p = 0.333) (Figure 3.33A). There was no difference in the variance of CD8 T cell density between compartments in the primary tumour and adjacent normal tissue (Figure 3.33B).

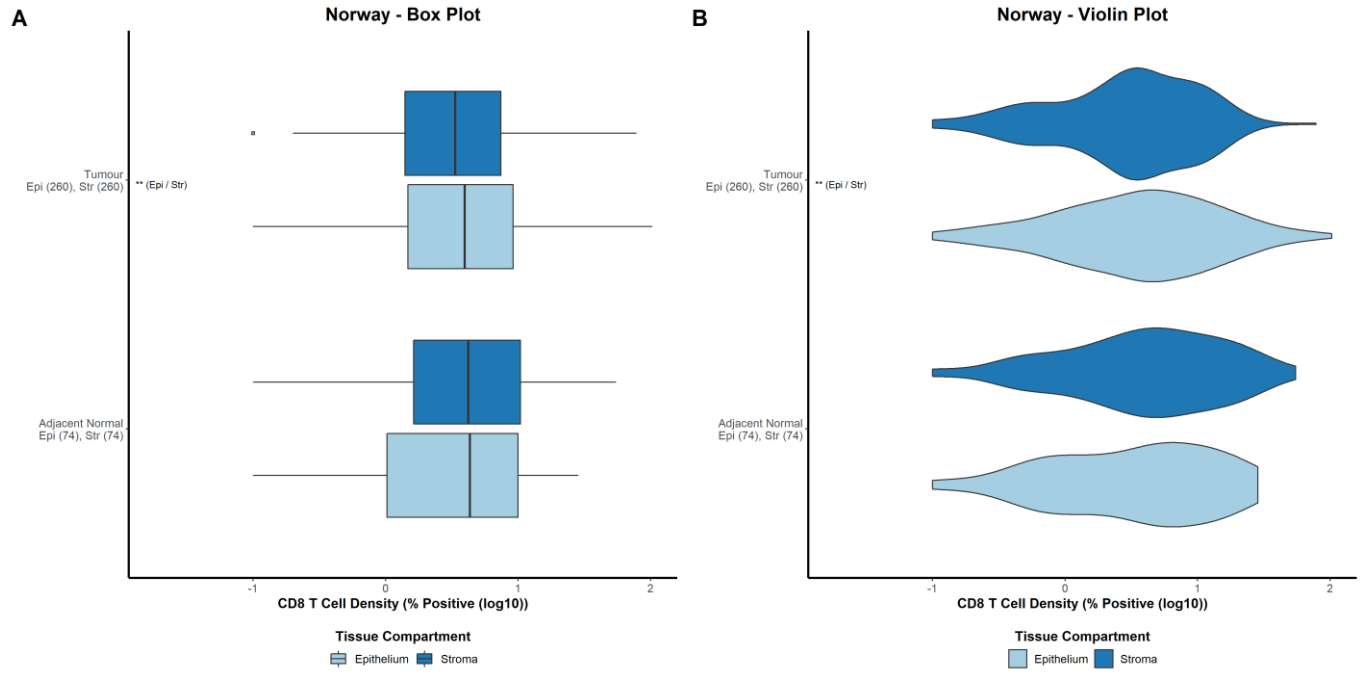

Figure 3.33 – Norway cohort. Assessment of CD8 T cell density in the stroma and epithelium. *Box plot presentation of CD8 T cell density in the stroma (dark blue) and epithelium (light blue). The box is representative of the interquartile range (middle 50% of data points), the vertical line denotes the median and the minimum and maximum are denoted by whiskers. Outliers are represented by an open triangle within an open square (A). Violin plot presentation of CD8 T cell density in the stroma (dark blue) and epithelium (light blue). The shape of the data reflects the distribution of the data points, which is not discernible in box plots (B). Y axis labels state the tissue compartment (primary tumour and adjacent normal tissue) and below, the test groups with number of cases in brackets. X axis is log10 of the % of total cells within a region positive for the marker of interest. Inline labels denote the lowest standard statistical significance threshold reached (non-significant not shown) using a Welch two sample t-test, <0.05 (*), <0.01 (**) or <0.001 (***), with test groups in brackets.*

3.4.10 CD8 T cell density by TNM stage

The primary tumour data consists of tumours at various stages of disease progression, stratified using the TNM staging system, which have variable tumour microenvironments and clinical outcomes. Thus, to understand whether data for the primary tumour is representative of all cases or stage dependent, CD8 T cell density was investigated across the four TNM stages. To conduct this analysis the standard exclusions were altered to include stage I and stage IV patients, although no stage IV patients had CD8 data available. In the adjacent normal stroma, there was no difference in CD8 T cell density between stage II-III patients (p = 0.761) (Figure 3.34A). In the primary tumour stroma, there was no difference in CD8 T cell density between stage II-III patients (p = 0.134) (Figure 3.34A). In the adjacent normal epithelium, there was no difference in CD8 T cell density between stage II-III patients (p = 0.523) (Figure 3.34A). In the primary tumour epithelium, there was no difference in CD8 T cell density between stage II-III patients (p = 0.085) (Figure 3.34A). In the adjacent normal tissue, there was no difference in CD8 T cell density between stage II-III patients (p = 0.641) (Figure 3.34A). In the primary tumour tissue, there was no difference in CD8 T cell density between stage II-III patients (p = 0.102) (Figure 3.34A). There was no difference in variance in CD8 T cell density in adjacent normal tissue compartments compared to the primary tumour compartments (Figure 3.34B).

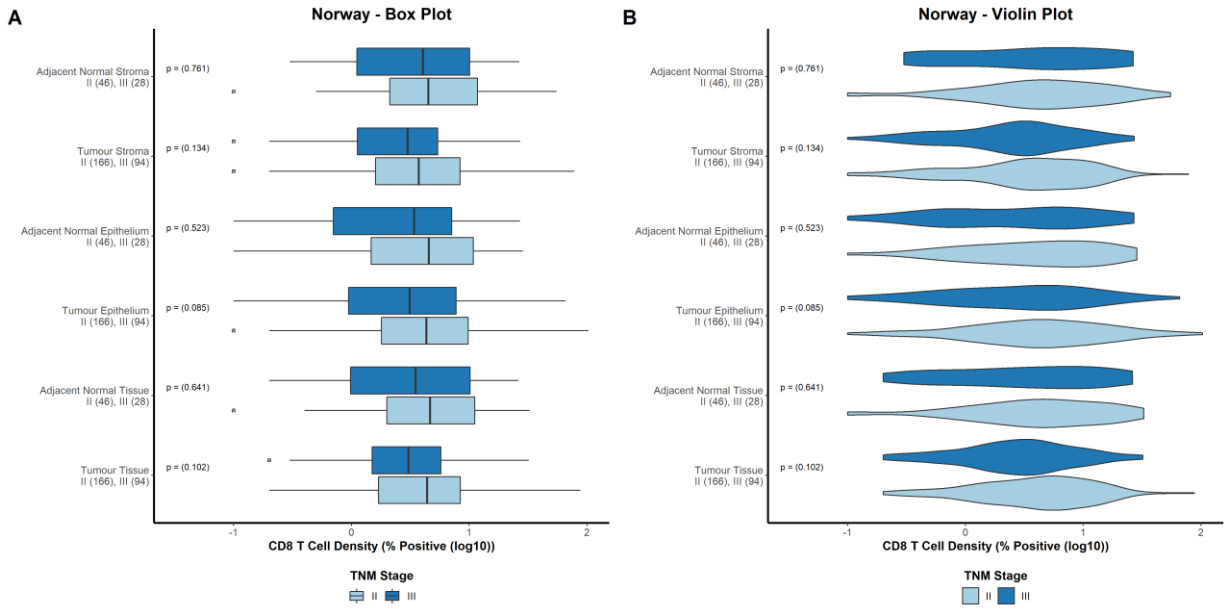

Figure 3.34 – Norway cohort. Assessment of CD8 T cell density across TNM stages. *Box plot presentation of CD8 T cell density in stage I (light blue), stage II (dark blue), stage III (light green) and stage IV (dark green) patients. The box is representative of the interquartile range (middle 50% of data points), the vertical line denotes the median and the minimum and maximum are denoted by whiskers. Outliers are represented by an open triangle within an open square (A). Violin plot presentation of CD8 T cell density in stage I (light blue), stage II (dark blue), stage III (light green) and stage IV (dark green) patients. The shape of the data reflects the distribution of the data points, which is not discernible in box plots (B). Y axis labels state the tissue compartment (primary tumour or adjacent normal tissue and epithelium, stroma or whole tissue) and below, the test groups with number of cases in brackets. X axis is log10 of the % of total cells within a region positive for the marker of interest. Inline labels denote the lowest standard statistical significance threshold reached (non-significant not shown) using a one-way ANOVA, <0.05 (*), <0.01 (**) or <0.001 (***), with statistically significant (<0.05) group comparisons noted below as determined by Tukey's post-hoc test.*

3.4.11 CD8 T cell density by age

Incidence of CRC increases with aged populations, although cases in younger populations are increasing, and so the density of CD8 T cells was investigated in patients aged < 65 years of age or ≥ 65 years of age [255]. In the adjacent normal stroma, there was a slight difference in CD8 T cell density in patients < 65 years of age compared to those ≥65 years of age (p = 0.869) (Figure 3.35A). In the primary tumour stroma, there was no difference in CD8 T cell density between patients < 65 years of age and those ≥65 years of age (p = 0.883) (Figure 3.35A). In the adjacent normal epithelium, there was no difference in CD8 T cell density between patients < 65 years of age and those ≥65 years of age (p = 0.874) (Figure 3.35A). In the primary tumour epithelium, there was no difference in CD8 T cell density in patients < 65 years of age compared to those ≥65 years of age (p = 0.144) (Figure 3.35A). In the adjacent normal tissue, there is a slightly greater CD8 T cell density in patients < 65 years of age compared to those ≥65 years of age (p = 0.968) (Figure 3.35A). In the primary tumour tissue, there was no difference in CD8 T cell density between patients < 65 years of age and those ≥65 years of age (p = 0.418) (Figure 3.35A). There was no difference in variance in CD8 T cell density between the adjacent normal and primary tumour tissue compartments (Figure 3.35B).

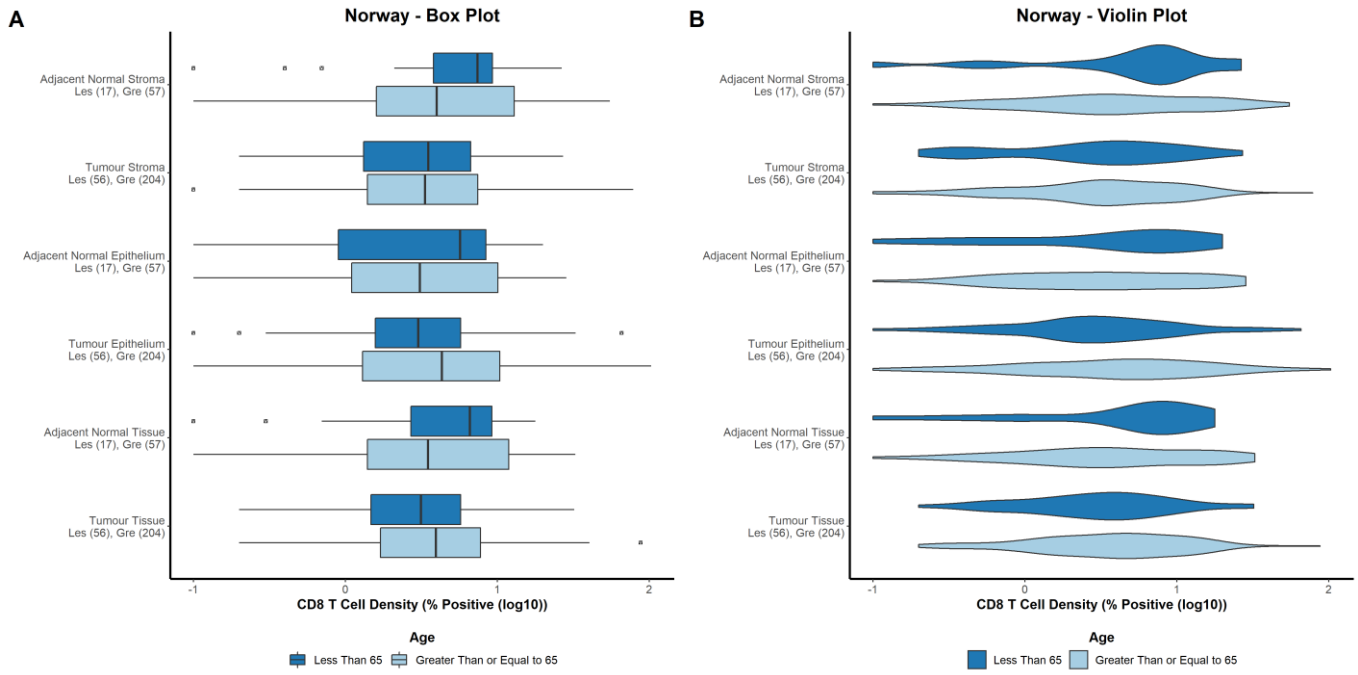

Figure 3.35 – Norway cohort. Assessment of CD8 T cell density in patients aged <65 or ≥65. *Box plot presentation of CD8 T cell density in patients aged <65 (dark blue) or ≥65 (light blue). The box is representative of the interquartile range (middle 50% of data points), the vertical line denotes the median and the minimum and maximum are denoted by whiskers. Outliers are represented by an open triangle within an open square (A). Violin plot presentation of CD8 T cell density in patients aged <65 (dark blue) or ≥65 (light blue). The shape of the data reflects the distribution of the data points, which is not discernible in box plots. Outliers are represented by an open triangle within an open square (B). Y axis labels state the tissue compartment (primary tumour or adjacent normal tissue and epithelium, stroma or whole tissue) and below, the test groups with number of cases in brackets. X axis is log10 of the % of total cells within a region positive for the marker of interest. Inline labels denote the lowest standard statistical significance threshold reached (non-significant not shown) using a Welch two sample t-test, <0.05 (*), <0.01 (**) or <0.001 (***), with test groups in brackets.*

3.4.12 CD8 T cell density by sex

Sex is a prominent factor in CRC incidence, with males having a greater incidence rate than females [256, 257], thus, the difference in CD8 T cell density between male and female patients was investigated. In the adjacent normal stroma, there was no difference in the density of CD8 T cells in male patients compared to female patients (p = 0.263) (Figure 3.36A). In the primary tumour stroma, there was no difference in the density of CD8 T cells in male patients compared to female patients (p = 0.863) (Figure 3.36A). In the adjacent normal epithelium, there was no difference in the density of CD8 T cells in male patients compared to female patients (p = 0.462) (Figure 3.36A). In the primary tumour epithelium, there was no difference in the density of CD8 T cells in male patients compared to female patients (p = 0.465) (Figure 3.36A). In the adjacent normal tissue, there was no difference in the density of CD8 T cells in male patients compared to female patients (p = 0.283) (Figure 3.36A). In the primary tumour tissue, there was no difference in the density of CD8 T cells in male patients compared to female patients (p = 0.862) (Figure 3.36A). There was no difference in variance in the density of CD8 T cells between compartments (Figure 3.36B).

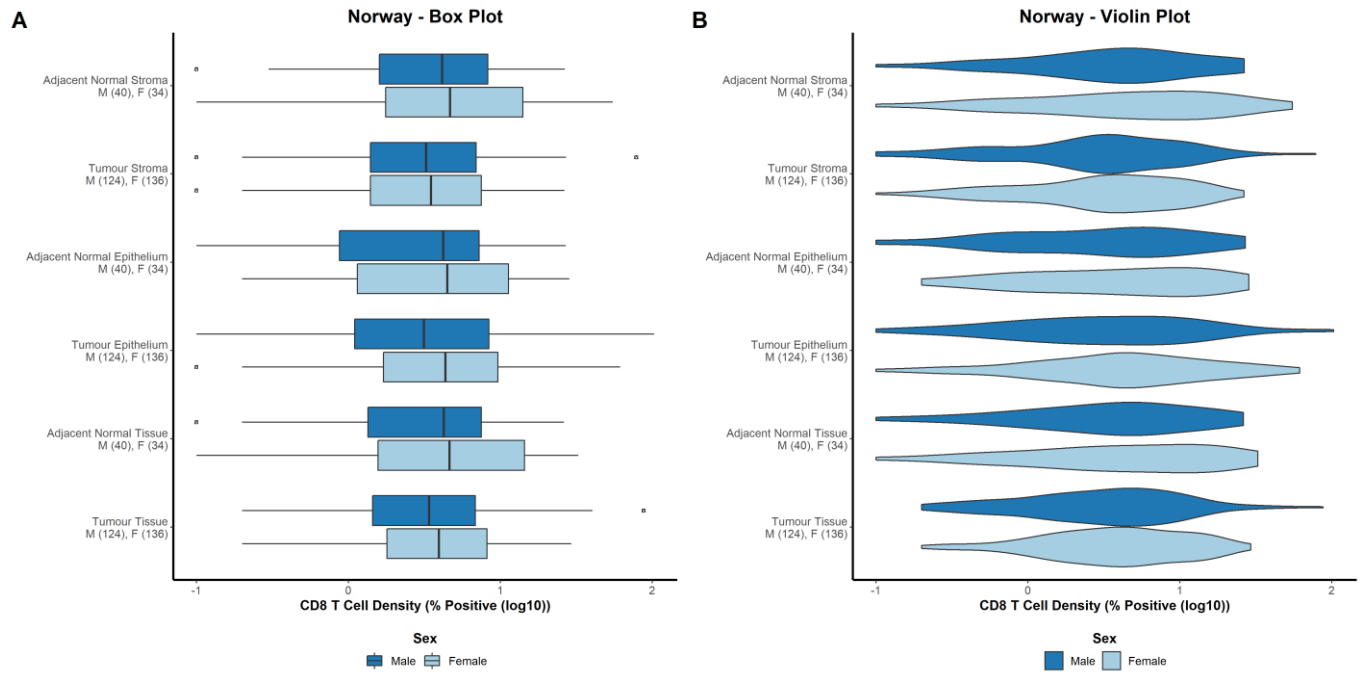

Figure 3.36 – Norway cohort. Assessment of CD8 T cell density in male and female patients. *Box plot presentation of CD8 T cell density in male patients (dark blue) or female patients (light blue). The box is representative of the interquartile range (middle 50% of data points), the vertical line denotes the median and the minimum and maximum are denoted by whiskers. Outliers are represented by an open triangle within an open square (A). Violin plot presentation of CD8 T cell density in male patients (dark blue) or female patients (light blue). The shape of the data reflects the distribution of the data points, which is not discernible in box plots. Outliers are represented by an open triangle within an open square (B). Y axis labels state the tissue compartment (primary tumour or adjacent normal tissue and epithelium, stroma or whole tissue) and below, the test groups with number of cases in brackets. X axis is log10 of the % of total cells within a region positive for the marker of interest. Inline labels denote the lowest standard statistical significance threshold reached (non-significant not shown) using a Welch two sample t-test, <0.05 (*), <0.01 (**) or <0.001 (***), with test groups in brackets.*

3.4.13 CD8 T cell density by site

There are molecular, histological, and prognostic differences associated with CRC tumours located in the proximal side of the splenic flexure (right-sided), distal side of the splenic flexure (left-sided) and the rectum. Thus, the density of CD8 T cells was investigated in the context of these tumour sites. In the adjacent normal stroma, there was a greater density of CD8 T cells in the right-sided cases compared to the left-sided (p = 0.0095) (Figure 3.37A). In the primary tumour stroma, there was no difference in the density of CD8 T cells between the right-sided and left-sided cases (p = 0.103) (Figure 3.37A). In the adjacent normal epithelium, there was a greater density of CD8 T cells in the right-sided cases compared to the left-sided (p = 0.0093) (Figure 3.37A). In the primary tumour epithelium, there was a slightly greater density of CD8 T cells in the right-sided compared to left-sided cases (p = 0.198) (Figure 3.37A). In the adjacent normal tissue, there was a greater density of CD8 T cells in the right-sided cases compared to the left-sided (p = 0.0033) (Figure 3.37A). In the primary tumour tissue, there was a slightly greater density of CD8 T cells in the right-sided compared to left-sided cases, although this result was not statistically significant (p = 0.098) (Figure 3.37A). There was no difference in the variance of CD8 T cell density between tissue compartments (Figure 3.37B).

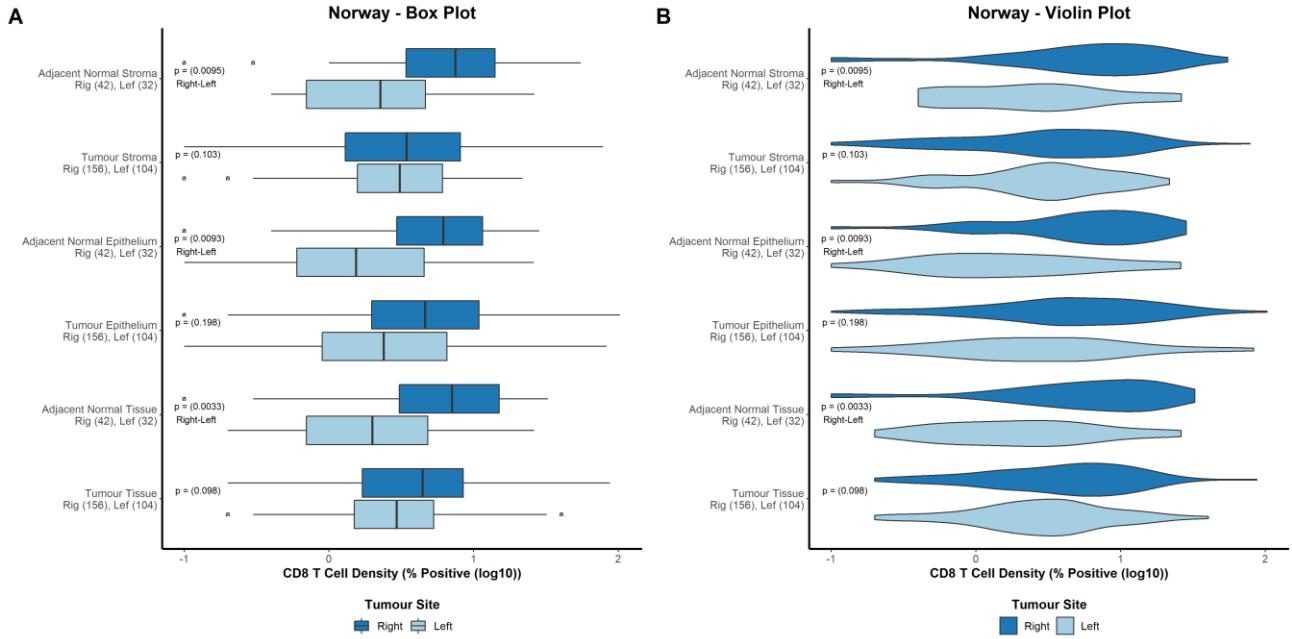

Figure 3.37 – Norway cohort. Assessment of CD8 T cell density in tumour sites. *Box plot presentation of CD8 T cell density in right-sided (dark blue) and left-sided (light blue)). The box is representative of the interquartile range (middle 50% of data points), the vertical line denotes the median and the minimum and maximum are denoted by whiskers. Outliers are represented by an open triangle within an open square (A). Violin plot presentation of CD8 T cell density in right-sided (dark blue) and left-sided (light blue)). The shape of the data reflects the distribution of the data points, which is not discernible in box plots. Outliers are represented by an open triangle within an open square (B). Y axis labels state the tissue compartment (primary tumour or adjacent normal tissue and epithelium, stroma or whole tissue) and below, the test groups with number of cases in brackets. X axis is log10 of the % of total cells within a region positive for the marker of interest. Inline labels denote the lowest standard statistical significance threshold reached (non-significant not shown) using a one-way ANOVA, <0.05 (*), <0.01 (**) or <0.001 (***), with statistically significant (<0.05) group comparisons noted below as determined by Tukey's post-hoc test.*

3.4.14 Comparison of γδ and CD8 T cell density

Compared to the expected density of CD8 T cells in tissue, the expected density of γδ T cells is hypothesised to be much less. In addition, the functional role of these lymphocyte populations is different and their comparative roles not clear [155]. Thus, the comparative density of γδ and CD8 T cells was investigated. In the adjacent normal stroma, CD8 T cells were present at a vastly greater density than γδ T cells (p = <0.001) (Figure 3.38A). In the primary tumour stroma, CD8 T cells were present at a vastly greater density than γδ T cells (p = <0.001) (Figure 3.38A). In the adjacent normal epithelium, CD8 T cells were present at a vastly greater density than γδ T cells (p = <0.001) (Figure 3.38A). In the primary tumour epithelium, CD8 T cells were present at a vastly greater density than γδ T cells (p = <0.001) (Figure 3.38A). In the adjacent normal tissue, CD8 T cells were present at a vastly greater density than γδ T cells (p = <0.001) (Figure 3.38A). In the primary tumour tissue, CD8 T cells were present at a vastly greater density than γδ T cells (p = <0.001) (Figure 3.38A). There was no difference in variance of lymphocyte density between groups (Figure 3.38B).

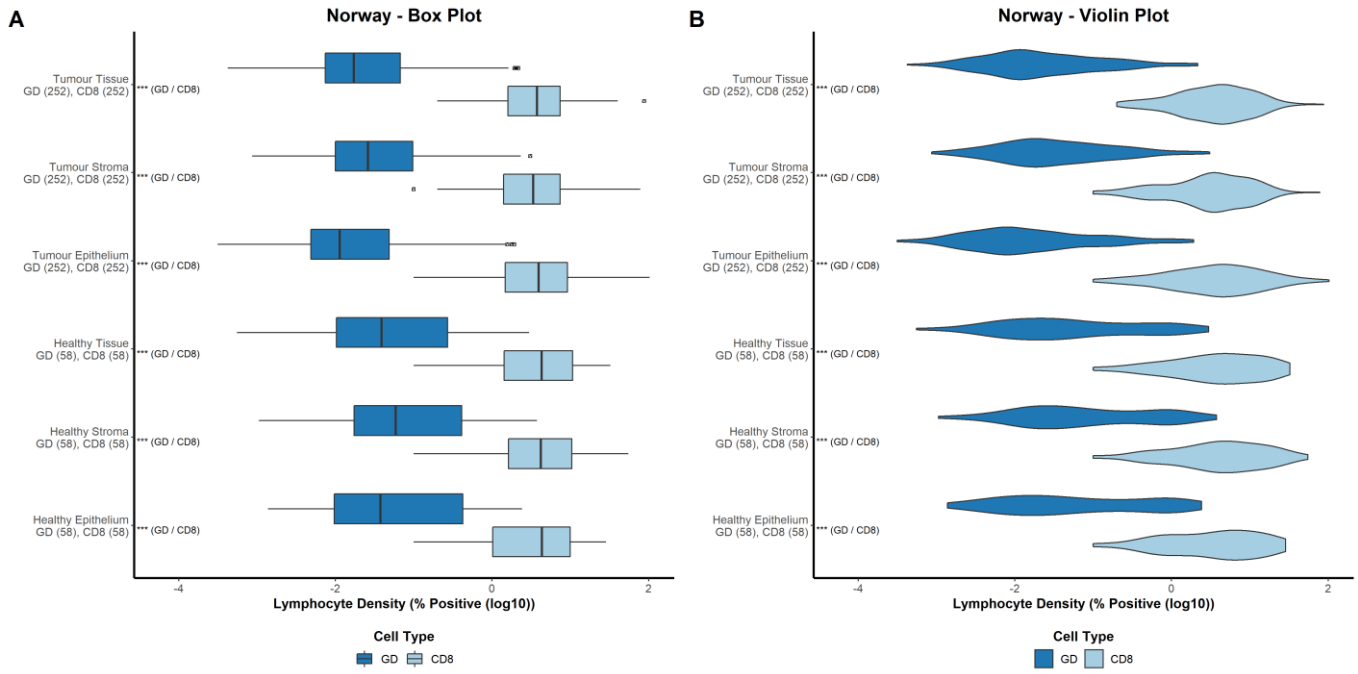

Figure 3.38 – Norway cohort. Assessment of comparative γδ and CD8 T cell density. *Box plot presentation of γδ T cell density (dark blue) and CD8 T cell density (light blue). The box is representative of the interquartile range (middle 50% of data points), the vertical line denotes the median and the minimum and maximum are denoted by whiskers. Outliers are represented by an open triangle within an open square (A). Violin plot presentation of γδ T cell density (dark blue) and CD8 T cell density (light blue). The shape of the data reflects the distribution of the data points, which is not discernible in box plots. Outliers are represented by an open triangle within an open square (B). Y axis labels state the tissue compartment (primary tumour or adjacent normal tissue and epithelium, stroma or whole tissue) and below, the test groups with number of cases in brackets. X axis is log10 of the % of total cells within a region positive for the marker of interest. Inline labels denote the lowest standard statistical significance threshold reached (non-significant not shown) using a paired t-test, <0.05 (*), <0.01 (**) or <0.001 (***), with test groups in brackets.*

3.5 Thailand Cohort

3.5.1 Clinicopathological characteristics of patient cohort

320 patients from the Thailand cohort were included in a sub-cohort for analysis. Patient cohort characteristics of the full cohort and sub-cohort are outlined in Table 3.3. The sub-cohort was comparable to the full cohort. Patient sex was skewed slightly towards males (56%) compared to females (44%). Patient age was roughly equal with 52% aged <65 and 48% aged ≥ 65. Patients were primarily T stage III (64%), evenly split across N stages 0/I/II (33%, 39%, 28%), M stage 0 (66%, 34.4% missing) and split across TNM stages II/III/IV (23%/43%/26%). Tumours were predominantly moderately/well differentiated (94%). Patients were slightly skewed towards not having vascular invasion (58%) compared to (40%). Patients had a close balance of tumour stroma percentage low (49%) and high (50%). Patients were mostly graded as Klintrup-Mäkinen weak (81%). Median follow-up (alive cases, n = 76) in the sub-cohort was 68 months. There was a total of 210 deaths in the sub-cohort. Patients were excluded if they had died within 30 days of surgery (n = 5) or had stage IV disease (n = 83) (Figure 3.39).

Table 3.3 - Clinicopathological characteristics of patients in the Thailand cohort. *Table showing the number (and %) of patients exhibiting clinical features and comparison between the full cohort and the sub-cohort included for analyses.*

Patient Characteristics - Thailand Cohort			
	Full cohort (N=411)	Sub-cohort (N=320)	P-Value
Sex			
Female	178 (43 %)	140 (44 %)	0.905
Male	233 (57 %)	180 (56 %)	
Age			
<65	216 (53 %)	165 (52 %)	0.79
≥65	195 (47 %)	155 (48 %)	
T Stage			
I	12 (3 %)	5 (2 %)	0.608
II	54 (13 %)	38 (12 %)	
III	253 (62 %)	205 (64 %)	
IV	91 (22 %)	71 (22 %)	
Missing	1 (0.2%)	1 (0.3%)	
N Stage			
0	151 (37 %)	107 (33 %)	0.563
I	145 (35 %)	124 (39 %)	
II	114 (28 %)	88 (28 %)	
Missing	1 (0.2%)	1 (0.3%)	
M Stage			
0	266 (65 %)	210 (66 %)	0.0103
Missing	145 (35.3%)	110 (34.4%)	
TNM Stage			
II	86 (21 %)	73 (23 %)	0.0659
III	126 (31 %)	138 (43 %)	
IV	117 (28 %)	83 (26 %)	
Missing	82 (20.0%)	26 (8.1%)	
Differentiation			
Moderate/Well	378 (92 %)	302 (94 %)	0.908
Poor	8 (2 %)	6 (2 %)	
Missing	25 (6.1%)	12 (3.8%)	
Vascular Invasion			
No	240 (58 %)	184 (58 %)	0.836
Yes	163 (40 %)	129 (40 %)	
Missing	8 (1.9%)	7 (2.2%)	
Tumour stroma percentage			
Low	200 (49 %)	157 (49 %)	0.979
High	203 (49 %)	160 (50 %)	
Missing	8 (1.9%)	3 (0.9%)	
Klintrup-Mäkinen Grade			
Strong	78 (19 %)	57 (18 %)	0.622
Weak	321 (78 %)	258 (81 %)	
Missing	12 (2.9%)	5 (1.6%)	

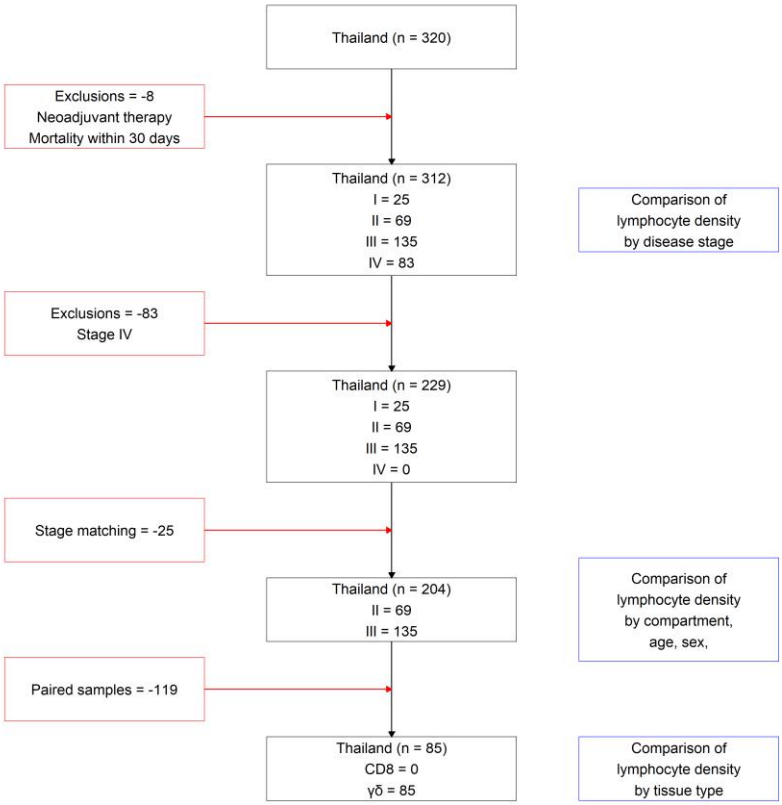

Figure 3.39 – Consort diagram for lymphocyte density analysis in the Thailand cohort. *Red boxes denote removal of cases. Blue boxes denote analyses that use cases present at that level of the consort diagram.*

3.5.2 γδ T cell density by tissue region

To understand whether lymphocyte density is altered in diseased tissue compared to the normal tissue environment, the density of γδ was investigated in the primary tumour and the adjacent normal tissue. To prevent any bias created by cases with exceptionally low or high lymphocyte density having only primary tumour tissue or only adjacent normal tissue available, standard exclusions were expanded to restrict cases to those with data available for both the primary tumour and the adjacent normal tissue. In the whole tissue, γδ T cells were present at a slightly greater density in the adjacent normal tissue than in the primary tumour (p = 0.0019) (Figure 3.40A). In the stroma, γδ T cells were present at a slightly greater density in the adjacent normal tissue than in the primary tumour (p = 0.055) (Figure 3.40A). In the epithelium, γδ T cells were present at a slightly greater density in the adjacent normal tissue than in the primary tumour (p = 0.0053) (Figure 3.40A). There was no difference in the variance of in γδ T cell density between groups (Figure 3.40B).

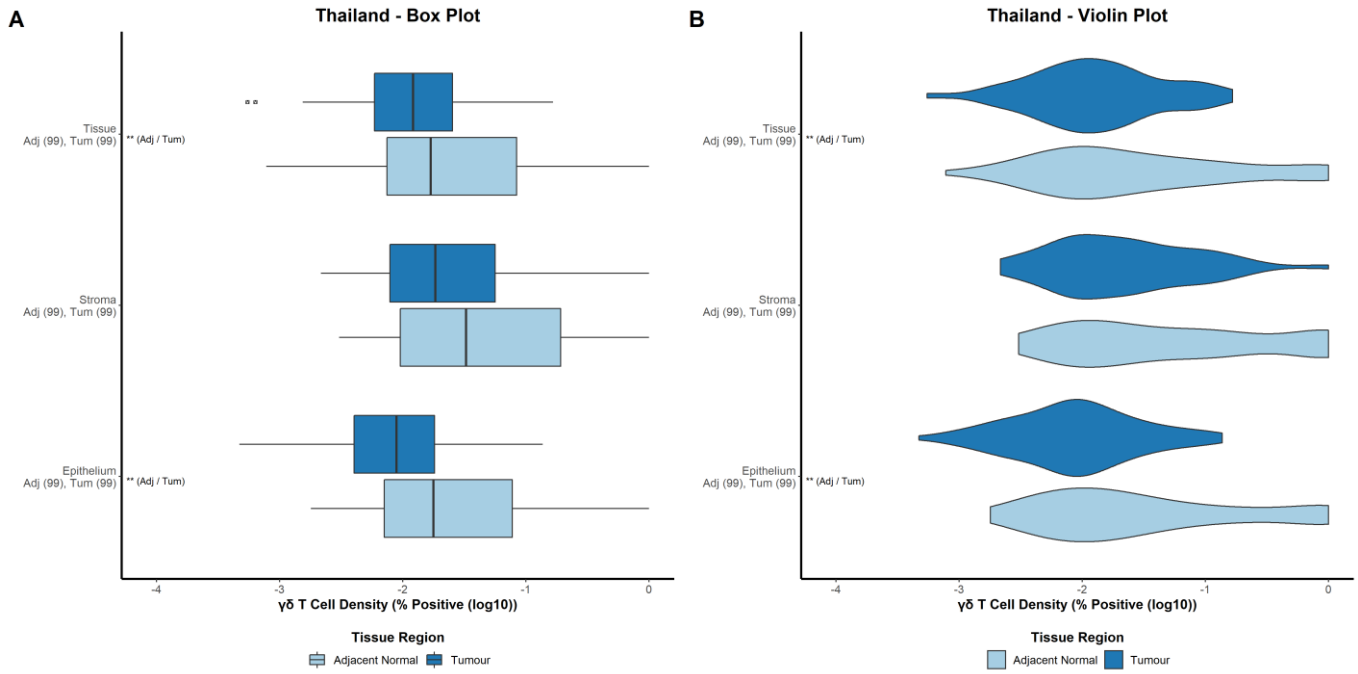

Figure 3.40 – Thailand cohort. Assessment of γδ T cell density in the primary tumour and adjacent normal tissue. *Box plot presentation of γδ T cell density in the primary tumour (dark blue) and adjacent normal tissue (light blue). The box is representative of the interquartile range (middle 50% of data points), the vertical line denotes the median and the minimum and maximum are denoted by whiskers. Outliers are represented by an open triangle within an open square (A). Violin plot presentation of γδ T cell density in the primary tumour (dark blue) and adjacent normal tissue (light blue). The shape of the data reflects the distribution of the data points, which is not discernible in box plots (B). Y axis labels state the tissue compartment (epithelium, stroma and whole tissue) and below, the test groups with number of cases in brackets. X axis is log10 of the % of total cells within a region positive for the marker of interest. Inline labels denote the lowest standard statistical significance threshold reached (non-significant not shown) using a paired t-test, <0.05 (*), <0.01 (**) or <0.001 (***), with test groups in brackets.*

3.5.3 γδ T cell density by tissue compartment

Lymphocyte localisation is vital to function [254], particularly γδ T cells which patrol the epithelium to maintain intestinal homeostasis [117]. Thus, lymphocytes were scored for the whole tissue (primary tumour or adjacent normal) and for the epithelium and stroma separately and these latter regions compared. In the primary tumour, γδ T cells were present at a greater density in the stroma than the epithelium (p = <0.001) (Figure 3.41A). In the adjacent normal tissue, there was no difference in the density of γδ T cells in the stroma and the epithelium (p = 0.281) (Figure 3.41A). γδ density showed greater variance in the adjacent normal tissue than in the primary tumour (Figure 3.41B).

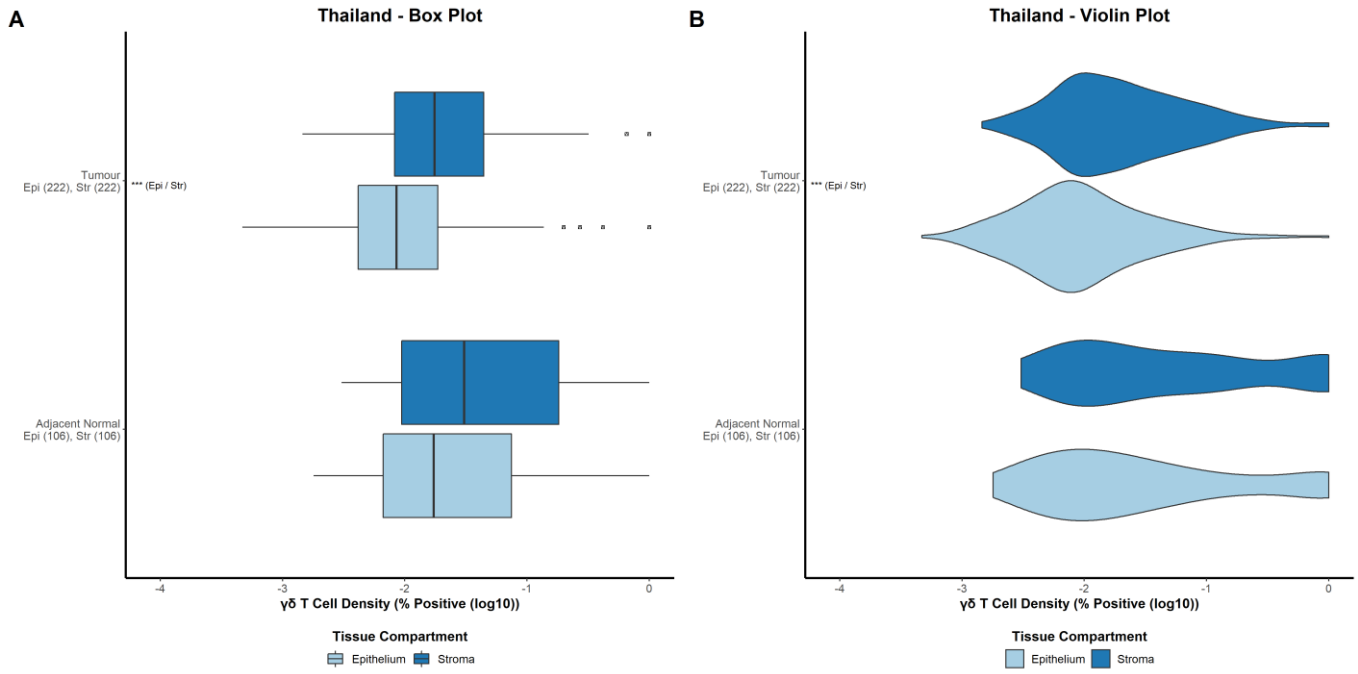

Figure 3.41 – Thailand cohort. Assessment of γδ T cell density in the stroma and epithelium. *Box plot presentation of γδ T cell density in the stroma (dark blue) and epithelium (light blue). The box is representative of the interquartile range (middle 50% of data points), the vertical line denotes the median and the minimum and maximum are denoted by whiskers. Outliers are represented by an open triangle within an open square (A). Violin plot presentation of γδ T cell density in the stroma (dark blue) and epithelium (light blue). The shape of the data reflects the distribution of the data points, which is not discernible in box plots (B). Y axis labels state the tissue compartment (primary tumour and adjacent normal tissue) and below, the test groups with number of cases in brackets. X axis is log10 of the % of total cells within a region positive for the marker of interest. Inline labels denote the lowest standard statistical significance threshold reached (non-significant not shown) using a Welch two sample t-test, <0.05 (*), <0.01 (**) or <0.001 (***), with test groups in brackets.*

3.5.4 γδ T cell density by TNM stage

The primary tumour data consists of tumours at various stages of disease progression, stratified using the TNM staging system, which have variable tumour microenvironments and clinical outcomes. Thus, to understand whether data for the primary tumour is representative of all cases or stage-dependent, γδ T cell density was investigated across the four TNM stages. To conduct this analysis the standard exclusions were altered to include stage I and stage IV patients. In the adjacent normal stroma, there was a difference in γδ T cell density between stage I-IV patients ($p = 0.0051$), with this difference being due to a lower density of γδ T cells between stage III and stage IV patients and to a lesser extent stage II and stage IV patients (Figure 3.42A). In the primary tumour stroma, there was a difference in γδ T cell density between stage I-IV patients ($p = 0.113$), with this difference being due to a lower density of γδ T cells between stage II and stage III patients and stage III and stage IV patients (Figure 3.42A). In the adjacent normal epithelium, there was a slight difference in γδ T cell density between stage I-IV patients ($p = 0.0034$), with this difference relating to stage IV patients compared to other stages (Figure 3.42A). In the primary tumour epithelium, there was a slight difference in γδ T cell density between stage I-IV patients ($p = 0.079$), with this difference relating to stage III patients compared to other stages, particularly stage IV (Figure 3.42A). In the adjacent normal tissue, there was a slight difference in γδ T cell density between stage I-IV patients ($p = 0.0025$), with this difference relating to stage IV patients compared to other stages (Figure 3.42A). In the primary tumour tissue, there was a slight difference in γδ T cell density between stage I-IV patients ($p = 0.104$), with this difference relating to stage IV patients compared to other stages, in addition to a slight difference between stage II and stage III patients (Figure 3.42A). There was no difference in variance between patients from stages I-IV (Figure 3.42B).

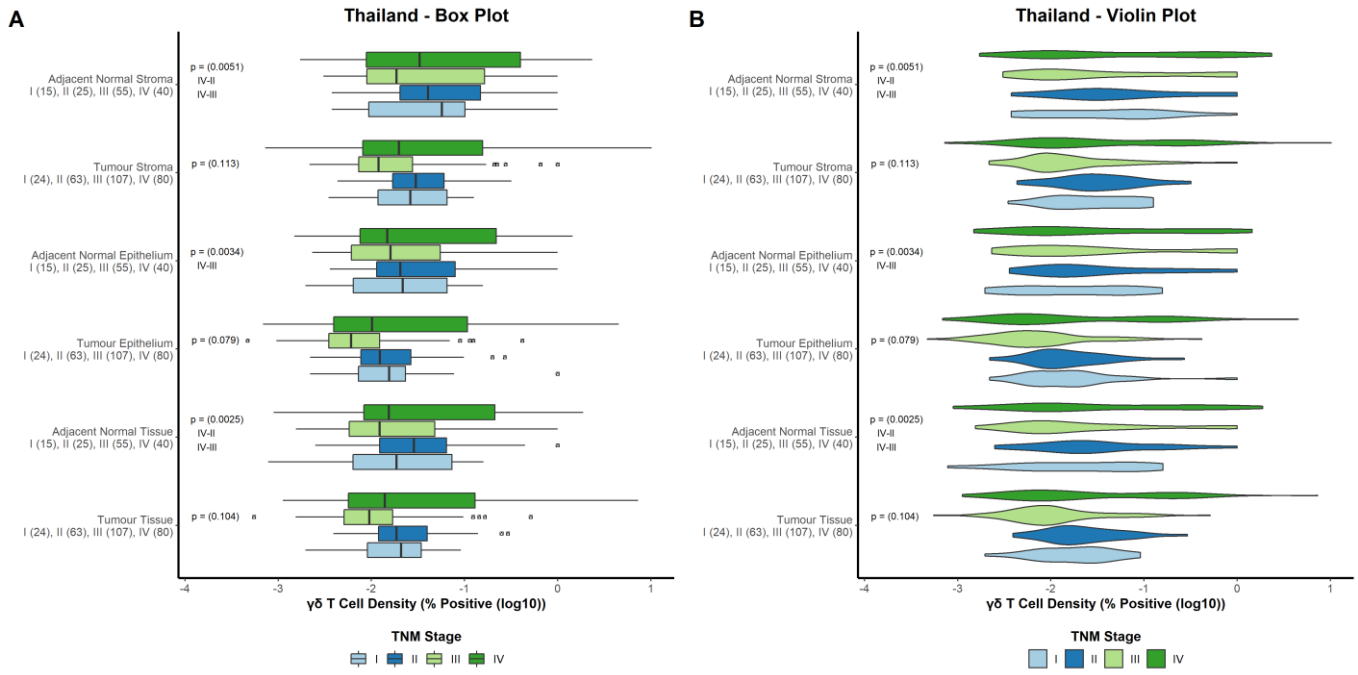

Figure 3.42 – Thailand cohort. Assessment of γδ T cell density across TNM stages. *Box plot presentation of γδ T cell density in stage I (light blue), stage II (dark blue), stage III (light green) and stage IV (dark green) patients. The box is representative of the interquartile range (middle 50% of data points), the vertical line denotes the median and the minimum and maximum are denoted by whiskers. Outliers are represented by an open triangle within an open square (A). Violin plot presentation of γδ T cell density in stage I (light blue), stage II (dark blue), stage III (light green) and stage IV (dark green) patients. The shape of the data reflects the distribution of the data points, which is not discernible in box plots. Outliers are represented by an open triangle within an open square (B). Y axis labels state the tissue compartment (primary tumour or adjacent normal tissue and epithelium, stroma or whole tissue) and below, the test groups with number of cases in brackets. X axis is log10 of the % of total cells within a region positive for the marker of interest. Inline labels denote the lowest standard statistical significance threshold reached (non-significant not shown) using a one-way ANOVA, <0.05 (*), <0.01 (**) or <0.001 (***), with statistically significant (<0.05) group comparisons noted below as determined by Tukey's post-hoc test.*

3.5.5 γδ T cell density by age

Incidence of CRC increases with aged populations, although cases in younger populations are increasing, and so the density of γδ T cells was investigated in patients aged < 65 years of age or ≥ 65 years of age [255]. In the adjacent normal stroma, patients < 65 years of age had a greater γδ T cell density than those ≥65 years of age (p = 0.046) (Figure 3.43A). In the primary tumour stroma, there was no difference in γδ T cell density between patients < 65 years of age and those ≥65 years of age (p = 0.349) (Figure 3.43A). In the adjacent normal epithelium, patients < 65 years of age had a greater γδ T cell density than those ≥65 years of age (p = 0.012) (Figure 3.43A). In the primary tumour epithelium, there was no difference in γδ T cell density between patients < 65 years of age and those ≥65 years of age (p = 0.198) (Figure 3.43A). In the adjacent normal tissue, patients < 65 years of age had a greater γδ T cell density than those ≥65 years of age (p = 0.019) (Figure 3.43A). In the primary tumour tissue, there was no difference in γδ T cell density between patients < 65 years of age and those ≥65 years of age (p = 0.216) (Figure 3.43A). There was no difference in variance in γδ T cell density between groups (Figure 3.43B).

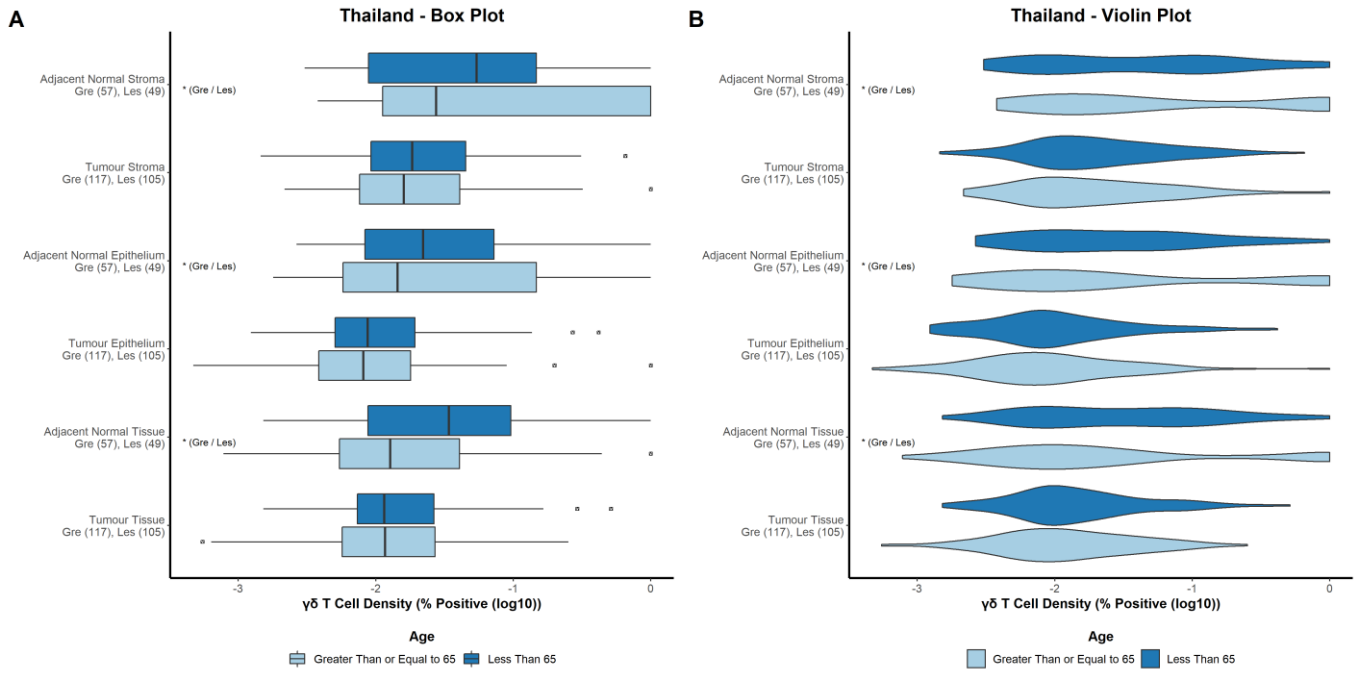

Figure 3.43 – Thailand cohort. Assessment of γδ T cell density in patients aged <65 or ≥65. *Box plot presentation of γδ T cell density in patients aged <65 (dark blue) or ≥65 (light blue). The box is representative of the interquartile range (middle 50% of data points), the vertical line denotes the median and the minimum and maximum are denoted by whiskers. Outliers are represented by an open triangle within an open square (A). Violin plot presentation of γδ T cell density in patients aged <65 (dark blue) or ≥65 (light blue). The shape of the data reflects the distribution of the data points, which is not discernible in box plots. Outliers are represented by an open triangle within an open square (B). Y axis labels state the tissue compartment (primary tumour or adjacent normal tissue and epithelium, stroma or whole tissue) and below, the test groups with number of cases in brackets. X axis is log10 of the % of total cells within a region positive for the marker of interest. Inline labels denote the lowest standard statistical significance threshold reached (non-significant not shown) using a Welch two sample t-test, <0.05 (*), <0.01 (**) or <0.001 (***), with test groups in brackets.*

3.5.6 γδ T cell density by sex

Sex is a prominent factor in CRC incidence, with males having a greater incidence rate than females [256, 257], thus, the difference in γδ T cell density between male and female patients was investigated. In the adjacent normal stroma, there was no difference in the density of γδ T cells in male patients compared to female patients (p = 0.968) (Figure 3.44A). In the primary tumour stroma, there was no difference in the density of γδ T cells in male patients compared to female patients (p = 0.202) (Figure 3.44A). In the adjacent normal epithelium, there was no difference in the density of γδ T cells in male patients compared to female patients (p = 0.857) (Figure 3.44A). In the primary tumour epithelium, there was no difference in the density of γδ T cells in male patients compared to female patients (p = 0.274) (Figure 3.44A). In the adjacent normal tissue, there was no difference in the density of γδ T cells in male patients compared to female patients (p = 0.868) (Figure 3.44A). In the primary tumour tissue, there was no difference in the density of γδ T cells in male patients compared to female patients (p = 0.193) (Figure 3.44A). Compartments in the primary tumour had a lesser variance in the density of γδ T cells compared to compartments in the adjacent normal tissue (Figure 3.44B).

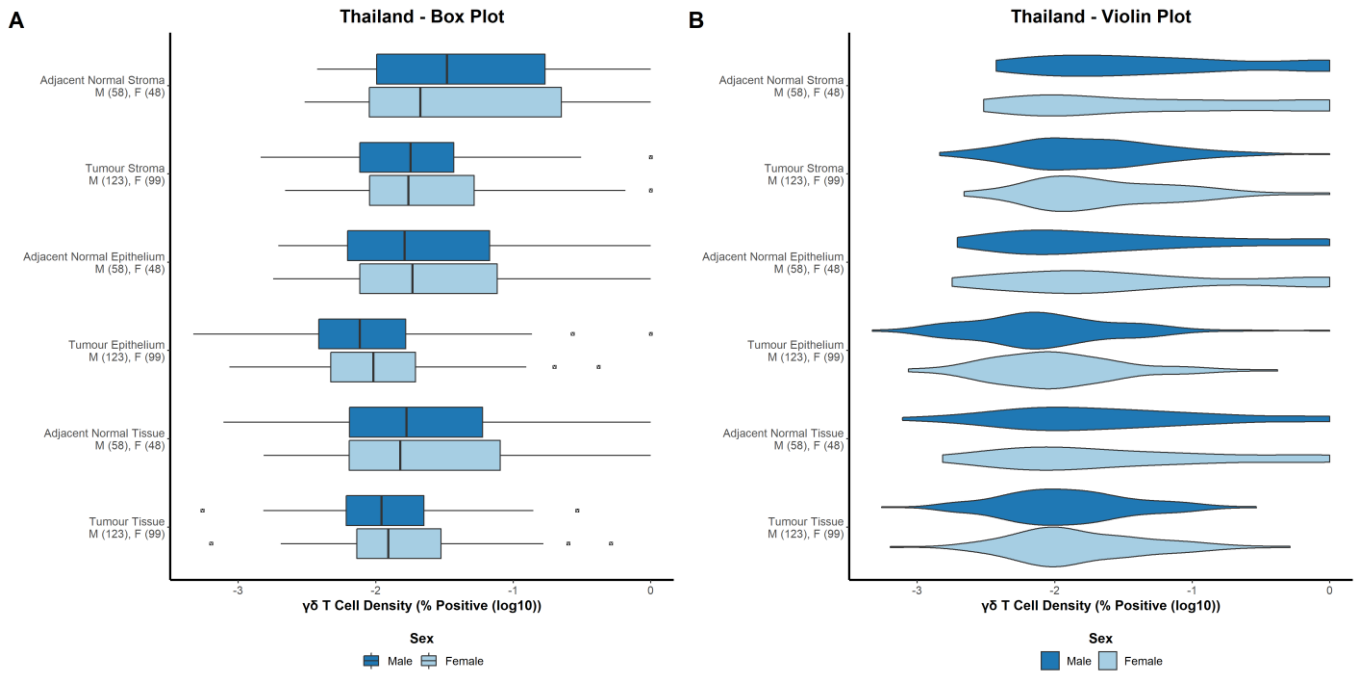

Figure 3.44 – Thailand cohort. Assessment of γδ T cell density in male and female patients. *Box plot presentation of γδ T cell density in male patients (dark blue) or female patients (light blue). The box is representative of the interquartile range (middle 50% of data points), the vertical line denotes the median and the minimum and maximum are denoted by whiskers. Outliers are represented by an open triangle within an open square (A). Violin plot presentation of γδ T cell density in male patients (dark blue) or female patients (light blue). The shape of the data reflects the distribution of the data points, which is not discernible in box plots. Outliers are represented by an open triangle within an open square (B). Y axis labels state the tissue compartment (primary tumour or adjacent normal tissue and epithelium, stroma or whole tissue) and below, the test groups with number of cases in brackets. X axis is log10 of the % of total cells within a region positive for the marker of interest. Inline labels denote the lowest standard statistical significance threshold reached (non-significant not shown) using a Welch two sample t-test, <0.05 (*), <0.01 (**) or <0.001 (***), with test groups in brackets.*

3.6 Discussion

In CRC, conventional T cell subsets are associated with patient outcome which is dependent on myriad factors such as tumour microenvironment components, cell density and localisation within the tissue [8, 9, 188, 239, 240]. To further the development of a comparative body of research for unconventional T cells, the density and localisation of unconventional γδ T cells, which are integral to intestinal maintenance [259] and enriched within the intestinal tract [241-244], was investigated in addition to conventional CD8 'effector' T cells. As a foundation, the density and localisation of these populations was investigated across three patient cohorts (Scotland, Norway, and Thailand), tissue factors (epithelium/stroma and primary tumour/adjacent normal tissue), patient characteristics (age and sex) and disease characteristics (TNM stage, tumour site and DNA mismatch repair status), thus forming a complete picture of the distribution of these lymphocyte populations.

To understand whether lymphocyte density is altered in diseased tissue compared to the normal tissue environment, the density of γδ T cells and CD8 T cells was investigated in the primary tumour and the adjacent normal tissue of patients with both tissue regions available for analysis. γδ T cells were present at a slightly lower density in the primary tumour of patients compared to the adjacent normal tissue and this was consistent across patient cohorts. CD8 T cells were present at a much lower density in the primary tumour compared to the adjacent normal tissue in the Scotland cohort, but patients in the Norway cohort showed no difference in the density of CD8 T cells. Both cohorts were predominantly moderately or well differentiated, had a weak Klintrup-Mäkinen grade and a low tumour stroma percentage, suggesting that this difference isn't due to any measured characteristic of the tumour. This difference was also not explained by the presence of rectal cases within the Scotland cohort, which are absent in the Norway cohort, the removal of which does not alter the result. Thus, there is a differentiating factor between these two populations, but it remains to be identified. The Norway cohort consists of patients who are slightly older, has a greater proportion of stage II patients, less vascular invasion, a weaker overall inflammatory grade (Klintrup–Mäkinen) and higher tumour stroma percentage (Table 3.2). Whether this effect is caused by one of these factors or the result of an environmental factor in this population (diet or genetic background for example) is not clear. This data shows a slight but well validated reduction in γδ T cells within the primary tumour compared to the adjacent normal tissue but is unable to provide clear answers in the context of CD8 T cells. The reduced presence of γδ T cells in tumour tissue compared to normal tissue aligns with work by Chabab *et al*, who have previously shown in a small not paired cohort of patients that γδ T cells in the colon are present at a lower density in tumour (n = 112) tissue compared to normal tissue (n = 62) in a [244].

Other tumour types show mixed results, with ovarian tumours showing an increase in γδ T cells in tumour tissue [260], but breast and pancreas showing no clear difference [244, 261]. This would suggest a difference that is specific to the colon, although the body of data is restricted in the variety of tumour types investigated to date. This result also raises the question of whether the reduction in γδ T cells is of functional relevance or just a bystander victim of generic immune exclusion, given the even more drastic depletion in CD8 T cells. Lymphocyte localisation is vital to function [254], particularly γδ T cells which patrol the epithelium [117, 118]. Referred to as intraepithelial T cells (IELs), consisting of both γδ T cells and CD8 T cells, these cells line the epithelium and make great contributions to the defence of the epithelial barrier [254, 259, 262]. Thus, these populations were investigated within the epithelium and the stroma to determine their relative proportion in these compartments and to understand whether this changes in diseased tissue. Across all cohorts, γδ T cells were present at a greater density in the stroma than in the epithelium, whilst CD8 T cells were present at a much greater density in stroma compared to epithelium in the Scotland cohort but showed no difference in the Norway cohort. This was true in both the primary tumour and the adjacent normal tissue. The greater density within the stroma is surprising but this issue is likely analytical as IELs are typically moving along the epithelial cells, not directly in between them but rather adjacent to the epithelial cells. Thus, they are effectively in the stroma.

The comparative density of γδ and CD8 T cells was also investigated in the context of the basic patient characteristics of sex and age, which are associated with CRC incidence and mortality, with males and those ≥ 65 years of age having greater incidence and mortality [2, 263]. Across all three cohorts, γδ T cells were consistently higher in patients <65 years of age whilst CD8 T cells were higher in the Norway cohort but not the Scotland cohort, with the latter previously suggested in the literature [264]. Likewise, male patients in the Scotland and Norway cohorts had a greater density of γδ T cells, but CD8 T cells showed no difference which contrasts with a stark difference shown by Nosho *et al* [264]. Correlation of lymphocyte density with CRC risk factors may aid hypothesis development for the prognostic role of these populations, but it is interesting to note that they correlate with the low-risk population by age but the high-risk population by sex.

The current gold standard method for stratifying CRC patients is the TNM staging system, and so γδ T cells and CD8 T cells were investigated across the four TNM stages. γδ T cells and CD8 T cells both showed no difference across TNM stages I-IV in both the Scotland cohort and the Norway cohort. In the Thailand cohort however, γδ T cells in stage IV patients were often slightly higher than in other stages, particularly compared to stage II and stage III patients and demonstrated a greater range. Others have shown a reduced density of CD8 T cells in stage IV patients [264]. Although there appears to be no relevant change in the density of these lymphocyte populations as disease progresses, it is quite possible that the T cells are in some way manipulated and remain relevant to disease progression despite their stable density. This may include exhaustion of T cells or be controlled by alterations to cytokine availability or access to antigen.

There are molecular, histological, and prognostic differences associated with CRC tumours located in the proximal side of the splenic flexure (right-sided), distal side of the splenic flexure (left-sided) and the rectum [265-268]. Right sided disease is considered to have a greater immune infiltrate [42] and more likely to be MMR deficient [43], which is also associated with immune infiltration [45, 269]. Thus, the density of γδ T cells was investigated in the context of these tumour sites and MMR status. γδ T cells and CD8 T cells in the Scotland cohort were slightly higher in adjacent normal tissue of right-sided patients, whilst γδ T cells in the Norway cohort were slightly higher in right-sided cases but CD8 T cells were present at a much higher density in right-sided cases. These results reflect the known correlation between right-sided disease and a higher immune infiltration, although Chabab *et al* found no difference in γδ T cell density between right-sided and left-sided patients in a small scale study conducted using a French cohort [244]. In the Scotland cohort, γδ T cells and CD8 T cells were present at a marginally higher density in MMR deficient patients compared to MMR proficient patients. Chabab *et al* found no difference in γδ T cell density in MMR proficient and deficient patients, although they were restricted by a very low number of MMR deficient cases [244]. This lack of a substantial difference in either lymphocyte population is a surprise given the strength of difference seen in the literature. In conclusion, there was some difference in lymphocyte density based on patient characteristics such as age and sex, but tumour specific factors showed little difference. The strongest finding was the stark difference in density of both lymphocyte subsets in the primary tumour of patients compared to the adjacent normal tissue. This demonstrates a link between tumour development (but not progression as lymphocyte density was stable across TNM stages) and lymphocyte density, but it is not clear whether alterations to lymphocyte density are a consequence of tumour development or precede and contribute to tumour development. The phenotype and activation status of these lymphocyte populations is also unknown and is likely to be highly relevant to how they exert any prospective influence on patient prognosis.

Chapter 4:
Assessment of the prognostic role of lymphocyte populations across patient cohorts

Chapter 4: Assessment of the prognostic role of lymphocyte populations across patient cohorts

4.0 Summary

To elucidate the prognostic role of γδ T cells and compare it to the established prognostic role of CD8 T cells, time-to-event analysis was conducted after classifying patients as 'high' or 'low'. CD8 T cells had a favourable prognostic role in the Scotland cohort, as predicted from the literature, whilst γδ T cells had an unfavourable prognostic role. This demonstrates opposing prognostic roles for these lymphocyte populations and suggests valuable prognostic information could be obtained from a wider analytical view of the immune landscape than the CD3/CD8 populations typically studied.

Interestingly, these results were not reflected in the Norway cohort (no difference). Clinical use of a biomarker requires a consistent cutpoint for classification and so data from one cohort (Scotland) was used to develop the classifications for all cohorts. When classification as 'high' or 'low' was conducted using data from the Norway cohort, the results were switched. The Scotland cohort has a larger inflammatory milieu than the Norway cohort. These results indicate that the effect of the populations is consistent but the clinical application of γδ T cells would be inappropriate due to the lack of a consistent classification cutpoint.

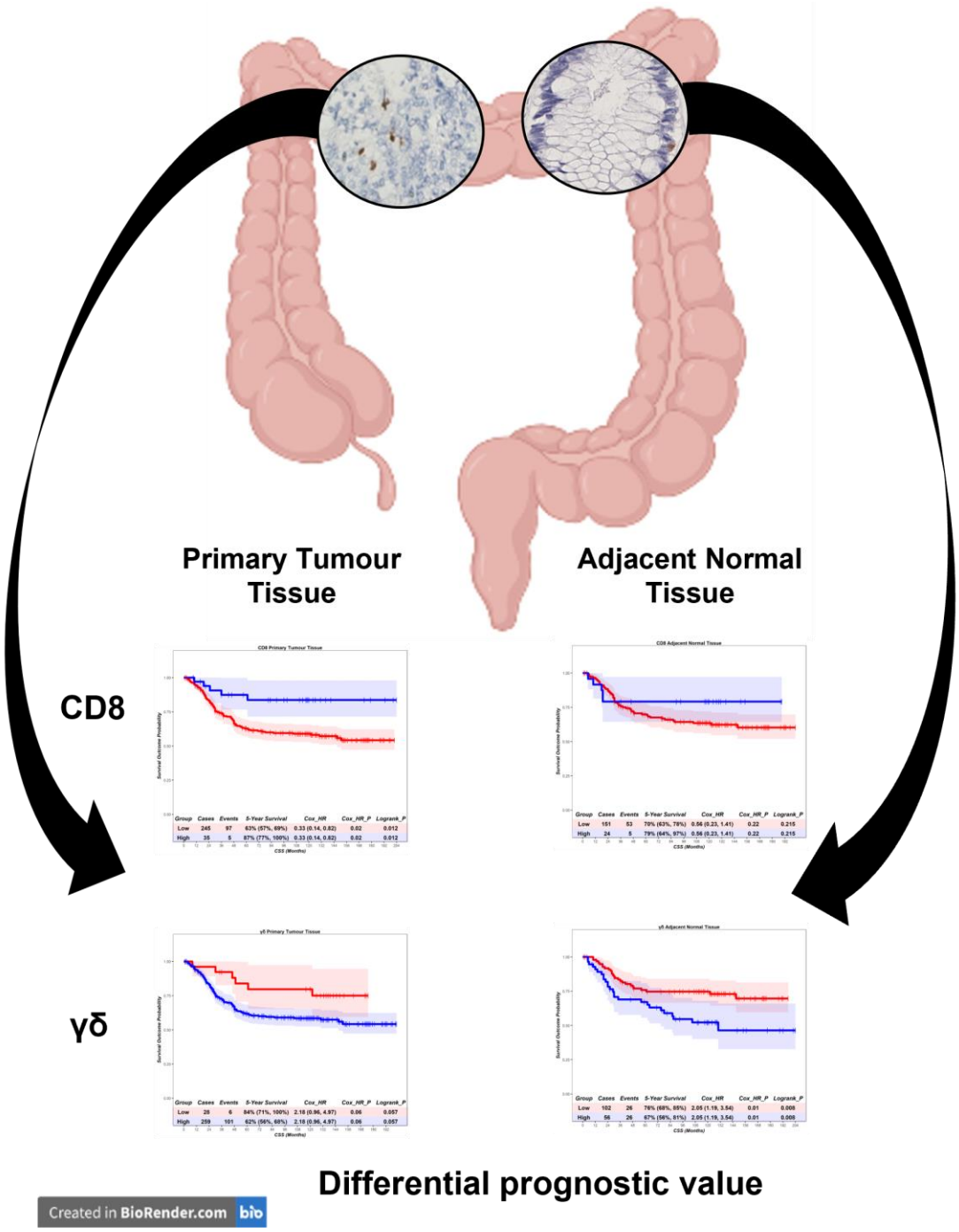
Primary Tumour Tissue
Adjacent Normal Tissue
CD8
γδ
Differential prognostic value
Created in BioRender.com

4.1 Introduction

The gold standard tumour burden/nodal status/metastasis, or TNM, staging system [65] is not sufficiently accurate for stage II and stage III patients with some proposing greater weight be given to T stage in discriminating between these stages [4]. Attempts to refine the TNM staging system have sought to adopt the immune landscape and led to the development of the Immunoscore® [9] which is based on the observation that T cells have a strong, favourable prognostic role in CRC. This originated from a study in 415 CRC patients showing that increased infiltration of CD3, CD8, or CD45RO (effector/memory) T cells at the tumour centre or invasive margin, but particularly when high in both, is associated with greater disease-free survival [8]. However, this work does not investigate the specific role of γδ T cells, although they would be included in CD3 staining.

Studies have investigated the prognostic role of γδ T cells in a transcriptomic setting using CIBERSORT, which infers immune cell populations from bulk transcriptomic data [11], and suggested that lymphocytes were prognostically favourable and γδ T cells were the most favourable sub-population [10]. However, this methodology was hindered by crossover of transcriptional signatures for lymphocyte populations and was subsequently refined using purified Vγ9Vδ2 T cells [187], highlighting a second drawback of this methodology; its refinement is based on circulating γδ T cells whilst the intestinal tract is populated primarily by $V\delta2^-$ T cells. Histological studies have demonstrated an unfavourable role for γδ T cells in cancers of the breast and gall bladder [185, 186], but to date there has been no comprehensive histological study of the prognostic role of γδ T cells in CRC.

4.2 Scotland Cohort

4.2.0 Summary Tables

Table 4.1 – Summary table of survival analysis for γδ T cells in the Scotland cohort. *Red rows are unfavourable. Green rows are favourable. Amber rows either present a mutual result or trend towards a result but with insufficient size effect.*

Survival	Compartment	Cox HR	Cox P Value	Logrank P Value	Prognostic Value
Cancer-specific (CSS)	γδ Adjacent Normal Epithelium	1.87	0.03	0.023	Unfavourable
Cancer-specific (CSS)	γδ Adjacent Normal Stroma	2.25	0	0.003	Unfavourable
Cancer-specific (CSS)	γδ Adjacent Normal Tissue	2.05	0.01	0.008	Unfavourable
Cancer-specific (CSS)	γδ Primary Tumour Epithelium	1.7	0.15	0.146	Unfavourable
Cancer-specific (CSS)	γδ Primary Tumour Stroma	2.36	0.04	0.035	Unfavourable
Cancer-specific (CSS)	γδ Primary Tumour Tissue	2.18	0.06	0.057	Unfavourable
Overall (OS)	γδ Adjacent Normal Epithelium	1.34	0.16	0.161	Unclear
Overall (OS)	γδ Adjacent Normal Stroma	1.3	0.22	0.22	Unclear
Overall (OS)	γδ Adjacent Normal Tissue	1.36	0.14	0.135	Unclear
Overall (OS)	γδ Primary Tumour Epithelium	1.39	0.17	0.171	Unclear
Overall (OS)	γδ Primary Tumour Stroma	1.97	0.01	0.013	Unfavourable
Overall (OS)	γδ Primary Tumour Tissue	1.85	0.03	0.024	Unfavourable
Disease-free (DFS)	γδ Adjacent Normal Epithelium	1.5	0.05	0.046	Unclear
Disease-free (DFS)	γδ Adjacent Normal Stroma	1.5	0.05	0.045	Unclear
Disease-free (DFS)	γδ Adjacent Normal Tissue	1.51	0.04	0.037	Unclear
Disease-free (DFS)	γδ Primary Tumour Epithelium	1.5	0.09	0.089	Unfavourable
Disease-free (DFS)	γδ Primary Tumour Stroma	2.08	0.01	0.007	Unfavourable
Disease-free (DFS)	γδ Primary Tumour Tissue	1.96	0.02	0.013	Unfavourable
Recurrence-free (RFS)	γδ Adjacent Normal Epithelium	1.64	0.1	0.1	Unclear
Recurrence-free (RFS)	γδ Adjacent Normal Stroma	2.18	0.01	0.009	Unfavourable
Recurrence-free (RFS)	γδ Adjacent Normal Tissue	1.72	0.08	0.074	Unclear
Recurrence-free (RFS)	γδ Primary Tumour Epithelium	1.87	0.53	0.527	Unclear
Recurrence-free (RFS)	γδ Primary Tumour Stroma	1.47	0.52	0.514	Unclear
Recurrence-free (RFS)	γδ Primary Tumour Tissue	1.63	0.5	0.491	Unclear

Table 4.2 – Summary table of survival analysis for CD8 T cells in the Scotland cohort. *Red rows are unfavourable. Green rows are favourable. Amber rows either present a mutual result or trend towards a result but with insufficient size effect.*

Survival	Compartment	Cox HR	Cox P Value	Logrank P Value	Prognostic Value
Cancer-specific (CSS)	CD8 Adjacent Normal Epithelium	0.65	0.15	0.15	Unclear
Cancer-specific (CSS)	CD8 Adjacent Normal Stroma	1.59	0.14	0.138	Unclear
Cancer-specific (CSS)	CD8 Adjacent Normal Tissue	0.56	0.22	0.215	Unclear
Cancer-specific (CSS)	CD8 Primary Tumour Epithelium	0.46	0.02	0.017	Favourable
Cancer-specific (CSS)	CD8 Primary Tumour Stroma	0.64	0.04	0.039	Favourable
Cancer-specific (CSS)	CD8 Primary Tumour Tissue	0.33	0.02	0.012	Favourable
Overall (OS)	CD8 Adjacent Normal Epithelium	0.62	0.04	0.035	Unclear
Overall (OS)	CD8 Adjacent Normal Stroma	1.11	0.62	0.623	Unclear
Overall (OS)	CD8 Adjacent Normal Tissue	0.91	0.75	0.746	Unclear
Overall (OS)	CD8 Primary Tumour Epithelium	0.96	0.81	0.805	Unclear
Overall (OS)	CD8 Primary Tumour Stroma	0.89	0.5	0.495	Unclear
Overall (OS)	CD8 Primary Tumour Tissue	0.83	0.42	0.419	Unclear
Disease-free (DFS)	CD8 Adjacent Normal Epithelium	0.67	0.08	0.077	Unclear
Disease-free (DFS)	CD8 Adjacent Normal Stroma	1.2	0.39	0.39	Unclear
Disease-free (DFS)	CD8 Adjacent Normal Tissue	0.84	0.52	0.523	Unclear
Disease-free (DFS)	CD8 Primary Tumour Epithelium	0.92	0.65	0.648	Unclear
Disease-free (DFS)	CD8 Primary Tumour Stroma	0.89	0.51	0.506	Unclear
Disease-free (DFS)	CD8 Primary Tumour Tissue	0.83	0.41	0.41	Unclear
Recurrence-free (RFS)	CD8 Adjacent Normal Epithelium	0.77	0.44	0.429	Unclear
Recurrence-free (RFS)	CD8 Adjacent Normal Stroma	2.01	0.05	0.046	Unfavourable
Recurrence-free (RFS)	CD8 Adjacent Normal Tissue	0.44	0.11	0.104	Favourable
Recurrence-free (RFS)	CD8 Primary Tumour Epithelium	0.25	0	0.001	Favourable
Recurrence-free (RFS)	CD8 Primary Tumour Stroma	0.67	0.1	0.095	Unclear
Recurrence-free (RFS)	CD8 Primary Tumour Tissue	0.24	0.01	0.007	Favourable

4.2.1 γδ T cells - cancer-specific survival

In the adjacent normal epithelium, patients deemed high for γδ T cells are associated with a worse prognosis (Figure 4.1). Patients with a high level of γδ T cells had a mean survival time of 81.08 months, compared to those with low levels of γδ T cells with a mean survival of 97.53 months (hazard ratio = 1.87, p = 0.03). 5-year survival for patients high for γδ T cells is 68% (56%, 82%), compared to 75% (67%, 84%) in the γδ low group. This suggests that γδ T cells in the epithelial compartment of the adjacent normal tissue have an unfavourable prognostic role. Multivariate analysis was not statistically significant (hazard ratio = 1.42, p = 0.25) (Table 4.3), suggesting that γδ T cells in the epithelial compartment of the adjacent normal tissue are not independently prognostic.

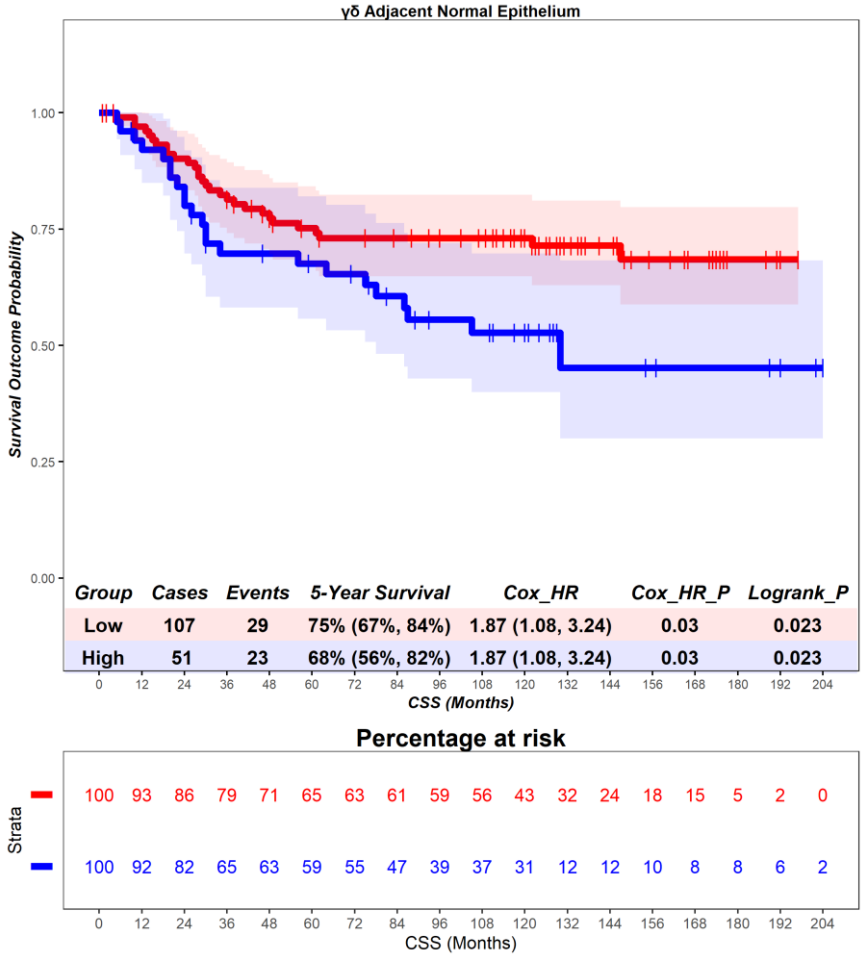

Figure 4.1 – Scotland cohort. Time-to-event (cancer-specific survival) analysis for γδ T cells in the adjacent normal epithelium*. Patients deemed 'High' or 'Low' for γδ T cells are shaded blue and red, respectively. Cox hazard ratio is univariate – see table 4.3 for multivariate. The 'Low' group is used as the reference group on cox regression modelling.*

In the adjacent normal stroma, patients deemed high for γδ T cells are associated with a worse prognosis (Figure 4.2). Patients with a high level of γδ T cells had a mean survival time of 81.02 months, compared to those with low levels of γδ T cells with a mean survival of 96.82 months (hazard ratio = 2.25, p = 0.03). 5-year survival for patients high for γδ T cells is 64% (52%, 80%), compared to 76% (69%, 85%) in the γδ low group. This suggests that γδ T cells in the stromal compartment of the adjacent normal tissue have an unfavourable prognostic role. Multivariate analysis was not statistically significant (hazard ratio = 1.6, p = 0.12) (Table 4.3), suggesting that γδ T cells in the stromal compartment of the adjacent normal tissue are not independently prognostic.

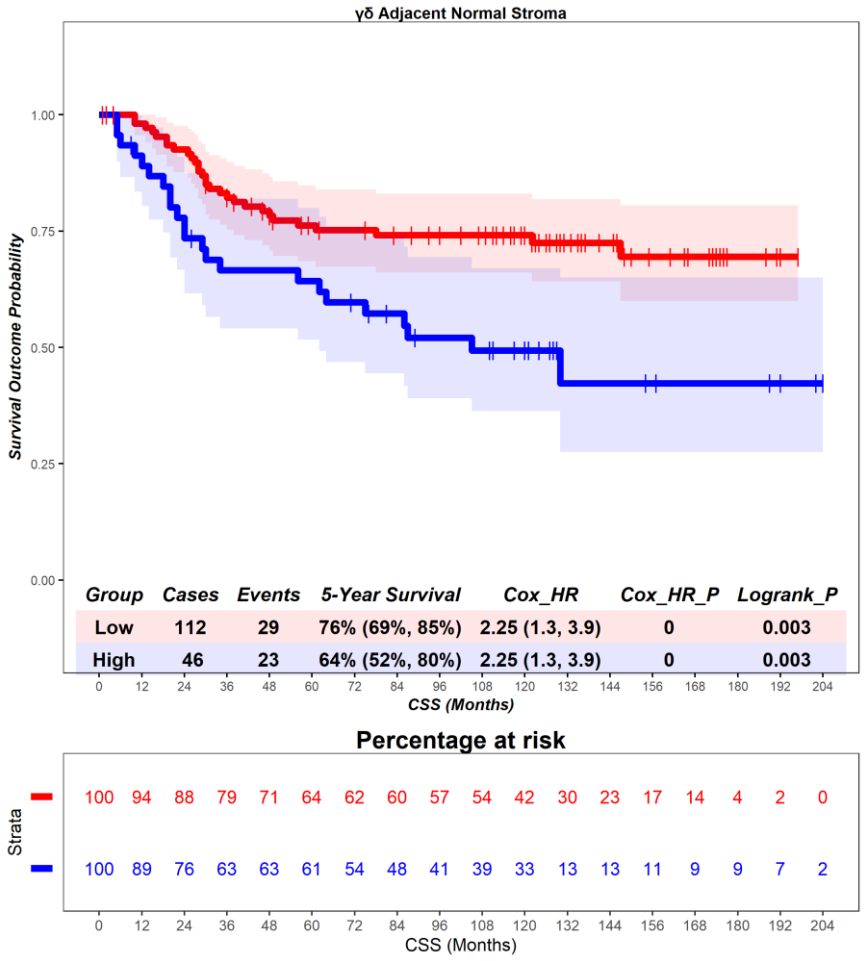

Figure 4.2 – Scotland cohort. Time-to-event (cancer-specific survival) analysis for γδ T cells in the adjacent normal stroma*. Patients deemed 'High' or 'Low' for γδ T cells are shaded blue and red, respectively. Cox hazard ratio is univariate – see table 4.3 for multivariate. The 'Low' group is used as the reference group on cox regression modelling.*

In the adjacent normal tissue, patients deemed high for γδ T cells are associated with a worse prognosis (Figure 4.3). Patients with a high level of γδ T cells had a mean survival time of 82.68 months, compared to those with low levels of γδ T cells with a mean survival of 97.46 months (hazard ratio = 2.05, p = 0.01). 5-year survival for patients high for γδ T cells is 67% (56%, 81%), compared to 76% (68%, 85%) in the γδ low group. This suggests that γδ T cells in the whole tissue of the adjacent normal tissue have an unfavourable prognostic role. Multivariate analysis was not statistically significant (hazard ratio = 1.49, p = 0.19) (Table 4.3), suggesting that γδ T cells in the whole tissue of the adjacent normal tissue are not independently prognostic.

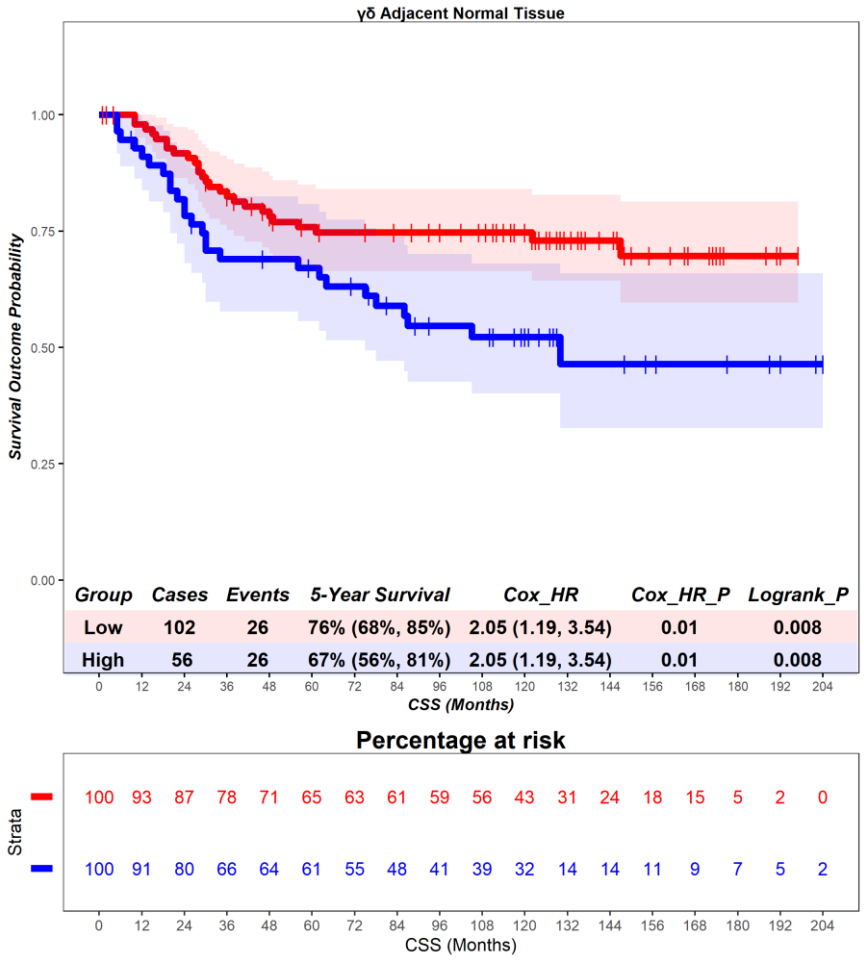

Figure 4.3 – Scotland cohort. Time-to-event (cancer-specific survival) analysis for γδ T cells in the adjacent normal tissue*. Patients deemed 'High' or 'Low' for γδ T cells are shaded blue and red, respectively. Cox hazard ratio is univariate – see table 4.3 for multivariate. The 'Low' group is used as the reference group on cox regression modelling.*

In the primary tumour epithelium, patients deemed high for γδ T cells are associated with a worse prognosis (Figure 4.4). Patients with a high level of γδ T cells had a mean survival time of 79.9 months, compared to those with low levels of γδ T cells with a mean survival of 100.71 months (hazard ratio = 1.7, p = 0.15). 5-year survival for patients high for γδ T cells is 62% (56%, 69%), compared to 79% (66%, 96%) in the γδ low group. This suggests that γδ T cells in the epithelial compartment of the primary tumour have an unfavourable prognostic role. Multivariate analysis was not statistically significant (hazard ratio = 1.7, p = 0.15) (Table 4.3), suggesting that γδ T cells in the epithelial compartment of the primary tumour are not independently prognostic.

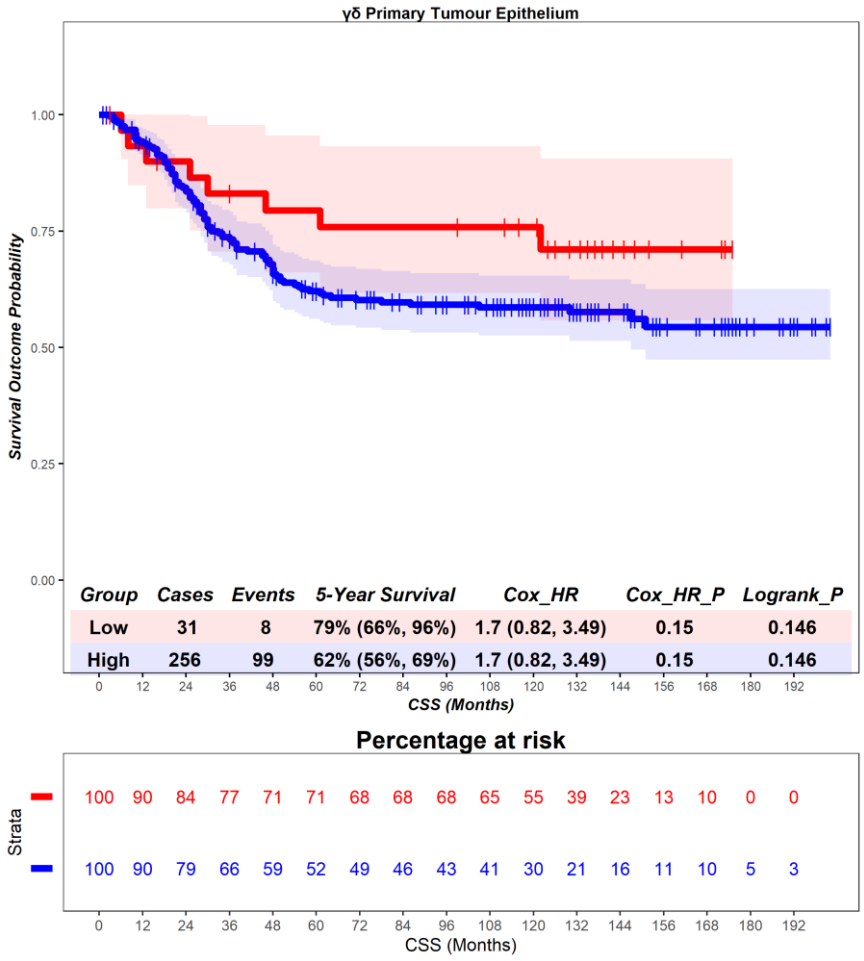

Figure 4.4 – Scotland cohort. Time-to-event (cancer-specific survival) analysis for γδ T cells in the primary tumour epithelium*. Patients deemed 'High' or 'Low' for γδ T are shaded blue and red, respectively. Cox hazard ratio is univariate – see table 4.3 for multivariate. The 'Low' group is used as the reference group on cox regression modelling.*

In the primary tumour stroma, patients deemed high for γδ T cells are associated with a worse prognosis (Figure 4.5). Patients with a high level of γδ T cells had a mean survival time of 79.02 months, compared to those with low levels of γδ T cells with a mean survival of 111.04 months (hazard ratio = 2.36, p = 0.04). 5-year survival for patients high for γδ T cells is 62% (56%, 68%), compared to 84% (71%, 100%) in the γδ low group. This suggests that γδ T cells in the stromal compartment of the primary tumour have an unfavourable prognostic role. Multivariate analysis was not statistically significant (hazard ratio = 1.51, p = 0.34) (Table 4.3), suggesting that γδ T cells in the stromal compartment of the primary tumour are not independently prognostic.

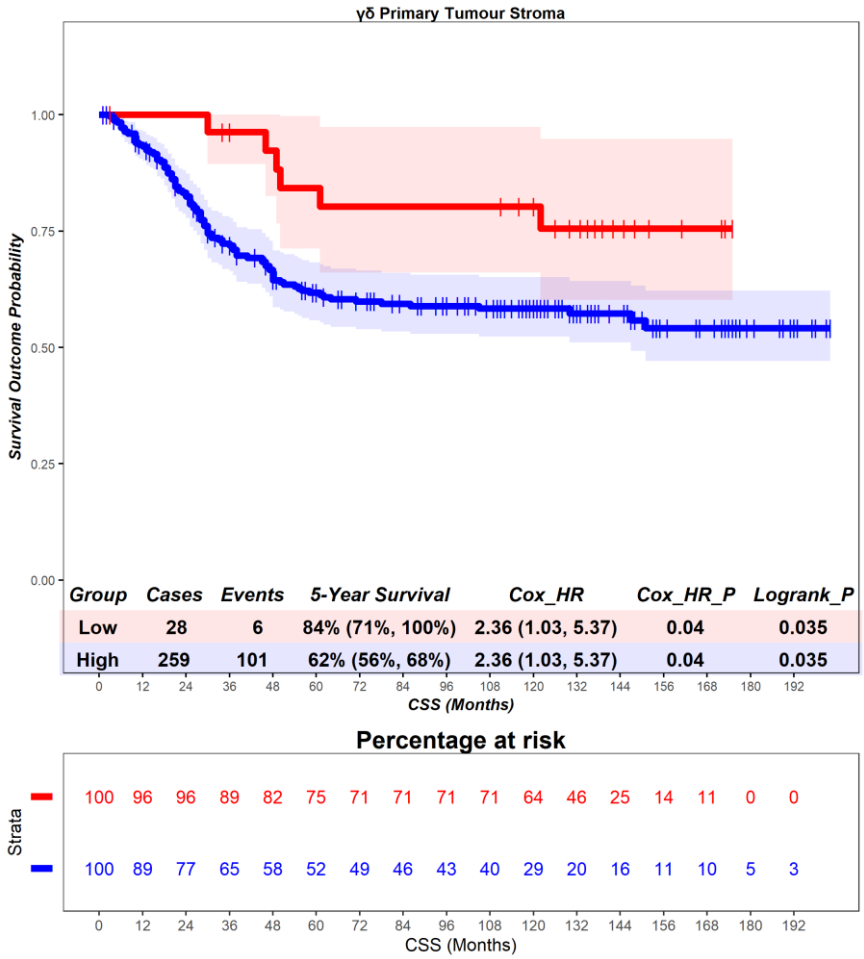

Figure 4.5 – Scotland cohort. Time-to-event (cancer-specific survival) analysis for γδ T cells in the primary tumour stroma*. Patients deemed 'High' or 'Low' for γδ T are shaded blue and red, respectively. Cox hazard ratio is univariate – see table 4.3 for multivariate. The 'Low' group is used as the reference group on cox regression modelling.*

In the primary tumour tissue, patients deemed high for γδ T cells are associated with a worse prognosis (Figure 4.6). Patients with a high level of γδ T cells had a mean survival time of 79.61 months, compared to those with low levels of γδ T cells with a mean survival of 105.61 months (hazard ratio = 2.18, p = 0.06). 5-year survival for patients high for γδ T cells is 62% (56%, 68%), compared to 84% (71%, 100%) in the γδ low group. This suggests that γδ T cells in the whole tissue of the primary tumour have an unfavourable prognostic role. Multivariate analysis was not statistically significant (hazard ratio = 1.23, p = 0.630) (Table 4.3), suggesting that γδ T cells in the whole tissue of the primary tumour are not independently prognostic.

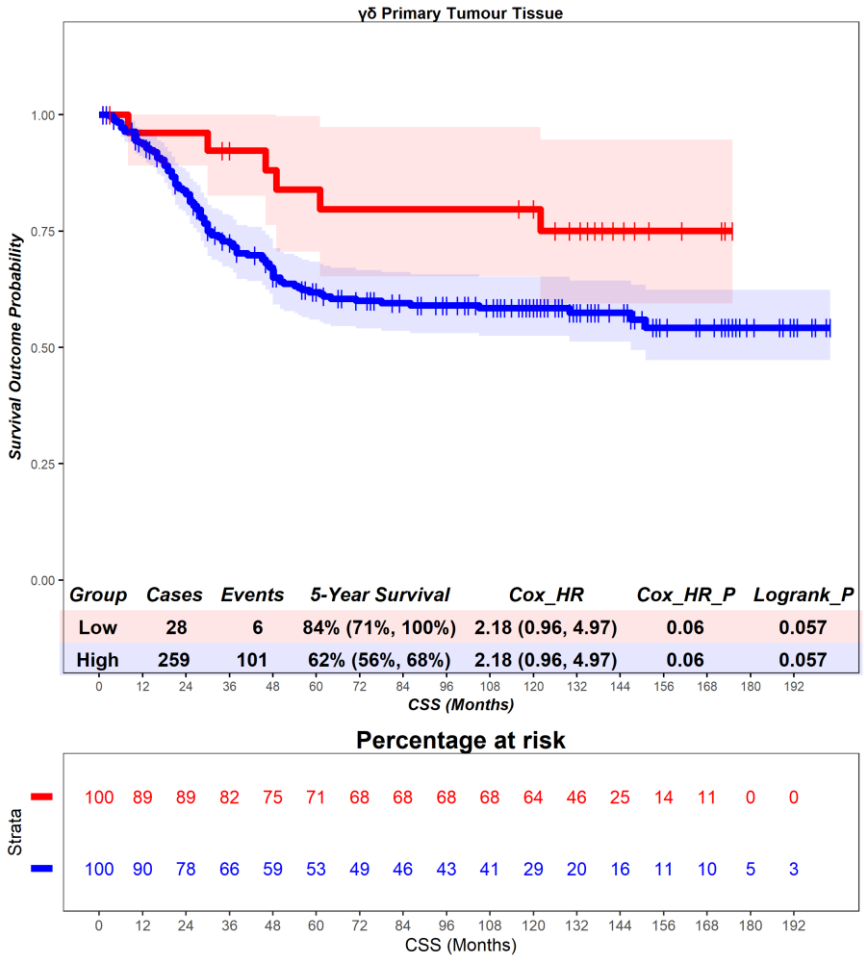

Figure 4.6 – Scotland cohort. Time-to-event (cancer-specific survival) analysis for γδ T cells in the primary tumour tissue*. Patients deemed 'High' or 'Low' for γδ T are shaded blue and red, respectively. Cox hazard ratio is univariate – see table 4.3 for multivariate. The 'Low' group is used as the reference group on cox regression modelling.*

4.2.2 γδ T cells - overall survival

In the adjacent normal epithelium, patients deemed high for γδ T cells are associated with a worse prognosis (Figure 4.7), although this result did not reach statistical significance. Patients with a high level of γδ T cells had a mean survival time of 81.08 months, compared to those with low levels of γδ T cells with a mean survival of 97.53 months (hazard ratio = 1.34, p = 0.16). 5-year survival for patients high for γδ T cells is 59% (47%, 74%), compared to 65% (57%, 75%) in the γδ low group. This suggests that γδ T cells in the epithelial compartment of the adjacent normal tissue are associated with an unfavourable prognostic role. Multivariate analysis was not statistically significant (hazard ratio = 1.36, p = 0.18) (Table 4.3), suggesting that γδ T cells in the epithelial compartment of the adjacent normal tissue are not independently prognostic.

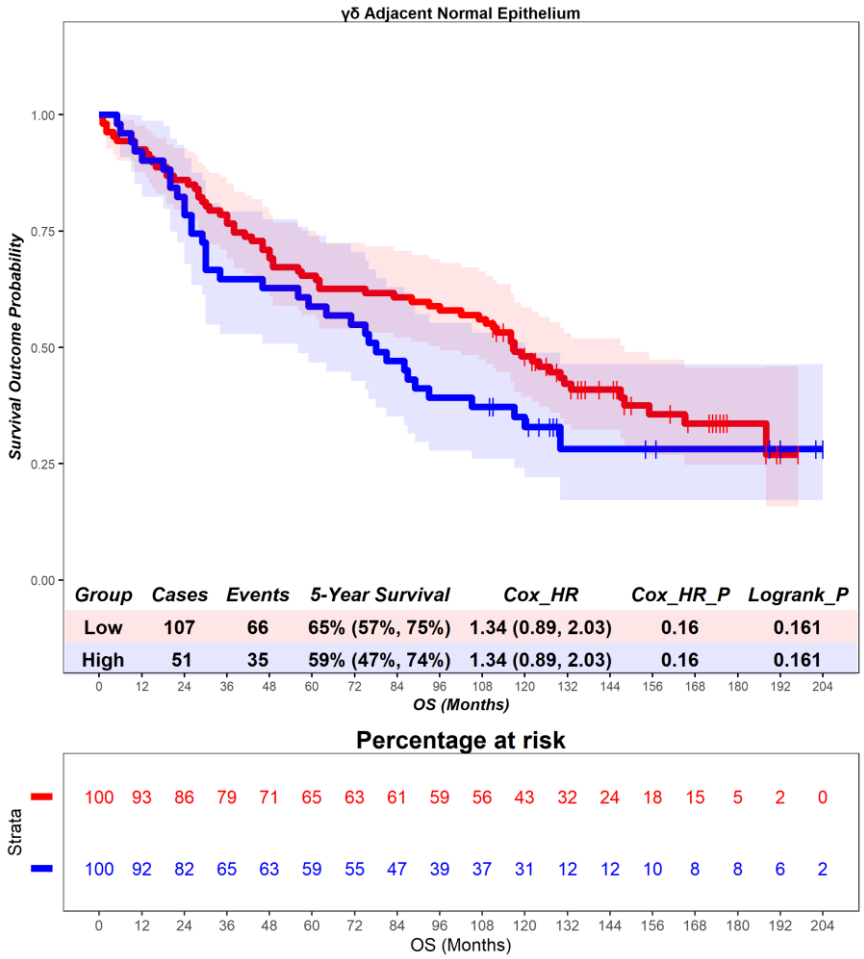

Figure 4.7 – Scotland cohort. Time-to-event (overall survival) analysis for γδ T cells in the adjacent normal epithelium*. Patients deemed 'High' or 'Low' for γδ T cells are shaded blue and red, respectively. Cox hazard ratio is univariate – see table 4.3 for multivariate. The 'Low' group is used as the reference group on cox regression modelling.*

In the adjacent normal stroma, patients deemed high for γδ T cells are associated with a worse prognosis (Figure 4.8), although this result did not reach statistical significance. Patients with a high level of γδ T cells had a mean survival time of 81.02 months, compared to those with low levels of γδ T cells with a mean survival of 96.82 months (hazard ratio = 1.3, p = 0.22). 5-year survival for patients high for γδ T cells is 61% (48%, 77%), compared to 64% (56%, 74%) in the γδ low group. This suggests that γδ T cells in the stromal compartment of the adjacent normal tissue are associated with an unfavourable prognostic role. Multivariate analysis was not statistically significant (hazard ratio = 1.32, p = 0.23) (Table 4.3), suggesting that γδ T cells in the epithelial compartment of the adjacent normal tissue are not independently prognostic.

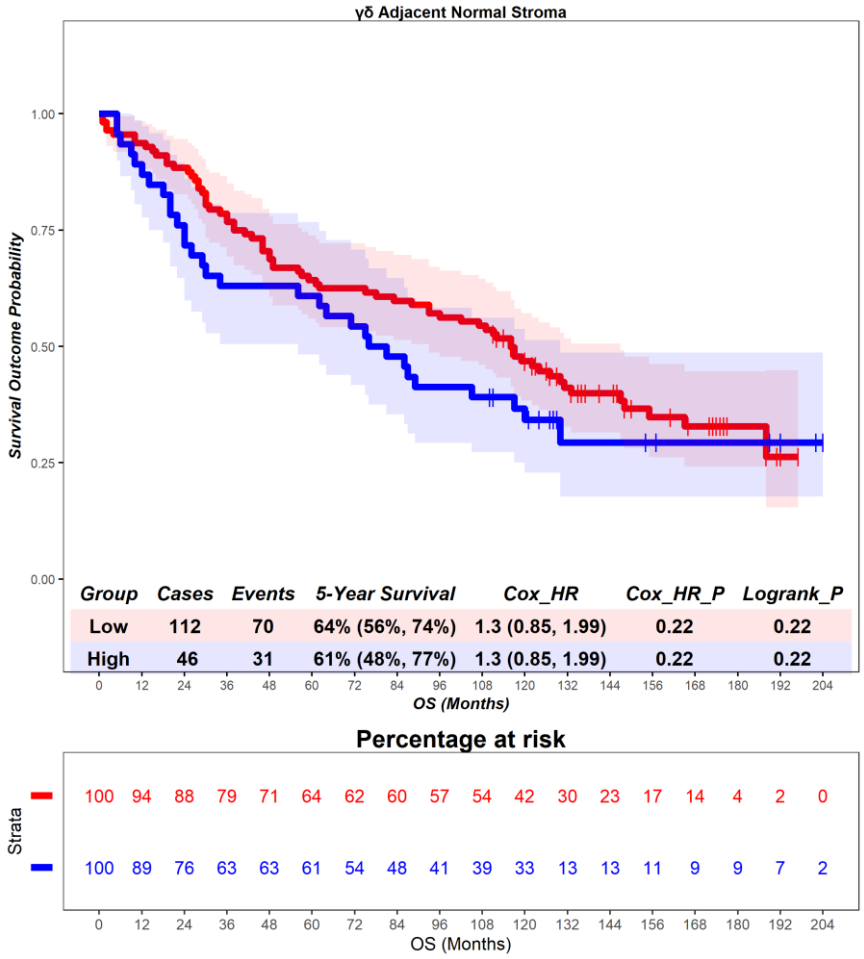

Figure 4.8 – Scotland cohort. Time-to-event (overall survival) analysis for γδ T cells in the adjacent normal stroma*. Patients deemed 'High' or 'Low' for γδ T cells are shaded blue and red, respectively. Cox hazard ratio is univariate – see table 4.3 for multivariate. The 'Low' group is used as the reference group on cox regression modelling.*

In the adjacent normal tissue, patients deemed high for γδ T cells are associated with a worse prognosis (Figure 4.9), although this result did not reach statistical significance. Patients with a high level of γδ T cells had a mean survival time of 82.68 months, compared to those with low levels of γδ T cells with a mean survival of 97.46 months (hazard ratio = 1.36, p = 0.14). 5-year survival for patients high for γδ T cells is 61% (49%, 75%), compared to 65% (56%, 75%) in the γδ low group. This suggests that γδ T cells in the whole tissue of the adjacent normal tissue are associated with an unfavourable prognostic role. Multivariate analysis was not statistically significant (hazard ratio = 1.37, p = 0.16) (Table 4.3), suggesting that γδ T cells in the epithelial compartment of the adjacent normal tissue are not independently prognostic.

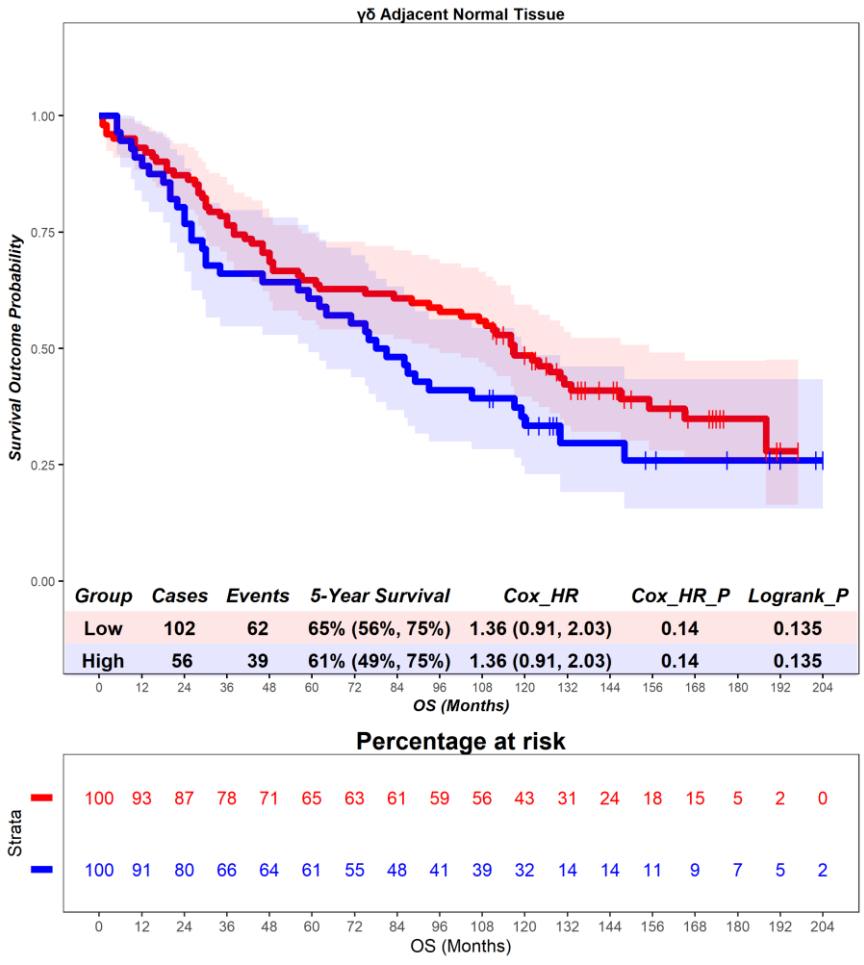

Figure 4.9 – Scotland cohort. Time-to-event (overall survival) analysis for γδ T cells in the adjacent normal tissue*. Patients deemed 'High' or 'Low' for γδ T cells are shaded blue and red, respectively. Cox hazard ratio is univariate – see table 4.3 for multivariate. The 'Low' group is used as the reference group on cox regression modelling.*

In the primary tumour epithelium, patients deemed high for γδ T cells are associated with a worse prognosis (Figure 4.10), although this result did not reach statistical significance. Patients with a high level of γδ T cells had a mean survival time of 79.9 months, compared to those with low levels of γδ T cells with a mean survival of 100.71 months (hazard ratio = 1.39, p = 0.17). 5-year survival for patients high for γδ T cells is 52% (46%, 58%), compared to 71% (57%, 89%) in the γδ low group. This suggests that γδ T cells in the epithelial compartment of the primary tumour are associated with an unfavourable prognostic role. Multivariate analysis was not statistically significant (hazard ratio = 1.24, p = 0.4) (Table 4.3), suggesting that γδ T cells in the epithelial compartment of the primary tumour are not independently prognostic.

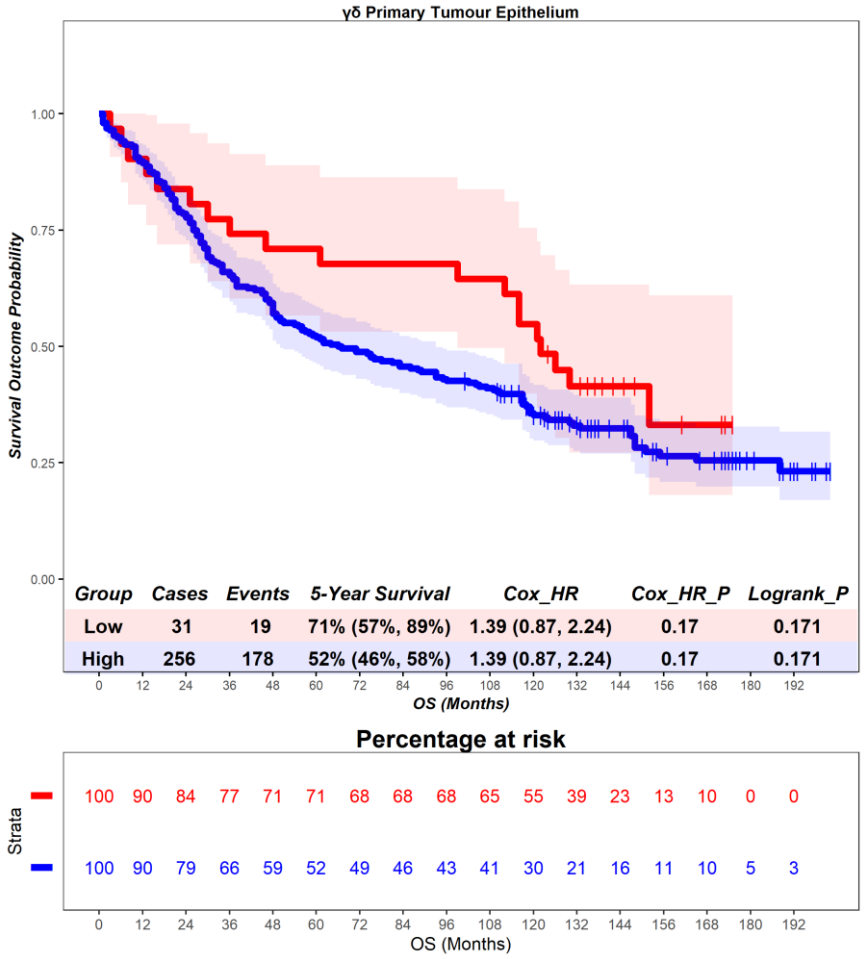

Figure 4.10 – Scotland cohort. Time-to-event (overall survival) analysis for γδ T cells in the primary tumour epithelium*. Patients deemed 'High' or 'Low' for γδ T cells are shaded blue and red, respectively. Cox hazard ratio is univariate – see table 4.3 for multivariate. The 'Low' group is used as the reference group on cox regression modelling.*

In the primary tumour stroma, patients deemed high for γδ T cells are associated with a worse prognosis (Figure 4.11). Patients with a high level of γδ T cells had a mean survival time of 79.02 months, compared to those with low levels of γδ T cells with a mean survival of 111.04 months (hazard ratio = 1.97, p = 0.01). 5-year survival for patients high for γδ T cells is 52% (46%, 58%), compared to 75% (61%, 93%) in the γδ low group. This suggests that γδ T cells in the stromal compartment of the primary tumour are associated with an unfavourable prognostic role. Multivariate analysis was not statistically significant (hazard ratio = 1.63, p = 0.08) (Table 4.3), suggesting that γδ T cells in the epithelial compartment of the primary tumour are not independently prognostic.

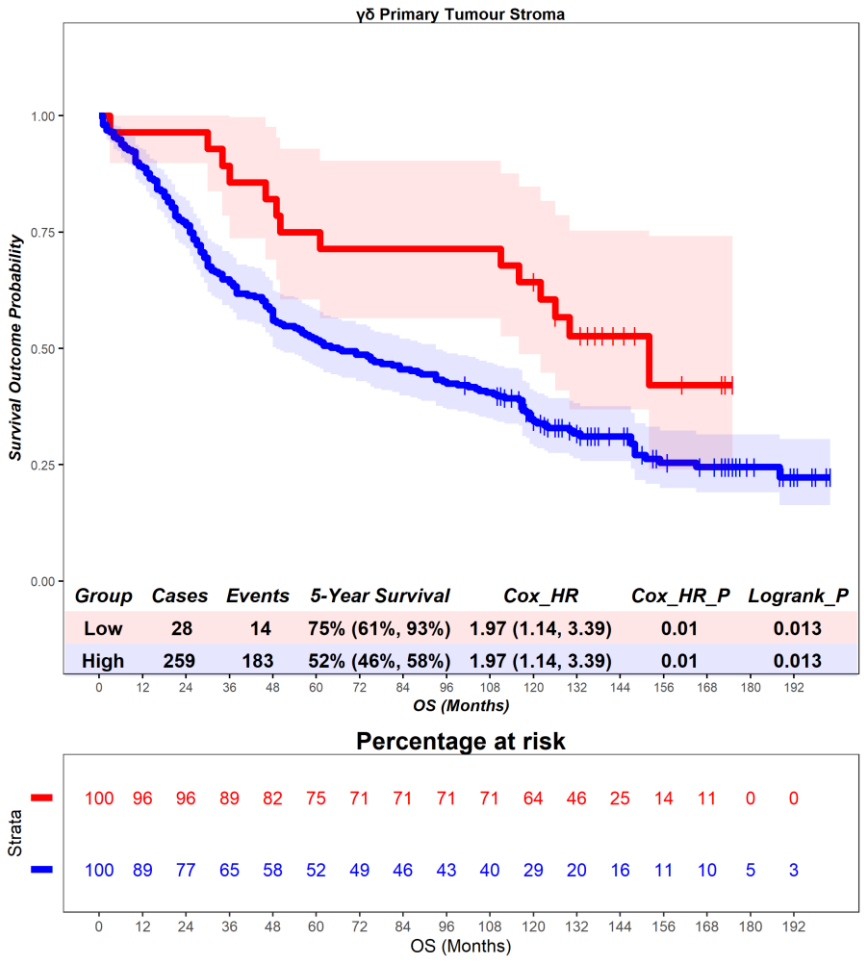

Figure 4.11 – Scotland cohort. Time-to-event (overall survival) analysis for γδ T cells in the primary tumour stroma*. Patients deemed 'High' or 'Low' for γδ T cells are shaded blue and red, respectively. Cox hazard ratio is univariate – see table 4.3 for multivariate. The 'Low' group is used as the reference group on cox regression modelling.*

In the primary tumour tissue, patients deemed high for γδ T cells are associated with a worse prognosis (Figure 4.12). Patients with a high level of γδ T cells had a mean survival time of 79.61 months, compared to those with low levels of γδ T cells with a mean survival of 105.61 months (hazard ratio = 1.85, p = 0.03). 5-year survival for patients high for γδ T cells is 52% (46%, 59%), compared to 71% (57%, 90%) in the γδ low group. This suggests that γδ T cells in the whole tissue of the primary tumour are associated with an unfavourable prognostic role. Multivariate analysis was not statistically significant (hazard ratio = 1.49, p = 0.4) (Table 4.3), suggesting that γδ T cells in the whole tissue of the adjacent normal tissue are not independently prognostic.

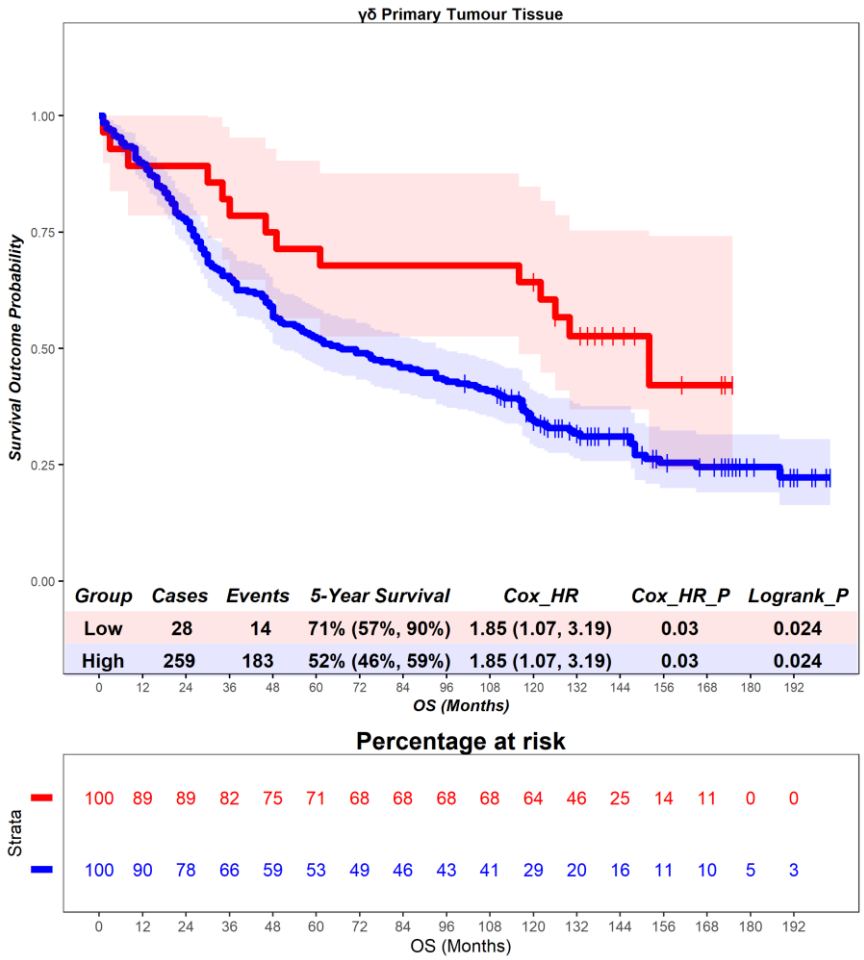

Figure 4.12 – Scotland cohort. Time-to-event (overall survival) analysis for γδ T cells in the primary tumour tissue*. Patients deemed 'High' or 'Low' for γδ T cells are shaded blue and red, respectively. Cox hazard ratio is univariate – see table 4.3 for multivariate. The 'Low' group is used as the reference group on cox regression modelling.*

4.2.3 γδ T cells - disease-free survival

In the adjacent normal epithelium, patients deemed high for γδ T cells are associated with a worse prognosis (Figure 4.13), although this result did not reach statistical significance. Patients with a high level of γδ T cells had a mean survival time of 69.25 months, compared to those with low levels of γδ T cells with a mean survival of 93.79 months (hazard ratio = 1.5, p = 0.05). 5-year survival for patients high for γδ T cells is 46% (34%, 62%), compared to 64% (55%, 73%) in the γδ low group. This suggests that γδ T cells in the epithelial compartment of the adjacent normal tissue are associated with an unfavourable prognostic role. Multivariate analysis was not statistically significant (hazard ratio = 1.45, p = 0.09) (Table 4.3), suggesting that γδ T cells in the epithelial compartment of the adjacent normal tissue are not independently prognostic.

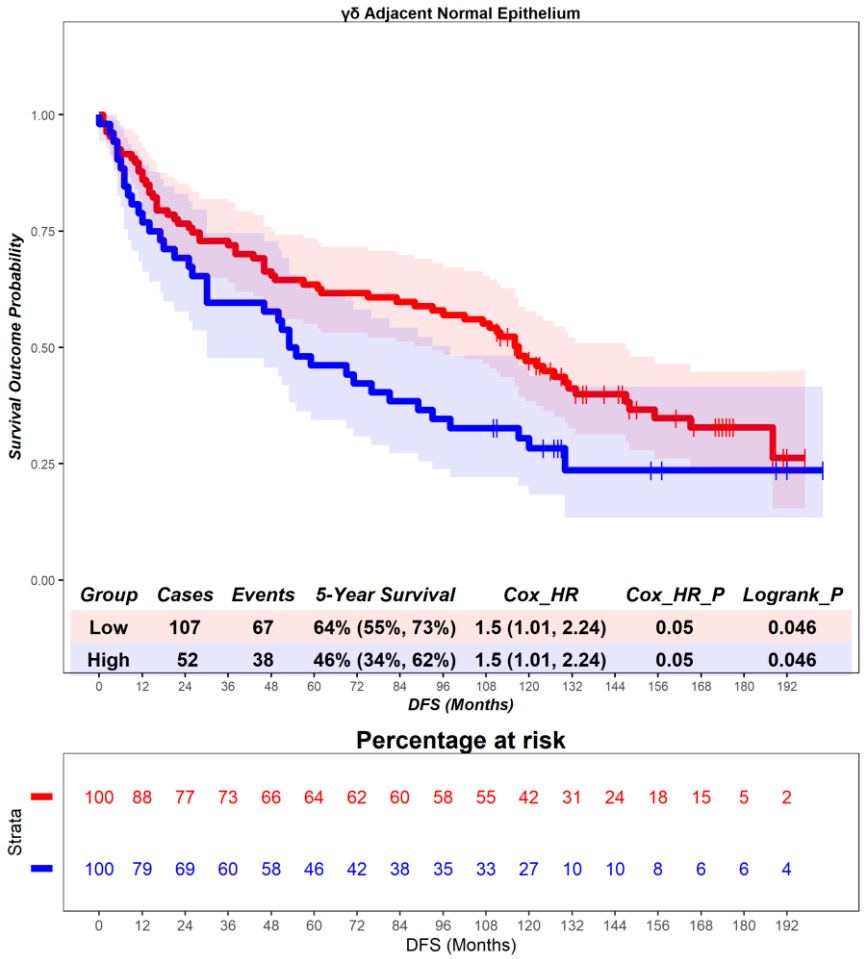

Figure 4.13 – Scotland cohort. Time-to-event (disease-free survival) analysis for γδ T cells in the adjacent normal epithelium*. Patients deemed 'High' or 'Low' for γδ T cells are shaded blue and red, respectively. Cox hazard ratio is univariate – see table 4.3 for multivariate. The 'Low' group is used as the reference group on cox regression modelling.*

In the adjacent normal stroma, patients deemed high for γδ T cells are associated with a worse prognosis (Figure 4.14), although this result did not reach statistical significance. Patients with a high level of γδ T cells had a mean survival time of 67.57 months, compared to those with low levels of γδ T cells with a mean survival of 93.4 months (hazard ratio = 1.52, p = 0.05). 5-year survival for patients high for γδ T cells is 46% (34%, 62%), compared to 64% (55%, 73%) in the γδ low group. This suggests that γδ T cells in the stromal compartment of the adjacent normal tissue are associated with an unfavourable prognostic role. Multivariate analysis was not statistically significant (hazard ratio = 1.44, p = 0.1) (Table 4.3), suggesting that γδ T cells in the stromal compartment of the adjacent normal tissue are not independently prognostic.

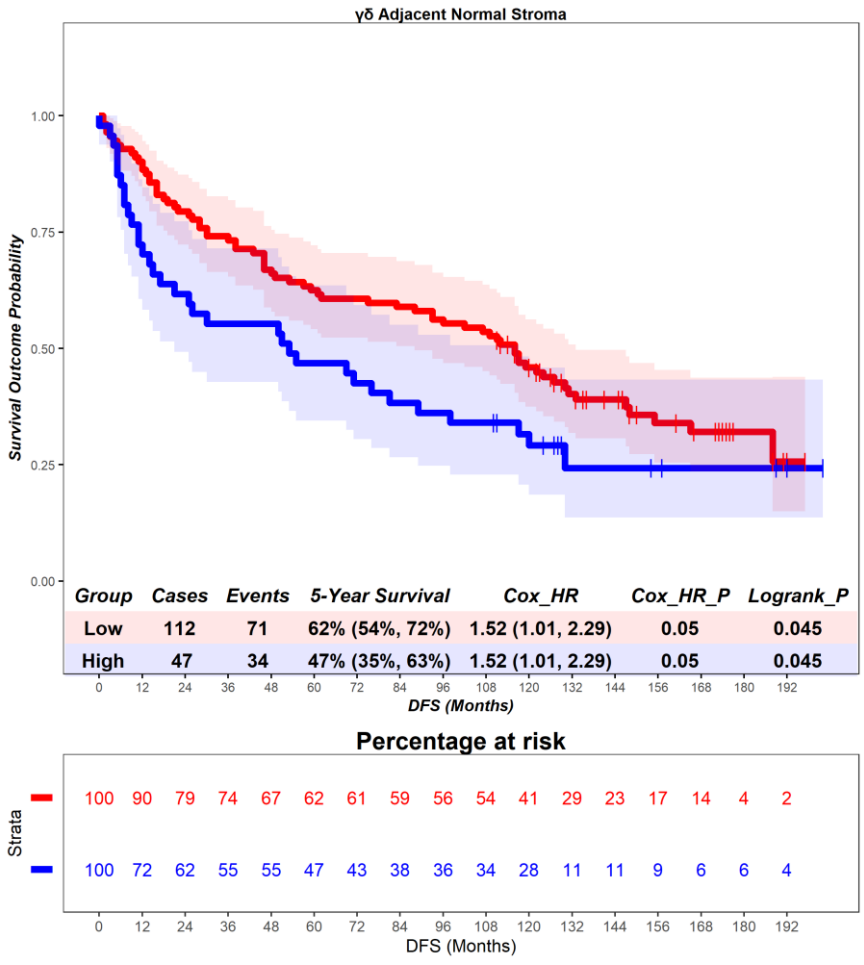

Figure 4.14 – Scotland cohort. Time-to-event (disease-free survival) analysis for γδ T cells in the adjacent normal stroma. *Patients deemed 'High' or 'Low' for γδ T cells are shaded blue and red, respectively. Cox hazard ratio is univariate – see table 4.3 for multivariate. The 'Low' group is used as the reference group on cox regression modelling.*

In the adjacent normal tissue, patients deemed high for γδ T cells are associated with a worse prognosis (Figure 4.15). Patients with a high level of γδ T cells had a mean survival time of 70.98 months, compared to those with low levels of γδ T cells with a mean survival of 94.03 months (hazard ratio = 1.51, p = 0.04). 5-year survival for patients high for γδ T cells is 47% (36%, 62%), compared to 64% (55%, 74%) in the γδ low group. This suggests that γδ T cells in the whole tissue of the adjacent normal tissue are associated with an unfavourable prognostic role. Multivariate analysis was not statistically significant (hazard ratio = 1.45, p = 0.09) (Table 4.3), suggesting that γδ T cells in the whole tissue of the adjacent normal tissue are not independently prognostic.

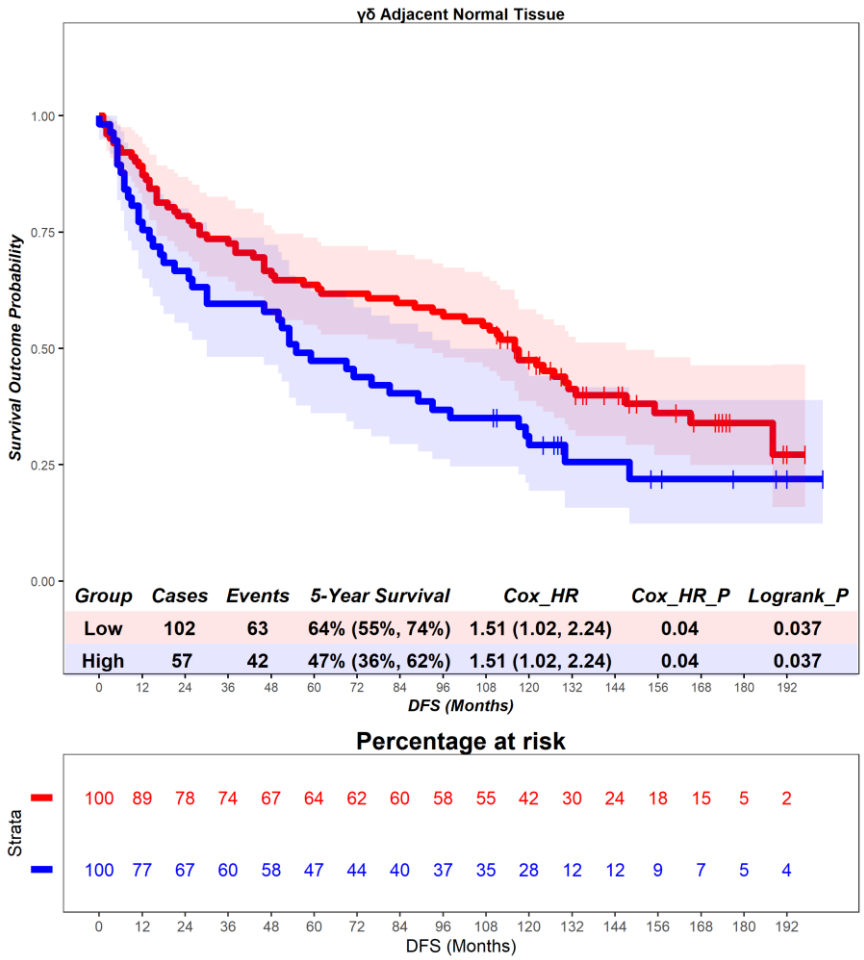

Figure 4.15 – Scotland cohort. Time-to-event (disease-free survival) analysis for γδ T cells in the adjacent normal tissue*. Patients deemed 'High' or 'Low' for γδ T cells are shaded blue and red, respectively. Cox hazard ratio is univariate – see table 4.3 for multivariate. The 'Low' group is used as the reference group on cox regression modelling.*

In the primary tumour epithelium, patients deemed high for γδ T cells are associated with a worse prognosis (Figure 4.16), although this result did not reach statistical significance. Patients with a high level of γδ T cells had a mean survival time of 73.76 months, compared to those with low levels of γδ T cells with a mean survival of 93.79 months (hazard ratio = 1.5, p = 0.09). 5-year survival for patients high for γδ T cells is 47% (42%, 54%), compared to 71% (57%, 89%) in the γδ low group. This suggests that γδ T cells in the epithelial compartment of the primary tumour are associated with an unfavourable prognostic role. Multivariate analysis was not statistically significant (hazard ratio = 1.35, p = 0.27) (Table 4.3), suggesting that γδ T cells in the epithelial compartment of the primary tumour are not independently prognostic.

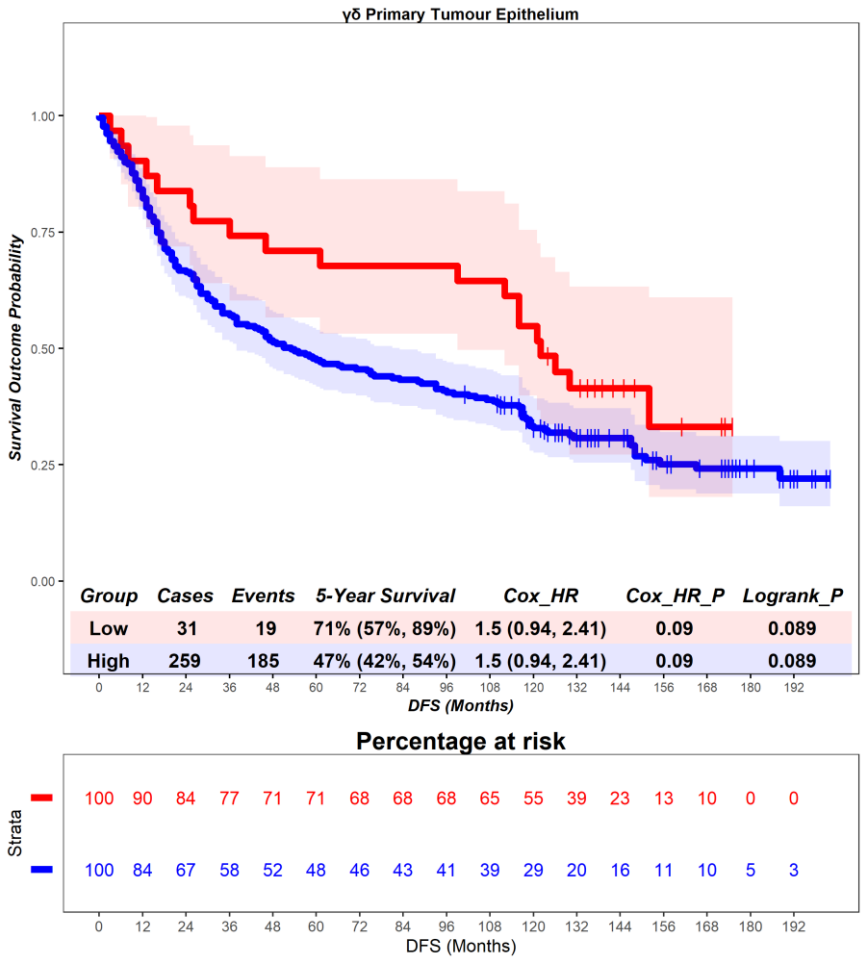

Figure 4.16 – Scotland cohort. Time-to-event (disease-free survival) analysis for γδ T cells in the primary tumour epithelium*. Patients deemed 'High' or 'Low' for γδ T cells are shaded blue and red, respectively. Cox hazard ratio is univariate – see table 4.3 for multivariate. The 'Low' group is used as the reference group on cox regression modelling.*

In the primary tumour stroma, patients deemed high for γδ T cells are associated with a worse prognosis (Figure 4.17). Patients with a high level of γδ T cells had a mean survival time of 73.08 months, compared to those with low levels of γδ T cells with a mean survival of 109.75 months (hazard ratio = 2.08, p = 0.01). 5-year survival for patients high for γδ T cells is 47% (42%, 54%), compared to 75% (61%, 93%) in the γδ low group. This suggests that γδ T cells in the stromal compartment of the primary tumour are associated with an unfavourable prognostic role. Multivariate analysis was not statistically significant (hazard ratio = 1.67, p = 0.07) (Table 4.3), suggesting that γδ T cells in the stromal compartment of the primary tumour are not independently prognostic.

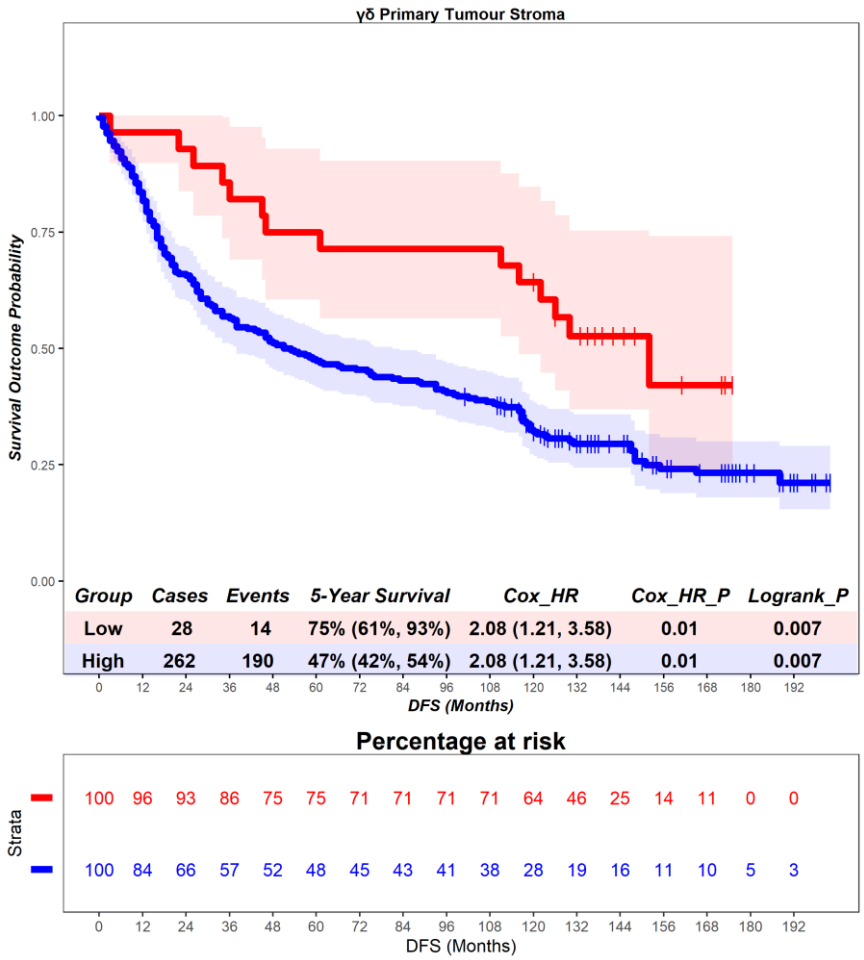

Figure 4.17 – Scotland cohort. Time-to-event (disease-free survival) analysis for γδ T cells in the primary tumour stroma*. Patients deemed 'High' or 'Low' for γδ T cells are shaded blue and red, respectively. Cox hazard ratio is univariate – see table 4.3 for multivariate. The 'Low' group is used as the reference group on cox regression modelling.*

In the primary tumour, patients deemed high for γδ T cells are associated with a worse prognosis (Figure 4.18). Patients with a high level of γδ T cells had a mean survival time of 73.65 months, compared to those with low levels of γδ T cells with a mean survival of 104.5 months (hazard ratio = 1.96, p = 0.02). 5-year survival for patients high for γδ T cells is 48% (42%, 54%), compared to 71% (57%, 90%) in the γδ low group. This suggests that γδ T cells in the whole tissue of the primary tumour are associated with an unfavourable prognostic role. Multivariate analysis was not statistically significant (hazard ratio = 1.53, p = 0.14) (Table 4.3), suggesting that γδ T cells in the whole tissue of the primary tumour are not independently prognostic.

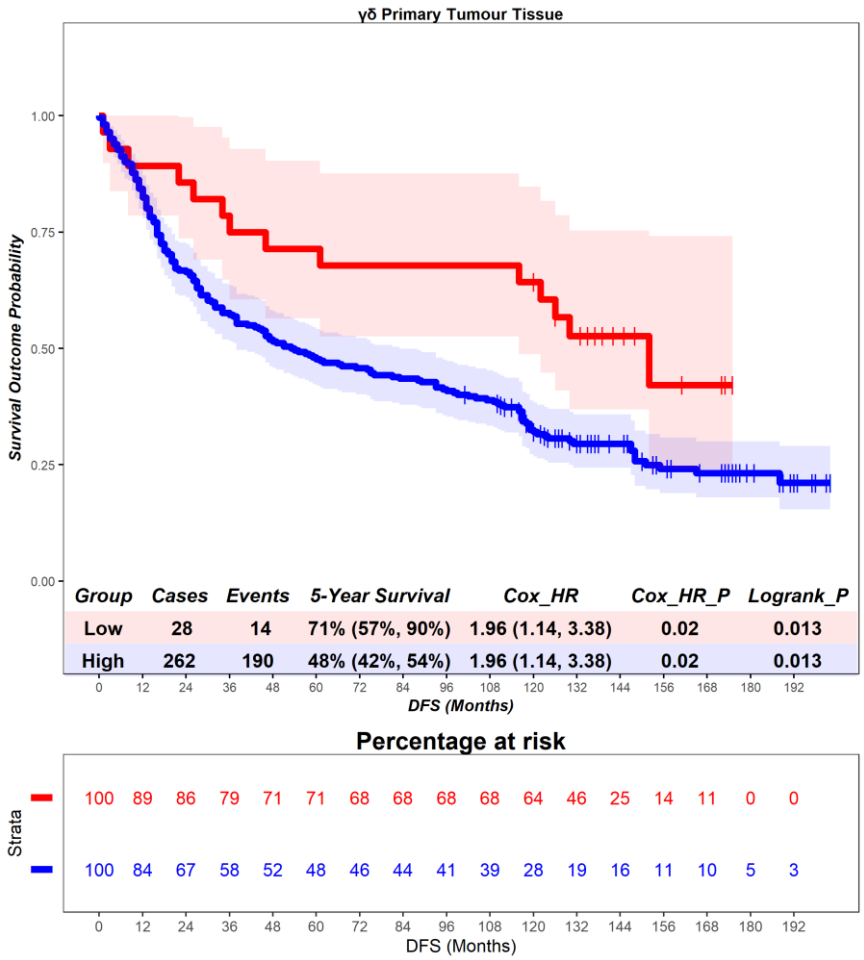

Figure 4.18 – Scotland cohort. Time-to-event (disease-free survival) analysis for γδ T cells in the primary tumour tissue*. Patients deemed 'High' or 'Low' for γδ T cells are shaded blue and red, respectively. Cox hazard ratio is univariate – see table 4.3 for multivariate. The 'Low' group is used as the reference group on cox regression modelling.*

4.2.4 γδ T cells - recurrence-free survival

In the adjacent normal epithelium, patients deemed high for γδ T cells are associated with a worse prognosis (Figure 4.19), although this result did not reach statistical significance. Patients with a high level of γδ T cells had a mean survival time of 68.08 months, compared to those with low levels of γδ T cells with a mean survival of 86.01 months (hazard ratio = 1.64, p = 0.1). 5-year survival for patients high for γδ T cells is 56% (43%, 73%), compared to 69% (59%, 81%) in the γδ low group. This suggests that γδ T cells in the epithelial compartment of the adjacent normal tissue are associated with an unfavourable prognostic role. Multivariate analysis was not statistically significant (hazard ratio = 1.62, p = 0.17) (Table 4.3), suggesting that γδ T cells in the epithelial compartment of the adjacent normal tissue are not independently prognostic.

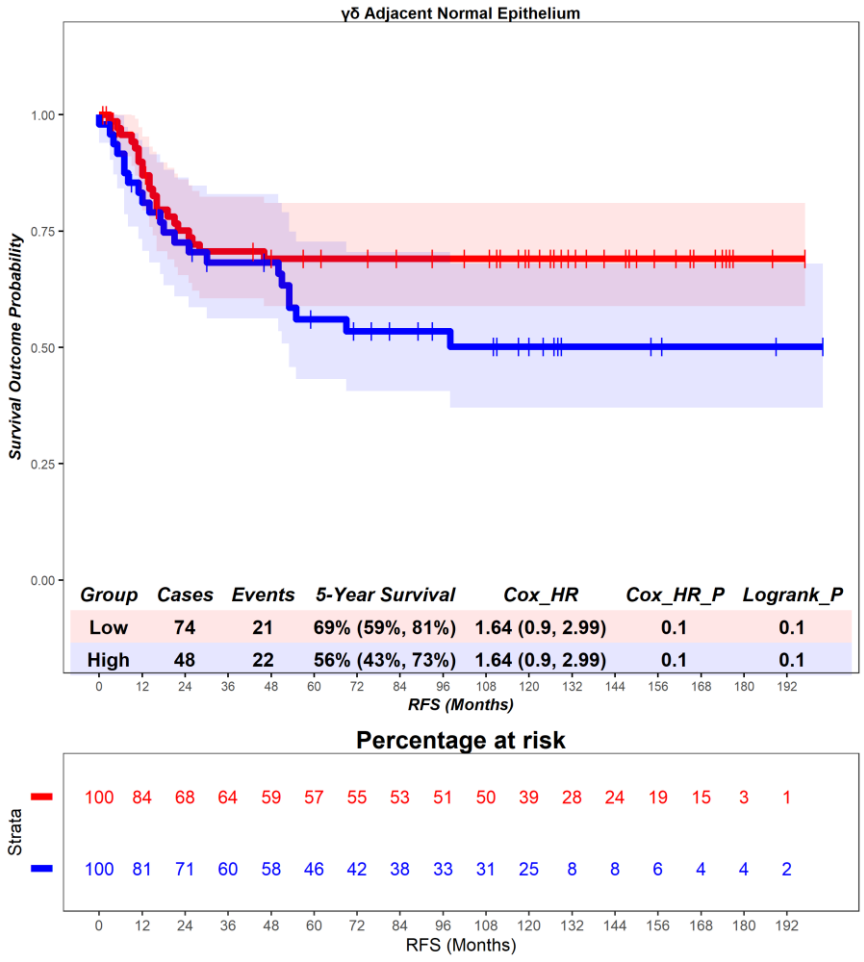

Figure 4.19 – Scotland cohort. Time-to-event (recurrence-free survival) analysis for γδ T cells in the adjacent normal epithelium*. Patients deemed 'High' or 'Low' for γδ T cells are shaded blue and red, respectively. Cox hazard ratio is univariate – see table 4.3 for multivariate. The 'Low' group is used as the reference group on cox regression modelling.*

In the adjacent normal stroma, patients deemed high for γδ T cells are associated with a worse prognosis (Figure 4.20). Patients with a high level of γδ T cells had a mean survival time of 66.12 months, compared to those with low levels of γδ T cells with a mean survival of 85.95 months (hazard ratio = 2.18, p = 0.01). 5-year survival for patients high for γδ T cells is 51% (38%, 69%), compared to 71% (62%, 82%) in the γδ low group. This suggests that γδ T cells in the stromal compartment of the adjacent normal tissue are associated with an unfavourable prognostic role. Multivariate analysis was not statistically significant (hazard ratio = 1.86, p = 0.07) (Table 4.3), suggesting that γδ T cells in the stromal compartment of the adjacent normal tissue are not independently prognostic.

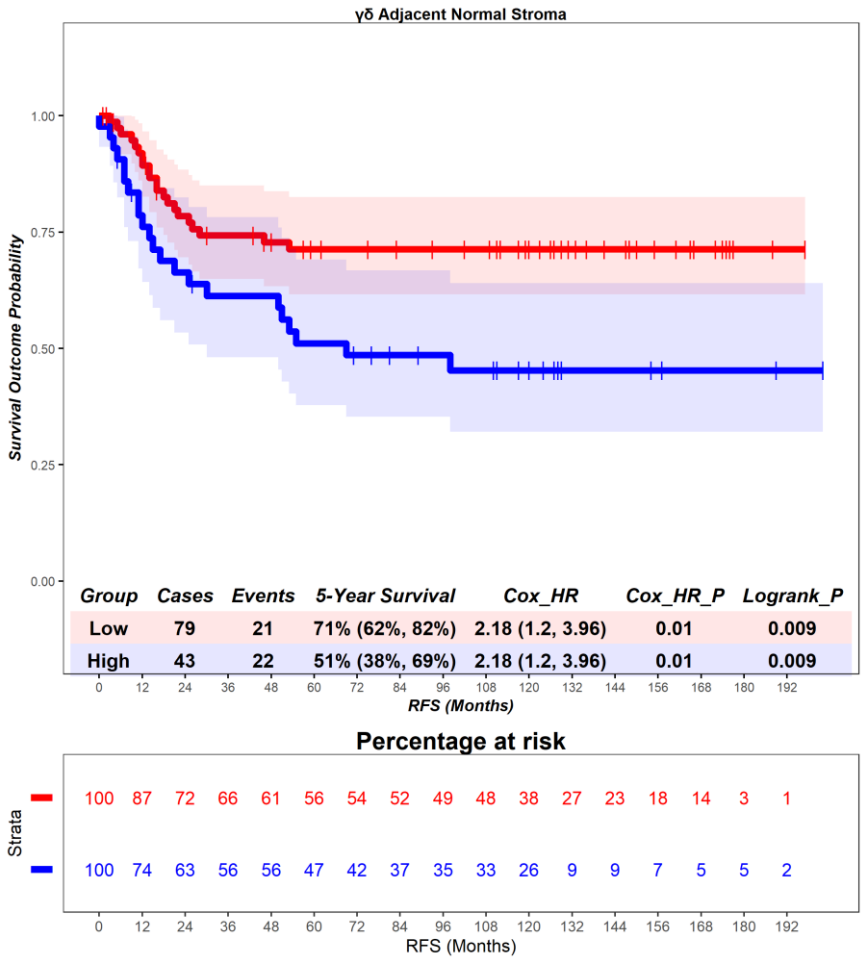

Figure 4.20 – Scotland cohort. Time-to-event (recurrence-free survival) analysis for γδ T cells in the adjacent normal stroma*. Patients deemed 'High' or 'Low' for γδ T cells are shaded blue and red, respectively. Cox hazard ratio is univariate – see table 4.3 for multivariate. The 'Low' group is used as the reference group on cox regression modelling.*

In the adjacent normal tissue, patients deemed high for γδ T cells are associated with a worse prognosis (Figure 4.21), although this result did not reach statistical significance. Patients with a high level of γδ T cells had a mean survival time of 70.06 months, compared to those with low levels of γδ T cells with a mean survival of 85.8 months (hazard ratio = 1.72, p = 0.08). 5-year survival for patients high for γδ T cells is 56% (44%, 72%), compared to 70% (60%, 82%) in the γδ low group. This suggests that γδ T cells in the whole tissue of the adjacent normal tissue are associated with an unfavourable prognostic role. Multivariate analysis was not statistically significant (hazard ratio = 1.49, p = 0.29) (Table 4.3), suggesting that γδ T cells in the whole tissue of the adjacent normal tissue are not independently prognostic.

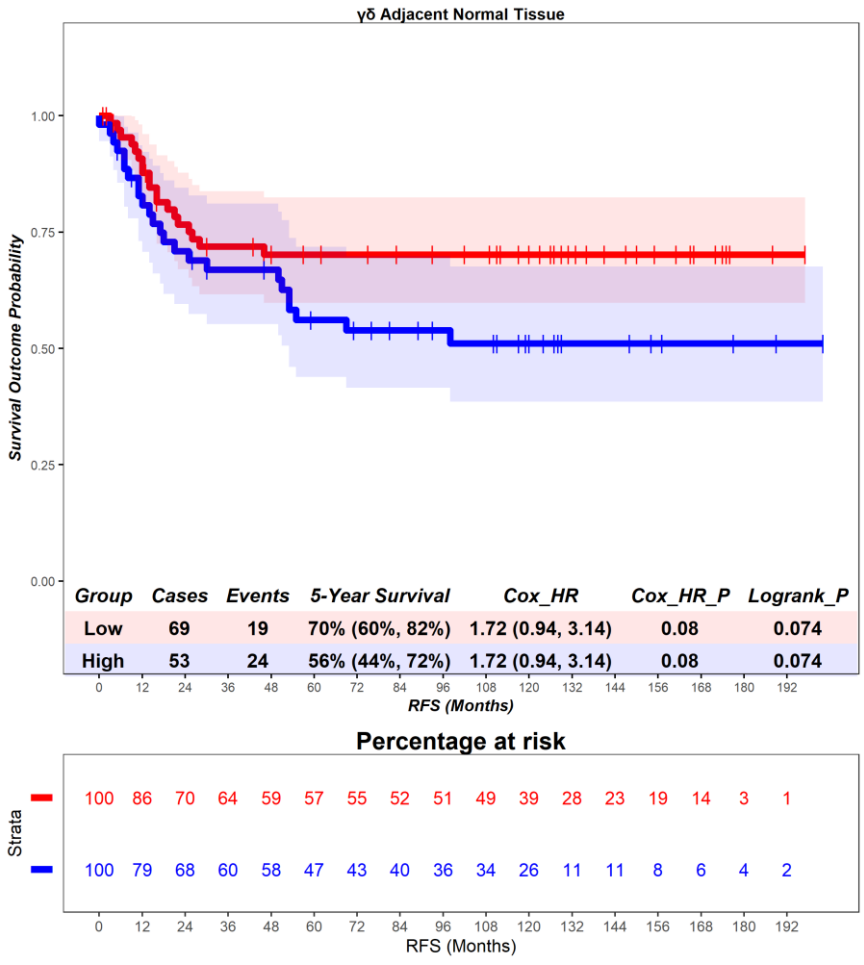

Figure 4.21 – Scotland cohort. Time-to-event (recurrence-free survival) analysis for γδ T cells in the adjacent normal tissue*. Patients deemed 'High' or 'Low' for γδ T cells are shaded blue and red, respectively. Cox hazard ratio is univariate – see table 4.3 for multivariate. The 'Low' group is used as the reference group on cox regression modelling.*

In the primary tumour epithelium, patients deemed high for γδ T cells are associated with a worse prognosis (Figure 4.22), although this result did not reach statistical significance. Patients with a high level of γδ T cells had a mean survival time of 71.07 months, compared to those with low levels of γδ T cells with a mean survival of 64.0 months (hazard ratio = 1.87, p = 0.53). 5-year survival for patients high for γδ T cells is 55% (48%, 63%), compared to 67% (30%, 100%) in the γδ low group. This suggests that γδ T cells in the epithelial compartment of the primary tumour are associated with an unfavourable prognostic role. Multivariate analysis was not statistically significant (hazard ratio = 0.65, p = 0.68) (Table 4.3), suggesting that γδ T cells in the epithelial compartment of the primary tumour are not independently prognostic.

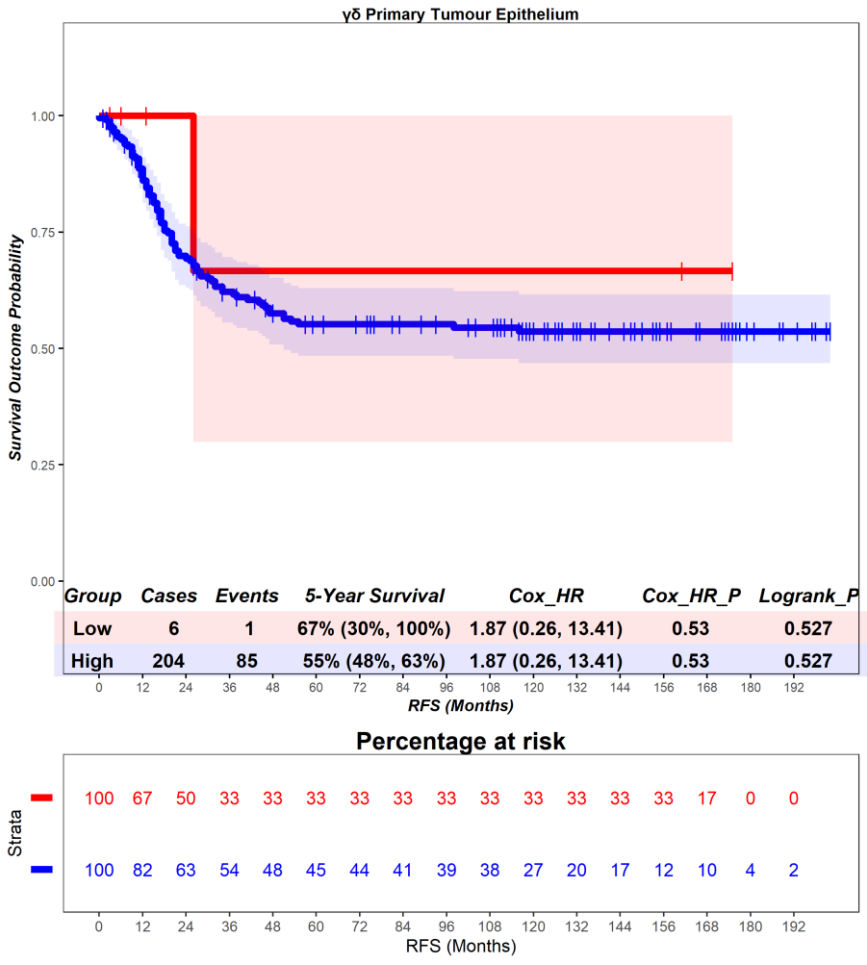

Figure 4.22 – Scotland cohort. Time-to-event (recurrence-free survival) analysis for γδ T cells in the primary tumour epithelium*. Patients deemed 'High' or 'Low' for γδ T cells are shaded blue and red, respectively. Cox hazard ratio is univariate – see table 4.3 for multivariate. The 'Low' group is used as the reference group on cox regression modelling.*

In the primary tumour stroma, patients deemed high for γδ T cells are associated with a worse prognosis (Figure 4.23), although this result did not reach statistical significance. Patients with a high level of γδ T cells had a mean survival time of 70.12 months, compared to those with low levels of γδ T cells with a mean survival of 87.67 months (hazard ratio = 1.47, p = 0.52). 5-year survival for patients high for γδ T cells is 55% (48%, 63%), compared to 62% (37%, 100%) in the γδ low group. This suggests that γδ T cells in the stromal compartment of the primary tumour are associated with an unfavourable prognostic role. Multivariate analysis was not statistically significant (hazard ratio = 0.87, p = 0.82) (Table 4.3), suggesting that γδ T cells in the stromal compartment of the primary tumour are not independently prognostic.

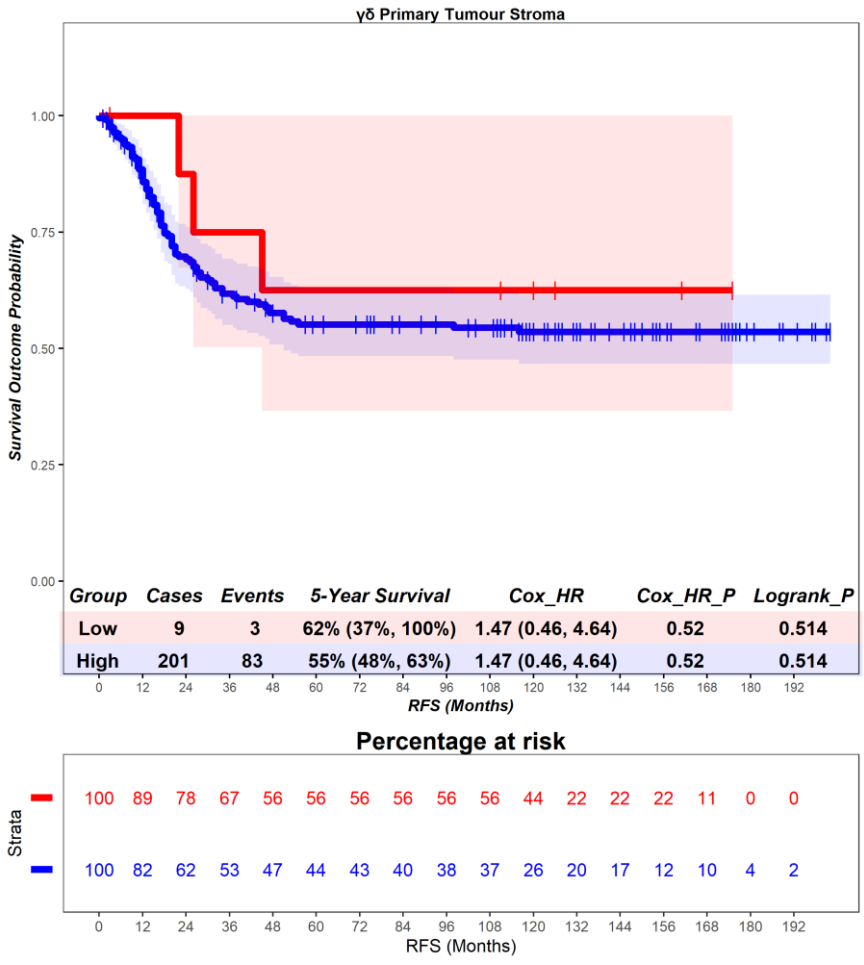

Figure 4.23 – Scotland cohort. Time-to-event (recurrence-free survival) analysis for γδ T cells in the primary tumour stroma*. Patients deemed 'High' or 'Low' for γδ T cells are shaded blue and red, respectively. Cox hazard ratio is univariate – see table 4.3 for multivariate. The 'Low' group is used as the reference group on cox regression modelling.*

In the primary tumour tissue, patients deemed high for γδ T cells are associated with a worse prognosis (Figure 4.24), although this result did not reach statistical significance. Patients with a high level of γδ T cells had a mean survival time of 70.2 months, compared to those with low levels of γδ T cells with a mean survival of 90.43 months (hazard ratio = 1.63, p = 0.5). 5-year survival for patients high for γδ T cells is 55% (48%, 63%), compared to 67% (38%, 100%) in the γδ low group. This suggests that γδ T cells in the whole tissue of the primary tumour are associated with an unfavourable prognostic role. Multivariate analysis was not statistically significant (hazard ratio = 0.54, p = 0.42) (Table 4.3), suggesting that γδ T cells in the whole tissue of the primary tumour are not independently prognostic.

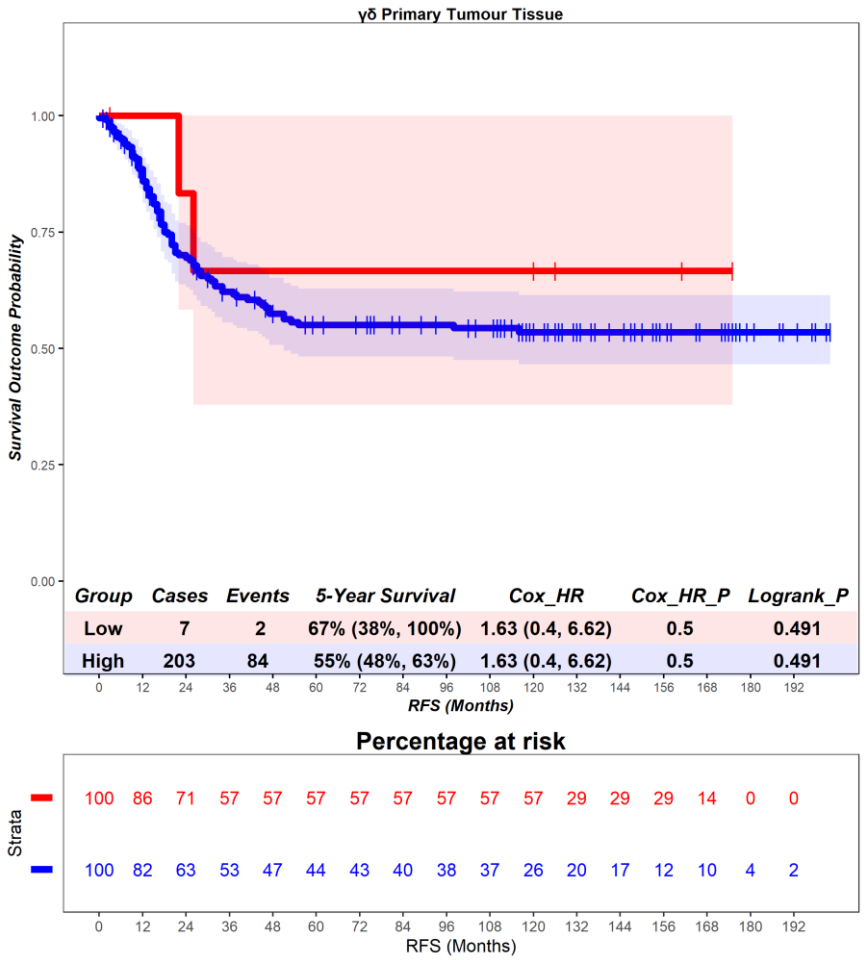

Figure 4.24 – Scotland cohort. Time-to-event (recurrence-free survival) analysis for γδ T cells in the primary tumour tissue*. Patients deemed 'High' or 'Low' for γδ T cells are shaded blue and red, respectively. Cox hazard ratio is univariate – see table 4.3 for multivariate. The 'Low' group is used as the reference group on cox regression modelling.*

4.2.5 CD8 T cells - cancer-specific survival

In the adjacent normal epithelium, patients deemed high for CD8 T cells are associated with a better prognosis (Figure 4.25), although this result did not reach statistical significance. Patients with a high level of CD8 T cells had a mean survival time of 94.12 months, compared to those with low levels of CD8 T cells with a mean survival of 78.68 months (hazard ratio = 0.65, p = 0.15). 5-year survival for patients high for CD8 T cells is 73% (66%, 81%), compared to 63% (48%, 83%) in the CD8 low group. This suggests that CD8 T cells in the epithelial compartment of the adjacent normal tissue are associated with a favourable prognostic role. Multivariate analysis was statistically significant (hazard ratio = 0.46, p = 0.03) (Table 4.3), suggesting that CD8 T cells in the epithelial compartment of the adjacent normal tissue are independently prognostic.

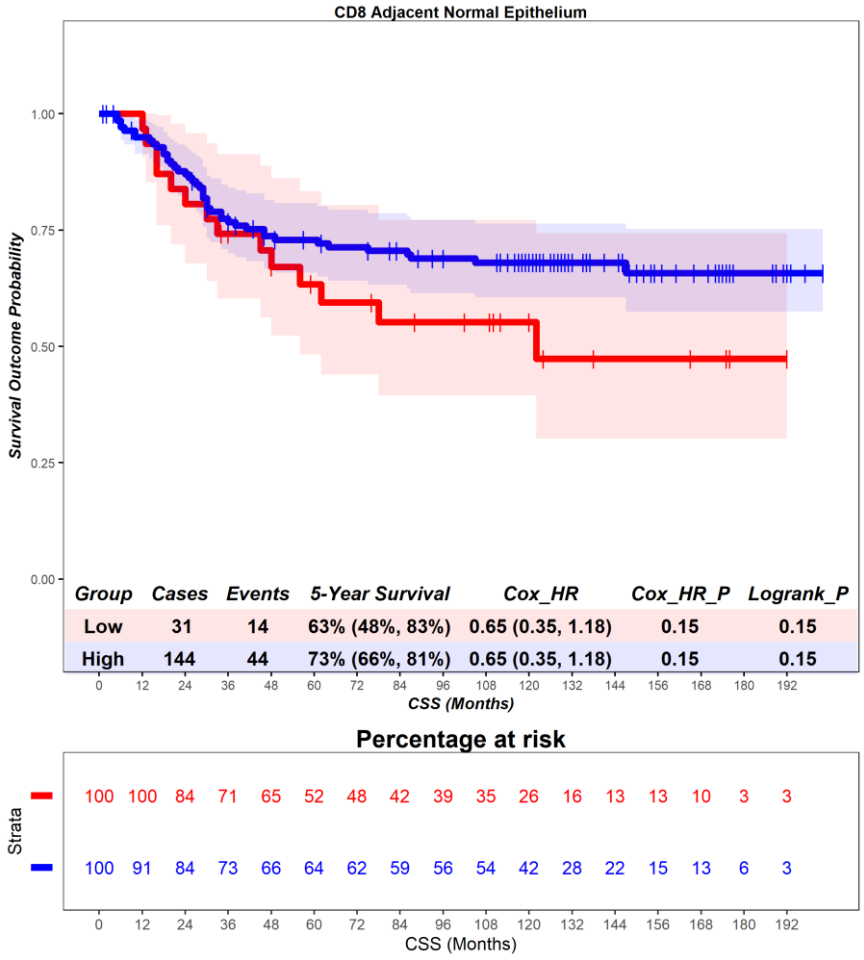

Figure 4.25 – Scotland cohort. Time-to-event (cancer-specific survival) analysis for CD8 T cells in the adjacent normal epithelium. *Patients deemed 'High' or 'Low' for CD8 T cells are shaded blue and red, respectively. Cox hazard ratio is univariate – see table 4.3 for multivariate. The 'Low' group is used as the reference group on cox regression modelling.*

In the adjacent normal stroma, patients deemed high for CD8 T cells are associated with a worse prognosis (Figure 4.26), although this result did not reach statistical significance. Patients with a high level of CD8 T cells had a mean survival time of 89.58 months, compared to those with low levels of CD8 T cells with a mean survival of 95.5 months (hazard ratio = 1.59, p = 0.14). 5-year survival for patients high for CD8 T cells is 69% (61%, 78%), compared to 77% (66%, 90%) in the CD8 low group. This suggests that CD8 T cells in the stromal compartment of the adjacent normal tissue are associated with an unfavourable prognostic role. Multivariate analysis was not statistically significant (hazard ratio = 1.39, p = 0.36) (Table 4.3), suggesting that CD8 T cells in the stromal compartment of the adjacent normal tissue are independently prognostic.

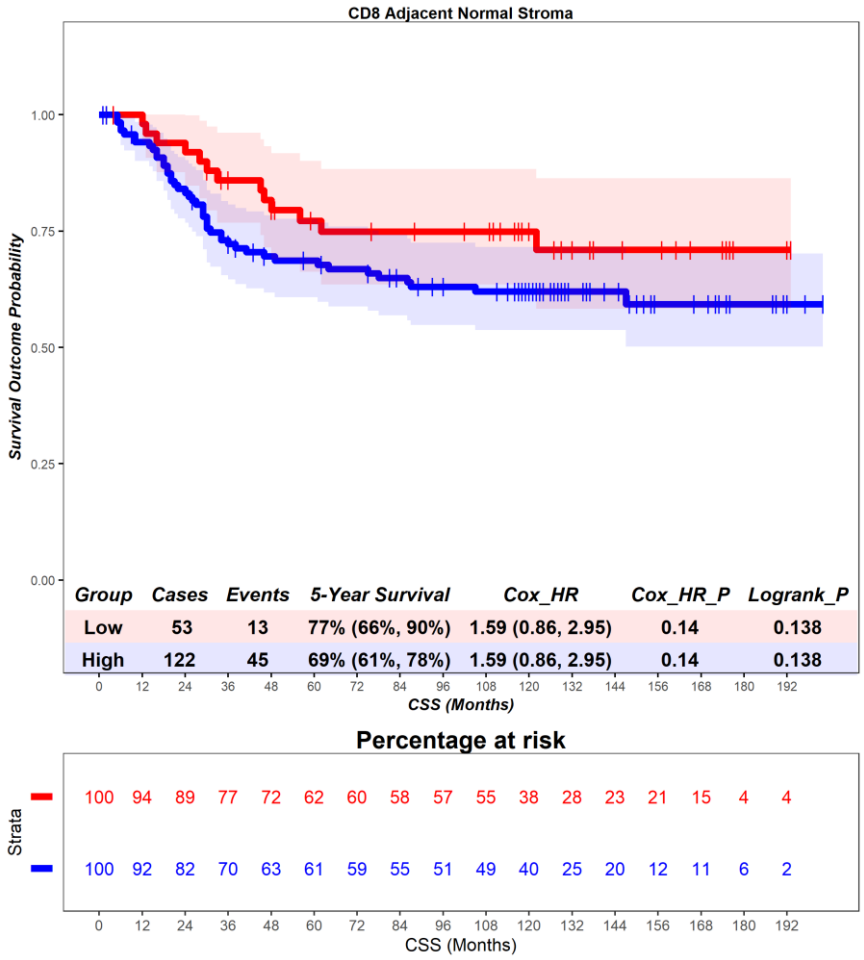

Figure 4.26 – Scotland cohort. Time-to-event (cancer-specific survival) analysis for CD8 T cells in the adjacent normal stroma. *Patients deemed 'High' or 'Low' for CD8 T cells are shaded blue and red, respectively. Cox hazard ratio is univariate – see table 4.3 for multivariate. The 'Low' group is used as the reference group on cox regression modelling.*

In the adjacent normal tissue, patients deemed high for CD8 T cells are associated with no differential prognosis (Figure 4.27), although this result did not reach statistical significance. Patients with a high level of CD8 T cells had a mean survival time of 99.29 months, compared to those with low levels of CD8 T cells with a mean survival of 90.13 months (hazard ratio = 0.56, p = 0.22). 5-year survival for patients high for CD8 T cells is 79% (64%, 97%), compared to 70% (63%, 78%) in the CD8 low group. This suggests that CD8 T cells in the whole tissue compartment of the adjacent normal tissue are associated with no differential prognostic role. Multivariate analysis was not statistically significant (hazard ratio = 0.74, p = 0.53) (Table 4.3), suggesting that CD8 T cells in the epithelial compartment of the adjacent normal tissue are not independently prognostic.

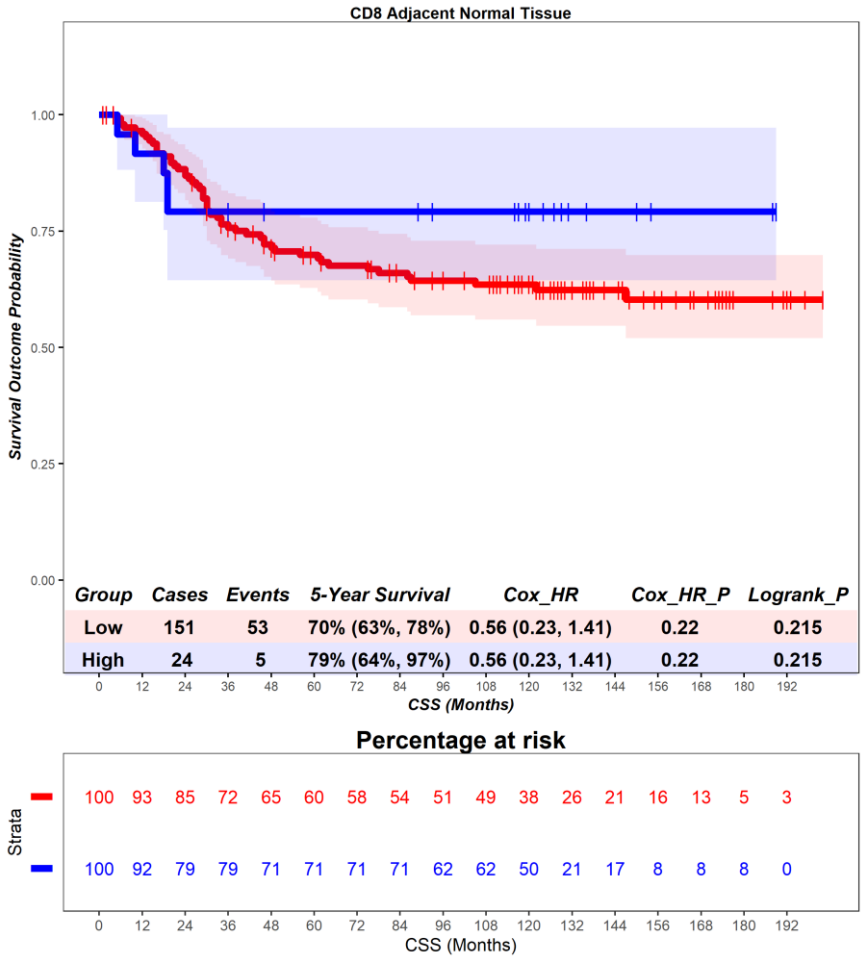

Figure 4.27 – Scotland cohort. Time-to-event (cancer-specific survival) analysis for CD8 T cells in the adjacent normal tissue. *Patients deemed 'High' or 'Low' for CD8 T cells are shaded blue and red, respectively. Cox hazard ratio is univariate – see table 4.3 for multivariate. The 'Low' group is used as the reference group on cox regression modelling.*

In the primary tumour epithelium, patients deemed high for CD8 T cells are associated with a better prognosis (Figure 4.28). Patients with a high level of CD8 T cells had a mean survival time of 87.9 months, compared to those with low levels of CD8 T cells with a mean survival of 83.97 months (hazard ratio = 0.46, p = 0.02). 5-year survival for patients high for CD8 T cells is 83% (73%, 95%), compared to 62% (56%, 69%) in the CD8 low group. This suggests that CD8 T cells in the epithelial compartment of the primary tumour are associated with a favourable prognostic role. Multivariate analysis was not statistically significant (hazard ratio = 0.52, p = 0.06) (Table 4.3), suggesting that CD8 T cells in the epithelial compartment of the primary tumour are not independently prognostic.

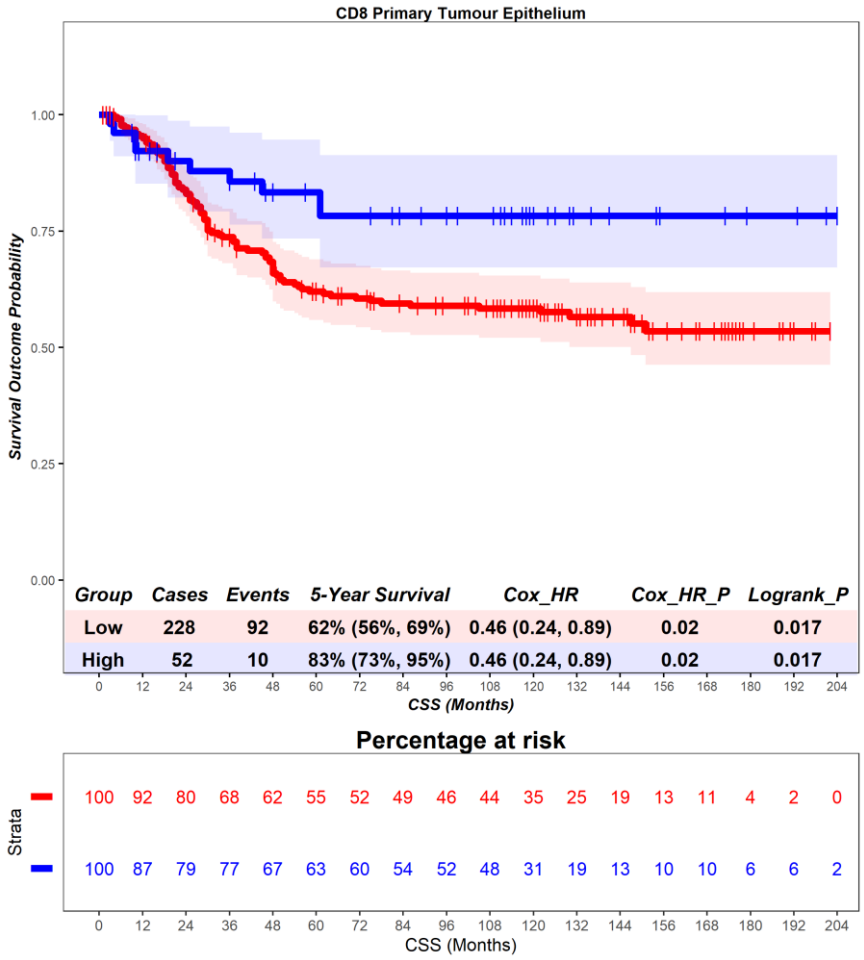

Figure 4.28 – Scotland cohort. Time-to-event (cancer-specific survival) analysis for CD8 T cells in the primary tumour epithelium. *Patients deemed 'High' or 'Low' for CD8 T are shaded blue and red, respectively. Cox hazard ratio is univariate – see table 4.3 for multivariate. The 'Low' group is used as the reference group on cox regression modelling.*

In the primary tumour stroma, patients deemed high for CD8 T cells are associated with a better prognosis (Figure 4.29). Patients with a high level of CD8 T cells had a mean survival time of 86.26 months, compared to those with low levels of CD8 T cells with a mean survival of 78.76 months (hazard ratio = 0.63, p = 0.04). 5-year survival for patients high for CD8 T cells is 69% (63%, 76%), compared to 52% (40%, 67%) in the CD8 low group. This suggests that CD8 T cells in the stromal compartment of the primary tumour are associated with a favourable prognostic role. Multivariate analysis was statistically significant (hazard ratio = 0.52, p = 0.01) (Table 4.3), suggesting that CD8 T cells in the stromal compartment of the primary tumour are independently prognostic.

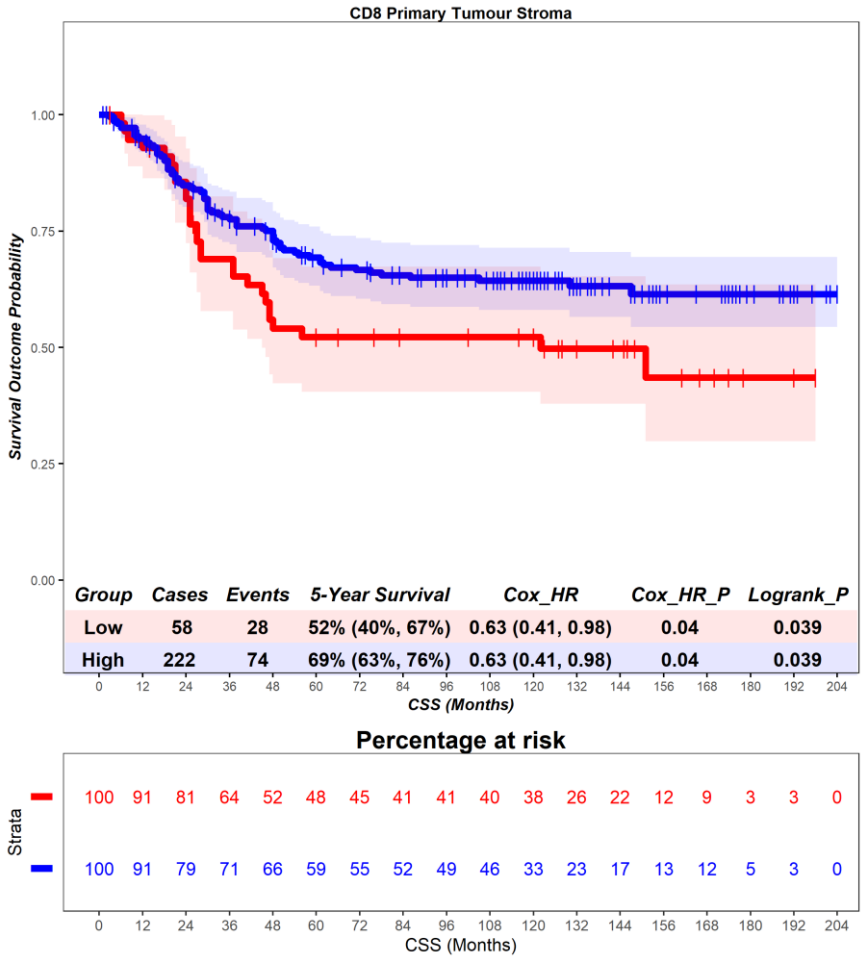

Figure 4.29 – Scotland cohort. Time-to-event (cancer-specific survival) analysis for CD8 T cells in the primary tumour stroma. *Patients deemed 'High' or 'Low' for CD8 T are shaded blue and red, respectively. Cox hazard ratio is univariate – see table 4.3 for multivariate. The 'Low' group is used as the reference group on cox regression modelling.*

In the primary tumour tissue, patients deemed high for CD8 T cells are associated with a better prognosis (Figure 4.30). Patients with a high level of CD8 T cells had a mean survival time of 93.71 months, compared to those with low levels of CD8 T cells with a mean survival of 83.42 months (hazard ratio = 0.33, p = 0.02). 5-year survival for patients high for CD8 T cells is 87% (77%, 100%), compared to 63% (57%, 69%) in the CD8 low group. This suggests that CD8 T cells in the whole tissue of the primary tumour are associated with a favourable prognostic role. Multivariate analysis was statistically significant (hazard ratio = 0.38, p = 0.04) (Table 4.3), suggesting that CD8 T cells in the whole tissue of the primary tumour are independently prognostic.

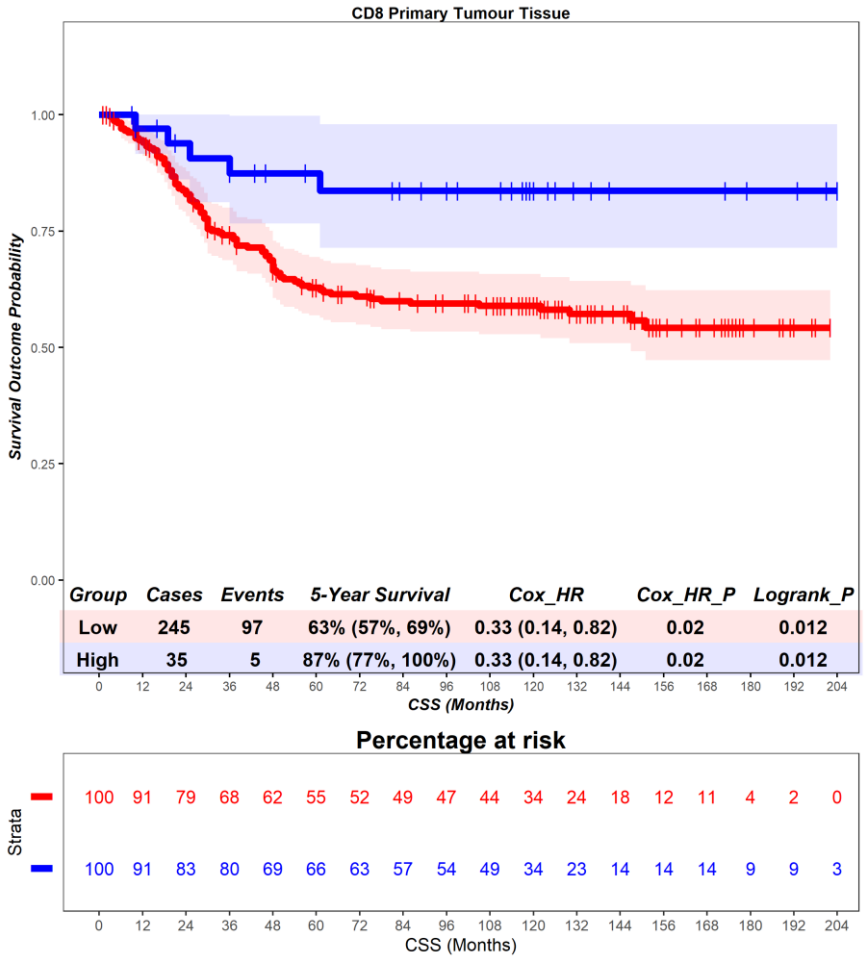

Figure 4.30 – Scotland cohort. Time-to-event (cancer-specific survival) analysis for CD8 T cells in the primary tumour tissue. *Patients deemed 'High' or 'Low' for CD8 T are shaded blue and red, respectively. Cox hazard ratio is univariate – see table 4.3 for multivariate. The 'Low' group is used as the reference group on cox regression modelling.*

4.2.6 CD8 T cells - overall survival

In the adjacent normal epithelium, patients deemed high for CD8 T cells are associated with a better prognosis (Figure 4.31). Patients with a high level of CD8 T cells had a mean survival time of 94.12 months, compared to those with low levels of CD8 T cells with a mean survival of 78.68 months (hazard ratio = 0.62, p = 0.04). 5-year survival for patients high for CD8 T cells is 64% (57%, 72%), compared to 52% (37%, 73%) in the CD8 low group. This suggests that CD8 T cells in the epithelial compartment of the adjacent normal tissue are associated with a favourable prognostic role. Multivariate analysis was statistically significant (hazard ratio = 0.59, p = 0.03) (Table 4.3), suggesting that CD8 T cells in the epithelial compartment of the adjacent normal tissue are independently prognostic.

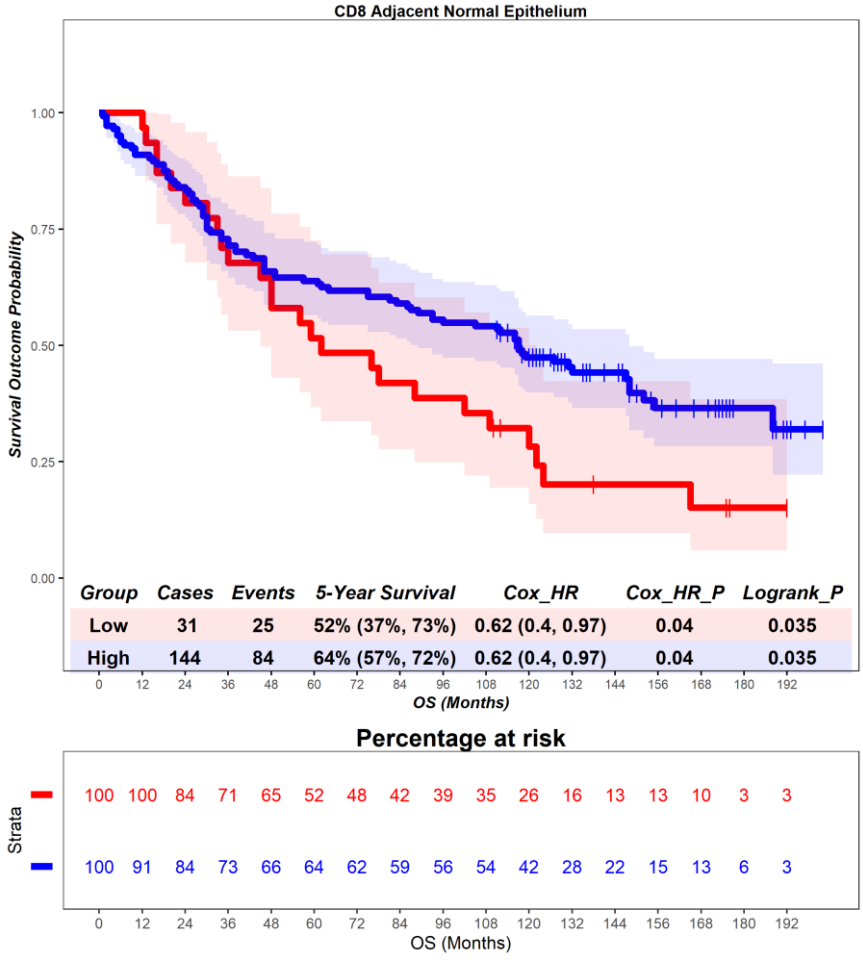

Figure 4.31 – Scotland cohort. Time-to-event (overall survival) analysis for CD8 T cells in the adjacent normal epithelium. *Patients deemed 'High' or 'Low' for CD8 T cells are shaded blue and red, respectively. Cox hazard ratio is univariate – see table 4.3 for multivariate. The 'Low' group is used as the reference group on cox regression modelling.*

In the adjacent normal stroma, patients deemed high for CD8 T cells are associated with no differential prognosis (Figure 4.32). Patients with a high level of CD8 T cells had a mean survival time of 89.58 months, compared to those with low levels of CD8 T cells with a mean survival of 95.55 months (hazard ratio = 1.11, p = 0.62). 5-year survival for patients high for CD8 T cells is 61% (53%, 71%), compared to 62% (50%, 77%) in the CD8 low group. This suggests that CD8 T cells in the stromal compartment of the adjacent normal tissue are associated with no differential prognostic role. Multivariate analysis was not statistically significant (hazard ratio = 1.12, p = 0.61) (Table 4.3), suggesting that CD8 T cells in the stromal compartment of the adjacent normal tissue are not independently prognostic.

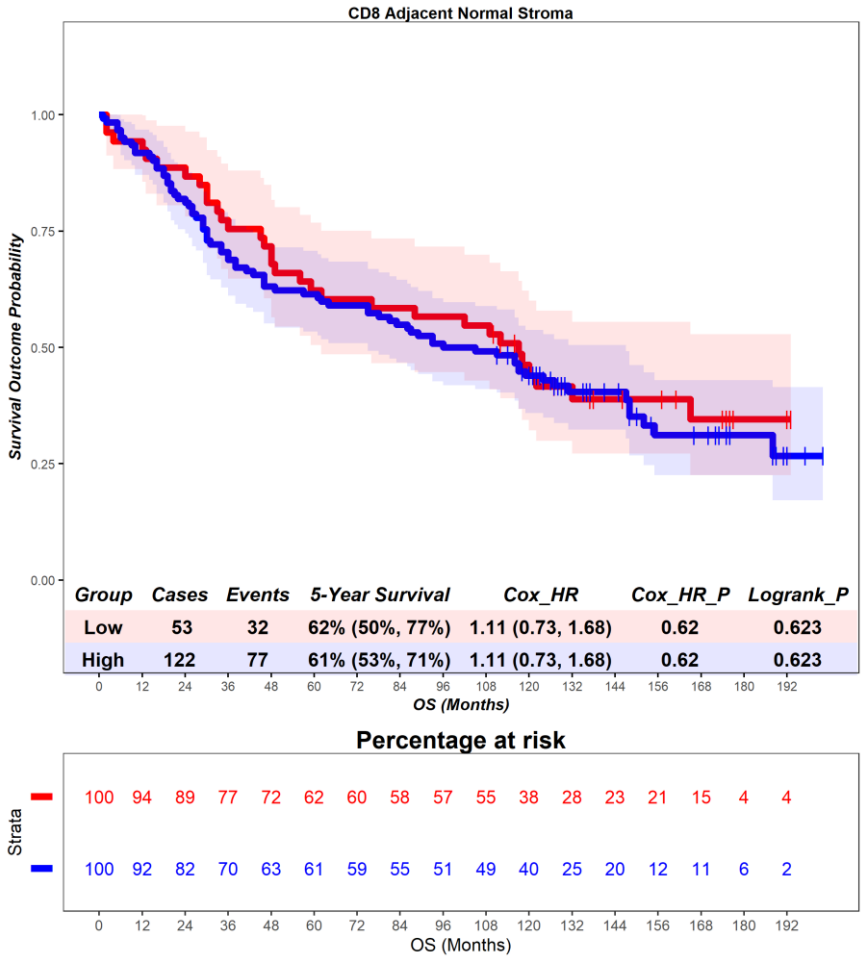

Figure 4.32 – Scotland cohort. Time-to-event (overall survival) analysis for CD8 T cells in the adjacent normal stroma. *Patients deemed 'High' or 'Low' for CD8 T cells are shaded blue and red, respectively. Cox hazard ratio is univariate – see table 4.3 for multivariate. The 'Low' group is used as the reference group on cox regression modelling.*

In the adjacent normal tissue, patients deemed high for CD8 T cells are associated with no differential prognosis (Figure 4.33). Patients with a high level of CD8 T cells had a mean survival time of 82.68 months, compared to those with low levels of CD8 T cells with a mean survival of 97.46 months (hazard ratio = 0.91, p = 0.75). 5-year survival for patients high for CD8 T cells is 71% (55%, 92%), compared to 60% (53%, 69%) in the CD8 low group. This suggests that CD8 T cells in the whole tissue of the adjacent normal tissue are associated with no differential prognostic role. Multivariate analysis was not statistically significant (hazard ratio = 0.87, p = 0.63) (Table 4.3), suggesting that CD8 T cells in the whole tissue of the adjacent normal tissue are not independently prognostic.

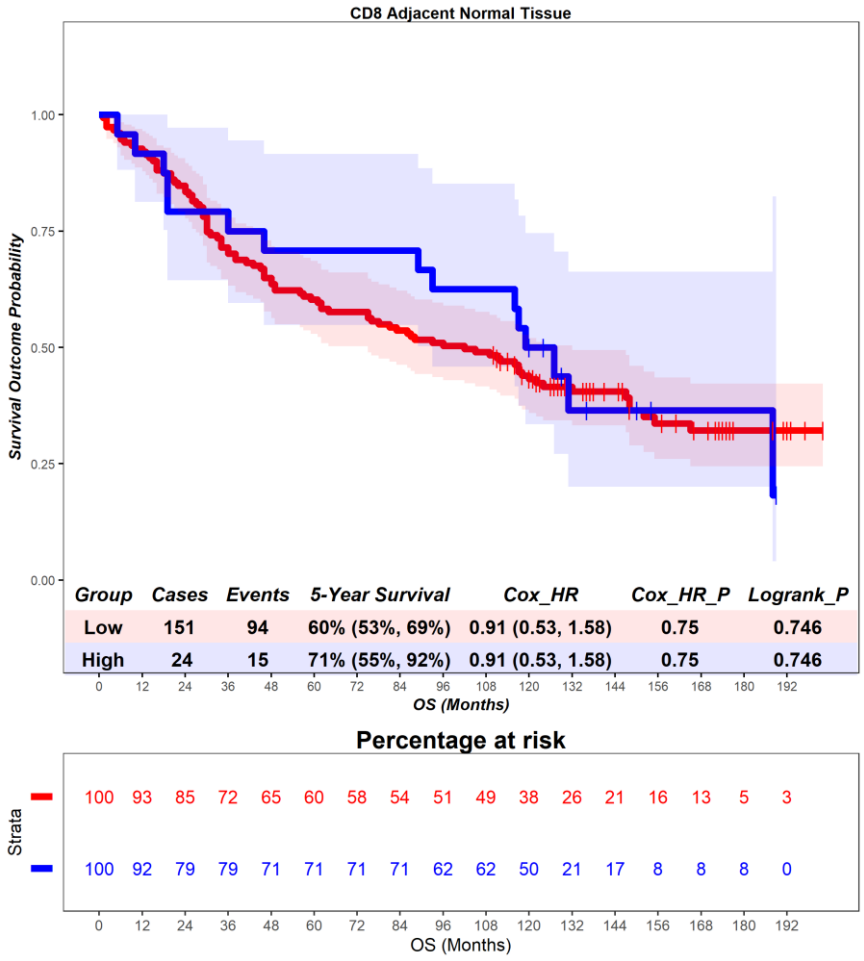

Figure 4.33 – Scotland cohort. Time-to-event (overall survival) analysis for CD8 T cells in the adjacent normal tissue. *Patients deemed 'High' or 'Low' for CD8 T cells are shaded blue and red, respectively. Cox hazard ratio is univariate – see table 4.3 for multivariate. The 'Low' group is used as the reference group on cox regression modelling.*

In the primary tumour epithelium, patients deemed high for CD8 T cells are associated with no differential prognosis (Figure 4.34). Patients with a high level of CD8 T cells had a mean survival time of 87.9 months, compared to those with low levels of CD8 T cells with a mean survival of 83.97 months (hazard ratio = 0.96, p = 0.81). 5-year survival for patients high for CD8 T cells is 63% (52%, 78%), compared to 54% (48%, 61%) in the CD8 low group. This suggests that CD8 T cells in the epithelial compartment of the primary tumour are associated with no differential prognostic role. Multivariate analysis was not statistically significant (hazard ratio = 0.85, p = 0.41) (Table 4.3), suggesting that CD8 T cells in the epithelial compartment of the primary tumour are not independently prognostic.

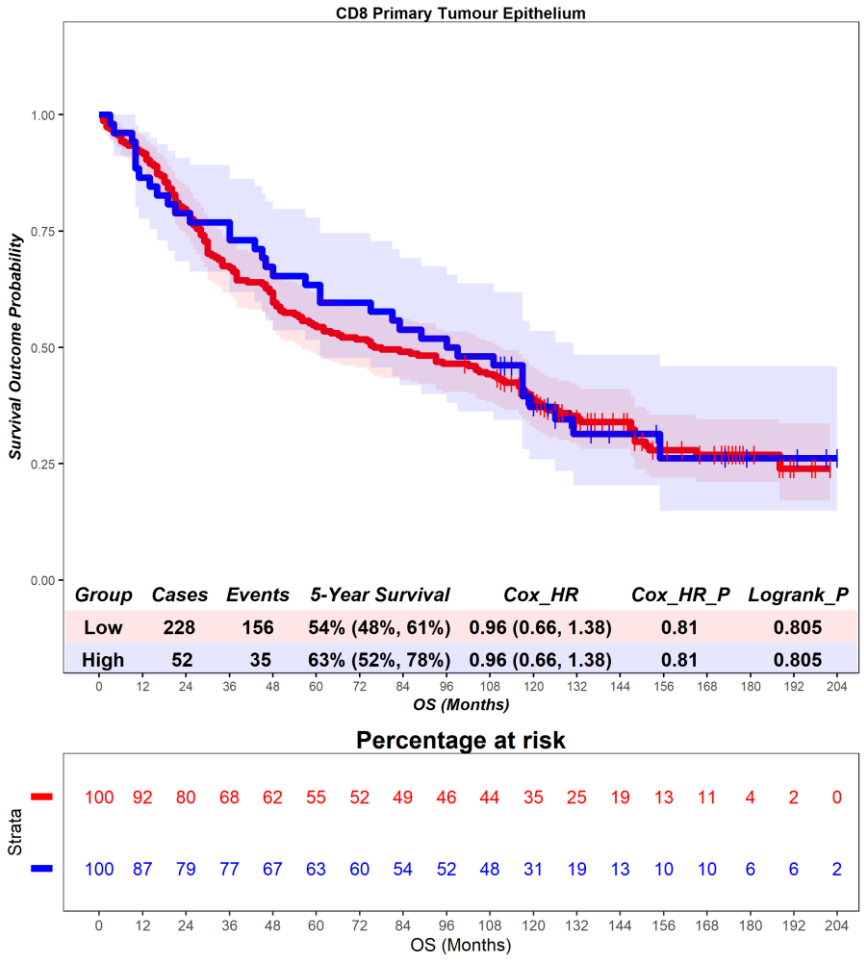

Figure 4.34 – Scotland cohort. Time-to-event (overall survival) analysis for CD8 T cells in the primary tumour epithelium. *Patients deemed 'High' or 'Low' for CD8 T cells are shaded blue and red, respectively. Cox hazard ratio is univariate – see table 4.3 for multivariate. The 'Low' group is used as the reference group on cox regression modelling.*

In the primary tumour stroma, patients deemed high for CD8 T cells are associated with no differential prognosis (Figure 4.35). Patients with a high level of CD8 T cells had a mean survival time of 86.26 months, compared to those with low levels of CD8 T cells with a mean survival of 78.76 months (hazard ratio = 0.89, p = 0.5). 5-year survival for patients high for CD8 T cells is 59% (52%, 65%), compared to 47% (35%, 61%) in the CD8 low group. This suggests that CD8 T cells in the stromal compartment of the primary tumour are associated with no differential prognostic role. Multivariate analysis was not statistically significant (hazard ratio = 0.82, p = 0.26) (Table 4.3), suggesting that CD8 T cells in the stromal compartment of the primary tumour are not independently prognostic.

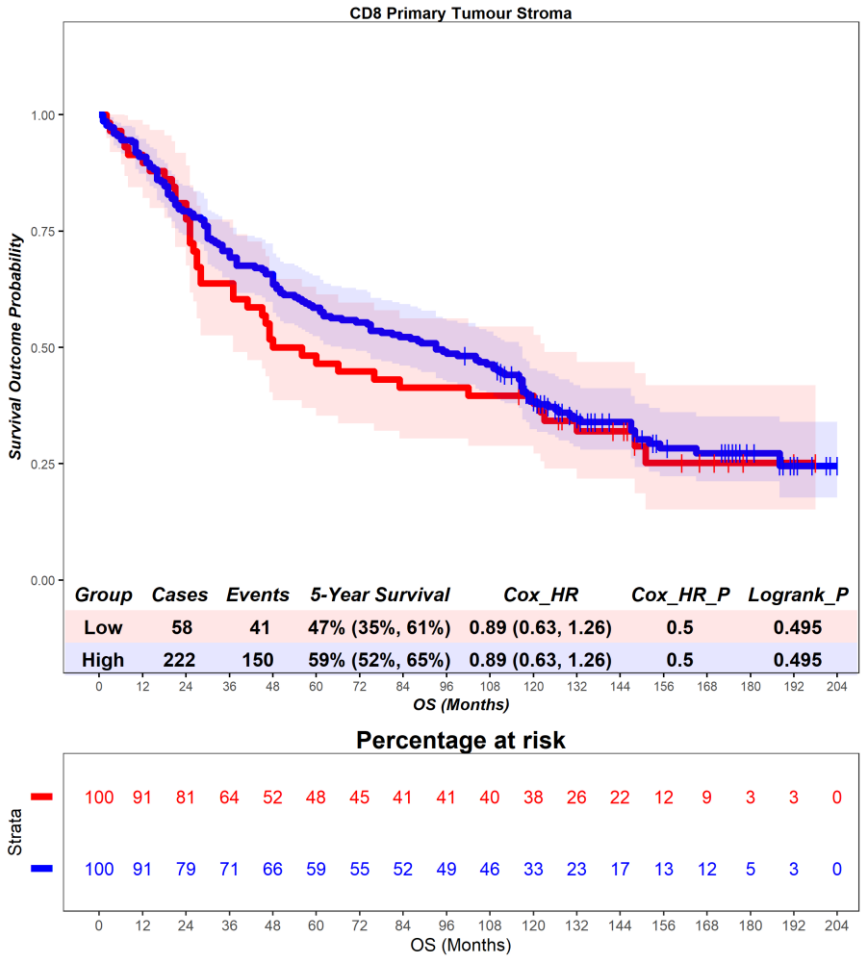

Figure 4.35 – Scotland cohort. Time-to-event (overall survival) analysis for CD8 T cells in the primary tumour stroma. *Patients deemed 'High' or 'Low' for CD8 T cells are shaded blue and red, respectively. Cox hazard ratio is univariate – see table 4.3 for multivariate. The 'Low' group is used as the reference group on cox regression modelling.*

In the primary tumour tissue, patients deemed high for CD8 T cells are associated with no differential prognosis (Figure 4.36). Patients with a high level of CD8 T cells had a mean survival time of 93.71 months, compared to those with low levels of CD8 T cells with a mean survival of 83.42 months (hazard ratio = 0.83, p = 0.42). 5-year survival for patients high for CD8 T cells is 66% (52%, 83%), compared to 55% (49%, 61%) in the CD8 low group. This suggests that CD8 T cells in the whole tissue of the primary tumour are associated with no differential prognostic role. Multivariate analysis was not statistically significant (hazard ratio = 0.65, p = 0.07) (Table 4.3), suggesting that CD8 T cells in the whole tissue of the primary tumour are not independently prognostic.

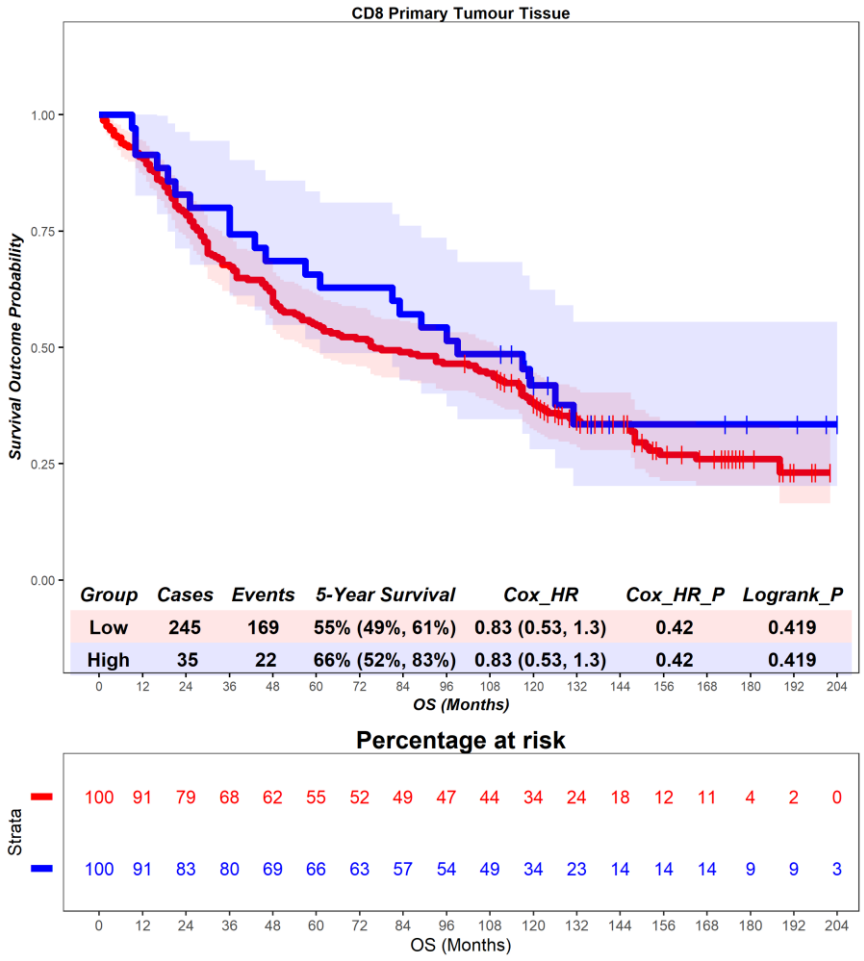

Figure 4.36 – Scotland cohort. Time-to-event (overall survival) analysis for CD8 T cells in the primary tumour tissue. *Patients deemed 'High' or 'Low' for CD8 T cells are shaded blue and red, respectively. Cox hazard ratio is univariate – see table 4.3 for multivariate. The 'Low' group is used as the reference group on cox regression modelling.*

4.2.7 CD8 T cells - disease-free survival

In the adjacent normal epithelium, patients deemed high for CD8 T cells are associated with a better prognosis (Figure 4.37), although this result did not reach statistical significance. Patients with a high level of CD8 T cells had a mean survival time of 87.32 months, compared to those with low levels of CD8 T cells with a mean survival of 73.16 months (hazard ratio = 0.67, p = 0.08). 5-year survival for patients high for CD8 T cells is 59% (51%, 67%), compared to 45% (31%, 67%) in the CD8 low group. This suggests that CD8 T cells in the epithelial compartment of the adjacent normal tissue are associated with a favourable prognostic role. Multivariate analysis was statistically significant (hazard ratio = 0.59, p = 0.03) (Table 4.3), suggesting that CD8 T cells in the epithelial compartment of the adjacent normal tissue are independently prognostic.

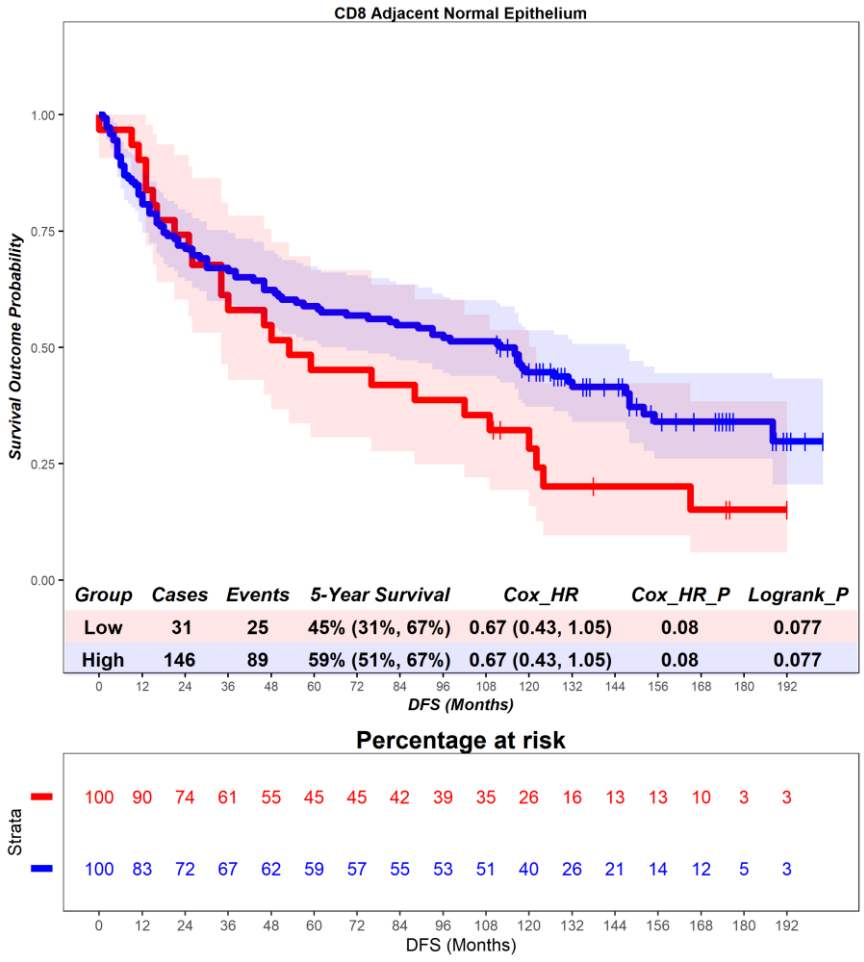

Figure 4.37 – Scotland cohort. Time-to-event (disease-free survival) analysis for CD8 T cells in the adjacent normal epithelium. *Patients deemed 'High' or 'Low' for CD8 T cells are shaded blue and red, respectively. Cox hazard ratio is univariate – see table 4.3 for multivariate. The 'Low' group is used as the reference group on cox regression modelling.*

In the adjacent normal stroma, patients deemed high for CD8 T cells are associated with a worse prognosis (Figure 4.38), although this result did not reach statistical significance. Patients with a high level of CD8 T cells had a mean survival time of 81.63 months, compared to those with low levels of CD8 T cells with a mean survival of 92.17 months (hazard ratio = 1.2, p = 0.39). 5-year survival for patients high for CD8 T cells is 55% (47%, 65%), compared to 59% (48%, 74%) in the CD8 low group. This suggests that CD8 T cells in the stromal compartment of the adjacent normal tissue are associated with an unfavourable prognostic role. Multivariate analysis was not statistically significant (hazard ratio = 1.11, p = 0.64) (Table 4.3), suggesting that CD8 T cells in the stromal compartment of the adjacent normal tissue are not independently prognostic.

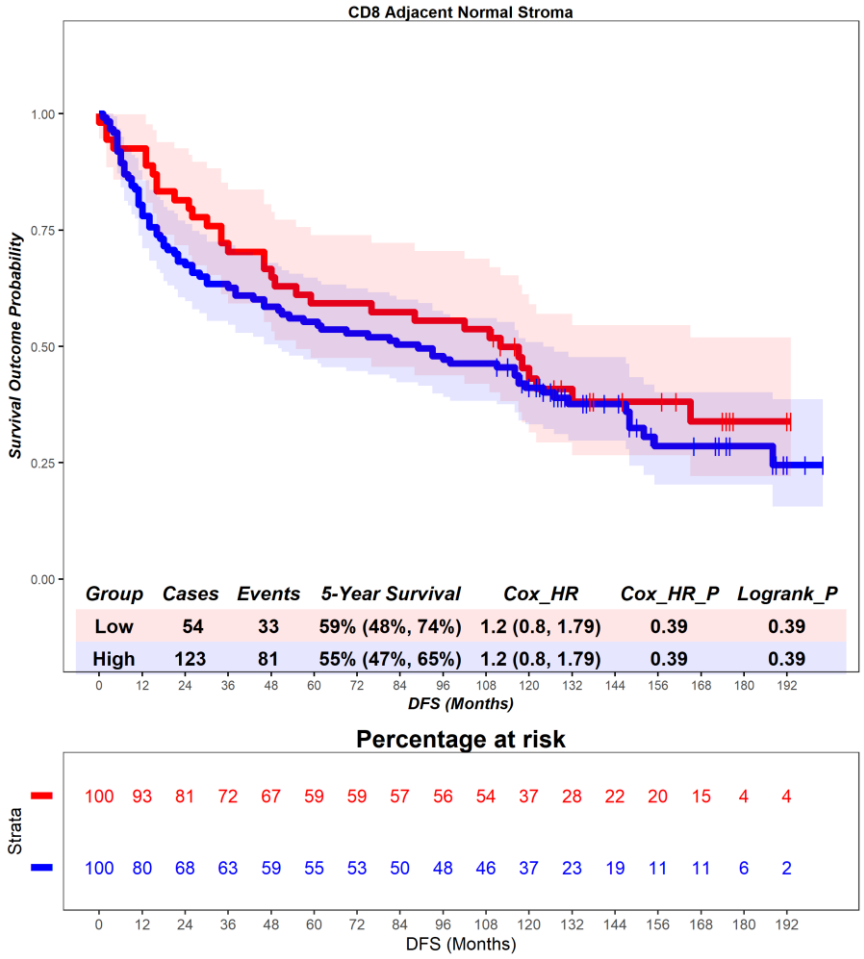

Figure 4.38 – Scotland cohort. Time-to-event (disease-free survival) analysis for CD8 T cells in the adjacent normal stroma. *Patients deemed 'High' or 'Low' for CD8 T cells are shaded blue and red, respectively. Cox hazard ratio is univariate – see table 4.3 for multivariate. The 'Low' group is used as the reference group on cox regression modelling.*

In the adjacent normal tissue, patients deemed high for CD8 T cells are associated with no differential prognosis (Figure 4.39). Patients with a high level of CD8 T cells had a mean survival time of 98.33 months, compared to those with low levels of CD8 T cells with a mean survival of 82.73 months (hazard ratio = 0.84, p = 0.52). 5-year survival for patients high for CD8 T cells is 71% (55%, 92%), compared to 54% (47%, 63%) in the CD8 low group. This suggests that CD8 T cells in the whole tissue of the adjacent normal tissue are associated with no differential prognostic role. Multivariate analysis was not statistically significant (hazard ratio = 0.82, p = 0.47) (Table 4.3), suggesting that CD8 T cells in the whole tissue of the adjacent normal tissue are not independently prognostic.

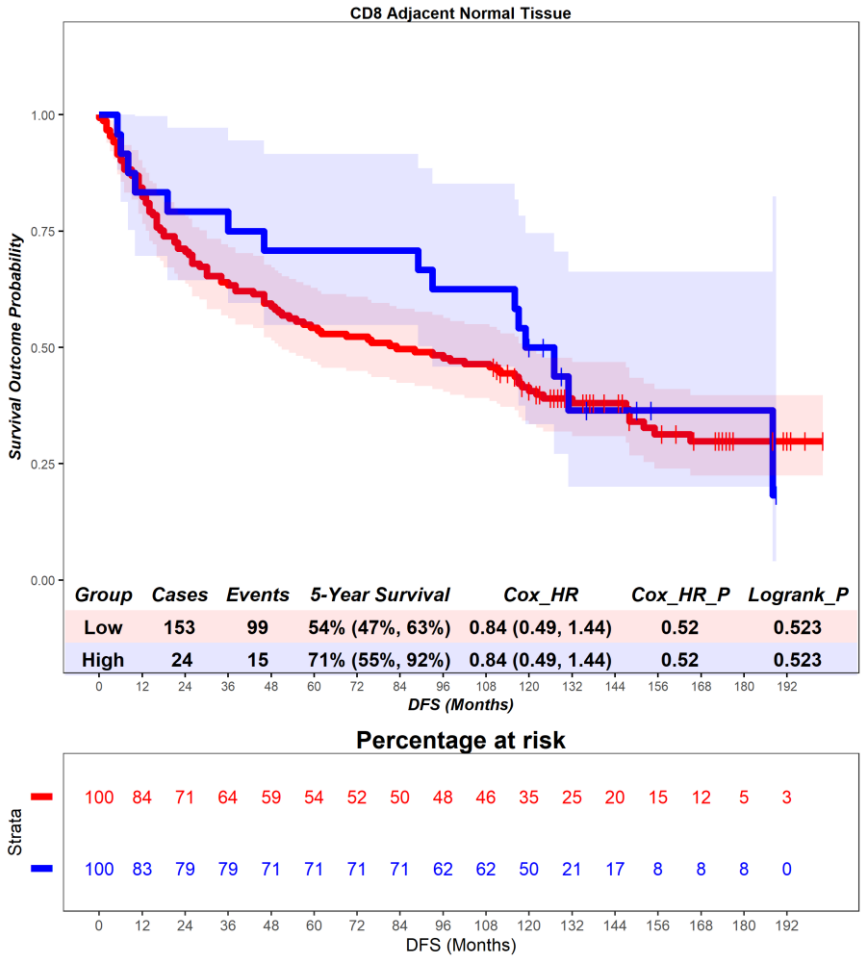

Figure 4.39 – Scotland cohort. Time-to-event (disease-free survival) analysis for CD8 T cells in the adjacent normal tissue. *Patients deemed 'High' or 'Low' for CD8 T cells are shaded blue and red, respectively. Cox hazard ratio is univariate – see table 4.3 for multivariate. The 'Low' group is used as the reference group on cox regression modelling.*

In the primary tumour epithelium, patients deemed high for CD8 T cells are associated with no differential prognosis (Figure 4.40). Patients with a high level of CD8 T cells had a mean survival time of 83.52 months, compared to those with low levels of CD8 T cells with a mean survival of 76.91 months (hazard ratio = 0.92, p = 0.65). 5-year survival for patients high for CD8 T cells is 62% (50%, 76%), compared to 49% (43%, 56%) in the CD8 low group. This suggests that CD8 T cells in the epithelial compartment of the primary tumour are associated with no differential prognostic role. Multivariate analysis was not statistically significant (hazard ratio = 0.87, p = 0.48) (Table 4.3), suggesting that CD8 T cells in the epithelial compartment of the primary tumour are not independently prognostic.

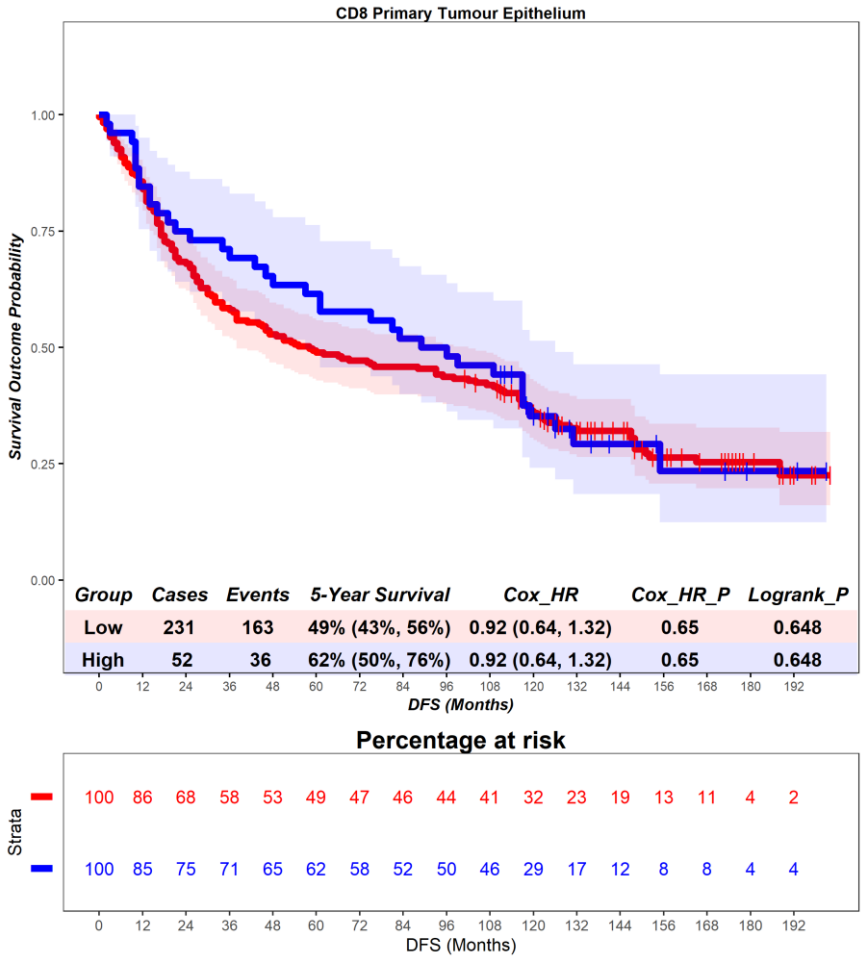

Figure 4.40 – Scotland cohort. Time-to-event (disease-free survival) analysis for CD8 T cells in the primary tumour epithelium. *Patients deemed 'High' or 'Low' for CD8 T cells are shaded blue and red, respectively. Cox hazard ratio is univariate – see table 4.3 X for multivariate. The 'Low' group is used as the reference group on cox regression modelling.*

In the primary tumour stroma, patients deemed high for CD8 T cells are associated with no differential prognosis (Figure 4.41). Patients with a high level of CD8 T cells had a mean survival time of 79.78 months, compared to those with low levels of CD8 T cells with a mean survival of 71.85 months (hazard ratio = 0.89, p = 0.51). 5-year survival for patients high for CD8 T cells is 54% (47%, 61%), compared to 42% (31%, 57%) in the CD8 low group. This suggests that CD8 T cells in the stromal compartment of the primary tumour are associated with no differential prognostic role. Multivariate analysis was not statistically significant (hazard ratio = 0.83, p = 0.3) (Table 4.3), suggesting that CD8 T cells in the stromal compartment of the primary tumour are not independently prognostic.

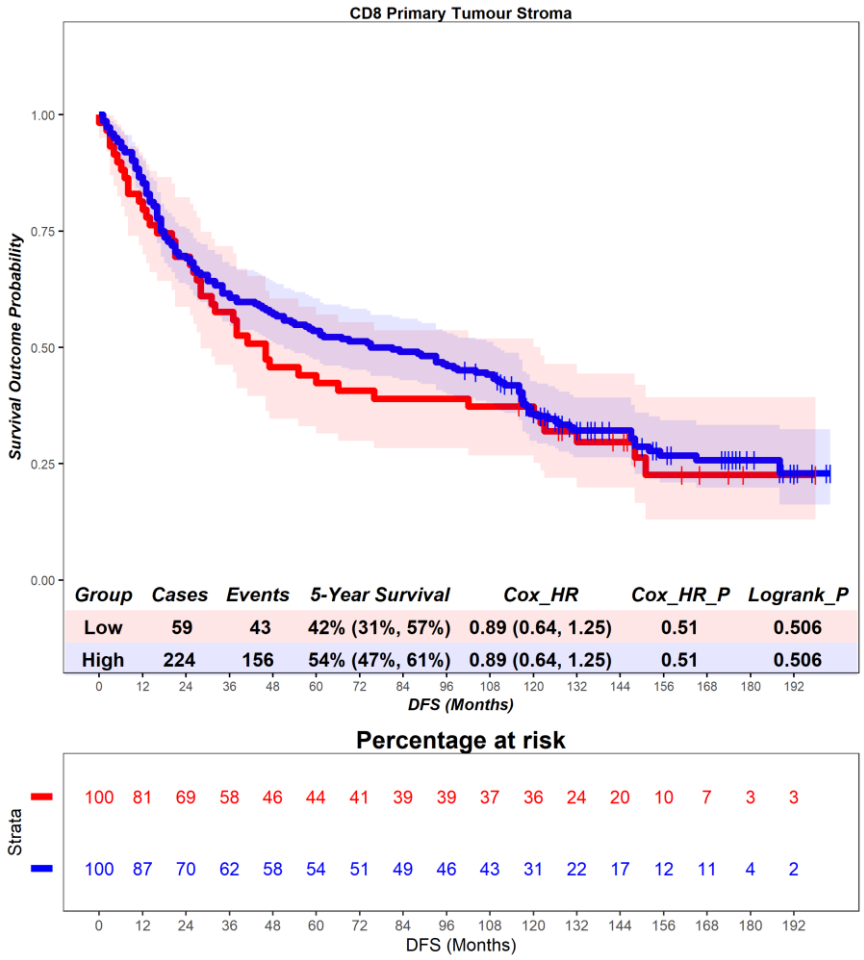

Figure 4.41 – Scotland cohort. Time-to-event (disease-free survival) analysis for CD8 T cells in the primary tumour stroma. *Patients deemed 'High' or 'Low' for CD8 T cells are shaded blue and red, respectively. Cox hazard ratio is univariate – see table 4.3 for multivariate. The 'Low' group is used as the reference group on cox regression modelling.*

In the primary tumour tissue, patients deemed high for CD8 T cells are associated with no differential prognosis (Figure 4.42). Patients with a high level of CD8 T cells had a mean survival time of 87.57 months, compared to those with low levels of CD8 T cells with a mean survival of 76.79 months (hazard ratio = 0.83, p = 0.41). 5-year survival for patients high for CD8 T cells is 63% (49%, 81%), compared to 50% (44%, 56%) in the CD8 low group. This suggests that CD8 T cells in the whole tissue of the primary tumour are associated with no differential prognostic role. Multivariate analysis was not statistically significant (hazard ratio = 0.69, p = 0.12) (Table 4.3), suggesting that CD8 T cells in the whole tissue of the primary tumour are not independently prognostic.

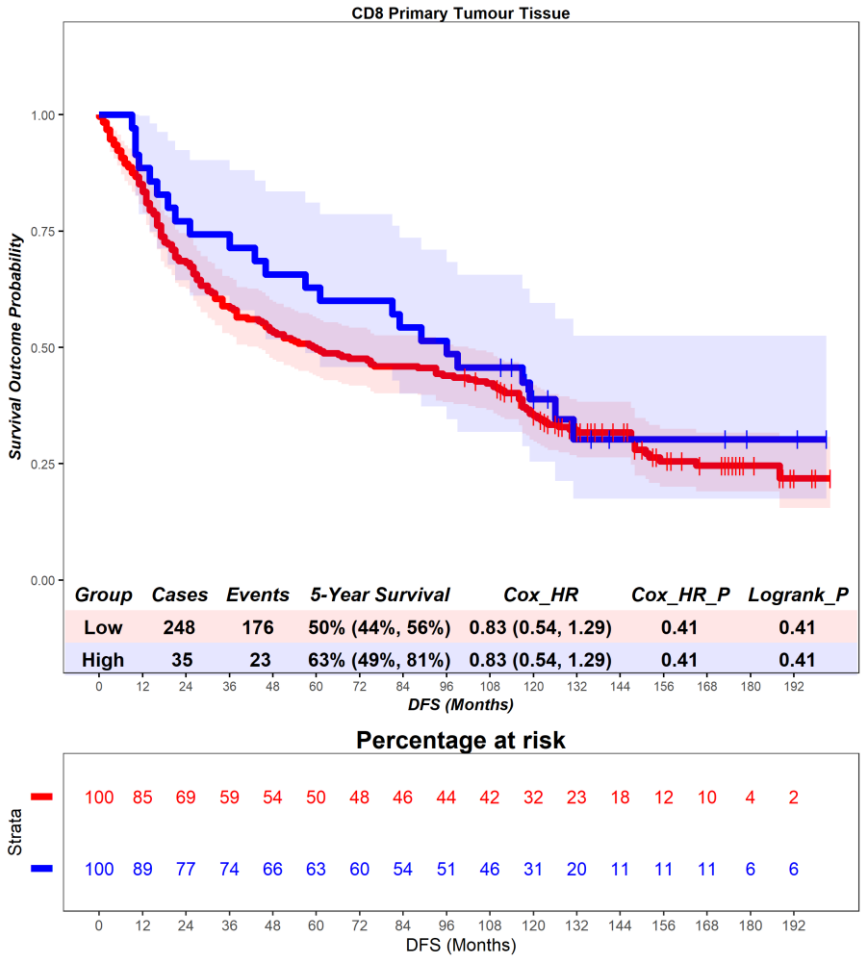

Figure 4.42 – Scotland cohort. Time-to-event (disease-free survival) analysis for CD8 T cells in the primary tumour tissue. *Patients deemed 'High' or 'Low' for CD8 T cells are shaded blue and red, respectively. Cox hazard ratio is univariate – see table 4.3 for multivariate. The 'Low' group is used as the reference group on cox regression modelling.*

4.2.8 CD8 T cells - recurrence-free survival

In the adjacent normal epithelium, patients deemed high for CD8 T cells are associated with a better prognosis (Figure 4.43), although this result did not reach statistical significance. Patients with a high level of CD8 T cells had a mean survival time of 82.75 months, compared to those with low levels of CD8 T cells with a mean survival of 62.72 months (hazard ratio = 0.77, p = 0.44). 5-year survival for patients high for CD8 T cells is 66% (57%, 75%), compared to 52% (35%, 78%) in the CD8 low group. This suggests that CD8 T cells in the epithelial compartment of the adjacent normal tissue are associated with a favourable prognostic role. Multivariate analysis was not statistically significant (hazard ratio = 0.49, p = 0.06) (Table 4.3), suggesting that CD8 T cells in the epithelial compartment of the adjacent normal tissue are independently prognostic.

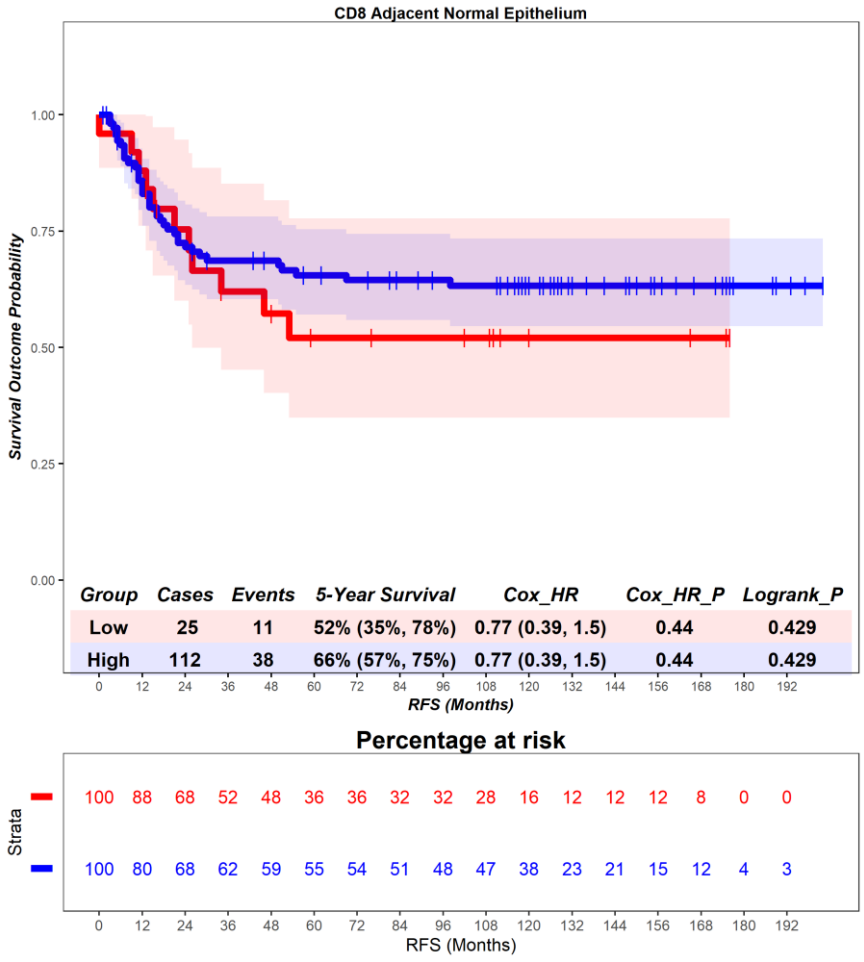

Figure 4.43 – Scotland cohort. Time-to-event (recurrence-free survival) analysis for CD8 T cells in the adjacent normal epithelium. *Patients deemed 'High' or 'Low' for CD8 T cells are shaded blue and red, respectively. Cox hazard ratio is univariate – see table 4.3 for multivariate. The 'Low' group is used as the reference group on cox regression modelling.*

In the adjacent normal stroma, patients deemed high for CD8 T cells are associated with a worse prognosis (Figure 4.44), although this result did not reach statistical significance. Patients with a high level of CD8 T cells had a mean survival time of 74.90 months, compared to those with low levels of CD8 T cells with a mean survival of 88.26 months (hazard ratio = 2.01, p = 0.05). 5-year survival for patients high for CD8 T cells is 59% (49%, 70%), compared to 74% (61%, 89%) in the CD8 low group. This suggests that CD8 T cells in the stromal compartment of the adjacent normal tissue are associated with an unfavourable prognostic role. Multivariate analysis was not statistically significant (hazard ratio = 1.67, p = 0.18) (Table 4.3), suggesting that CD8 T cells in the stromal compartment of the adjacent normal tissue are not independently prognostic.

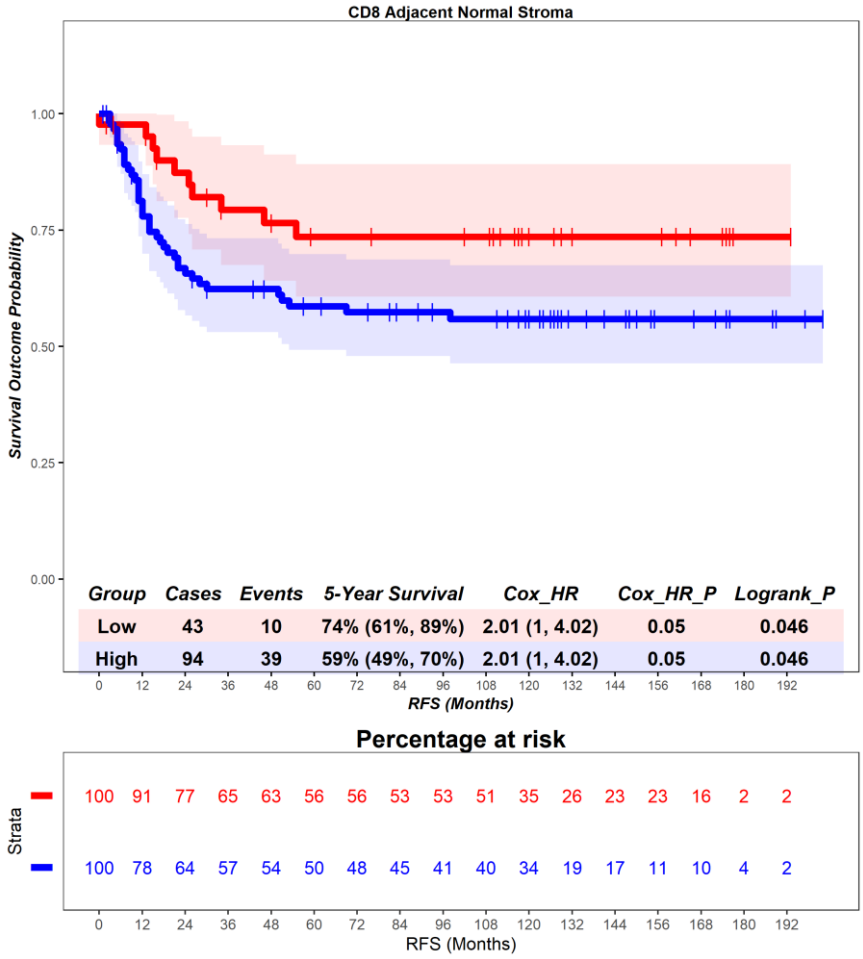

Figure 4.44 – Scotland cohort. Time-to-event (recurrence-free survival) analysis for CD8 T cells in the adjacent normal stroma. *Patients deemed 'High' or 'Low' for CD8 T cells are shaded blue and red, respectively. Cox hazard ratio is univariate – see table 4.3 for multivariate. The 'Low' group is used as the reference group on cox regression modelling.*

In the adjacent normal tissue, patients deemed high for CD8 T cells are associated with a better prognosis (Figure 4.45), although this result did not reach statistical significance. Patients with a high level of CD8 T cells had a mean survival time of 98.67 months, compared to those with low levels of CD8 T cells with a mean survival of 75.55 months (hazard ratio = 0.44, p = 0.11). 5-year survival for patients high for CD8 T cells is 80% (64%, 100%), compared to 60% (51%, 70%) in the CD8 low group. This suggests that CD8 T cells in the stromal compartment of the adjacent normal tissue are associated with a favourable prognostic role. Multivariate analysis was not statistically significant (hazard ratio = 0.74, p = 0.58) (Table 4.3), suggesting that CD8 T cells in the whole tissue compartment of the adjacent normal tissue are not independently prognostic.

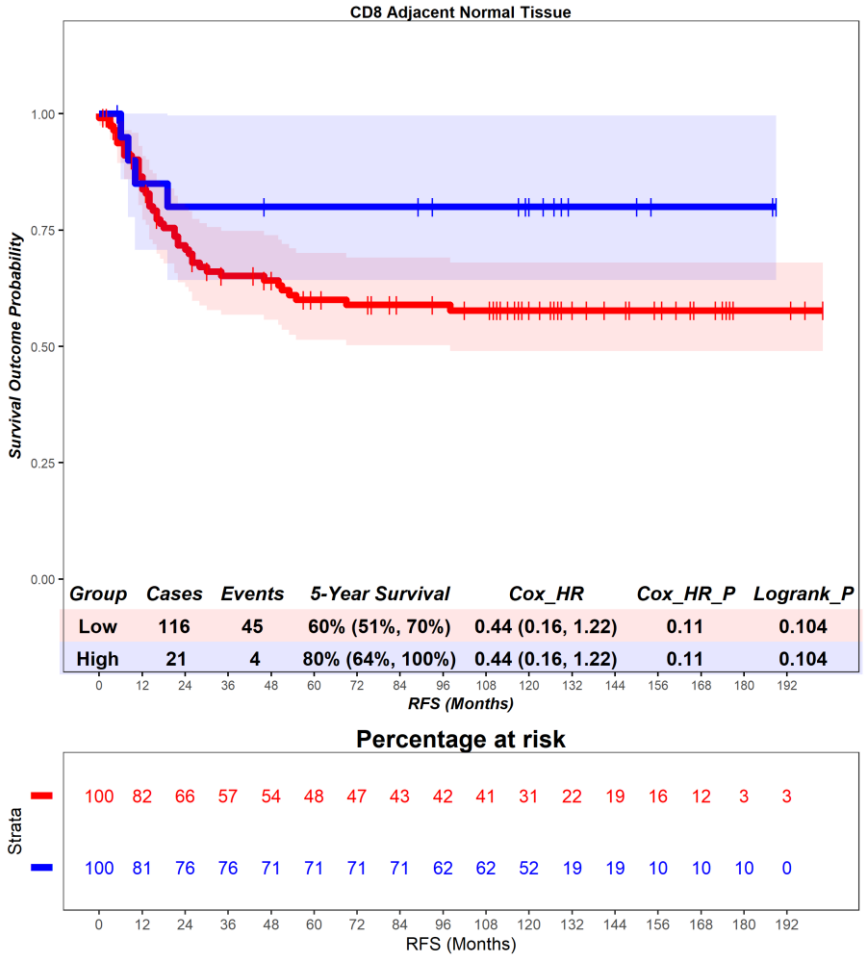

Figure 4.45 – Scotland cohort. Time-to-event (recurrence-free survival) analysis for CD8 T cells in the adjacent normal tissue. *Patients deemed 'High' or 'Low' for CD8 T cells are shaded blue and red, respectively. Cox hazard ratio is univariate – see table 4.3 for multivariate. The 'Low' group is used as the reference group on cox regression modelling.*

In the primary tumour epithelium, patients deemed high for CD8 T cells are associated with a better prognosis (Figure 4.46), and this resulted reached statistical significance. Patients with a high level of CD8 T cells had a mean survival time of 86.03 months, compared to those with low levels of CD8 T cells with a mean survival of 70.62 months (hazard ratio = 0.25, p = 0). 5-year survival for patients high for CD8 T cells is 85% (73%, 98%), compared to 51% (43%, 59%) in the CD8 low group. This suggests that CD8 T cells in the epithelial compartment of the primary tumour are associated with a favourable prognostic role. Multivariate analysis was statistically significant (hazard ratio = 0.29, p = 0.01) (Table 4.3), suggesting that CD8 T cells in the epithelial compartment of the primary tumour are independently prognostic.

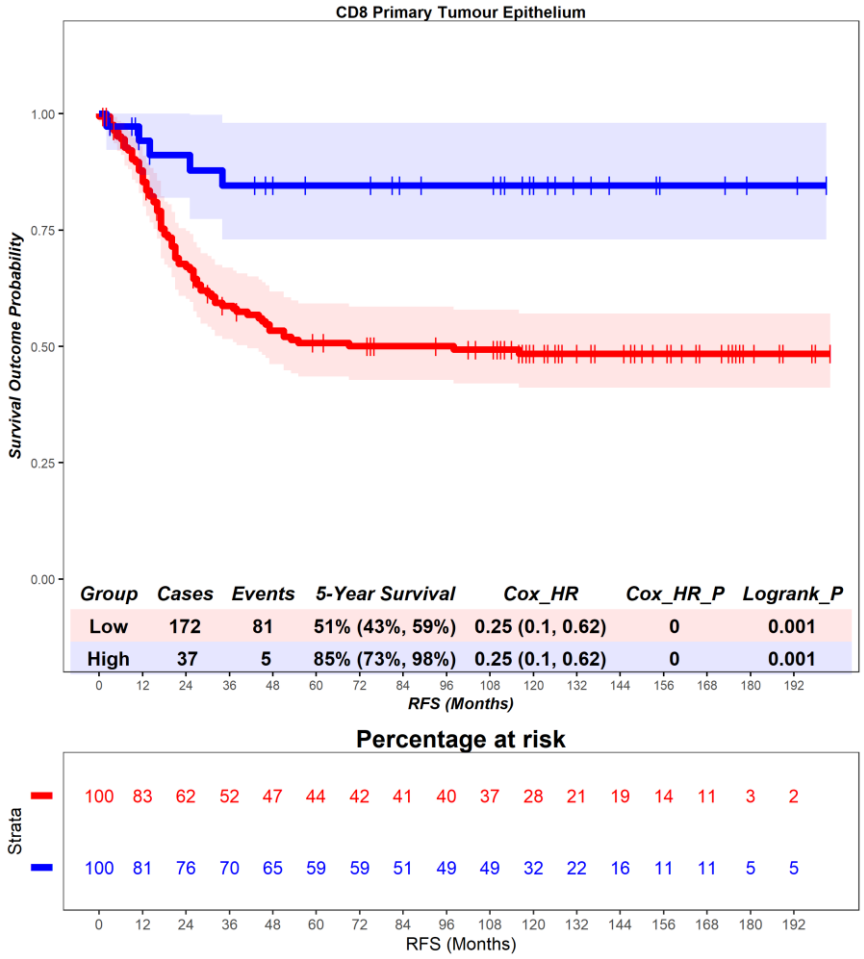

Figure 4.46 – Scotland cohort. Time-to-event (recurrence-free survival) analysis for CD8 T cells in the primary tumour epithelium. *Patients deemed 'High' or 'Low' for CD8 T cells are shaded blue and red, respectively. Cox hazard ratio is univariate – see table 4.3 for multivariate. The 'Low' group is used as the reference group on cox regression modelling.*

In the primary tumour stroma, patients deemed high for CD8 T cells are associated with a better prognosis (Figure 4.47), although this result did not reach statistical significance. Patients with a high level of CD8 T cells had a mean survival time of 75.33 months, compared to those with low levels of CD8 T cells with a mean survival of 65.22 months (hazard ratio = 0.67, p = 0.1). 5-year survival for patients high for CD8 T cells is 60% (52%, 68%), compared to 42% (29%, 61%) in the CD8 low group. This suggests that CD8 T cells in the stromal compartment of the primary tumour are associated with a favourable prognostic role. Multivariate analysis was not statistically significant (hazard ratio = 0.64, p = 0.09) (Table 4.3), suggesting that CD8 T cells in the stromal compartment of the primary tumour are not independently prognostic.

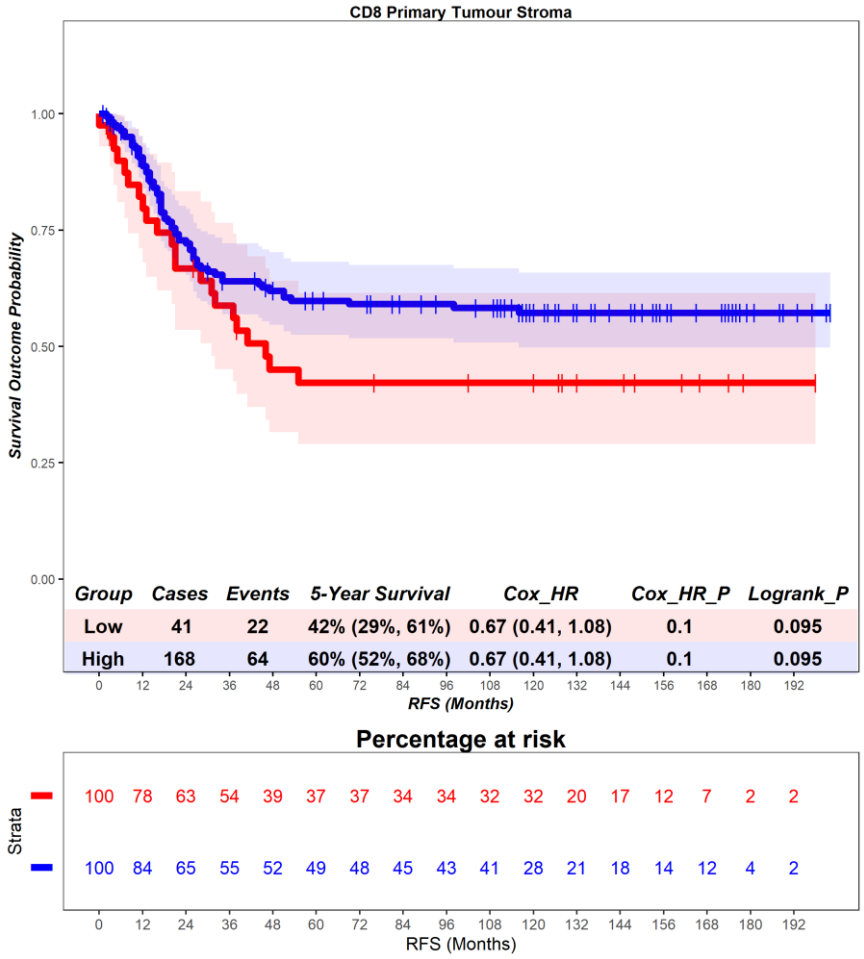

Figure 4.47 – Scotland cohort. Time-to-event (recurrence-free survival) analysis for CD8 T cells in the primary tumour stroma. *Patients deemed 'High' or 'Low' for CD8 T cells are shaded blue and red, respectively. Cox hazard ratio is univariate – see table 4.3 for multivariate. The 'Low' group is used as the reference group on cox regression modelling.*

In the primary tumour tissue, patients deemed high for CD8 T cells are associated with a better prognosis (Figure 4.48), and this result reached statistical significance. Patients with a high level of CD8 T cells had a mean survival time of 96.22 months, compared to those with low levels of CD8 T cells with a mean survival of 70.52 months (hazard ratio = 0.24, p = 0.01). 5-year survival for patients high for CD8 T cells is 86% (72%, 100%), compared to 53% (46%, 61%) in the CD8 low group. This suggests that CD8 T cells in the whole tissue of the primary tumour are associated with a favourable prognostic role. Multivariate analysis was statistically significant (hazard ratio = 0.24, p = 0.02) (Table 4.3), suggesting that CD8 T cells in the whole tissue of the primary tumour are independently prognostic.

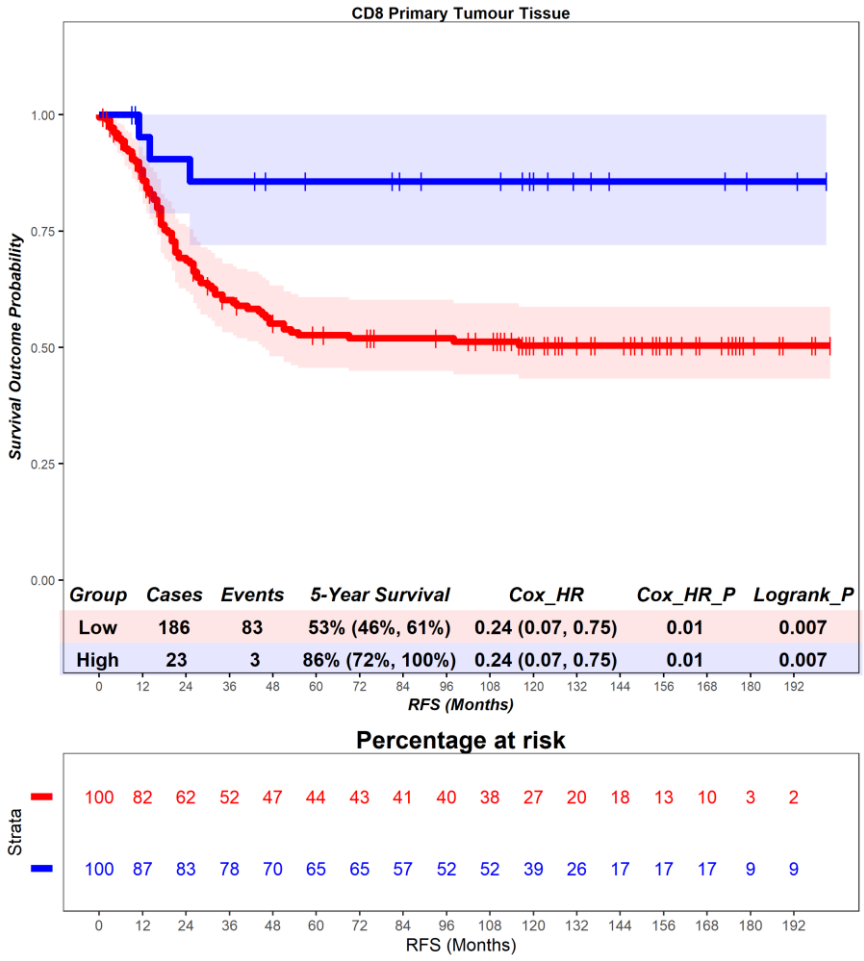

Figure 4.48 – Scotland cohort. Time-to-event (recurrence-free survival) analysis for CD8 T cells in the primary tumour tissue. *Patients deemed 'High' or 'Low' for CD8 T cells are shaded blue and red, respectively. Cox hazard ratio is univariate – see table 4.3 for multivariate. The 'Low' group is used as the reference group on cox regression modelling.*

4.2.9 Relationship between CD8 and γδ T cells

In the adjacent normal epithelium, there was a poor positive correlation between γδ T cells and CD8 T cells (R = 0.12) and this result did not reach statistical significance (p = 0.17) (Figure 4.49A). γδ T cells were consistently present at a lower than CD8 T cells (Figure 4.49B/C). Thus, the data show no relationship between the density of γδ T cells and CD8 T cells in the adjacent normal epithelium.

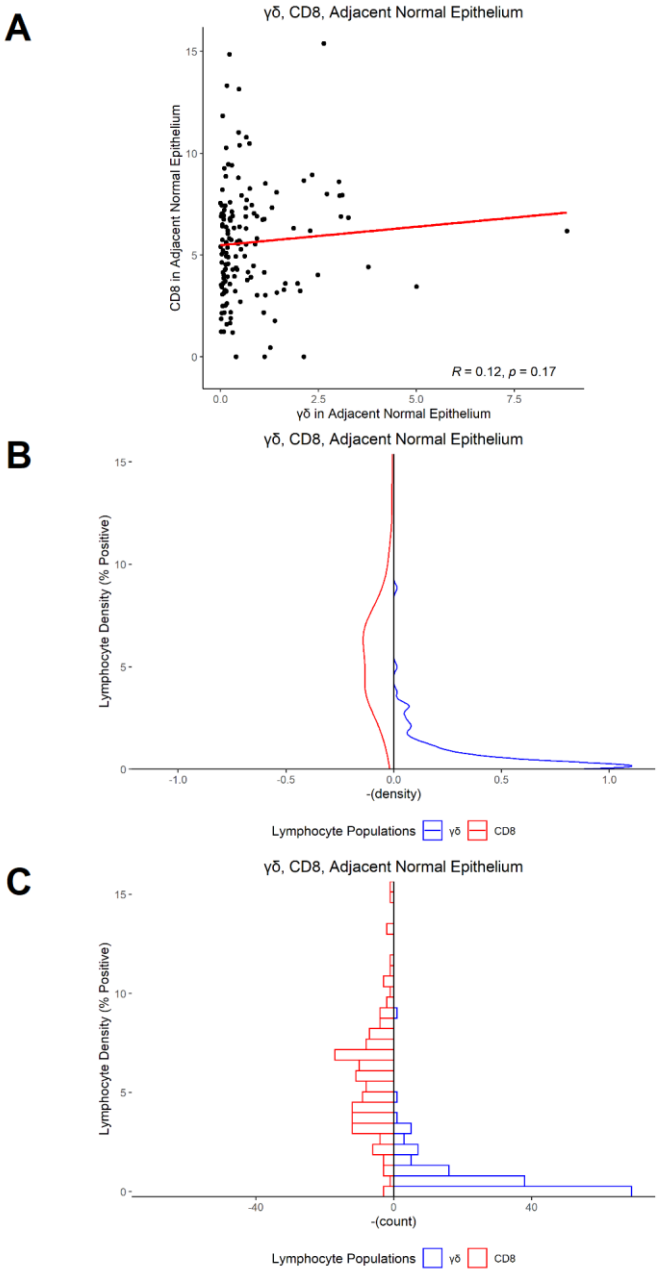

Figure 4.49 – Scotland cohort. Correlation analysis for γδ T cells and CD8 T cells in the adjacent normal epithelium. *A - Scatter plot depicts the density (% positive) of γδ T cells (X axis) and CD8 T cells (Y axis), restricted to cases for which data is available for both populations. Correlation is described using Spearman's rank correlation coefficient. R values >0 and <0.3 are poor, >0.3 are fair, >0.6 are moderate, >0.8 are very strong and 1 are perfect. Correlation coefficients are considered statistically significant if p <0.05. B – Density plot of lymphocyte density for CD8 T cells (red) and γδ T cells (blue). C – Histogram plot of lymphocyte density for CD8 T cells (red) and γδ T cells (blue).*

In the adjacent normal stroma, there was a poor positive correlation between γδ T cells and CD8 T cells (R = 0.16) and this result did not reach statistical significance (p = 0.053) Figure (4.50A). γδ T cells were consistently present at a lower than CD8 T cells (Figure 4.50B/C). Thus, the data show no relationship between the density of γδ T cells and CD8 T cells in the adjacent normal stroma.

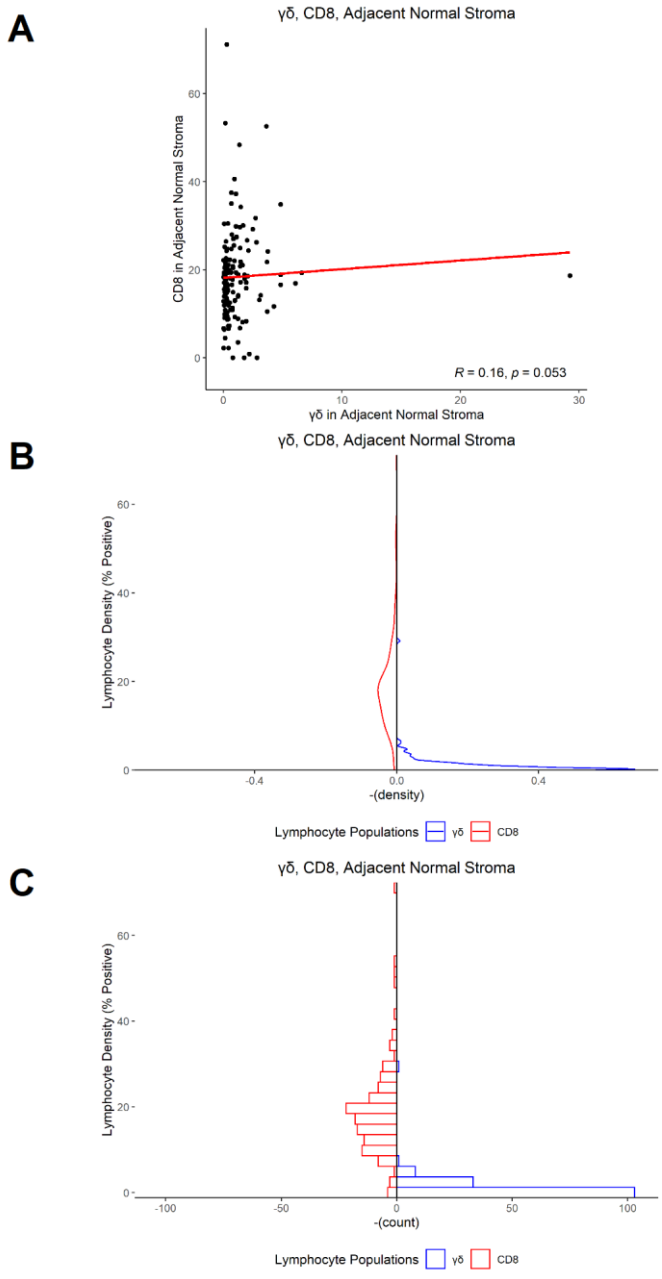

Figure 4.50 – Scotland cohort. Correlation analysis for γδ T cells and CD8 T cells in the adjacent normal stroma. *A - Scatter plot depicts the density (% positive) of γδ T cells (X axis) and CD8 T cells (Y axis), restricted to cases for which data is available for both populations. Correlation is described using Spearman's rank correlation coefficient. R values >0 and <0.3 are poor, >0.3 are fair, >0.6 are moderate, >0.8 are very strong and 1 are perfect. Correlation coefficients are considered statistically significant if p <0.05. B – Density plot of lymphocyte density for CD8 T cells (red) and γδ T cells (blue). C – Histogram plot of lymphocyte density for CD8 T cells (red) and γδ T cells (blue).*

In the adjacent normal tissue, there was a poor positive correlation between γδ T cells and CD8 T cells (R = 0.12) and this result did not reach statistical significance (p = 0.16) Figure (4.51A). γδ T cells were consistently present at a lower than CD8 T cells (Figure 4.51B/C). Thus, the data show no relationship between the density of γδ T cells and CD8 T cells in the adjacent normal tissue.

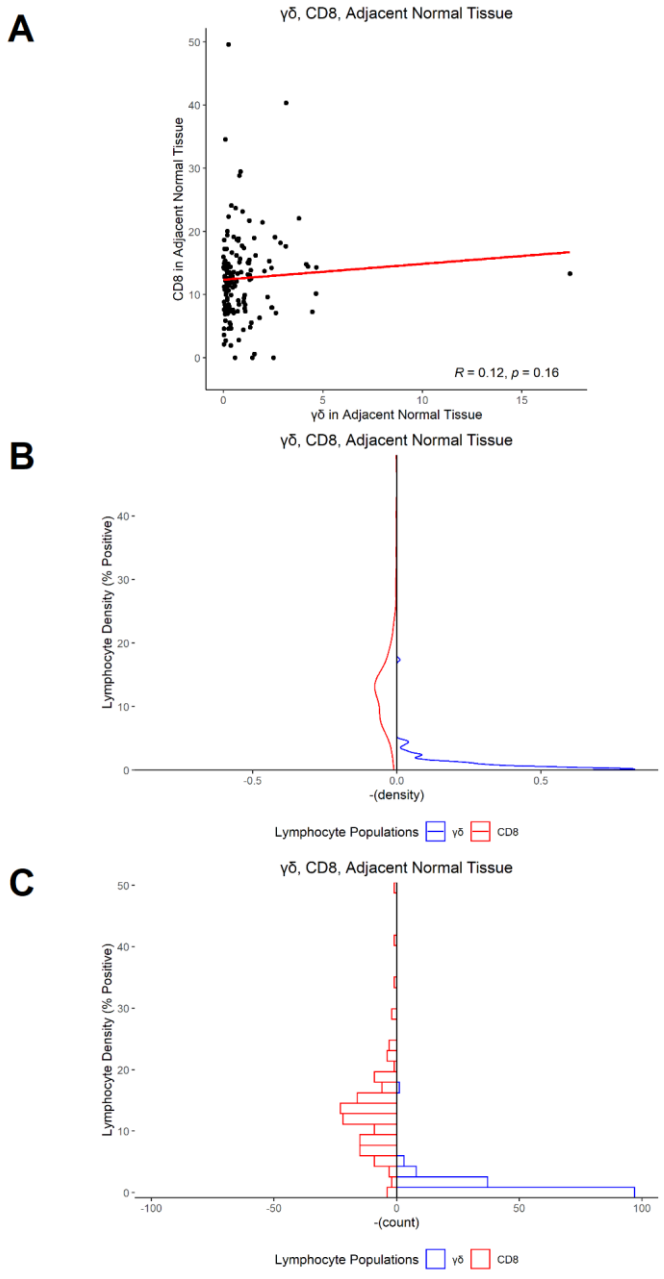

Figure 4.51 – Scotland cohort. Correlation analysis for γδ T cells and CD8 T cells in the adjacent normal tissue. *A - Scatter plot depicts the density (% positive) of γδ T cells (X axis) and CD8 T cells (Y axis), restricted to cases for which data is available for both populations. Correlation is described using Spearman's rank correlation coefficient. R values >0 and <0.3 are poor, >0.3 are fair, >0.6 are moderate, >0.8 are very strong and 1 are perfect. Correlation coefficients are considered statistically significant if p <0.05. B – Density plot of lymphocyte density for CD8 T cells (red) and γδ T cells (blue). C – Histogram plot of lymphocyte density for CD8 T cells (red) and γδ T cells (blue).*

In the primary tumour epithelium, there was a poor positive correlation between γδ T cells and CD8 T cells (R = 0.11) and this result did not reach statistical significance (p = 0.061) Figure (4.52A). γδ T cells were consistently present at a lower than CD8 T cells (Figure 4.52B/C). Thus, the data show no relationship between the density of γδ T cells and CD8 T cells in the primary tumour epithelium.

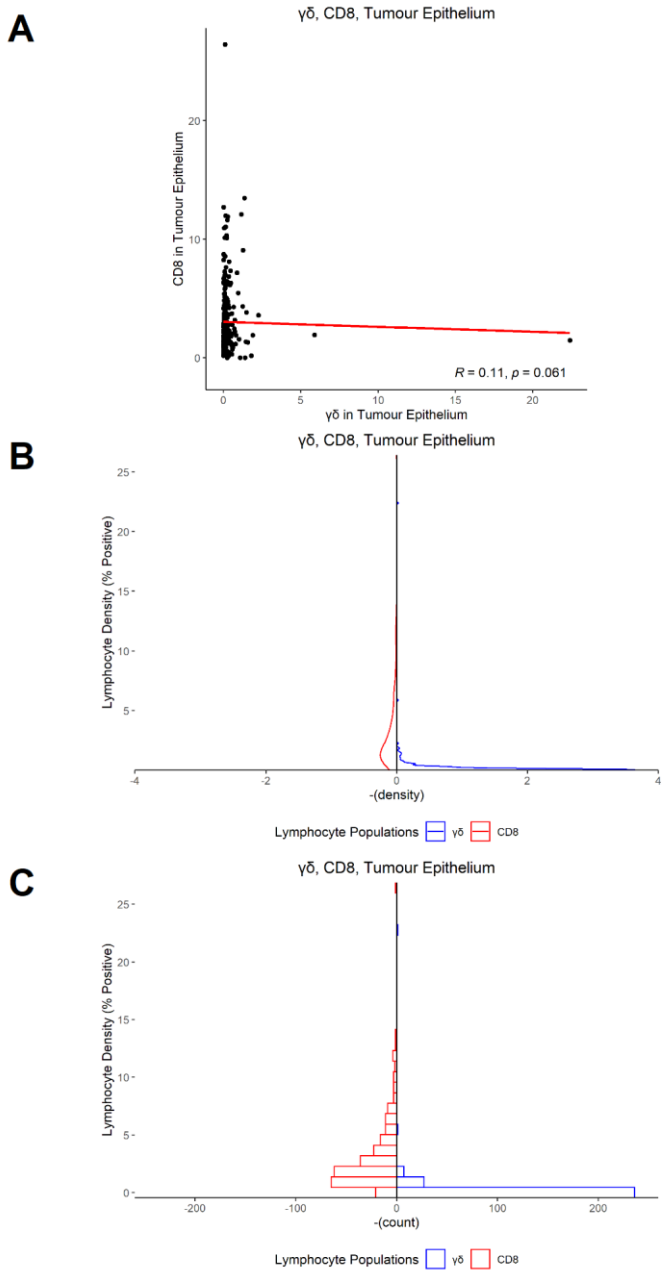

Figure 4.52 – Scotland cohort. Correlation analysis for γδ T cells and CD8 T cells in the primary tumour epithelium. *A - Scatter plot depicts the density (% positive) of γδ T cells (X axis) and CD8 T cells (Y axis), restricted to cases for which data is available for both populations. Correlation is described using Spearman's rank correlation coefficient. R values >0 and <0.3 are poor, >0.3 are fair, >0.6 are moderate, >0.8 are very strong and 1 are perfect. Correlation coefficients are considered statistically significant if p <0.05. B – Density plot of lymphocyte density for CD8 T cells (red) and γδ T cells (blue). C – Histogram plot of lymphocyte density for CD8 T cells (red) and γδ T cells (blue).*

In the primary tumour stroma, there was a poor positive correlation between γδ T cells and CD8 T cells (R = 0.078) and this result did not reach statistical significance (p = 0.2) Figure (4.53A). γδ T cells were consistently present at a lower than CD8 T cells (Figure 4.53B/C). Thus, the data show no relationship between the density of γδ T cells and CD8 T cells in the primary tumour stroma.

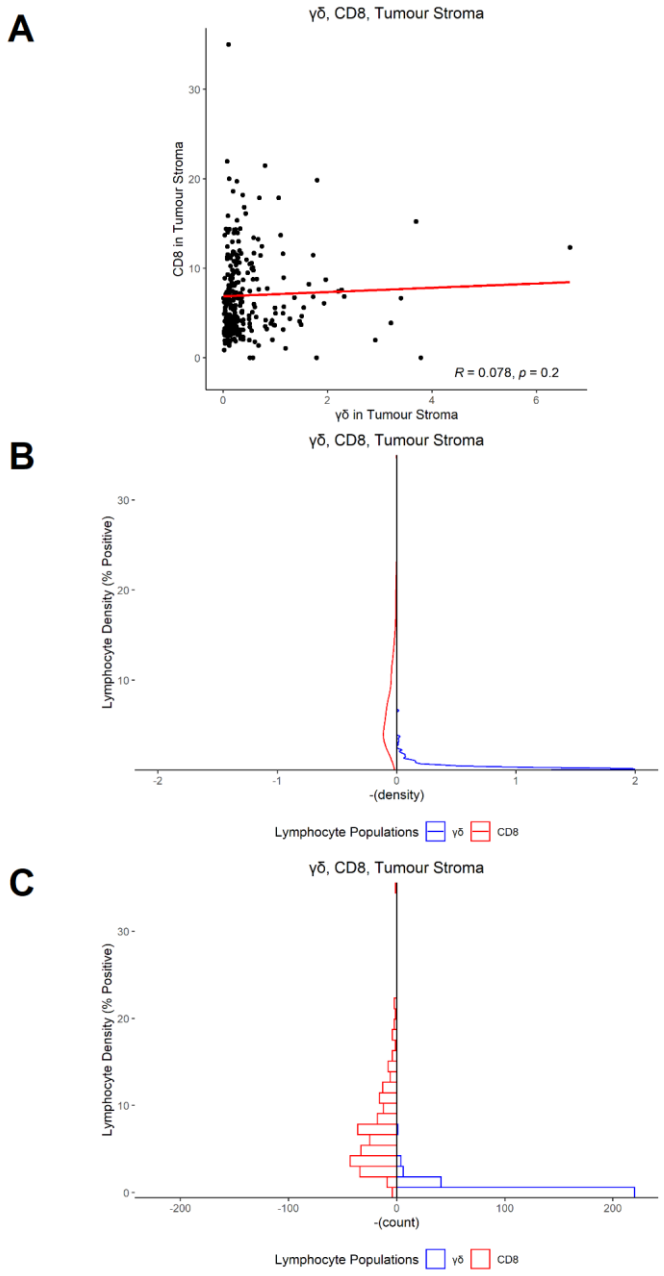

Figure 4.53 – Scotland cohort. Correlation analysis for γδ T cells and CD8 T cells in the primary tumour stroma. *A - Scatter plot depicts the density (% positive) of γδ T cells (X axis) and CD8 T cells (Y axis), restricted to cases for which data is available for both populations. Correlation is described using Spearman's rank correlation coefficient. R values >0 and <0.3 are poor, >0.3 are fair, >0.6 are moderate, >0.8 are very strong and 1 are perfect. Correlation coefficients are considered statistically significant if p <0.05. B – Density plot of lymphocyte density for CD8 T cells (red) and γδ T cells (blue). C – Histogram plot of lymphocyte density for CD8 T cells (red) and γδ T cells (blue).*

In the primary tumour tissue, there was a poor positive correlation between γδ T cells and CD8 T cells (R = 0.083) and this result did not reach statistical significance (p = 0.17) Figure (4.54A). γδ T cells were consistently present at a lower than CD8 T cells (Figure 4.54B/C). Thus, the data show no relationship between the density of γδ T cells and CD8 T cells in the primary tumour tissue.

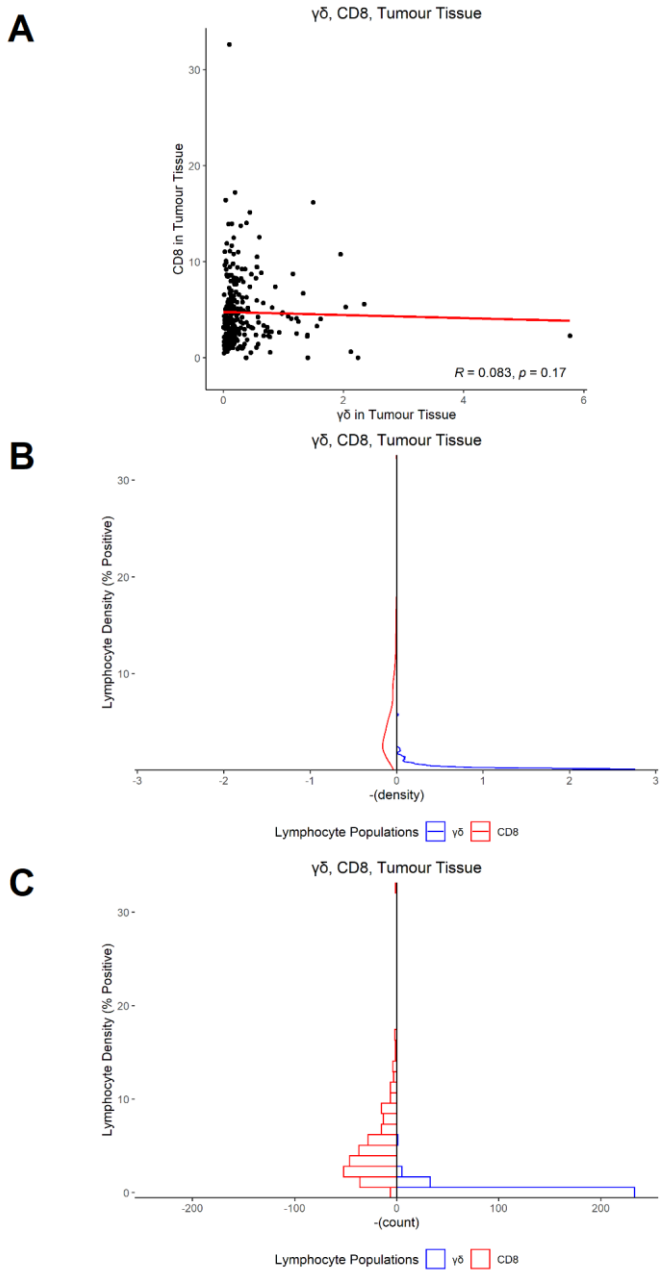

Figure 4.54 – Scotland cohort. Correlation analysis for γδ T cells and CD8 T cells in the primary tumour tissue. *A - Scatter plot depicts the density (% positive) of γδ T cells (X axis) and CD8 T cells (Y axis), restricted to cases for which data is available for both populations. Correlation is described using Spearman's rank correlation coefficient. R values >0 and <0.3 are poor, >0.3 are fair, >0.6 are moderate, >0.8 are very strong and 1 are perfect. Correlation coefficients are considered statistically significant if p <0.05. B – Density plot of lymphocyte density for CD8 T cells (red) and γδ T cells (blue). C – Histogram plot of lymphocyte density for CD8 T cells (red) and γδ T cells (blue).*

4.2.10 Scotland - multivariate analysis

Table 4.3 – Results of multivariate cox regression modelling in the Scotland cohort. *Covariates were selected by extracting univariate variables that were statistically significant in univariate models. Covariates are listed in Table S4.*

Group Descriptors			Multivariate Values							
Cohort	Status	variable	p.value	estimate	conf.low	conf.high	N_obs	N_event	std.error	statistic
Scotland	CSS	GD_PercPositiveCellsinHealthyTissue_Coded	0.190	1.49	0.83	2.70	152	50	0.303	1.325
Scotland	CSS	GD_PercPositiveCellsinTumourTissue_Coded	0.630	1.23	0.52	2.89	273	102	0.436	0.476
Scotland	CSS	GD_PercPositiveCellsinHealthyEpithelium_Coded	0.250	1.42	0.78	2.58	152	50	0.304	1.157
Scotland	CSS	GD_PercPositiveCellsinTumourEpithelium_Coded	0.540	1.31	0.55	3.08	273	102	0.438	0.609
Scotland	CSS	GD_PercPositiveCellsinHealthyStroma_Coded	0.120	1.60	0.89	2.87	152	50	0.299	1.571
Scotland	CSS	GD_PercPositiveCellsinTumourStroma_Coded	0.340	1.51	0.65	3.52	273	102	0.431	0.958
Scotland	CSS	CD8_PercPositiveCellsinHealthyTissue_Coded	0.530	0.74	0.29	1.89	168	56	0.479	-0.634
Scotland	CSS	CD8_PercPositiveCellsinTumourTissue_Coded	0.040	0.38	0.15	0.94	267	98	0.468	-2.089
Scotland	CSS	CD8_PercPositiveCellsinHealthyEpithelium_Coded	0.030	0.46	0.23	0.92	168	56	0.355	-2.209
Scotland	CSS	CD8_PercPositiveCellsinTumourEpithelium_Coded	0.060	0.52	0.27	1.02	267	98	0.339	-1.902
Scotland	CSS	CD8_PercPositiveCellsinHealthyStroma_Coded	0.360	1.39	0.69	2.80	168	56	0.357	0.921
Scotland	CSS	CD8_PercPositiveCellsinTumourStroma_Coded	0.010	0.52	0.33	0.84	267	98	0.239	-2.706
Scotland	OS	GD_PercPositiveCellsinHealthyTissue_Coded	0.160	1.37	0.88	2.13	155	99	0.225	1.408
Scotland	OS	GD_PercPositiveCellsinTumourTissue_Coded	0.160	1.49	0.85	2.61	280	193	0.286	1.400
Scotland	OS	GD_PercPositiveCellsinHealthyEpithelium_Coded	0.180	1.36	0.87	2.12	155	99	0.227	1.353
Scotland	OS	GD_PercPositiveCellsinTumourEpithelium_Coded	0.400	1.24	0.75	2.06	280	193	0.259	0.834
Scotland	OS	GD_PercPositiveCellsinHealthyStroma_Coded	0.230	1.32	0.84	2.07	155	99	0.229	1.204
Scotland	OS	GD_PercPositiveCellsinTumourStroma_Coded	0.080	1.63	0.93	2.85	280	193	0.284	1.723
Scotland	OS	CD8_PercPositiveCellsinHealthyTissue_Coded	0.630	0.87	0.50	1.52	171	107	0.286	-0.487
Scotland	OS	CD8_PercPositiveCellsinTumourTissue_Coded	0.070	0.65	0.40	1.03	274	188	0.240	-1.822
Scotland	OS	CD8_PercPositiveCellsinHealthyEpithelium_Coded	0.030	0.59	0.37	0.94	171	107	0.241	-2.200
Scotland	OS	CD8_PercPositiveCellsinTumourEpithelium_Coded	0.410	0.85	0.58	1.25	274	188	0.198	-0.824
Scotland	OS	CD8_PercPositiveCellsinHealthyStroma_Coded	0.610	1.12	0.72	1.73	171	107	0.221	0.504
Scotland	OS	CD8_PercPositiveCellsinTumourStroma_Coded	0.260	0.82	0.57	1.16	274	188	0.180	-1.132
Scotland	DFS	GD_PercPositiveCellsinHealthyTissue_Coded	0.090	1.45	0.94	2.21	153	102	0.218	1.691
Scotland	DFS	GD_PercPositiveCellsinTumourTissue_Coded	0.140	1.53	0.87	2.68	276	194	0.286	1.484
Scotland	DFS	GD_PercPositiveCellsinHealthyEpithelium_Coded	0.090	1.45	0.95	2.23	153	102	0.218	1.705
Scotland	DFS	GD_PercPositiveCellsinTumourEpithelium_Coded	0.270	1.35	0.79	2.31	276	194	0.273	1.106
Scotland	DFS	GD_PercPositiveCellsinHealthyStroma_Coded	0.100	1.44	0.94	2.21	153	102	0.220	1.656
Scotland	DFS	GD_PercPositiveCellsinTumourStroma_Coded	0.070	1.67	0.96	2.92	276	194	0.284	1.805
Scotland	DFS	CD8_PercPositiveCellsinHealthyTissue_Coded	0.470	0.82	0.47	1.43	170	110	0.286	-0.716
Scotland	DFS	CD8_PercPositiveCellsinTumourTissue_Coded	0.120	0.69	0.43	1.10	270	190	0.239	-1.575
Scotland	DFS	CD8_PercPositiveCellsinHealthyEpithelium_Coded	0.030	0.59	0.37	0.95	170	110	0.241	-2.190
Scotland	DFS	CD8_PercPositiveCellsinTumourEpithelium_Coded	0.480	0.87	0.59	1.28	270	190	0.196	-0.714
Scotland	DFS	CD8_PercPositiveCellsinHealthyStroma_Coded	0.640	1.11	0.72	1.70	170	110	0.220	0.467
Scotland	DFS	CD8_PercPositiveCellsinTumourStroma_Coded	0.300	0.83	0.58	1.19	270	190	0.184	-1.033
Scotland	RFS	GD_PercPositiveCellsinHealthyTissue_Coded	0.290	1.49	0.71	3.13	119	42	0.378	1.058
Scotland	RFS	GD_PercPositiveCellsinTumourTissue_Coded	0.420	0.54	0.12	2.39	203	82	0.758	-0.810
Scotland	RFS	GD_PercPositiveCellsinHealthyEpithelium_Coded	0.170	1.62	0.81	3.23	119	42	0.353	1.363
Scotland	RFS	GD_PercPositiveCellsinTumourEpithelium_Coded	0.680	0.65	0.08	5.03	203	82	1.044	-0.413
Scotland	RFS	GD_PercPositiveCellsinHealthyStroma_Coded	0.070	1.86	0.94	3.70	119	42	0.349	1.781
Scotland	RFS	GD_PercPositiveCellsinTumourStroma_Coded	0.820	0.87	0.26	2.87	203	82	0.609	-0.226
Scotland	RFS	CD8_PercPositiveCellsinHealthyTissue_Coded	0.580	0.74	0.25	2.16	133	47	0.546	-0.548
Scotland	RFS	CD8_PercPositiveCellsinTumourTissue_Coded	0.020	0.24	0.07	0.79	203	83	0.603	-2.353
Scotland	RFS	CD8_PercPositiveCellsinHealthyEpithelium_Coded	0.060	0.49	0.23	1.04	133	47	0.387	-1.846
Scotland	RFS	CD8_PercPositiveCellsinTumourEpithelium_Coded	0.010	0.29	0.11	0.73	203	83	0.473	-2.612
Scotland	RFS	CD8_PercPositiveCellsinHealthyStroma_Coded	0.180	1.67	0.79	3.57	133	47	0.386	1.334
Scotland	RFS	CD8_PercPositiveCellsinTumourStroma_Coded	0.090	0.64	0.38	1.08	203	83	0.265	-1.682

4.3 Norway cohort

4.3.0 Summary Tables

Table 4.4 – Summary table of survival analysis for γδ T cells in the Norway cohort. *Red rows are unfavourable. Green rows are favourable. Amber rows either present a mutual result or trend towards a result but with insufficient size effect.*

Survival	Compartment	Cox HR	Cox P Value	Logrank P Value	Prognostic Value
Cancer-specific (CSS)	γδ Adjacent Normal Epithelium	1.24	0.84	0.835	Unclear
Cancer-specific (CSS)	γδ Adjacent Normal Stroma	1.24	0.84	0.835	Unclear
Cancer-specific (CSS)	γδ Adjacent Normal Tissue	1.05	0.96	0.96	Unclear
Cancer-specific (CSS)	γδ Primary Tumour Epithelium	0.49	0.11	0.099	Favourable
Cancer-specific (CSS)	γδ Primary Tumour Stroma	0.83	0.66	0.655	Unclear
Cancer-specific (CSS)	γδ Primary Tumour Tissue	0.58	0.22	0.211	Unclear
Overall (OS)	γδ Adjacent Normal Epithelium	1.79	0.28	0.272	Unclear
Overall (OS)	γδ Adjacent Normal Stroma	1.38	0.6	0.597	Unclear
Overall (OS)	γδ Adjacent Normal Tissue	1.56	0.41	0.403	Unclear
Overall (OS)	γδ Primary Tumour Epithelium	0.56	0.01	0.008	Favourable
Overall (OS)	γδ Primary Tumour Stroma	0.67	0.08	0.078	Unclear
Overall (OS)	γδ Primary Tumour Tissue	0.56	0.01	0.012	Favourable
Disease-free (DFS)	γδ Adjacent Normal Epithelium	2.52	0.23	0.219	Unclear
Disease-free (DFS)	γδ Adjacent Normal Stroma	2.52	0.23	0.219	Unclear
Disease-free (DFS)	γδ Adjacent Normal Tissue	2.09	0.34	0.332	Unclear
Disease-free (DFS)	γδ Primary Tumour Epithelium	0.52	0.09	0.081	Favourable
Disease-free (DFS)	γδ Primary Tumour Stroma	0.83	0.63	0.628	Unclear
Disease-free (DFS)	γδ Primary Tumour Tissue	0.61	0.2	0.198	Unclear
Recurrence-free (RFS)	γδ Adjacent Normal Epithelium	12.24	0.08	0.023	Unclear
Recurrence-free (RFS)	γδ Adjacent Normal Stroma	12.24	0.08	0.023	Unclear
Recurrence-free (RFS)	γδ Adjacent Normal Tissue	10.35	0.1	0.04	Unclear
Recurrence-free (RFS)	γδ Primary Tumour Epithelium	0.63	0.58	0.577	Unclear
Recurrence-free (RFS)	γδ Primary Tumour Stroma	0.86	0.85	0.854	Unclear
Recurrence-free (RFS)	γδ Primary Tumour Tissue	0.74	0.72	0.724	Unclear

Table 4.5 – Summary table of survival analysis for CD8 T cells in the Norway cohort. *Red rows are unfavourable. Green rows are favourable. Amber rows either present a mutual result or trend towards a result but with insufficient size effect.*

Survival	Compartment	Cox HR	Cox P Value	Logrank P Value	Prognostic Value
Cancer-specific (CSS)	CD8 Adjacent Normal Epithelium	1.29	0.74	0.738	Unclear
Cancer-specific (CSS)	CD8 Adjacent Normal Stroma	1.56	0.59	0.591	Unclear
Cancer-specific (CSS)	CD8 Adjacent Normal Tissue	0	1	0.308	Unclear
Cancer-specific (CSS)	CD8 Primary Tumour Epithelium	0.6	0.19	0.185	Unclear
Cancer-specific (CSS)	CD8 Primary Tumour Stroma	0.27	0	0.001	Favourable
Cancer-specific (CSS)	CD8 Primary Tumour Tissue	0.35	0.09	0.074	Favourable
Overall (OS)	CD8 Adjacent Normal Epithelium	2	0.14	0.127	Unclear
Overall (OS)	CD8 Adjacent Normal Stroma	1.91	0.19	0.181	Unclear
Overall (OS)	CD8 Adjacent Normal Tissue	0.76	0.71	0.709	Unclear
Overall (OS)	CD8 Primary Tumour Epithelium	1	0.99	0.991	Unclear
Overall (OS)	CD8 Primary Tumour Stroma	0.83	0.38	0.378	Unclear
Overall (OS)	CD8 Primary Tumour Tissue	0.97	0.89	0.889	Unclear
Disease-free (DFS)	CD8 Adjacent Normal Epithelium	1.46	0.56	0.559	Unclear
Disease-free (DFS)	CD8 Adjacent Normal Stroma	2.76	0.12	0.101	Unclear
Disease-free (DFS)	CD8 Adjacent Normal Tissue	0.81	0.84	0.84	Unclear
Disease-free (DFS)	CD8 Primary Tumour Epithelium	0.47	0.03	0.028	Favourable
Disease-free (DFS)	CD8 Primary Tumour Stroma	0.35	0	0.002	Favourable
Disease-free (DFS)	CD8 Primary Tumour Tissue	0.26	0.03	0.016	Favourable
Recurrence-free (RFS)	CD8 Adjacent Normal Epithelium	1.85	0.62	0.61	Unclear
Recurrence-free (RFS)	CD8 Adjacent Normal Stroma	7.4	0.1	0.055	Unclear
Recurrence-free (RFS)	CD8 Adjacent Normal Tissue	3.62	0.29	0.261	Unclear
Recurrence-free (RFS)	CD8 Primary Tumour Epithelium	0.16	0.08	0.046	Unclear
Recurrence-free (RFS)	CD8 Primary Tumour Stroma	0.76	0.69	0.688	Unclear
Recurrence-free (RFS)	CD8 Primary Tumour Tissue	0	1	0.103	Unclear

4.3.1 γδ T cells - cancer-specific survival

In the adjacent normal epithelium, patients deemed high for γδ T cells are associated with no differential prognosis (Figure 4.55). Patients with a high level of γδ T cells had a mean survival time of 74.29 months, compared to those with low levels of γδ T cells with a mean survival of 77.17 months (hazard ratio = 1.24, p = 0.84). 5-year survival for patients high for γδ T cells is 86% (63%, 100%), compared to 87% (80%, 95%) in the γδ low group. This suggests that γδ T cells in the epithelial compartment of the adjacent normal tissue are associated with no differential prognostic role. Multivariate analysis was not statistically significant (hazard ratio = 3.63, p = 0.26) (Table 4.6), suggesting that γδ T cells in the epithelial compartment of the adjacent normal tissue are not independently prognostic.

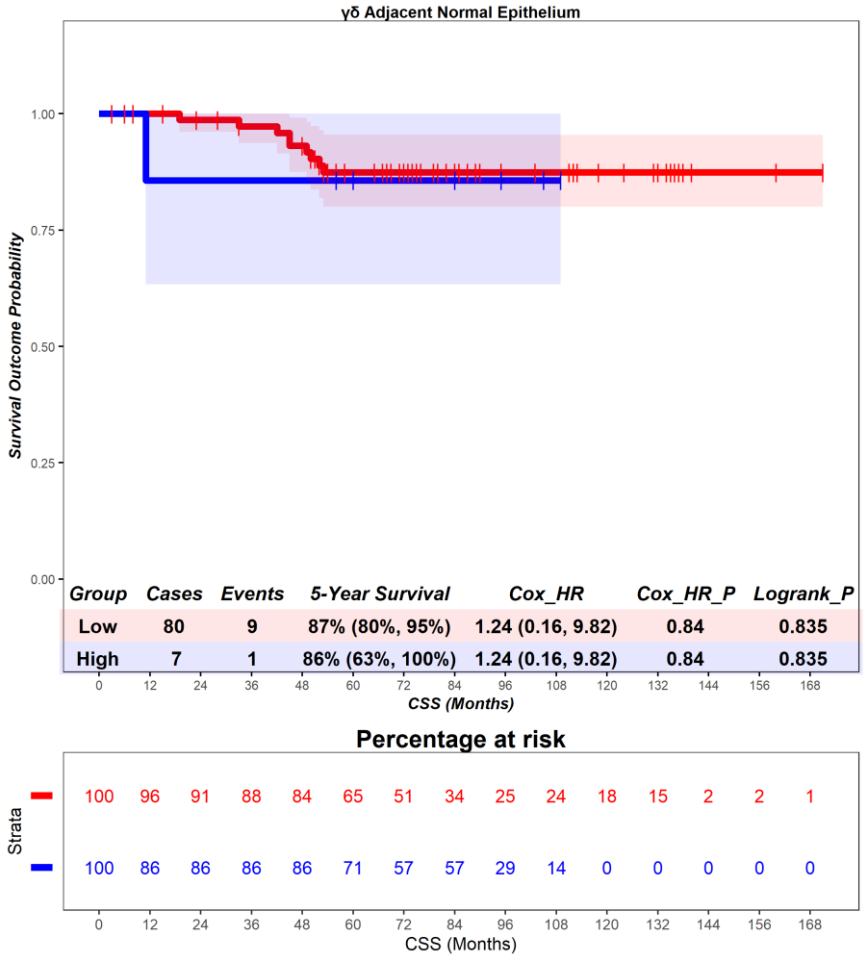

Figure 4.55 – Norway cohort. Time-to-event (cancer-specific survival) analysis for γδ T cells in the adjacent normal epithelium. *Patients deemed 'High' or 'Low' for γδ T cells are shaded blue and red, respectively. Cox hazard ratio is univariate – see table 4.6 for multivariate. The 'Low' group is used as the reference group on cox regression modelling.*

In the adjacent normal stroma, patients deemed high for γδ T cells are associated with no differential prognosis (Figure 4.56). Patients with a high level of γδ T cells had a mean survival time of 71.0 months, compared to those with low levels of γδ T cells with a mean survival of 77.46 months (hazard ratio = 1.24, p = 0.84). 5-year survival for patients high for γδ T cells is 86% (63%, 100%), compared to 87% (80%, 95%) in the γδ low group. This suggests that γδ T cells in the stromal compartment of the adjacent normal tissue are associated with no differential prognostic role. Multivariate analysis was not statistically significant (hazard ratio = Inf, p = 1.0) (Table 4.6), suggesting that γδ T cells in the stromal compartment of the adjacent normal tissue are not independently prognostic.

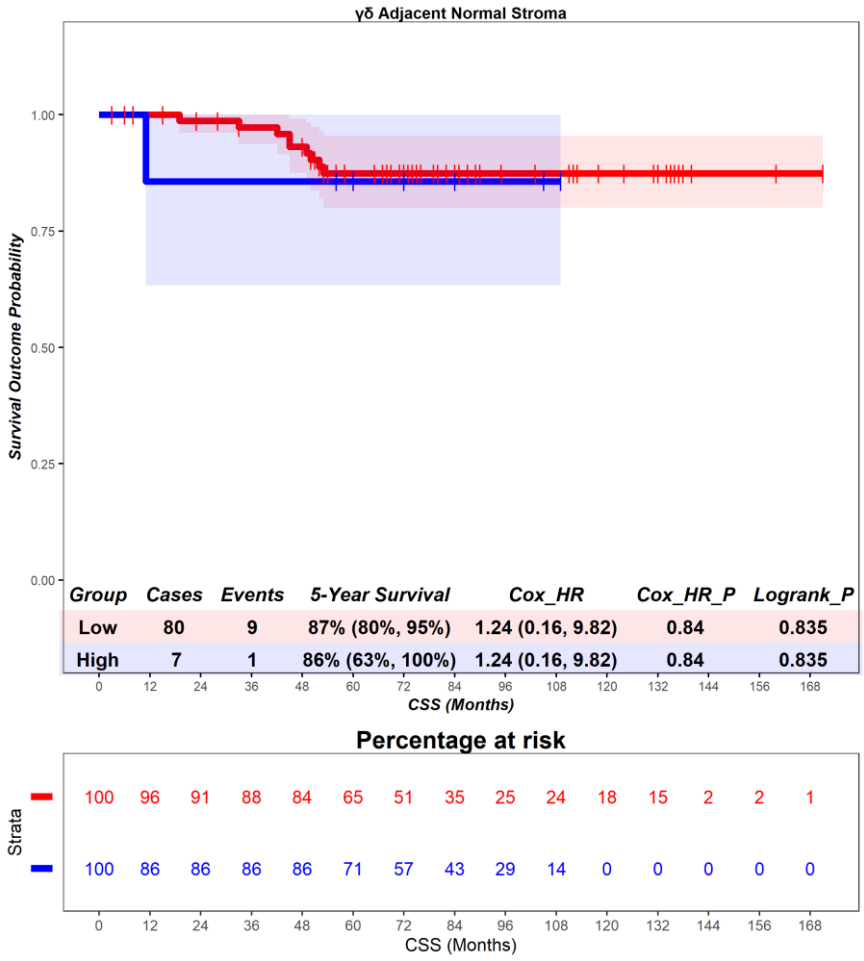

Figure 4.56 – Norway cohort. Time-to-event (cancer-specific survival) analysis for γδ T cells in the adjacent normal stroma. *Patients deemed 'High' or 'Low' for γδ T cells are shaded blue and red, respectively. Cox hazard ratio is univariate – see table 4.6 for multivariate. The 'Low' group is used as the reference group on cox regression modelling.*

In the adjacent normal tissue, patients deemed high for γδ T cells are associated with no differential prognosis (Figure 4.57). Patients with a high level of γδ T cells had a mean survival time of 74.0 months, compared to those with low levels of γδ T cells with a mean survival of 77.24 months (hazard ratio = 1.05, p = 0.96). 5-year survival for patients high for γδ T cells is 88% (67%, 100%), compared to 87% (80%, 95%) in the γδ low group. This suggests that γδ T cells in the whole tissue of the adjacent normal tissue are associated with no differential prognostic role. Multivariate analysis was not statistically significant (hazard ratio = 3.63, p = 0.26) (Table 4.6), suggesting that γδ T cells in the whole tissue of the adjacent normal tissue are not independently prognostic.

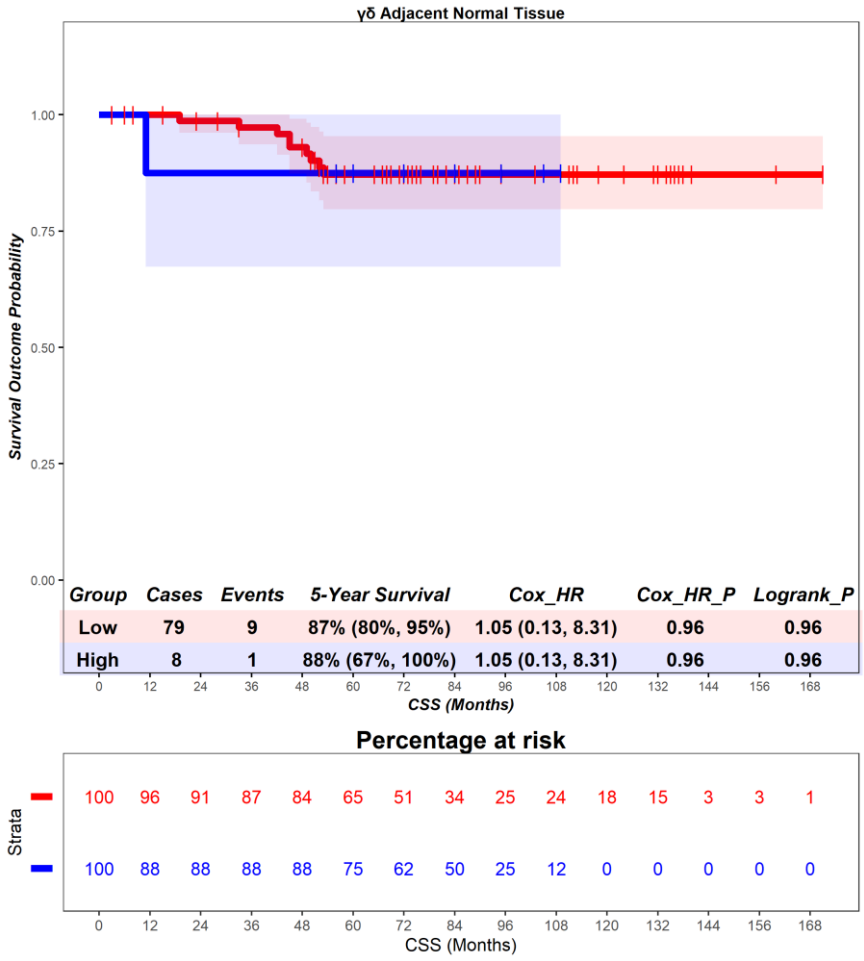

Figure 4.57 - Norway cohort. Time-to-event (cancer-specific survival) analysis for γδ T cells in the adjacent normal tissue. *Patients deemed 'High' or 'Low' for γδ T cells are shaded blue and red, respectively. Cox hazard ratio is univariate – see table 4.6 for multivariate. The 'Low' group is used as the reference group on cox regression modelling.*

In the primary tumour epithelium, patients deemed high for γδ T cells are associated with no differential prognosis (Figure 4.58). Patients with a high level of γδ T cells had a mean survival time of 77.11 months, compared to those with low levels of γδ T cells with a mean survival of 70.54 months (hazard ratio = 0.49, p = 0.11). 5-year survival for patients high for γδ T cells is 93% (88%, 98%), compared to 88% (83%, 94%) in the γδ low group. This suggests that γδ T cells in the epithelial compartment of the primary tumour are associated with no differential prognostic role. Multivariate analysis was not statistically significant (hazard ratio = 0.7, p = 0.42) (Table 4.6), suggesting that γδ T cells in the epithelial compartment of the primary tumour are not independently prognostic.

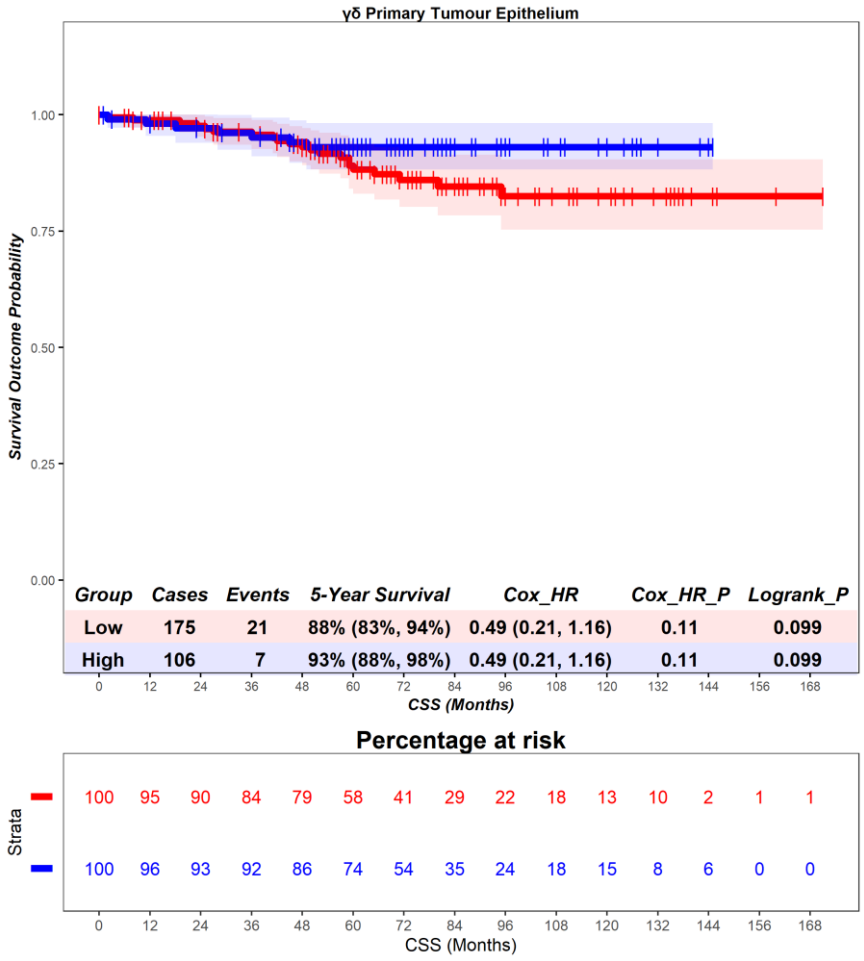

Figure 4.58 – Norway cohort. Time-to-event (cancer-specific survival) analysis for γδ T cells in the primary tumour epithelium. *Patients deemed 'High' or 'Low' for γδ T cells are shaded blue and red, respectively. Cox hazard ratio is univariate – see table 4.6 for multivariate. The 'Low' group is used as the reference group on cox regression modelling.*

In the primary tumour stroma, patients deemed high for γδ T cells are associated with no differential prognosis (Figure 4.59). Patients with a high level of γδ T cells had a mean survival time of 75.58 months, compared to those with low levels of γδ T cells with a mean survival of 71.85 months (hazard ratio = 0.83, p = 0.66). 5-year survival for patients high for γδ T cells is 90% (84%, 97%), compared to 90% (86%, 95%) in the γδ low group. This suggests that γδ T cells in the stromal compartment of the primary tumour are associated with no differential prognostic role. Multivariate analysis was not statistically significant (hazard ratio = 1.05, p = 0.91) (Table 4.6), suggesting that γδ T cells in the stromal compartment of the primary tumour are not independently prognostic.

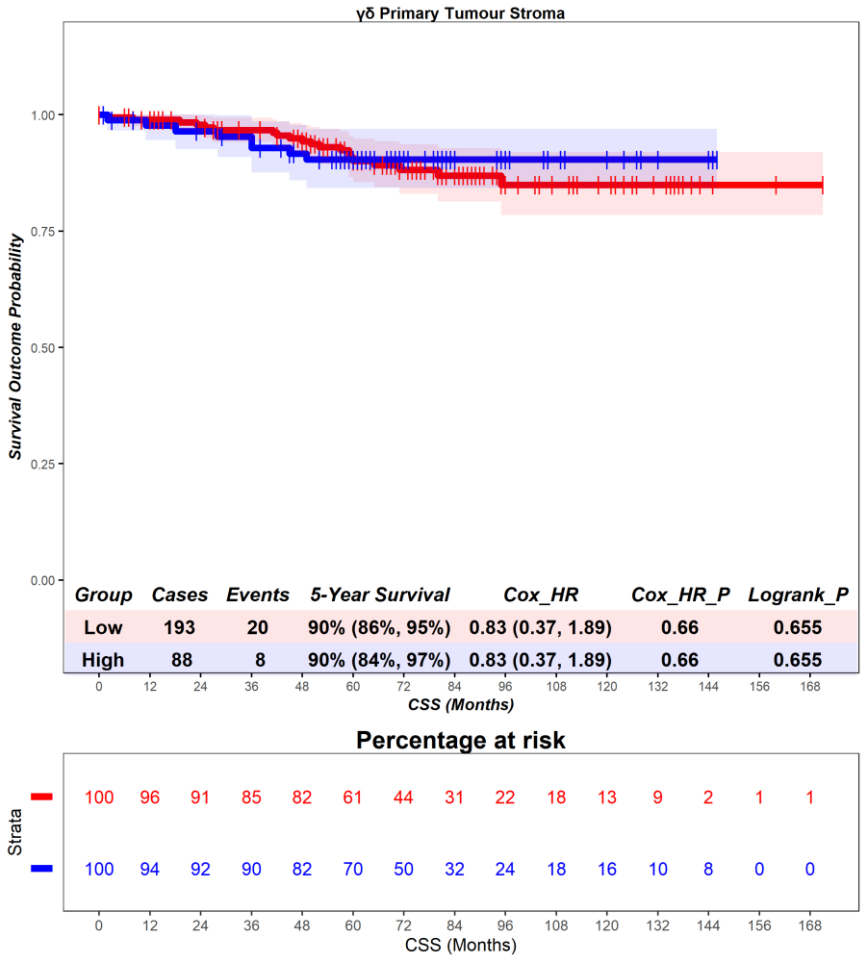

Figure 4.59 – Norway cohort. Time-to-event (cancer-specific survival) analysis for γδ T cells in the primary tumour stroma. *Patients deemed 'High' or 'Low' for γδ T cells are shaded blue and red, respectively. Cox hazard ratio is univariate – see table 4.6 for multivariate. The 'Low' group is used as the reference group on cox regression modelling.*

In the primary tumour tissue, patients deemed high for γδ T cells are associated with no differential prognosis (Figure 4.60). Patients with a high level of γδ T cells had a mean survival time of 77.07 months, compared to those with low levels of γδ T cells with a mean survival of 70.91 months (hazard ratio = 0.58, p = 0.22). 5-year survival for patients high for γδ T cells is 92% (87%, 98%), compared to 89% (84%, 94%) in the γδ low group. This suggests that γδ T cells in the whole tissue of the primary tumour are associated with no differential prognostic role. Multivariate analysis was not statistically significant (hazard ratio = 0.79, p = 0.6) (Table 4.6), suggesting that γδ T cells in the whole tissue of the primary tumour are not independently prognostic.

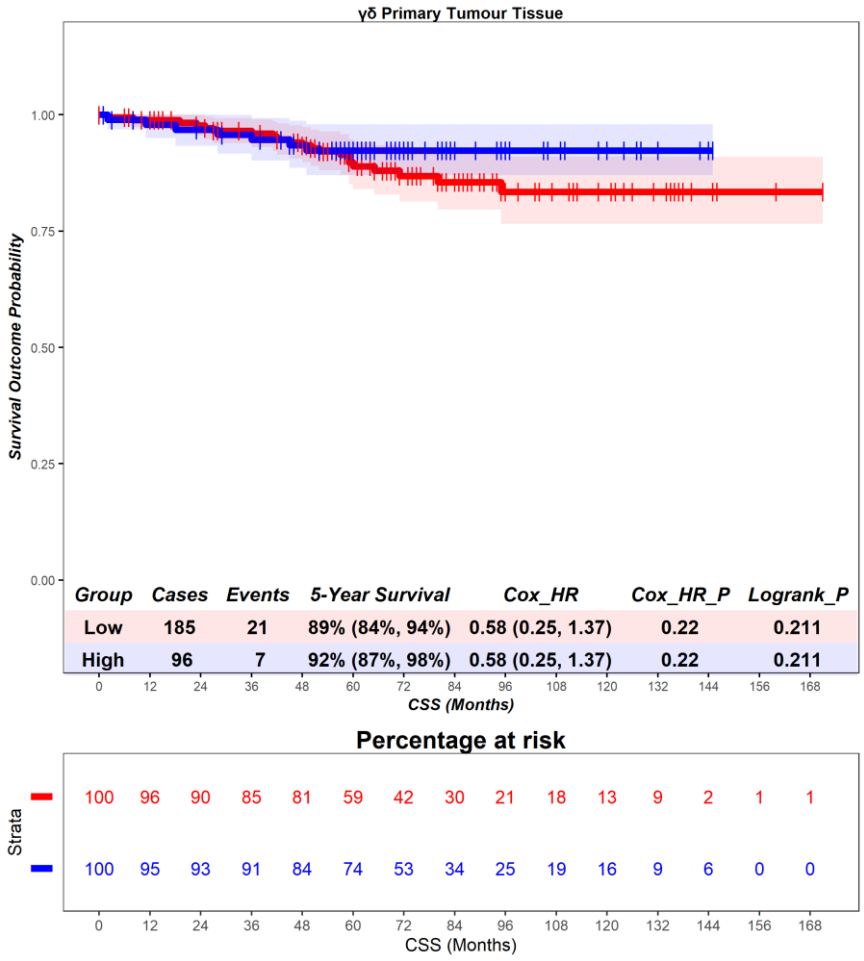

Figure 4.60 – Norway cohort. Time-to-event (cancer-specific survival) analysis for γδ T cells in the primary tumour tissue. *Patients deemed 'High' or 'Low' for γδ T cells are shaded blue and red, respectively. Cox hazard ratio is univariate – see table 4.6 for multivariate. The 'Low' group is used as the reference group on cox regression modelling.*

4.3.2 γδ T cells - overall survival

In the adjacent normal epithelium, patients deemed high for γδ T cells are associated with no differential prognosis (Figure 4.61). Patients with a high level of γδ T cells had a mean survival time of 74.29 months, compared to those with low levels of γδ T cells with a mean survival of 77.17 months (hazard ratio = 1.79, p = 0.28). 5-year survival for patients high for γδ T cells is 69% (40%, 100%), compared to 76% (67%, 86%) in the γδ low group. This suggests that γδ T cells in the epithelial compartment of the adjacent normal tissue are associated with no differential prognostic role. Multivariate analysis was not statistically significant (hazard ratio = 2.33, p = 0.13) (Table 4.6), suggesting that γδ T cells in the epithelial compartment of the adjacent normal tissue are not independently prognostic.

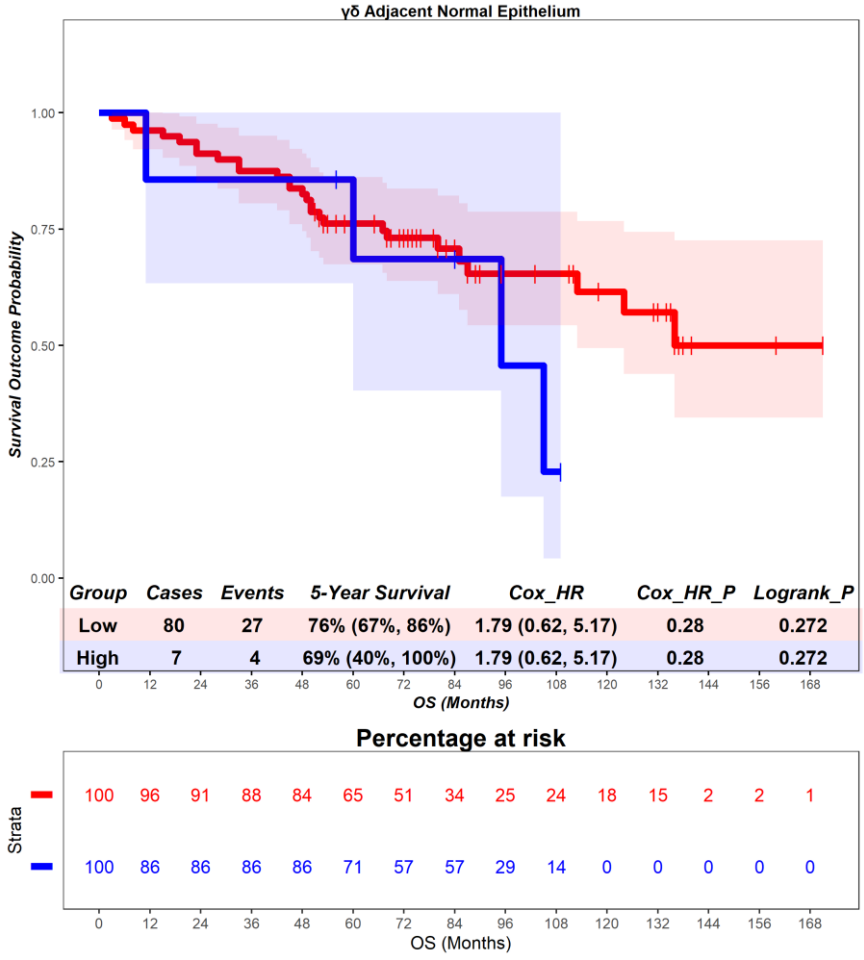

Figure 4.61 – Norway cohort. Time-to-event (overall survival) analysis for γδ T cells in the adjacent normal epithelium. *Patients deemed 'High' or 'Low' for γδ T cells are shaded blue and red, respectively. Cox hazard ratio is univariate – see table 4.6 for multivariate. The 'Low' group is used as the reference group on cox regression modelling.*

In the adjacent normal stroma, patients deemed high for γδ T cells are associated with no differential prognosis (Figure 4.62). Patients with a high level of γδ T cells had a mean survival time of 71.0 months, compared to those with low levels of γδ T cells with a mean survival of 77.46 months (hazard ratio = 1.38, p = 0.6). 5-year survival for patients high for γδ T cells is 69% (40%, 100%), compared to 76% (67%, 86%) in the γδ low group. This suggests that γδ T cells in the stromal compartment of the adjacent normal tissue are associated with no differential prognostic role. Multivariate analysis was not statistically significant (hazard ratio = 1.38, p = 0.6) (Table 4.6), suggesting that γδ T cells in the stromal compartment of the adjacent normal tissue are not independently prognostic.

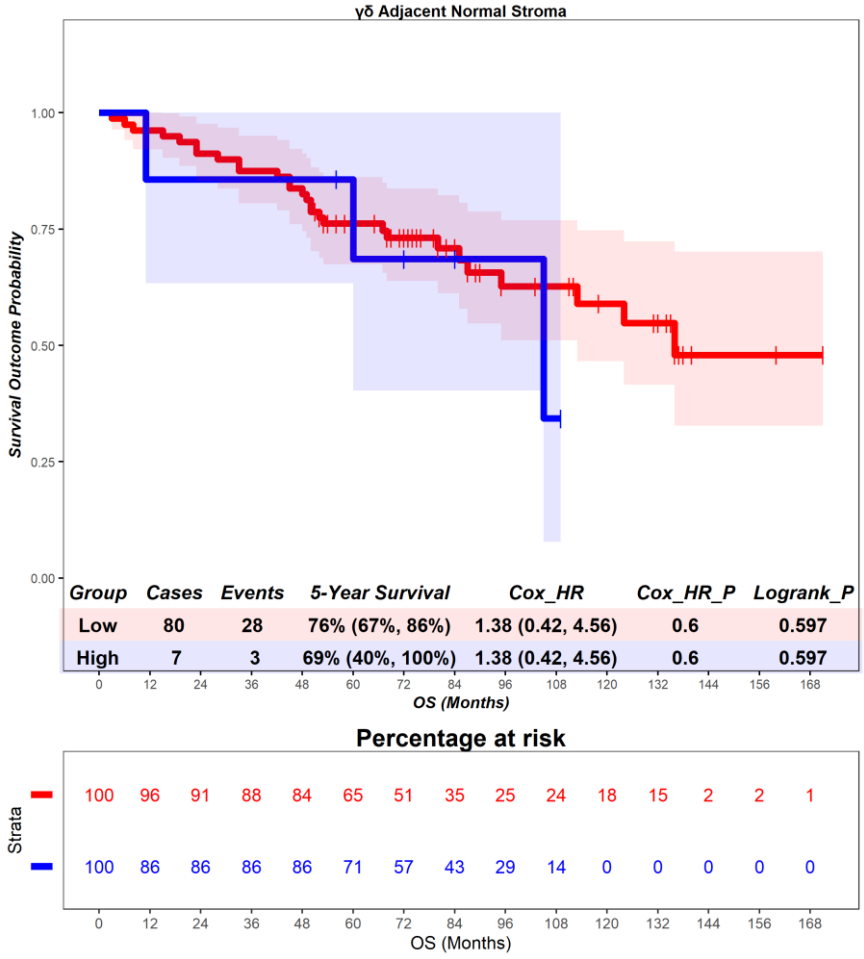

Figure 4.62 – Norway cohort. Time-to-event (overall survival) analysis for γδ T cells in the adjacent normal stroma. *Patients deemed 'High' or 'Low' for γδ T cells are shaded blue and red, respectively. Cox hazard ratio is univariate – see table 4.6 for multivariate. The 'Low' group is used as the reference group on cox regression modelling.*

In the adjacent normal tissue, patients deemed high for γδ T cells are associated with no differential prognosis (Figure 4.63). Patients with a high level of γδ T cells had a mean survival time of 74.00 months, compared to those with low levels of γδ T cells with a mean survival of 77.24 months (hazard ratio = 1.56, p = 0.41). 5-year survival for patients high for γδ T cells is 73% (47%, 100%), compared to 76% (67%, 86%) in the γδ low group. This suggests that γδ T cells in the whole tissue of the adjacent normal tissue are associated with no differential prognostic role. Multivariate analysis was not statistically significant (hazard ratio = 2.29, p = 0.14) (Table 4.6), suggesting that γδ T cells in the whole tissue of the adjacent normal tissue are not independently prognostic.

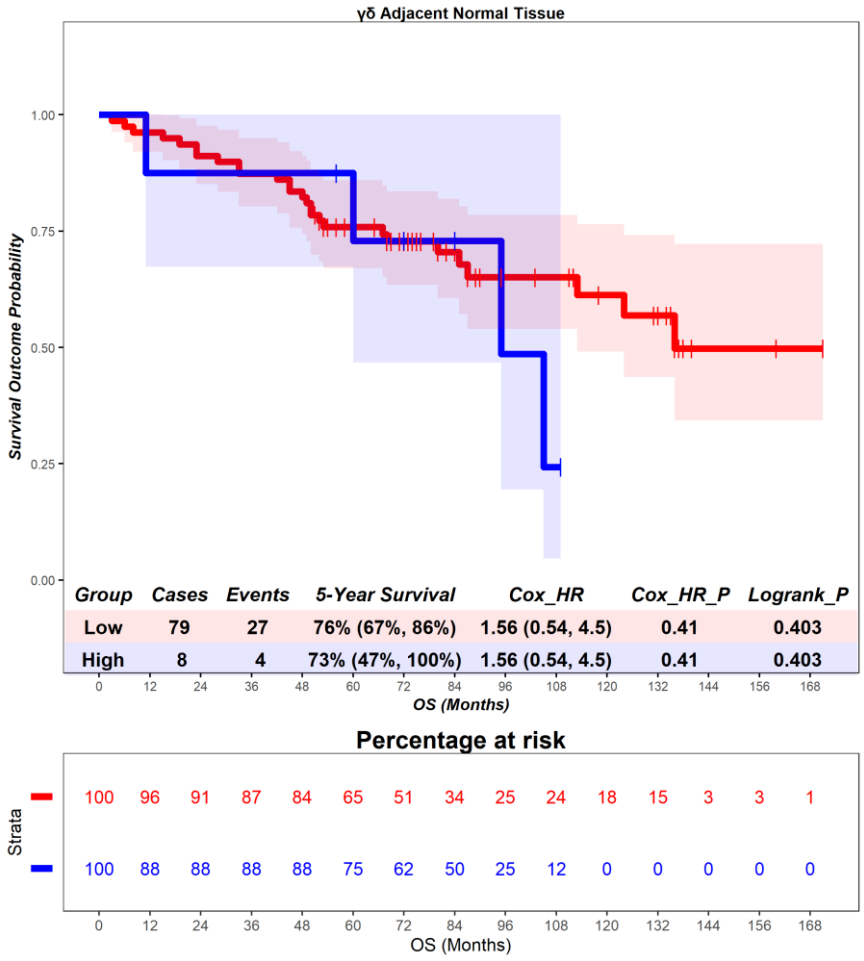

Figure 4.63 – Norway cohort. Time-to-event (overall survival) analysis for γδ T cells in the adjacent normal tissue. *Patients deemed 'High' or 'Low' for γδ T cells are shaded blue and red, respectively. Cox hazard ratio is univariate – see table 4.6 for multivariate. The 'Low' group is used as the reference group on cox regression modelling.*

In the primary tumour epithelium, patients deemed high for γδ T cells are associated with a better prognosis (Figure 4.64). Patients with a high level of γδ T cells had a mean survival time of 77.11 months, compared to those with low levels of γδ T cells with a mean survival of 70.54 months (hazard ratio = 0.56, p = 0.01). 5-year survival for patients high for γδ T cells is 83% (76%, 90%), compared to 69% (63%, 77%) in the γδ low group. This suggests that γδ T cells in the epithelial compartment of the primary tumour are associated with no differential prognostic role. Multivariate analysis was statistically significant (hazard ratio = 0.55, p = 0.01) (Table 4.6), suggesting that γδ T cells in the epithelial compartment of the primary tumour are independently prognostic.

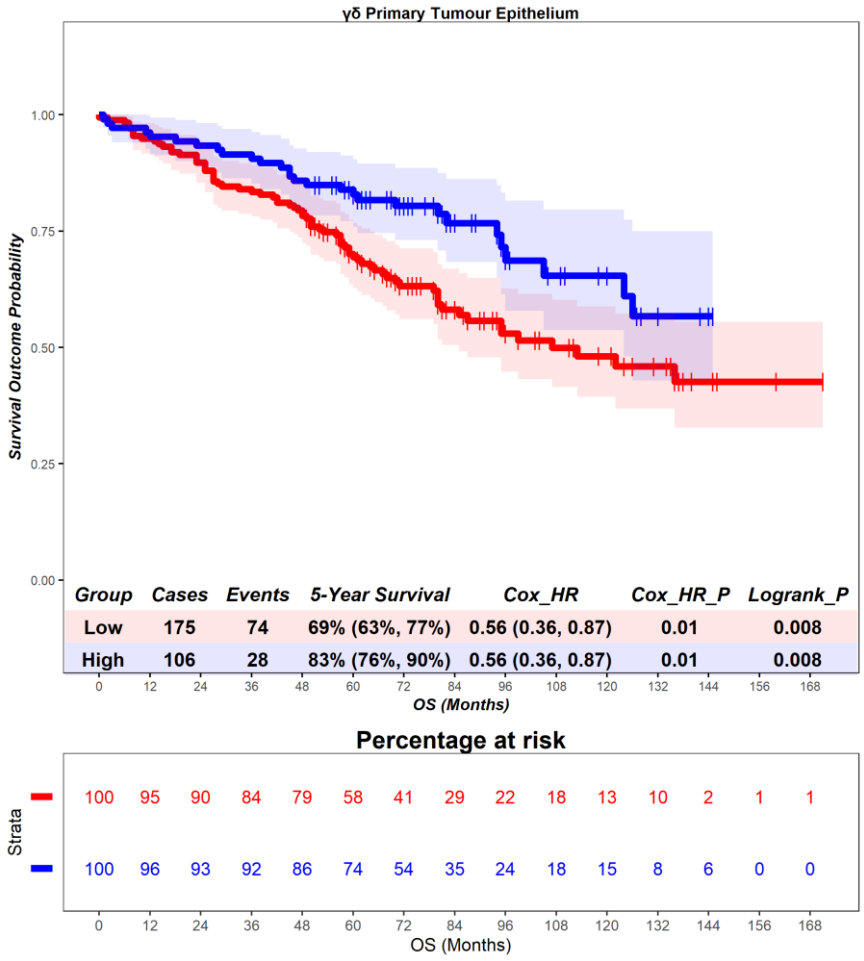

Figure 4.64 – Norway cohort. Time-to-event (overall survival) analysis for γδ T cells in the primary tumour epithelium. *Patients deemed 'High' or 'Low' for γδ T cells are shaded blue and red, respectively. Cox hazard ratio is univariate – see table 4.6 for multivariate. The 'Low' group is used as the reference group on cox regression modelling.*

In the primary tumour stroma, patients deemed high for γδ T cells are associated with a better prognosis (Figure 4.65). Patients with a high level of γδ T cells had a mean survival time of 75.58 months, compared to those with low levels of γδ T cells with a mean survival of 71.85 months (hazard ratio = 0.67, p = 0.08). 5-year survival for patients high for γδ T cells is 78% (70%, 87%), compared to 73% (67%, 80%) in the γδ low group. This suggests that γδ T cells in the stromal compartment of the primary tumour are associated with no differential prognostic role. Multivariate analysis was not statistically significant (hazard ratio = 0.64, p = 0.06) (Table 4.6), suggesting that γδ T cells in the stromal compartment of the primary tumour are not independently prognostic.

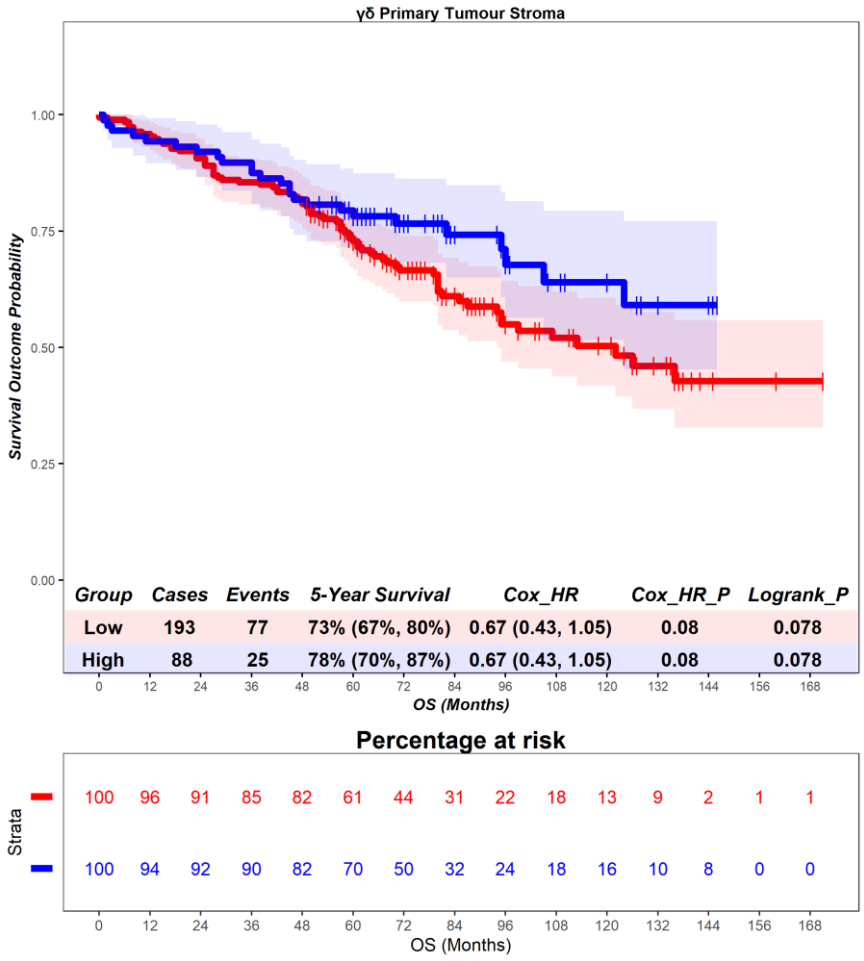

Figure 4.65 – Norway cohort. Time-to-event (overall survival) analysis for γδ T cells in the primary tumour stroma. *Patients deemed 'High' or 'Low' for γδ T cells are shaded blue and red, respectively. Cox hazard ratio is univariate – see table 4.6 for multivariate. The 'Low' group is used as the reference group on cox regression modelling.*

In the primary tumour tissue, patients deemed high for γδ T cells are associated with a better prognosis (Figure 4.66). Patients with a high level of γδ T cells had a mean survival time of 77.07 months, compared to those with low levels of γδ T cells with a mean survival of 70.91 months (hazard ratio = 0.56, p = 0.01). 5-year survival for patients high for γδ T cells is 81% (74%, 89%), compared to 71% (65%, 78%) in the γδ low group. This suggests that γδ T cells in the whole tissue of the primary tumour are associated with no differential prognostic role. Multivariate analysis was statistically significant (hazard ratio = 0.57, p = 0.02) (Table 4.6), suggesting that γδ T cells in the whole tissue of the primary tumour are independently prognostic.

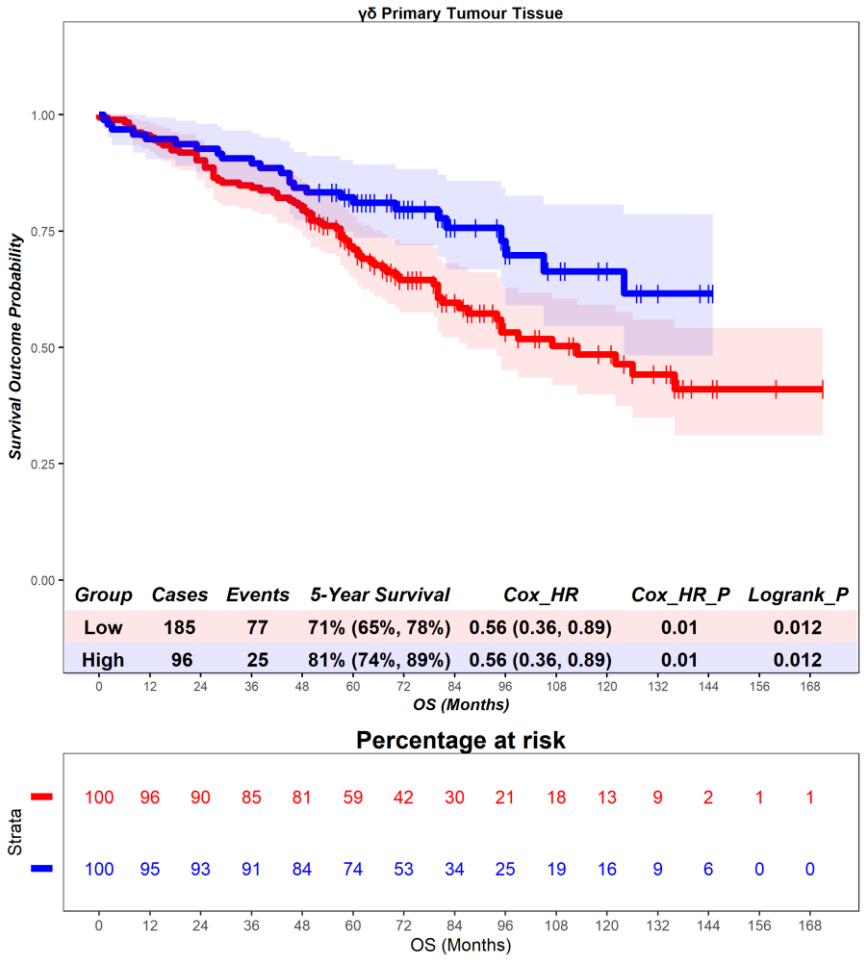

Figure 4.66 – Norway cohort. Time-to-event (overall survival) analysis for γδ T cells in the primary tumour tissue. *Patients deemed 'High' or 'Low' for γδ T cells are shaded blue and red, respectively. Cox hazard ratio is univariate – see table 4.6 for multivariate. The 'Low' group is used as the reference group on cox regression modelling.*

4.3.3 γδ T cells - disease-free survival

In the adjacent normal epithelium, patients deemed high for γδ T cells are associated with a worse prognosis (Figure 4.67). Patients with a high level of γδ T cells had a mean survival time of 67.0 months, compared to those with low levels of γδ T cells with a mean survival of 76.7 months (hazard ratio = 2.52, p = 0.23). 5-year survival for patients high for γδ T cells is 71% (45%, 100%), compared to 86% (78%, 94%) in the γδ low group. This suggests that γδ T cells in the epithelial compartment of the adjacent normal tissue are associated with an unfavourable prognostic role. Multivariate analysis was statistically significant (hazard ratio = 6.18, p = 0.03) (Table 4.6), suggesting that γδ T cells in the epithelial compartment of the adjacent normal tissue are independently prognostic.

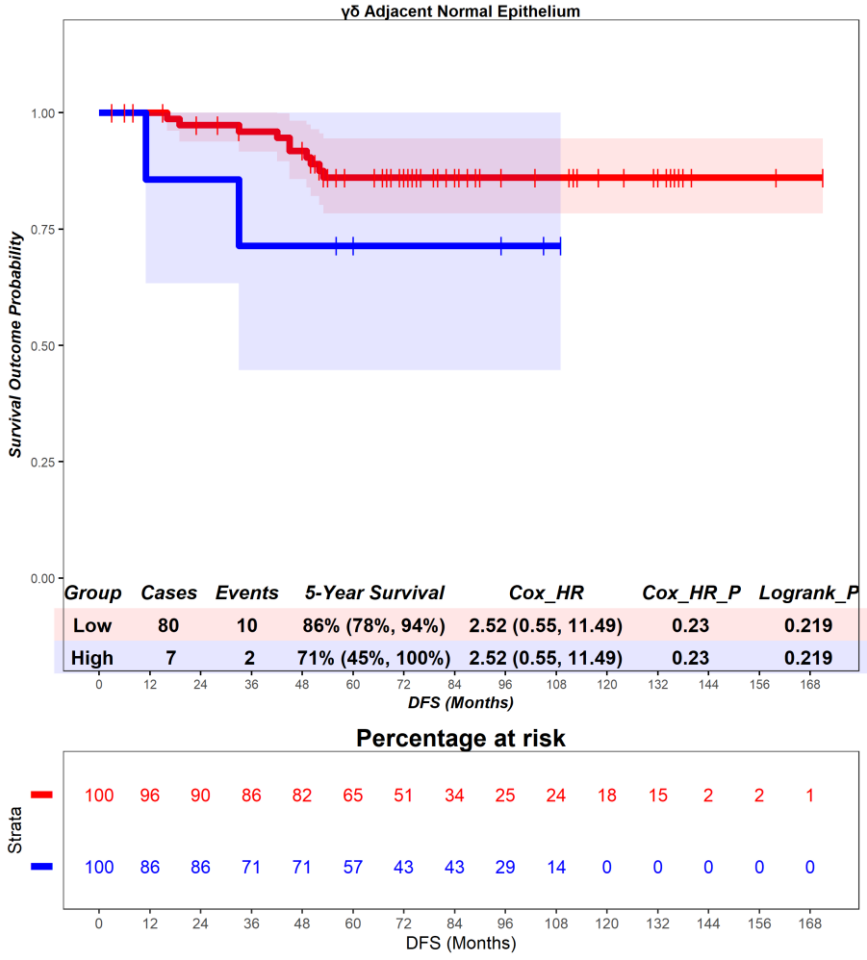

Figure 4.67 – Norway cohort. Time-to-event (disease-free survival) analysis for γδ T cells in the adjacent normal epithelium. *Patients deemed 'High' or 'Low' for γδ T cells are shaded blue and red, respectively. Cox hazard ratio is univariate – see table 4.6 for multivariate. The 'Low' group is used as the reference group on cox regression modelling.*

In the adjacent normal stroma, patients deemed high for γδ T cells are associated with a worse prognosis (Figure 4.68). Patients with a high level of γδ T cells had a mean survival time of 63.71 months, compared to those with low levels of γδ T cells with a mean survival of 76.99 months (hazard ratio = 2.52, p = 0.23). 5-year survival for patients high for γδ T cells is 71% (45%, 100%), compared to 86% (78%, 94%) in the γδ low group. This suggests that γδ T cells in the stromal compartment of the adjacent normal tissue are associated with an unfavourable prognostic role. Multivariate analysis was not statistically significant (hazard ratio = Inf, p = 1) (Table 4.6), suggesting that γδ T cells in the stromal compartment of the adjacent normal tissue are independently prognostic.

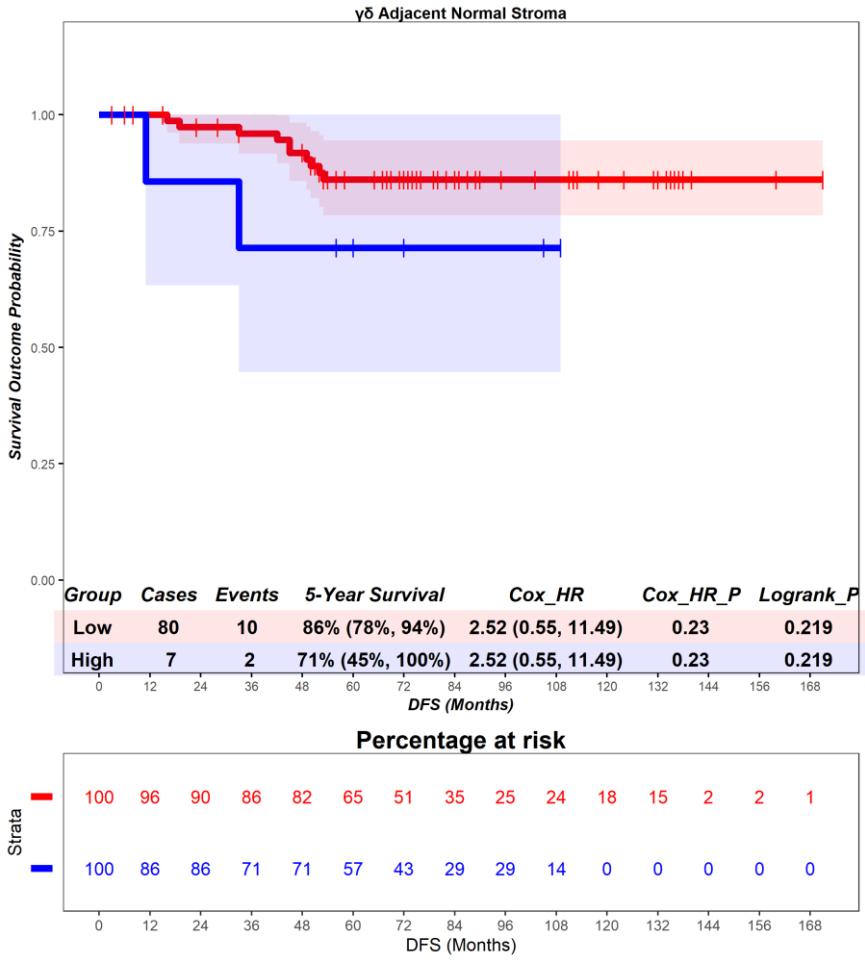

Figure 4.68 – Norway cohort. Time-to-event (disease-free survival) analysis for γδ T cells in the adjacent normal stroma. *Patients deemed 'High' or 'Low' for γδ T cells are shaded blue and red, respectively. Cox hazard ratio is univariate – see table 4.6 for multivariate. The 'Low' group is used as the reference group on cox regression modelling.*

In the adjacent normal tissue, patients deemed high for γδ T cells are associated with a worse prognosis (Figure 4.69). Patients with a high level of γδ T cells had a mean survival time of 67.0 months, compared to those with low levels of γδ T cells with a mean survival of 76.7 months (hazard ratio = 2.09, p = 0.34). 5-year survival for patients high for γδ T cells is 75% (50%, 100%), compared to 86% (78%, 94%) in the γδ low group. This suggests that γδ T cells in the whole tissue of the adjacent normal tissue are associated with an unfavourable prognostic role. Multivariate analysis was statistically significant (hazard ratio = 5.97, p = 0.04) (Table 4.6), suggesting that γδ T cells in the whole tissue of the adjacent normal tissue are independently prognostic.

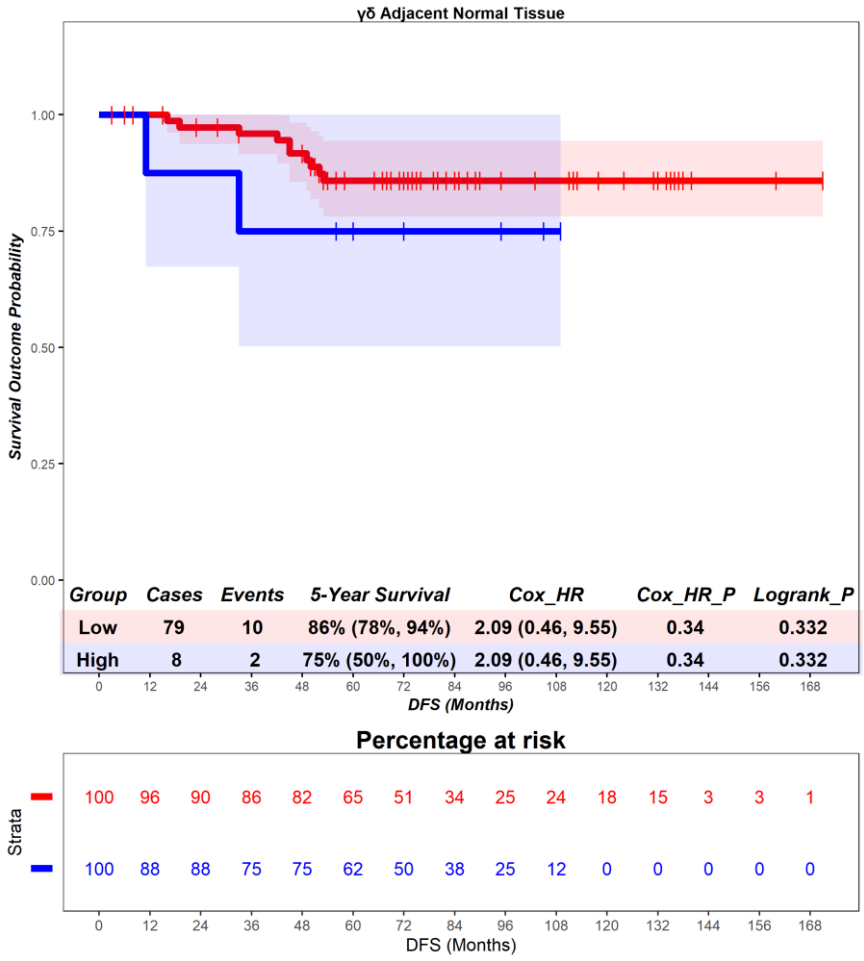

Figure 4.69 – Norway cohort. Time-to-event (disease-free survival) analysis for γδ T cells in the adjacent normal tissue. *Patients deemed 'High' or 'Low' for γδ T cells are shaded blue and red, respectively. Cox hazard ratio is univariate – see table 4.6 for multivariate. The 'Low' group is used as the reference group on cox regression modelling.*

In the primary tumour epithelium, patients deemed high for γδ T cells are associated with a better prognosis (Figure 4.70), although this result did not reach statistical significance. Patients with a high level of γδ T cells had a mean survival time of 76.18 months, compared to those with low levels of γδ T cells with a mean survival of 69.02 months (hazard ratio = 0.52, p = 0.09). 5-year survival for patients high for γδ T cells is 91% (86%, 97%), compared to 85% (80%, 91%) in the γδ low group. This suggests that γδ T cells in the epithelial compartment of the primary tumour are associated with a favourable prognostic role. Multivariate analysis was not statistically significant (hazard ratio = 0.67, p = 0.3) (Table 4.6), suggesting that γδ T cells in the epithelial compartment of the primary tumour are not independently prognostic.

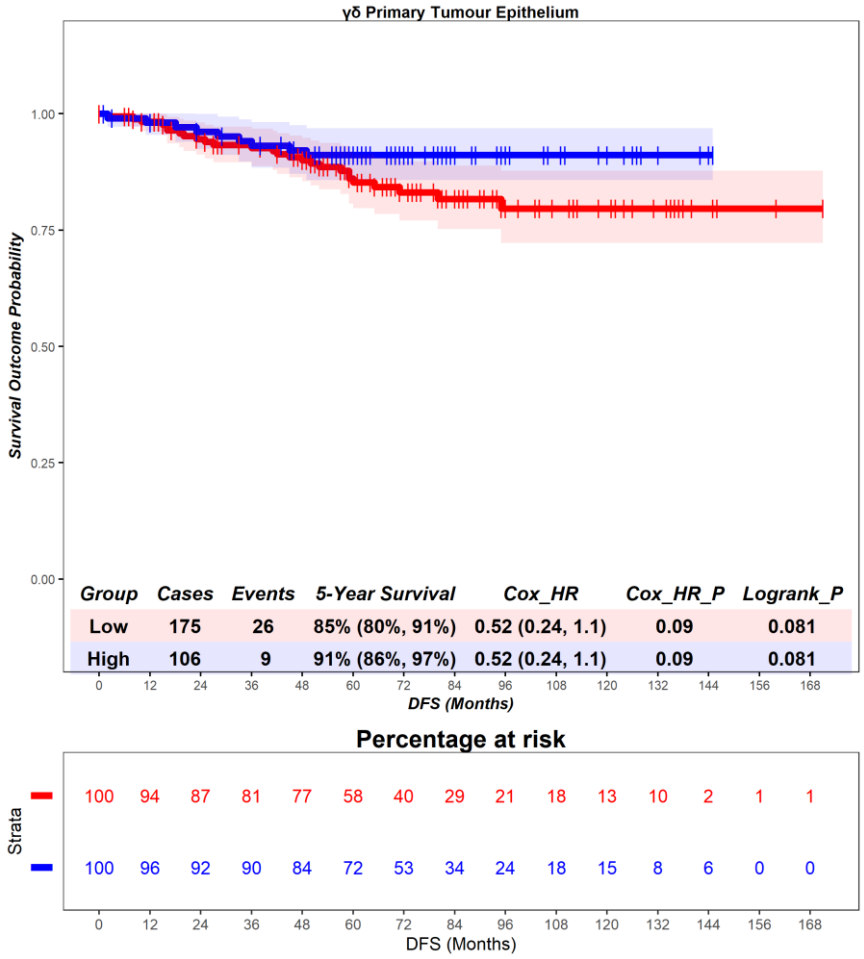

Figure 4.70 – Norway cohort. Time-to-event (disease-free survival) analysis for γδ T cells in the primary tumour epithelium. *Patients deemed 'High' or 'Low' for γδ T cells are shaded blue and red, respectively. Cox hazard ratio is univariate – see table 4.6 for multivariate. The 'Low' group is used as the reference group on cox regression modelling.*

In the primary tumour stroma, patients deemed high for γδ T cells are associated with no differential prognosis (Figure 4.71), although this result did not reach statistical significance. Patients with a high level of γδ T cells had a mean survival time of 74.45 months, compared to those with low levels of γδ T cells with a mean survival of 70.48 months (hazard ratio = 0.83, p = 0.63). 5-year survival for patients high for γδ T cells is 88% (81%, 95%), compared to 87% (82%, 93%) in the γδ low group. This suggests that γδ T cells in the stromal compartment of the primary tumour are associated with no differential prognostic role. Multivariate analysis was not statistically significant (hazard ratio = 1.04, p = 0.92) (Table 4.6), suggesting that γδ T cells in the stromal compartment of the primary tumour are not independently prognostic.

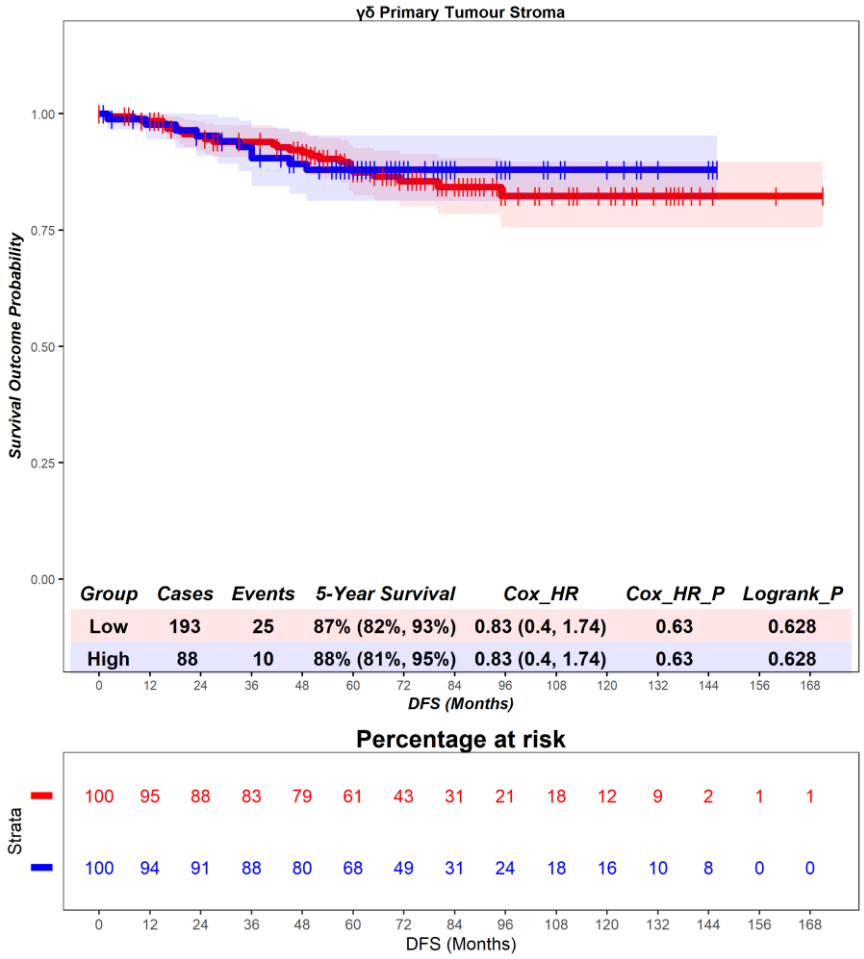

Figure 4.71 – Norway cohort. Time-to-event (disease-free survival) analysis for γδ T cells in the primary tumour stroma. *Patients deemed 'High' or 'Low' for γδ T cells are shaded blue and red, respectively. Cox hazard ratio is univariate – see table 4.6 for multivariate. The 'Low' group is used as the reference group on cox regression modelling.*

In the primary tumour tissue, patients deemed high for γδ T cells are associated with a better prognosis (Figure 4.72), although this result did not reach statistical significance. Patients with a high level of γδ T cells had a mean survival time of 76.04 months, compared to those with low levels of γδ T cells with a mean survival of 69.48 months (hazard ratio = 0.61, p = 0.2). 5-year survival for patients high for γδ T cells is 90% (84%, 96%), compared to 86% (81%, 92%) in the γδ low group. This suggests that γδ T cells in the whole tissue of the primary tumour are associated with a favourable prognostic role. Multivariate analysis was not statistically significant (hazard ratio = 0.77, p = 0.52) (Table 4.6), suggesting that γδ T cells in the whole tissue of the primary tumour are not independently prognostic.

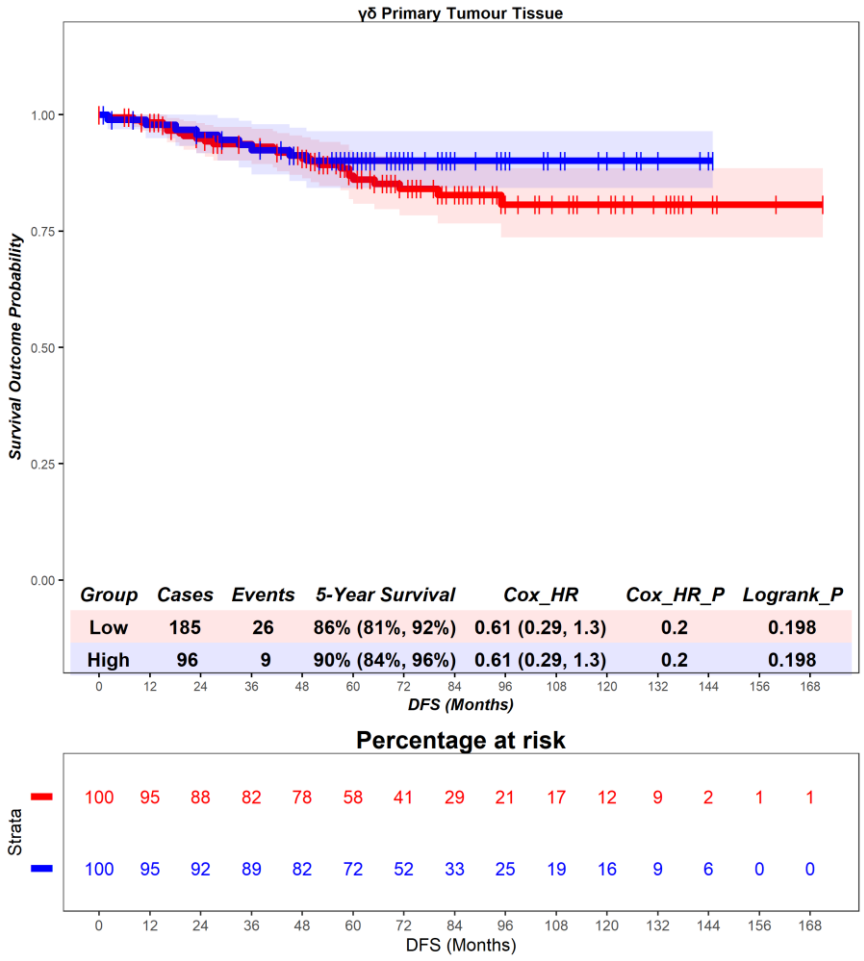

Figure 4.72 – Norway cohort. Time-to-event (disease-free survival) analysis for γδ T cells in the primary tumour tissue. *Patients deemed 'High' or 'Low' for γδ T cells are shaded blue and red, respectively. Cox hazard ratio is univariate – see table 4.6 for multivariate. The 'Low' group is used as the reference group on cox regression modelling.*

4.3.4 γδ T cells - recurrence-free survival

In the adjacent normal epithelium, patients deemed high for γδ T cells are associated with no differential prognosis (Figure 4.73). Patients with a high level of γδ T cells had a mean survival time of 67.0 months, compared to those with low levels of γδ T cells with a mean survival of 76.7 months (hazard ratio = 12.24, p = 0.08). 5-year survival for patients high for γδ T cells is 83% (58%, 100%), compared to 99% (96%, 100%) in the γδ low group. This suggests that γδ T cells in the epithelial compartment of the adjacent normal tissue are associated with no differential prognostic role. Multivariate analysis was not statistically significant (hazard ratio = 9.91, p = 0.11) (Table 4.6), suggesting that γδ T cells in the epithelial compartment of the adjacent normal tissue are not independently prognostic.

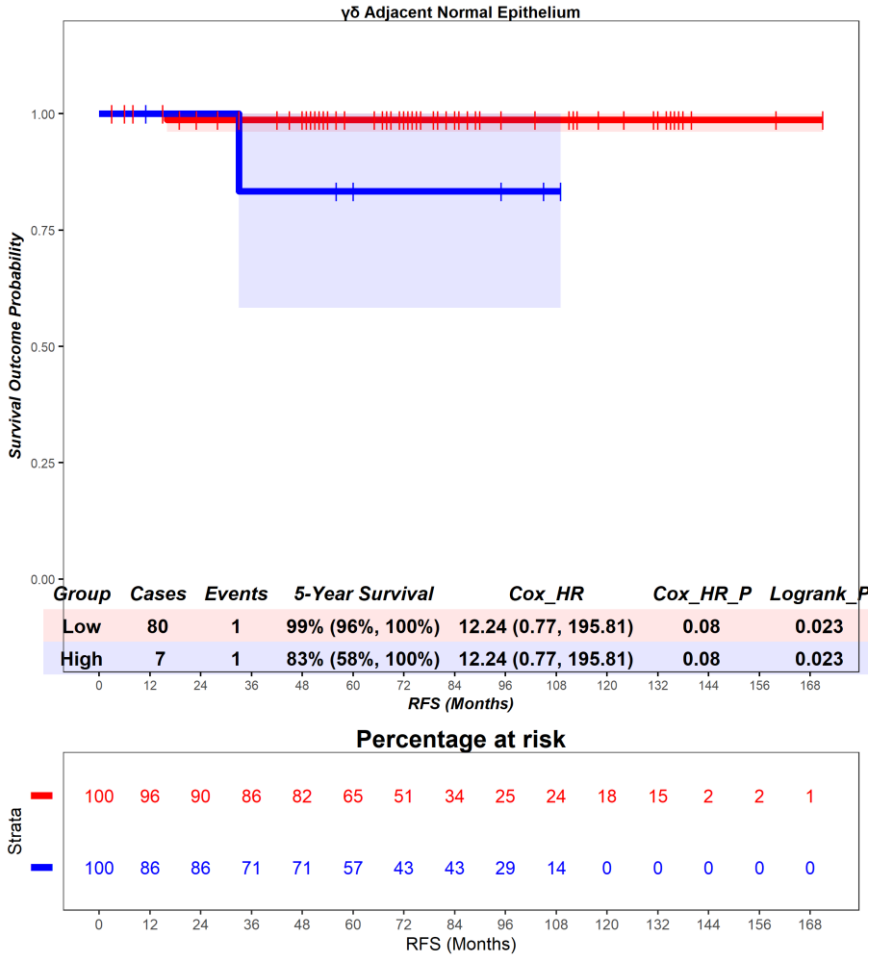

Figure 4.73 – Norway cohort Time-to-event (recurrence-free survival) analysis for γδ T cells in the adjacent normal epithelium. *Patients deemed 'High' or 'Low' for γδ T cells are shaded blue and red, respectively. Cox hazard ratio is univariate – see table 4.6 for multivariate. The 'Low' group is used as the reference group on cox regression modelling.*

In the adjacent normal stroma, patients deemed high for γδ T cells are associated with no differential prognosis (Figure 4.74). Patients with a high level of γδ T cells had a mean survival time of 63.71 months, compared to those with low levels of γδ T cells with a mean survival of 76.99 months (hazard ratio = 12.24, p = 0.08). 5-year survival for patients high for γδ T cells is 83% (58%, 100%), compared to 99% (96%, 100%) in the γδ low group. This suggests that γδ T cells in the stromal compartment of the adjacent normal tissue are associated with no differential prognostic role. Multivariate analysis was not statistically significant (hazard ratio = 9.05, p = 0.15) (Table 4.6), suggesting that γδ T cells in the stromal compartment of the adjacent normal tissue are not independently prognostic.

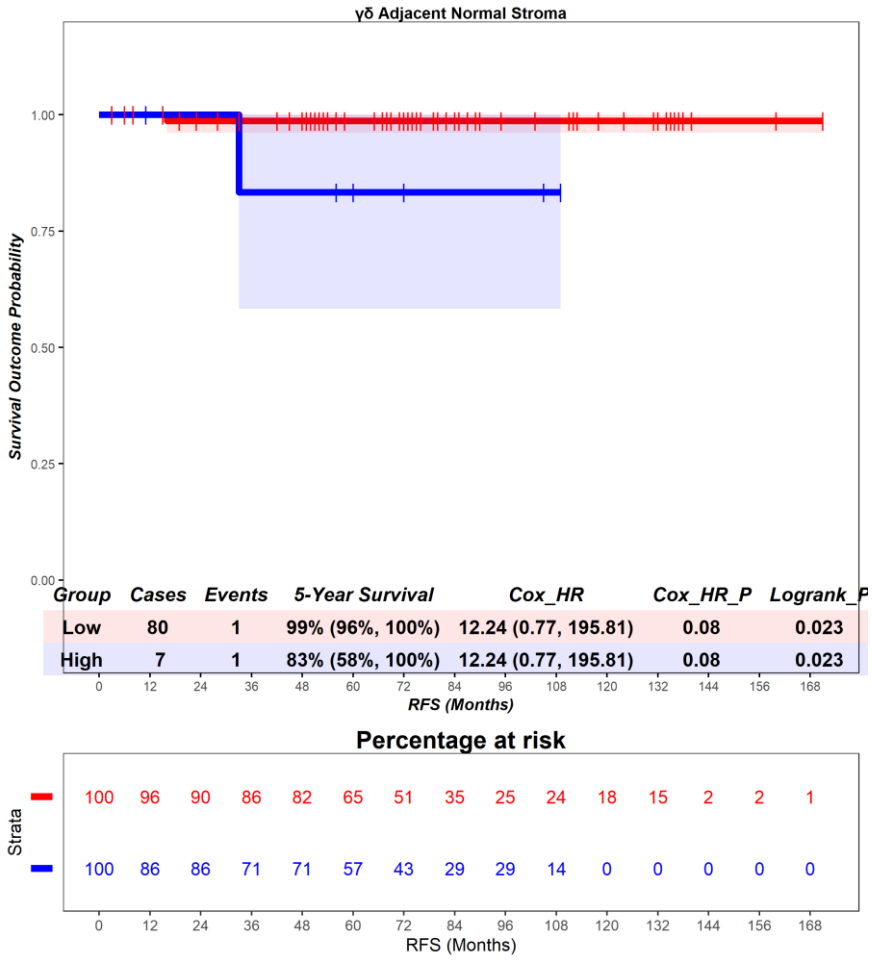

Figure 4.74 – Norway cohort. Time-to-event (recurrence-free survival) analysis for γδ T cells in the adjacent normal stroma. *Patients deemed 'High' or 'Low' for γδ T cells are shaded blue and red, respectively. Cox hazard ratio is univariate – see table 4.6 for multivariate. The 'Low' group is used as the reference group on cox regression modelling.*

In the adjacent normal tissue, patients deemed high for γδ T cells are associated with no differential prognosis (Figure 4.75). Patients with a high level of γδ T cells had a mean survival time of 67.62 months, compared to those with low levels of γδ T cells with a mean survival of 76.76 months (hazard ratio = 10.35, p = 0.1). 5-year survival for patients high for γδ T cells is 86% (63%, 100%), compared to 99% (96%, 100%) in the γδ low group. This suggests that γδ T cells in the whole tissue of the adjacent normal tissue are associated with no differential prognostic role. Multivariate analysis was not statistically significant (hazard ratio = 7.78, p = 0.17) (Table 4.6), suggesting that γδ T cells in the whole tissue of the adjacent normal tissue are not independently prognostic.

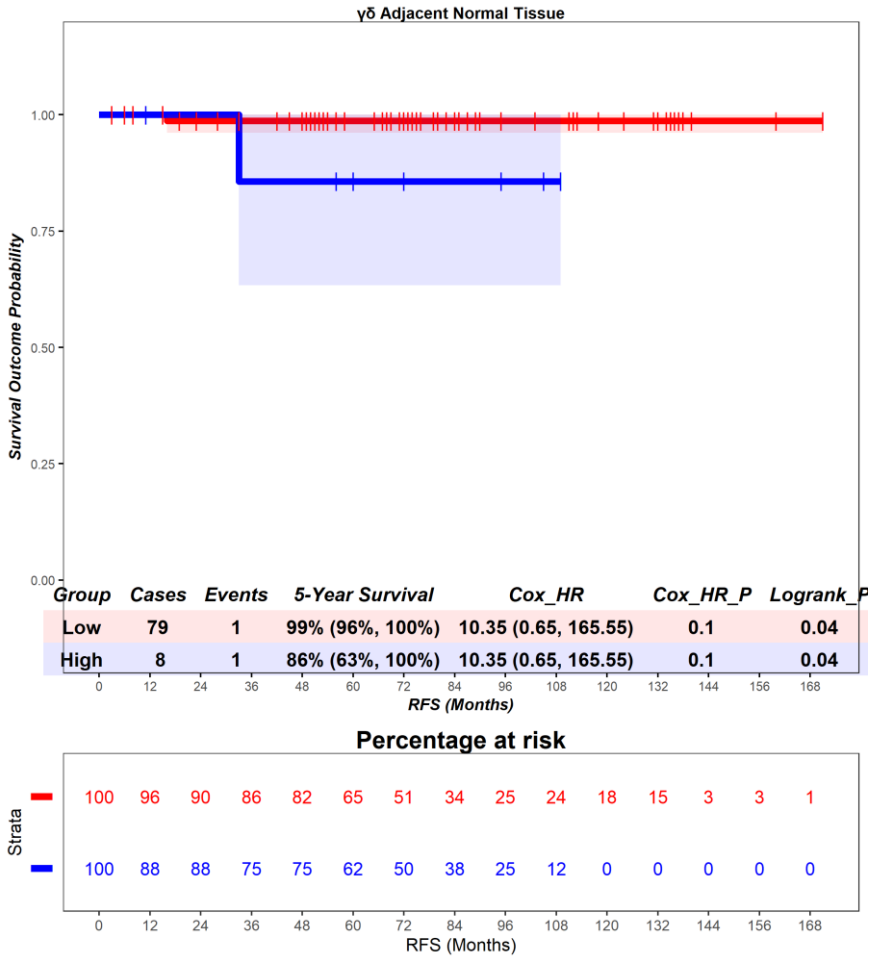

Figure 4.75 – Norway cohort. Time-to-event (recurrence-free survival) analysis for γδ T cells in the adjacent normal tissue. *Patients deemed 'High' or 'Low' for γδ T cells are shaded blue and red, respectively. Cox hazard ratio is univariate – see table 4.6 for multivariate. The 'Low' group is used as the reference group on cox regression modelling.*

In the primary tumour epithelium, patients deemed high for γδ T cells are associated with no differential prognosis (Figure 4.76). Patients with a high level of γδ T cells had a mean survival time of 76.18 months, compared to those with low levels of γδ T cells with a mean survival of 69.02 months (hazard ratio = 0.63, p = 0.58). 5-year survival for patients high for γδ T cells is 98% (95%, 100%), compared to 97% (94%, 100%) in the γδ low group. This suggests that γδ T cells in the epithelial compartment of the primary tumour are associated with no differential prognostic role. Multivariate analysis was not statistically significant (hazard ratio = 0.56, p = 0.49) (Table 4.6), suggesting that γδ T cells in the epithelial compartment of the primary tumour are not independently prognostic.

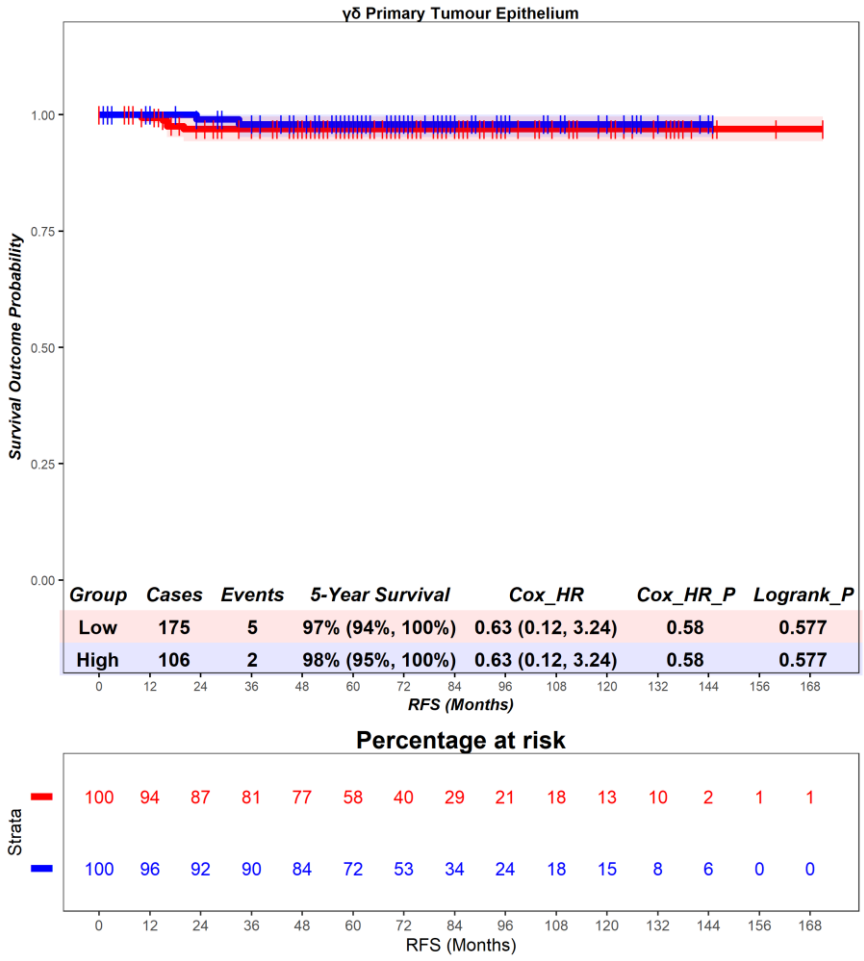

Figure 4.76 – Norway cohort. Time-to-event (recurrence-free survival) analysis for γδ T cells in the primary tumour epithelium. *Patients deemed 'High' or 'Low' for γδ T cells are shaded blue and red, respectively. Cox hazard ratio is univariate – see table 4.6 for multivariate. The 'Low' group is used as the reference group on cox regression modelling.*

In the primary tumour stroma, patients deemed high for γδ T cells are associated with no differential prognosis (Figure 4.77). Patients with a high level of γδ T cells had a mean survival time of 74.45 months, compared to those with low levels of γδ T cells with a mean survival of 70.48 months (hazard ratio = 0.86, p = 0.85). 5-year survival for patients high for γδ T cells is 98% (94%, 100%), compared to 97% (95%, 100%) in the γδ low group. This suggests that γδ T cells in the stromal compartment of the primary tumour are associated with no differential prognostic role. Multivariate analysis was not statistically significant (hazard ratio = 0.82, p = 0.81) (Table 4.6), suggesting that γδ T cells in the stromal compartment of the primary tumour are not independently prognostic.

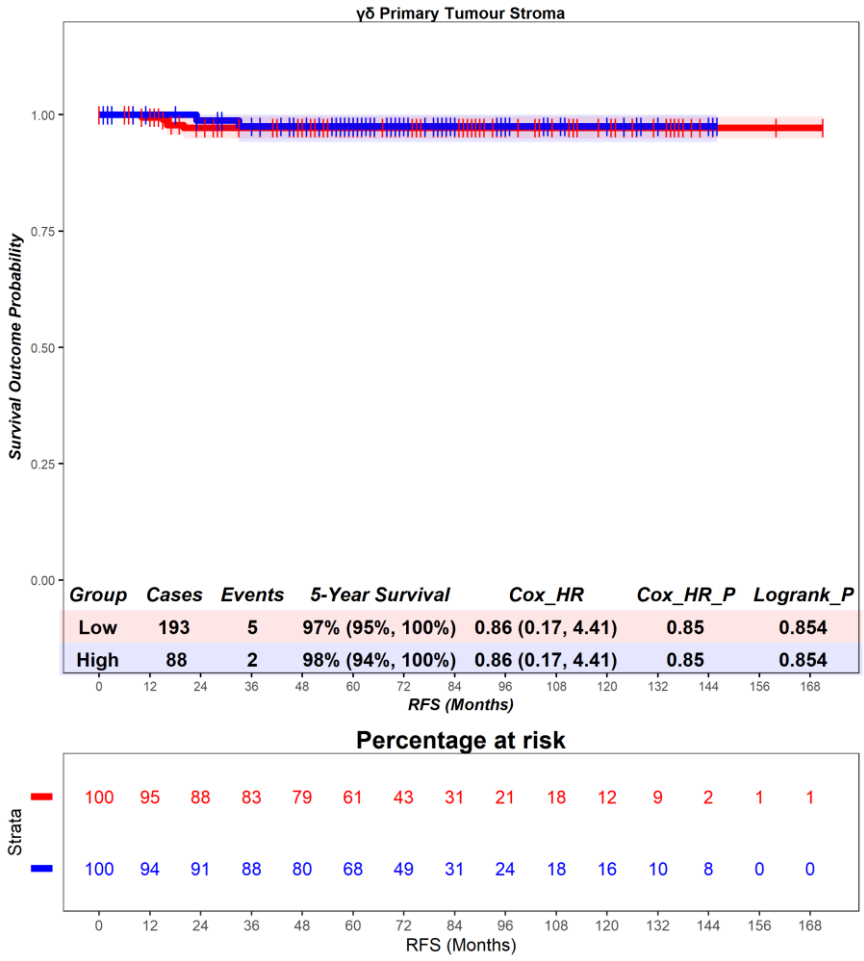

Figure 4.77 – Norway cohort. Time-to-event (recurrence-free survival) analysis for γδ T cells in the primary tumour stroma. *Patients deemed 'High' or 'Low' for γδ T cells are shaded blue and red, respectively. Cox hazard ratio is univariate – see table 4.6 for multivariate. The 'Low' group is used as the reference group on cox regression modelling.*

In the primary tumour tissue, patients deemed high for γδ T cells are associated with no differential prognosis (Figure 4.78). Patients with a high level of γδ T cells had a mean survival time of 76.04 months, compared to those with low levels of γδ T cells with a mean survival of 69.48 months (hazard ratio = 0.74, p = 0.72). 5-year survival for patients high for γδ T cells is 98% (95%, 100%), compared to 97% (95%, 100%) in the γδ low group. This suggests that γδ T cells in the whole tissue of the primary tumour are associated with no differential prognostic role. Multivariate analysis was not statistically significant (hazard ratio = 0.66, p = 0.62) (Table 4.6), suggesting that γδ T cells in the whole tissue of the primary tumour are not independently prognostic.

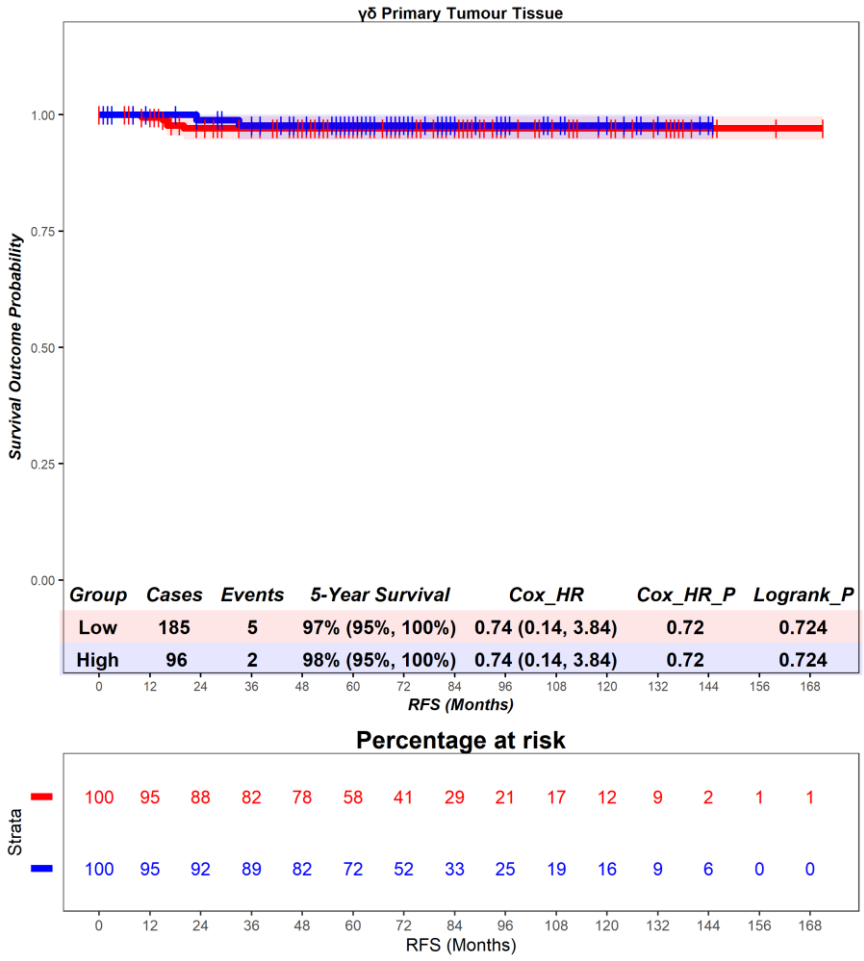

Figure 4.78 – Norway cohort. Time-to-event (recurrence-free survival) analysis for γδ T cells in the primary tumour tissue. *Patients deemed 'High' or 'Low' for γδ T cells are shaded blue and red, respectively. Cox hazard ratio is univariate – see table 4.6 for multivariate. The 'Low' group is used as the reference group on cox regression modelling.*

4.3.5 CD8 T cells - cancer-specific survival

In the adjacent normal epithelium, patients deemed high for γδ T cells are associated with no differential prognosis (Figure 4.79). Patients with a high level of γδ T cells had a mean survival time of 76.12 months, compared to those with low levels of γδ T cells with a mean survival of 88.53 months (hazard ratio = 1.29, p = 0.74). 5-year survival for patients high for γδ T cells is 92% (83%, 100%), compared to 91% (82%, 100%) in the γδ low group. This suggests that γδ T cells in the epithelial compartment of the adjacent normal tissue are associated with no differential prognostic role. Multivariate analysis was not statistically significant (hazard ratio = 0.38, p = 0.46) (Table 4.6), suggesting that γδ T cells in the epithelial compartment of the adjacent normal tissue are not independently prognostic.

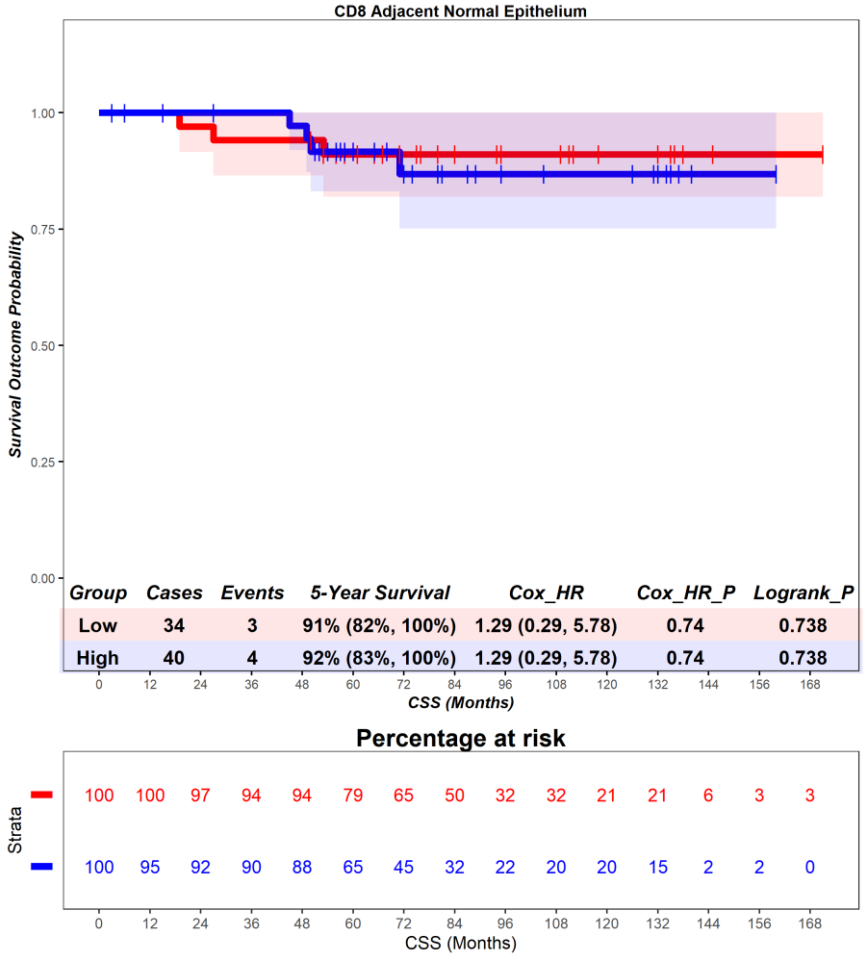

Figure 4.79 – Norway cohort. Time-to-event (cancer-specific survival) analysis for CD8 T cells in the adjacent normal epithelium. *Patients deemed 'High' or 'Low' for CD8 T cells are shaded blue and red, respectively. Cox hazard ratio is univariate – see table 4.6 for multivariate. The 'Low' group is used as the reference group on cox regression modelling.*

In the adjacent normal stroma, patients deemed high for γδ T cells are associated with no differential prognosis (Figure 4.80). Patients with a high level of γδ T cells had a mean survival time of 66.41 months, compared to those with low levels of γδ T cells with a mean survival of 86.42 months (hazard ratio = 1.56, p = 0.59). 5-year survival for patients high for γδ T cells is 87% (71%, 100%), compared to 93% (86%, 100%) in the γδ low group. This suggests that γδ T cells in the stromal compartment of the adjacent normal tissue are associated with no differential prognostic role. Multivariate analysis was not statistically significant (hazard ratio = Inf, p = 1.0) (Table 4.6), suggesting that γδ T cells in the stromal compartment of the adjacent normal tissue are not independently prognostic.

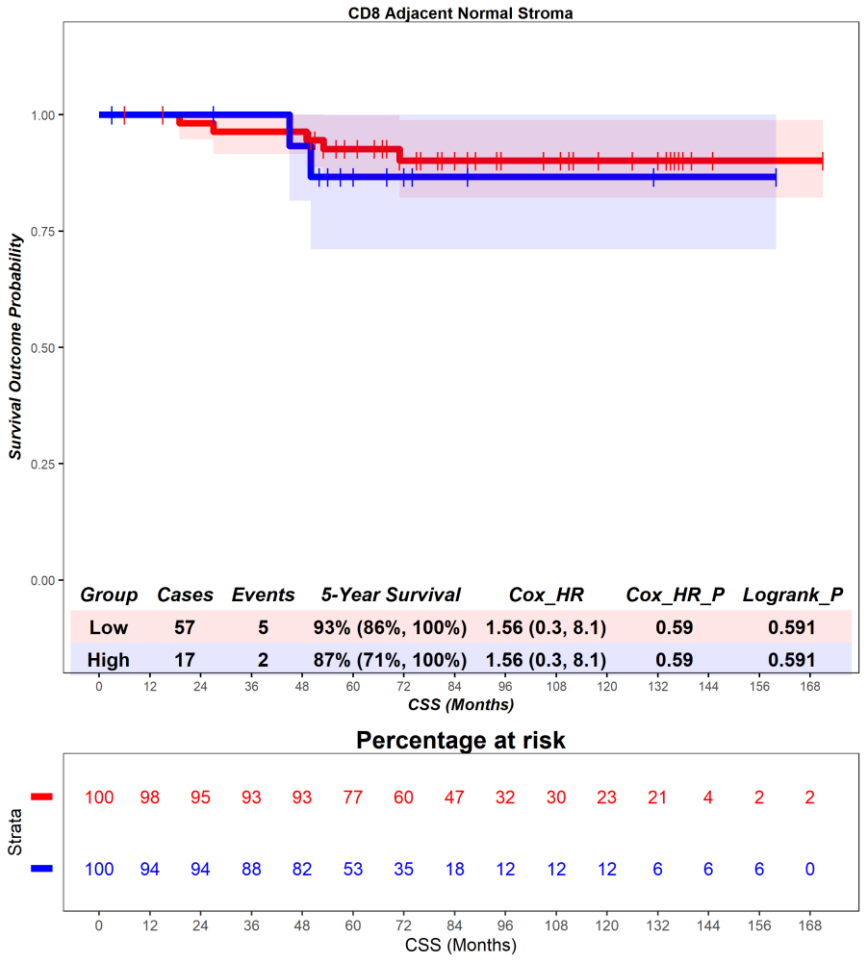

Figure 4.80 – Norway cohort. Time-to-event (cancer-specific survival) analysis for CD8 T cells in the adjacent normal stroma. *Patients deemed 'High' or 'Low' for CD8 T cells are shaded blue and red, respectively. Cox hazard ratio is univariate – see table 4.6 for multivariate. The 'Low' group is used as the reference group on cox regression modelling.*

In the adjacent normal tissue, patients deemed high for γδ T cells are associated with no differential prognosis (Figure 4.81). Patients with a high level of γδ T cells had a mean survival time of 83.89 months, compared to those with low levels of γδ T cells with a mean survival of 81.54 months (hazard ratio = 0, p = 1.0). 5-year survival for patients high for γδ T cells is 100% (100%, 100%), compared to 90% (83%, 98%) in the γδ low group. This suggests that γδ T cells in the whole tissue of the adjacent normal tissue are associated with no differential prognostic role. Multivariate analysis was not statistically significant (hazard ratio = 0.0, p = 1.0) (Table 4.6), suggesting that γδ T cells in the whole tissue of the adjacent normal tissue are not independently prognostic.

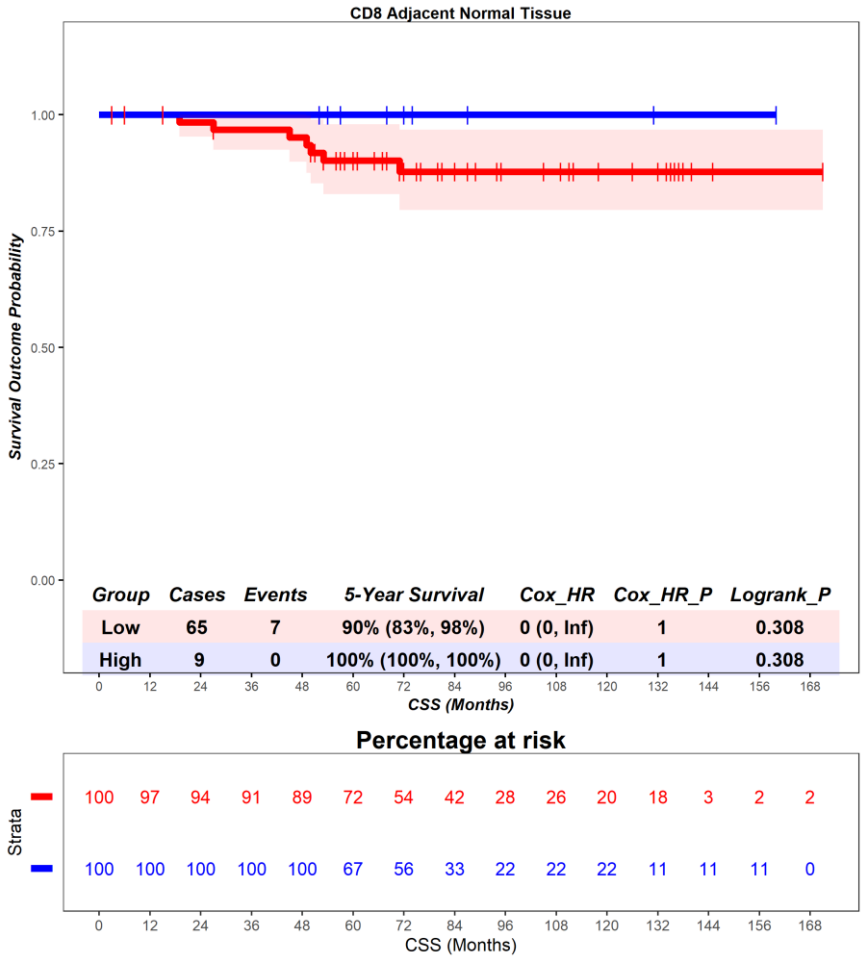

Figure 4.81 – Norway cohort. Time-to-event (cancer-specific survival) analysis for CD8 T cells in the adjacent normal tissue. *Patients deemed 'High' or 'Low' for CD8 T cells are shaded blue and red, respectively. Cox hazard ratio is univariate – see table 4.6 for multivariate. The 'Low' group is used as the reference group on cox regression modelling.*

In the primary tumour epithelium, patients deemed high for γδ T cells are associated with a better prognosis (Figure 4.82), although this result did not reach statistical significance. Patients with a high level of γδ T cells had a mean survival time of 75.26 months, compared to those with low levels of γδ T cells with a mean survival of 69.41 months (hazard ratio = 0.6, p = 0.19). 5-year survival for patients high for γδ T cells is 90% (84%, 96%), compared to 86% (81%, 93%) in the γδ low group. This suggests that γδ T cells in the epithelial compartment of the primary tumour are associated with a favourable prognostic role. Multivariate analysis was not statistically significant (hazard ratio = 0.84, p = 0.66) (Table 4.6), suggesting that γδ T cells in the epithelial compartment of the primary tumour are not independently prognostic.

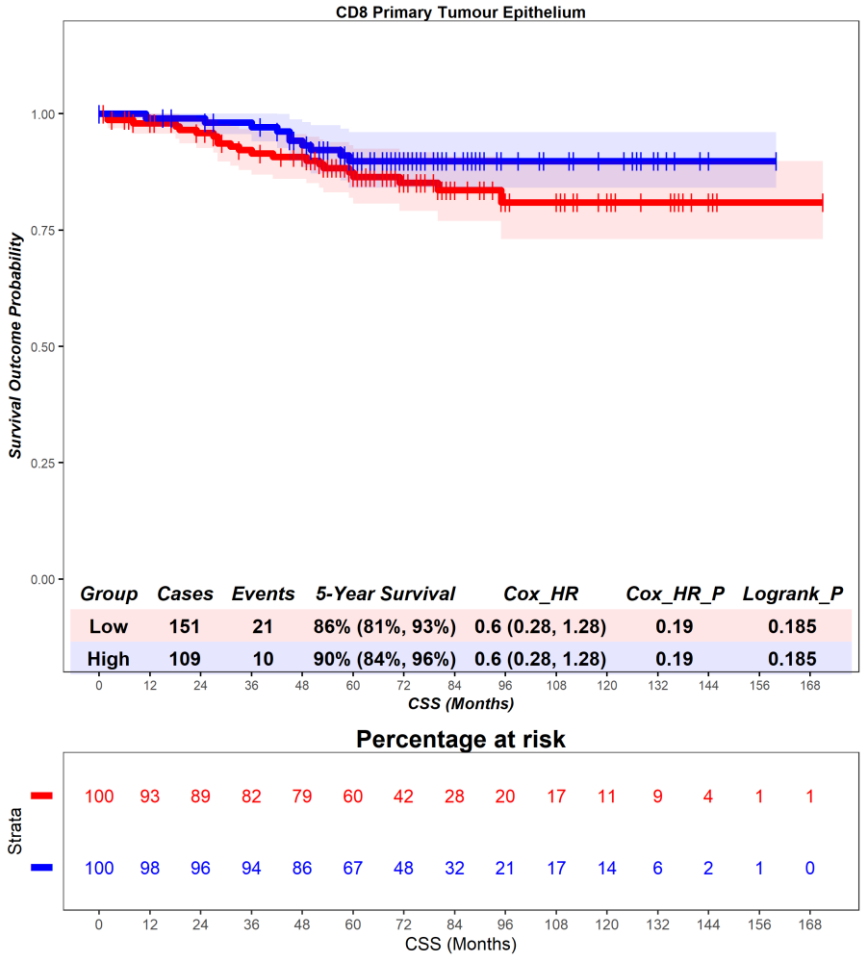

Figure 4.82 – Norway cohort. Time-to-event (cancer-specific survival) analysis for CD8 T cells in the primary tumour epithelium. *Patients deemed 'High' or 'Low' for CD8 T cells are shaded blue and red, respectively. Cox hazard ratio is univariate – see table 4.6 for multivariate. The 'Low' group is used as the reference group on cox regression modelling.*

In the primary tumour stroma, patients deemed high for γδ T cells are associated with a better prognosis (Figure 4.83). Patients with a high level of γδ T cells had a mean survival time of 72.77 months, compared to those with low levels of γδ T cells with a mean survival of 70.91 months (hazard ratio = 0.27, p = 0.001). 5-year survival for patients high for γδ T cells is 94% (90%, 98%), compared to 82% (75%, 89%) in the γδ low group. This suggests that γδ T cells in the stromal compartment of the primary tumour are associated with a favourable prognostic role. Multivariate analysis was statistically significant (hazard ratio = 0.37, p = 0.03) (Table 4.6), suggesting that γδ T cells in the stromal compartment of the primary tumour are independently prognostic.

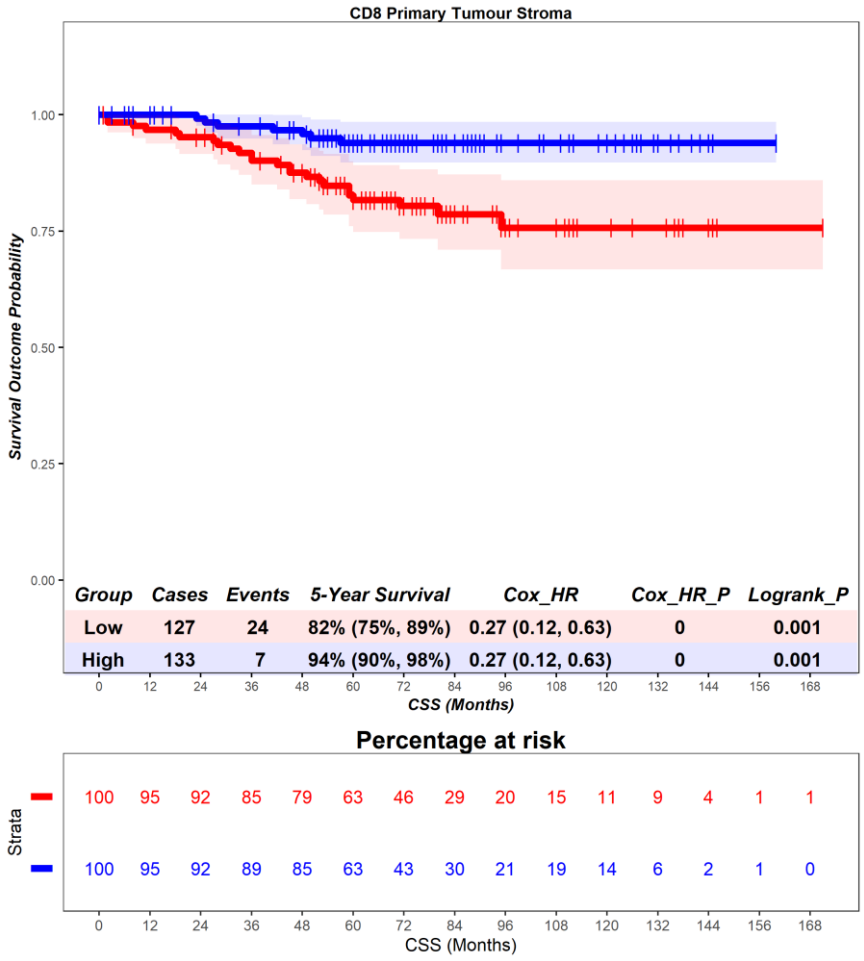

Figure 4.83 – Norway cohort. Time-to-event (cancer-specific survival) analysis for CD8 T cells in the primary tumour stroma. *Patients deemed 'High' or 'Low' for CD8 T cells are shaded blue and red, respectively. Cox hazard ratio is univariate – see table 4.6 for multivariate. The 'Low' group is used as the reference group on cox regression modelling.*

In the primary tumour tissue, patients deemed high for γδ T cells are associated with a better prognosis (Figure 4.84), although this result did not reach statistical significance. Patients with a high level of γδ T cells had a mean survival time of 78.05 months, compared to those with low levels of γδ T cells with a mean survival of 70.2 months (hazard ratio = 0.35, p = 0.09). 5-year survival for patients high for γδ T cells is 94% (87%, 100%), compared to 86% (81%, 91%) in the γδ low group. This suggests that γδ T cells in the whole tissue of the primary tumour are associated with a favourable prognostic role. Multivariate analysis was not statistically significant (hazard ratio = 0.6, p = 0.41) (Table 4.6), suggesting that γδ T cells in the whole tissue of the primary tumour are not independently prognostic.

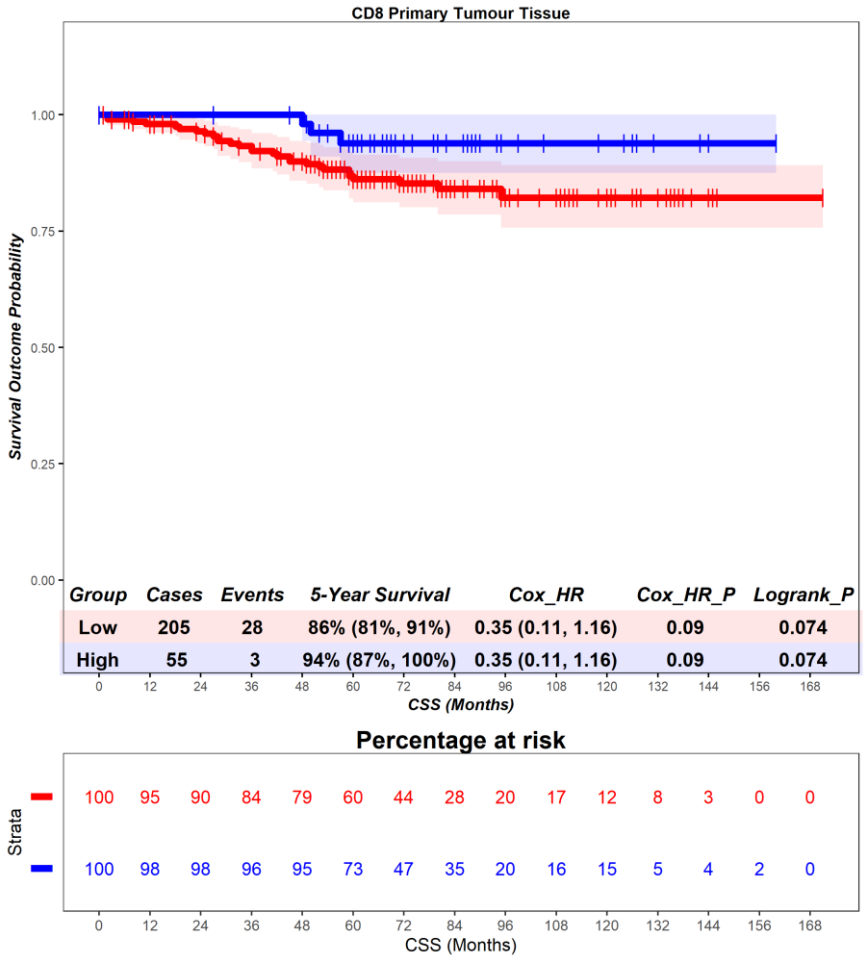

Figure 4.84 – Norway cohort. Time-to-event (cancer-specific survival) analysis for CD8 T cells in the primary tumour tissue. *Patients deemed 'High' or 'Low' for CD8 T cells are shaded blue and red, respectively. Cox hazard ratio is univariate – see table 4.6 for multivariate. The 'Low' group is used as the reference group on cox regression modelling.*

4.3.6 CD8 T cells - overall survival

In the adjacent normal epithelium, patients deemed high for γδ T cells are associated with an unfavourable prognosis (Figure 4.85), although this result did not reach statistical significance. Patients with a high level of γδ T cells had a mean survival time of 76.12 months, compared to those with low levels of γδ T cells with a mean survival of 88.53 months (hazard ratio = 2, p = 0.14). 5-year survival for patients high for γδ T cells is 80% (68%, 93%), compared to 88% (78%, 100%) in the γδ low group. This suggests that γδ T cells in the epithelial compartment of the adjacent normal tissue are associated with an unfavourable prognostic role. Multivariate analysis was not statistically significant (hazard ratio = 2.32, p = 0.07) (Table 4.6), suggesting that γδ T cells in the epithelial compartment of the adjacent normal tissue are not independently prognostic.

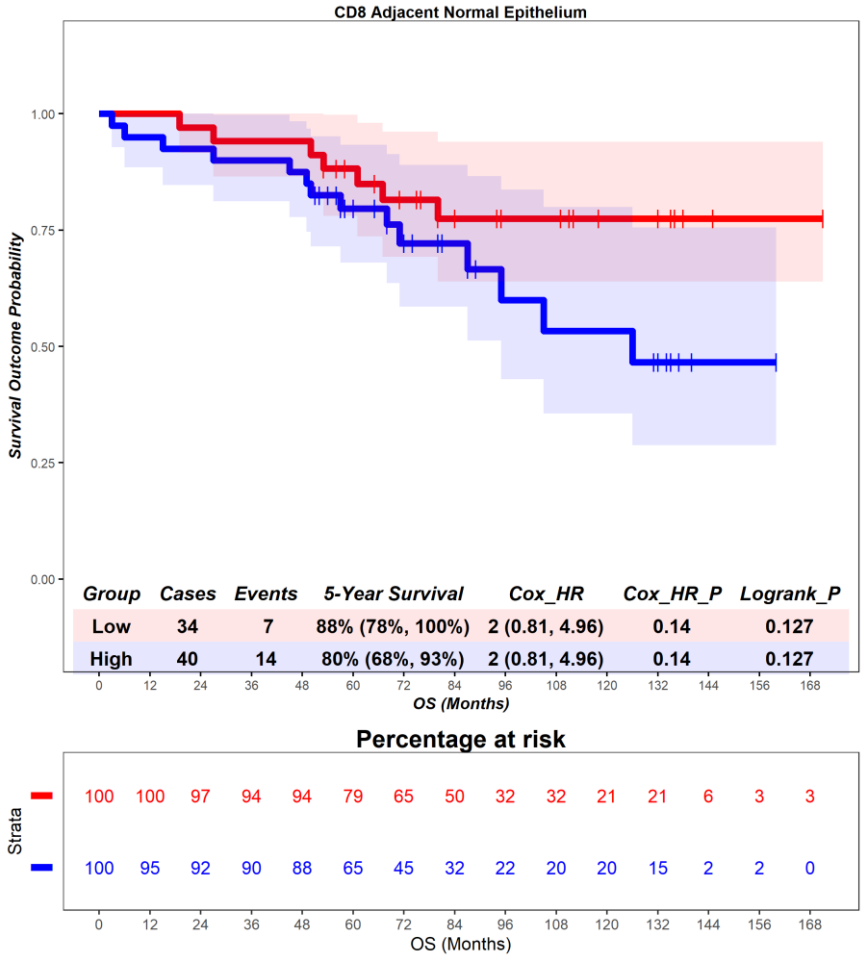

Figure 4.85 – Norway cohort. Time-to-event (overall survival) analysis for CD8 T cells in the adjacent normal epithelium. *Patients deemed 'High' or 'Low' for CD8 T cells are shaded blue and red, respectively. Cox hazard ratio is univariate – see table 4.6 for multivariate. The 'Low' group is used as the reference group on cox regression modelling.*

In the adjacent normal stroma, patients deemed high for γδ T cells are associated with an unfavourable prognosis (Figure 4.86), although this result did not reach statistical significance. Patients with a high level of γδ T cells had a mean survival time of 66.41 months, compared to those with low levels of γδ T cells with a mean survival of 86.42 months (hazard ratio = 1.91, p = 0.19). 5-year survival for patients high for γδ T cells is 70% (50%, 96%), compared to 88% (80%, 97%) in the γδ low group. This suggests that γδ T cells in the stromal compartment of the adjacent normal tissue are associated with an unfavourable prognostic role. Multivariate analysis was not statistically significant (hazard ratio = 2.08, p = 0.16) (Table 4.6), suggesting that γδ T cells in the stromal compartment of the adjacent normal tissue are not independently prognostic.

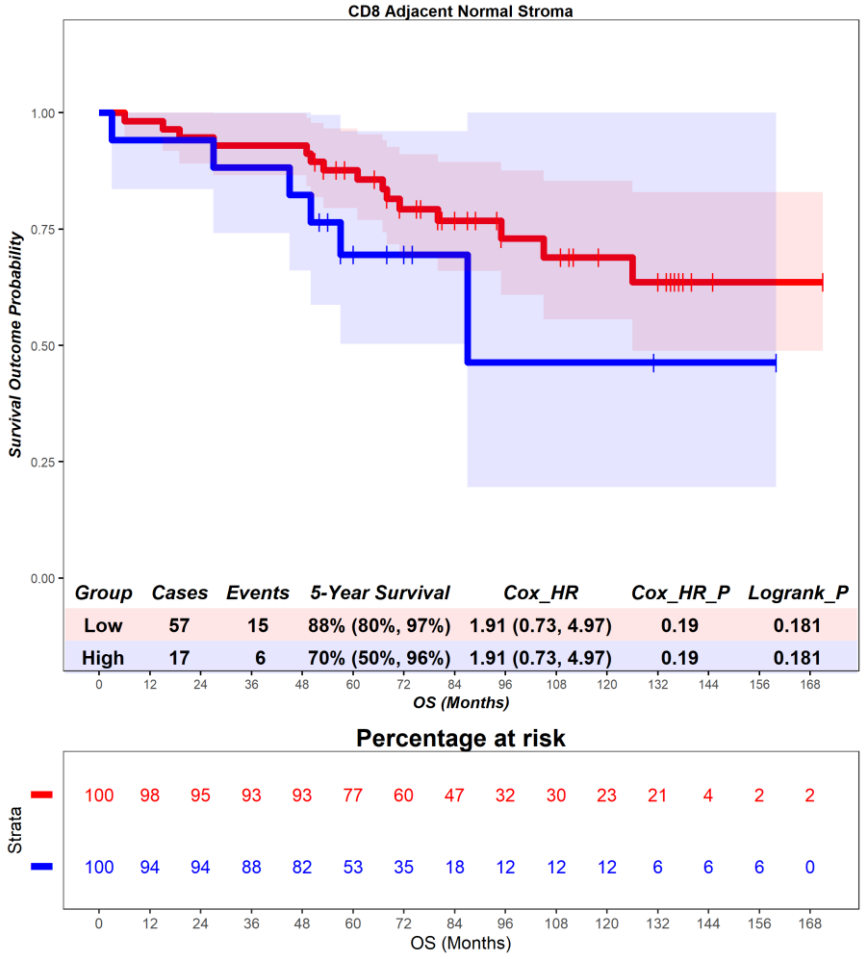

Figure 4.86 – Norway cohort. Time-to-event (overall survival) analysis for CD8 T cells in the adjacent normal stroma. *Patients deemed 'High' or 'Low' for CD8 T cells are shaded blue and red, respectively. Cox hazard ratio is univariate – see table 4.6 for multivariate. The 'Low' group is used as the reference group on cox regression modelling.*

In the adjacent normal tissue, patients deemed high for γδ T cells are associated with no differential prognosis (Figure 4.87). Patients with a high level of γδ T cells had a mean survival time of 83.89 months, compared to those with low levels of γδ T cells with a mean survival of 81.54 months (hazard ratio = 0.76, p = 0.71). 5-year survival for patients high for γδ T cells is 86% (63%, 100%), compared to 83% (74%, 93%) in the γδ low group. This suggests that γδ T cells in the whole tissue of the adjacent normal tissue are associated with no differential prognostic role. Multivariate analysis was not statistically significant (hazard ratio = 0.75, p = 0.71) (Table 4.6), suggesting that γδ T cells in the whole tissue of the adjacent normal tissue are not independently prognostic.

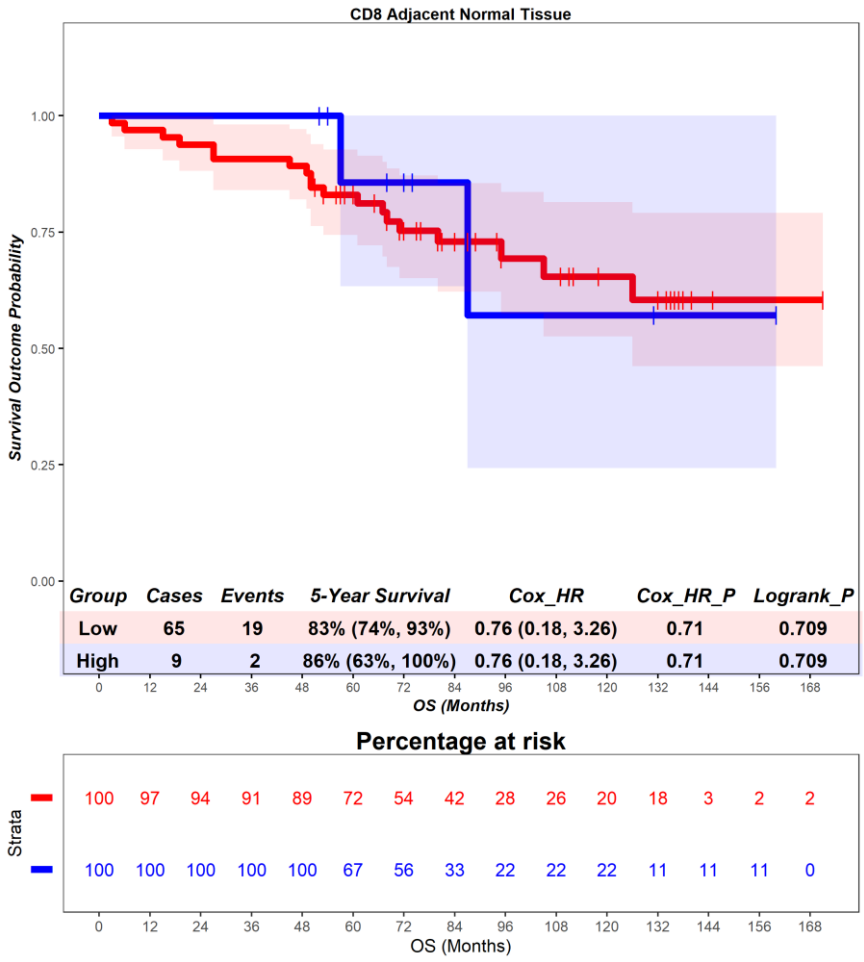

Figure 4.87 – Norway cohort. Time-to-event (overall survival) analysis for CD8 T cells in the adjacent normal tissue. *Patients deemed 'High' or 'Low' for CD8 T cells are shaded blue and red, respectively. Cox hazard ratio is univariate – see table 4.6 for multivariate. The 'Low' group is used as the reference group on cox regression modelling.*

In the primary tumour epithelium, patients deemed high for γδ T cells are associated with no differential prognosis (Figure 4.88). Patients with a high level of γδ T cells had a mean survival time of 75.26 months, compared to those with low levels of γδ T cells with a mean survival of 69.41 months (hazard ratio = 1, p = 0.99). 5-year survival for patients high for γδ T cells is 75% (67%, 83%), compared to 73% (66%, 81%) in the γδ low group. This suggests that γδ T cells in the epithelial compartment of the primary tumour are associated with no differential prognostic role. Multivariate analysis was not statistically significant (hazard ratio = 1.01, p = 0.98) (Table 4.6), suggesting that γδ T cells in the epithelial compartment of the primary tumour are not independently prognostic.

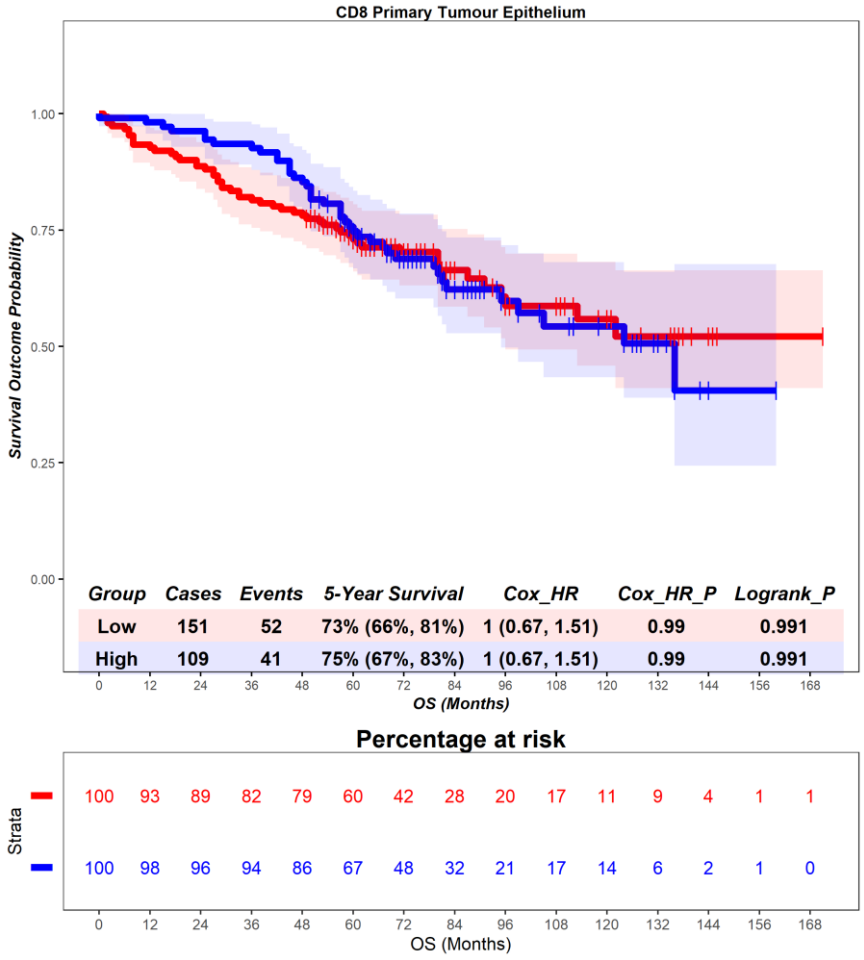

Figure 4.88 – Norway cohort. Time-to-event (overall survival) analysis for CD8 T cells in the primary tumour epithelium. *Patients deemed 'High' or 'Low' for CD8 T cells are shaded blue and red, respectively. Cox hazard ratio is univariate – see table 4.6 for multivariate. The 'Low' group is used as the reference group on cox regression modelling.*

In the primary tumour stroma, patients deemed high for γδ T cells are associated with no differential prognosis (Figure 4.89). Patients with a high level of γδ T cells had a mean survival time of 72.77 months, compared to those with low levels of γδ T cells with a mean survival of 70.91 months (hazard ratio = 0.83, p = 0.38). 5-year survival for patients high for γδ T cells is 79% (60%, 77%), compared to 68% (69%, 77%) in the γδ low group. This suggests that γδ T cells in the stromal compartment of the primary tumour are associated with no differential prognostic role. Multivariate analysis was not statistically significant (hazard ratio = 0.92, p = 0.69) (Table 4.6), suggesting that γδ T cells in the stromal compartment of the primary tumour are not independently prognostic.

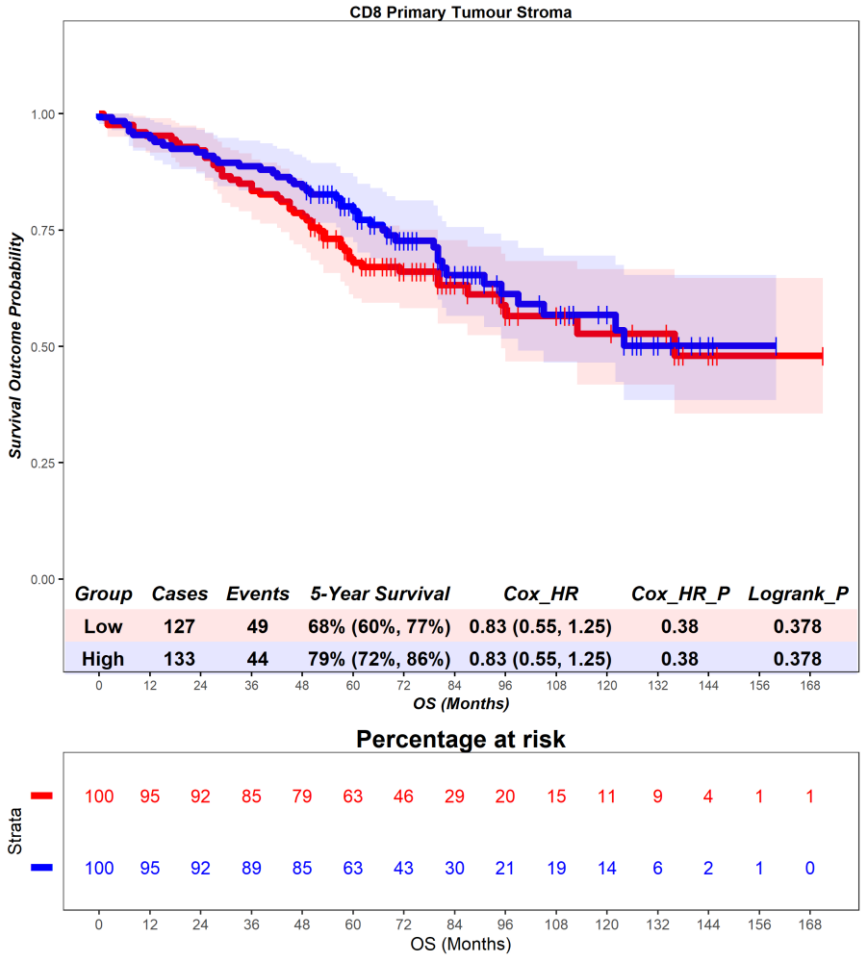

Figure 4.89 – Norway cohort. Time-to-event (overall survival) analysis for CD8 T cells in the primary tumour stroma. *Patients deemed 'High' or 'Low' for CD8 T cells are shaded blue and red, respectively. Cox hazard ratio is univariate – see table 4.6 for multivariate. The 'Low' group is used as the reference group on cox regression modelling.*

In the primary tumour tissue, patients deemed high for γδ T cells are associated with no differential prognosis (Figure 4.90). Patients with a high level of γδ T cells had a mean survival time of 78.05 months, compared to those with low levels of γδ T cells with a mean survival of 70.2 months (hazard ratio = 0.97, p = 0.89). 5-year survival for patients high for γδ T cells is 83% (73%, 94%), compared to 71% (65%, 78%) in the γδ low group. This suggests that γδ T cells in the whole tissue of the primary tumour are associated with no differential prognostic role. Multivariate analysis was not statistically significant (hazard ratio = 1.03, p = 0.89) (Table 4.6), suggesting that γδ T cells in the whole tissue of the primary tumour are not independently prognostic.

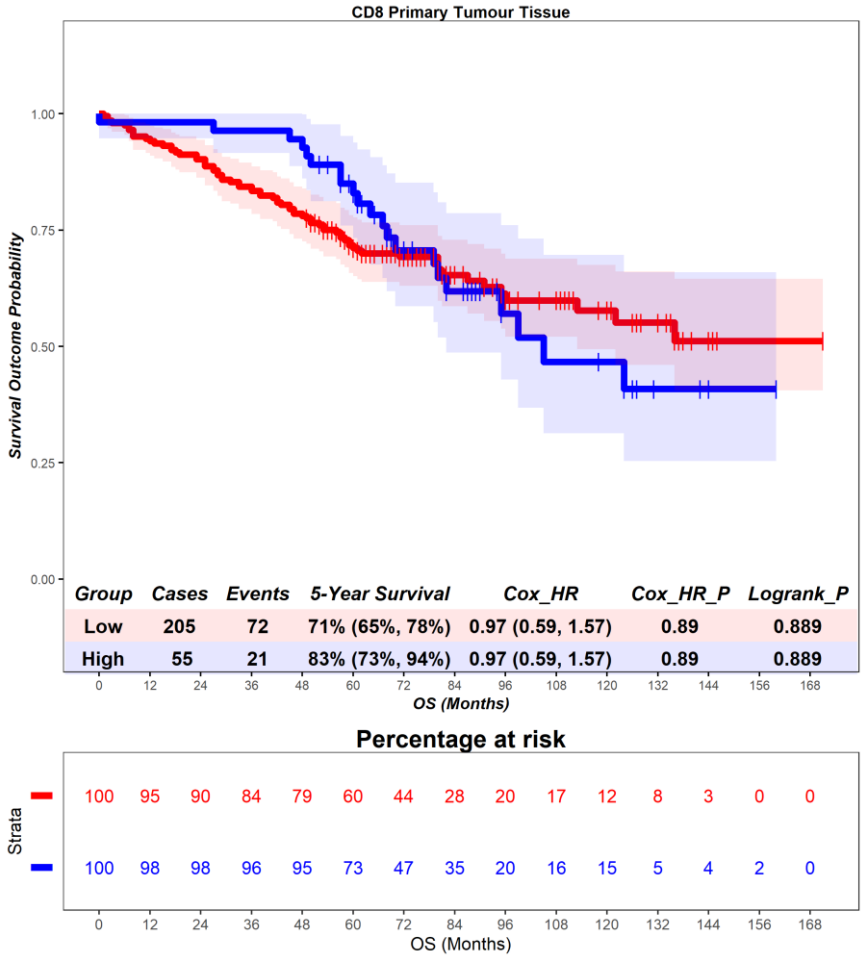

Figure 4.90 – Norway cohort. Time-to-event (overall survival) analysis for CD8 T cells in the primary tumour tissue. *Patients deemed 'High' or 'Low' for CD8 T cells are shaded blue and red, respectively. Cox hazard ratio is univariate – see table 4.6 for multivariate. The 'Low' group is used as the reference group on cox regression modelling.*

4.3.7 CD8 T cells - disease-free survival

In the adjacent normal epithelium, patients deemed high for γδ T cells are associated with no differential prognosis (Figure 4.91). Patients with a high level of γδ T cells had a mean survival time of 74.25 months, compared to those with low levels of γδ T cells with a mean survival of 87.03 months (hazard ratio = 1.46, p = 0.56). 5-year survival for patients high for γδ T cells is 86% (76%, 98%), compared to 88% (78%, 100%) in the γδ low group. This suggests that γδ T cells in the epithelial compartment of the adjacent normal tissue are associated with no differential prognostic role. Multivariate analysis was not statistically significant (hazard ratio = 2.73, p = 0.39) (Table 4.6), suggesting that γδ T cells in the epithelial compartment of the adjacent normal tissue are not independently prognostic.

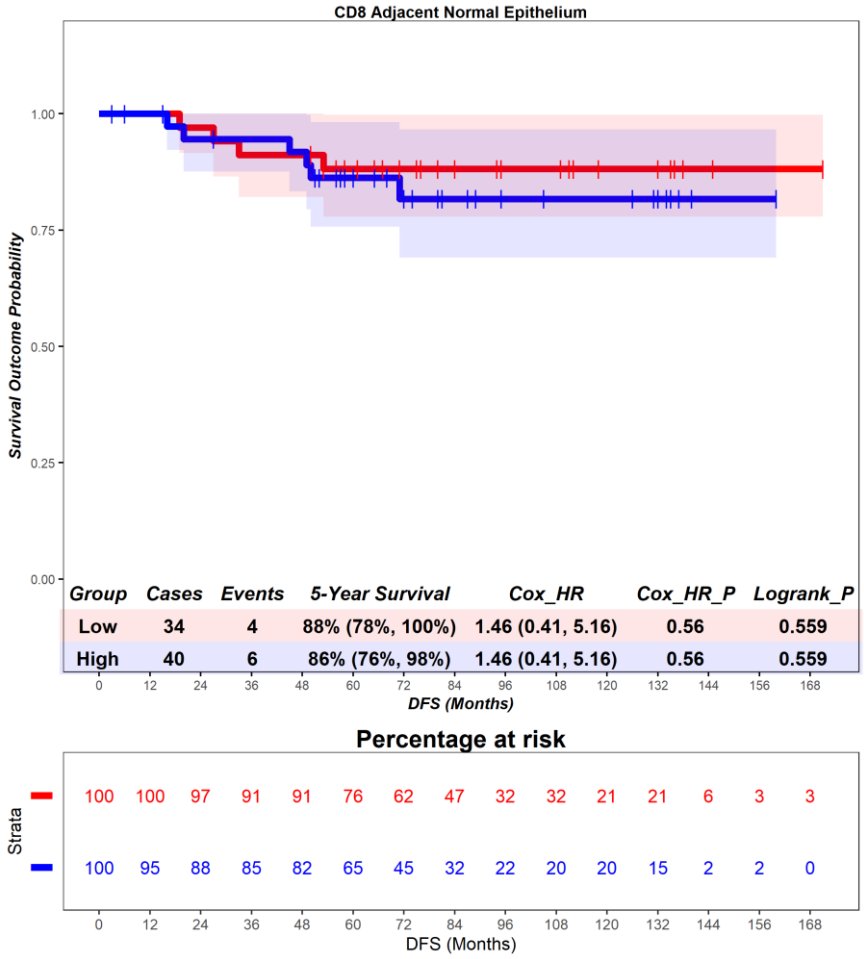

Figure 4.91 – Norway cohort. Time-to-event (disease-free survival) analysis for CD8 T cells in the adjacent normal epithelium. *Patients deemed 'High' or 'Low' for CD8 T cells are shaded blue and red, respectively. Cox hazard ratio is univariate – see table 4.6 for multivariate. The 'Low' group is used as the reference group on cox regression modelling.*

In the adjacent normal stroma, patients deemed high for γδ T cells are associated with an unfavourable prognosis (Figure 4.92), although this result did not reach statistical significance. Patients with a high level of γδ T cells had a mean survival time of 62.0 months, compared to those with low levels of γδ T cells with a mean survival of 85.53 months (hazard ratio = 2.76, p = 0.12). 5-year survival for patients high for γδ T cells is 74% (55%, 100%), compared to 91% (83%, 99%) in the γδ low group. This suggests that γδ T cells in the stromal compartment of the adjacent normal tissue are associated with an unfavourable prognostic role. Multivariate analysis was not statistically significant (hazard ratio = 8.82, p = 0.08) (Table 4.6), suggesting that γδ T cells in the stromal compartment of the adjacent normal tissue are not independently prognostic.

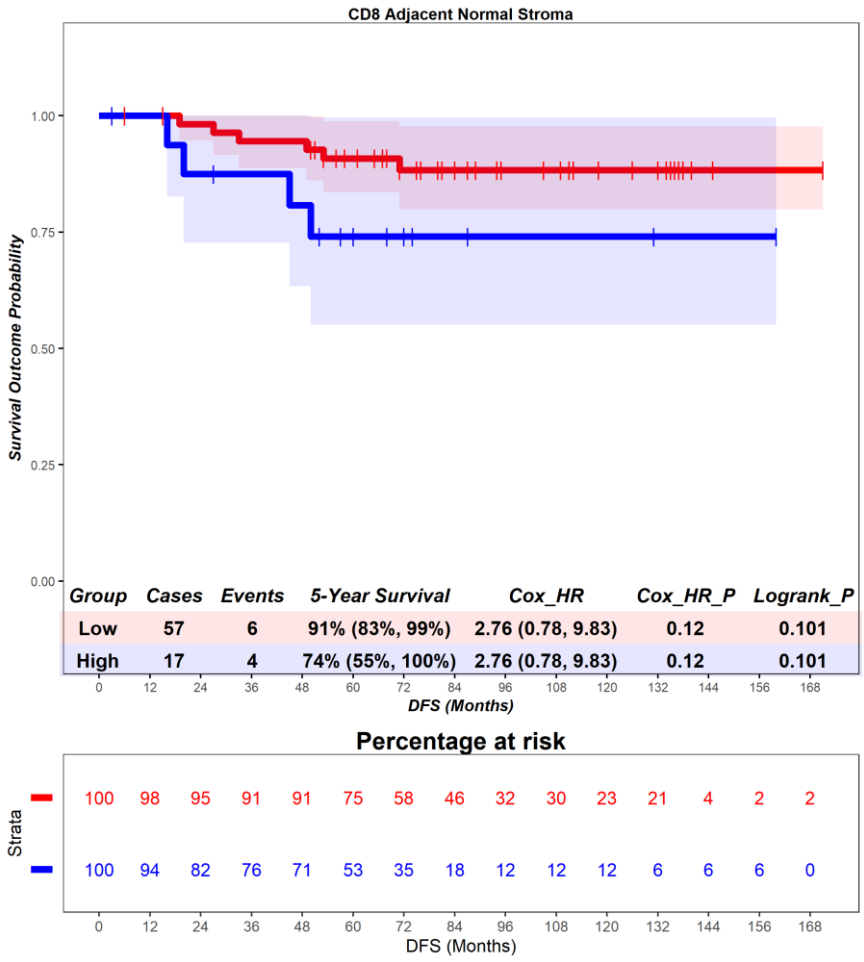

Figure 4.92 – Norway cohort. Time-to-event (disease-free survival) analysis for CD8 T cells in the adjacent normal stroma. *Patients deemed 'High' or 'Low' for CD8 T cells are shaded blue and red, respectively. Cox hazard ratio is univariate – see table 4.6 for multivariate. The 'Low' group is used as the reference group on cox regression modelling.*

In the adjacent normal tissue, patients deemed high for γδ T cells are associated with no differential prognosis (Figure 4.93). Patients with a high level of γδ T cells had a mean survival time of 79.67 months, compared to those with low levels of γδ T cells with a mean survival of 80.18 months (hazard ratio = 0.81, p = 0.84). 5-year survival for patients high for γδ T cells is 89% (71%, 100%), compared to 87% (79%, 96%) in the γδ low group. This suggests that γδ T cells in the whole tissue of the adjacent normal tissue are associated with no differential prognostic role. Multivariate analysis was not statistically significant (hazard ratio = 5.38, p = 0.18) (Table 4.6), suggesting that γδ T cells in the whole tissue of the adjacent normal tissue are not independently prognostic.

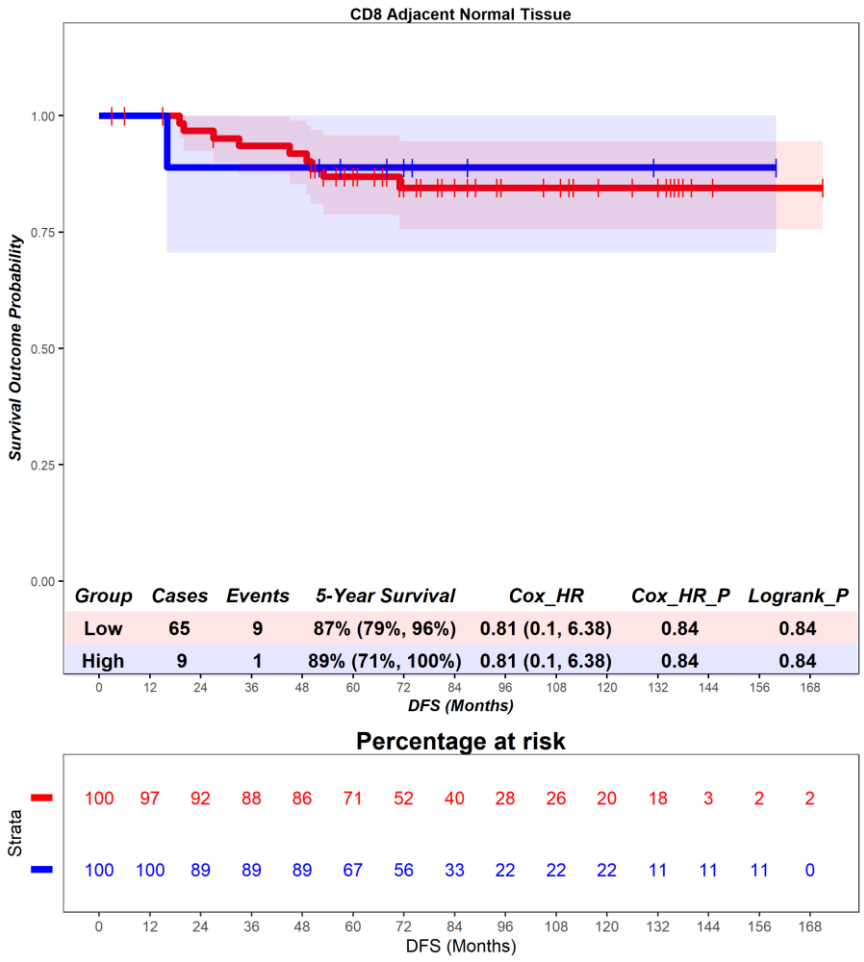

Figure 4.93 – Norway cohort. Time-to-event (disease-free survival) analysis for CD8 T cells in the adjacent normal tissue. *Patients deemed 'High' or 'Low' for CD8 T cells are shaded blue and red, respectively. Cox hazard ratio is univariate – see table 4.6 for multivariate. The 'Low' group is used as the reference group on cox regression modelling.*

In the primary tumour epithelium, patients deemed high for γδ T cells are associated with a better prognosis (Figure 4.94). Patients with a high level of γδ T cells had a mean survival time of 74.24 months, compared to those with low levels of γδ T cells with a mean survival of 66.82 months (hazard ratio = 0.47, p = 0.028). 5-year survival for patients high for γδ T cells is 89% (83%, 95%), compared to 81% (74%, 88%) in the γδ low group. This suggests that γδ T cells in the epithelial compartment of the primary tumour are associated with a favourable prognostic role. Multivariate analysis was not statistically significant (hazard ratio = 0.18, p = 0.11) (Table 4.6), suggesting that γδ T cells in the epithelial compartment of the primary tumour are not independently prognostic.

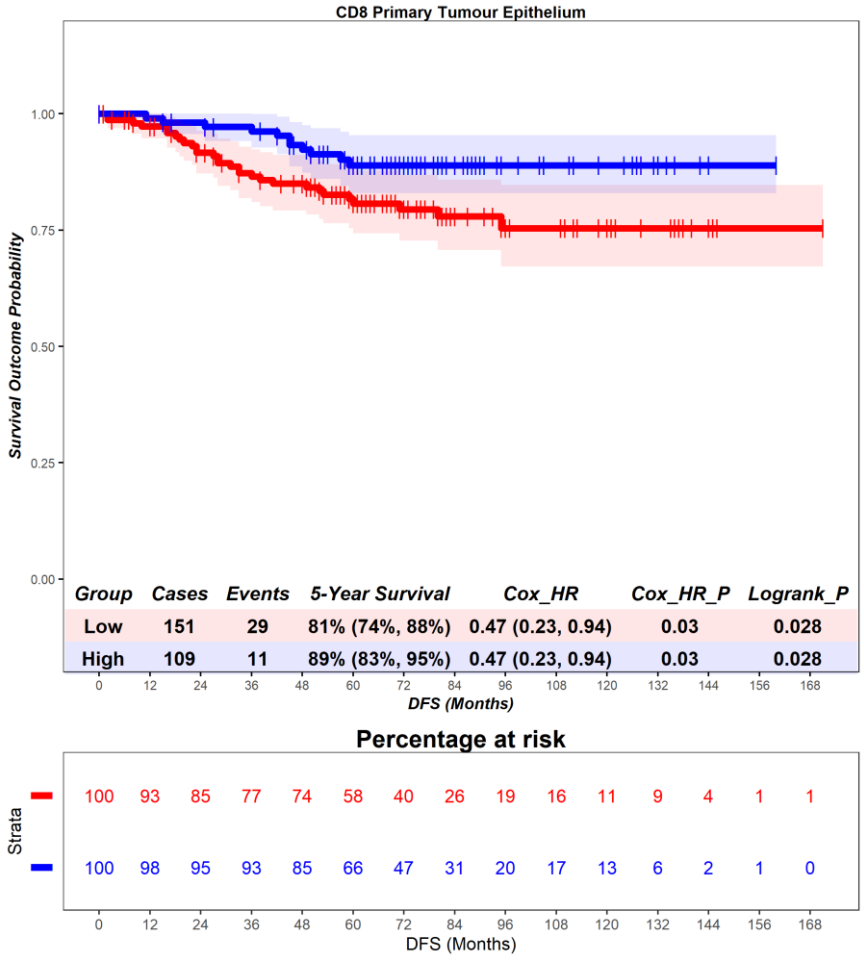

Figure 4.94 – Norway cohort. Time-to-event (disease-free survival) analysis for CD8 T cells in the primary tumour epithelium. *Patients deemed 'High' or 'Low' for CD8 T cells are shaded blue and red, respectively. Cox hazard ratio is univariate – see table 4.6 for multivariate. The 'Low' group is used as the reference group on cox regression modelling.*

In the primary tumour stroma, patients deemed high for γδ T cells are associated with a better prognosis (Figure 4.95). Patients with a high level of γδ T cells had a mean survival time of 71.38 months, compared to those with low levels of γδ T cells with a mean survival of 68.41 months (hazard ratio = 0.35, p = <0.001). 5-year survival for patients high for γδ T cells is 91% (86%, 96%), compared to 78% (70%, 86%) in the γδ low group. This suggests that γδ T cells in the stromal compartment of the primary tumour are associated with a favourable prognostic role. Multivariate analysis was not statistically significant (hazard ratio = 0.77, p = 0.69) (Table 4.6), suggesting that γδ T cells in the stromal compartment of the primary tumour are not independently prognostic.

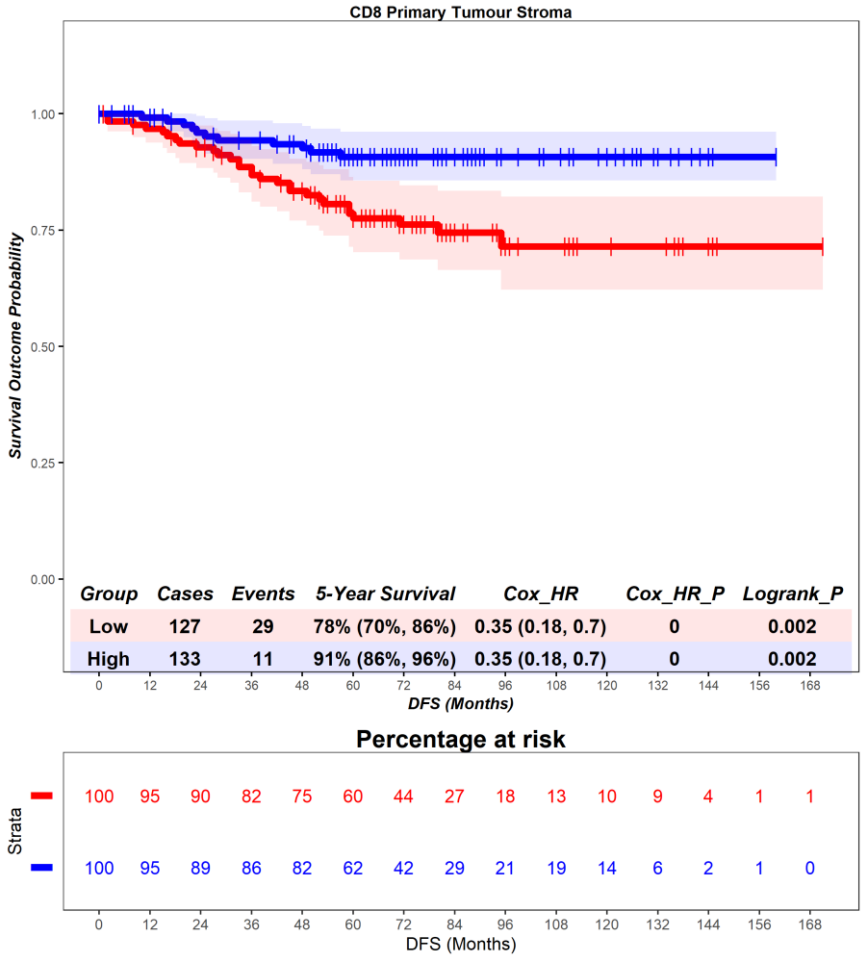

Figure 4.95 – Norway cohort. Time-to-event (disease-free survival) analysis for CD8 T cells in the primary tumour stroma. *Patients deemed 'High' or 'Low' for CD8 T cells are shaded blue and red, respectively. Cox hazard ratio is univariate – see table 4.6 for multivariate. The 'Low' group is used as the reference group on cox regression modelling.*

In the primary tumour tissue, patients deemed high for γδ T cells are associated with a better prognosis (Figure 4.96). Patients with a high level of γδ T cells had a mean survival time of 78.05 months, compared to those with low levels of γδ T cells with a mean survival of 67.75 months (hazard ratio = 0.26, p = 0.03). 5-year survival for patients high for γδ T cells is 94% (87%, 100%), compared to 82% (76%, 87%) in the γδ low group. This suggests that γδ T cells in the whole tissue of the primary tumour are associated with a favourable prognostic role. Multivariate analysis was not statistically significant (hazard ratio = 0.44, p = 0.18) (Table 4.6), suggesting that γδ T cells in the whole tissue of the primary tumour are not independently prognostic.

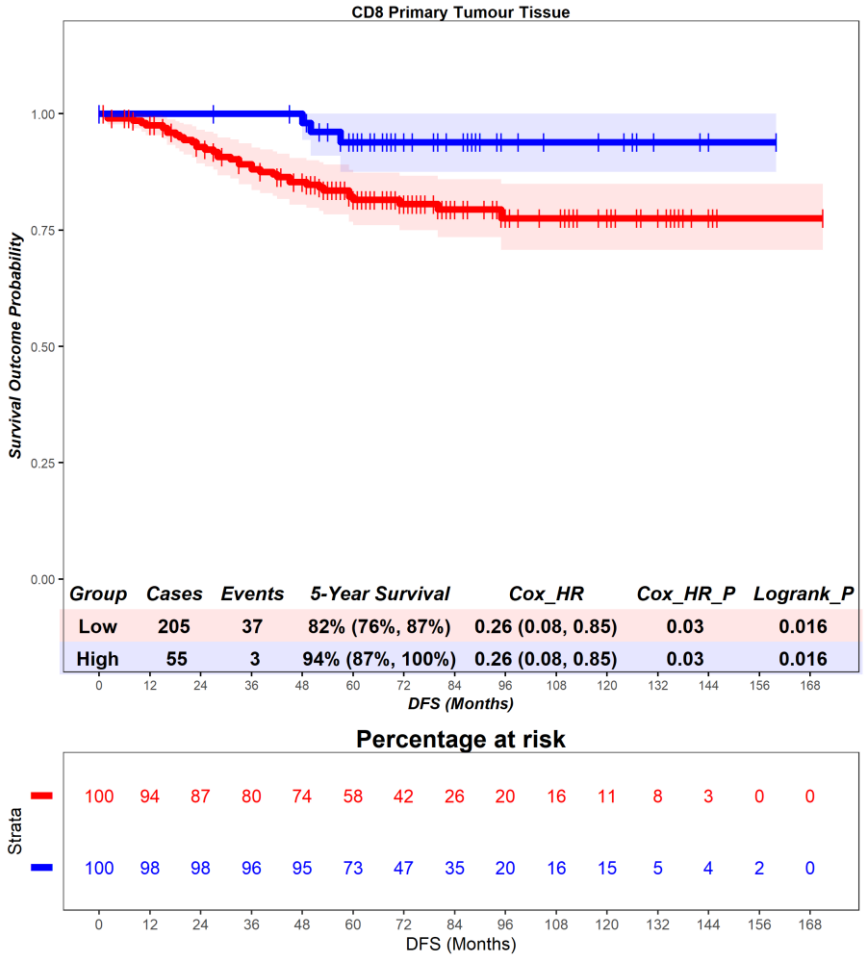

Figure 4.96 – Norway cohort. Time-to-event (disease-free survival) analysis for CD8 T cells in the primary tumour tissue. *Patients deemed 'High' or 'Low' for CD8 T cells are shaded blue and red, respectively. Cox hazard ratio is univariate – see table 4.6 for multivariate. The 'Low' group is used as the reference group on cox regression modelling.*

4.3.8 CD8 T cells - recurrence-free survival

In the adjacent normal epithelium, patients deemed high for γδ T cells are associated with no differential prognosis (Figure 4.97). Patients with a high level of γδ T cells had a mean survival time of 74.25 months, compared to those with low levels of γδ T cells with a mean survival of 87.03 months (hazard ratio = 1.85, p = 0.62). 5-year survival for patients high for γδ T cells is 95% (88%, 100%), compared to 97% (91%, 100%) in the γδ low group. This suggests that γδ T cells in the epithelial compartment of the adjacent normal tissue are associated with no differential prognostic role. Multivariate analysis was not statistically significant (hazard ratio = 1.29, p = 0.84) (Table 4.6), suggesting that γδ T cells in the epithelial compartment of the adjacent normal tissue are not independently prognostic.

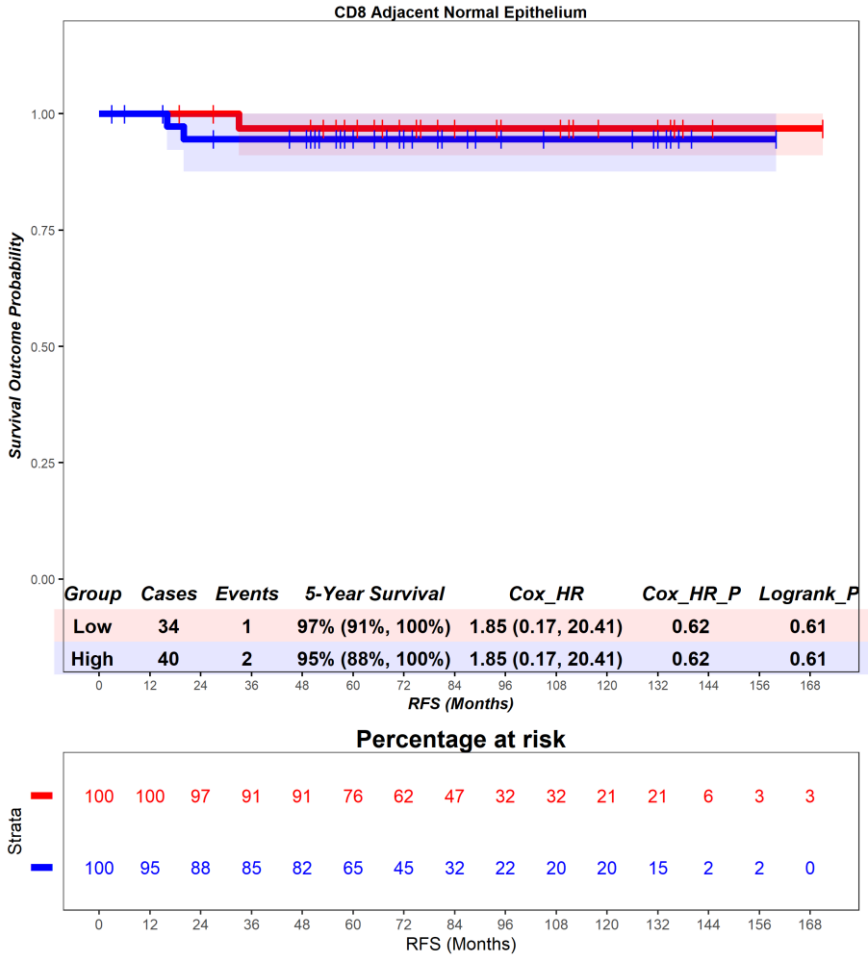

Figure 4.97 – Norway cohort. Time-to-event (recurrence-free survival) analysis for CD8 T cells in the adjacent normal epithelium. *Patients deemed 'High' or 'Low' for CD8 T cells are shaded blue and red, respectively. Cox hazard ratio is univariate – see table 4.6 for multivariate. The 'Low' group is used as the reference group on cox regression modelling.*

In the adjacent normal stroma, patients deemed high for γδ T cells are associated with a worse prognosis (Figure 4.98), although this result did not reach statistical significance. Patients with a high level of γδ T cells had a mean survival time of 62.0 months, compared to those with low levels of γδ T cells with a mean survival of 85.53 months (hazard ratio = 7.4, p = 0.1). 5-year survival for patients high for γδ T cells is 88% (73%, 100%), compared to 98% (95%, 100%) in the γδ low group. This suggests that γδ T cells in the stromal compartment of the adjacent normal tissue are associated with a worse prognostic role. Multivariate analysis was not statistically significant (hazard ratio = 8.82, p = 0.08) (Table 4.6), suggesting that γδ T cells in the stromal compartment of the adjacent normal tissue are not independently prognostic.

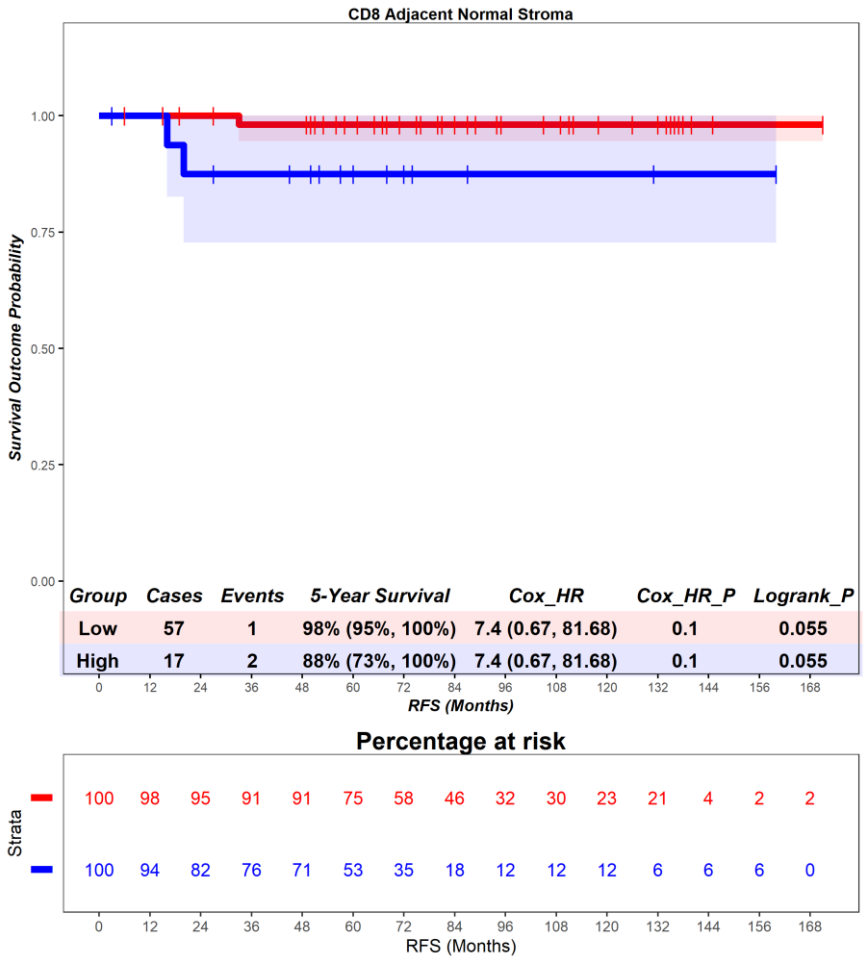

Figure 4.98 – Norway cohort. Time-to-event (recurrence-free survival) analysis for CD8 T cells in the adjacent normal stroma. *Patients deemed 'High' or 'Low' for CD8 T cells are shaded blue and red, respectively. Cox hazard ratio is univariate – see table 4.6 for multivariate. The 'Low' group is used as the reference group on cox regression modelling.*

In the adjacent normal tissue, patients deemed high for γδ T cells are associated with a worse prognosis (Figure 4.99), although this result did not reach statistical significance. Patients with a high level of γδ T cells had a mean survival time of 79.67 months, compared to those with low levels of γδ T cells with a mean survival of 80.18 months (hazard ratio = 3.62, p = 0.29). 5-year survival for patients high for γδ T cells is 89% (71%, 100%), compared to 97% (92%, 100%) in the γδ low group. This suggests that γδ T cells in the whole tissue of the adjacent normal tissue are associated with a worse prognostic role. Multivariate analysis was not statistically significant (hazard ratio = 5.38, p = 0.18) (Table 4.6), suggesting that γδ T cells in the whole tissue of the adjacent normal tissue are not independently prognostic.

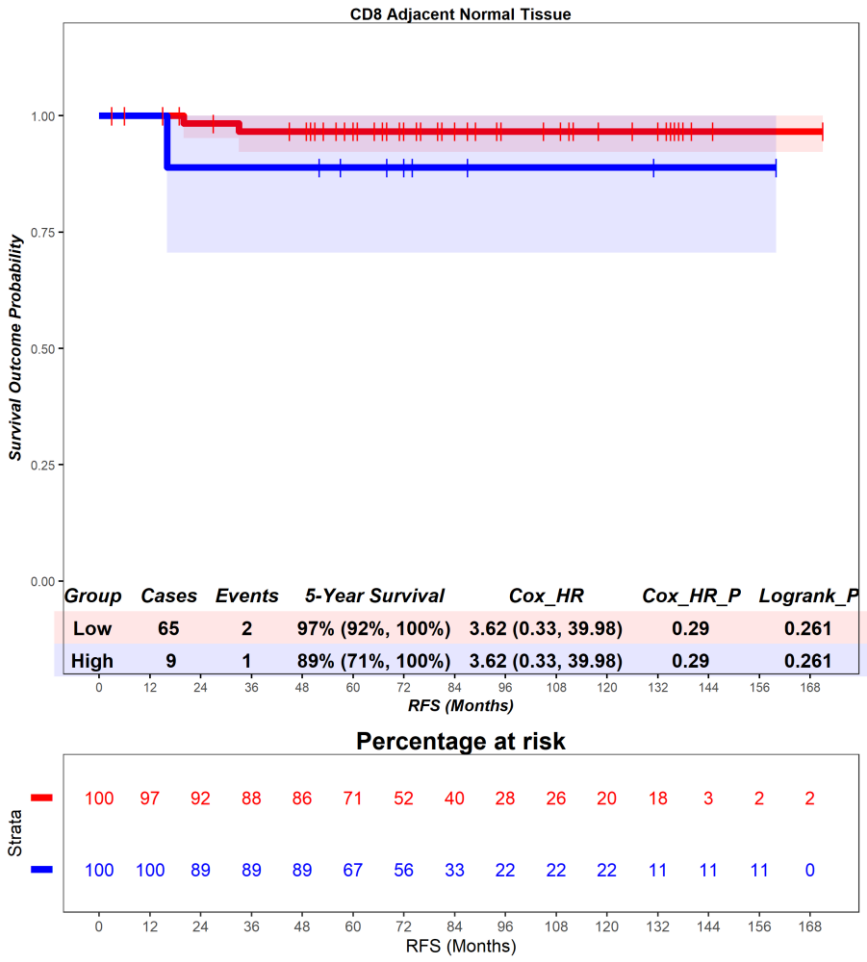

Figure 4.99 – Norway cohort. Time-to-event (recurrence-free survival) analysis for CD8 T cells in the adjacent normal tissue. *Patients deemed 'High' or 'Low' for CD8 T cells are shaded blue and red, respectively. Cox hazard ratio is univariate – see table 4.6 for multivariate. The 'Low' group is used as the reference group on cox regression modelling.*

In the primary tumour epithelium, patients deemed high for γδ T cells are associated with a better prognosis (Figure 4.100), although this result did not reach statistical significance. Patients with a high level of γδ T cells had a mean survival time of 74.24 months, compared to those with low levels of γδ T cells with a mean survival of 66.82 months (hazard ratio = 0.16, p = 0.08). 5-year survival for patients high for γδ T cells is 99% (97%, 100%), compared to 94% (90%, 98%) in the γδ low group. This suggests that γδ T cells in the epithelial compartment of the primary tumour are associated with a favourable prognostic role. Multivariate analysis was not statistically significant (hazard ratio = 0.18, p = 0.11) (Table 4.6), suggesting that γδ T cells in the epithelial compartment of the primary tumour are not independently prognostic.

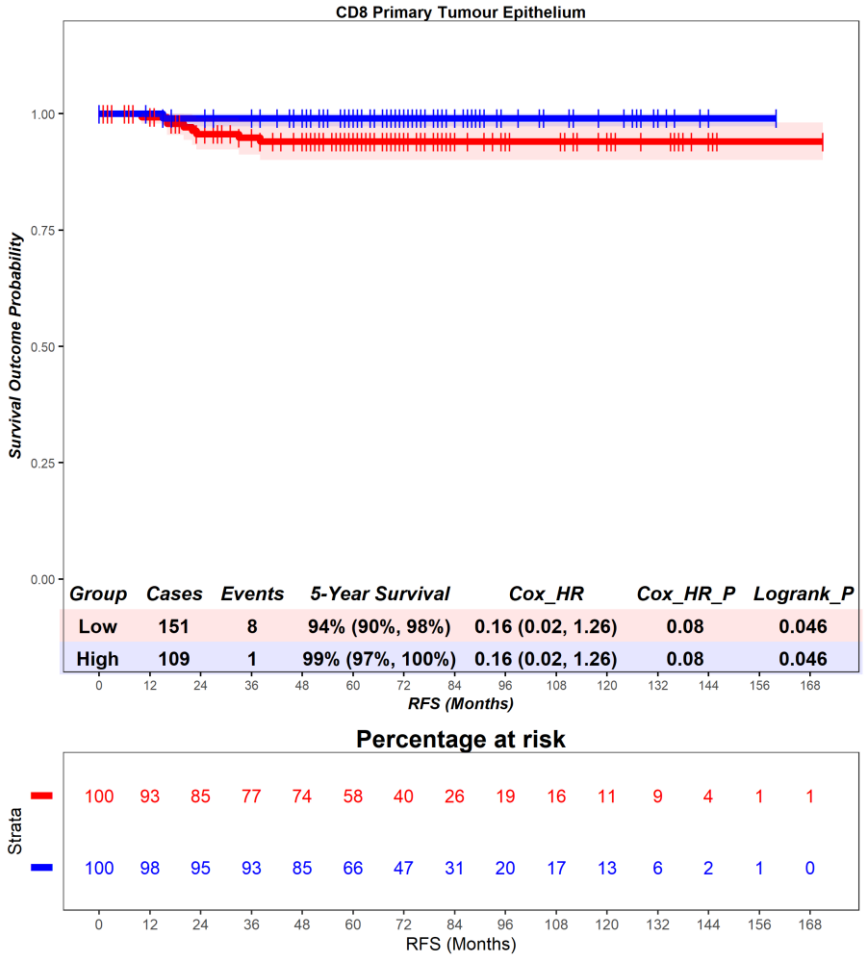

Figure 4.100 – Norway cohort. Time-to-event (recurrence-free survival) analysis for CD8 T cells in the primary tumour epithelium. *Patients deemed 'High' or 'Low' for CD8 T cells are shaded blue and red, respectively. Cox hazard ratio is univariate – see table 4.6 for multivariate. The 'Low' group is used as the reference group on cox regression modelling.*

In the primary tumour stroma, patients deemed high for γδ T cells are associated with no differential prognsis (Figure 4.101). Patients with a high level of γδ T cells had a mean survival time of 71.38 months, compared to those with low levels of γδ T cells with a mean survival of 68.41 months (hazard ratio = 0.76, p = 0.69). 5-year survival for patients high for γδ T cells is 97% (94%, 100%), compared to 96% (92%, 99%) in the γδ low group. This suggests that γδ T cells in the stromal compartment of the primary tumour are associated with no differential prognostic role. Multivariate analysis was not statistically significant (hazard ratio = 0.77, p = 0.69) (Table 4.6), suggesting that γδ T cells in the stromal compartment of the primary tumour are not independently prognostic.

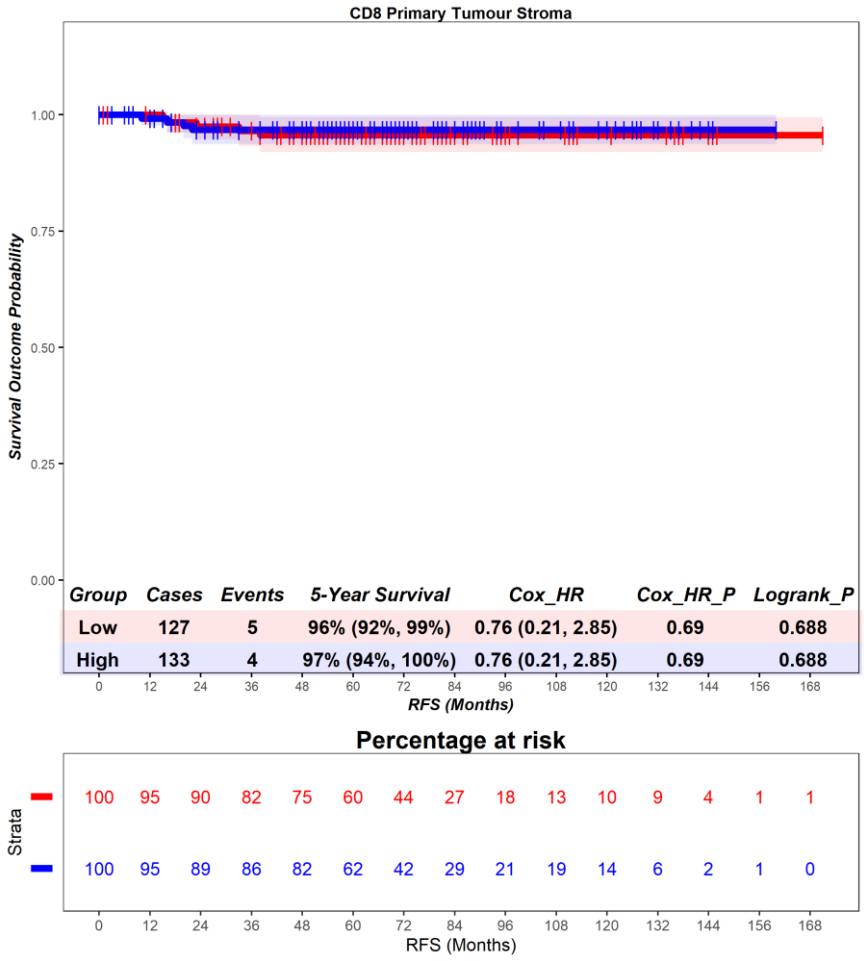

Figure 4.101 – Norway cohort. Time-to-event (recurrence-free survival) analysis for CD8 T cells in the primary tumour stroma. *Patients deemed 'High' or 'Low' for CD8 T cells are shaded blue and red, respectively. Cox hazard ratio is univariate – see table 4.6 for multivariate. The 'Low' group is used as the reference group on cox regression modelling.*

In the primary tumour tissue, patients deemed high for γδ T cells are associated with a better prognosis (Figure 4.102), although this result did not reach statistical significance. Patients with a high level of γδ T cells had a mean survival time of 78.05 months, compared to those with low levels of γδ T cells with a mean survival of 67.75 months (hazard ratio = Inf, p = 1). 5-year survival for patients high for γδ T cells is 100% (100%, 100%), compared to 95% (92%, 98%) in the γδ low group. This suggests that γδ T cells in the whole tissue of the primary tumour are associated with a favourable prognostic role. Multivariate analysis was not statistically significant (hazard ratio = Inf, p = 1.0) (Table 4.6), suggesting that γδ T cells in the whole tissue of the primary tumour are not independently prognostic.

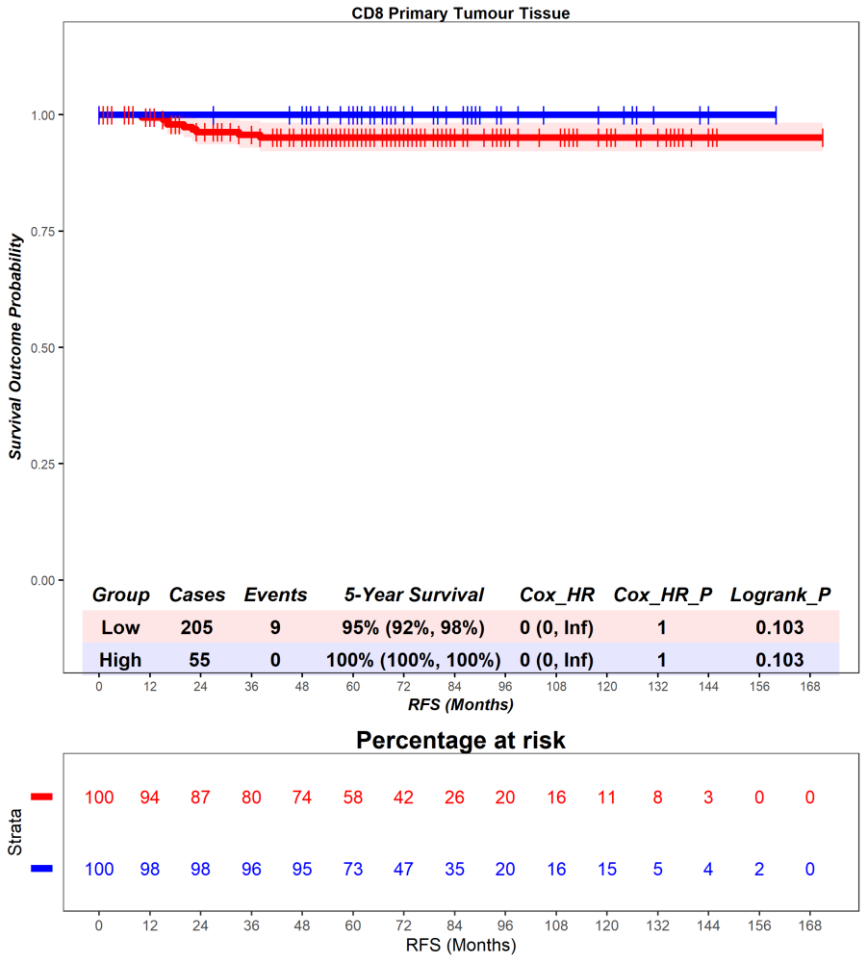

Figure 4.102 – Norway cohort. Time-to-event (recurrence-free survival) analysis for CD8 T cells in the primary tumour tissue. *Patients deemed 'High' or 'Low' for CD8 T cells are shaded blue and red, respectively. Cox hazard ratio is univariate – see table 4.6 for multivariate. The 'Low' group is used as the reference group on cox regression modelling.*

4.3.9 Relationship between CD8 and γδ T cells

In the adjacent normal epithelium, there was a poor positive correlation between γδ T cells and CD8 T cells (R = 0.19) and this result did not reach statistical significance (p = 0.15) Figure (4.103A). γδ T cells were consistently present at a lower than CD8 T cells (Figure 4.103B/C). Thus, the data show no relationship between the density of γδ T cells and CD8 T cells in the adjacent normal epithelium.

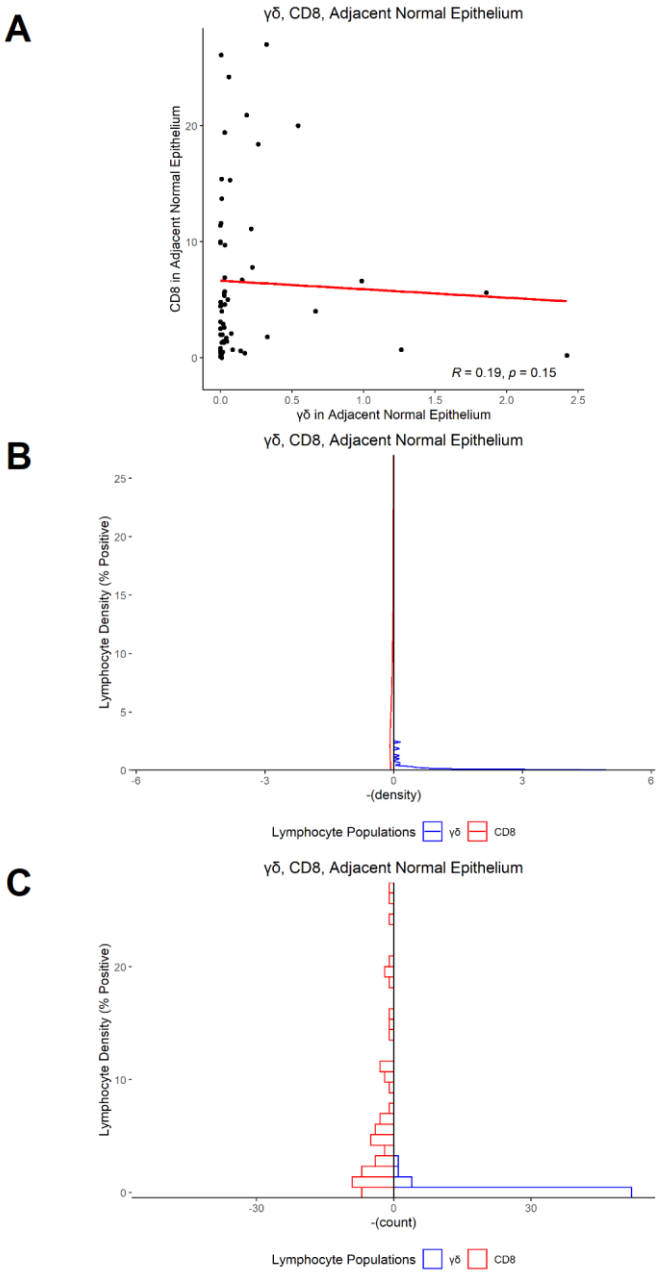

Figure 4.103 – Norway cohort. Correlation analysis for γδ T cells and CD8 T cells in the adjacent normal epithelium. *A - Scatter plot depicts the density (% positive) of γδ T cells (X axis) and CD8 T cells (Y axis), restricted to cases for which data is available for both populations. Correlation is described using Spearman's rank correlation coefficient. R values >0 and <0.3 are poor, >0.3 are fair, >0.6 are moderate, >0.8 are very strong and 1 are perfect. Correlation coefficients are considered statistically significant if p <0.05. B – Density plot of lymphocyte density for CD8 T cells (red) and γδ T cells (blue). C – Histogram plot of lymphocyte density for CD8 T cells (red) and γδ T cells (blue).*

In the adjacent normal stroma, there was a poor positive correlation between γδ T cells and CD8 T cells (R = 0.13) and this result did not reach statistical significance (p = 0.32) Figure (4.104A). γδ T cells were consistently present at a lower than CD8 T cells (Figure 4.104B/C). Thus, the data show no relationship between the density of γδ T cells and CD8 T cells in the adjacent normal stroma.

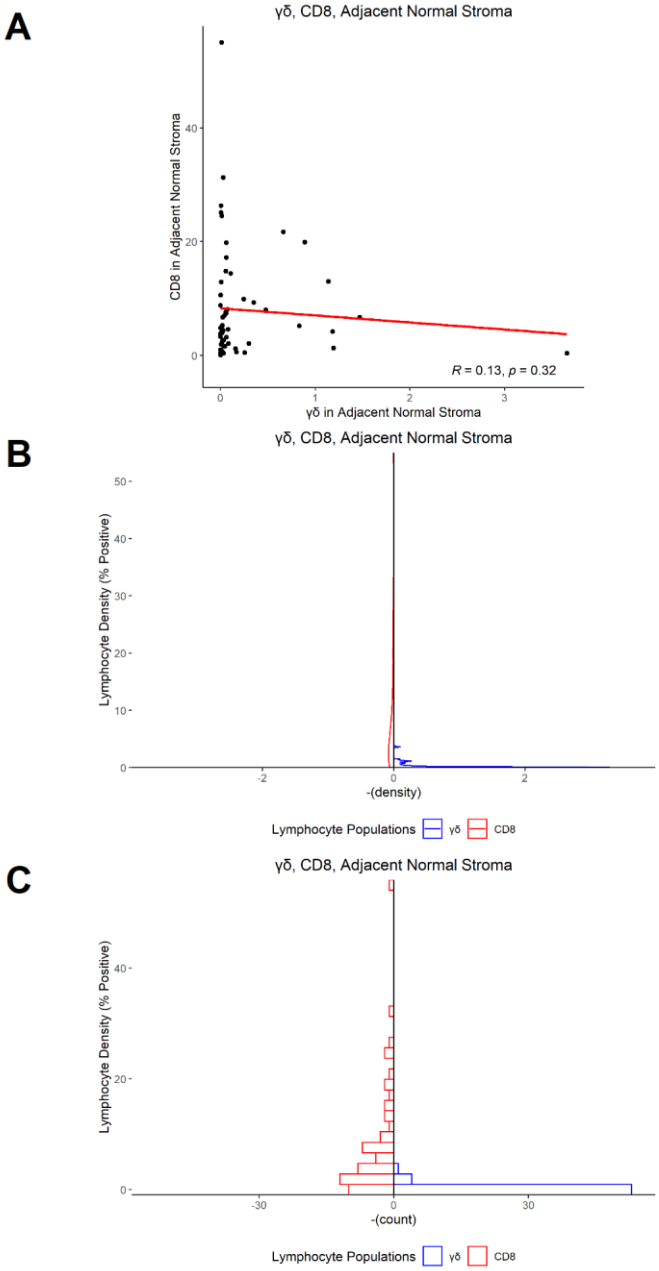

Figure 4.104 Correlation analysis for γδ T cells and CD8 T cells in the adjacent normal stroma. *A - Scatter plot depicts the density (% positive) of γδ T cells (X axis) and CD8 T cells (Y axis), restricted to cases for which data is available for both populations. Correlation is described using Spearman's rank correlation coefficient. R values >0 and <0.3 are poor, >0.3 are fair, >0.6 are moderate, >0.8 are very strong and 1 are perfect. Correlation coefficients are considered statistically significant if p <0.05. B – Density plot of lymphocyte density for CD8 T cells (red) and γδ T cells (blue). C – Histogram plot of lymphocyte density for CD8 T cells (red) and γδ T cells (blue).*

In the adjacent normal tissue, there was a poor positive correlation between γδ T cells and CD8 T cells (R = 0.19) and this result did not reach statistical significance (p = 0.15) Figure (4.105A). γδ T cells were consistently present at a lower than CD8 T cells (Figure 4.105B/C). Thus, the data show no relationship between the density of γδ T cells and CD8 T cells in the adjacent normal tissue.

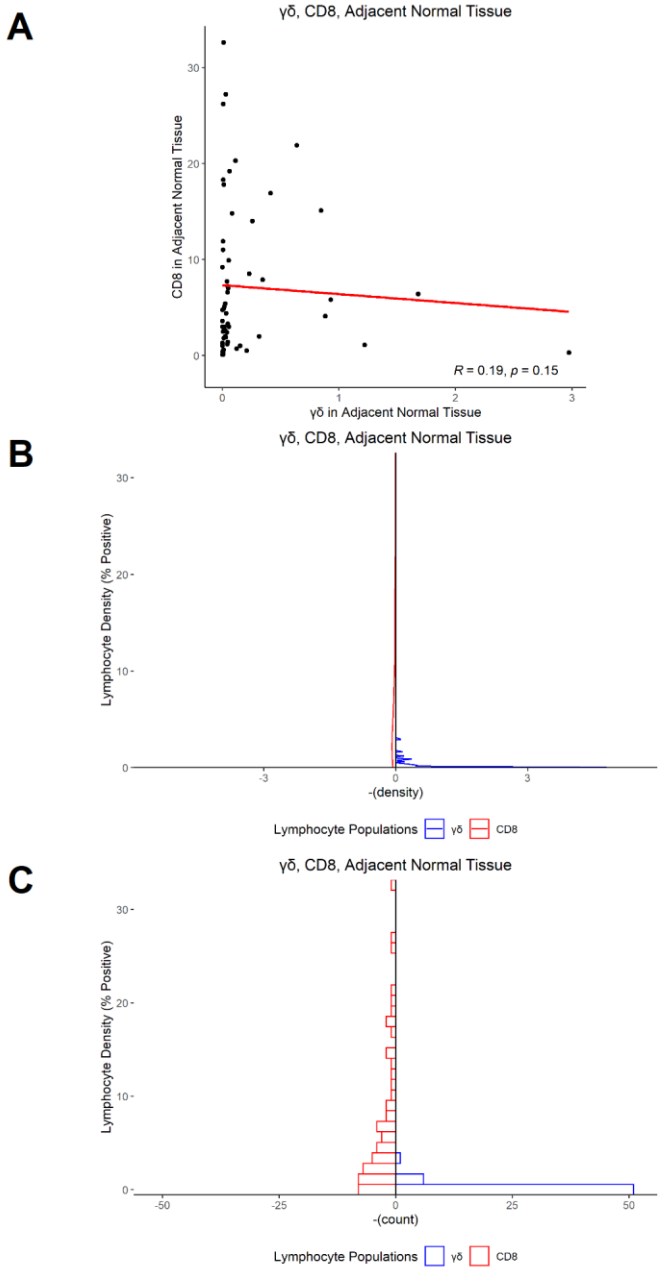

Figure 4.105 – Norway cohort. Correlation analysis for γδ T cells and CD8 T cells in the adjacent normal tissue. *A - Scatter plot depicts the density (% positive) of γδ T cells (X axis) and CD8 T cells (Y axis), restricted to cases for which data is available for both populations. Correlation is described using Spearman's rank correlation coefficient. R values >0 and <0.3 are poor, >0.3 are fair, >0.6 are moderate, >0.8 are very strong and 1 are perfect. Correlation coefficients are considered statistically significant if p <0.05. B – Density plot of lymphocyte density for CD8 T cells (red) and γδ T cells (blue). C – Histogram plot of lymphocyte density for CD8 T cells (red) and γδ T cells (blue).*

In the primary tumour epithelium, there was a poor positive correlation between γδ T cells and CD8 T cells (R = 0.11) and this result did not reach statistical significance (p = 0.072) Figure (4.106A). γδ T cells were consistently present at a lower than CD8 T cells (Figure 4.106B/C). Thus, the data show no relationship between the density of γδ T cells and CD8 T cells in the primary tumour epithelium.

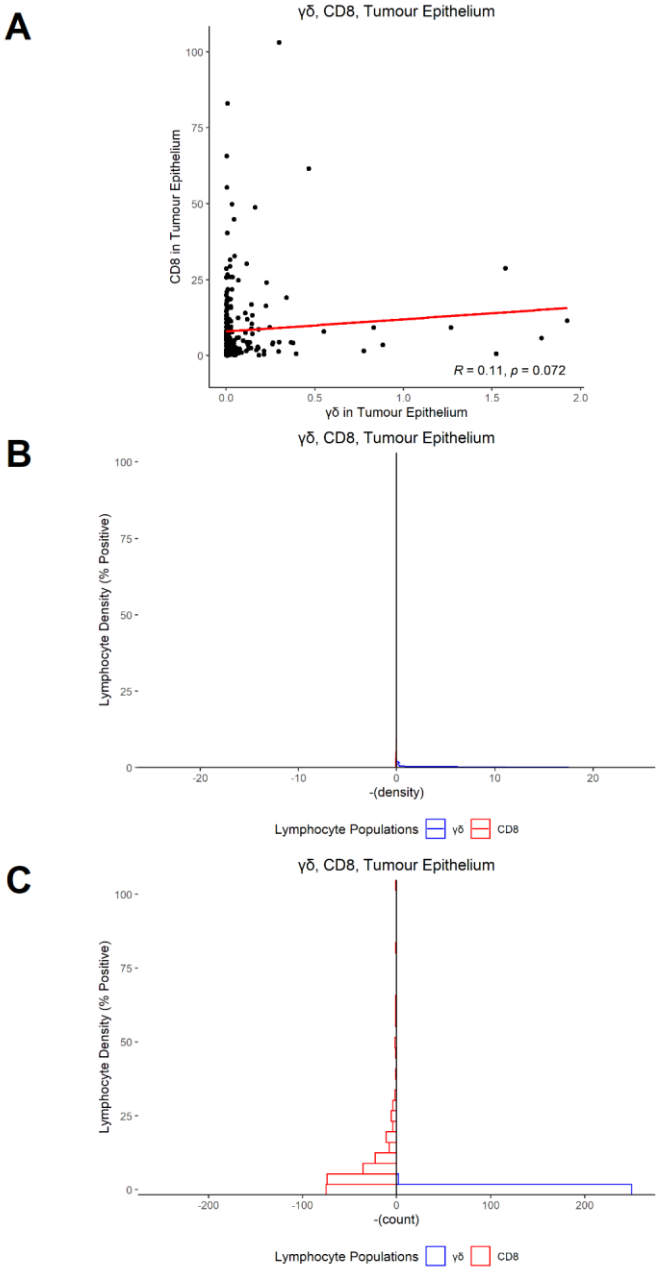

Figure 4.106 – Norway cohort. Correlation analysis for γδ T cells and CD8 T cells in the primary tumour epithelium. *A - Scatter plot depicts the density (% positive) of γδ T cells (X axis) and CD8 T cells (Y axis), restricted to cases for which data is available for both populations. Correlation is described using Spearman's rank correlation coefficient. R values >0 and <0.3 are poor, >0.3 are fair, >0.6 are moderate, >0.8 are very strong and 1 are perfect. Correlation coefficients are considered statistically significant if p <0.05. B – Density plot of lymphocyte density for CD8 T cells (red) and γδ T cells (blue). C – Histogram plot of lymphocyte density for CD8 T cells (red) and γδ T cells (blue).*

In the primary tumour stroma, there was a poor positive correlation between γδ T cells and CD8 T cells (R = 0.15) and this result did reach statistical significance (p = 0.014) Figure (4.107A). γδ T cells were consistently present at a lower than CD8 T cells (Figure 4.107B/C). Thus, the data show no relationship between the density of γδ T cells and CD8 T cells in the primary tumour stroma.

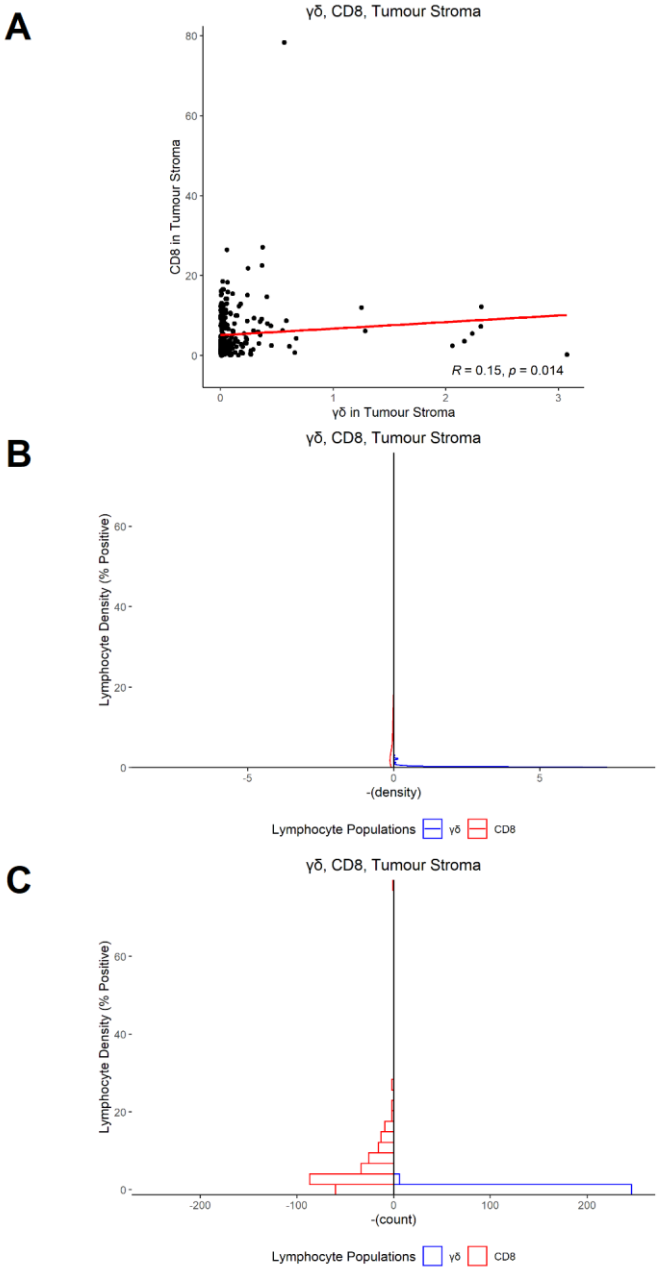

Figure 4.107 – Norway cohort. Correlation analysis for γδ T cells and CD8 T cells in the primary tumour stroma. *A - Scatter plot depicts the density (% positive) of γδ T cells (X axis) and CD8 T cells (Y axis), restricted to cases for which data is available for both populations. Correlation is described using Spearman's rank correlation coefficient. R values >0 and <0.3 are poor, >0.3 are fair, >0.6 are moderate, >0.8 are very strong and 1 are perfect. Correlation coefficients are considered statistically significant if p <0.05. B – Density plot of lymphocyte density for CD8 T cells (red) and γδ T cells (blue). C – Histogram plot of lymphocyte density for CD8 T cells (red) and γδ T cells (blue).*

In the primary tumour tissue, there was a poor positive correlation between γδ T cells and CD8 T cells (R = 0.15) and this result did reach statistical significance (p = 0.016) Figure (4.108A). γδ T cells were consistently present at a lower than CD8 T cells (Figure 4.108B/C). Thus, the data show no relationship between the density of γδ T cells and CD8 T cells in the primary tumour tissue.

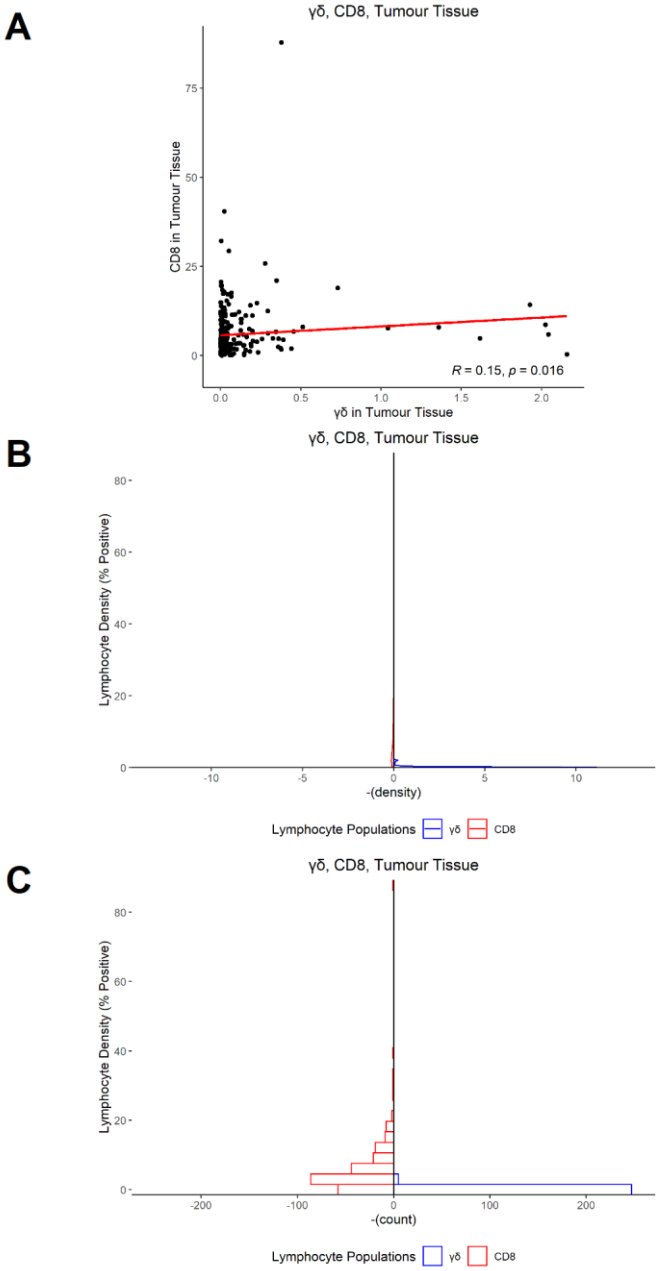

Figure 4.108. Norway cohort. Correlation analysis for γδ T cells and CD8 T cells in the primary tumour tissue. *A - Scatter plot depicts the density (% positive) of γδ T cells (X axis) and CD8 T cells (Y axis), restricted to cases for which data is available for both populations. Correlation is described using Spearman's rank correlation coefficient. R values >0 and <0.3 are poor, >0.3 are fair, >0.6 are moderate, >0.8 are very strong and 1 are perfect. Correlation coefficients are considered statistically significant if p <0.05. B – Density plot of lymphocyte density for CD8 T cells (red) and γδ T cells (blue). C – Histogram plot of lymphocyte density for CD8 T cells (red) and γδ T cells (blue).*

4.3.10 Norway - multivariate analysis

Table 4.6 – Results of multivariate cox regression modelling in the Norway cohort. *Covariates were selected by extracting univariate variables that were statistically significant in univariate models. Covariates are listed in Table S4.*

Group Descriptors			Multivariate Values							
Cohort	Status	variable	p.value	estimate	conf.low	conf.high	N_obs	N_event	std.error	statistic
Norway	CSS	GD_PercPositiveCellsinHealthyTissue_Coded	0.260	3.63	0.39	34.25	87	10	1.145	1.127
Norway	CSS	GD_PercPositiveCellsinTumourTissue_Coded	0.600	0.79	0.33	1.90	281	28	0.447	-0.519
Norway	CSS	GD_PercPositiveCellsinHealthyEpithelium_Coded	0.260	3.63	0.39	34.25	87	10	1.145	1.127
Norway	CSS	GD_PercPositiveCellsinTumourEpithelium_Coded	0.420	0.70	0.29	1.68	281	28	0.450	-0.808
Norway	CSS	GD_PercPositiveCellsinHealthyStroma_Coded	1.000	16954305 22.08	0.00	Inf	87	10	14451.817	0.001
Norway	CSS	GD_PercPositiveCellsinTumourStroma_Coded	0.910	1.05	0.45	2.42	281	28	0.427	0.112
Norway	CSS	CD8_PercPositiveCellsinHealthyTissue_Coded	1.000	0.00	0.00	Inf	74	7	27281.346	-0.001
Norway	CSS	CD8_PercPositiveCellsinTumourTissue_Coded	0.410	0.60	0.18	2.03	260	31	0.622	-0.823
Norway	CSS	CD8_PercPositiveCellsinHealthyEpithelium_Coded	0.460	0.38	0.03	4.94	74	7	1.315	-0.745
Norway	CSS	CD8_PercPositiveCellsinTumourEpithelium_Coded	0.660	0.84	0.38	1.84	260	31	0.399	-0.439
Norway	CSS	CD8_PercPositiveCellsinHealthyStroma_Coded	<0.001	51372352 1.40	95313333. 81	27688870 57.87	74	7	0.859	23.337
Norway	CSS	CD8_PercPositiveCellsinTumourStroma_Coded	0.030	0.37	0.16	0.89	260	31	0.441	-2.232
Norway	OS	GD_PercPositiveCellsinHealthyTissue_Coded	0.140	2.29	0.77	6.76	87	31	0.553	1.495
Norway	OS	GD_PercPositiveCellsinTumourTissue_Coded	0.020	0.57	0.36	0.90	281	102	0.231	-2.411
Norway	OS	GD_PercPositiveCellsinHealthyEpithelium_Coded	0.130	2.33	0.79	6.90	87	31	0.553	1.530
Norway	OS	GD_PercPositiveCellsinTumourEpithelium_Coded	0.010	0.55	0.36	0.86	281	102	0.223	-2.640
Norway	OS	GD_PercPositiveCellsinHealthyStroma_Coded	0.060	3.56	0.95	13.36	87	31	0.675	1.883
Norway	OS	GD_PercPositiveCellsinTumourStroma_Coded	0.060	0.64	0.41	1.01	281	102	0.231	-1.908
Norway	OS	CD8_PercPositiveCellsinHealthyTissue_Coded	0.710	0.75	0.16	3.43	74	21	0.775	-0.369
Norway	OS	CD8_PercPositiveCellsinTumourTissue_Coded	0.890	1.03	0.62	1.72	260	93	0.258	0.133
Norway	OS	CD8_PercPositiveCellsinHealthyEpithelium_Coded	0.070	2.32	0.93	5.81	74	21	0.468	1.804
Norway	OS	CD8_PercPositiveCellsinTumourEpithelium_Coded	0.980	1.01	0.66	1.53	260	93	0.213	0.029
Norway	OS	CD8_PercPositiveCellsinHealthyStroma_Coded	0.160	2.08	0.74	5.80	74	21	0.524	1.394
Norway	OS	CD8_PercPositiveCellsinTumourStroma_Coded	0.690	0.92	0.60	1.40	260	93	0.215	-0.396
Norway	DFS	GD_PercPositiveCellsinHealthyTissue_Coded	0.040	5.97	1.08	33.08	87	12	0.874	2.045
Norway	DFS	GD_PercPositiveCellsinTumourTissue_Coded	0.520	0.77	0.36	1.68	281	35	0.395	-0.647
Norway	DFS	GD_PercPositiveCellsinHealthyEpithelium_Coded	0.030	6.18	1.14	33.59	87	12	0.864	2.109
Norway	DFS	GD_PercPositiveCellsinTumourEpithelium_Coded	0.300	0.67	0.31	1.44	281	35	0.395	-1.033
Norway	DFS	GD_PercPositiveCellsinHealthyStroma_Coded	1.000	10626890 63.76	0.00	Inf	87	12	8139.972	0.003
Norway	DFS	GD_PercPositiveCellsinTumourStroma_Coded	0.920	1.04	0.49	2.19	281	35	0.380	0.097
Norway	DFS	CD8_PercPositiveCellsinHealthyTissue_Coded	0.390	2.73	0.27	27.40	74	10	1.177	0.853
Norway	DFS	CD8_PercPositiveCellsinTumourTissue_Coded	0.180	0.44	0.13	1.45	260	40	0.610	-1.349
Norway	DFS	CD8_PercPositiveCellsinHealthyEpithelium_Coded	0.900	0.90	0.19	4.24	74	10	0.790	-0.131
Norway	DFS	CD8_PercPositiveCellsinTumourEpithelium_Coded	0.250	0.66	0.32	1.35	260	40	0.367	-1.139
Norway	DFS	CD8_PercPositiveCellsinHealthyStroma_Coded	0.010	16.65	1.74	159.61	74	10	1.153	2.439
Norway	DFS	CD8_PercPositiveCellsinTumourStroma_Coded	0.090	0.54	0.26	1.10	260	40	0.366	-1.692
Norway	RFS	GD_PercPositiveCellsinHealthyTissue_Coded	0.170	7.78	0.42	145.11	87	2	1.493	1.374
Norway	RFS	GD_PercPositiveCellsinTumourTissue_Coded	0.620	0.66	0.13	3.42	281	7	0.839	-0.496
Norway	RFS	GD_PercPositiveCellsinHealthyEpithelium_Coded	0.110	9.91	0.58	168.63	87	2	1.446	1.586
Norway	RFS	GD_PercPositiveCellsinTumourEpithelium_Coded	0.490	0.56	0.11	2.92	281	7	0.839	-0.682
Norway	RFS	GD_PercPositiveCellsinHealthyStroma_Coded	0.150	9.05	0.45	182.98	87	2	1.534	1.436
Norway	RFS	GD_PercPositiveCellsinTumourStroma_Coded	0.810	0.82	0.16	4.21	281	7	0.837	-0.242
Norway	RFS	CD8_PercPositiveCellsinHealthyTissue_Coded	0.180	5.38	0.47	62.15	74	3	1.249	1.347
Norway	RFS	CD8_PercPositiveCellsinTumourTissue_Coded	1.000	0.00	0.00	Inf	260	9	6263.109	-0.003
Norway	RFS	CD8_PercPositiveCellsinHealthyEpithelium_Coded	0.840	1.29	0.11	14.90	74	3	1.250	0.202
Norway	RFS	CD8_PercPositiveCellsinTumourEpithelium_Coded	0.110	0.18	0.02	1.48	260	9	1.064	-1.594
Norway	RFS	CD8_PercPositiveCellsinHealthyStroma_Coded	0.080	8.82	0.79	98.59	74	3	1.232	1.768
Norway	RFS	CD8_PercPositiveCellsinTumourStroma_Coded	0.690	0.77	0.21	2.85	260	9	0.671	-0.398

4.4 Thailand Cohort

4.4.0 Summary Tables

Table 4.7 – Summary table of survival analysis for γδ T cells in the Thailand cohort. *Red rows are unfavourable. Green rows are favourable. Amber rows either present a mutual result or trend towards a result but with insufficient size effect.*

Survival	Compartment	Cox HR	Cox P Value	Logrank P Value	Prognostic Value
Overall (OS)	γδ Primary Tumour Epithelium	0.85	0.44	0.435	Unclear
Overall (OS)	γδ Primary Tumour Stroma	0.94	0.81	0.813	Unclear
Overall (OS)	γδ Primary Tumour Tissue	0.96	0.86	0.857	Unclear

4.4.1 γδ T cells - overall survival

In the primary tumour epithelium, patients deemed high for γδ T cells are associated with a better prognosis (Figure 4.109), although this result did not reach statistical significance. Patients with a high level of γδ T cells had a mean survival time of 53.66 months, compared to those with low levels of γδ T cells with a mean survival of 48.11 months (hazard ratio = 0.85, p = 0.44). 5-year survival for patients high for γδ T cells is 35% (23%, 53%), compared to 34% (28%, 43%) in the γδ low group. This suggests that γδ T cells in the epithelial compartment of the primary tumour are associated with a favourable prognostic role. Multivariate analysis was not statistically significant (hazard ratio = 1.14, p = 0.57) (Table 4.8), suggesting that γδ T cells in the epithelial compartment of the primary tumour are not independently prognostic.

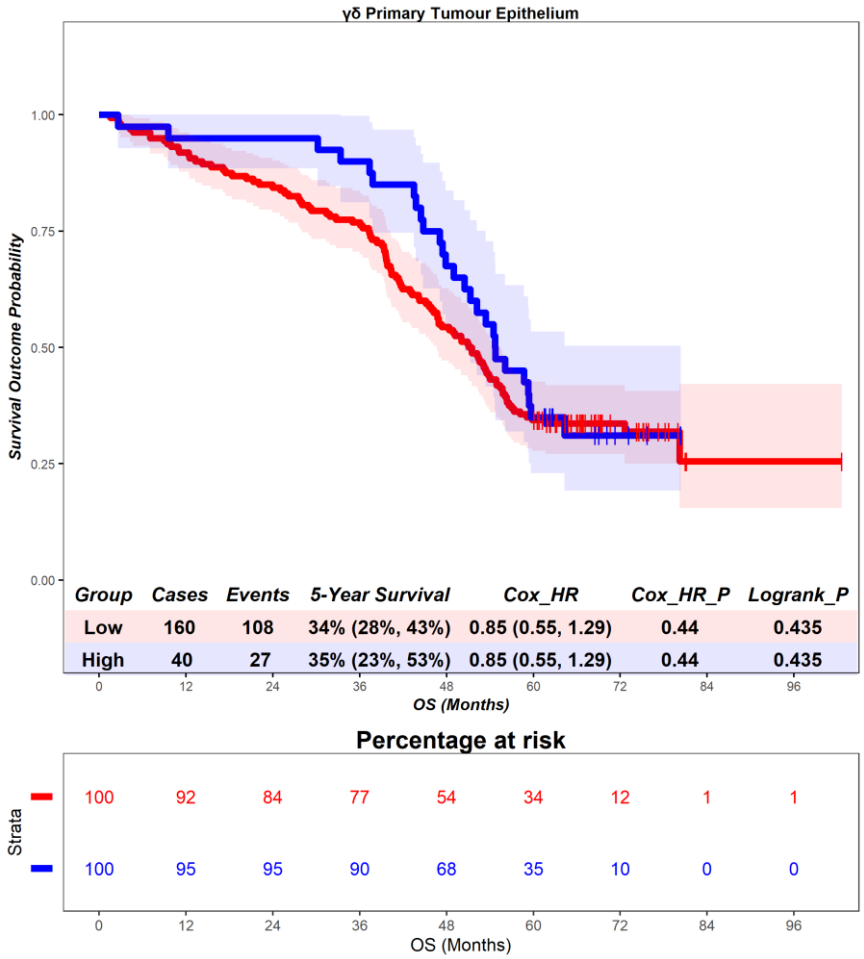

Figure 4.109 – Thailand cohort. Time-to-event (overall survival) analysis for γδ T cells in the primary tumour epithelium. *Patients deemed 'High' or 'Low' for γδ T cells are shaded blue and red, respectively. Cox hazard ratio is univariate – see table 4.8 for multivariate. The 'Low' group is used as the reference group on cox regression modelling.*

In the primary tumour stroma, patients deemed high for γδ T cells are associated with no differential prognosis (Figure 4.110). Patients with a high level of γδ T cells had a mean survival time of 51.78 months, compared to those with low levels of γδ T cells with a mean survival of 48.79 months (hazard ratio = 0.94, p = 0.81). 5-year survival for patients high for γδ T cells is 34% (21%, 57%), compared to 35% (28%, 42%) in the γδ low group. This suggests that γδ T cells in the stromal compartment of the primary tumour are associated with no differential prognostic role. Multivariate analysis was not statistically significant (hazard ratio = 1.26, p = 0.36) (Table 4.8), suggesting that γδ T cells in the stromal compartment of the primary tumour are not independently prognostic.

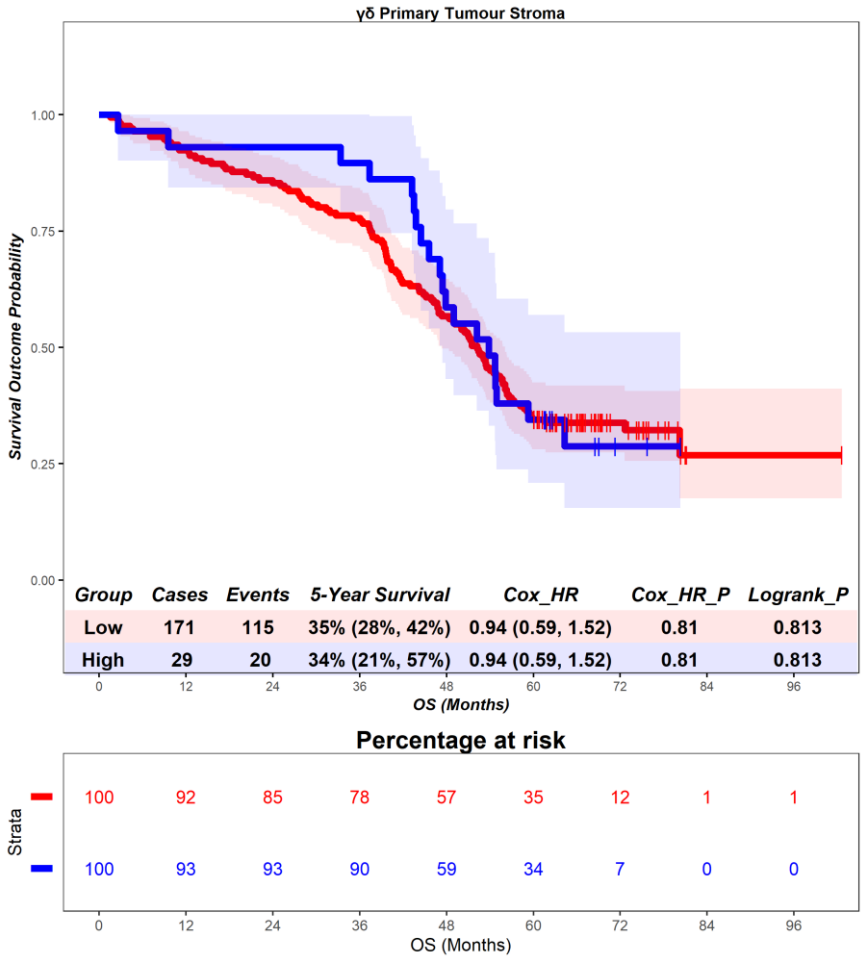

Figure 4.110 – Thailand cohort. Time-to-event (overall survival) analysis for γδ T cells in the primary tumour stroma. *Patients deemed 'High' or 'Low' for γδ T cells are shaded blue and red, respectively. Cox hazard ratio is univariate – see table 4.8 for multivariate. The 'Low' group is used as the reference group on cox regression modelling.*

In the primary tumour tissue, patients deemed high for γδ T cells are associated with no differential prognosis (Figure 4.111). Patients with a high level of γδ T cells had a mean survival time of 51.75 months, compared to those with low levels of γδ T cells with a mean survival of 48.78 months (hazard ratio = 0.96, p = 0.857). 5-year survival for patients high for γδ T cells is 33% (20%, 55%), compared to 35% (28%, 43%) in the γδ low group. This suggests that γδ T cells in the whole tissue of the primary tumour are associated with no differential prognostic role. Multivariate analysis was not statistically significant (hazard ratio = 1.27, p = 0.34) (Table 4.8), suggesting that γδ T cells in the whole tissue compartment of the primary tumour are not independently prognostic.

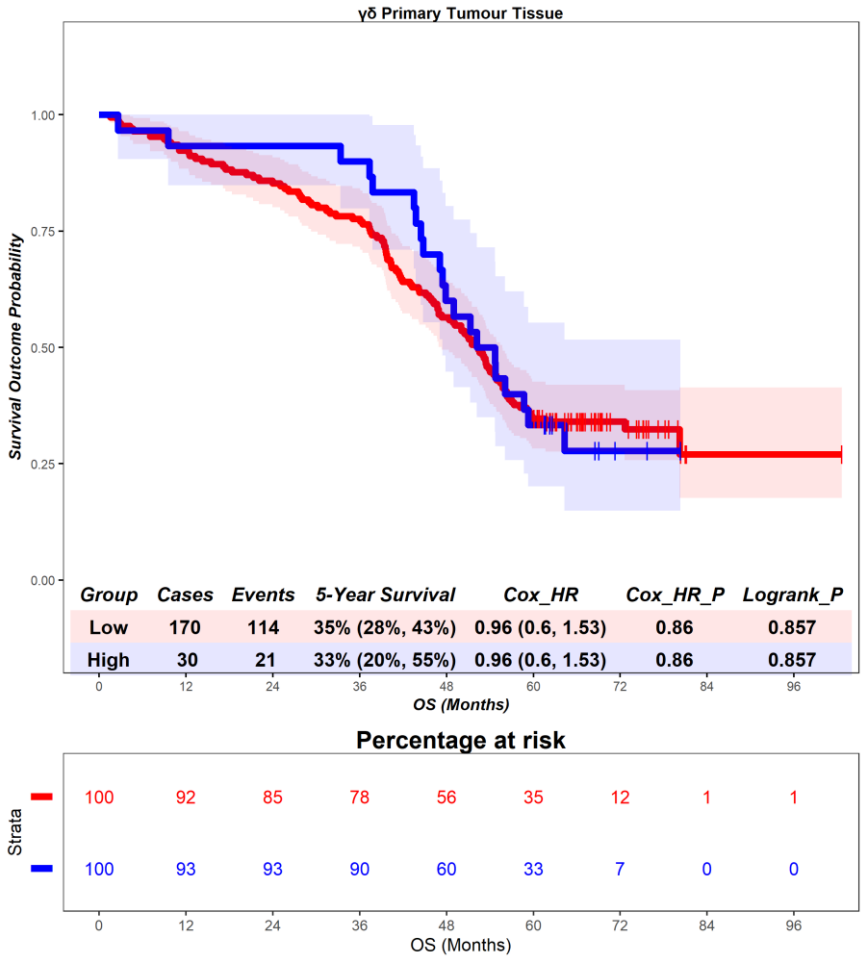

Figure 4.111 – Thailand cohort. Time-to-event (overall survival) analysis for γδ T cells in the primary tumour tissue. *Patients deemed 'High' or 'Low' for γδ T cells are shaded blue and red, respectively. Cox hazard ratio is univariate – see table 4.8 for multivariate. The 'Low' group is used as the reference group on cox regression modelling.*

4.4.2 Thailand - multivariate analysis

Table 4.8 - Results of multivariate cox regression modelling in the Thailand cohort. *Covariates were selected by extracting univariate variables that were statistically significant in univariate models. Covariates are listed in Table S4.*

Group Descriptors			Multivariate Values							
Cohort	Status	variable	p.value	estimate	conf.low	conf.high	N_obs	N_event	std.error	statistic
Thailand	OS	GD_PercPositiveCellsinTumourTissue_Coded	0.340	1.27	0.78	2.08	200	135	0.250	0.963
Thailand	OS	GD_PercPositiveCellsinTumourEpithelium_Coded	0.570	1.14	0.73	1.79	200	135	0.231	0.575
Thailand	OS	GD_PercPositiveCellsinTumourStroma_Coded	0.360	1.26	0.77	2.07	200	135	0.253	0.915

4.5 Discussion

The prognostic role of γδ T cells in CRC remains to be elucidated despite attempts to both rectify this gap in our understanding of γδ T cell biology and improve stratification tools to provide the optimal outcome for patients. Attempts to date have relied on transcriptomic methodologies which whilst very successful in investigating the influence of the greater lymphocyte populations, fail to accurately identify specific subsets such as γδ T cells. To take a histological approach to tackling this problem, the density of two target lymphocyte populations, γδ T cells and CD8 T cells, was determined and used to categorise patients as being 'Low' or 'High' for these populations. By applying survival analysis to three cohorts of patients representative of populations in Scotland, Norway and Thailand, the effect of γδ T cells and CD8 T cells on cancer-specific, overall, disease-free and recurrence-free survival is described, revealing contrasting prognostic roles for γδ T cells and CD8 T cells.

γδ T cells in the Scotland cohort demonstrated a clear unfavourable prognostic role in the context of cancer-specific survival, regardless of the tissue region (primary tumour or adjacent normal tissue) or compartment (epithelial, stromal or whole tissue). A similar result was seen in the context of overall survival, although with a lesser effect size in the adjacent normal tissue, disease-free survival and recurrence-free survival, although the primary tumour tissue was uninformative due to extremely low numbers of cases and events in the 'Low' group. In stark contrast, CD8 T cells in the Scotland cohort demonstrated a favourable prognostic role in the context of cancer-specific survival, although CD8 T cells in the adjacent normal tissue did have contrasting roles in the epithelium and stroma. However, CD8 T cells did not demonstrate a clear impact on overall survival. In the context of disease-free survival, CD8 T cells were a favourable factor in the epithelium and whole tissue of the adjacent normal tissue but not the stroma, with no clear role in the tumour. In the context of recurrence free survival, CD8 T cells were favourable in the epithelium and whole tissue of the adjacent normal tissue but unfavourable in the stroma but were favourable in all compartments of the primary tumour.

γδ T cells in the Norway cohort demonstrated no prognostic value in the context of cancer-specific survival, with the exception of the epithelial compartment in the primary tumour, although this effect was not present until the five-year point. In the context of overall survival, no effect could be observed in the adjacent normal tissue but γδ T cells in the primary tumour were favourable. In the context of disease-free survival, the adjacent normal tissue showed a trend towards a favourable role but with very low numbers of cases and events and subsequently high variance, whilst the primary tumour tissue showed an effect like that seen in the context of cancer-specific survival. In the context of recurrence-free survival, the adjacent normal tissue showed a similar result to that observed in the context of disease-free survival, whilst the primary tumour showed no effect. CD8 T cells in the Norway cohort had no prognostic value in the context of cancer-specific survival in the adjacent normal tissue, but were favourable in the primary tumour, particularly in the stroma. In the context of overall survival, CD8 T cells were not observably prognostic in the adjacent normal tissue (the stroma did present an unfavourable effect but with significant variance) or in the primary tumour. In the context of disease-free survival, CD8 T cells were not prognostic in the adjacent normal tissue (there was some favourable effect in the stromal compartment but with significant variance) whilst in the primary tumour they were a clear favourable prognostic factor. There was no observable prognostic effect of CD8 T cells in the context of recurrence-free survival.

In the context of overall survival, γδ T cells in the primary tumour of patients in the Thailand cohort showed a favourable effect up to the three-to-four-year point, but thereafter survival times merged again, suggesting that γδ T cells did not have a lasting prognostic effect but perhaps delayed death.

γδ T cells in the Scotland cohort were a distinctly unfavourable prognostic factor regardless of the survival outcome of interest, whilst CD8 T cells were a favourable factor in the context of cancer-specific survival but were either inconclusive or contradictive between the epithelium and stroma. The cut points used to define patients as ‘Low’ or ‘High’ for γδ T cells or CD8 T cells were generated from the Scotland cohort, and these cut points applied to two additional cohorts of patients representative of Norway and Thailand. Due to the limited availability of survival outcome data and lack of CD8 staining, no conclusion can be drawn on whether the results seen in the Scotland cohort are reflected in the Thailand cohort.

γδ T cells and CD8 T cells in the Norway cohort failed to reflect the results observed in the Scotland cohort. This was not due to a contrasting result but rather a lack of any discernible effects. When cut points are generated using the Norway cohort, the Norway cohort shows clear results in the context of cancer-specific, overall survival and disease-free survival, whilst the Scotland cohort shows inconclusive results. Much of the results seen in the Scotland cohort when cut points are generated from the Scotland cohort and results in the Norway cohort when cut points are generated from the Norway cohort, are largely in agreement (Appendices, chapter 4). This would suggest that γδ T cells and CD8 T cells do have prognostic value but that the appropriate cut points to stratify patients are inconsistent across patient populations (Figure 4.112), with some difference in prognosis.

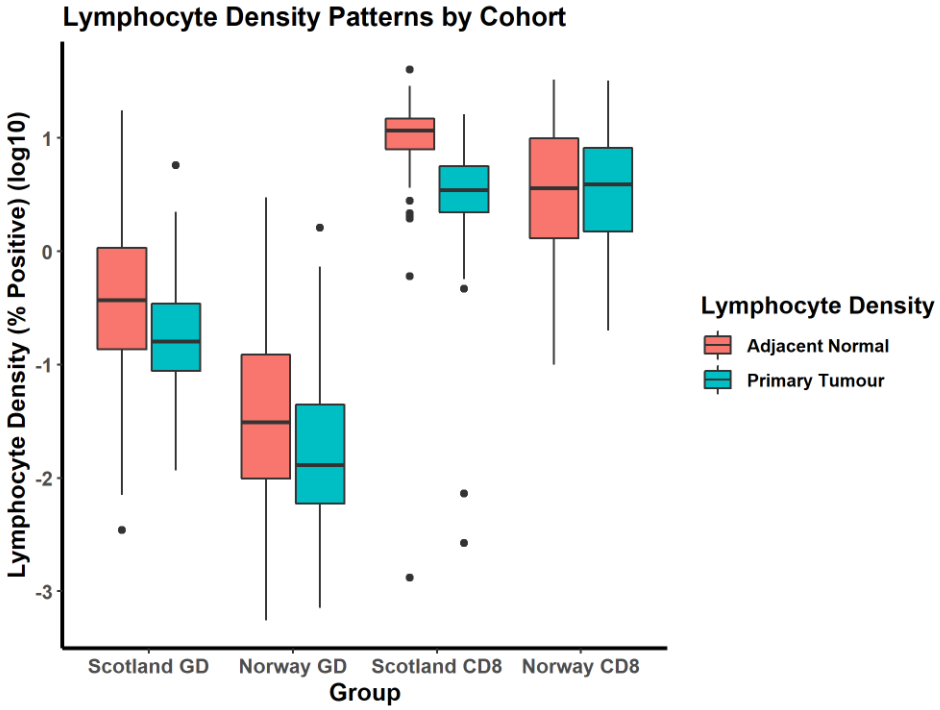

Figure 4.112 – Patterns of lymphocyte density across cohorts. *Y axis is log10 of the lymphocyte density previously described.*

In the context of all three disease-specific survival outcomes; cancer-specific, disease-free and recurrence-free; γδ T cells were unfavourable whilst CD8 T cells were largely favourable with some indifferent effects. Overall survival, which encompassed those who experienced a cancer death or a non-cancer death, was only impacted (unfavourably) by γδ T cells in the primary tumour. This would suggest that the prognostic effect of CD8 T cells is disease specific, whilst γδ T cells may be impacting the general wellbeing of patients. In conclusion, whilst the conventional CD8 T cell population are a favourable prognostic factor for CRC patients, unconventional γδ T cells are an unfavourable factor. This highlights both the divergent roles of T cell subsets and the need to understand their respective effects and how they might interact. Specifically, what is the prognosis for patients subjected to the effects of both populations and is there a threshold for one population or the other to have a dominant effect? Given that there is no correlation between γδ T cells and CD8 T cells it may be that these populations are either antagonistic or differentially regulated within the microenvironment and therefore do not colocalise at a high density. Unfortunately, the data presented lacks the appropriate power to answer this question within the scope of this study, but if an immune landscape beyond CD3 or CD8 T cells is to be clinically utilised, such questions would be key to an accurate prognosis.

Chapter 5:
Assessment of the mutational landscape by lymphocyte density

Chapter 5: Assessment of the mutational landscape by lymphocyte density

5.0 Summary

To identify biological themes underlying cases classed as ‘high’ or ‘low’ for lymphocytes, and potentially direct future mechanistic research, we conducted mutational analysis on a subset of the Scotland cohort. Mutations associated with a greater density of CD8 T cells consisted of mutations in genes related to DNA repair and cellular survival. Of interest are mutations in *ASTE1* and *TTK*. From the literature, in patients with microsatellite instability stemming from deficiencies in the DNA mismatch repair system, mutations occur in the microsatellite regions of genes including *ASTE1* and *TTK*, and these mutations are associated with CD8 T cell infiltration in the tumour due to the development of neoantigens. These data suggest that CD8 T cell density in this cohort is linked to microsatellite instability, an established biological process in colorectal cancer. γδ T cells did not show these themes, suggesting that they may be driven by an alternative mechanism.

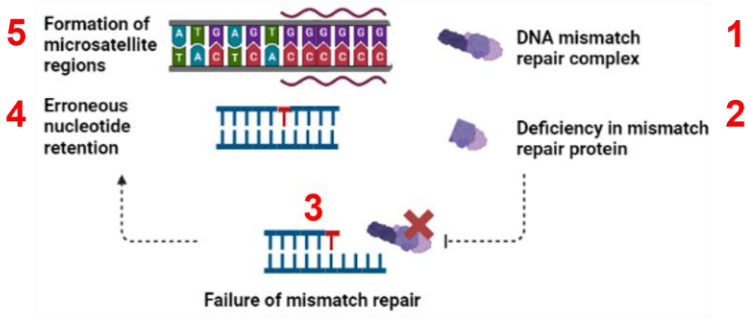

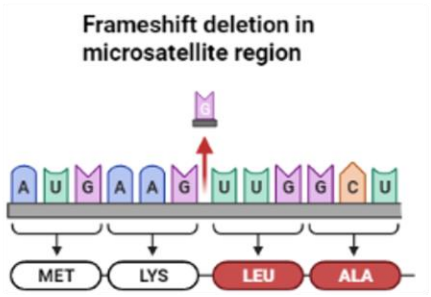

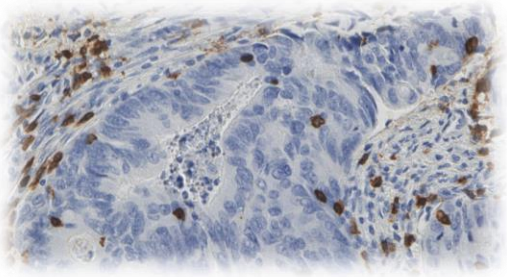

Mutations in MSI associate with CD8 T cell density

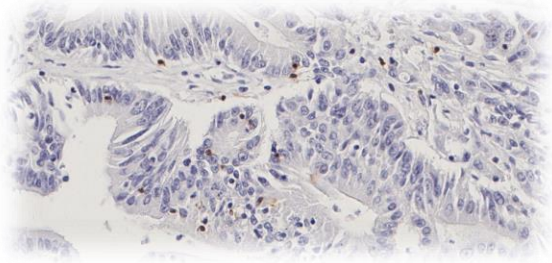

No association with γδ T cells

5.1 Introduction

As CRC develops from an adenoma it does so with a progression of key genetic aberrations, *BRAF* mutations, CIMP and MSI in the case of sessile serrated polyps and mutations in *APC*, *KRAS*, *TGFβ* and *TP53* in the case of adenocarcinomas [16, 33, 270]. Mutational profiles further differ in the context of metastasis, MSI and anatomical sites [271, 272]. In addition, mutational profiles are key to the infiltration of T cells into CRC tissue where the increased neoantigen load favours T cells infiltration, including specific mutations such as frameshift mutations in *ASTE1*, *TTK*, *HNF1A* and *TCF7L2* [45, 273]. Thus, the mutational landscape is of clear importance not just to the progression of CRC but also to the immune response.

Given that both γδ T cells and CD8 T cells were demonstrated to have prognostic value, mutational analysis was conducted on a sub-cohort of the Scotland cohort to determine whether lymphocyte status is influenced by the mutational landscape. The mutational landscape of patients low or high for γδ T cells and CD8 T cells were compared, and the resultant genes investigated in the context of survival, determining which genes influence lymphocyte density, whether these genes also influence survival and additionally whether that influence on survival matches the prognostic effect seen in the lymphocyte density group that they are associated with.

5.2 Summary analysis of cohort

Patient characteristics table

The cohort of patients with mutational data were largely reflective of the parent cohort. In terms of patient characteristics, the proportion of patients that were male or female and below or above the age of 65 were comparable. Tumour characteristics were less consistent with TNM stage being higher in the mutational cohort whilst other tumour characteristics were comparable, such as tumour site, differentiation, vascular invasion, Klintrup-Mäkinen grade, tumour stroma percentage and DNA mismatch repair status. With the exception of adjuvant therapy, treatment characteristics were not comparable with the mutational cohort having no cases with neoadjuvant therapy, mortality within 30 days and a higher rate of emergency surgery.

Table 5.1 – clinicopathologic characteristics of mutational sub-cohort of Scotland cohort. *Table of clinicopathologic characteristics of the cohort with distribution of cases (number of cases (% of cases)) and comparison to the parent cohort via 2-sample t-test (numerical variable) or chi-squared test (categorical variable).*

Patient Characteristics - Mutational Cohort			
	Full Cohort (N=1030)	**Mutational Cohort (N=200)**	**P-Value**
Sex			
Female	539 (52 %)	101 (50 %)	0.635
Male	491 (48 %)	99 (50 %)	
Age			
≥65	708 (69 %)	146 (73 %)	0.231
<65	322 (31 %)	54 (27 %)	
Surgery Type			
Elective	801 (78 %)	132 (66 %)	<0.001
Emergency	228 (22 %)	68 (34 %)	
Missing	1 (0.1%)	0 (0%)	
Tumour Site			
Right	430 (42 %)	93 (46 %)	0.125
Left	340 (33 %)	70 (35 %)	
Rectum	253 (25 %)	36 (18 %)	
Missing	7 (0.7%)	1 (0.5%)	
T Stage			
I	44 (4 %)	6 (3 %)	0.12
II	122 (12 %)	15 (8 %)	
III	560 (54 %)	107 (54 %)	
IV	304 (30 %)	72 (36 %)	
N Stage			
0	629 (61 %)	98 (49 %)	0.015
I	273 (27 %)	68 (34 %)	
II	123 (12 %)	33 (16 %)	
III	1 (0 %)	0 (0 %)	
Missing	4 (0.4%)	1 (0.5%)	
M Stage			
0	1004 (97 %)	199 (100 %)	0.0417
I	21 (2 %)	0 (0 %)	
Missing	5 (0.5%)	1 (0.5%)	
TNM Stage			
I	138 (13 %)	13 (6 %)	<0.001
II	483 (47 %)	84 (42 %)	
III	388 (38 %)	103 (52 %)	
IV	21 (2 %)	0 (0 %)	
Differentiation			
Moderate/Well	919 (89 %)	176 (88 %)	0.613
Poor	111 (11 %)	24 (12 %)	
Vascular Invasion			
No	681 (66 %)	128 (64 %)	0.564
Yes	349 (34 %)	72 (36 %)	
MMR Status			
Proficient	822 (80 %)	153 (76 %)	0.0789
Deficient	178 (17 %)	46 (23 %)	
Missing	30 (2.9%)	1 (0.5%)	
Klintrup-Mäkinen Grade			
Weak	696 (68 %)	139 (70 %)	0.647
Strong	314 (30 %)	58 (29 %)	
Missing	20 (1.9%)	3 (1.5%)	
Tumour Stroma Percentage			
Low	747 (73 %)	142 (71 %)	0.286
High	254 (25 %)	58 (29 %)	
Missing	29 (2.8%)	0 (0%)	
Adjuvant Therapy			
No	222 (22 %)	9 (4 %)	0.251
Yes	112 (11 %)	8 (4 %)	
Missing	696 (67.6%)	183 (91.5%)	
Neoadjuvant Therapy			
No	984 (96 %)	200 (100 %)	0.0056
Yes	38 (4 %)	0 (0 %)	
Missing	8 (0.8%)	0 (0%)	
Mortality Within 30 Days			
No	968 (94 %)	200 (100 %)	0.00153
Yes	49 (5 %)	0 (0 %)	
Missing	13 (1.3%)	0 (0%)	

Consort diagram of analysis groups

The whole cohort (n = 1030) was reduced to those that had matched mutational data (n = 200). This sub-cohort is further subset by availability of data for the tissue compartments for which analysis is to be run.

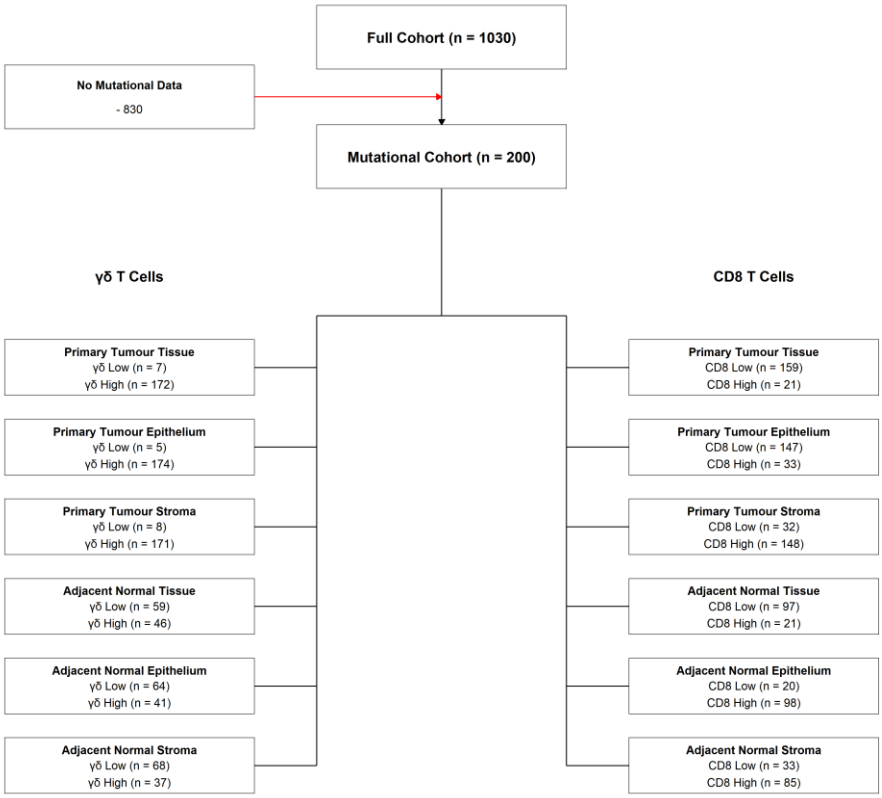

Figure 5.1 – Consort diagram for mutational analysis.

Mutational Overview

Within the cohort the dominant mutations were *APC*, *TP53* and *KRAS*, the key mutations for development of CRC from adenocarcinomas. Androgen receptor, the expression of which has been shown to be absent in normal mucosa but highly expressed (40%~) in adenomas and CRC, was mutated in 24% of cases [274]. Also mutated in 24% of cases is *PIK3CA*, the catalytic subunit of *PIK3*, in which gain of function mutations are associated with progression of CRC and a poor prognosis in *KRAS* wildtype patients [275-277]. 15% of cases had a mutation in *BRAF*, a key component of progression from serrated polyp to CRC [16], which leads to MAPK activated cell proliferation and is considered mutually exclusive to *KRAS [278]*, a key component of the process from adenocarcinoma to CRC [35]. *BRAF* mutations are predominantly found in right sided cases [61]. Other mutations present in the top 20 included the DNA damage response genes *ATM*, *ATR* and *BRCA2*, ubiquitination factors *FBXW7* and *RNF43*, chromatin regulating genes *ARID1A* and *ASXL1*, Wnt associated component *TGFBR2* and regulator *SMAD4*, DNA mismatch repair gene *MSH2* and additional genes *ALK*, *NOTCH1*, *NOTCH3* and *RPL22*.

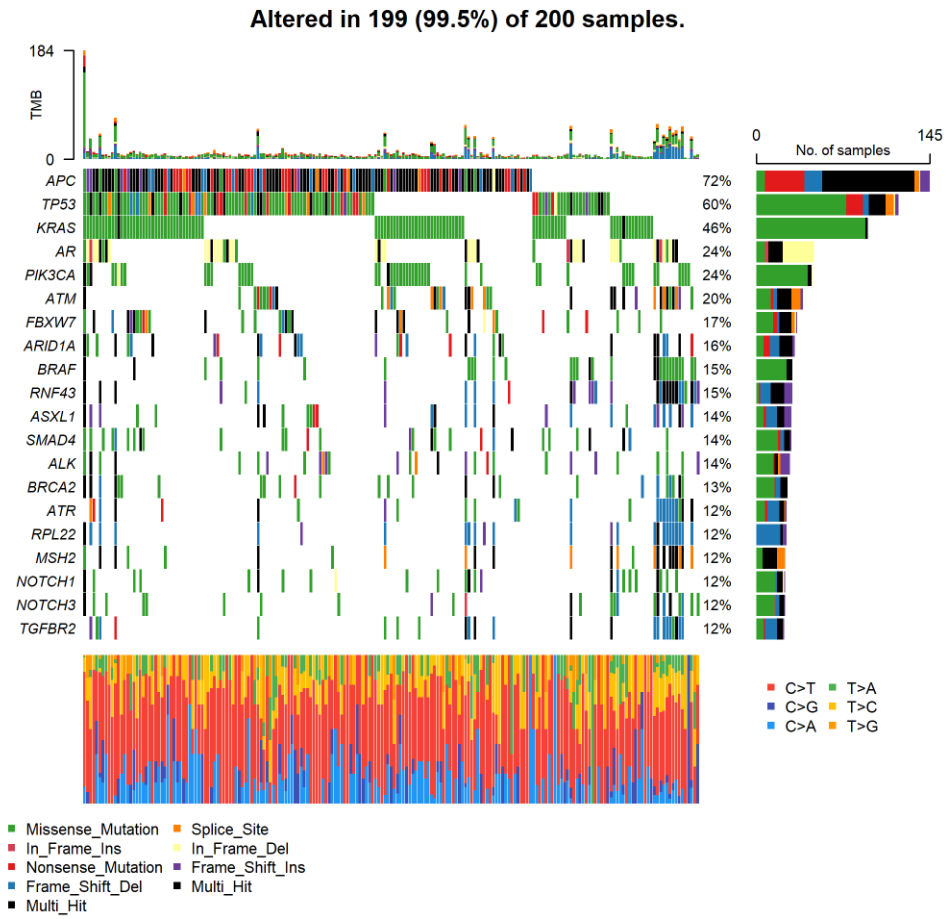

Figure 5.2 – Oncoplot for mutational cohort. *Top bar shows tumour burden. Right bar shows the number of altered samples for each gene. Bottom bar shows transitions and transversions.*

Among the top 20 mutated, mutations were predominantly classed as missense mutations with an even distribution of frameshift deletions and frameshift insertions. The exception was APC which had few missense mutations and consisted primarily of nonsense mutations and frameshift deletions. Androgen receptor mutations were primarily classed as in frame deletions and was the only representative of this variant class. Variants were largely single nucleotide polymorphisms with a sizeable contribution of deletions. Single nucleotide variants were primarily transitions from cytosine to thymine.

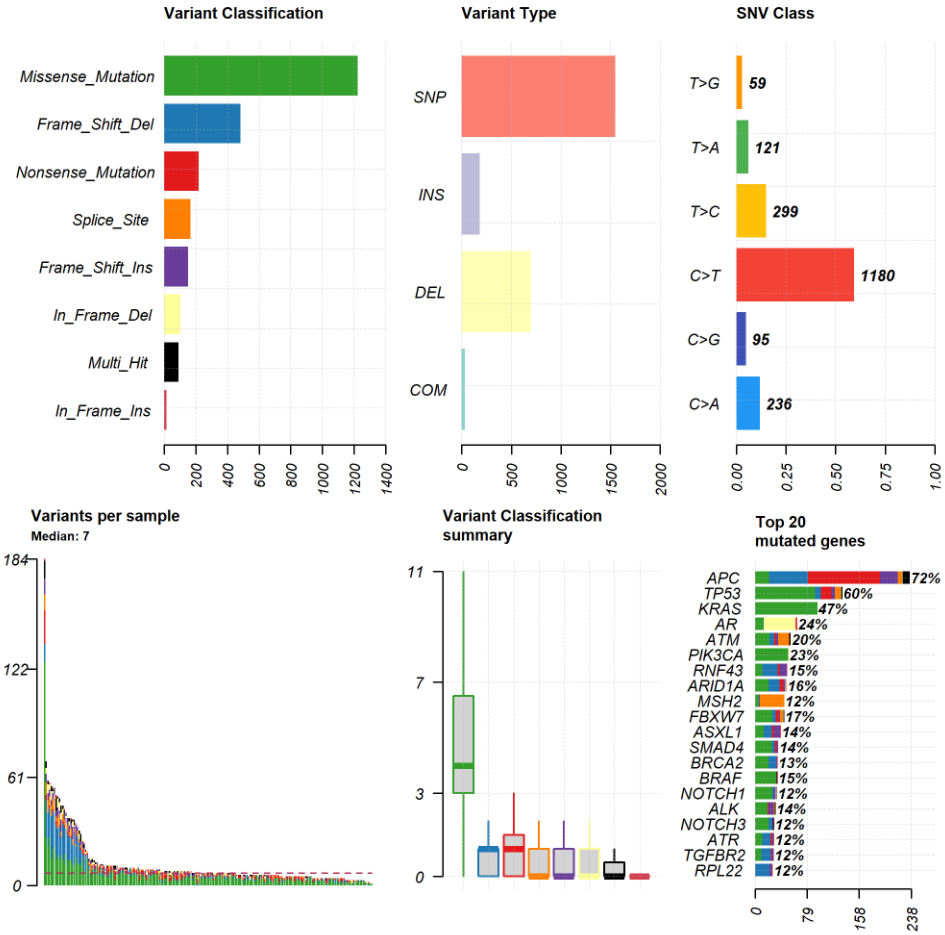

Figure 5.3 – Summary of mutational cohort. *Summary data including variant classifications, variant types, SNV classes, variant counts and top 20 mutated genes.*

5.3 Mutations associated with lymphocyte density and prognosis

5.3.1 Mutations associated with γδ T cells in the adjacent normal tissue

To understand if there was a genetic profile representative of lymphocyte density, mutational analysis was conducted to determine differentially mutated genes between those classed as low or high, previously determined via immunohistochemistry, for γδ T cells or CD8 T cells. For each gene in the panel, a contingency table was formed between these groups and wildtype/mutant status and a Fisher's test applied to produce an odds ratio and associated p value.

A high density of γδ T cells was associated with mutations in the endonuclease *ASTE1* and the solute transporter *SLC23A2* (Figure 5.4A), which showed significant co-occurrence (Figure 5.4B-D). *ASTE1* has previously been reported to be a key frameshift mutation in the generation of neopeptides, contributing to immune infiltration ($CD3^+$ cells) in MSI CRC cases [44, 45]. A low density of γδ T cells was not associated with mutations in any genes (Figure 5.4A, Table 5.2).

Table 5.2 – Mutated genes associated with γδ T cell density in the adjacent normal tissue. *Association between mutated genes and lymphocyte density is determined by performing a Fisher's test on a 2x2 contingency table consisting of WT/mutant and lymphocyte low/high, with the low group used as a reference for the odds ratio. Genes are highlighted if the odds ratio is > 2 or < 0.5, and the associated p value is < 0.05.*

Mutant Gene	P Value	OR	OR Low	OR High	FDR
ASTE1	0.010	11.96	1.50	549.36	0.677
SLC23A2	0.040	5.04	0.90	52.20	1.000

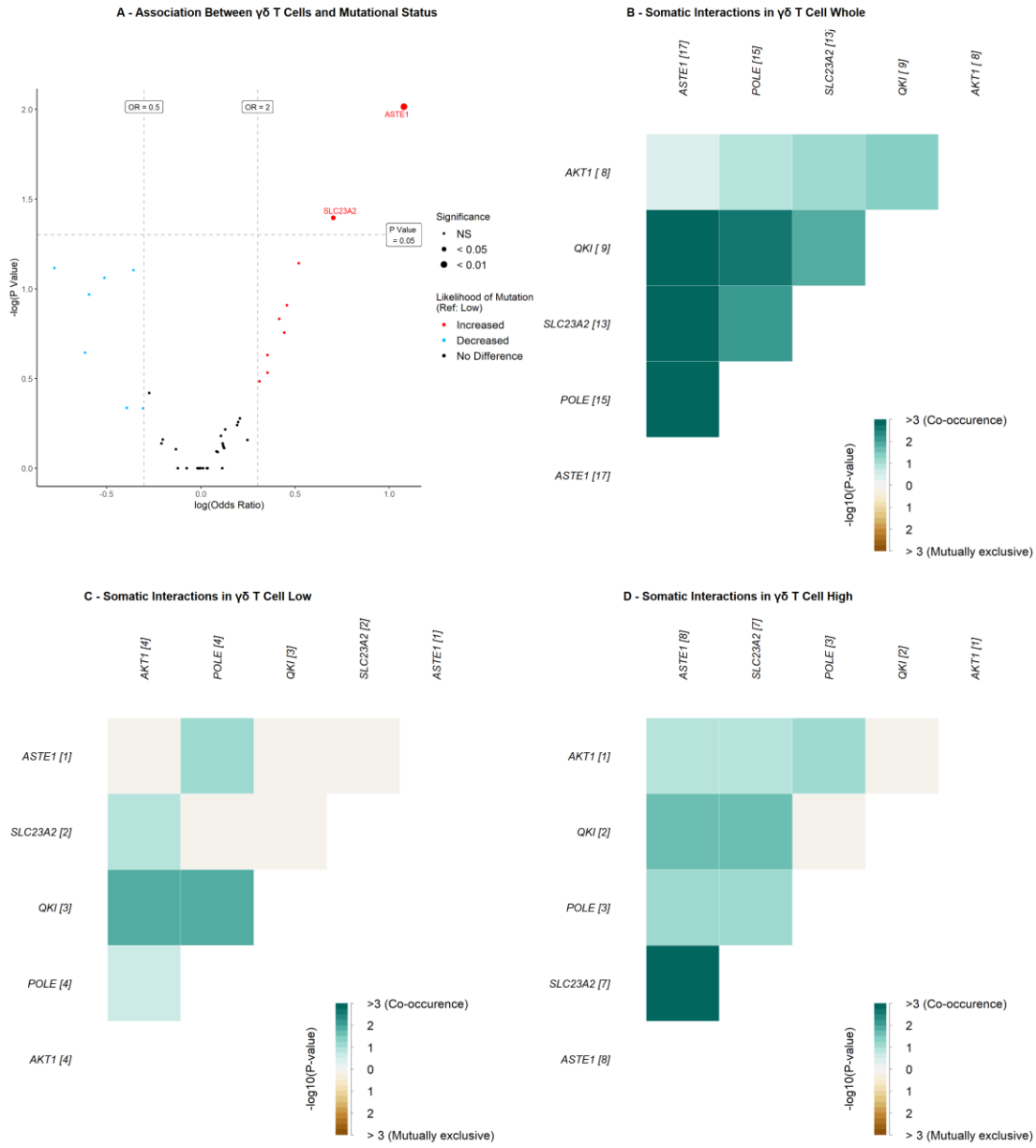

Figure 5.4 – Single mutations, and their somatic interactions, associated with γδ T cell density in the adjacent normal tissue. *A – Single mutated genes associated with patients classed as low or high for γδ T cells in the adjacent normal tissue. B – Somatic interactions for γδ high cases. C – Somatic interactions for γδ low cases. D – Somatic interactions for the whole cohort.The number of altered samples for each gene is denoted in square brackets. Association between mutated genes and lymphocyte density is determined by performing a Fisher's test on a 2x2 contingency table consisting of WT/mutant and lymphocyte low/high, with the low group used as a reference for the odds ratio. Genes are highlighted if the odds ratio is > 2 or < 0.5, and the associated p value is < 0.05.*

The variant classification and location of key mutations were analysed using lollipop plots to reveal any specific mutations associated with lymphocyte density. There was no difference in the classification of mutations in *ASTE1* and *SCL23A2* between γδ T cell low and high cases (Figure 5.5).

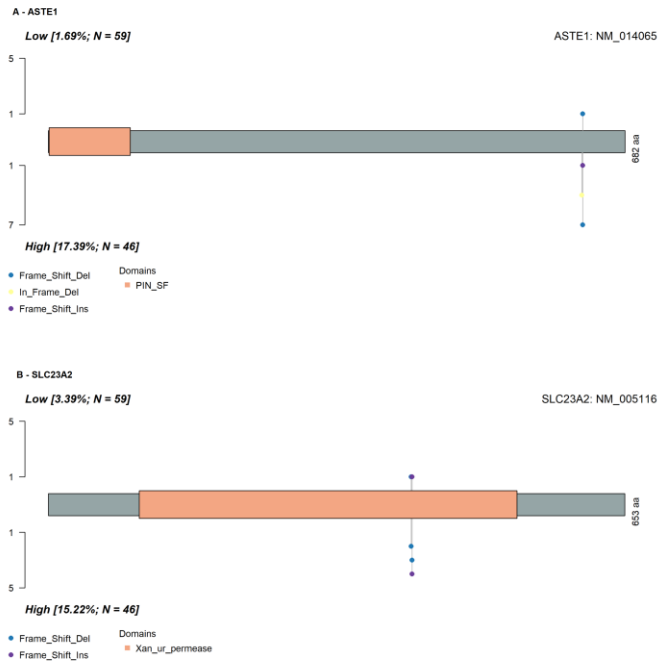

Figure 5.5 – Location and variant classification of mutations associated with γδ T cell density in the adjacent normal tissue. *A – Lollipop plot for ASTE1.* B *– Lollipop plot for SLC23A2. % in square brackets indicates the % of cases with the mutation. Y axis indicates the sum of occurrences of a particular mutation.*

As there are known associations between some mutations and MMR deficiency and MSI, associations between mutation status in these genes and MMR status was analysed using a chi squared test and mosaic plots. In this cohort, almost all cases with a mutation in *ASTE1* are MMR deficient (Figure 5.6A). However, previous data did not show a difference in lymphocyte density between MMR deficient and MMR proficient cases (Figure 3.16), and only a third of cases that were MMR deficient had a mutation in *ASTE1* (Figure 5.6B). This would suggest that being MMR deficient is not enough to associate with high lymphocyte density but that when these additional mutations (such as *ASTE1*) occur in these cases, high lymphocyte density is significantly more likely.

Table 5.3 – Contingency table of ASTE1 mutation status and MMR status for chi squared test.

	Mutant	Wildtype
Deficient	16	30
Proficient	1	152

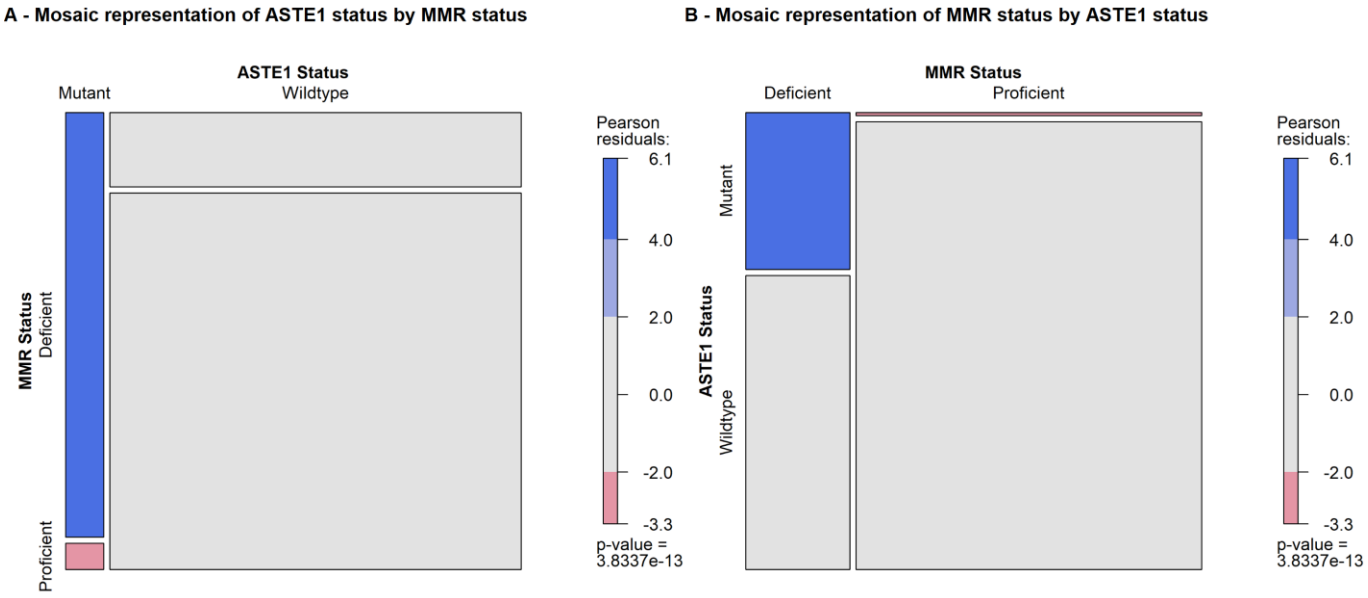

Figure 5.6 – Mosaic plot of contingency table for ASTE1 mutation status and MMR status. *A – Mosaic representation of ASTE1 status by MMR status. B – Mosaic representation of MMR status by ASTE1 status. X axis denotes mutation status of the ASTE1 gene. Y axis denotes MMR deficiency status.*

MMR status associated with CSS and RFS, with MMR deficient cases having a favourable prognosis (Figure 5.7A/D). This contrasts with the unfavourable prognostic effect of the high γδ T cell density with which these mutations are associated, and again this is likely due to MMR deficiency only being a factor in lymphocyte density when these mutations do occur.

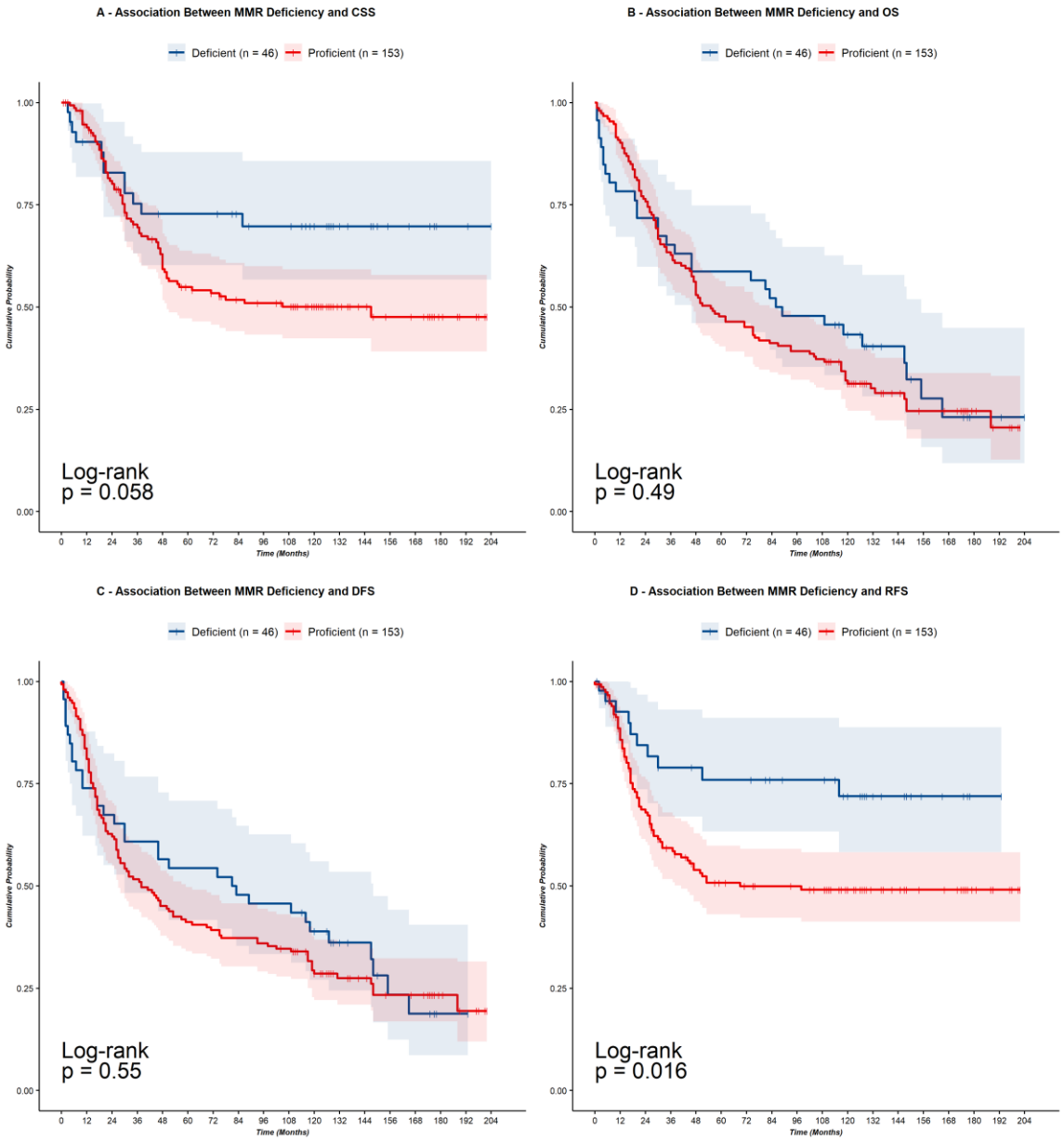

Figure 5.7 – Associations between MMR status and survival. *A – Time to event analysis for MMR deficient vs MMR proficient cases, in the context of CSS. B – Time to event analysis for MMR deficient vs MMR proficient cases, in the context of OS. C – Time to event analysis for MMR deficient vs MMR proficient cases, in the context of DFS. D – Time to event analysis for MMR deficient vs MMR proficient cases, in the context of RFS. Patients deemed MMR deficient and MMR proficient are shaded blue and red, respectively.*

To further link mutations with lymphocyte density, the prognostic effect of key mutations were investigated to determine if they shared a prognostic effect with the lymphocyte classification (low or high) with which they are associated. None of the genes in which mutations were associated with a high γδ T cell density demonstrated a prognostic effect (Figure 5.8A-D and Figure 5.9A-B).

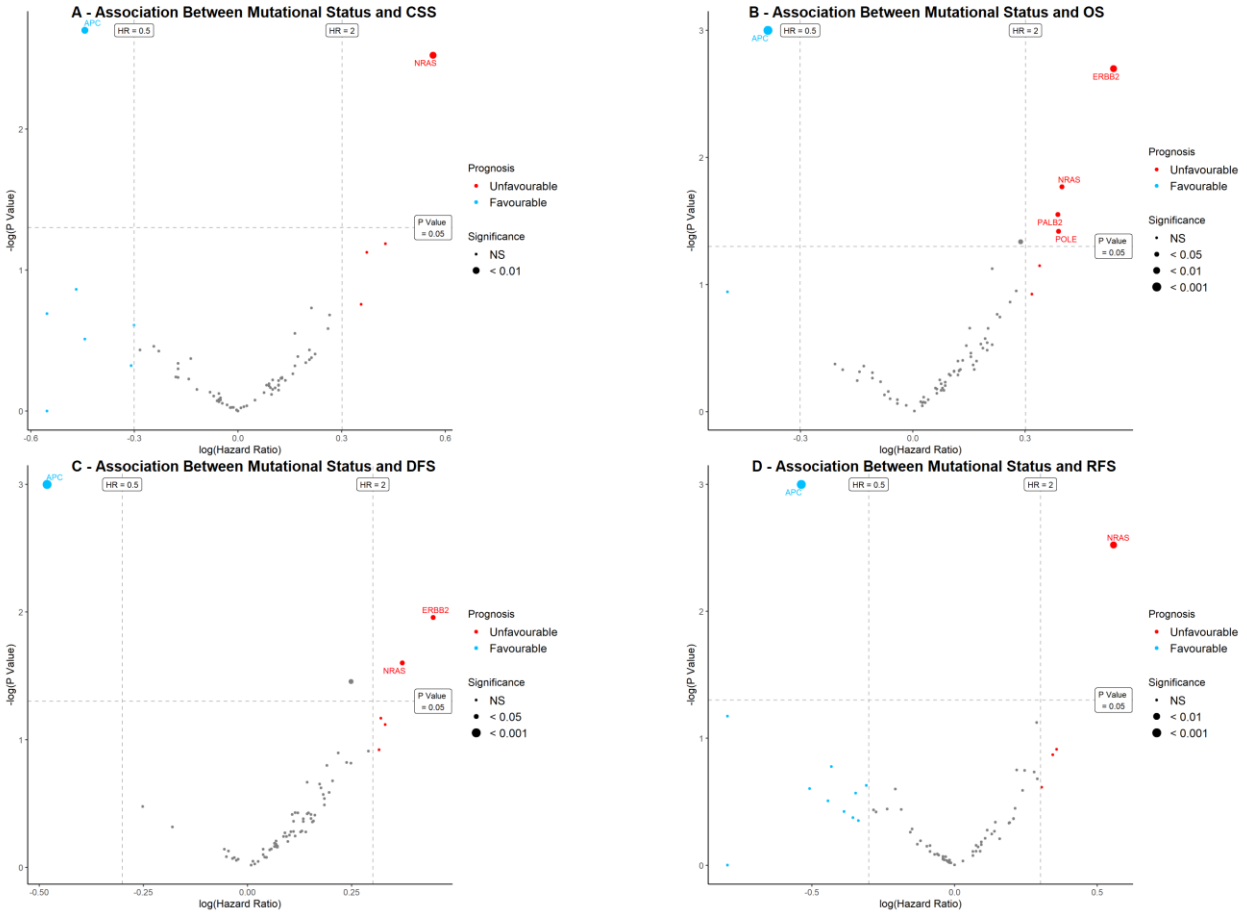

Figure 5.8 – Single mutated genes associated with survival outcomes in the adjacent normal tissue γδ population. *A – Single mutated genes associated with cancer-specific survival. B - Single mutated genes associated with overall survival. C - Single mutated genes associated with disease-free survival. D - Single mutated genes associated with recurrence-free survival. Association between mutated genes and survival is determined by building a univariate cox regression model, with the low group used as a reference for the hazard ratio. Genes are highlighted if the hazard ratio is > 2 or < 0.5, and the associated p value is < 0.05. Genes in the upper right segment are statistically significant and associated with an unfavourable prognosis (red) whilst genes in the upper left are statistically significant and associated with a favourable prognosis (blue).*

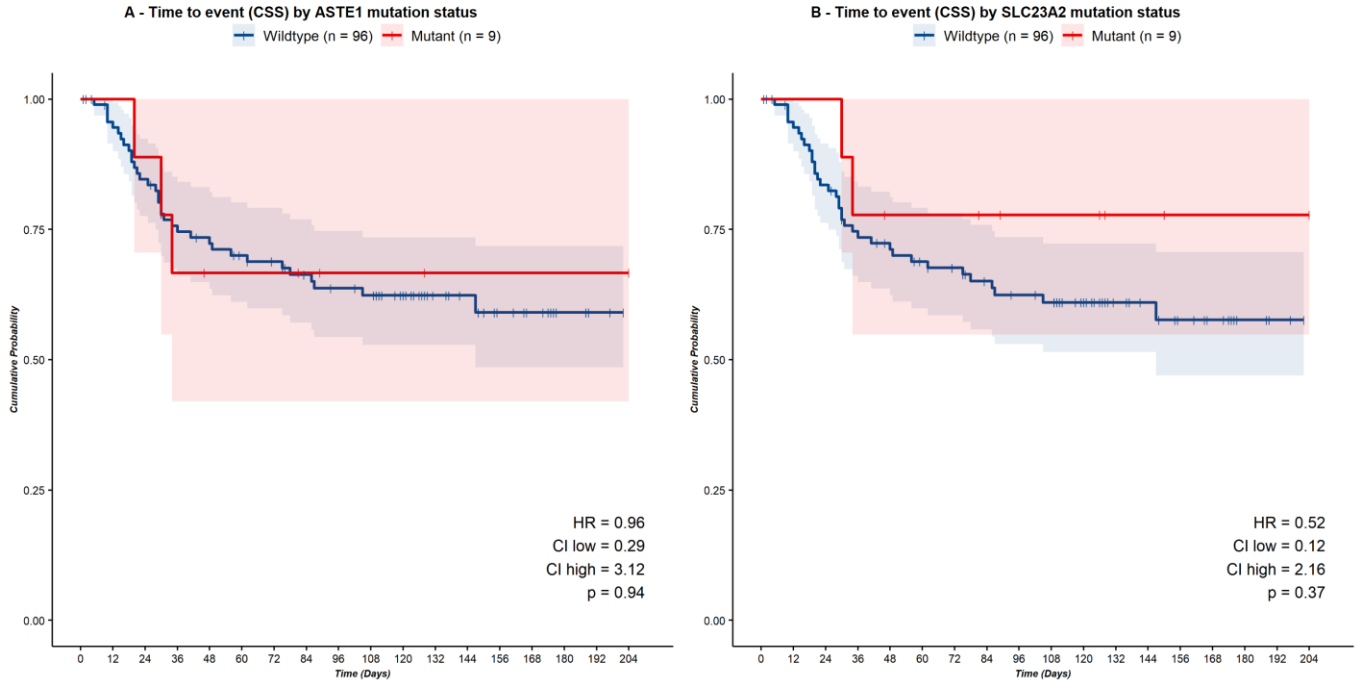

Figure 5.9 – Time to event (CSS) analysis in the adjacent normal γδ population. *A – Time to event analysis for ASTE1. B – Time to event analysis for SLC23A2.HR is determined with the Cox proportional hazards model. Mutant group is coloured red. Wildtype group is coloured blue. Shaded areas represent confidence intervals.*

5.3.2 Mutations associated with γδ T cells in the primary tumour tissue

A high density of γδ T cells was not associated with mutations in any genes (Figure 5.10A). This is likely due to the disparity in the number of cases available for γδ low and high in the tumour tissue, just 7 and 8 cases present in the γδ low group in the primary tumour tissue and stroma, respectively. A low density of γδ T cells was not associated with mutations in any genes (Figure 5.10A).

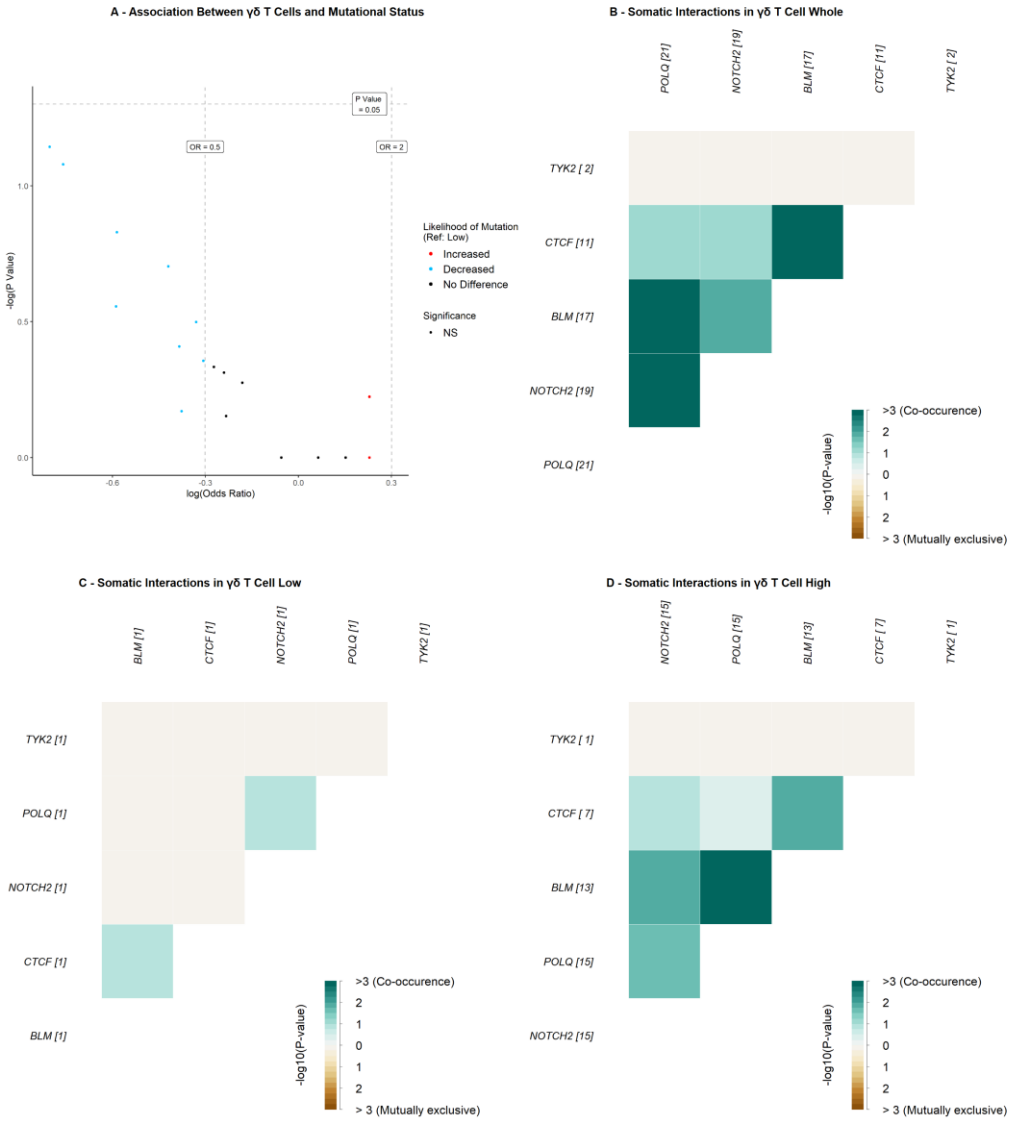

Figure 5.10 – Single mutations, and their somatic interactions, associated with γδ T cell density in the primary tumour tissue. *A – Single mutated genes associated with patients classed as low or high for γδ T cells in the primary tumour tissue. B – Somatic interactions for γδ high cases. C – Somatic interactions for γδ low cases. D – Somatic interactions for the whole cohort. The number of altered samples for each gene is denoted in square brackets. Association between mutated genes and lymphocyte density is determined by performing a Fisher's test on a 2x2 contingency table consisting of WT/mutant and lymphocyte low/high, with the low group used as a reference for the odds ratio. Genes are highlighted if the odds ratio is > 2 or < 0.5, and the associated p value is < 0.05.*

5.3.3 Mutations associated with CD8 T cells in the adjacent normal tissue

A high density of CD8 T cells was associated with mutations in genes including *AR*, *BRAF* [61, 279]and *TTK* (Figure 5.11A and Table 5.4). *BRAF*, acting downstream of the RAS proteins, codes for a protein that activates *MEK/MAPK* to induce transcription. *BRAF* inhibition results in a greater infiltration of T cells in melanoma [280, 281]. Mutations are associated with right sided disease and are predominantly V600E mutations which result in constitutively active BRAF [282] and are thus oncogenic. *AR* encodes the androgen receptor, a ligand-activated transcription factor, which is expressed on T cells [283] and its inhibition induces a more cytotoxic cytokine profile from $CD8^+$ T cells [284]. Mutations in *AR* associated with cancer are predominantly gain-of-function mutations [285], potentially exacerbating their immunosuppressive function [286]. *PIK3R1* is involved in insulin signalling [287] and is a component of PI3K, key to a signalling pathway that has demonstrated cross regulation with that of AR [288] (although no co-occurrence between these mutations is seen in this data (Figure 5.11B-D)), and its inhibition has been linked with a higher density of $CD8^+$ T cells in CRC [289]. Mutations in *AR* and *BRAF* co-occurred (Figure 5.11B-D) and data in melanoma shows that blocking the AR can improve response to BRAF inhibitors [286], and given that they are consistent across compartments within the tissue, this would strengthen the possibility that they interact. *ATM* is a serine/threonine protein kinase which activates DNA damage checkpoint proteins [290], and *POLQ* is a polymerase that functions within double strand break repair [291] – these mutations show no co-occurrence however (Figure 5.11B-D). *SETD2* is a histone methyltransferase which methylates transcription promoting histone modification H3K3me3 to the repressive H3K4me3, the loss of which results in *DVL2* mediated promotion of Wnt signalling and tumourigenesis [292]. Mutations in *TTK*, *AR*, *ATM* and *BRAF* were co-occurring (Figure 5.11B-D), raising the possibility that these mutations are a core set of mutations contributing to CD8 T cell density in the adjacent normal tissue.

Table 5.4 – Mutated genes associated with CD8 T cell density in the adjacent normal tissue. *Association between mutated genes and lymphocyte density is determined by performing a Fisher's test on a 2x2 contingency table consisting of WT/mutant and lymphocyte low/high, with the low group used as a reference for the odds ratio. Genes are highlighted if the odds ratio is > 2 or < 0.5, and the associated p value is < 0.05.*

Mutant Gene	P Value	OR	OR Low	OR High	FDR
AR	0.002	5.08	1.67	15.87	0.115
BRAF	0.004	4.76	1.47	15.39	0.146
PIK3R1	0.009	10.82	1.43	128.52	0.220
POLQ	0.012	5.04	1.22	20.41	0.220
TP53	0.024	0.31	0.10	0.89	0.317
ATM	0.026	3.60	1.09	11.56	0.317
SETD2	0.033	5.36	0.91	31.78	0.321
TTK	0.038	3.95	0.88	16.66	0.321

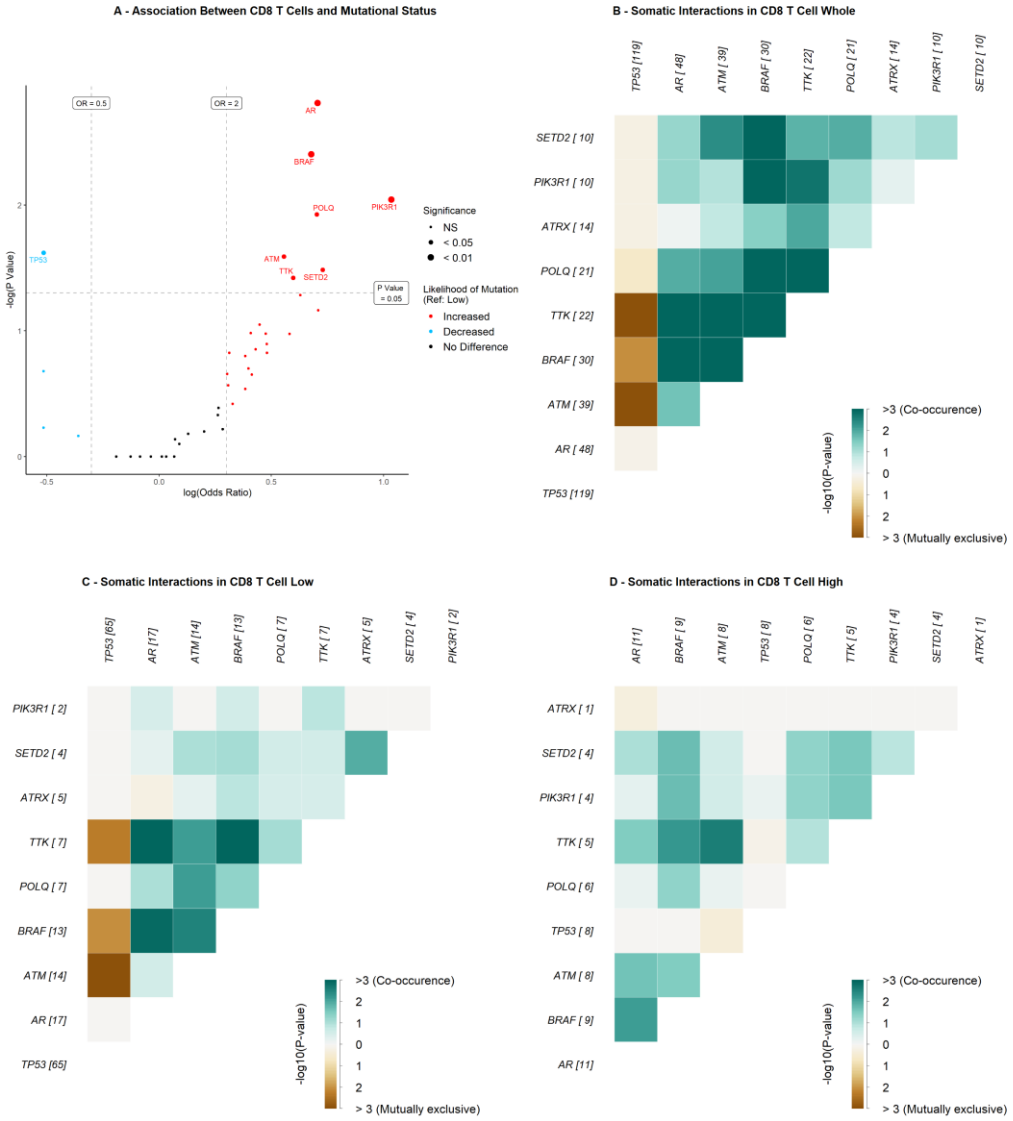

Figure 5.11 – Single mutations, and their somatic interactions, associated with CD8 T cell density in the adjacent normal tissue. *A – Single mutated genes associated with patients classed as low or high for CD8 T cells in the adjacent normal tissue. B – Somatic interactions for CD8 high cases. C – Somatic interactions for CD8 low cases. D – Somatic interactions for the whole cohort. The number of altered samples for each gene is denoted in square brackets. Association between mutated genes and lymphocyte density is determined by performing a Fisher's test on a 2x2 contingency table consisting of WT/mutant and lymphocyte low/high, with the low group used as a reference for the odds ratio. Genes are highlighted if the odds ratio is > 2 or < 0.5, and the associated p value is < 0.05.*

There was no difference in the classification of mutations between CD8 T cell low and high cases (Figure 5.12).

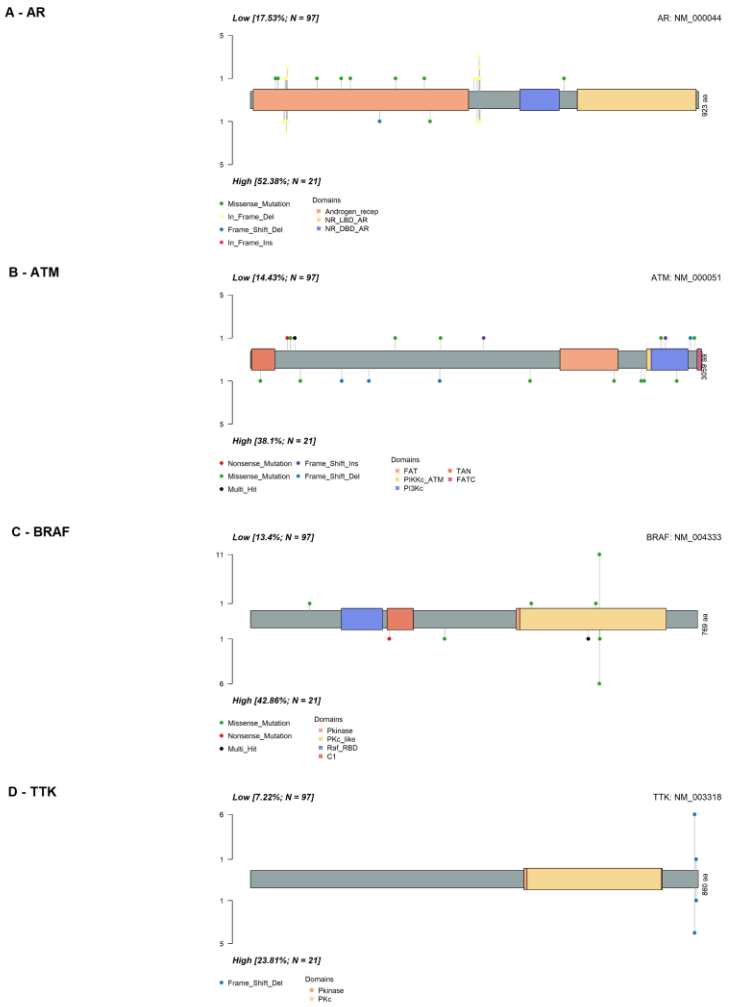

Figure 5.12 – Location and variant classification of mutations associated with CD8 T cell density in the adjacent normal tissue. *A – Lollipop plot for AR.* B *– Lollipop plot for ATM. C – Lollipop plot for BRAF. D – Lollipop plot for TTK. % in square brackets indicates the % of cases with the mutation. Y axis indicates the sum of occurrences of a particular mutation.*

TTK is a common source of frameshift mutations in MSI CRC which lead to neoantigens and increased immune infiltration [46]. In this cohort, mutations in *TTK* correlate with MMR status (Figure 5.13A and Table 5.5) with all cases with a mutation in *TTK* being MMR deficient whilst of those cases deficient in MMR, only half carried a mutation in *TTK* (Figure 5.13B). As previously seen in *ASTE1*, this would suggest that it is not MMR deficiency itself that correlates with lymphocyte density, but these specific mutations occurring in the microsatellites of cases that are MMR deficient. It is interesting that γδ T cells (*ASTE1*) and CD8 T cells (*TTK*) in the adjacent normal tissue feature different MSI related frameshift mutations, raising the possibility the specific frameshift mutations may drive different immune subsets, although the significance of *ASTE1* mutations in $CD8^+$ T cell infiltration specifically would suggest that this is unlikely [45].

Table 5.5 – Contingency table of TTK mutation status and MMR status for chi squared test.

	Mutant	**Wildtype**
Deficient	22	24
Proficient	0	153

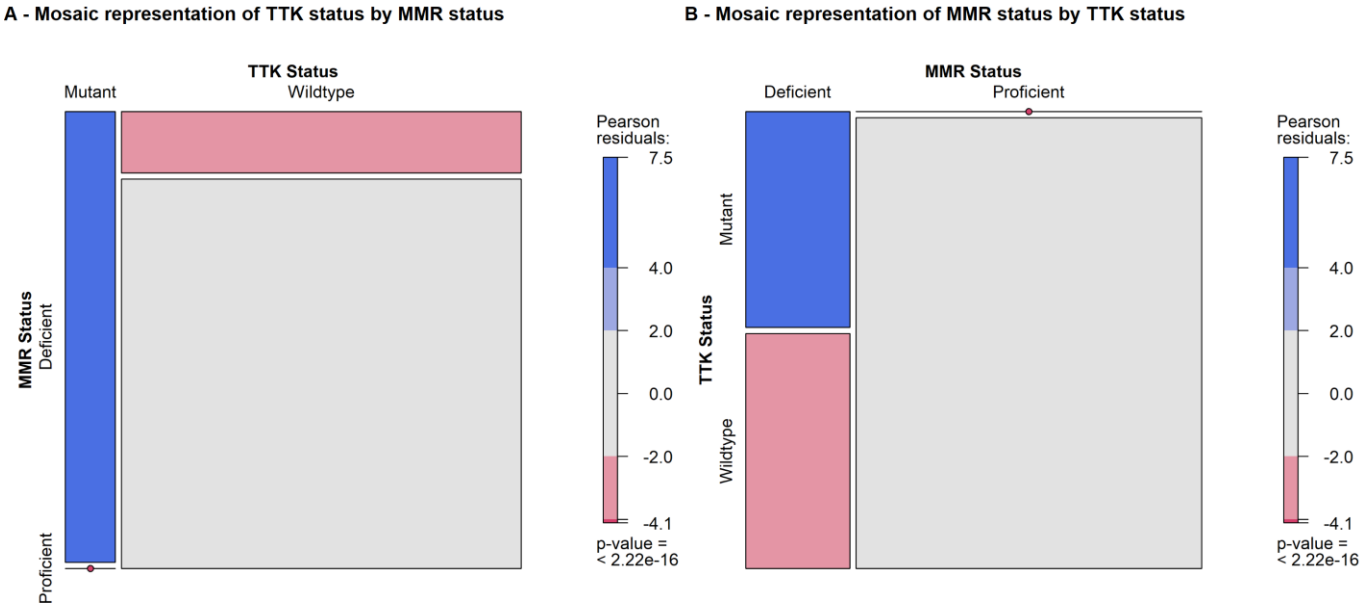

Figure 5.13 – Mosaic plot of contingency table for TTK mutation status and MMR status. *A – Mosaic representation of TTK status by MMR status. B – Mosaic representation of MMR status by TTK status. X axis denotes mutation status of the TTK gene. Y axis denotes MMR deficiency status.*

None of the genes in which mutations were associated with a high CD8 T cell density demonstrated a prognostic effect (Figure 5.14A-D and Figure 5.15A A-D). Of the mutated genes associated with low CD8 T cell density, *APC* was associated with a favourable prognosis across all survival outcomes (Figure 5.14A A-D, Figure 5.14A A-D and Figure 5.14A A-D).

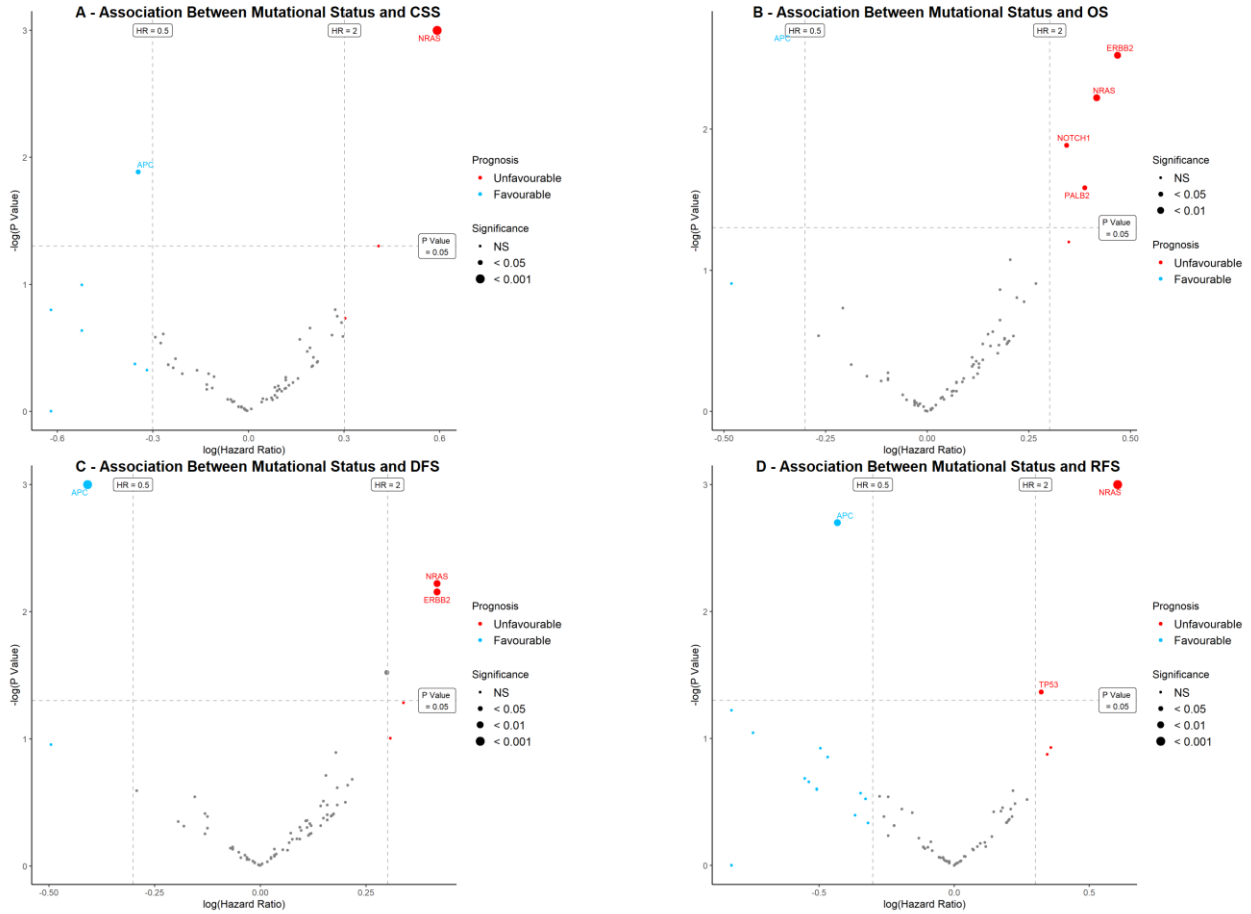

Figure 5.14 – Single mutated genes associated with survival outcomes in the adjacent normal tissue CD8 population. *A – Single mutated genes associated with cancer-specific survival. B - Single mutated genes associated with overall survival. C - Single mutated genes associated with disease-free survival. D - Single mutated genes associated with recurrence-free survival. Association between mutated genes and survival is determined by building a univariate cox regression model, with the low group used as a reference for the hazard ratio. Genes are highlighted if the hazard ratio is > 2 or < 0.5, and the associated p value is < 0.05. Genes in the upper right segment are statistically significant and associated with an unfavourable prognosis (red) whilst genes in the upper left are statistically significant and associated with a favourable prognosis (blue).*

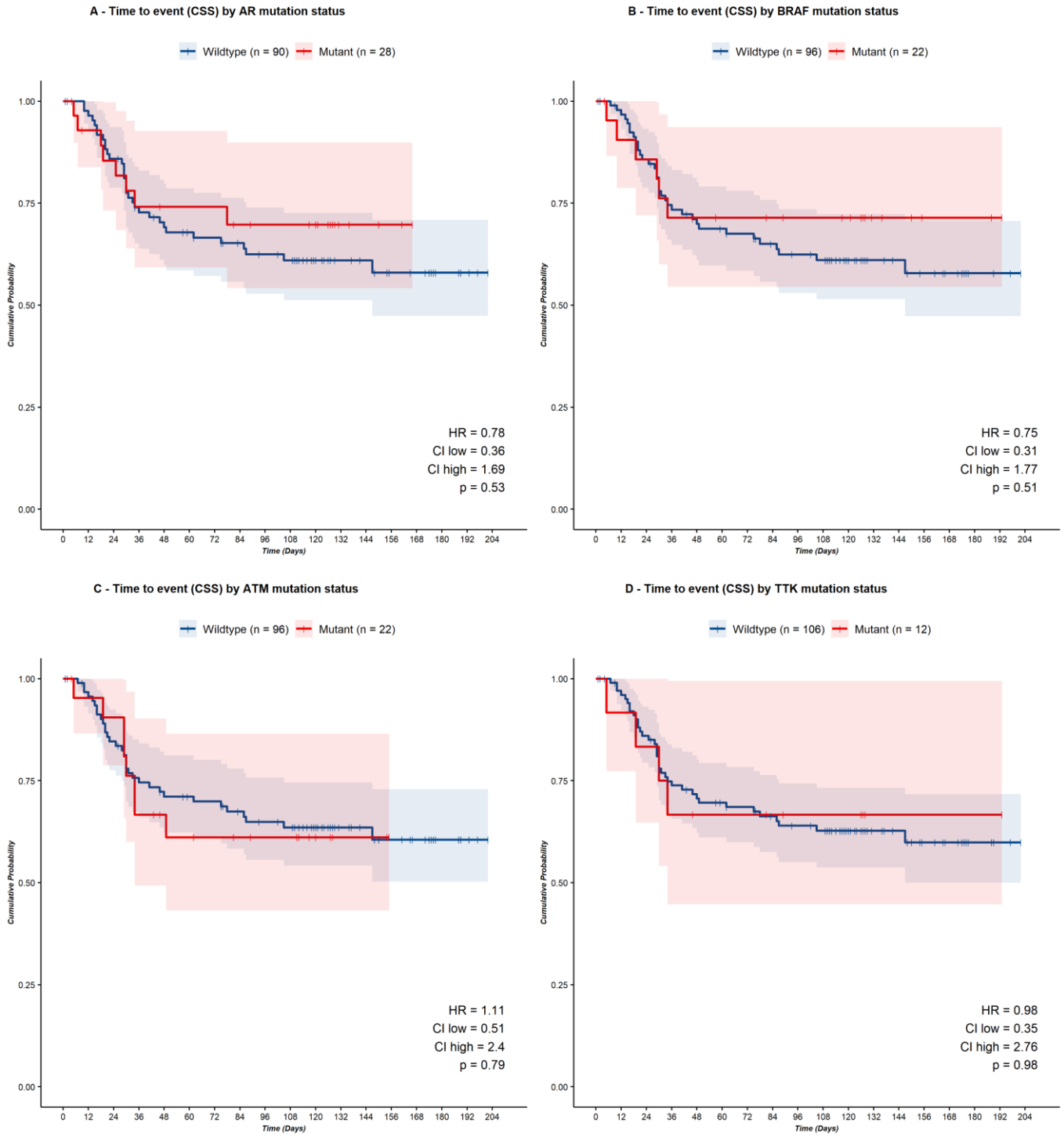

Figure 5.15 – Time to event (CSS) analysis in the adjacent normal CD8 population. *A – Time to event analysis for AR. B – Time to event analysis for BRAF. C – Time to event analysis for ATM. D – Time to event analysis for TTK. HR is determined with the Cox proportional hazards model. Mutant group is coloured red. Wildtype group is coloured blue. Shaded areas represent confidence intervals.*

5.3.4 Mutations associated with CD8 T cells in the primary tumour tissue

In the primary tumour tissue, as in the adjacent normal tissue, cases high for CD8 T cells were more likely to have mutations in multiple genes (Figure 5.16 and Table 5.6) including *BRAF* and *AR* but lacked the previously observed co-occurrence (Figure 5.16B-D). This group also featured both *ASTE1* and *TTK* mutations which were previously noted in the adjacent normal tissue population for cases high for γδ T cells and CD8 T cells, respectively. Mutations in these genes occur frequently in colorectal MSI cases, as do mutations in *RPL22* and *RNF43* [293], and survival analysis indicates that they may associate with a favourable prognosis although due to the number of mutant cases the analysis is likely underpowered (Figure 5.19C/D). MSI has a demonstrated favourable effect on overall and recurrence-free survival [258, 294]. *RPL22* encodes a cytoplasmic ribosomal protein and its ablation in mice inhibits αβ T cell development whilst sparing γδ T cells [293]. *RNF43* encodes a protein which negatively regulates Wnt signalling by degrading the Frizzled receptor, and mutations in *RNF43* are believed to prevent the required phosphorylation of the RNF43 protein, thus encouraging Wnt signalling [295].

Also present is *SLC23A2*, noted in the adjacent normal tissue γδ high group. *IDH1* is critical in cellular metabolism with roles in both the TCA cycle and β-oxidation of fatty acids and mutations alter metabolism [296, 297]. Mutations in *IDH1* have been suggested to be more common in *BRAF* mutant p.V600E cases compared to *BRAF* mutant non p.V600E cases in CRC, although it should be noted the *IDH1* groups is very small [298]. *DNMT3A* is also more likely to be mutated in cases classed as high for CD8 T cells in the primary tumour, which downregulates *DAB2IP* to activate MEK/ERK signalling and drive cell growth in CRC [299] and has a similar effect on the androgen receptor in prostate cancer [300].

MTOR encodes the mTOR protein which forms part of the mTOR complexes to regulate cellular survival and interacts with PI3K/Akt signalling [301, 302] – these mutations show no co-occurrence. In addition, mutations in *MTOR* are higher in MSI CRC [303]. There were additional mutations in chromatin remodelling genes (*CTCF*, *PBRM1*), DNA damage response genes (*RAD50* and *BLM*).

Table 5.6 – Mutated genes associated with CD8 T cell density in the primary tumour tissue. *Association between mutated genes and lymphocyte density is determined by performing a Fisher's test on a 2x2 contingency table consisting of WT/mutant and lymphocyte low/high, with the low group used as a reference for the odds ratio. Genes are highlighted if the odds ratio is > 2 or < 0.5, and the associated p value is < 0.05.*

Mutant Gene	P Value	OR	OR Low	OR High	FDR
BRAF	<0.001	7.07	2.25	22.03	0.017
TTK	<0.001	9.22	2.46	34.38	0.017
IDH1	0.004	11.90	1.85	88.14	0.085
ASTE1	0.004	7.80	1.69	34.77	0.085
CTCF	0.007	8.91	1.52	52.59	0.125
SLC23A2	0.012	7.11	1.28	36.66	0.173
RAD50	0.018	5.90	1.11	27.90	0.174
AR	0.019	3.33	1.13	9.58	0.174
TP53	0.019	0.32	0.10	0.91	0.174
COBLL1	0.022	8.47	1.06	68.04	0.174
EGFR	0.022	8.47	1.06	68.04	0.174
SMO	0.027	5.03	0.98	22.36	0.192
RNF43	0.033	3.31	0.93	10.66	0.200
DNMT3A	0.035	6.34	0.86	40.88	0.200
PBRM1	0.035	6.34	0.86	40.88	0.200
BLM	0.037	4.38	0.87	18.60	0.200
RPL22	0.041	3.48	0.86	12.23	0.211
MTOR	0.049	3.88	0.79	15.87	0.236

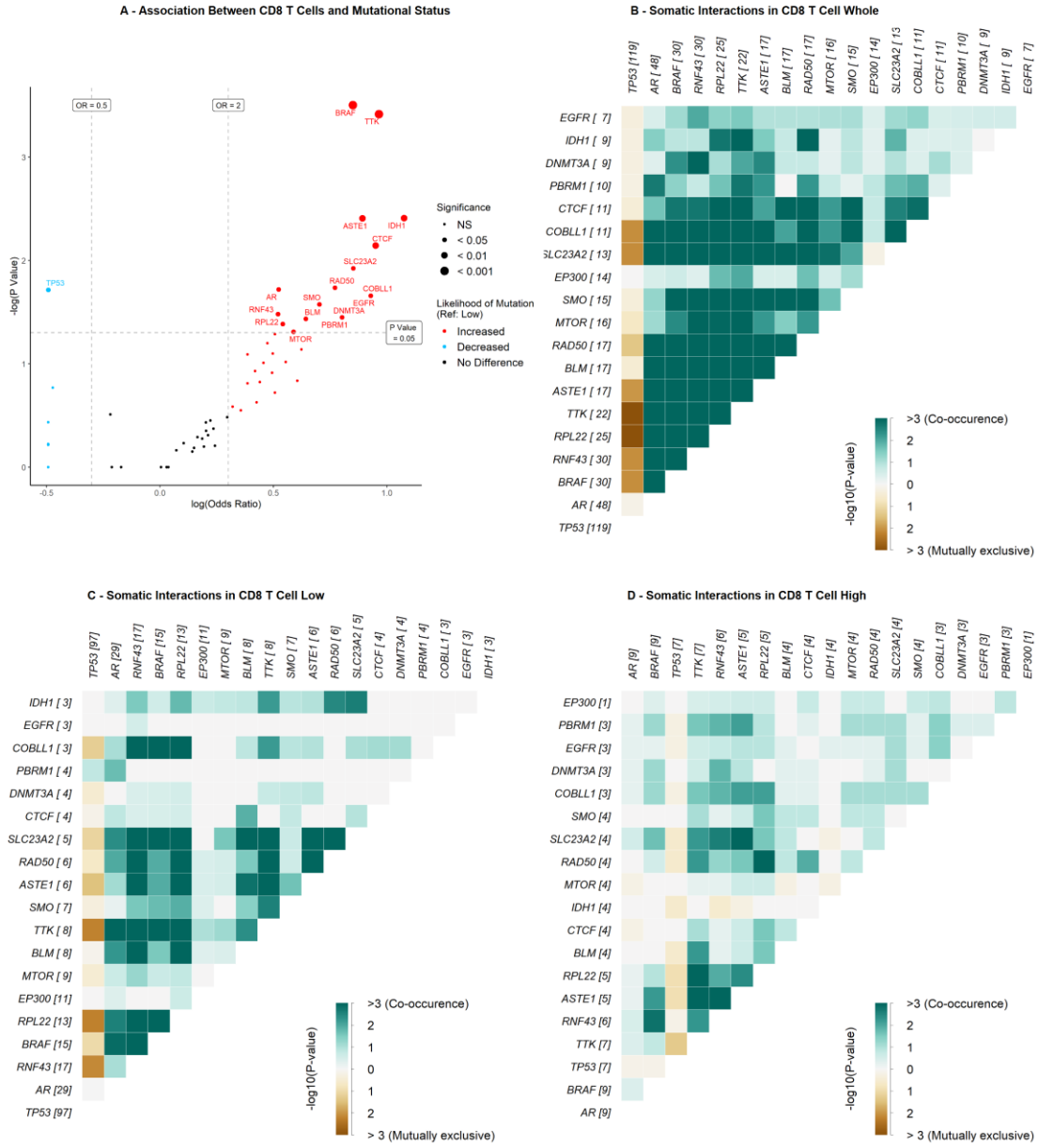

Figure 5.16 – Single mutations, and their somatic interactions, associated with CD8 T cell density in the primary tumour tissue. *A – Single mutated genes associated with patients classed as low or high for CD8 T cells in the primary tumour tissue. B – Somatic interactions for CD8 high cases. C – Somatic interactions for CD8 low cases. D – Somatic interactions for the whole cohort. The number of altered samples for each gene is denoted in square brackets. Association between mutated genes and lymphocyte density is determined by performing a Fisher's test on a 2x2 contingency table consisting of WT/mutant and lymphocyte low/high, with the low group used as a reference for the odds ratio. Genes are highlighted if the odds ratio > 2 or < 0.5, and the associated p value is < 0.05.*

Despite *MTOR* being associated with MSI in the literature, in this cohort mutations in *MTOR* only weakly correlate with MMR status with *MTOR* mutant cases being equally likely to be MMR deficient or proficient (Figure 5.17A and Table 5.7). However, of those lacking a mutation in *MTOR*, the majority were MMR proficient (Figure 5.17B and Table 5.7), suggesting that the effect is like that seen in *ASTE1* and *TTK* but much weaker.

Table 5.7 – Contingency table of MTOR mutation status and MMR status for chi squared test.

	Mutant	**Wildtype**
Deficient	8	38
Proficient	8	145

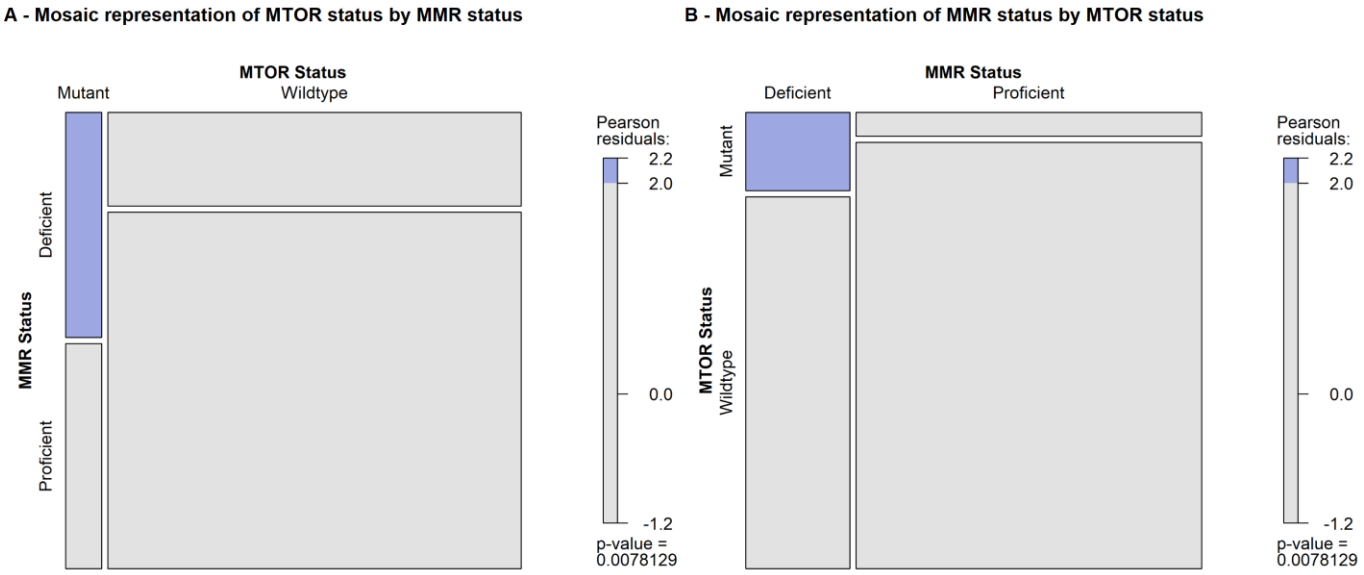

Figure 5.17 – Mosaic plot of contingency table for TTK mutation status and MMR status. *A – Mosaic representation of MTOR status by MMR status. B – Mosaic representation of MMR status by MTOR status. X axis denotes mutation status of the MTOR gene. Y axis denotes MMR deficiency status.*

None of the genes in which mutations were associated with a high CD8 T cell density demonstrated a prognostic effect for any survival outcome (Figure 5.18A-D and Figure 5.19A-D). Of the mutated genes associated with low CD8 T cell density, none were associated with a prognostic effect for any survival outcome (Figure 5.18A-D and Figure 5.19A-D).

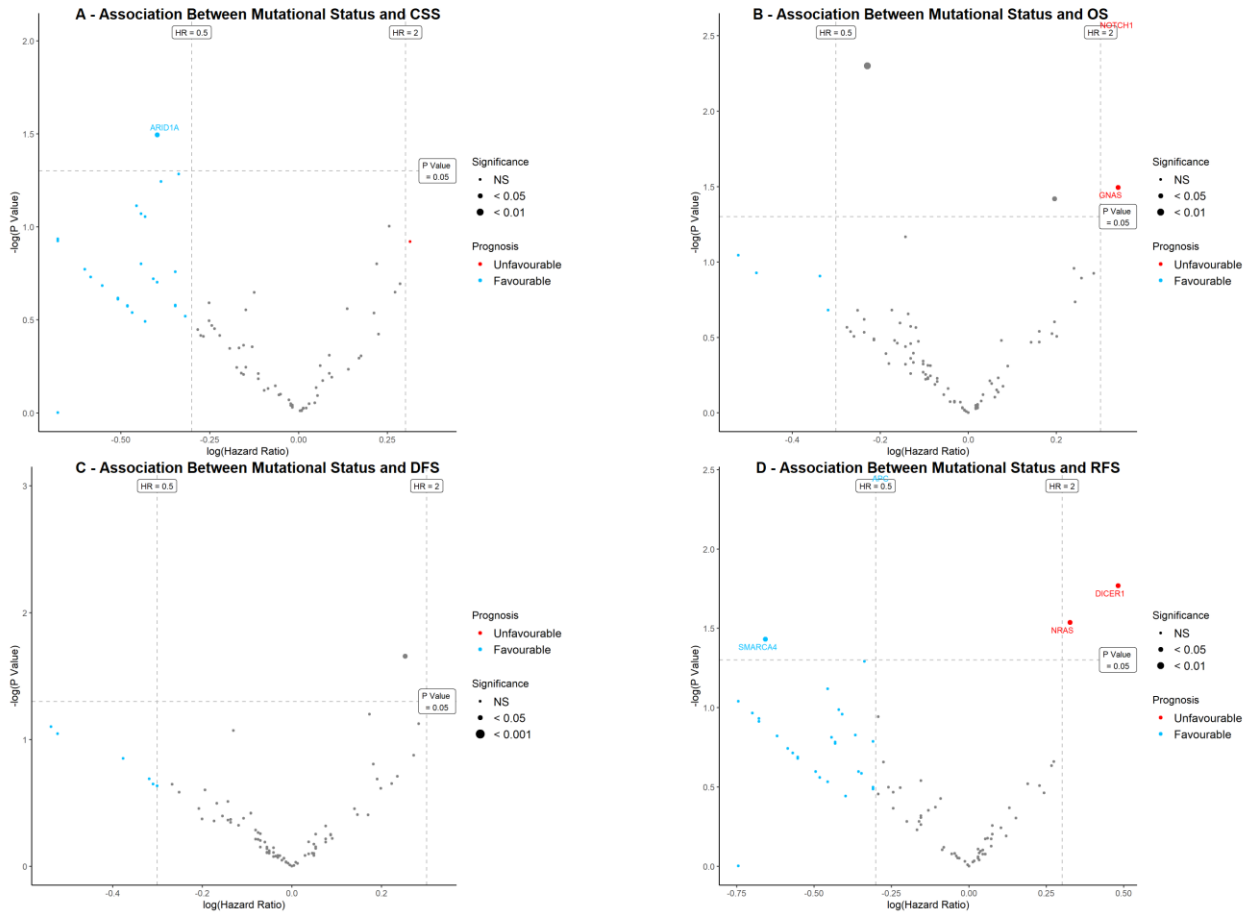

Figure 5.18 – Single mutated genes associated with survival outcomes in the primary tumour CD8 population. *A – Single mutated genes associated with cancer-specific survival. B - Single mutated genes associated with overall survival. C - Single mutated genes associated with disease-free survival. D - Single mutated genes associated with recurrence-free survival. Association between mutated genes and survival is determined by building a univariate cox regression model, with the low group used as a reference for the hazard ratio. Genes are highlighted if the hazard ratio is > 2 or < 0.5, and the associated p value is < 0.05. Genes in the upper right segment are statistically significant and associated with an unfavourable prognosis (red) whilst genes in the upper left are statistically significant and associated with a favourable prognosis (blue).*

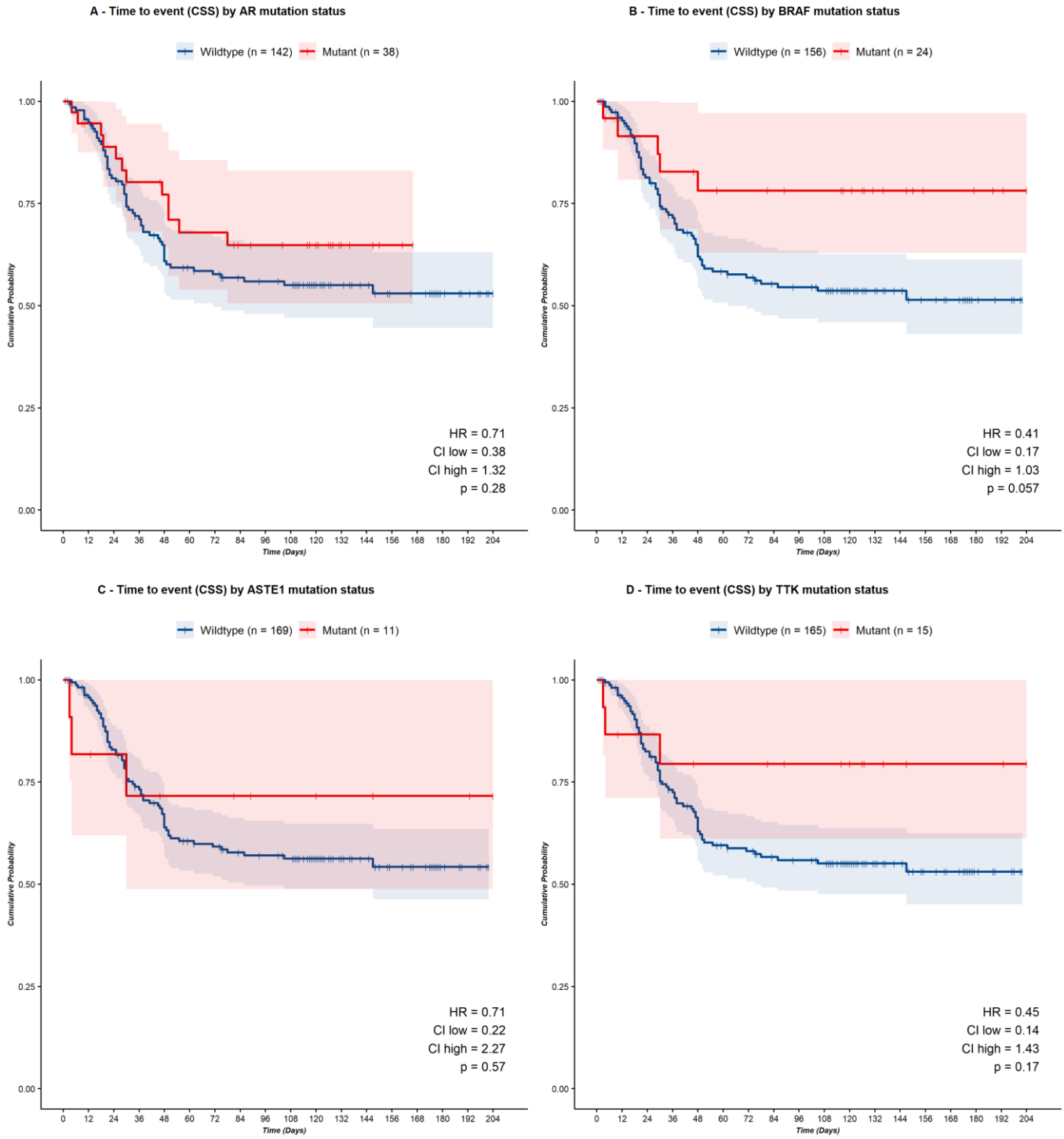

Figure 5.19 – Time to event (CSS) analysis in the primary tumour CD8 population. *A – Time to event analysis for AR. B – Time to event analysis for BRAF. C – Time to event analysis for ATM. D – Time to event analysis for TTK. HR is determined with the Cox proportional hazards model. Mutant group is coloured red. Wildtype group is coloured blue. Shaded areas represent confidence intervals.*

5.4 Discussion

As CRC develops from an adenoma it does so with a progression of key genetic aberrations; BRAF mutations, CIMP and MSI in the case of sessile serrated polyps and mutations in *APC, KRAS, TGFβ* and *TP53* in the case of the more frequent adenocarcinomas [48-50]. These key mutations are represented within this cohort with *APC (72%)*, *KRAS* (46%) and *TP53* (60%) being the most mutated genes, with 14% of cases also carrying a mutation in *BRAF* (Figure 5.2). Other mutated genes frequently featured in this cohort are also established mutations in CRC include *AR* at 24% [274, 304-306], *FBXW7* at 17% [307, 308], *ARID1A* at 16% [309-311] and *SMAD4* at 14% [312-314]. Thus, the Scotland cohort included in mutational analysis is representative of the current literature and reflects other colorectal cohorts. Across tissue compartments there were mutations in genes with demonstrated importance in MSI derived lymphocyte density [44-46], including *ASTE1* and *TTK*, suggesting that MSI may be an additional and potentially cooperative factor with alterations to the Wnt signalling pathway. However, this data did not show a difference in lymphocyte density between MMR deficient and MMR proficient cases (Figure 3.16 and Figure 3.23), but MMR deficiency was associated with a favourable CSS and RFS (Figure 5.7A/D). The mutations associated with lymphocyte density in MSI cases (*ASTE1* and *TTK*) occur in the microsatellite regions of the genes but being MMR deficient and developing MSI does not require these mutations to exist, so it may be that MMR deficiency alone does not lead to a greater lymphocyte density unless these specific mutations do occur. γδ T cells in the adjacent normal tissue were associated with *ASTE1* whilst *TTK* was associated with CD8 T cells in the same compartment, raising the question of whether the specific mutation is a factor in which T cell subsets are present at greater density. Mutations in both genes were enriched in cases high for CD8 T cells in the primary tumour however, so this is unlikely to be the case but cannot be discounted. *BRAF* is associated with right sided disease and MSI [279]. In this data *BRAF* is mutated in 15% of cases in the whole cohort but 28% of right sided cases, and *BRAF* status associates with MMR status in the whole cohort ($X^2 = 32.15$, $p = < 0.001$) and surprisingly to a lesser extent in right sided cases ($X^2 = 12.93$, $p = < 0.001$). In *BRAF* mutant and wildtype cases, CD8 T cells have been found to be higher in MSI cases compared to MSS cases [315]. In the case of CD8 T cells, both *BRAF* and mutations associated with MSI (*ASTE1/TTK*) are also present and co-occur with *BRAF* mutations. This is reflective of a right sided pathology, of which 46% of the mutational cohort are. Overall, the mutational landscape of this cohort, which reflects that seen in the literature, is representative of Wnt signalling and MSI with mutations associated with these pathways being differential between cases low and high for γδ and CD8 T cells.

Chapter 6: Assessment of the transcriptional landscape by lymphocyte density

Chapter 6: Assessment of the transcriptional landscape by lymphocyte density

6.0 Summary

Previous attempts to elucidate the prognostic role of γδ T cells have relied on transcriptional deconvolution for classification of cases by lymphocyte density. These methods have demonstrated flaws in their ability to accurately identify γδ T cells. To validate our findings based on histological data, cases were reclassified as 'high' or 'low' for either lymphocyte population (γδ or CD8) based on their expression of genes specific to these lymphocytes. CD8 T cells were represented by expression of genes encoding the CD8α and CD8β co-receptors. γδ T cells were represented by expression of genes encoding specific γ and δ chains.

Survival analysis conducted using cases reclassified by their transcriptional profile as 'high' or 'low' reflected the results seen using histological classification. These data further validate the initial histological findings and encourage the use of these lymphocyte subtype specific genes in future lymphocyte deconvolution methods.

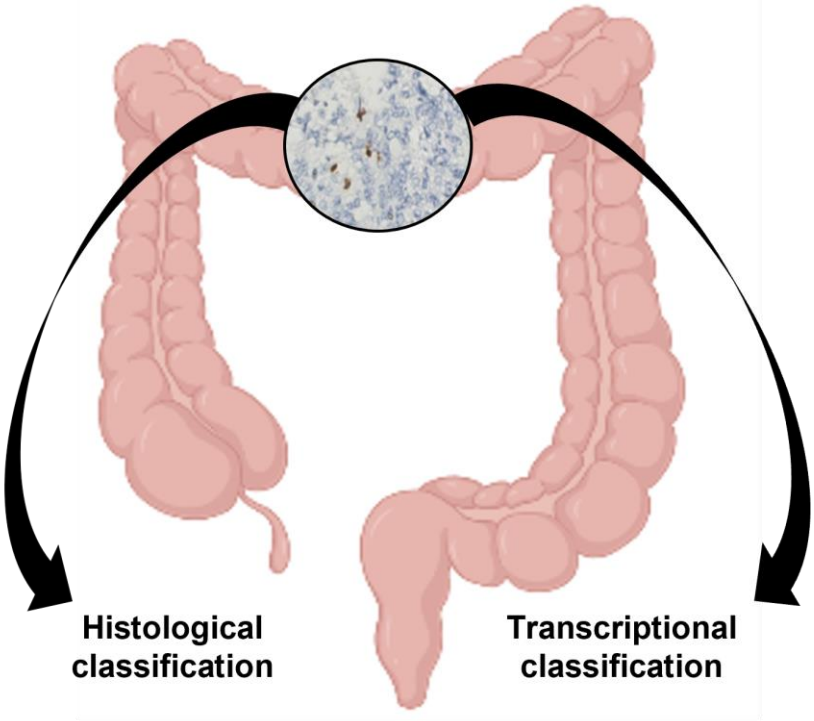

CD8

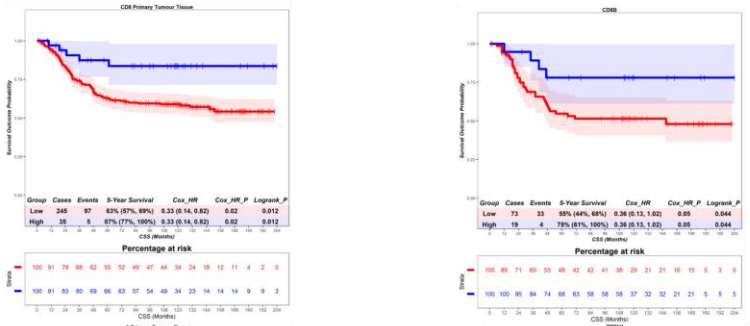

γδ

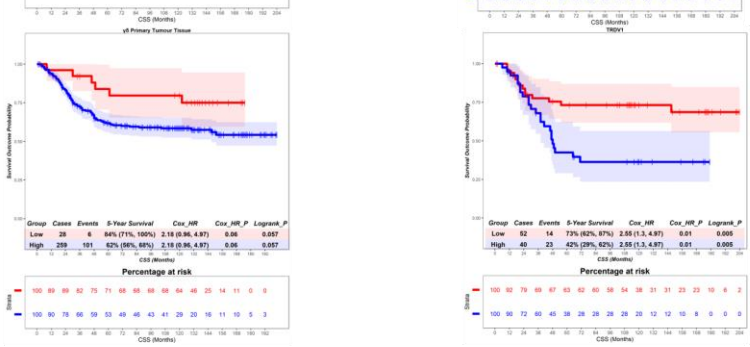

Transcriptional classification validates histological

6.1 Introduction

Although analysis of genomic data is valuable for understanding the genetic blueprint that underlies the cohort, this does not necessarily reflect the degree to which gene transcription occurs and so it is important to also understand the transcriptional landscape of the cohort whilst keeping in mind the RNA is not always translated and can be translated multiple times, and thus is not a true reflection of functional protein within the tissue environment.

First, transcriptional validation of histological classification of T cell density was performed to understand whether the histological findings are supported by the preceding transcriptional landscape. Next, transcriptional investigation of BTNL proteins, which are responsible for the development and maintenance of γδ T cell compartments, was used to determine if the histological findings can be in part explained by differences in established regulatory molecules. This was followed by further validation by replicating the survival analysis performed using histological data, with cases classified as low or high based on transcriptional data. Finally, the presence of differential genes was explored within the cohort.

6.2 Transcriptional validation of γδ T cell and CD8 T cell density

Previous attempts to identify the prognostic role of γδ T cells has relied on transcriptional identification of lymphocyte populations using the flawed algorithm CIBERSORT previously discussed [11, 187]. To transcriptionally validate our histological classification of cases as 'Low' or 'High' for γδ T cells and CD8 T cells, the expression of genes encoding for the γδ chain [93] and the CD8 co-receptor were compared between classifications. Statistical significance was determined using a Welch two sample t-test. It should be noted that the group sizes were imbalanced.

In the primary tumour, cases histologically classed as high for γδ T cells had a higher expression of both the CD8α (CD8A) and CD8β (CD8B) chains (Figure 6.1A), suggesting a higher density of CD8 T cells – this is likely a result of a generally higher inflammatory density. The γδ high cases exhibited a higher expression of the intestine associated Vγ4 (TRGV4) chain, although no difference could be seen in the expression of its common partner the tissue resident associated Vδ1 chain (TRDV1) (Figure 6.1A), although this was the only Vδ chain present as there was no expression of the Vδ2 chain (TRDV2) or Vδ3 chain (TRDV3) (Figure 6.1A). The restriction of Vδ expression to Vδ1 suggests that the γδ population likely consists of tissue resident cells. In addition to no expression of the blood associated Vδ2 (TRDV2) chain, its associated partner Vγ9 (TRGV9) was expressed only in γδ high cases and at a very low level (Figure 6.1A). This also reflects the expectation that γδ T cells in the primary tumour tissue would be of the Vγ4Vδ1 variety, although the presence of Vγ9 expression may be due to an influx of circulating γδ T cells in those cases with a high density, but the lack of expression of its partner chain Vδ2 is unexplained. It is possible that the Vδ1 chain is partnering with alternative Vγ chains as although there was no expression of Vγ1 (TRGV1), Vγ2 (TRGV2) or Vγ11 (TRGV11), there was minor expression of Vγ5 (TRGV5) and Vγ8 (TRGV8) and strong expression of Vγ3 (TRGV3). Vγ5 is a pseudogene and thus is not utilised in functioning γδ T cells, whilst Vγ8 is a functional chain but its low expression would suggest that it is not of significant contribution to the immune landscape. Vγ3 is also a functional chain, and its expression is substantial, but Vγ3 is not associated with functionality in the literature. There was substantial expression of Vγ10 (TRGV10) in both low and high cases (Figure 6.1A). Vγ10 is a pseudogene in humans (although functional in other primates [316]), so it being so highly expressed is interesting. Although, their being expressed does not necessarily require that they are functional. As the group sizes were imbalanced, the correlation between the histological count (% positive) and transcriptomic counts were determined. Histological γδ density did not correlate with expression of any lymphocyte genes (Figure 6.2).

In the primary tumour, cases histologically classed as high for CD8 T cells had a higher expression of CD8α (CD8A) but no difference in the expression of CD8β (CD8B) (Figure 6.1B), suggesting that significant expansion of CD8 T cells may be biased towards expression of the α chain, which aligns with the literature as CD8 T cells are expected to be CD8αβ or CD8αα [125]. There was no difference in expression of the Vδ1 chain and no expression of the Vδ2 or Vδ3 chains and the Vγ chains with the highest expression (Vγ4 and Vγ10) showed no difference (Figure 6.1B), suggesting that γδ T cell density is not associated with CD8 T cell density. As the group sizes were imbalanced, the correlation between the histological count (% positive) and transcriptomic counts were determined. Histological CD8 density did not correlate with expression of any lymphocyte genes (Figure 6.3).

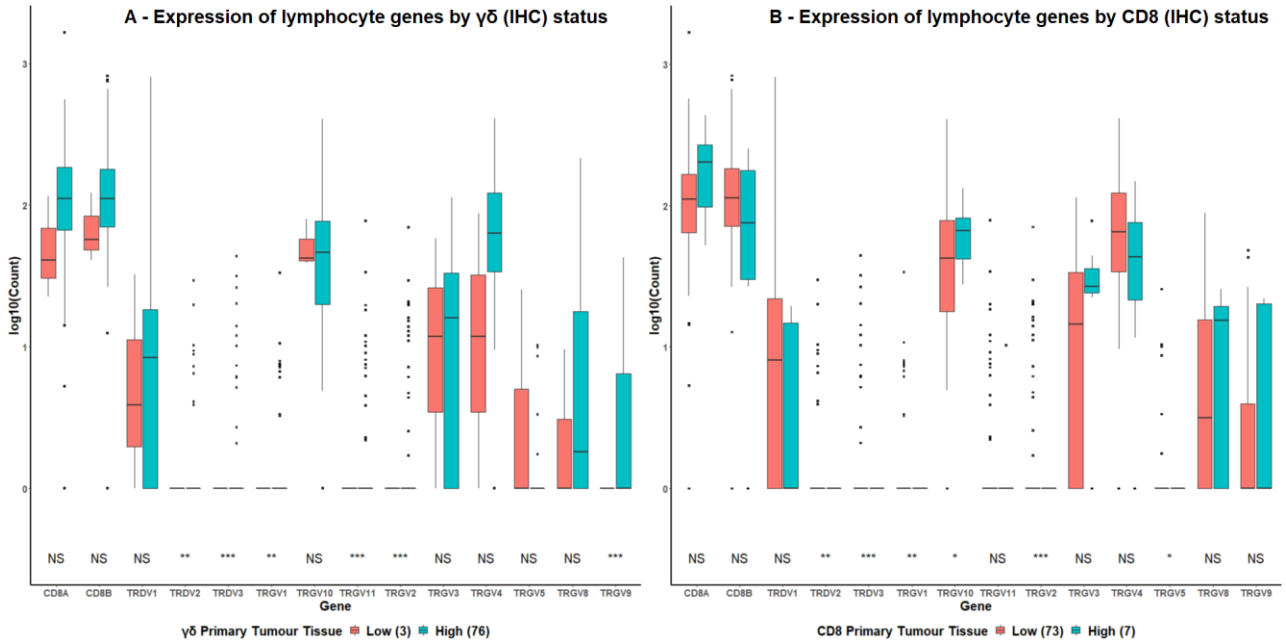

Figure 6.1 – Expression of lymphocyte genes by lymphocyte density status (IHC). *A – Lymphocyte gene expression by γδ T cell status. B – Lymphocyte gene expression by CD8 T cell status. X axis denotes lymphocyte gene. Y axis denotes the expression count of the lymphocyte gene, expressed as log10. Statistical significance is denoted below groups and is calculated via a Welch two sample t-test, <0.05 (*), <0.01 (**) or <0.001 (***).*

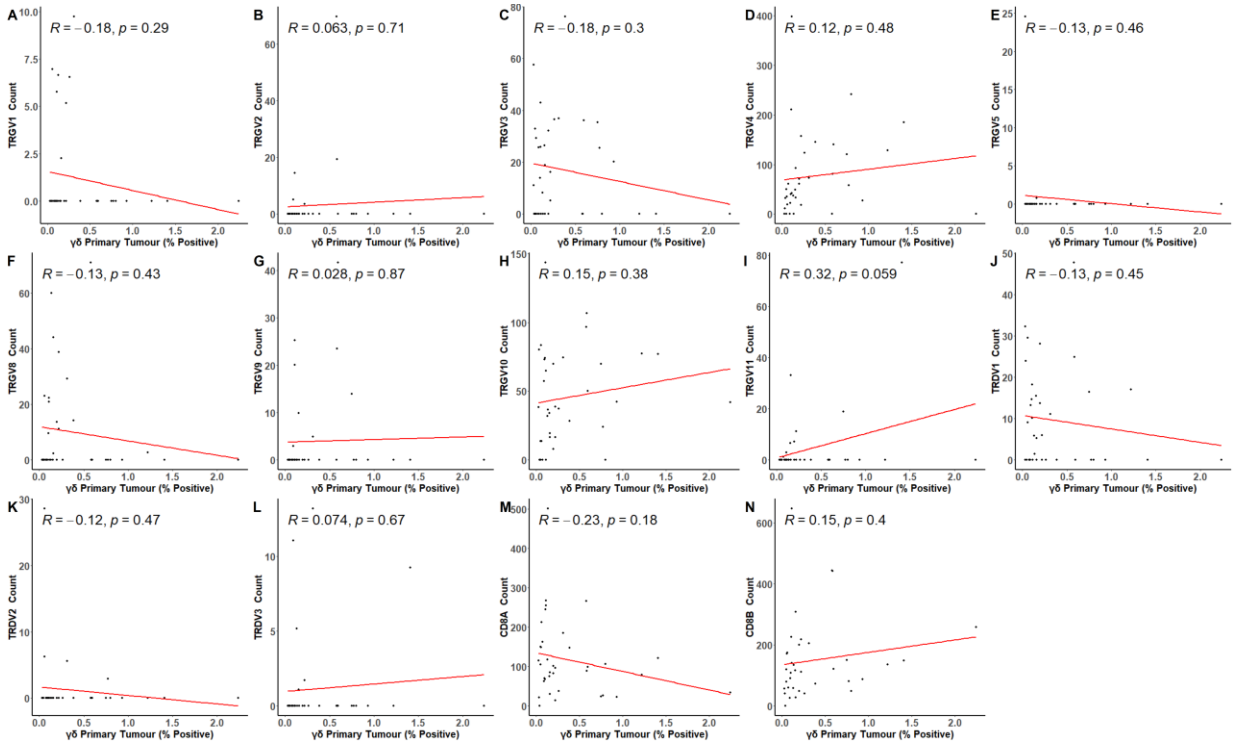

Figure 6.2 – Correlation matrix for histological γδ density and gene expression of lymphocyte genes. *A – Correlation between γδ T cell density and TRGV1 expression. B – Correlation between γδ T cell density and TRGV2 expression. C – Correlation between γδ T cell density and TRGV3 expression. D – Correlation between γδ T cell density and TRGV4 expression. E – Correlation between γδ T cell density and TRGV5 expression. F – Correlation between γδ T cell density and TRGV8 expression. G – Correlation between γδ T cell density and TRGV9 expression. H – Correlation between γδ T cell density and TRGV10 expression. I – Correlation between γδ T cell density and TRGV11 expression. J – Correlation between γδ T cell density and TRDV1 expression. K – Correlation between γδ T cell density and TRDV2 expression. L – Correlation between γδ T cell density and TRDV3 expression. M – Correlation between γδ T cell density and CD8A expression. N – Correlation between γδ T cell density and CD8B expression. X axis denotes γδ T cell density (% positive). Y axis denotes gene expression. Linear correlation is determined by a Pearson correlation (R = Pearson coefficient).*

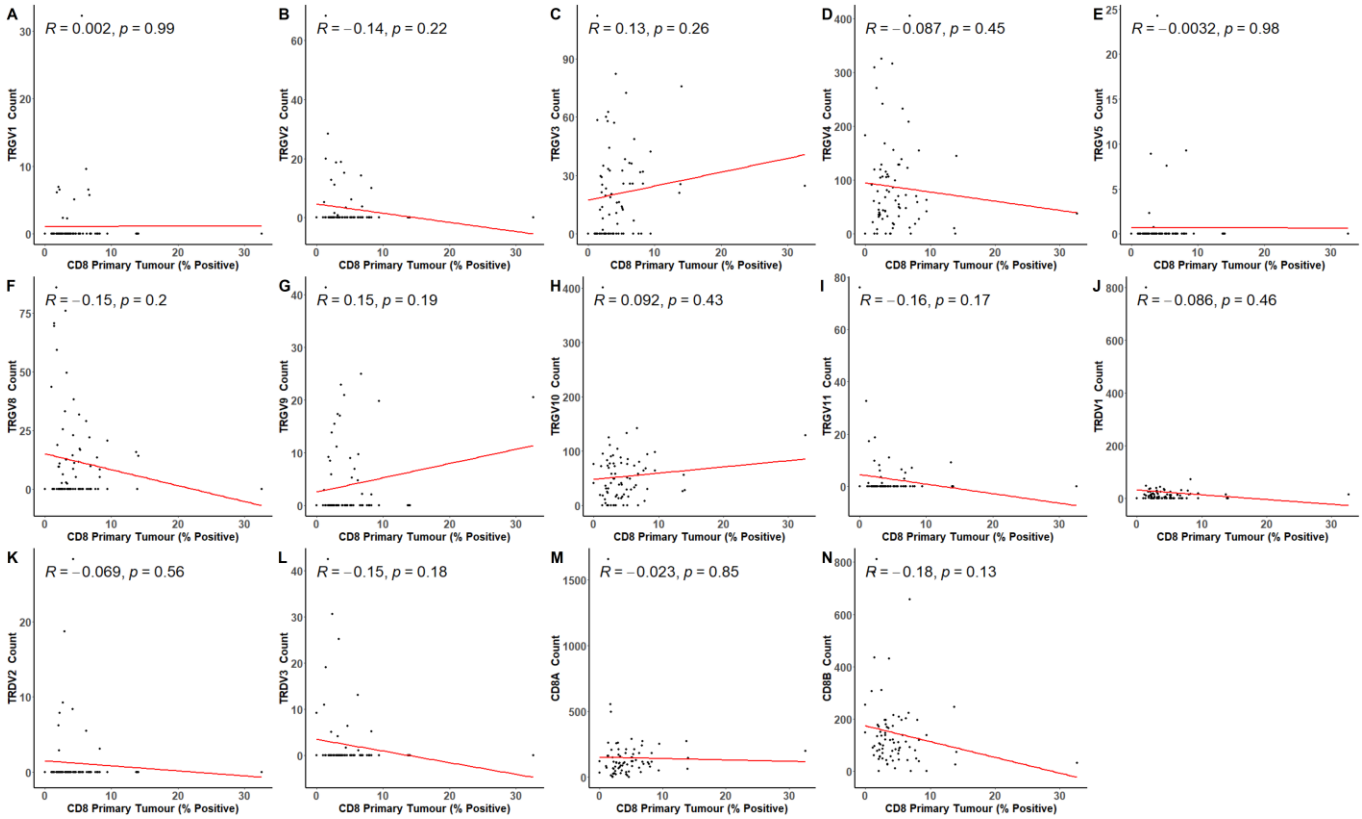

Figure 6.3 – Correlation matrix for histological CD8 density and gene expression of lymphocyte genes. *A – Correlation between CD8 T cell density and TRGV1 expression. B – Correlation between CD8 T cell density and TRGV2 expression. C – Correlation between CD8 T cell density and TRGV3 expression. D – Correlation between CD8 T cell density and TRGV4 expression. E – Correlation between CD8 T cell density and TRGV5 expression. F – Correlation between CD8 T cell density and TRGV8 expression. G – Correlation between CD8 T cell density and TRGV9 expression. H – Correlation between CD8 T cell density and TRGV10 expression. I – Correlation between CD8 T cell density and TRGV11 expression. J – Correlation between CD8 T cell density and TRDV1 expression. K – Correlation between CD8 T cell density and TRDV2 expression. L – Correlation between CD8 T cell density and TRDV3 expression. M – Correlation between CD8 T cell density and CD8A expression. N – Correlation between CD8 T cell density and CD8B expression. X axis denotes CD8 T cell density (% positive). Y axis denotes gene expression. Linear correlation is determined by a Pearson correlation (R = Pearson coefficient).*

To further attempt to validate the histological data using the transcriptional data, contingency tables were formed consisting of histological classification (columns) and transcriptional classification (rows) (Table 6.1 and Table 6.2), on which mosaic plots were built (Figure 6.4 and Figure 6.5). Transcriptional classification was performed as previously described for histological data but using transcription data. This analysis showed no relationship between histological and transcriptional classifications; however, it should be stressed that the number of cases histologically classified as low for γδ T cells and high for CD8 T cells are too small to rely on these findings.

Table 6.1 – Contingency tables of histological classification (columns) and transcriptional classification (rows) of γδ density.

	GD High	GD Low
TRGV1 High	9	0
TRGV1 Low	67	3

	GD High	GD Low
TRGV10 High	59	3
TRGV10 Low	17	0

	GD High	GD Low
TRGV2 High	9	0
TRGV2 Low	67	3

	GD High	GD Low
TRGV11 High	10	0
TRGV11 Low	66	3

	GD High	GD Low
TRGV3 High	10	1
TRGV3 Low	66	2

	GD High	GD Low
TRDV1 High	33	1
TRDV1 Low	43	2

	GD High	GD Low
TRGV4 High	11	0
TRGV4 Low	65	3

	GD High	GD Low
TRDV2 High	9	0
TRDV2 Low	67	3

	GD High	GD Low
TRGV5 High	4	1
TRGV5 Low	72	2

	GD High	GD Low
TRGV3 High	13	0
TRGV3 Low	63	3

	GD High	GD Low
TRGV8 High	8	0
TRGV8 Low	68	3

	GD High	GD Low
CD8A High	37	0
CD8A Low	39	3

	GD High	GD Low
TRGV9 High	11	0
TRGV9 Low	65	3

	GD High	GD Low
CD8B High	15	0
CD8B Low	61	3

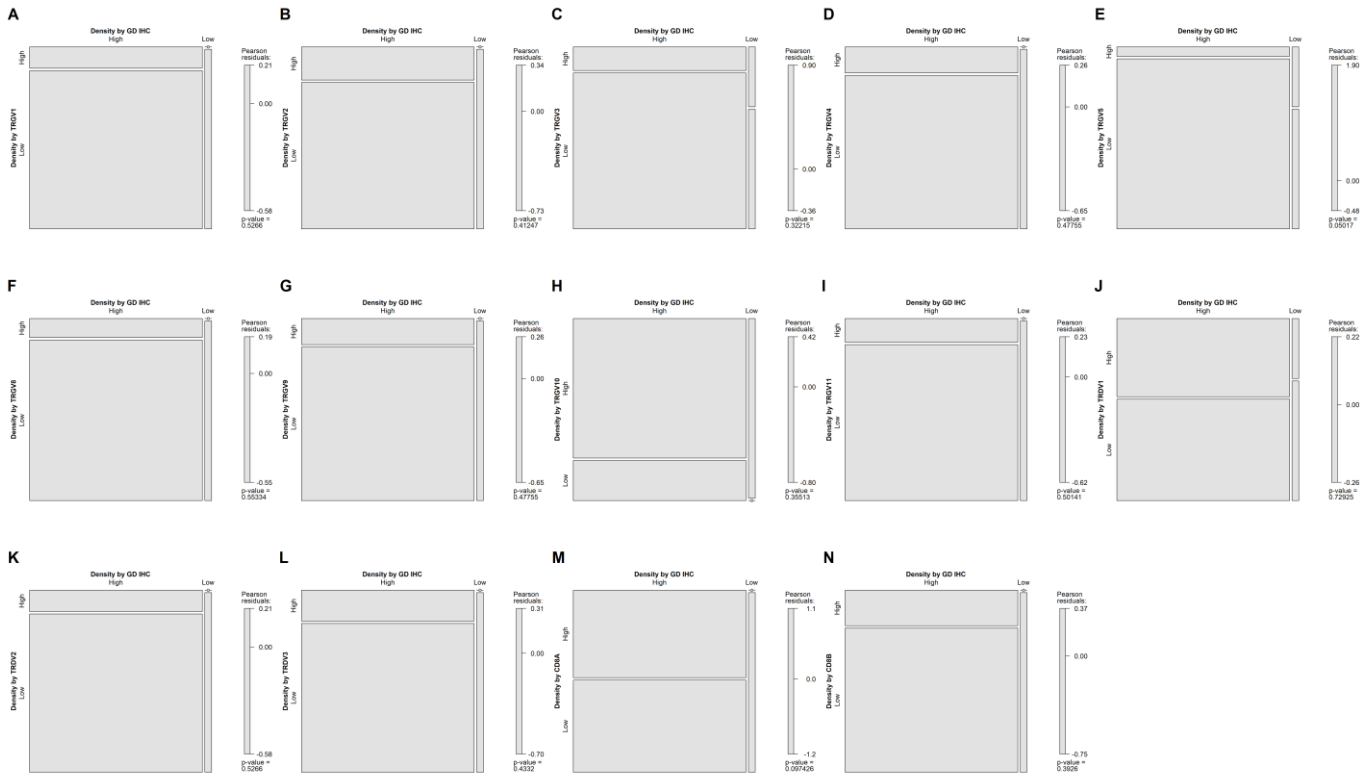

Figure 6.4 – Mosaic plots of contingency tables of histological classification (columns) and transcriptional classification (rows). *A – Mosaic representation of γδ T cell status by TRGV1 status. B – Mosaic representation of γδ T cell status by TRGV2 status. C – Mosaic representation of γδ T cell status by TRGV3 status. D – Mosaic representation of γδ T cell status by TRGV4 status. E – Mosaic representation of γδ T cell status by TRGV5 status. F – Mosaic representation of γδ T cell status by TRGV8 status. G – Mosaic representation of γδ T cell status by TRGV9 status. H – Mosaic representation of γδ T cell status by TRGV10 status. I – Mosaic representation of γδ T cell status by TRGV11 status. J – Mosaic representation of γδ T cell status by TRDV1 status. K – Mosaic representation of γδ T cell status by TRDV2 status. L – Mosaic representation of γδ T cell status by TRDV3 status. M – Mosaic representation of γδ T cell status by CD8A status. N– Mosaic representation of γδ T cell status by CD8B status. X axis denotes histological classification of γδ T cell status. Y axis denotes transcriptional classification by gene expression.*

Table 6.2 – Contingency tables of histological classification (columns) and transcriptional classification (rows) of CD8 density.

	CD8 High	CD8 Low
TRGV1 High	0	9
TRGV1 Low	7	64

	CD8 High	CD8 Low
TRGV10 High	7	55
TRGV10 Low	0	18

	CD8 High	CD8 Low
TRGV2 High	0	13
TRGV2 Low	7	60

	CD8 High	CD8 Low
TRGV11 High	1	9
TRGV11 Low	6	64

	CD8 High	CD8 Low
TRGV3 High	1	10
TRGV3 Low	6	63

	CD8 High	CD8 Low
TRDV1 High	3	31
TRDV1 Low	4	42

	CD8 High	CD8 Low
TRGV4 High	0	11
TRGV4 Low	7	62

	CD8 High	CD8 Low
TRDV2 High	0	9
TRDV2 Low	7	64

	CD8 High	CD8 Low
TRGV5 High	0	5
TRGV5 Low	7	68

	CD8 High	CD8 Low
TRGV3 High	0	13
TRGV3 Low	7	60

	CD8 High	CD8 Low
TRGV8 High	0	8
TRGV8 Low	7	65

	CD8 High	CD8 Low
CD8A High	5	33
CD8A Low	2	40

	CD8 High	CD8 Low
TRGV9 High	3	9
TRGV9 Low	4	64

	CD8 High	CD8 Low
CD8BHigh	2	13
CD8B Low	5	60

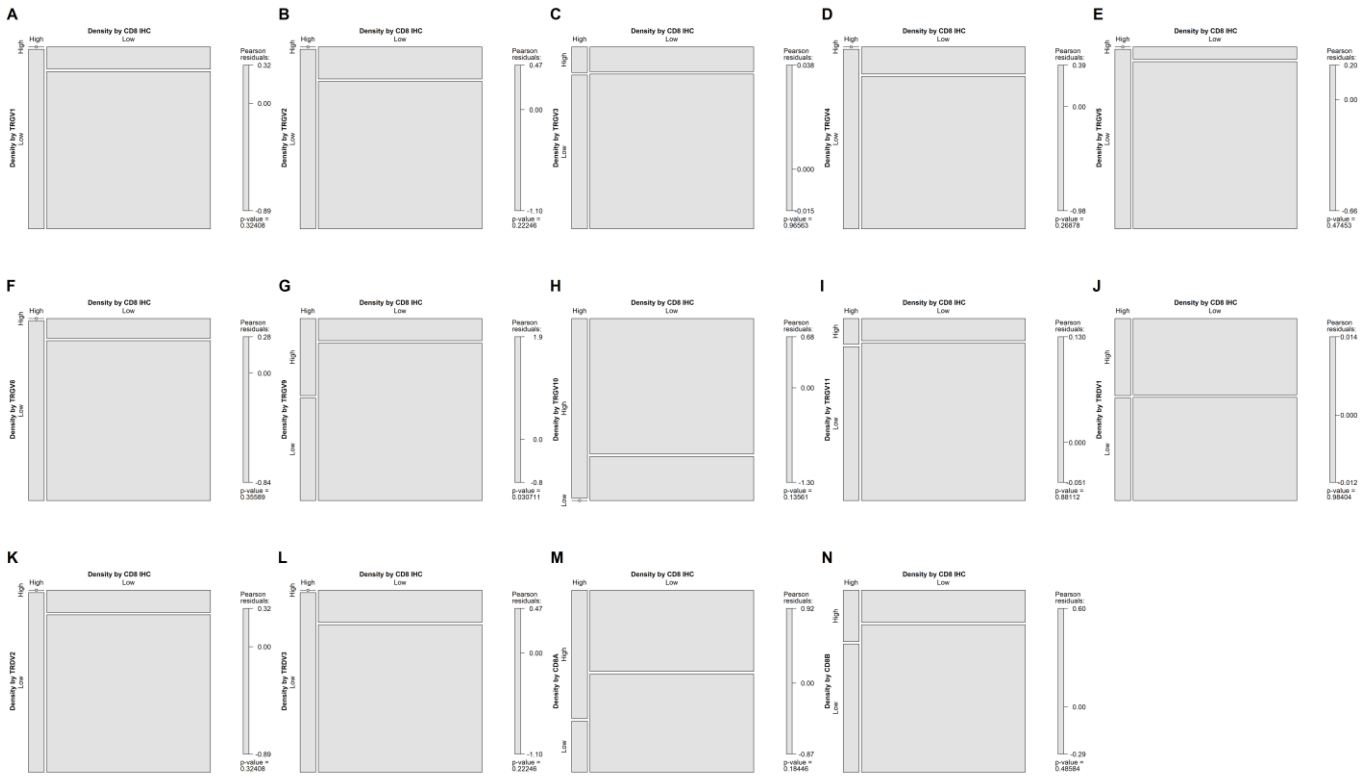

Figure 6.5 – Mosaic plots of contingency tables of histological classification (columns) and transcriptional classification (rows). *A – Mosaic representation of CD8 T cell status by TRGV1 status. B – Mosaic representation of CD8 T cell status by TRGV2 status. C – Mosaic representation of CD8 T cell status by TRGV3 status. D – Mosaic representation of CD8 T cell status by TRGV4 status. E – Mosaic representation of CD8 T cell status by TRGV5 status. F – Mosaic representation of CD8 T cell status by TRGV8 status. G – Mosaic representation of CD8 T cell status by TRGV9 status. H – Mosaic representation of CD8 T cell status by TRGV10 status. I – Mosaic representation of CD8 T cell status by TRGV11 status. J – Mosaic representation of CD8 T cell status by TRDV1 status. K – Mosaic representation of CD8 T cell status by TRDV2 status. L – Mosaic representation of CD8 T cell status by TRDV3 status. M – Mosaic representation of CD8 T cell status by CD8A status. N– Mosaic representation of CD8 T cell status by CD8B status. X axis denotes histological classification of CD8 T cell status. Y axis denotes transcriptional classification by gene expression.*

6.3 Transcriptional investigation of γδ T cell regulatory molecules

To understand if regulatory molecules are key factors in lymphocyte density, associations were explored with the intestine restricted butyrophilin like molecules BTNL3 and BTNL8, which dimerise and bind the γ chain of γδ T cells to enable their development and maintenance within the intestine [111-113].

There was no difference in the expression of any BTNL genes between those histologically classed as γδ low or γδ high (Figure 6.6). BTNL3, BTNL8 and BTNL9 were highly expressed (median count (log10) = 1.72, 1.71 and 2.33, respectively) and BTNL2 and BTNL10 were lowly expressed (median count (log10) = 0.00 and 0.00, respectively) (Figure 6.6). *Lebrero-Fernández et al* found a similar expression profile in 17 normal tissue samples adjacent to the primary tumour (BTNL9 was lowly expressed in their data) with a reduction of BTNL3 and BTNL8, but not BTNL2 or BTNL9, in the primary tumour [317]. The comparative expression of the BTNL genes in the primary tumour in this study may reflect that state of BTNL3/BTNL8 reduction without a change in BTNL9, resulting in similar expression of the three BTNL genes. Correlation analysis was performed between expression of the BTNL genes and γδ T cell density (% positive) in the primary tumour (Figure 6.7), and between expression of the BTNL genes and expression of the T cell genes (Figure 6.8). None of these analyses showed a strong correlation (Figure 6.7 and Figure 6.8). Our understanding of the interaction between the Btnl proteins and γδ T cells would lead us to hypothesise that their expression would correlate, but it may be that the need for *BTNL* expression is closer to a binary requirement, so the level of expression doesn't necessarily need to increase for γδ T cells to increase in density.

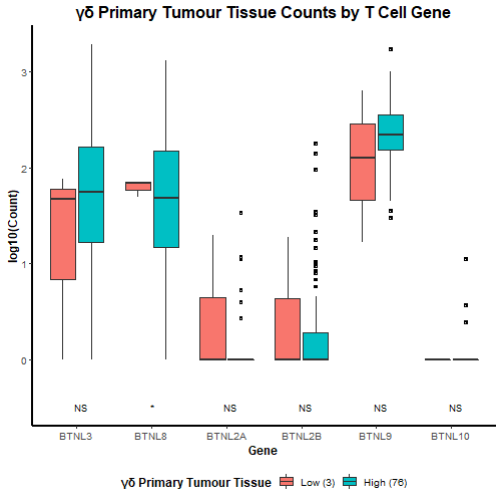

Figure 6.6 – Expression of BTNL genes by lymphocyte density status (IHC). *X axis denotes lymphocyte gene. Y axis denotes the expression count of the lymphocyte gene, expressed as log10. Statistical significance is denoted below groups and is calculated via a Welch two sample t-test, <0.05 (*), <0.01 (**) or <0.001 (***).*

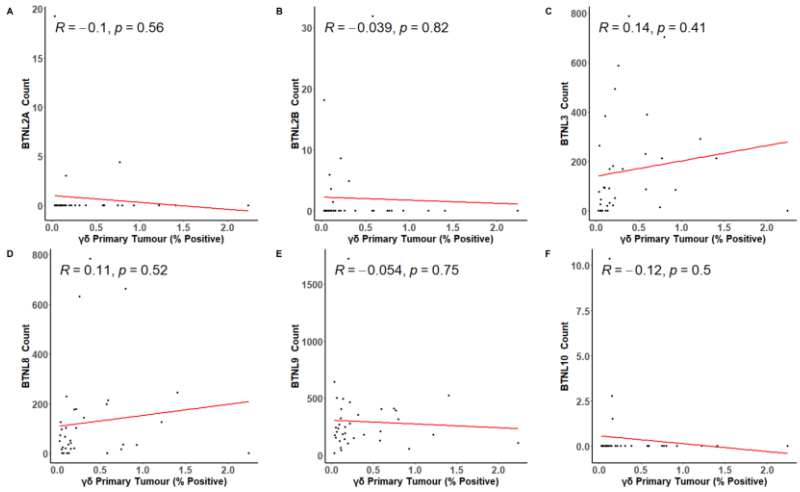

Figure 6.7 – Correlation matrix for histological γδ density and gene expression of BTNL genes. *A – Correlation between γδ T cell density and BTNL2A expression. B – Correlation between γδ T cell density and BTNL2B expression. C – Correlation between γδ T cell density and BTNL3 expression. D – Correlation between γδ T cell density and BTNL8 expression. E – Correlation between γδ T cell density and BTNL9 expression. F – Correlation between γδ T cell density and BTNL10 expression. X axis denotes γδ T cell density (% positive). Y axis denotes gene expression. Linear correlation is determined by a Pearson correlation (R = Pearson coefficient).*

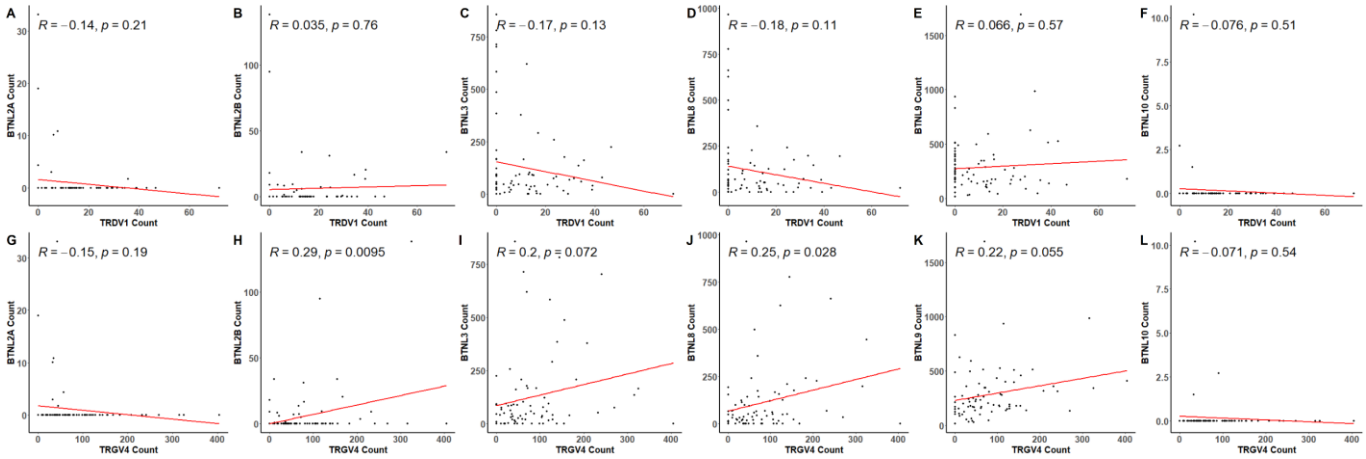

Figure 6.8 – Correlation matrix for gene expression of Vγ1 (TRDV1) or Vδ4 (TRGV4) and gene expression of BTNL genes. *A – Correlation between TRDV1 expression and BTNL2A expression. B – Correlation between TRDV1 expression and BTNL2B expression. C – Correlation between TRDV1 expression and BTNL3 expression. D – Correlation between TRDV1 expression and BTNL8 expression. E – Correlation between TRDV1 expression and BTNL9 expression. F – Correlation between TRDV1 expression and BTNL10 expression. G – Correlation between TRGV4 expression and BTNL2A expression. H – Correlation between TRGV4 expression and BTNL2B expression. I – Correlation between TRGV4 expression and BTNL3 expression. J – Correlation between TRGV4 expression and BTNL8 expression. K – Correlation between TRGV4 expression and BTNL9 expression. L – Correlation between TRGV4 expression and BTNL10 expression. X axis denotes γδ T cell density (% positive). Y axis denotes gene expression. Linear correlation is determined by a Pearson correlation (R = Pearson coefficient). A significant outlier (a minimum of 10x the expression of any other case), TMA_ID = 228, was removed as it drastically altered the results of some genes towards a positive correlation. Correlation matrix including this outlier are available in the appendix.*

6.4 Assessment of the prognostic role of lymphocyte populations

Survival analysis was performed using transcriptional data for case classification. As the transcriptional data originates from bulk tumour sequencing, no adjacent normal tissue is available, and analysis cannot be subset by epithelial/stromal compartments. Classification as ‘low’ or ‘high’ is determined by applying the previously used maximally selected rank statistic to gene expression data for genes that encode TCR chains and co-receptor chains that are structurally integral to γδ T cells and CD8 T cells.

6.4.1 γδ T cells - cancer-specific survival

CSS was investigated in the context of transcriptional classification by *TRDV1*, which encodes the Vδ1 chain. In the primary tumour, patients deemed high for *TRDV1* expression are associated with a worse prognosis (Figure 6.9). Patients with a high expression of *TRDV1* had a mean survival time of 63.98 months, compared to those with low expression of *TRDV1* with a mean survival of 97.25 months (hazard ratio = 2.55, p = 0.01). 5-year survival for patients high for *TRDV1* expression is 42% (29%, 62%), compared to 73% (62%, 87%) in the *TRDV1* low group. This suggests that *TRDV1* expression in the primary tumour has an unfavourable prognostic role.

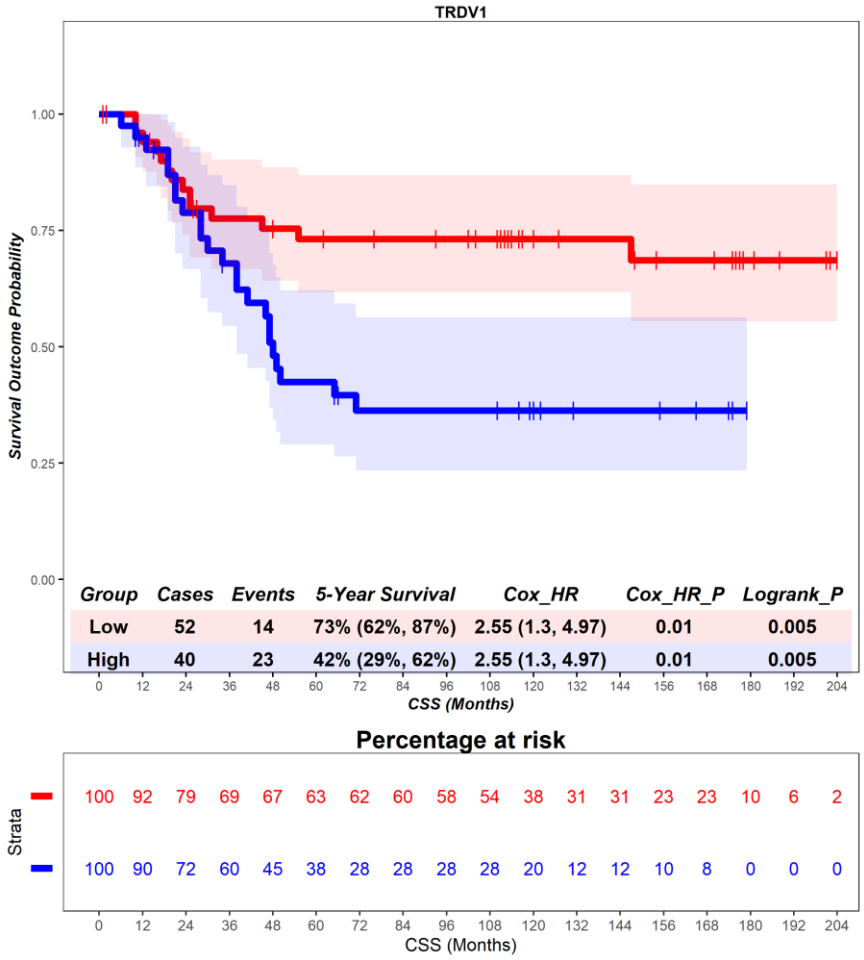

Figure 6.9 – Time-to-event (cancer-specific survival) analysis for TRDV1 expression in the primary tumour. *Patients deemed 'High' or 'Low' for TRDV1 expression are shaded blue and red, respectively. Cox hazard ratio is univariate. The 'Low' group is used as the reference group on cox regression modelling.*

CSS was investigated in the context of transcriptional classification by *TRDV2*, which encodes the Vδ2 chain. In the primary tumour, patients deemed high for *TRDV2* expression are associated with no difference in prognosis (Figure 6.10). Patients with a high expression of *TRDV2* had a mean survival time of 65.6 months, compared to those with low expression of *TRDV2* with a mean survival of 84.88 months (hazard ratio = 0.86, p = 0.81). 5-year survival for patients high for *TRDV2* expression is 64% (39%, 100%), compared to 59% (49%, 72%) in the *TRDV2* low group. This suggests that *TRDV2* expression in the primary tumour has no prognostic role.

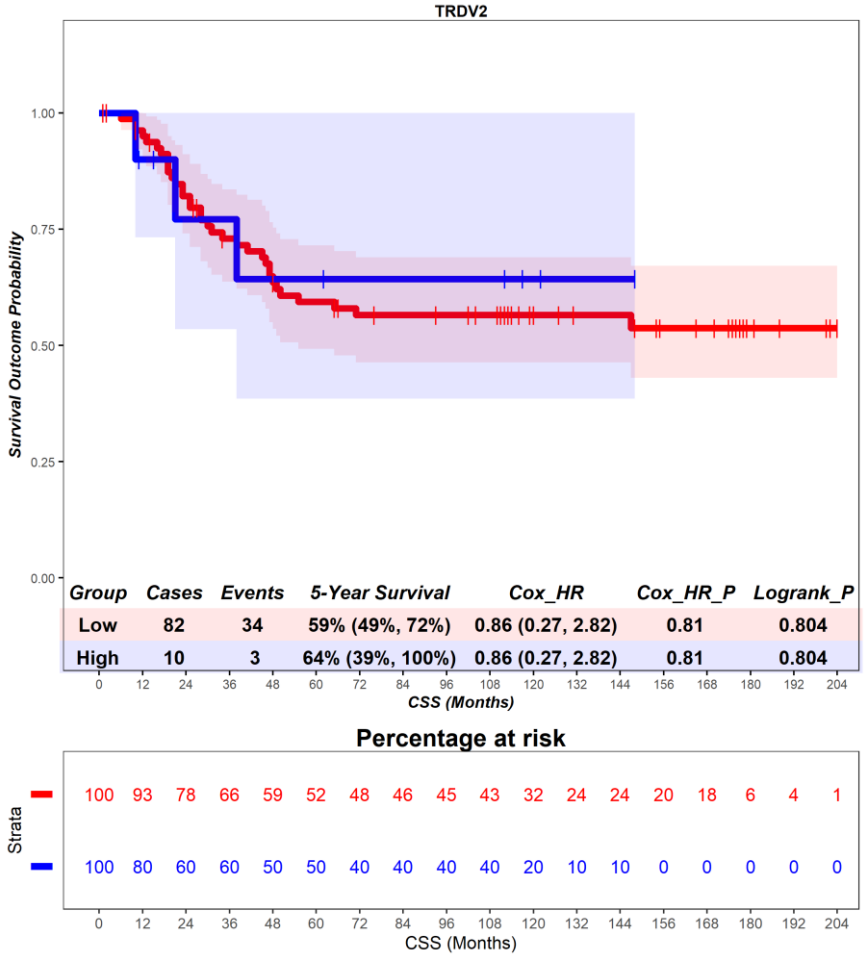

Figure 6.10 – Time-to-event (cancer-specific survival) analysis for TRDV2 expression in the primary tumour. *Patients deemed 'High' or 'Low' for TRDV2 expression are shaded blue and red, respectively. Cox hazard ratio is univariate. The 'Low' group is used as the reference group on cox regression modelling.*

CSS was investigated in the context of transcriptional classification by *TRDV3*, which encodes the Vδ3 chain. In the primary tumour, patients deemed high for *TRDV3* expression are associated with no difference in prognosis (Figure 6.11). Patients with a high expression of *TRDV3* had a mean survival time of 85.21 months, compared to those with low expression of *TRDV3* with a mean survival of 82.35 months (hazard ratio = 0.82, p = 0.67). 5-year survival for patients high for *TRDV3* expression is 62% (40%, 95%), compared to 59% (49%, 72%) in the *TRDV3* low group. This suggests that *TRDV3* expression in the primary tumour has no prognostic role.

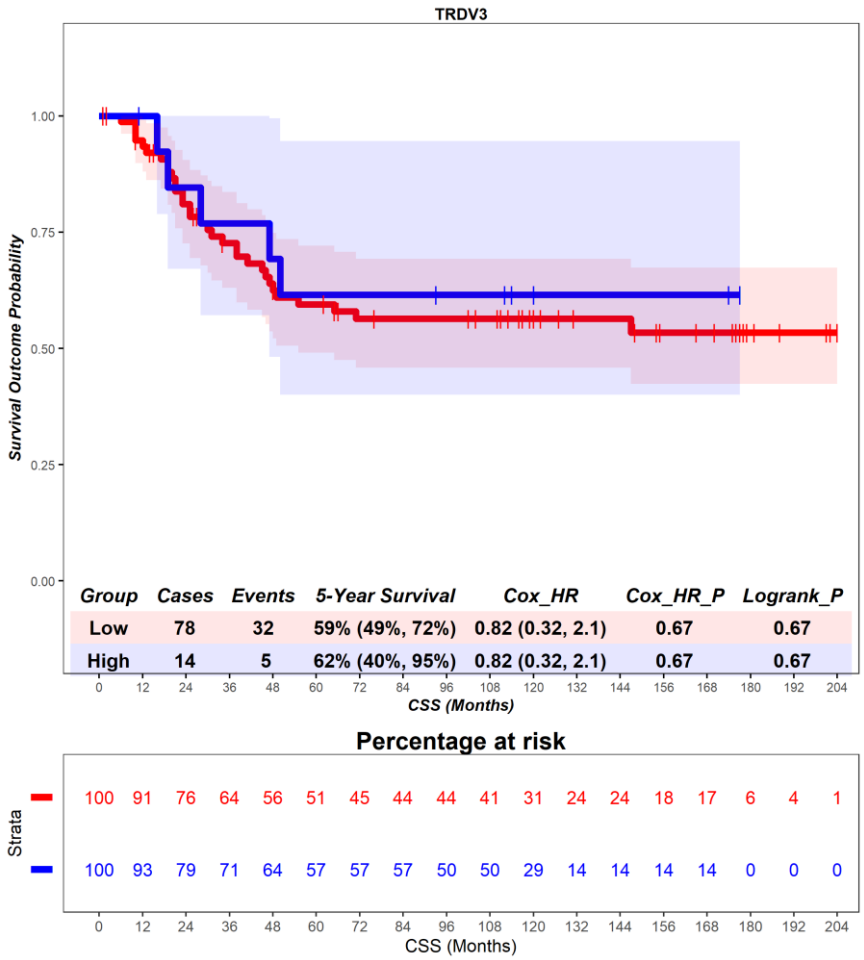

Figure 6.11 – Time-to-event (cancer-specific survival) analysis for TRDV3 expression in the primary tumour. *Patients deemed 'High' or 'Low' for TRDV3 expression are shaded blue and red, respectively. Cox hazard ratio is univariate. The 'Low' group is used as the reference group on cox regression modelling.*

CSS was investigated in the context of transcriptional classification by *TRGV1*, which encodes the Vγ1 chain. In the primary tumour, patients deemed high for *TRGV1* expression are associated with a better prognosis (Figure 6.12). Patients with a high expression of *TRGV1* had a mean survival time of 96.30 months, compared to those with low expression of *TRGV1* with a mean survival of 81.13 months (hazard ratio = 0.18, p = 0.09). 5-year survival for patients high for *TRGV1* expression is 89% (71%, 100%), compared to 56% (46%, 69%) in the *TRGV1* low group. This suggests that *TRGV1* expression in the primary tumour has a favourable prognostic role.

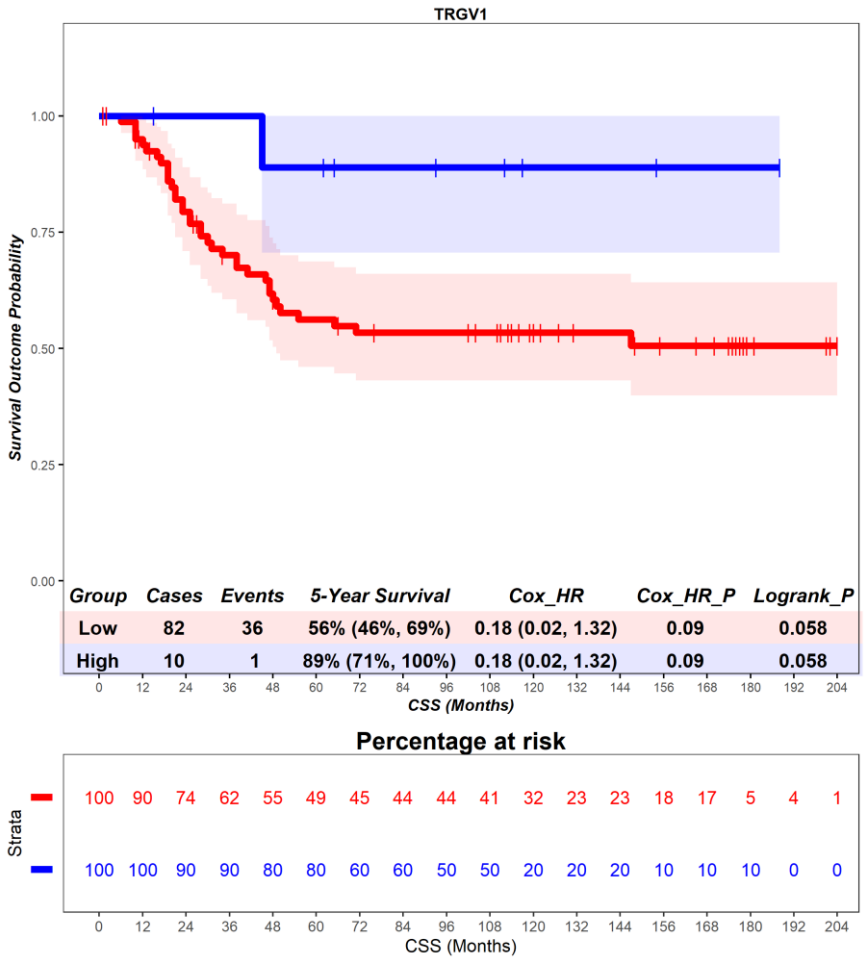

Figure 6.12 – Time-to-event (cancer-specific survival) analysis for TRGV1 expression in the primary tumour. *Patients deemed 'High' or 'Low' for TRGV1 expression are shaded blue and red, respectively. Cox hazard ratio is univariate. The 'Low' group is used as the reference group on cox regression modelling.*

CSS was investigated in the context of transcriptional classification by *TRGV2*, which encodes the Vγ2 chain. In the primary tumour, patients deemed high for *TRGV2* expression are associated with no difference in prognosis (Figure 6.13). Patients with a high expression of *TRGV2* had a mean survival time of 67.88 months, compared to those with low expression of *TRGV2* with a mean survival of 86.16 months (hazard ratio = 1.7, p = 0.16). 5-year survival for patients high for *TRGV2* expression is 38% (20%, 71%), compared to 65% (55%, 78%) in the *TRGV2* low group. This suggests that *TRGV2* expression in the primary tumour has no prognostic role.

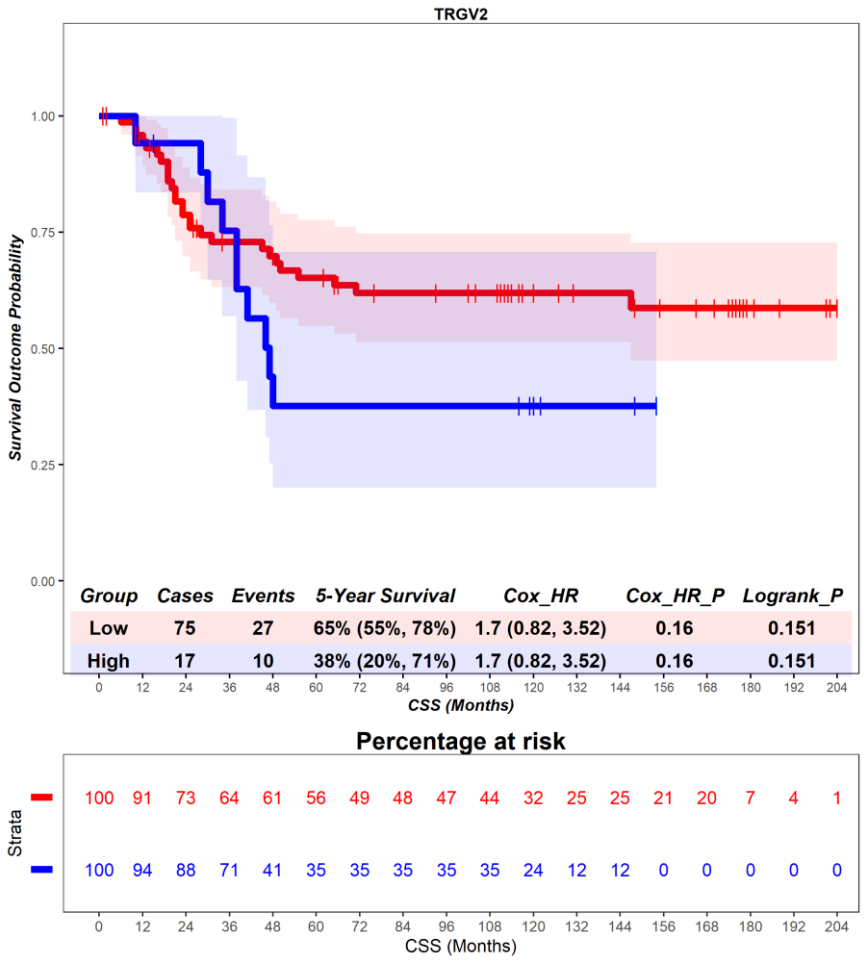

Figure 6.13 – Time-to-event (cancer-specific survival) analysis for TRGV2 expression in the primary tumour. *Patients deemed 'High' or 'Low' for TRGV2 expression are shaded blue and red, respectively. Cox hazard ratio is univariate. The 'Low' group is used as the reference group on cox regression modelling.*

CSS was investigated in the context of transcriptional classification by *TRGV3*, which encodes the Vγ3 chain. In the primary tumour, patients deemed high for *TRGV3* expression are associated with an unfavourable prognosis (Figure 6.14). Patients with a high expression of *TRGV3* had a mean survival time of 59.58 months, compared to those with low expression of *TRGV3* with a mean survival of 86.26 months (hazard ratio = 2.1, p = 0.06). 5-year survival for patients high for *TRGV3* expression is 37% (17%, 80%), compared to 63% (53%, 75%) in the *TRGV3* low group. This suggests that *TRGV3* expression in the primary tumour has an unfavourable prognostic role.

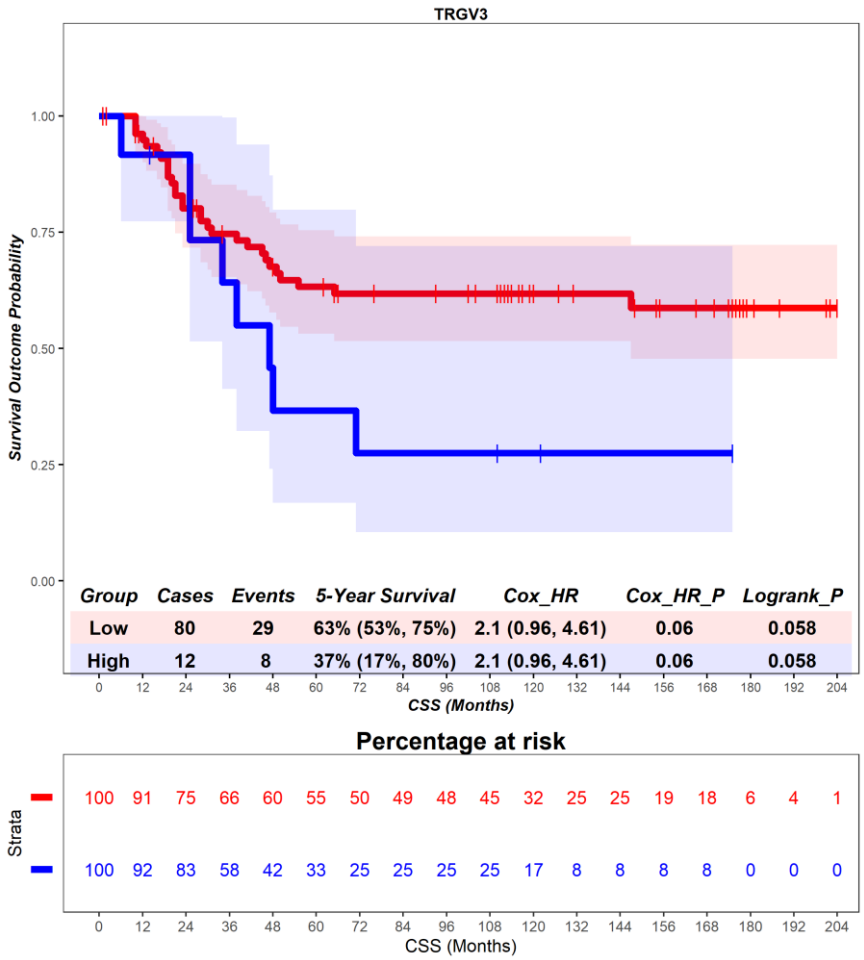

Figure 6.14 – Time-to-event (cancer-specific survival) analysis for TRGV3 expression in the primary tumour. *Patients deemed 'High' or 'Low' for TRGV3 expression are shaded blue and red, respectively. Cox hazard ratio is univariate. The 'Low' group is used as the reference group on cox regression modelling.*

CSS was investigated in the context of transcriptional classification by *TRGV4*, which encodes the Vγ4 chain. In the primary tumour, patients deemed high for *TRGV4* expression are associated with a favourable prognosis (Figure 6.15). Patients with a high expression of *TRGV4* had a mean survival time of 116.82 months, compared to those with low expression of *TRGV4* with a mean survival of 78.16 months (hazard ratio = 0.3, p = 0.07). 5-year survival for patients high for *TRGV4* expression is 82% (62%, 100%), compared to 57% (46%, 69%) in the TRGV4 low group. This suggests that *TRGV4* expression in the primary tumour has a favourable prognostic role.

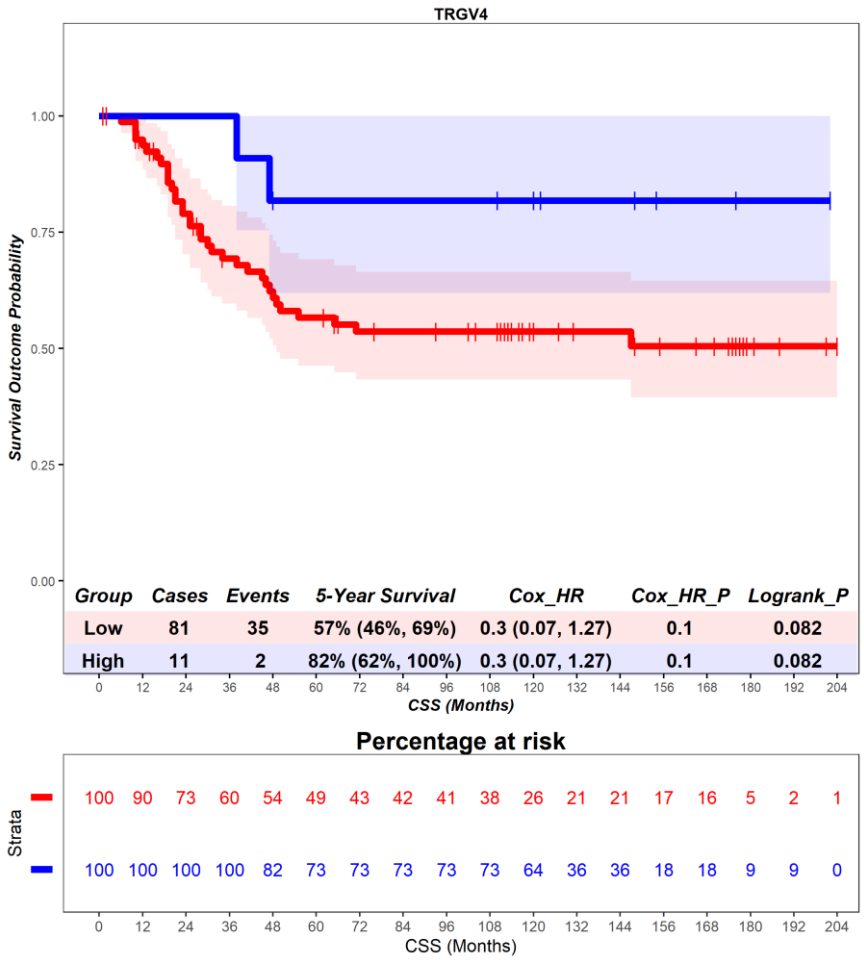

Figure 6.15 – Time-to-event (cancer-specific survival) analysis for TRGV4 expression in the primary tumour. *Patients deemed 'High' or 'Low' for TRGV4 expression are shaded blue and red, respectively. Cox hazard ratio is univariate. The 'Low' group is used as the reference group on cox regression modelling.*

CSS was investigated in the context of transcriptional classification by *TRGV5*, which encodes the Vγ5 chain. In the primary tumour, patients deemed high for *TRGV5* expression are associated with no difference in prognosis (Figure 6.16). Patients with a high expression of *TRGV5* had a mean survival time of 66.20 months, compared to those with low expression of *TRGV5* with a mean survival of 84.8 months (hazard ratio = 0.77, p = 0.67). 5-year survival for patients high for *TRGV5* expression is 62% (37%, 100%), compared to 59% (49%, 72%) in the *TRGV5* low group. This suggests that *TRGV5* expression in the primary tumour has no prognostic role.

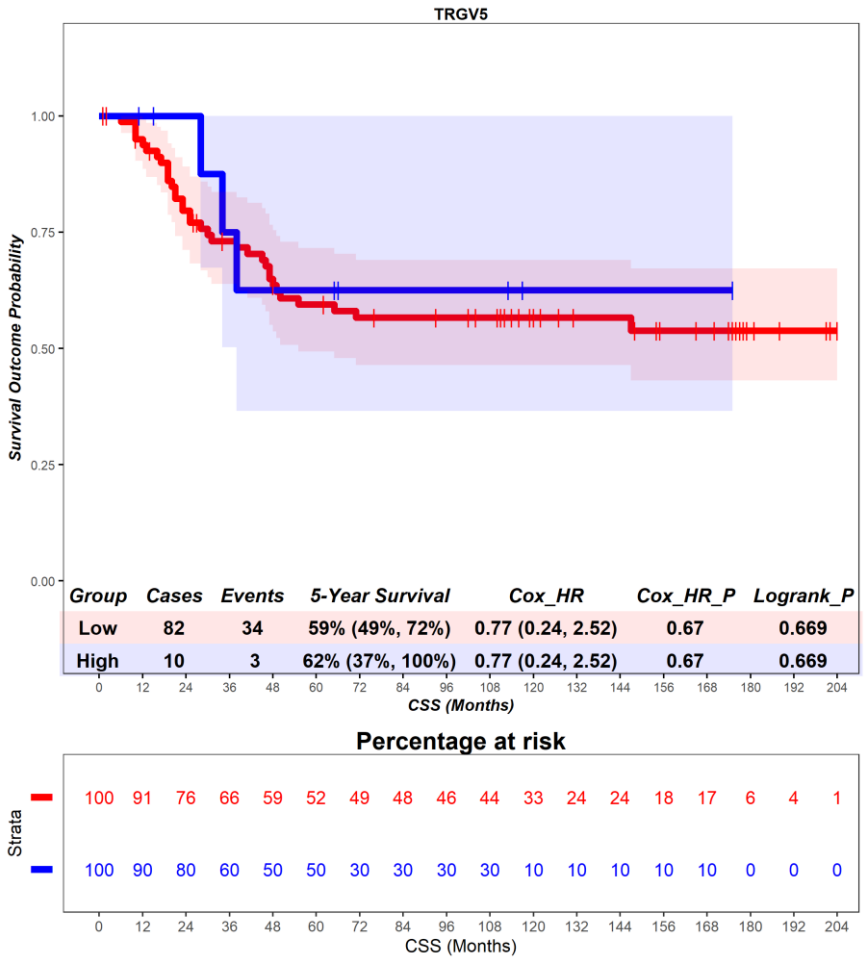

Figure 6.16 – Time-to-event (cancer-specific survival) analysis for TRGV5 expression in the primary tumour. *Patients deemed 'High' or 'Low' for TRGV5 expression are shaded blue and red, respectively. Cox hazard ratio is univariate. The 'Low' group is used as the reference group on cox regression modelling.*

CSS was investigated in the context of transcriptional classification by *TRGV8*, which encodes the Vγ8 chain. In the primary tumour, patients deemed high for *TRGV8* expression are associated with no difference in prognosis (Figure 6.17). Patients with a high expression of *TRGV8* had a mean survival time of 69.90 months, compared to those with low expression of *TRGV8* with a mean survival of 84.35 months (hazard ratio = 1.76, p = 0.21). 5-year survival for patients high for *TRGV8* expression is 35% (14%, 86%), compared to 63% (53%, 75%) in the *TRGV8* low group. This suggests that *TRGV8* expression in the primary tumour has no prognostic role.

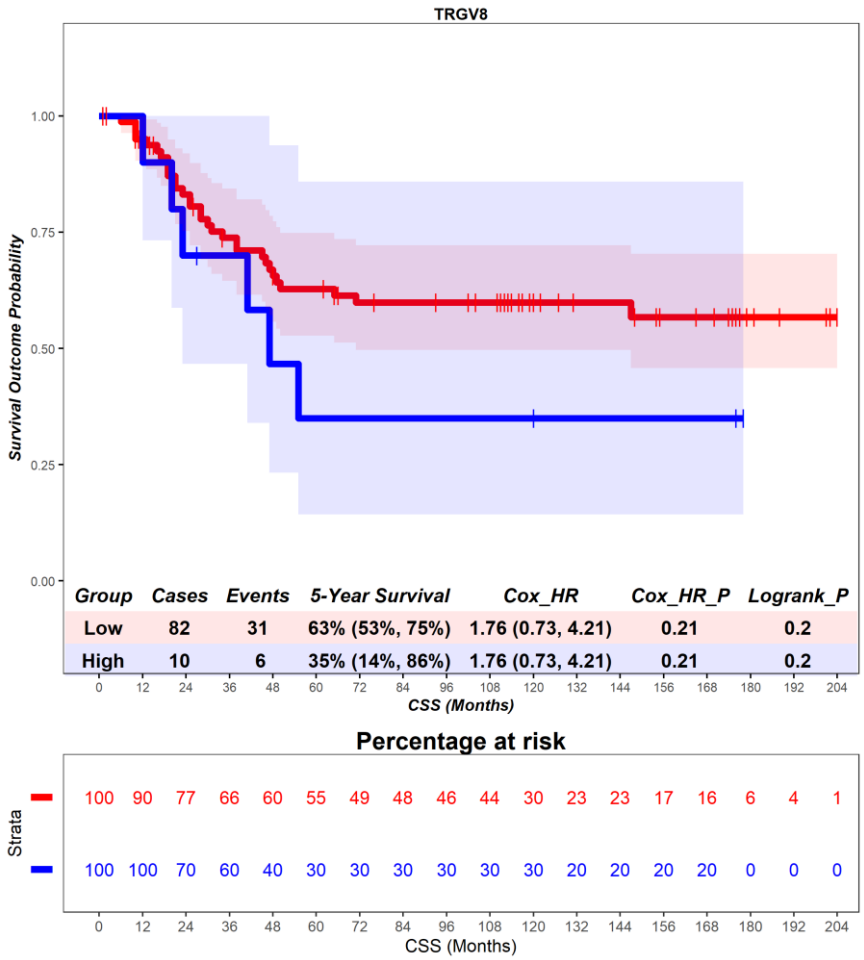

Figure 6.17 – Time-to-event (cancer-specific survival) analysis for TRGV8 expression in the primary tumour. *Patients deemed 'High' or 'Low' for TRGV8 expression are shaded blue and red, respectively. Cox hazard ratio is univariate. The 'Low' group is used as the reference group on cox regression modelling.*

CSS was investigated in the context of transcriptional classification by *TRGV9*, which encodes the Vγ9 chain. In the primary tumour, patients deemed high for *TRGV9* expression are associated with a favourable prognosis (Figure 6.18). Patients with a high expression of *TRGV9* had a mean survival time of 106.57 months, compared to those with low expression of *TRGV9* with a mean survival of 78.51 months (hazard ratio = 0.25, p = 0.06). 5-year survival for patients high for *TRGV9* expression is 84% (66%, 100%), compared to 56% (45%, 68%) in the *TRGV9* low group. This suggests that *TRGV9* expression in the primary tumour has a favourable prognostic role.

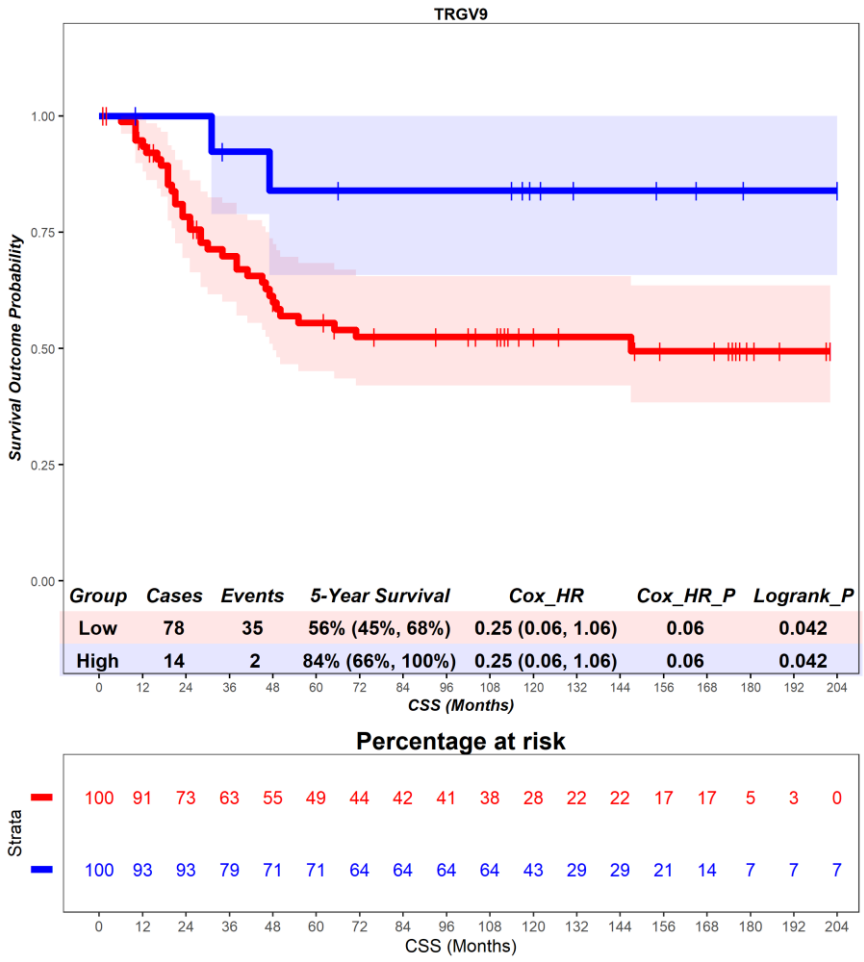

Figure 6.18 – Time-to-event (cancer-specific survival) analysis for TRGV9 expression in the primary tumour. *Patients deemed 'High' or 'Low' for TRGV9 expression are shaded blue and red, respectively. Cox hazard ratio is univariate. The 'Low' group is used as the reference group on cox regression modelling.*

CSS was investigated in the context of transcriptional classification by *TRGV10*, which encodes the Vγ10 chain. In the primary tumour, patients deemed high for *TRGV10* expression are associated with an unfavourable prognosis (Figure 6.19). Patients with a high expression of *TRGV10* had a mean survival time of 78.20 months, compared to those with low expression of *TRGV10* with a mean survival of 98.29 months (hazard ratio = 2.13, p = 0.12). 5-year survival for patients high for *TRGV10* expression is 54% (43%, 68%), compared to 79% (63%, 100%) in the *TRGV10* low group. This suggests that *TRGV10* expression in the primary tumour has an unfavourable prognostic role.

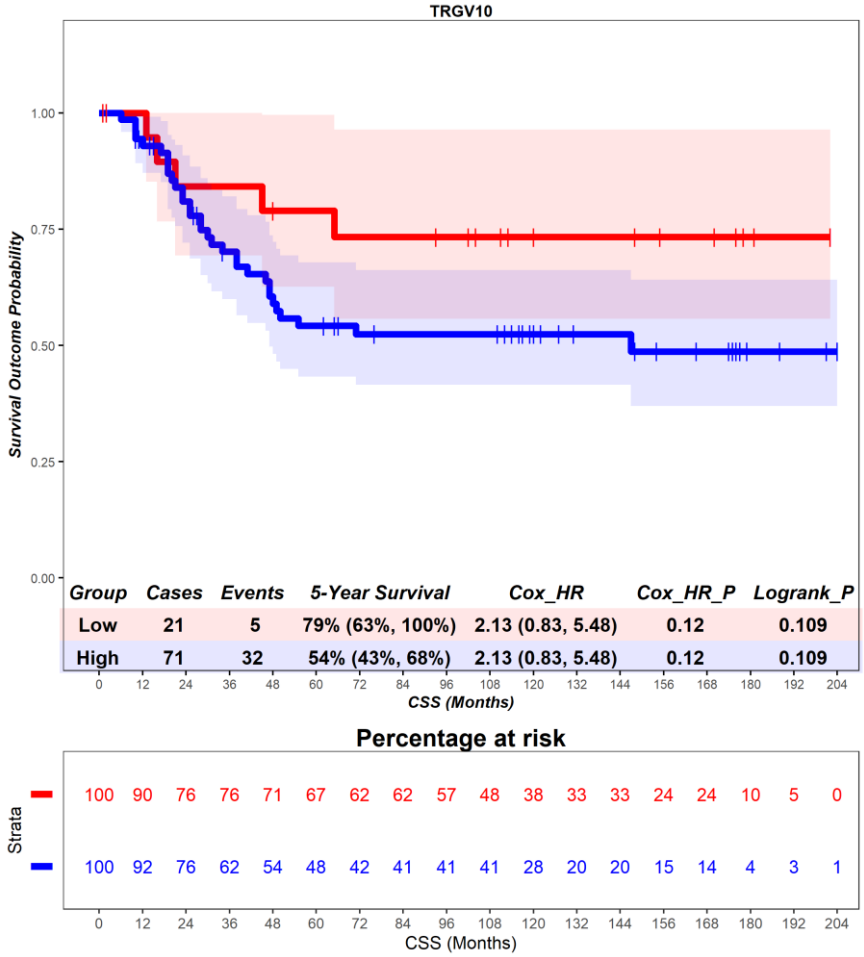

Figure 6.19 – Time-to-event (cancer-specific survival) analysis for TRGV10 expression in the primary tumour. *Patients deemed 'High' or 'Low' for TRGV10 expression are shaded blue and red, respectively. Cox hazard ratio is univariate. The 'Low' group is used as the reference group on cox regression modelling.*

CSS was investigated in the context of transcriptional classification by *TRGV11*, which encodes the Vγ11 chain. In the primary tumour, patients deemed high for *TRGV11* expression are associated with no difference in prognosis (Figure 6.20). Patients with a high expression of TRGV11 had a mean survival time of 102.18 months, compared to those with low expression of *TRGV11* with a mean survival of 80.15 months (hazard ratio = 0.59, p = 0.38). 5-year survival for patients high for *TRGV11* expression is 71% (48%, 100%), compared to 58% (48%, 71%) in the *TRGV11* low group. This suggests that *TRGV11* expression in the primary tumour has no prognostic role.

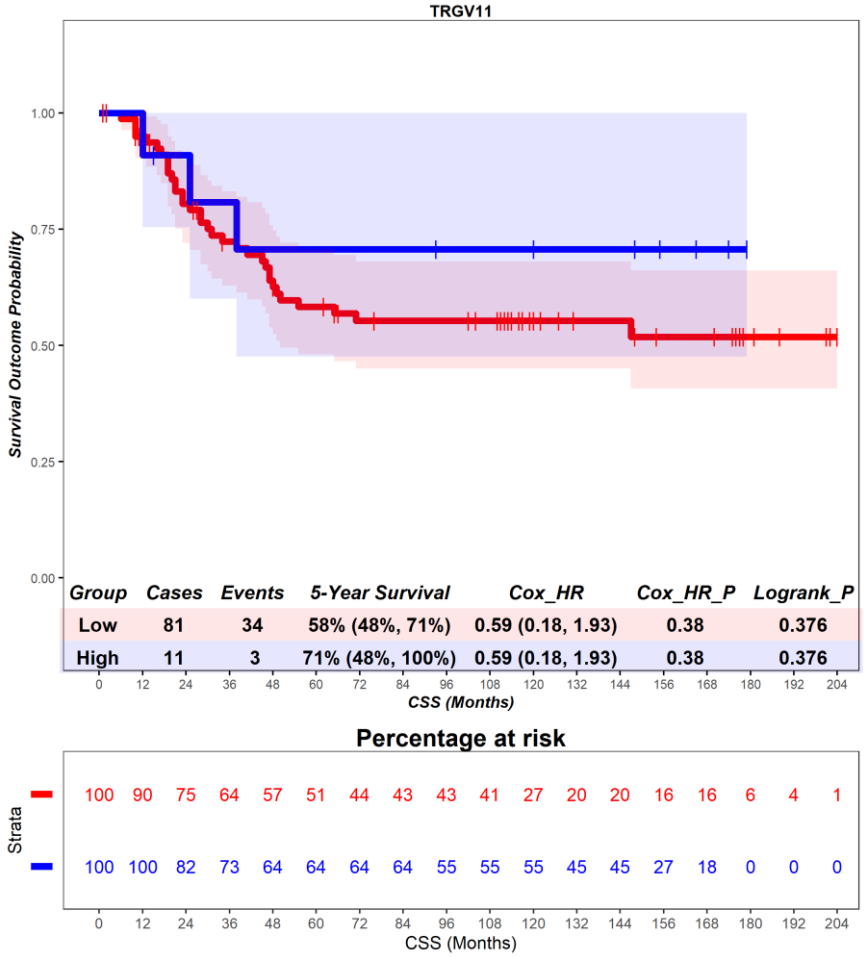

Figure 6.20 – Time-to-event (cancer-specific survival) analysis for TRGV11 expression in the primary tumour. *Patients deemed 'High' or 'Low' for TRGV11 expression are shaded blue and red, respectively. Cox hazard ratio is univariate. The 'Low' group is used as the reference group on cox regression modelling.*

6.4.2 γδ T cells - overall survival

OS was investigated in the context of transcriptional classification by *TRDV1*, which encodes the Vδ1 chain. In the primary tumour, patients deemed high for *TRDV1* expression are associated with an unfavourable prognosis (Figure 6.21). Patients with a high expression of *TRDV1* had a mean survival time of 63.98 months, compared to those with low expression of *TRDV1* with a mean survival of 97.25 months (hazard ratio = 1.85, p = 0.02). 5-year survival for patients high for *TRDV1* expression is 37% (25%, 56%), compared to 63% (52%, 78%) in the *TRDV1* low group. This suggests that *TRDV1* expression in the primary tumour has an unfavourable prognostic role.

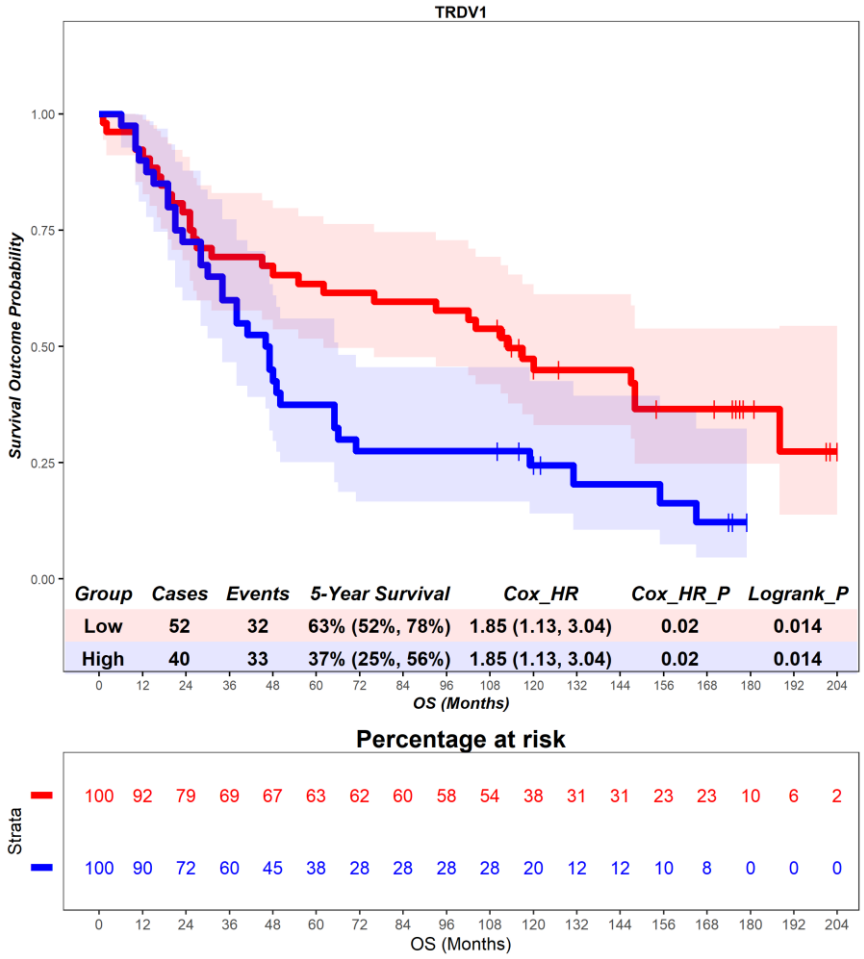

Figure 6.21 – Time-to-event (overall survival) analysis for TRDV1 expression in the primary tumour. *Patients deemed 'High' or 'Low' for TRDV1 expression are shaded blue and red, respectively. Cox hazard ratio is univariate. The 'Low' group is used as the reference group on cox regression modelling.*

OS was investigated in the context of transcriptional classification by *TRDV2*, which encodes the Vδ2 chain. In the primary tumour, patients deemed high for *TRDV2* expression are associated with no difference in prognosis (Figure 6.22). Patients with a high expression of *TRDV2* had a mean survival time of 65.60 months, compared to those with low expression of *TRDV2* with a mean survival of 84.88 months (hazard ratio = 1.48, p = 0.3). 5-year survival for patients high for *TRDV2* expression is 50% (27%, 93%), compared to 52% (43%, 64%) in the *TRDV2* low group. This suggests that *TRDV2* expression in the primary tumour has no prognostic role.

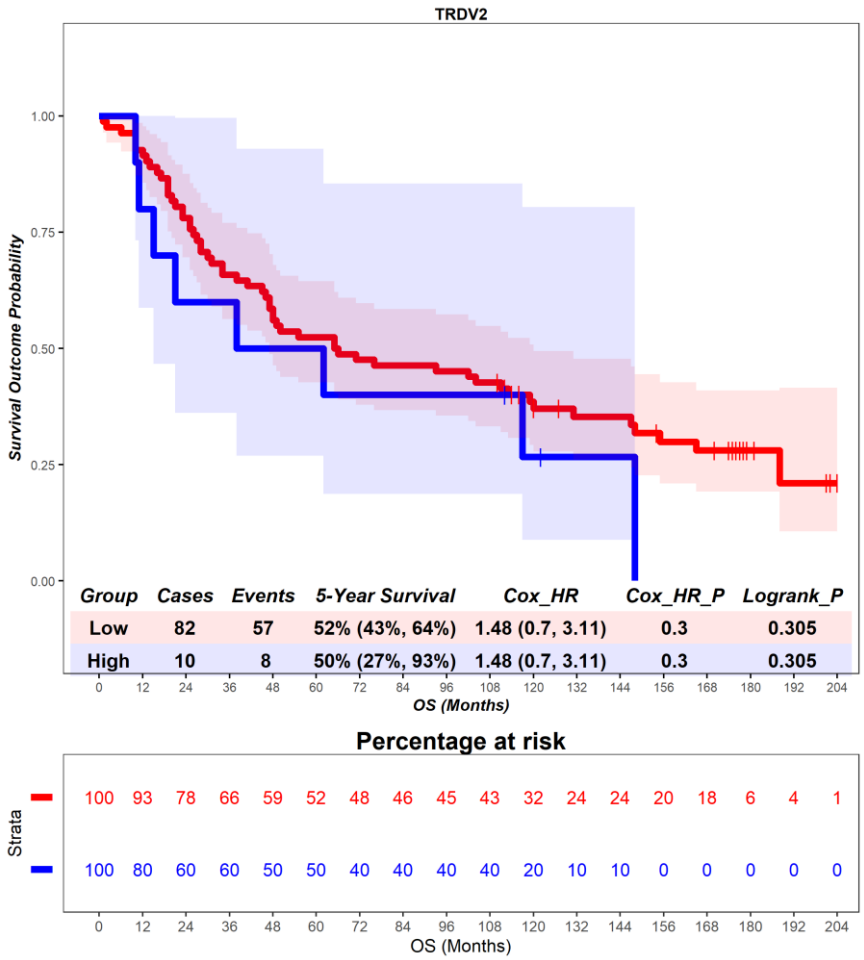

Figure 6.22 – Time-to-event (overall survival) analysis for TRDV2 expression in the primary tumour. *Patients deemed 'High' or 'Low' for TRDV2 expression are shaded blue and red, respectively. Cox hazard ratio is univariate. The 'Low' group is used as the reference group on cox regression modelling.*

OS was investigated in the context of transcriptional classification by *TRDV3*, which encodes the Vδ3 chain. In the primary tumour, patients deemed high for *TRDV3* expression are associated with no difference in prognosis (Figure 6.23). Patients with a high expression of *TRDV3* had a mean survival time of 85.21 months, compared to those with low expression of *TRDV3* with a mean survival of 82.35 months (hazard ratio = 0.76, p = 0.47). 5-year survival for patients high for *TRDV3* expression is 57% (36%, 90%), compared to 51% (41%, 64%) in the *TRDV3* low group. This suggests that *TRDV3* expression in the primary tumour has no prognostic role.

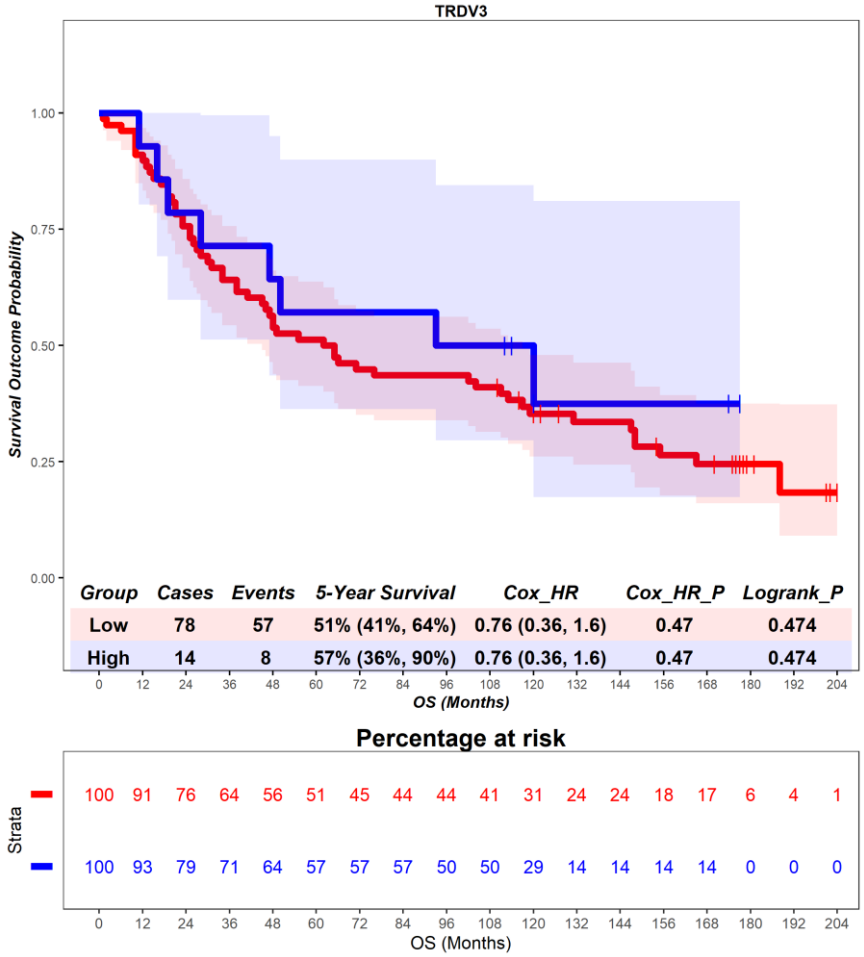

Figure 6.23 – Time-to-event (overall survival) analysis for TRDV3 expression in the primary tumour. *Patients deemed 'High' or 'Low' for TRDV3 expression are shaded blue and red, respectively. Cox hazard ratio is univariate. The 'Low' group is used as the reference group on cox regression modelling.*

OS was investigated in the context of transcriptional classification by *TRGV1*, which encodes the Vγ1 chain. In the primary tumour, patients deemed high for *TRGV1* expression are associated with no difference in prognosis (Figure 6.24). Patients with a high expression of *TRGV1* had a mean survival time of 96.30 months, compared to those with low expression of *TRGV1* with a mean survival of 81.13 months (hazard ratio = 0.83, p = 0.63). 5-year survival for patients high for *TRGV1* expression is 80% (59%, 100%), compared to 49% (39%, 61%) in the *TRGV1* low group. This suggests that *TRGV1* expression in the primary tumour has no prognostic role.

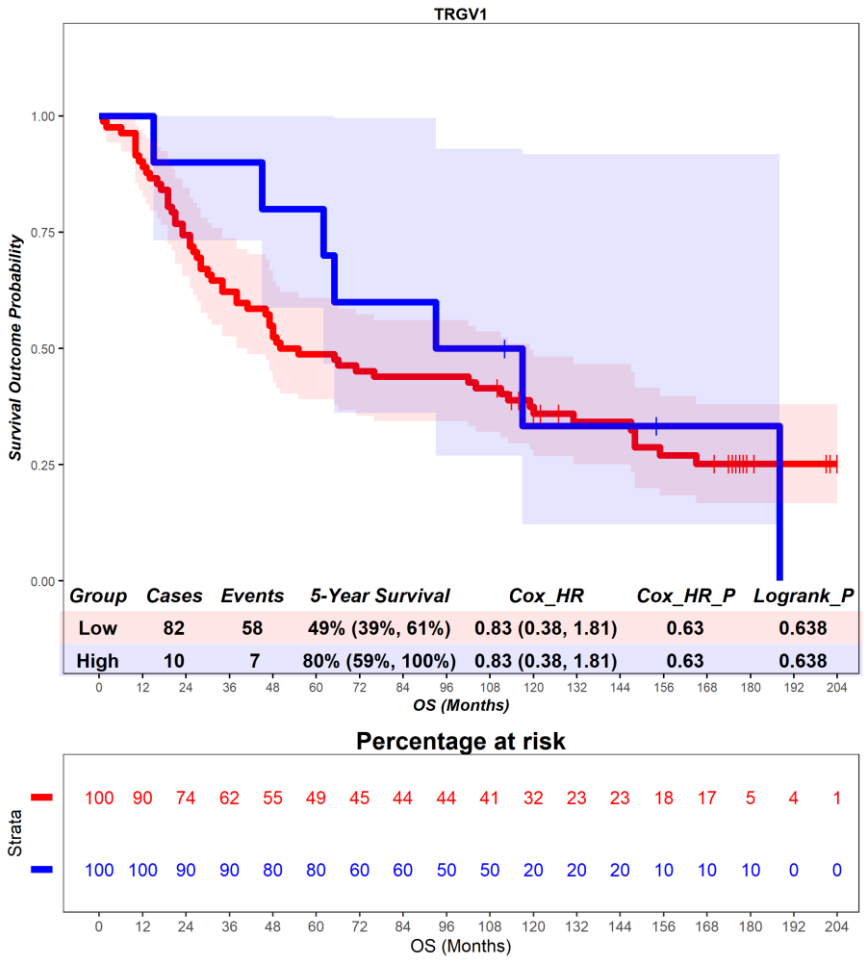

Figure 6.24 – Time-to-event (overall survival) analysis for TRGV1 expression in the primary tumour. *Patients deemed 'High' or 'Low' for TRGV1 expression are shaded blue and red, respectively. Cox hazard ratio is univariate. The 'Low' group is used as the reference group on cox regression modelling.*

OS was investigated in the context of transcriptional classification by *TRGV2*, which encodes the Vγ2 chain. In the primary tumour, patients deemed high for *TRGV2* expression are associated with no difference in prognosis (Figure 6.25). Patients with a high expression of *TRGV2* had a mean survival time of 67.88 months, compared to those with low expression of *TRGV2* with a mean survival of 86.16 months (hazard ratio = 1.28, p = 0.42). 5-year survival for patients high for *TRGV2* expression is 35% (19%, 67%), compared to 56% (46%, 68%) in the *TRGV2* low group. This suggests that *TRGV2* expression in the primary tumour has no prognostic role.

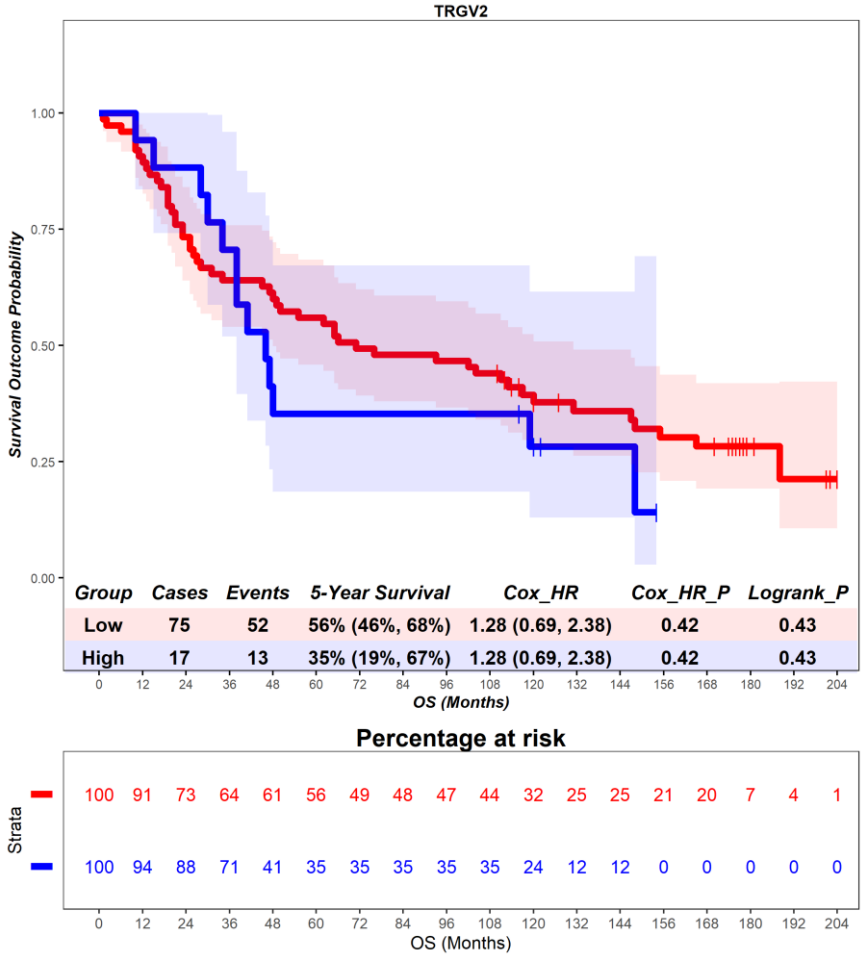

Figure 6.25 – Time-to-event (overall survival) analysis for TRGV2 expression in the primary tumour. *Patients deemed 'High' or 'Low' for TRGV2 expression are shaded blue and red, respectively. Cox hazard ratio is univariate. The 'Low' group is used as the reference group on cox regression modelling.*

OS was investigated in the context of transcriptional classification by *TRGV3*, which encodes the Vγ3 chain. In the primary tumour, patients deemed high for *TRGV3* expression are associated with no difference in prognosis (Figure 6.26). Patients with a high expression of *TRGV3* had a mean survival time of 59.58 months, compared to those with low expression of *TRGV3* with a mean survival of 86.26 months (hazard ratio = 1.41, p = 0.34). 5-year survival for patients high for *TRGV3* expression is 33% (15%, 74%), compared to 55% (45%, 67%) in the *TRGV3* low group. This suggests that *TRGV3* expression in the primary tumour has no prognostic role.

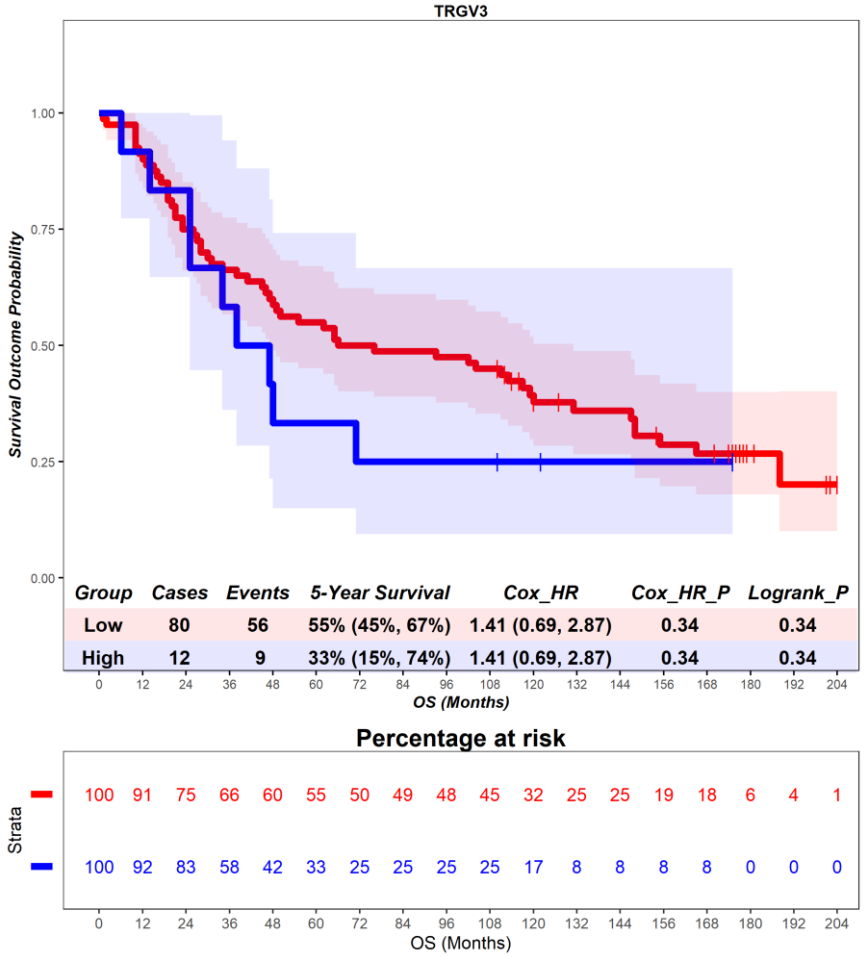

Figure 6.26 – Time-to-event (overall survival) analysis for TRGV3 expression in the primary tumour. *Patients deemed 'High' or 'Low' for TRGV3 expression are shaded blue and red, respectively. Cox hazard ratio is univariate. The 'Low' group is used as the reference group on cox regression modelling.*

OS was investigated in the context of transcriptional classification by *TRGV4*, which encodes the Vγ4 chain. In the primary tumour, patients deemed high for *TRGV4* expression are associated with a favourable prognosis (Figure 6.27). Patients with a high expression of *TRGV4* had a mean survival time of 116.82 months, compared to those with low expression of *TRGV4* with a mean survival of 78.16 months (hazard ratio = 0.42, p = 0.06). 5-year survival for patients high for *TRGV4* expression is 73% (51%, 100%), compared to 49% (40%, 62%) in the *TRGV4* low group. This suggests that *TRGV4* expression in the primary tumour has a favourable prognostic role.

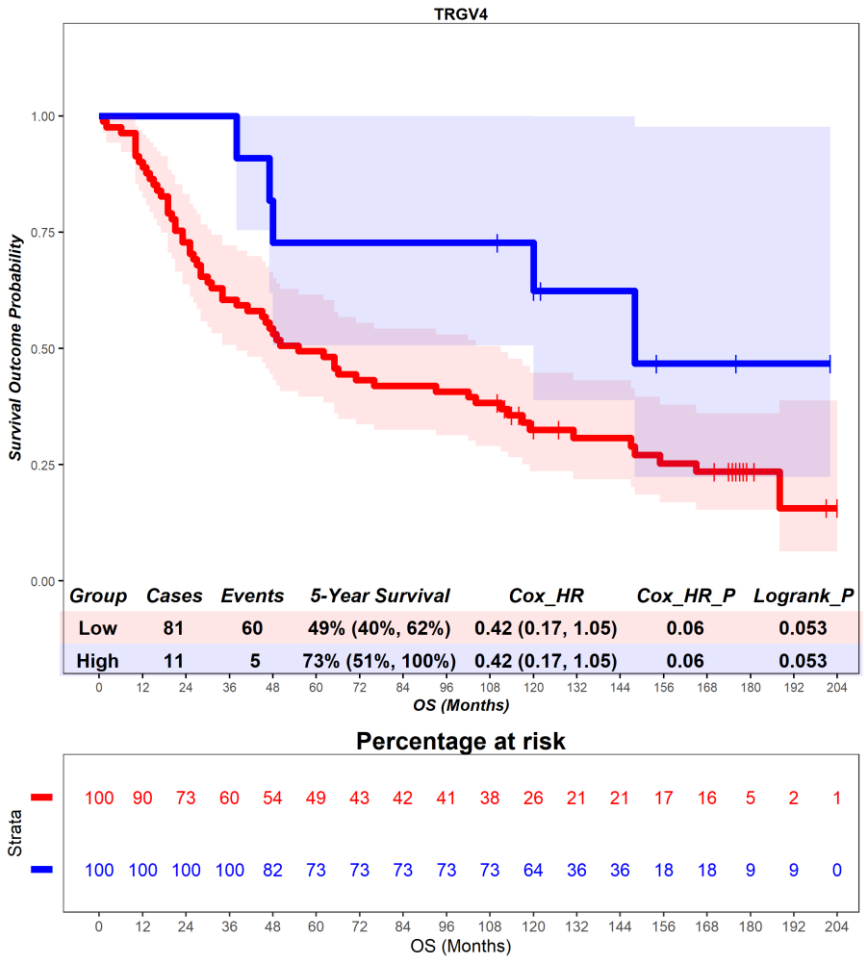

Figure 6.27 – Time-to-event (overall survival) analysis for TRGV4 expression in the primary tumour. *Patients deemed 'High' or 'Low' for TRGV4 expression are shaded blue and red, respectively. Cox hazard ratio is univariate. The 'Low' group is used as the reference group on cox regression modelling.*

OS was investigated in the context of transcriptional classification by *TRGV5*, which encodes the Vγ5 chain. In the primary tumour, patients deemed high for *TRGV5* expression are associated with no difference in prognosis (Figure 6.28). Patients with a high expression of *TRGV5* had a mean survival time of 66.20 months, compared to those with low expression of *TRGV5* with a mean survival of 84.80 months (hazard ratio = 1.57, p = 0.21). 5-year survival for patients high for *TRGV5* expression is 50% (27%, 93%), compared to 52% (43%, 64%) in the *TRGV5* low group. This suggests that *TRGV5* expression in the primary tumour has no prognostic role.

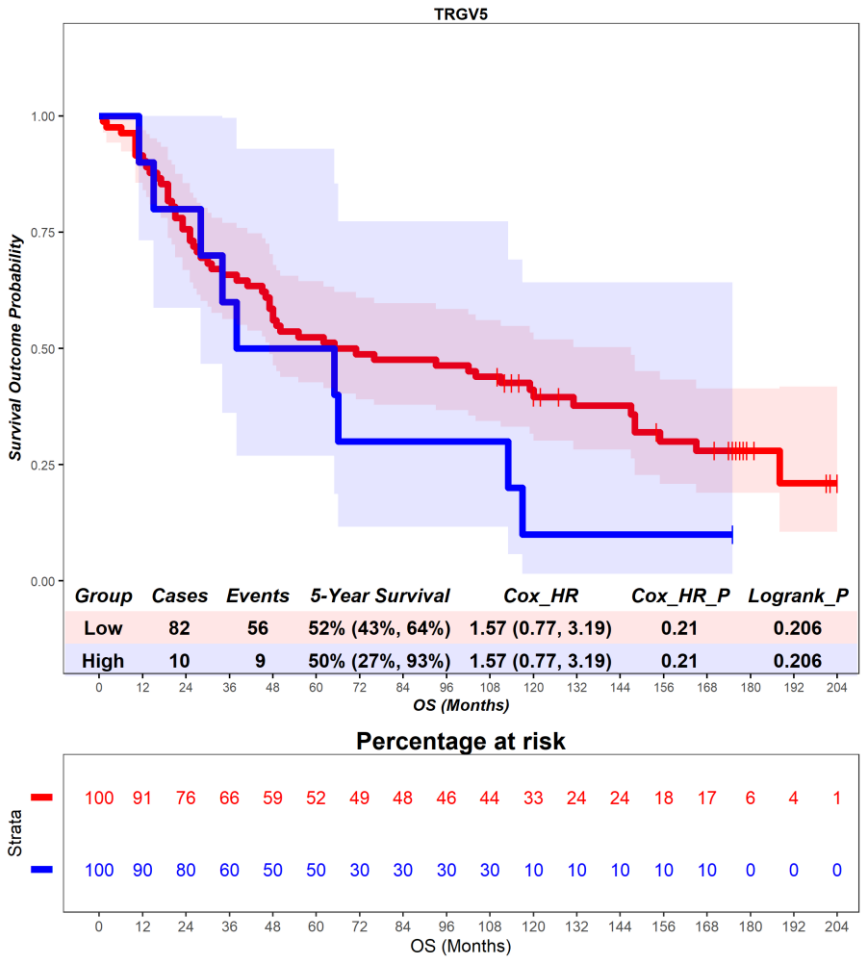

Figure 6.28 – Time-to-event (overall survival) analysis for TRGV5 expression in the primary tumour. *Patients deemed 'High' or 'Low' for TRGV5 expression are shaded blue and red, respectively. Cox hazard ratio is univariate. The 'Low' group is used as the reference group on cox regression modelling.*

OS was investigated in the context of transcriptional classification by *TRGV8*, which encodes the Vγ8 chain. In the primary tumour, patients deemed high for *TRGV8* expression are associated with no difference in prognosis (Figure 6.29). Patients with a high expression of *TRGV8* had a mean survival time of 69.90 months, compared to those with low expression of *TRGV8* with a mean survival of 84.35 months (hazard ratio = 1.14, p = 0.75). 5-year survival for patients high for *TRGV8* expression is 30% (12%, 77%), compared to 55% (45%, 67%) in the *TRGV8* low group. This suggests that *TRGV8* expression in the primary tumour has no prognostic role.

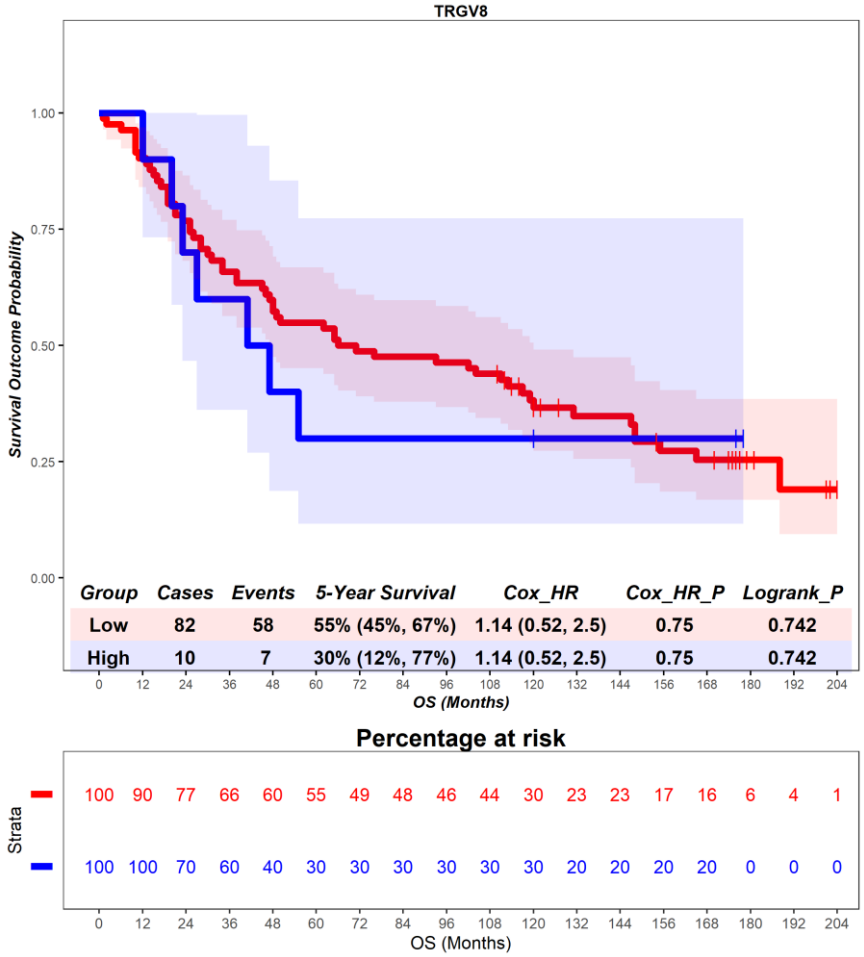

Figure 6.29 – Time-to-event (overall survival) analysis for TRGV8 expression in the primary tumour. *Patients deemed 'High' or 'Low' for TRGV8 expression are shaded blue and red, respectively. Cox hazard ratio is univariate. The 'Low' group is used as the reference group on cox regression modelling.*

OS was investigated in the context of transcriptional classification by *TRGV9*, which encodes the Vγ9 chain. In the primary tumour, patients deemed high for *TRGV9* expression are associated with no difference in prognosis (Figure 6.30). Patients with a high expression of *TRGV9* had a mean survival time of 106.57 months, compared to those with low expression of *TRGV9* with a mean survival of 78.51 months (hazard ratio = 0.68, p = 0.28). 5-year survival for patients high for *TRGV9* expression is 71% (51%, 99%), compared to 49% (39%, 61%) in the *TRGV9* low group. This suggests that *TRGV9* expression in the primary tumour has no prognostic role.

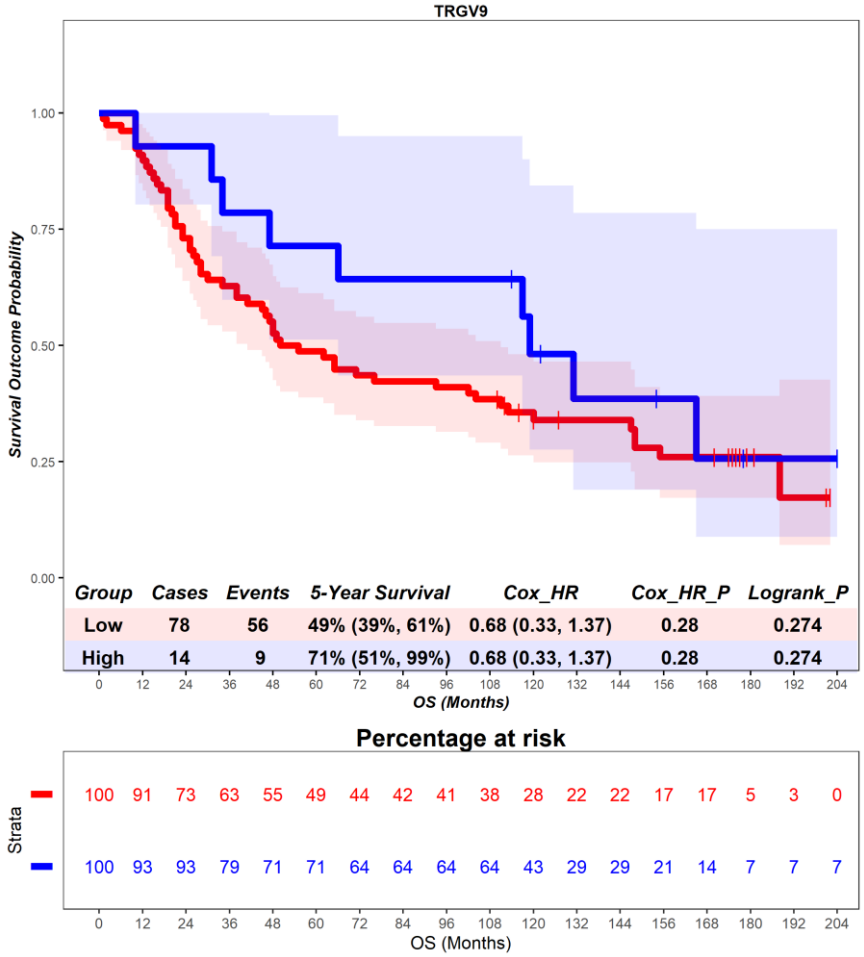

Figure 6.30 – Time-to-event (overall survival) analysis for TRGV9 expression in the primary tumour. *Patients deemed 'High' or 'Low' for TRGV9 expression are shaded blue and red, respectively. Cox hazard ratio is univariate. The 'Low' group is used as the reference group on cox regression modelling.*

OS was investigated in the context of transcriptional classification by *TRGV10*, which encodes the Vγ10 chain. In the primary tumour, patients deemed high for *TRGV10* expression are associated with no difference in prognosis (Figure 6.31). Patients with a high expression of *TRGV10* had a mean survival time of 78.20 months, compared to those with low expression of *TRGV10* with a mean survival of 98.29 months (hazard ratio = 1.17, p = 0.59). 5-year survival for patients high for *TRGV10* expression is 48% (38%, 61%), compared to 67% (49%, 90%) in the *TRGV10* low group. This suggests that *TRGV10* expression in the primary tumour has no prognostic role.

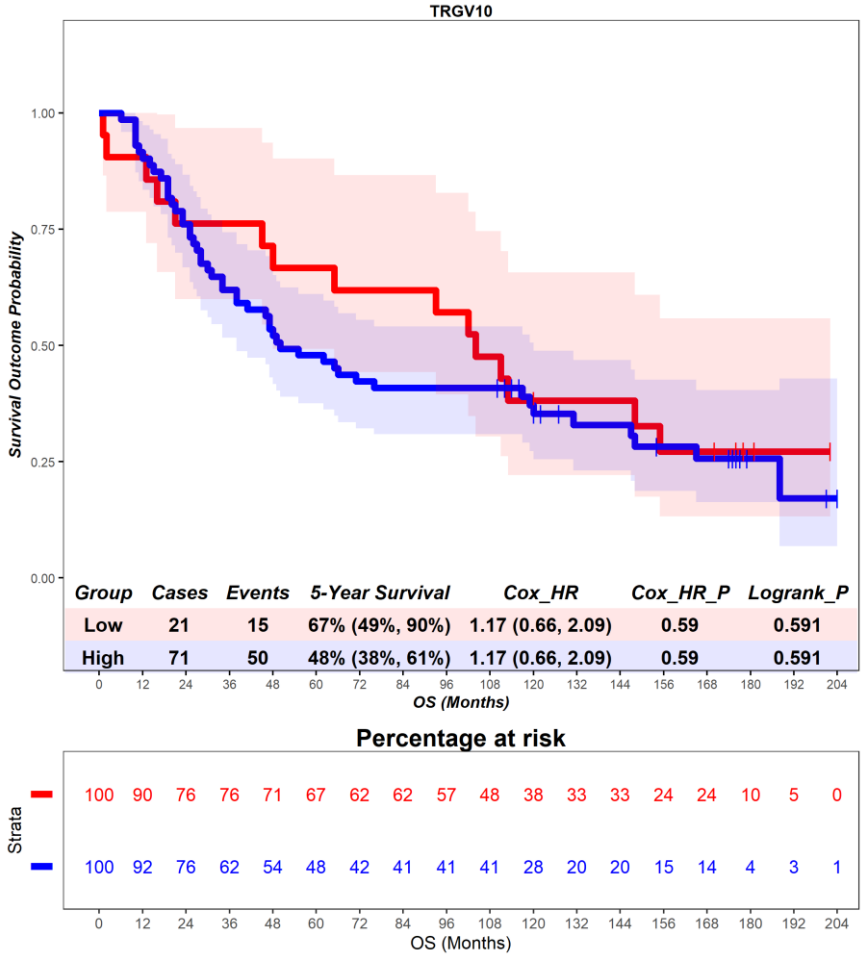

Figure 6.31 – Time-to-event (overall survival) analysis for TRGV10 expression in the primary tumour. *Patients deemed 'High' or 'Low' for TRGV10 expression are shaded blue and red, respectively. Cox hazard ratio is univariate. The 'Low' group is used as the reference group on cox regression modelling.*

OS was investigated in the context of transcriptional classification by *TRGV11*, which encodes the Vγ11 chain. In the primary tumour, patients deemed high for *TRGV11* expression are associated with no difference in prognosis (Figure 6.32). Patients with a high expression of *TRGV11* had a mean survival time of 102.18 months, compared to those with low expression of *TRGV11* with a mean survival of 80.15 months (hazard ratio = 0.97, p = 0.94). 5-year survival for patients high for *TRGV11* expression is 64% (41%, 99%), compared to 51% (41%, 63%) in the *TRGV11* low group. This suggests that *TRGV11* expression in the primary tumour has no prognostic role.

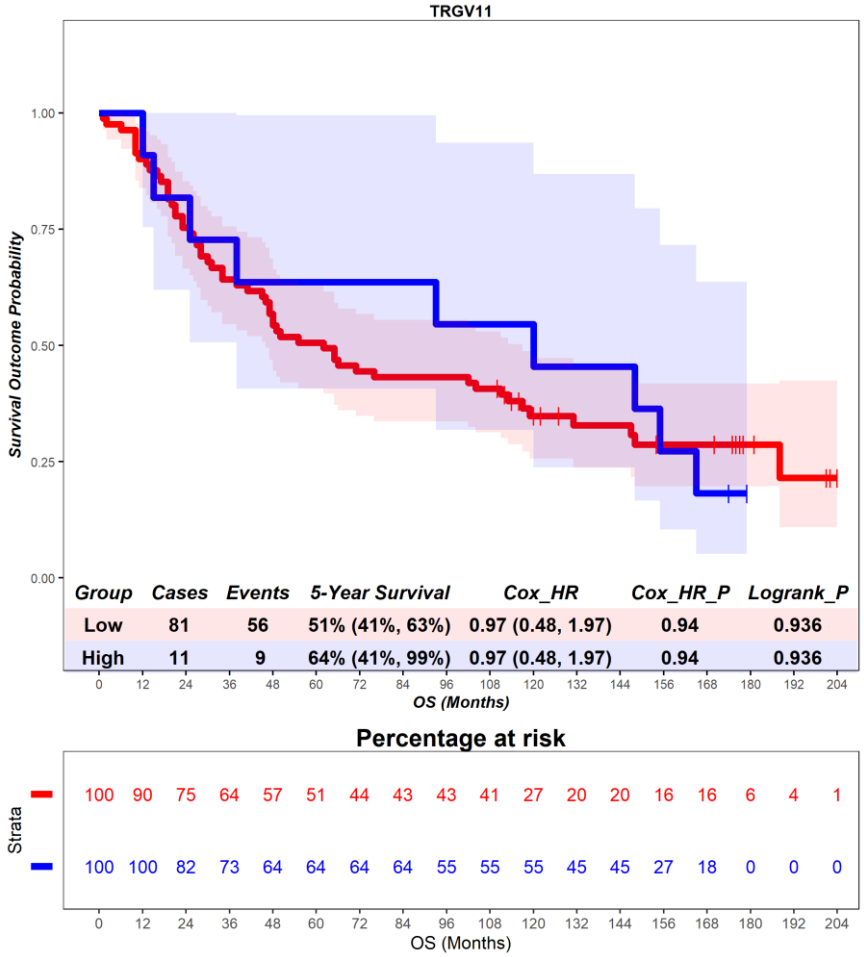

Figure 6.32 – Time-to-event (overall survival) analysis for TRGV11 expression in the primary tumour. *Patients deemed 'High' or 'Low' for TRGV11 expression are shaded blue and red, respectively. Cox hazard ratio is univariate. The 'Low' group is used as the reference group on cox regression modelling.*

6.4.3 γδ T cells – disease-free survival

DFS was investigated in the context of transcriptional classification by *TRDV1*, which encodes the Vδ1 chain. In the primary tumour, patients deemed high for *TRDV1* expression are associated with a favourable prognosis (Figure 6.33). Patients with a high expression of *TRDV1* had a mean survival time of 56.02 months, compared to those with low expression of *TRDV1* with a mean survival of 92.57 months (hazard ratio = 1.85, p = 0.01). 5-year survival for patients high for *TRDV1* expression is 32% (21%, 51%), compared to 62% (50%, 77%) in the *TRDV1* low group. This suggests that *TRDV1* expression in the primary tumour has an unfavourable prognostic role.

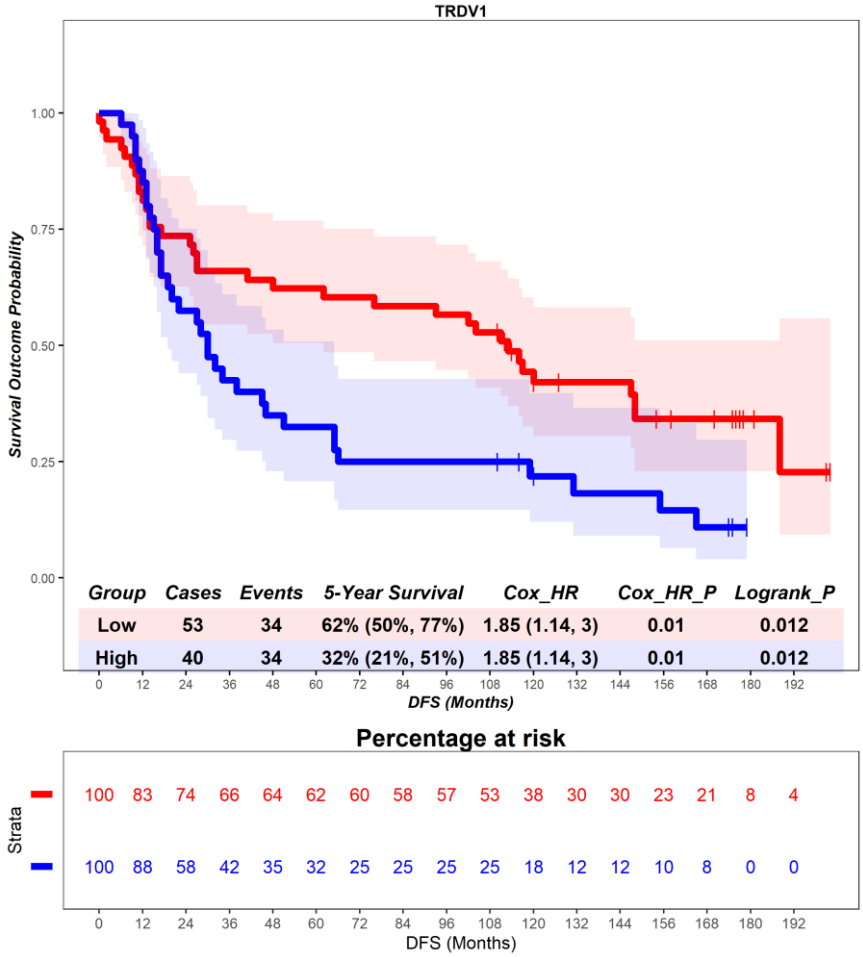

Figure 6.33 – Time-to-event (disease-free survival) analysis for TRDV1 expression in the primary tumour. *Patients deemed 'High' or 'Low' for TRDV1 expression are shaded blue and red, respectively. Cox hazard ratio is univariate. The 'Low' group is used as the reference group on cox regression modelling.*

DFS was investigated in the context of transcriptional classification by *TRDV2*, which encodes the Vδ2 chain. In the primary tumour, patients deemed high for *TRDV2* expression are associated with no difference in prognosis (Figure 6.34). Patients with a high expression of *TRDV2* had a mean survival time of 52.60 months, compared to those with low expression of *TRDV2* with a mean survival of 79.77 months (hazard ratio = 1.80, p = 0.10). 5-year survival for patients high for *TRDV2* expression is 40% (19%, 85%), compared to 51% (41%, 63%) in the *TRDV2* low group. This suggests that *TRDV2* expression in the primary tumour has no prognostic role.

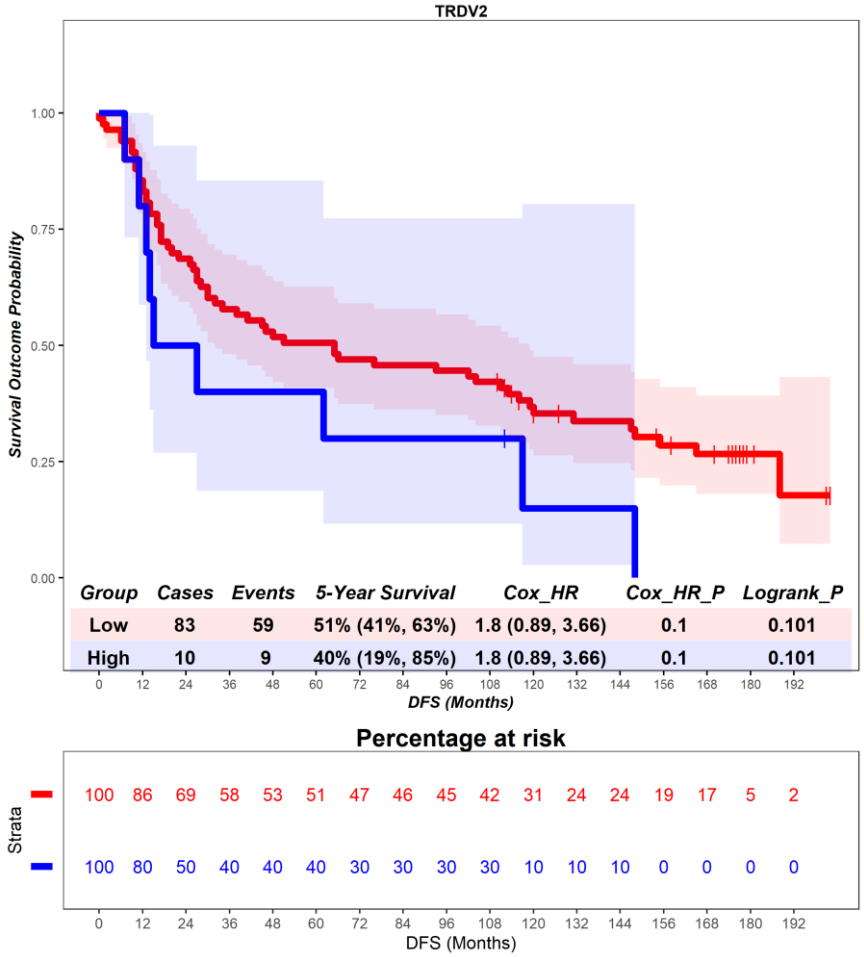

Figure 6.34 – Time-to-event (disease-free survival) analysis for TRDV2 expression in the primary tumour. *Patients deemed 'High' or 'Low' for TRDV2 expression are shaded blue and red, respectively. Cox hazard ratio is univariate. The 'Low' group is used as the reference group on cox regression modelling.*

DFS was investigated in the context of transcriptional classification by *TRDV3*, which encodes the Vδ3 chain. In the primary tumour, patients deemed high for *TRDV3* expression are associated with no difference in prognosis (Figure 6.35). Patients with a high expression of *TRDV3* had a mean survival time of 82.21 months, compared to those with low expression of *TRDV3* with a mean survival of 75.90 months (hazard ratio = 0.73, p = 0.41). 5-year survival for patients high for *TRDV3* expression is 57% (36%, 90%), compared to 48% (38%, 60%) in the *TRDV3* low group. This suggests that *TRDV3* expression in the primary tumour has no prognostic role.

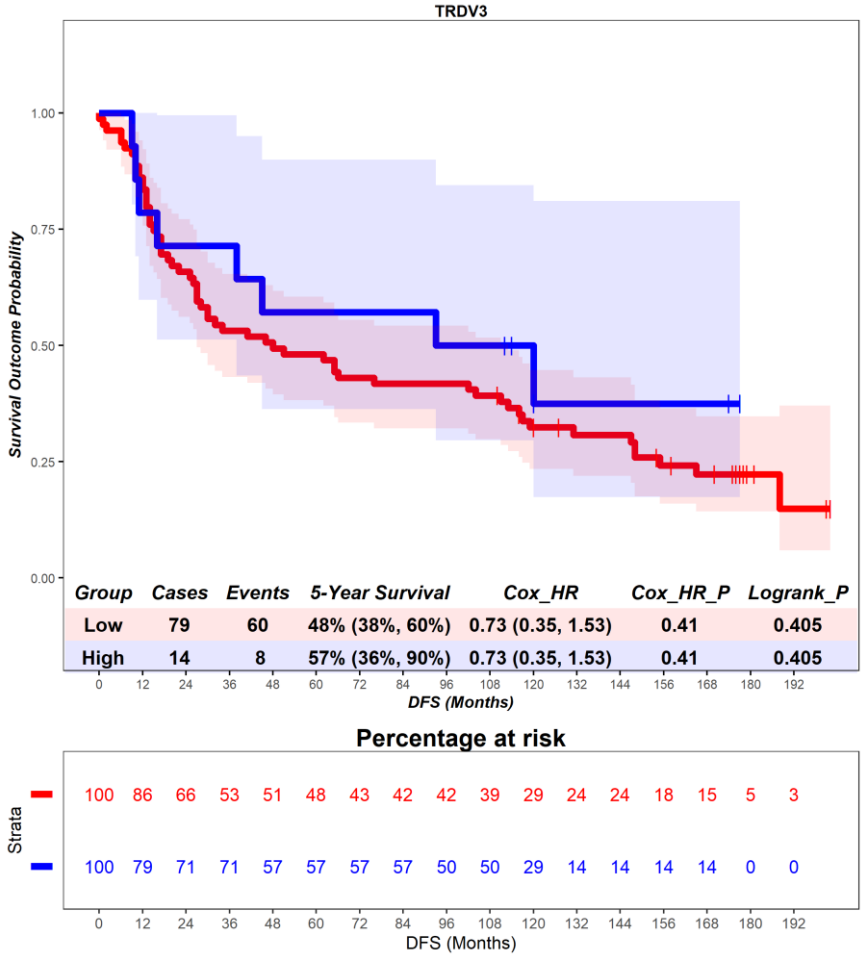

Figure 6.35 – Time-to-event (disease-free survival) analysis for TRDV3 expression in the primary tumour. *Patients deemed 'High' or 'Low' for TRDV3 expression are shaded blue and red, respectively. Cox hazard ratio is univariate. The 'Low' group is used as the reference group on cox regression modelling.*

DFS was investigated in the context of transcriptional classification by *TRGV1*, which encodes the Vγ1 chain. In the primary tumour, patients deemed high for *TRGV1* expression are associated with no difference in prognosis (Figure 6.36). Patients with a high expression of *TRGV1* had a mean survival time of 101.55 months, compared to those with low expression of *TRGV1* with a mean survival of 73.54 months (hazard ratio = 0.63, p = 0.25). 5-year survival for patients high for *TRGV1* expression is 82% (62%, 100%), compared to 45% (36%, 57%) in the *TRGV1* low group. This suggests that *TRGV1* expression in the primary tumour has no prognostic role.

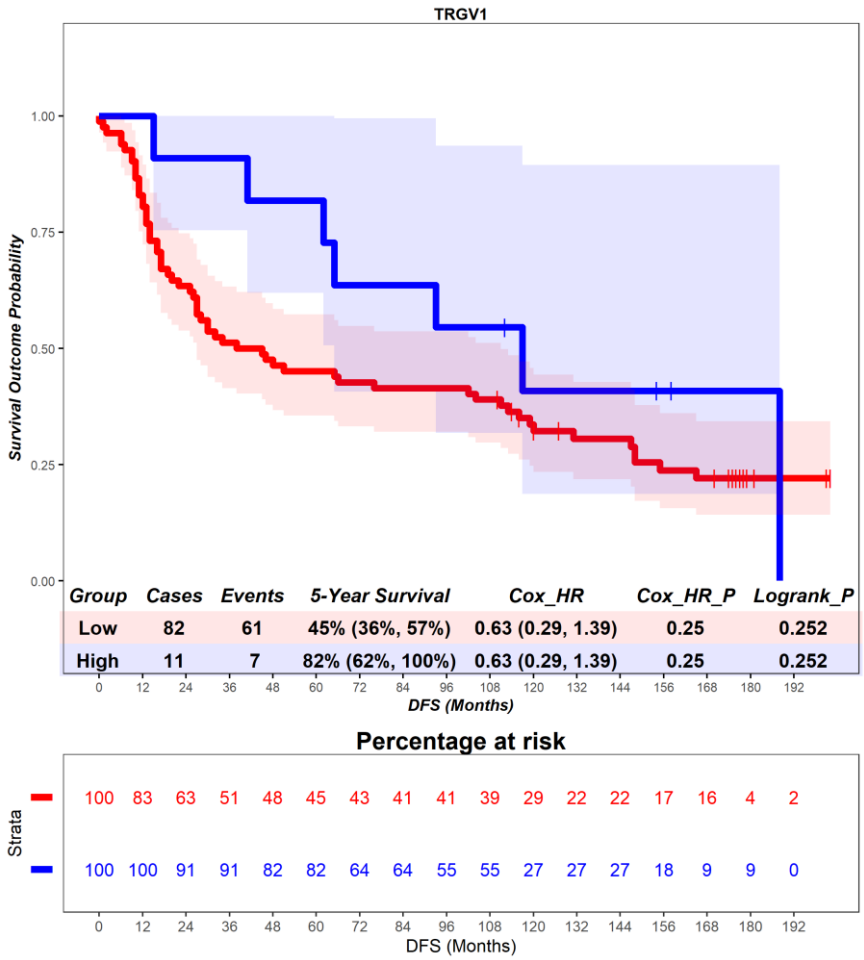

Figure 6.36 – Time-to-event (disease-free survival) analysis for TRGV1 expression in the primary tumour. *Patients deemed 'High' or 'Low' for TRGV1 expression are shaded blue and red, respectively. Cox hazard ratio is univariate. The 'Low' group is used as the reference group on cox regression modelling.*

DFS was investigated in the context of transcriptional classification by *TRGV2*, which encodes the Vγ2 chain. In the primary tumour, patients deemed high for *TRGV2* expression are associated with no difference in prognosis (Figure 6.37). Patients with a high expression of *TRGV2* had a mean survival time of 54.94 months, compared to those with low expression of *TRGV2* with a mean survival of 81.75 months (hazard ratio = 1.61, p = 0.11). 5-year survival for patients high for *TRGV2* expression is 29% (14%, 61%), compared to 54% (44%, 66%) in the *TRGV2* low group. This suggests that *TRGV2* expression in the primary tumour has no prognostic role.

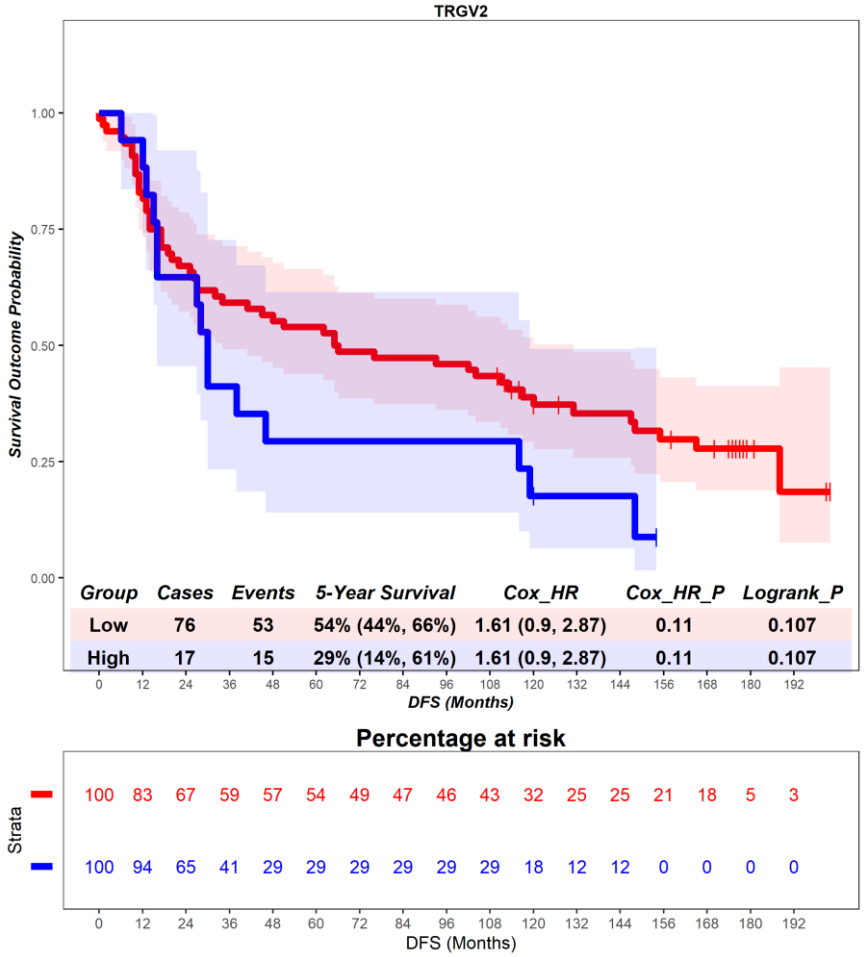

Figure 6.37 – Time-to-event (disease-free survival) analysis for TRGV2 expression in the primary tumour. *Patients deemed 'High' or 'Low' for TRGV2 expression are shaded blue and red, respectively. Cox hazard ratio is univariate. The 'Low' group is used as the reference group on cox regression modelling.*

DFS was investigated in the context of transcriptional classification by *TRGV3*, which encodes the Vγ3 chain. In the primary tumour, patients deemed high for *TRGV3* expression are associated with no difference in prognosis (Figure 6.38). Patients with a high expression of *TRGV3* had a mean survival time of 43.17 months, compared to those with low expression of *TRGV3* with a mean survival of 81.84 months (hazard ratio = 1.8, p = 0.09). 5-year survival for patients high for *TRGV3* expression is 17% (5%, 59%), compared to 54% (44%, 66%) in the *TRGV3* low group. This suggests that *TRGV3* expression in the primary tumour has no prognostic role.

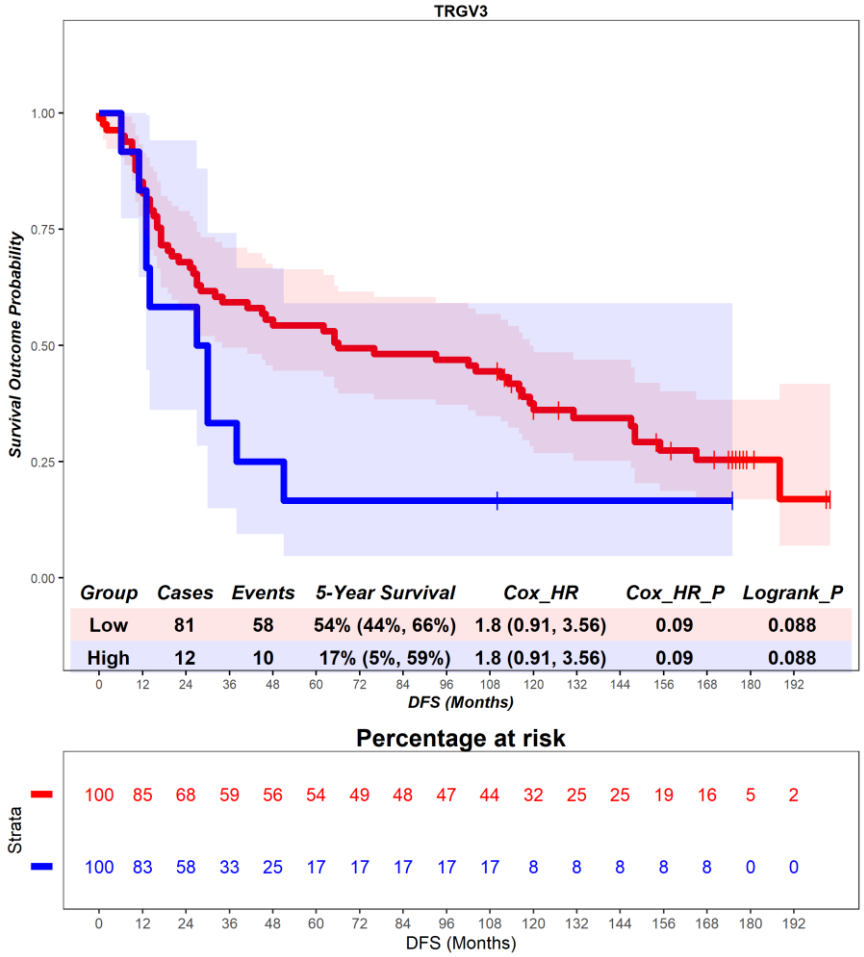

Figure 6.38 – Time-to-event (disease-free survival) analysis for TRGV3 expression in the primary tumour. *Patients deemed 'High' or 'Low' for TRGV3 expression are shaded blue and red, respectively. Cox hazard ratio is univariate. The 'Low' group is used as the reference group on cox regression modelling.*

DFS was investigated in the context of transcriptional classification by *TRGV4*, which encodes the Vγ4 chain. In the primary tumour, patients deemed high for *TRGV4* expression are associated with a favourable prognosis (Figure 6.39). Patients with a high expression of *TRGV4* had a mean survival time of 105.09 months, compared to those with low expression of *TRGV4* with a mean survival of 73.06 months (hazard ratio = 0.52, p = 0.12). 5-year survival for patients high for *TRGV4* expression is 64% (41%, 99%), compared to 48% (38%, 60%) in the *TRGV4* low group. This suggests that *TRGV4* expression in the primary tumour has a favourable prognostic role.

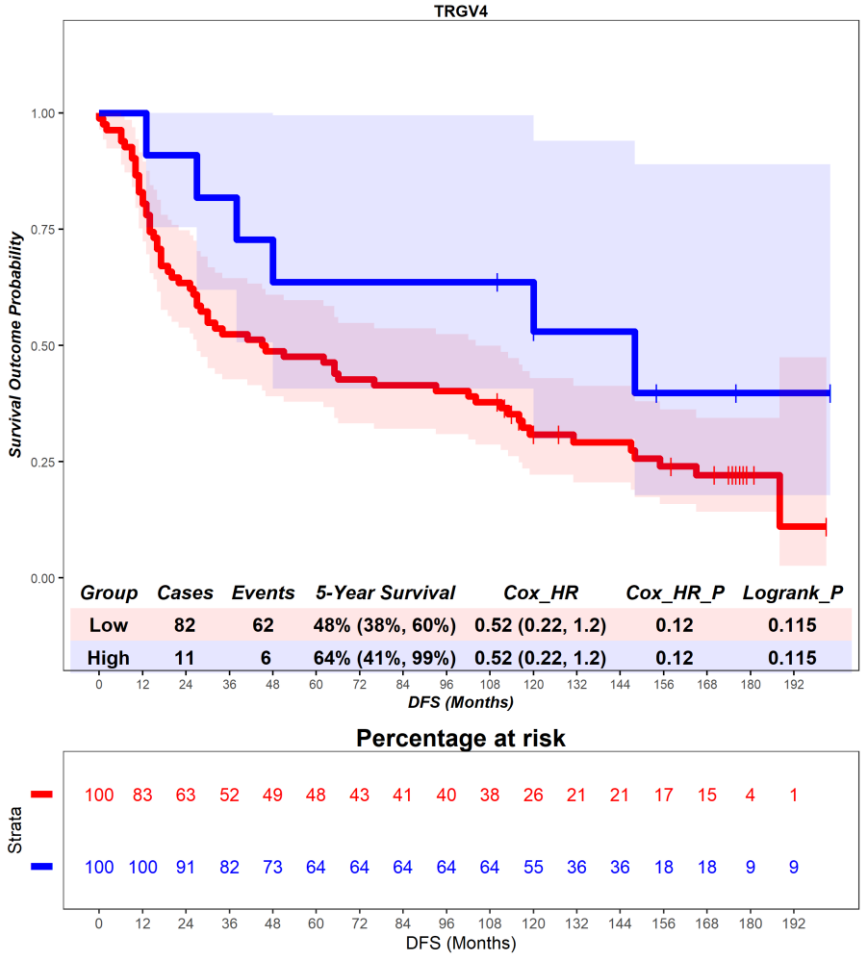

Figure 6.39 – Time-to-event (disease-free survival) analysis for TRGV4 expression in the primary tumour. *Patients deemed 'High' or 'Low' for TRGV4 expression are shaded blue and red, respectively. Cox hazard ratio is univariate. The 'Low' group is used as the reference group on cox regression modelling.*

DFS was investigated in the context of transcriptional classification by *TRGV5*, which encodes the Vγ5 chain. In the primary tumour, patients deemed high for *TRGV5* expression are associated with no difference in prognosis (Figure 6.40). Patients with a high expression of *TRGV5* had a mean survival time of 61.50 months, compared to those with low expression of *TRGV5* with a mean survival of 78.70 months (hazard ratio = 1.53, p = 0.24). 5-year survival for patients high for *TRGV5* expression is 50% (27%, 93%), compared to 49% (40%, 61%) in the *TRGV5* low group. This suggests that *TRGV5* expression in the primary tumour has no prognostic role.

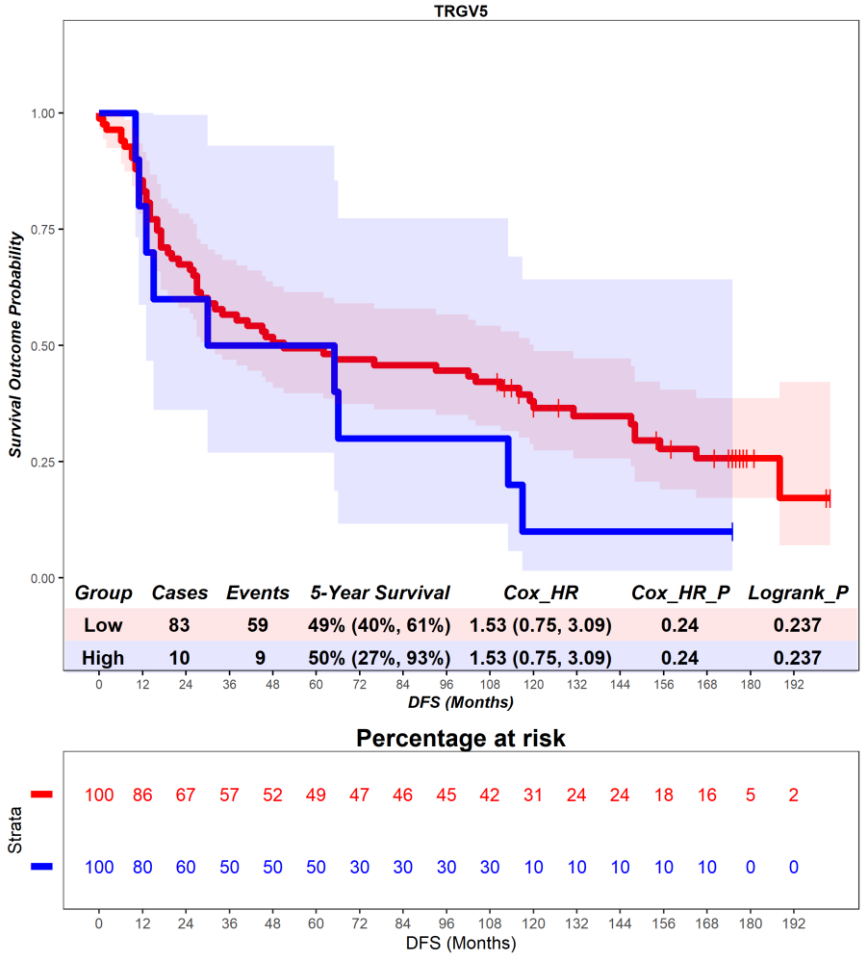

Figure 6.40 – Time-to-event (disease-free survival) analysis for TRGV5 expression in the primary tumour. *Patients deemed 'High' or 'Low' for TRGV5 expression are shaded blue and red, respectively. Cox hazard ratio is univariate. The 'Low' group is used as the reference group on cox regression modelling.*

DFS was investigated in the context of transcriptional classification by *TRGV8*, which encodes the Vγ8 chain. In the primary tumour, patients deemed high for *TRGV8* expression are associated with no difference in prognosis (Figure 6.41). Patients with a high expression of *TRGV8* had a mean survival time of 61.90 months, compared to those with low expression of *TRGV8* with a mean survival of 78.65 months (hazard ratio = 1.11, p = 0.79). 5-year survival for patients high for *TRGV8* expression is 30% (12%, 77%), compared to 52% (42%, 64%) in the *TRGV8* low group. This suggests that *TRGV8* expression in the primary tumour has no prognostic role.

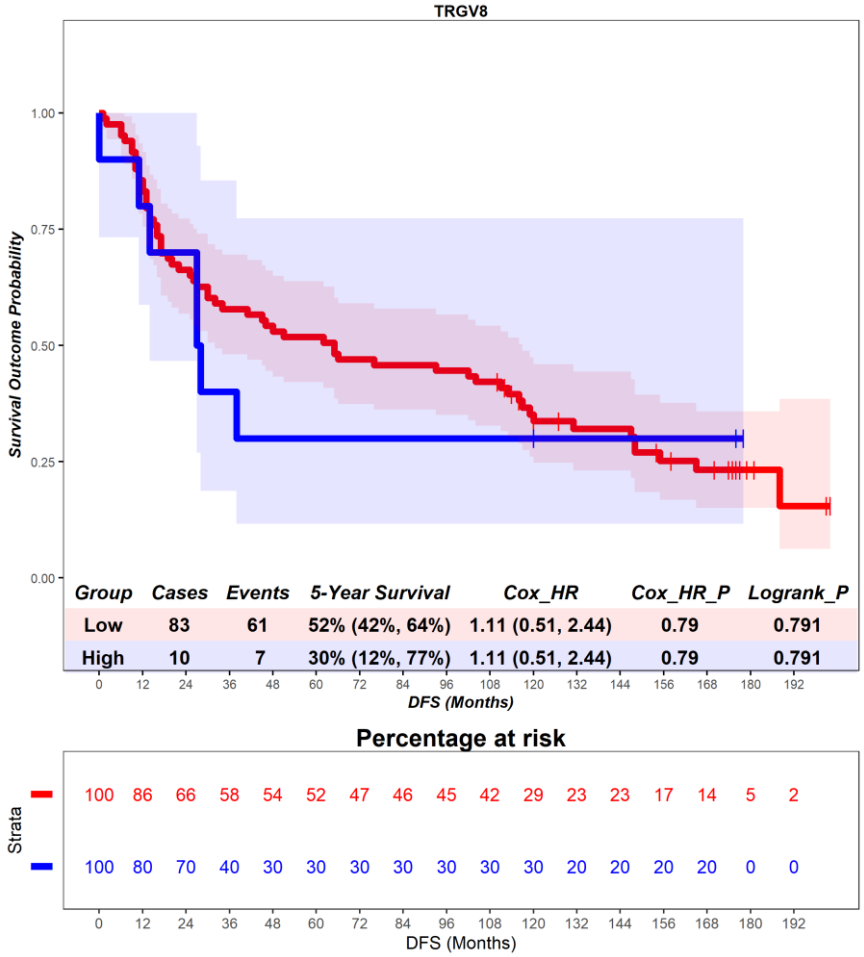

Figure 6.41 – Time-to-event (disease-free survival) analysis for TRGV8 expression in the primary tumour. *Patients deemed 'High' or 'Low' for TRGV8 expression are shaded blue and red, respectively. Cox hazard ratio is univariate. The 'Low' group is used as the reference group on cox regression modelling.*

DFS was investigated in the context of transcriptional classification by *TRGV9*, which encodes the Vγ9 chain. In the primary tumour, patients deemed high for *TRGV9* expression are associated with no difference in prognosis (Figure 6.42). Patients with a high expression of *TRGV9* had a mean survival time of 85.00 months, compared to those with low expression of *TRGV9* with a mean survival of 75.41 months (hazard ratio = 0.96, p = 0.9). 5-year survival for patients high for *TRGV9* expression is 57% (36%, 90%), compared to 48% (38%, 60%) in the *TRGV9* low group. This suggests that *TRGV9* expression in the primary tumour has no prognostic role.

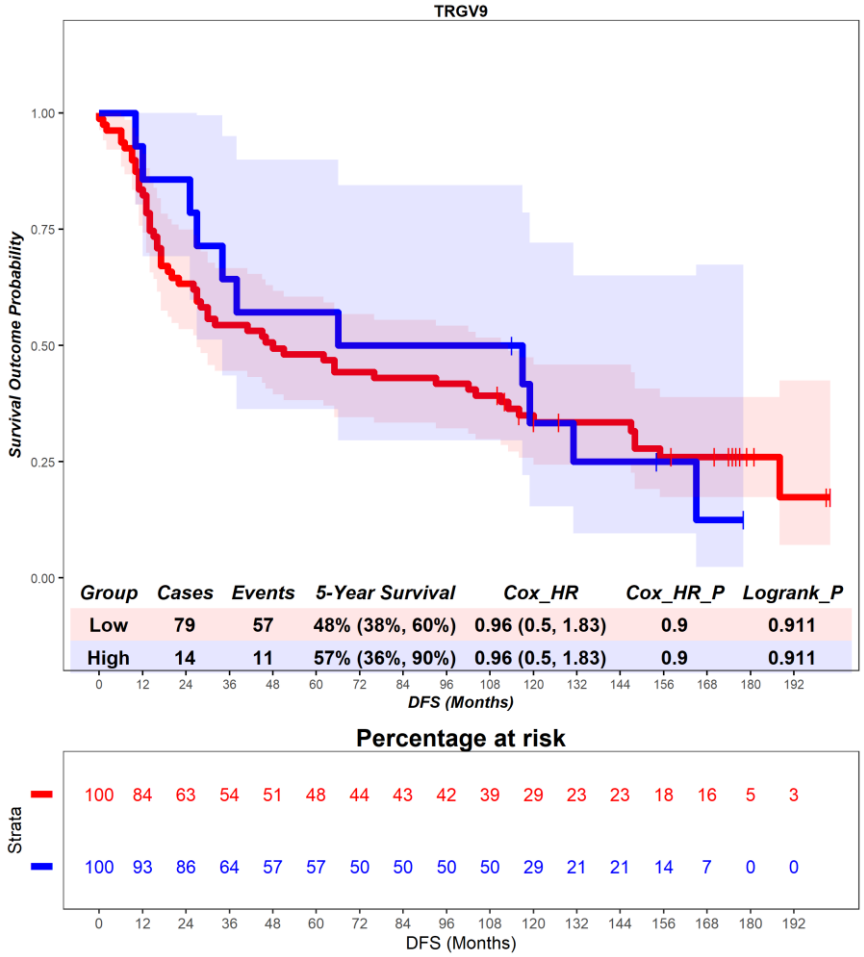

Figure 6.42 – Time-to-event (disease-free survival) analysis for TRGV9 expression in the primary tumour. *Patients deemed 'High' or 'Low' for TRGV9 expression are shaded blue and red, respectively. Cox hazard ratio is univariate. The 'Low' group is used as the reference group on cox regression modelling.*

DFS was investigated in the context of transcriptional classification by *TRGV10*, which encodes the Vγ10 chain. In the primary tumour, patients deemed high for *TRGV10* expression are associated with no difference in prognosis (Figure 6.43). Patients with a high expression of *TRGV10* had a mean survival time of 70.85 months, compared to those with low expression of *TRGV10* with a mean survival of 97.43 months (hazard ratio = 1.29, p = 0.39). 5-year survival for patients high for *TRGV10* expression is 44% (34%, 58%), compared to 67% (49%, 90%) in the *TRGV10* low group. This suggests that *TRGV10* expression in the primary tumour has no prognostic role.

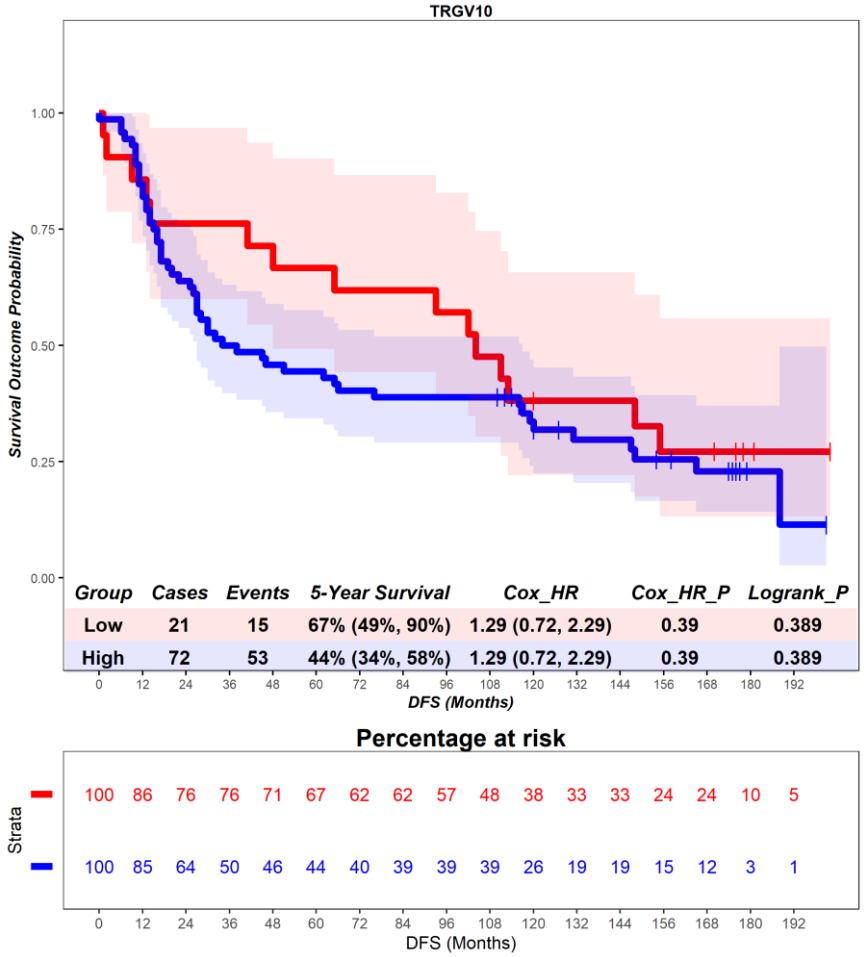

Figure 6.43 – Time-to-event (disease-free survival) analysis for TRGV10 expression in the primary tumour. *Patients deemed 'High' or 'Low' for TRGV10 expression are shaded blue and red, respectively. Cox hazard ratio is univariate. The 'Low' group is used as the reference group on cox regression modelling.*

DFS was investigated in the context of transcriptional classification by *TRGV11*, which encodes the Vγ11 chain. In the primary tumour, patients deemed high for *TRGV11* expression are associated with no difference in prognosis (Figure 6.44). Patients with a high expression of *TRGV11* had a mean survival time of 97.73 months, compared to those with low expression of *TRGV11* with a mean survival of 74.05 months (hazard ratio = 0.94, p = 0.87). 5-year survival for patients high for *TRGV11* expression is 64% (41%, 99%), compared to 48% (38%, 60%) in the *TRGV11* low group. This suggests that *TRGV11* expression in the primary tumour has no prognostic role.

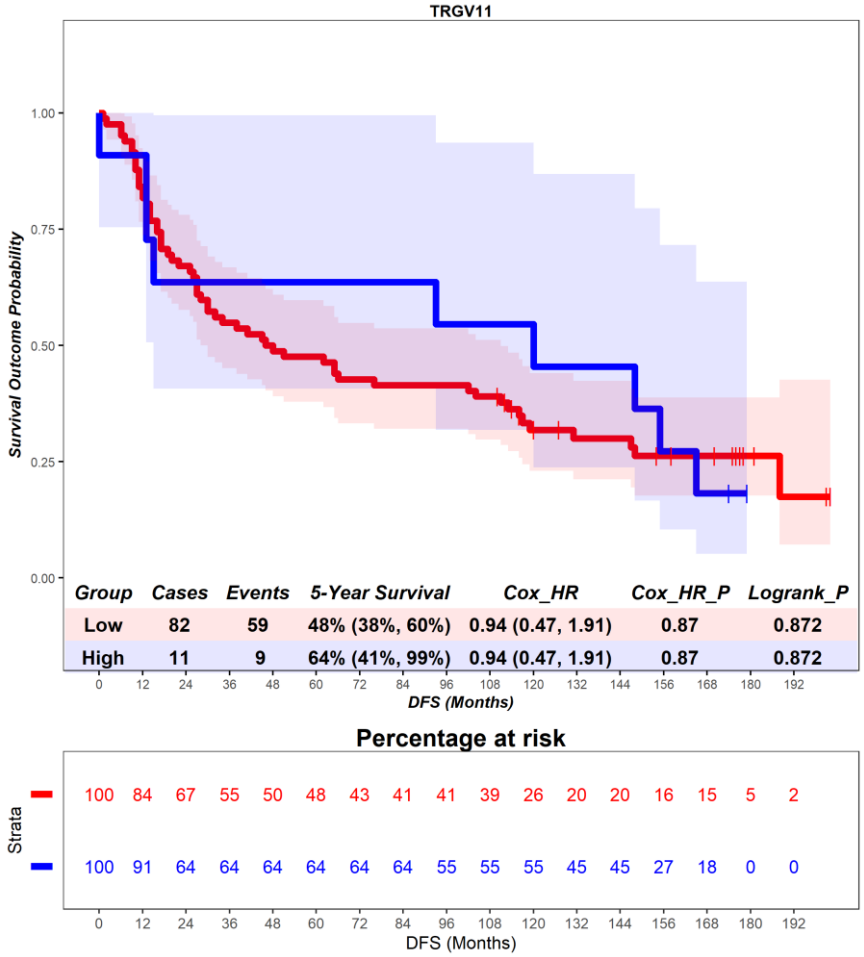

Figure 6.44 – Time-to-event (disease-free survival) analysis for TRGV11 expression in the primary tumour. *Patients deemed 'High' or 'Low' for TRGV11 expression are shaded blue and red, respectively. Cox hazard ratio is univariate. The 'Low' group is used as the reference group on cox regression modelling.*

6.4.4 γδ T cells – recurrence-free survival

RFS was investigated in the context of transcriptional classification by *TRDV1*, which encodes the Vδ1 chain. In the primary tumour, patients deemed high for *TRDV1* expression are associated with a worse prognosis (Figure 6.45). Patients with a high expression of *TRDV1* had a mean survival time of 56.02 months, compared to those with low expression of *TRDV1* with a mean survival of 92.57 months (hazard ratio = 1.89, p = 0.06). 5-year survival for patients high for *TRDV1* expression is 43% (29%, 63%), compared to 70% (59%, 84%) in the *TRDV1* low group. This suggests that *TRDV1* expression in the primary tumour has an unfavourable prognostic role.

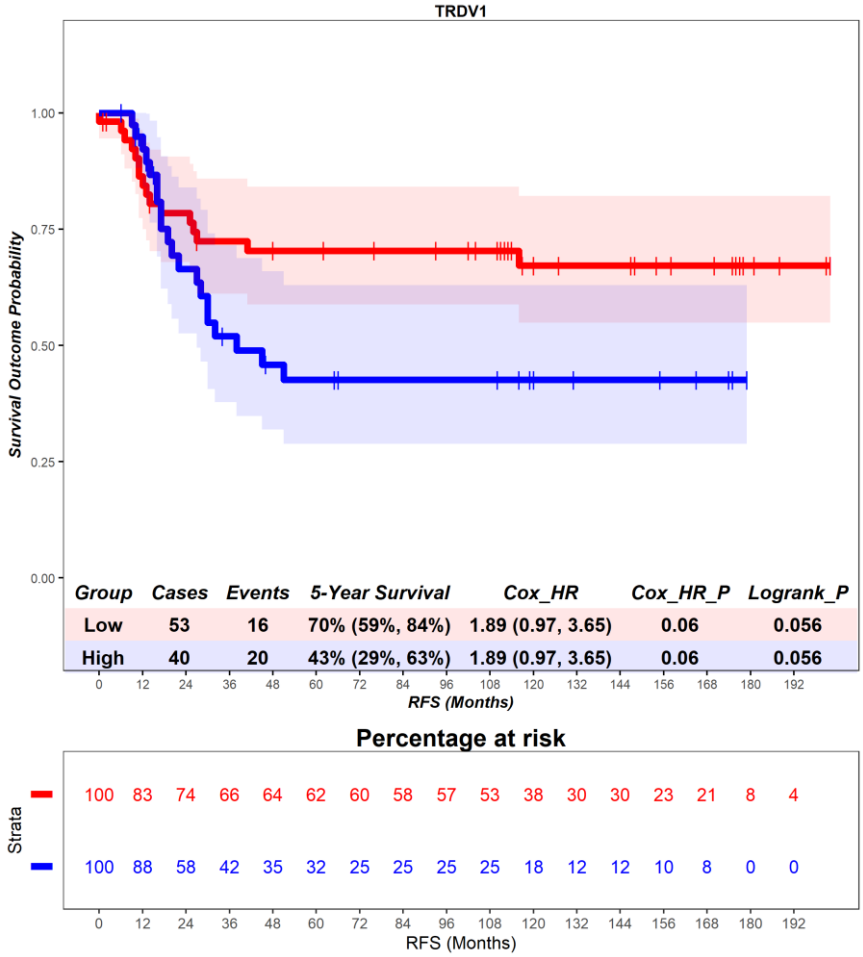

Figure 6.45 – Time-to-event (recurrence-free survival) analysis for TRDV1 expression in the primary tumour. *Patients deemed 'High' or 'Low' for TRDV1 expression are shaded blue and red, respectively. Cox hazard ratio is univariate. The 'Low' group is used as the reference group on cox regression modelling.*

RFS was investigated in the context of transcriptional classification by *TRDV2*, which encodes the Vδ2 chain. In the primary tumour, patients deemed high for *TRDV2* expression are associated with no difference in prognosis (Figure 6.46). Patients with a high expression of *TRDV2* had a mean survival time of 52.60 months, compared to those with low expression of *TRDV2* with a mean survival of 79.77 months (hazard ratio = 1.3, p = 0.62). 5-year survival for patients high for *TRDV2* expression is 54% (29%, 100%), compared to 60% (50%, 72%) in the *TRDV2* low group. This suggests that *TRDV2* expression in the primary tumour has no prognostic role.

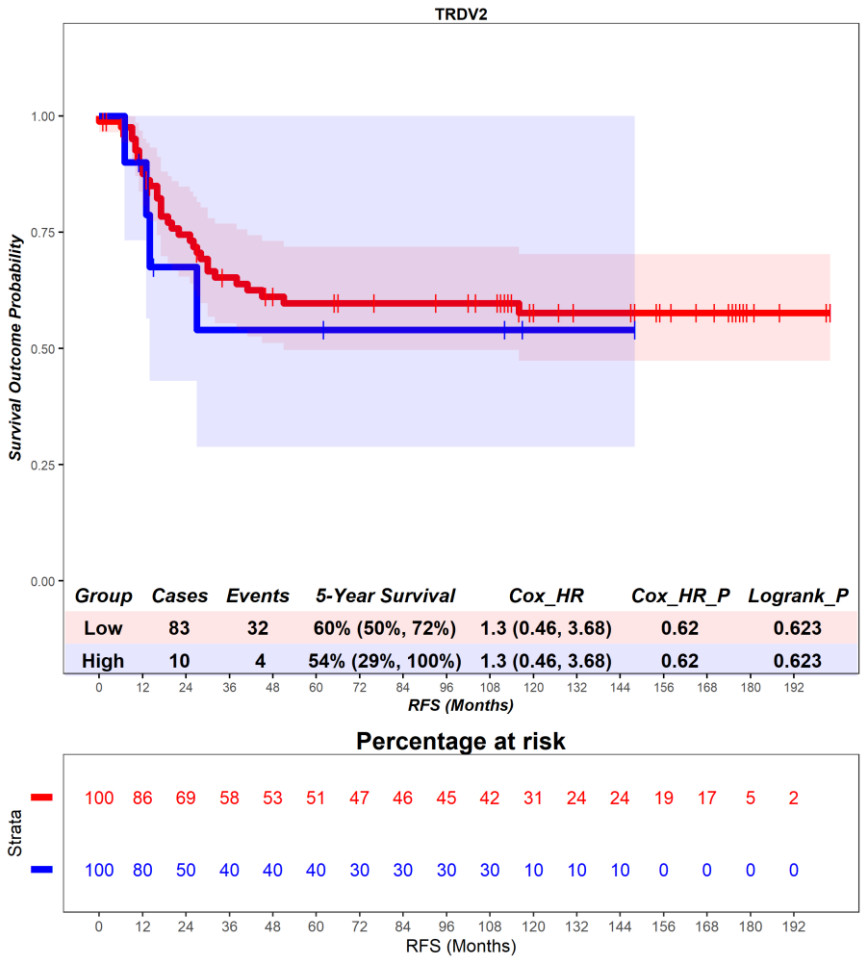

Figure 6.46 – Time-to-event (recurrence-free survival) analysis for TRDV2 expression in the primary tumour. *Patients deemed 'High' or 'Low' for TRDV2 expression are shaded blue and red, respectively. Cox hazard ratio is univariate. The 'Low' group is used as the reference group on cox regression modelling.*

RFS was investigated in the context of transcriptional classification by *TRDV3*, which encodes the Vδ3 chain. In the primary tumour, patients deemed high for *TRDV3* expression are associated with no difference in prognosis (Figure 6.47). Patients with a high expression of *TRDV3* had a mean survival time of 82.21 months, compared to those with low expression of *TRDV3* with a mean survival of 75.90 months (hazard ratio = 0.86, p = 0.75). 5-year survival for patients high for *TRDV3* expression is 62% (41%, 95%), compared to 59% (48%, 71%) in the *TRDV3* low group. This suggests that *TRDV3* expression in the primary tumour has no prognostic role.

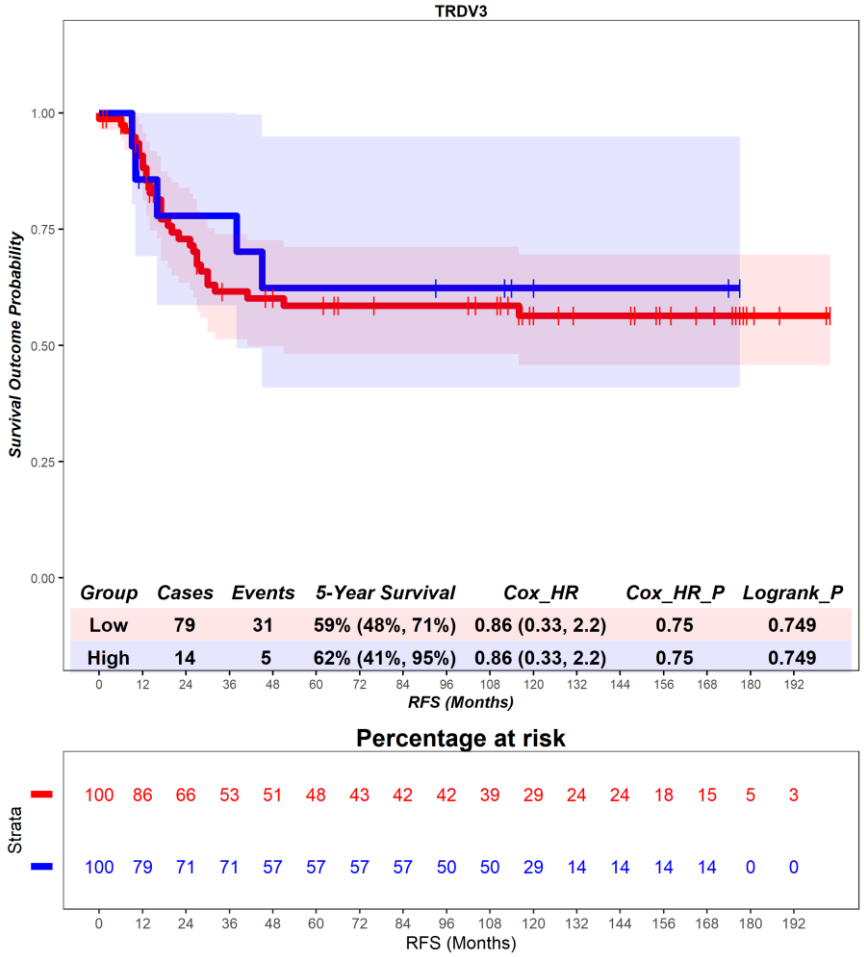

Figure 6.47 – Time-to-event (recurrence-free survival) analysis for TRDV3 expression in the primary tumour. *Patients deemed 'High' or 'Low' for TRDV3 expression are shaded blue and red, respectively. Cox hazard ratio is univariate. The 'Low' group is used as the reference group on cox regression modelling.*

RFS was investigated in the context of transcriptional classification by *TRGV1*, which encodes the Vγ1 chain. In the primary tumour, patients deemed high for *TRGV1* expression are associated with a better prognosis (Figure 6.48). Patients with a high expression of *TRGV1* had a mean survival time of 101.55 months, compared to those with low expression of *TRGV1* with a mean survival of 73.54 months (hazard ratio = 0.16, p = 0.07). 5-year survival for patients high for *TRGV1* expression is 90% (73%, 100%), compared to 55% (45%, 67%) in the *TRGV1* low group. This suggests that *TRGV1* expression in the primary tumour has a favourable prognostic role.

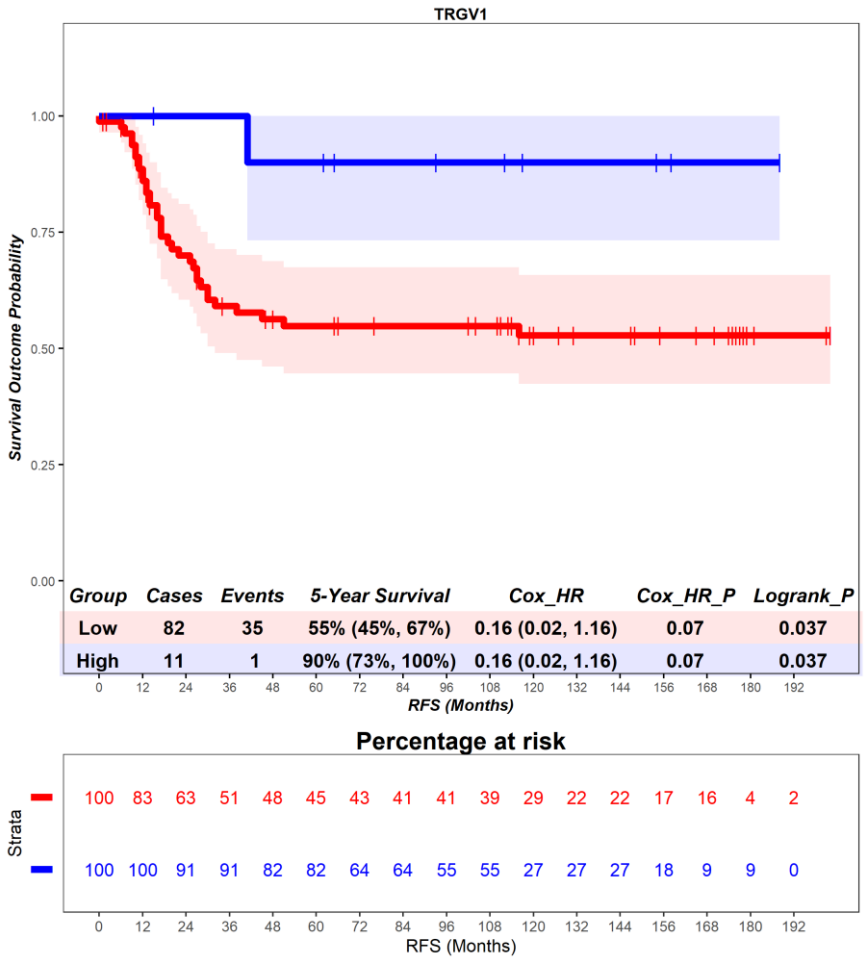

Figure 6.48 – Time-to-event (recurrence-free survival) analysis for TRGV1 expression in the primary tumour. *Patients deemed 'High' or 'Low' for TRGV1 expression are shaded blue and red, respectively. Cox hazard ratio is univariate. The 'Low' group is used as the reference group on cox regression modelling.*

RFS was investigated in the context of transcriptional classification by *TRGV2*, which encodes the Vγ2 chain. In the primary tumour, patients deemed high for *TRGV2* expression are associated with a worse prognosis (Figure 6.49). Patients with a high expression of *TRGV2* had a mean survival time of 54.94 months, compared to those with low expression of *TRGV2* with a mean survival of 81.75 months (hazard ratio = 2.12, p = 0.04). 5-year survival for patients high for *TRGV2* expression is 38% (20%, 71%), compared to 64% (54%, 76%) in the *TRGV2* low group. This suggests that *TRGV2* expression in the primary tumour has an unfavourable prognostic role.

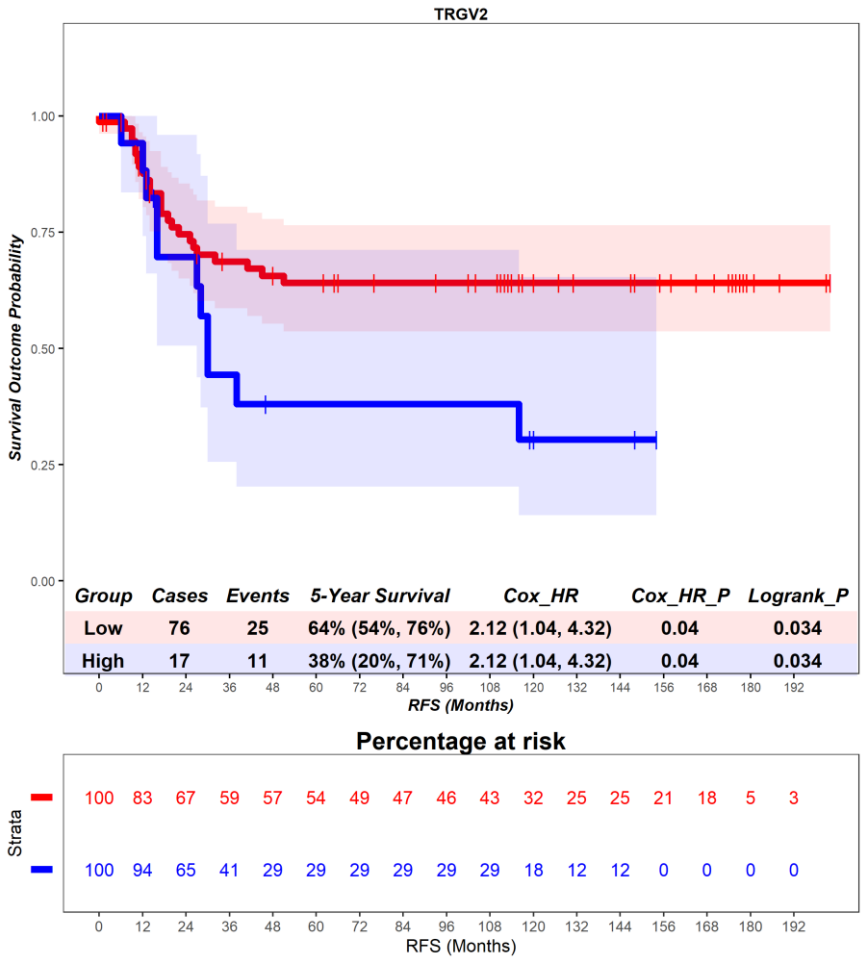

Figure 6.49 – Time-to-event (recurrence-free survival) analysis for TRGV2 expression in the primary tumour. *Patients deemed 'High' or 'Low' for TRGV2 expression are shaded blue and red, respectively. Cox hazard ratio is univariate. The 'Low' group is used as the reference group on cox regression modelling.*

RFS was investigated in the context of transcriptional classification by *TRGV3*, which encodes the Vγ3 chain. In the primary tumour, patients deemed high for *TRGV3* expression are associated with a worse prognosis (Figure 6.50). Patients with a high expression of *TRGV3* had a mean survival time of 43.17 months, compared to those with low expression of *TRGV3* with a mean survival of 81.84 months (hazard ratio = 2.4, p = 0.03). 5-year survival for patients high for *TRGV3* expression is 21% (6%, 71%), compared to 64% (54%, 76%) in the *TRGV3* low group. This suggests that *TRGV3* expression in the primary tumour has an unfavourable prognostic role.

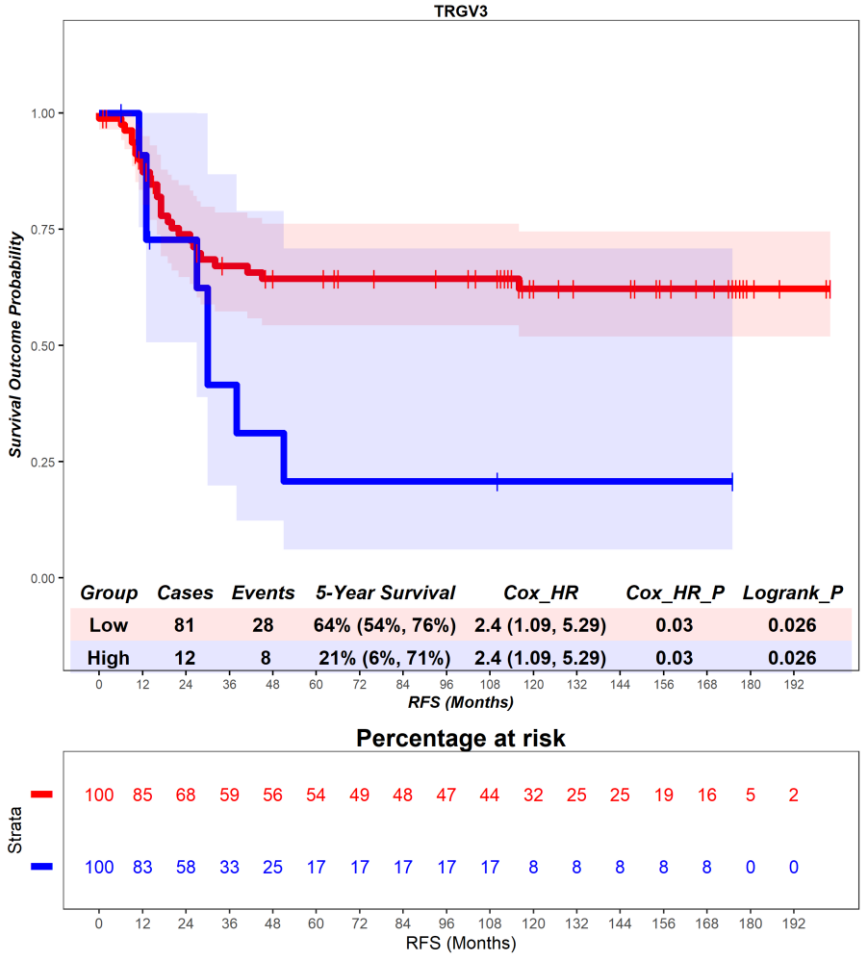

Figure 6.50 – Time-to-event (recurrence-free survival) analysis for TRGV3 expression in the primary tumour. *Patients deemed 'High' or 'Low' for TRGV3 expression are shaded blue and red, respectively. Cox hazard ratio is univariate. The 'Low' group is used as the reference group on cox regression modelling.*

RFS was investigated in the context of transcriptional classification by *TRGV4*, which encodes the Vγ4 chain. In the primary tumour, patients deemed high for *TRGV4* expression are associated with a better prognosis (Figure 6.51). Patients with a high expression of *TRGV4* had a mean survival time of 105.09 months, compared to those with low expression of *TRGV4* with a mean survival of 73.06 months (hazard ratio = 0.52, p = 0.28). 5-year survival for patients high for *TRGV4* expression is 73% (51%, 100%), compared to 57% (47%, 70%) in the *TRGV4* low group. This suggests that *TRGV4* expression in the primary tumour has a favourable prognostic role.

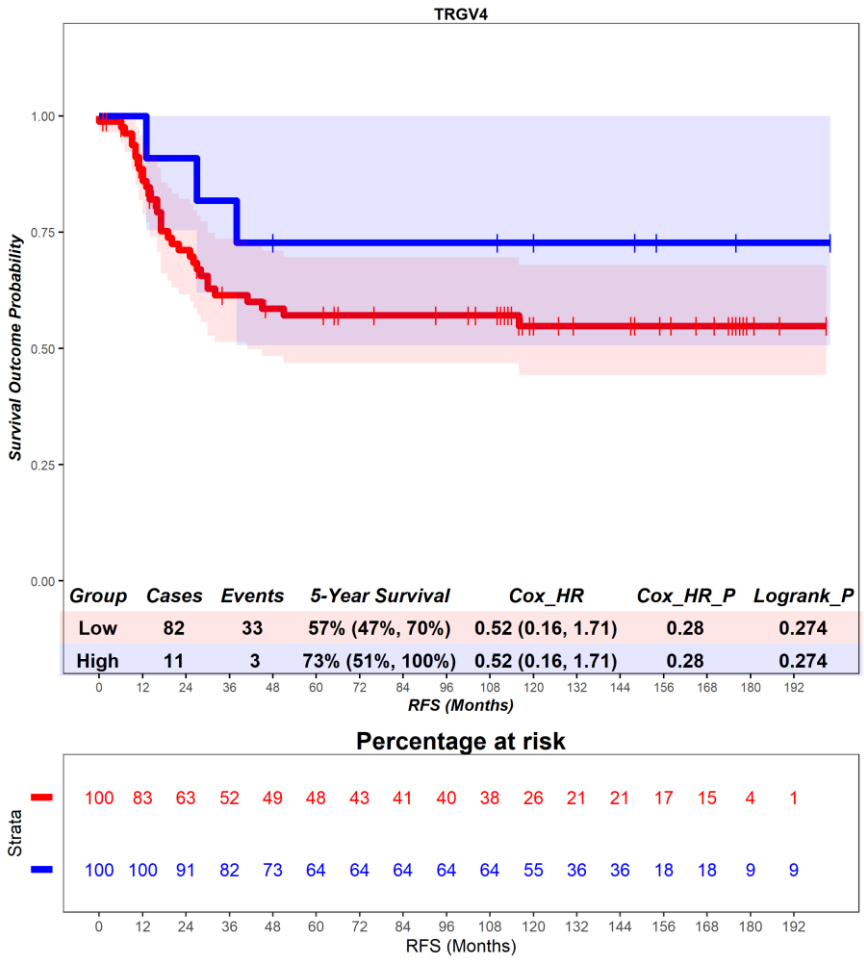

Figure 6.51 – Time-to-event (recurrence-free survival) analysis for TRGV4 expression in the primary tumour. *Patients deemed 'High' or 'Low' for TRGV4 expression are shaded blue and red, respectively. Cox hazard ratio is univariate. The 'Low' group is used as the reference group on cox regression modelling.*

RFS was investigated in the context of transcriptional classification by *TRGV5*, which encodes the Vγ5 chain. In the primary tumour, patients deemed high for *TRGV5* expression are associated with no difference in prognosis (Figure 6.52). Patients with a high expression of *TRGV5* had a mean survival time of 61.50 months, compared to those with low expression of *TRGV5* with a mean survival of 78.70 months (hazard ratio = 0.82, p = 0.74). 5-year survival for patients high for *TRGV5* expression is 66% (10%, 100%), compared to 58% (48%, 71%) in the *TRGV5* low group. This suggests that *TRGV5* expression in the primary tumour has no prognostic role.

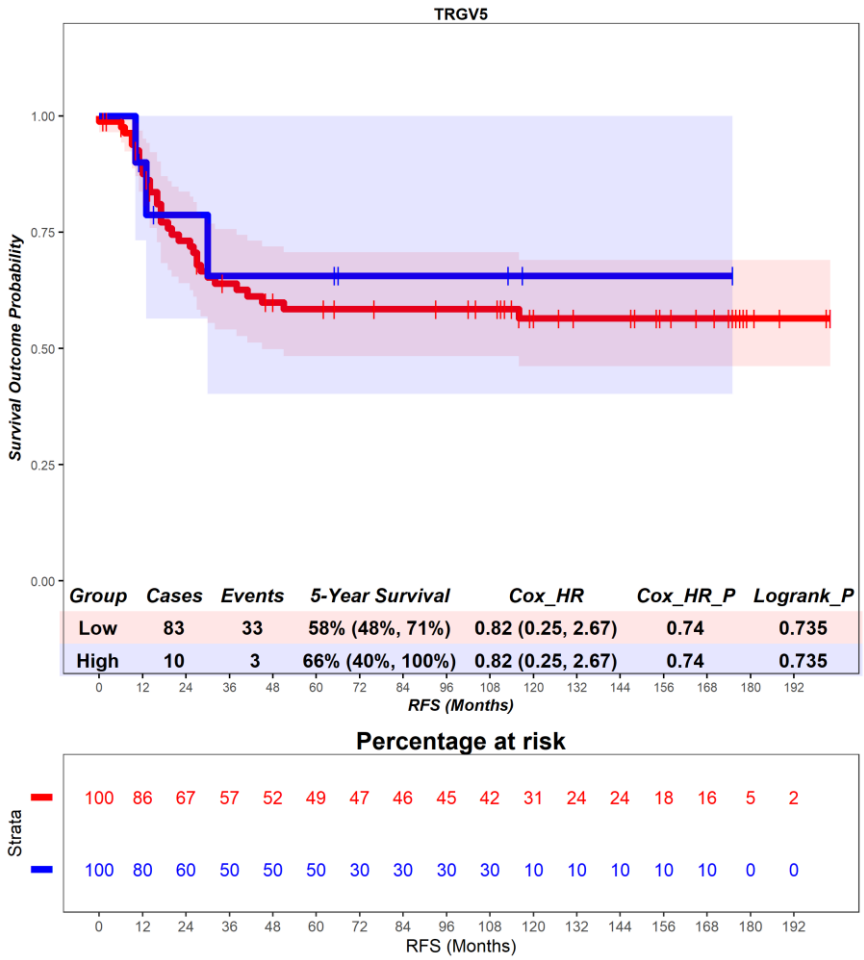

Figure 6.52 – Time-to-event (recurrence-free survival) analysis for TRGV5 expression in the primary tumour. *Patients deemed 'High' or 'Low' for TRGV5 expression are shaded blue and red, respectively. Cox hazard ratio is univariate. The 'Low' group is used as the reference group on cox regression modelling.*

RFS was investigated in the context of transcriptional classification by *TRGV8*, which encodes the Vγ8 chain. In the primary tumour, patients deemed high for *TRGV8* expression are associated with no difference in prognosis (Figure 6.53). Patients with a high expression of *TRGV8* had a mean survival time of 61.90 months, compared to those with low expression of *TRGV8* with a mean survival of 78.65 months (hazard ratio = 1.84, p = 0.17). 5-year survival for patients high for *TRGV8* expression is 36% (15%, 86%), compared to 62% (52%, 74%) in the *TRGV8* low group. This suggests that *TRGV8* expression in the primary tumour has no prognostic role.

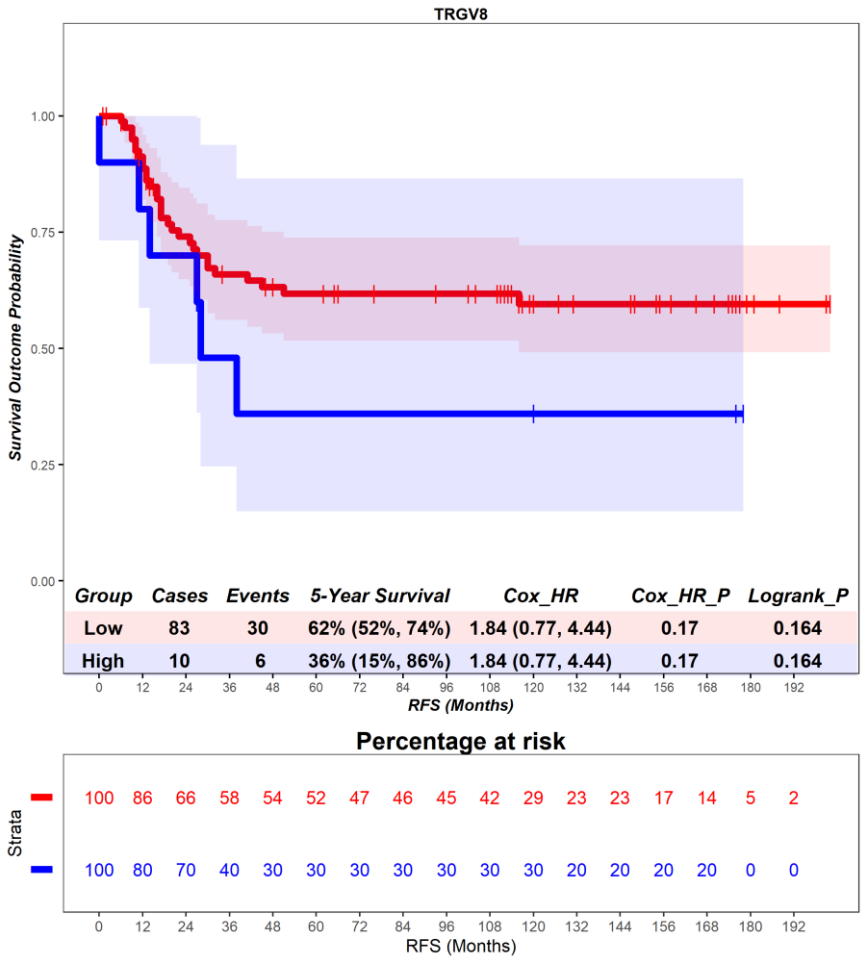

***Figure 6.53 – Time-to-event (recurrence-free survival) analysis for TRGV8 expression in the primary tumour**. Patients deemed 'High' or 'Low' for TRGV8 expression are shaded blue and red, respectively. Cox hazard ratio is univariate. The 'Low' group is used as the reference group on cox regression modelling.*

RFS was investigated in the context of transcriptional classification by *TRGV9*, which encodes the Vγ9 chain. In the primary tumour, patients deemed high for *TRGV9* expression are associated with a better prognosis (Figure 6.54). Patients with a high expression of *TRGV9* had a mean survival time of 85.00 months, compared to those with low expression of *TRGV9* with a mean survival of 75.41 months (hazard ratio = 0.61, p = 0.34). 5-year survival for patients high for *TRGV9* expression is 68% (47%, 100%), compared to 57% (47%, 70%) in the *TRGV9* low group. This suggests that *TRGV9* expression in the primary tumour has a favourable prognostic role.

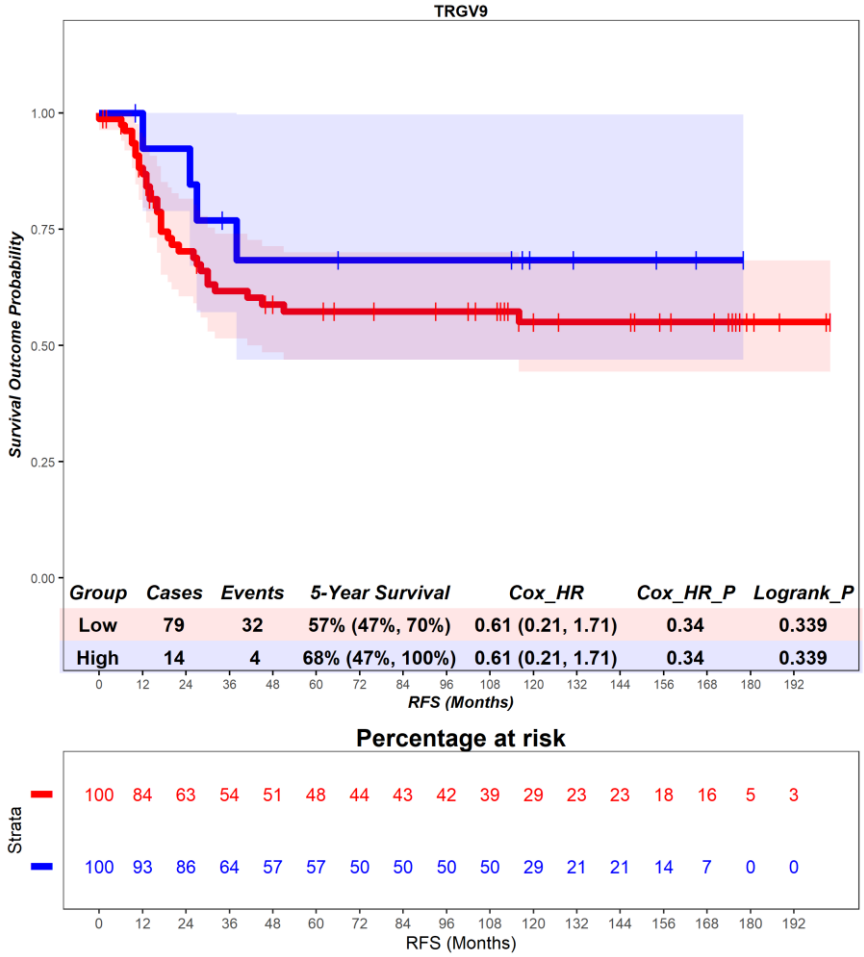

Figure 6.54 – Time-to-event (recurrence-free survival) analysis for TRGV9 expression in the primary tumour. *Patients deemed 'High' or 'Low' for TRGV9 expression are shaded blue and red, respectively. Cox hazard ratio is univariate. The 'Low' group is used as the reference group on cox regression modelling.*

RFS was investigated in the context of transcriptional classification by *TRGV10*, which encodes the Vγ10 chain. In the primary tumour, patients deemed high for *TRGV10* expression are associated with a worse prognosis (Figure 6.55). Patients with a high expression of *TRGV10* had a mean survival time of 70.85 months, compared to those with low expression of *TRGV10* with a mean survival of 97.43 months (hazard ratio = 3.66, p = 0.03). 5-year survival for patients high for *TRGV10* expression is 52% (42%, 66%), compared to 84% (68%, 100%) in the *TRGV10* low group. This suggests that *TRGV10* expression in the primary tumour has an unfavourable prognostic role.

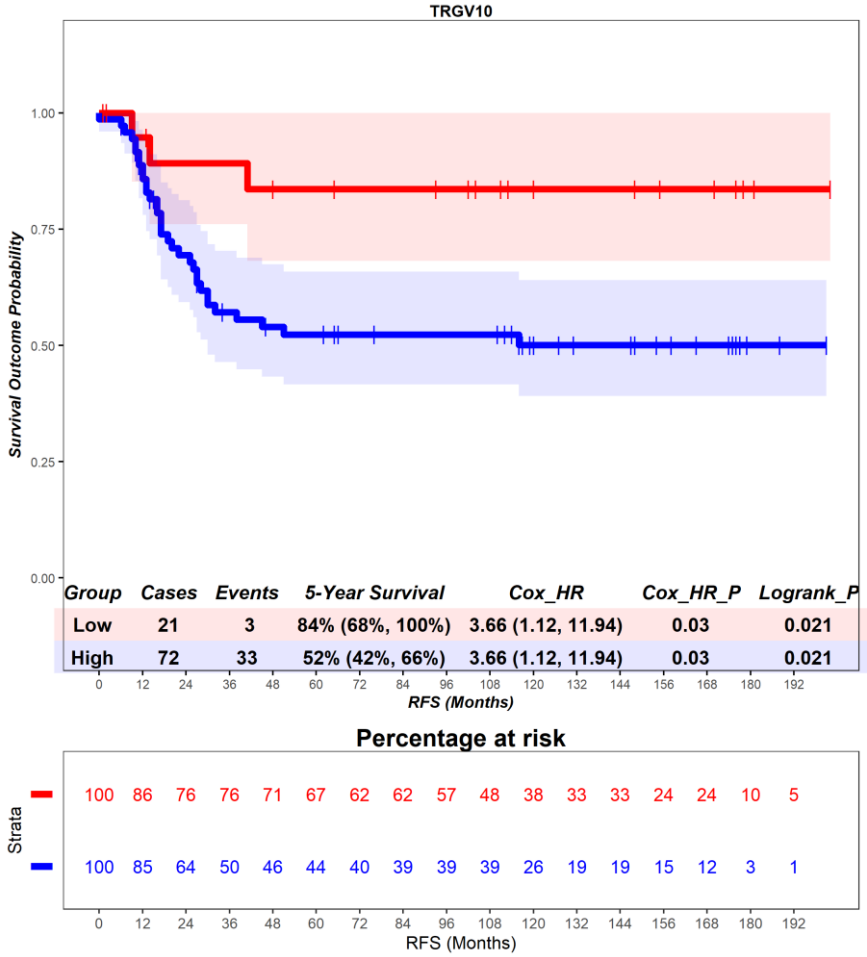

Figure 6.55 – Time-to-event (recurrence-free survival) analysis for TRGV10 expression in the primary tumour. *Patients deemed 'High' or 'Low' for TRGV10 expression are shaded blue and red, respectively. Cox hazard ratio is univariate. The 'Low' group is used as the reference group on cox regression modelling.*

RFS was investigated in the context of transcriptional classification by *TRGV11*, which encodes the Vγ11 chain. In the primary tumour, patients deemed high for *TRGV11* expression are associated with no difference in prognosis (Figure 6.66). Patients with a high expression of *TRGV11* had a mean survival time of 97.73 months, compared to those with low expression of *TRGV11* with a mean survival of 74.05 months (hazard ratio = 0.66, p = 0.49). 5-year survival for patients high for *TRGV11* expression is 73% (51%, 100%), compared to 57% (47%, 70%) in the *TRGV11* low group. This suggests that *TRGV11* expression in the primary tumour has no prognostic role.

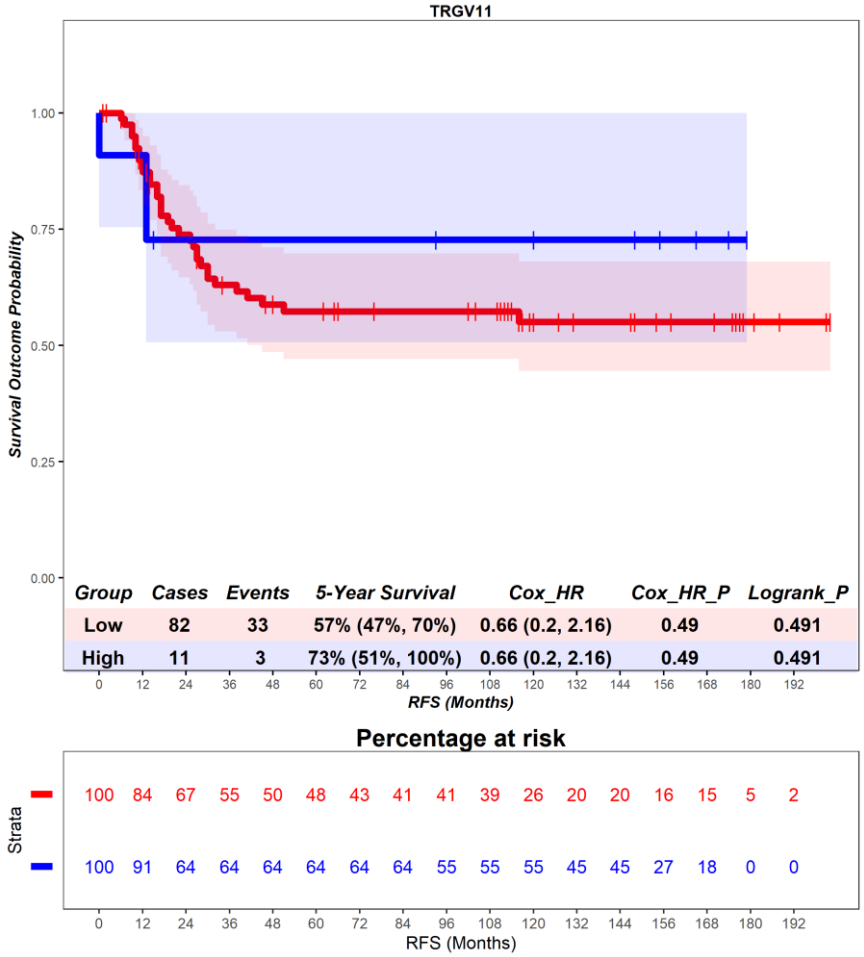

Figure 6.66 – Time-to-event (recurrence-free survival) analysis for TRGV11 expression in the primary tumour. *Patients deemed 'High' or 'Low' for TRGV11 expression are shaded blue and red, respectively. Cox hazard ratio is univariate. The 'Low' group is used as the reference group on cox regression modelling.*

6.4.5 CD8 T cells - cancer-specific survival

CSS was investigated in the context of transcriptional classification by *CD8A*, which encodes the CD8α chain. In the primary tumour, patients deemed high for *CD8A* expression are associated with no difference in prognosis (Figure 6.67). Patients with a high expression of *CD8A* had a mean survival time of 66.20 months, compared to those with low expression of *CD8A* with a mean survival of 98.66 months (hazard ratio = 1.51, p = 0.22). 5-year survival for patients high for *CD8A* expression is 51% (37%, 69%), compared to 68% (56%, 84%) in the *CD8A* low group. This suggests that *CD8A* expression in the primary tumour has no prognostic role.

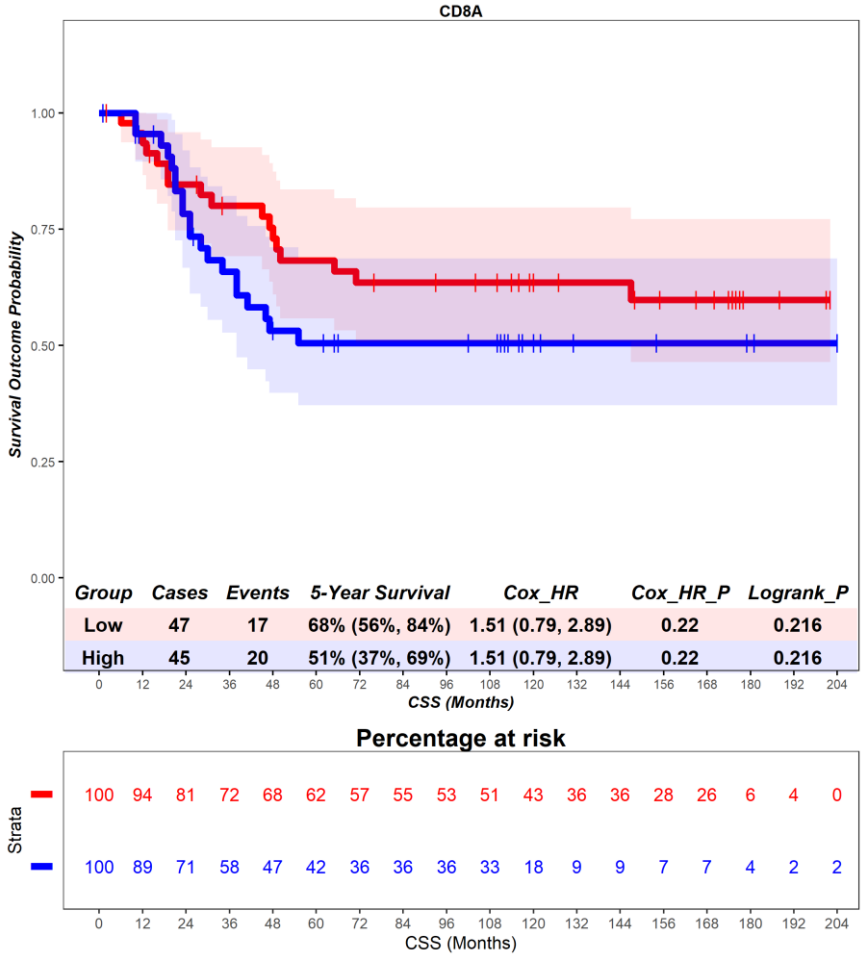

Figure 6.67 – Time-to-event (cancer-specific survival) analysis for CD8A expression in the primary tumour. *Patients deemed 'High' or 'Low' for CD8A expression are shaded blue and red, respectively. Cox hazard ratio is univariate. The 'Low' group is used as the reference group on cox regression modelling.*

CSS was investigated in the context of transcriptional classification by *CD8B*, which encodes the CD8β chain. In the primary tumour, patients deemed high for *CD8B* expression are associated with a better prognosis (Figure 6.68). Patients with a high expression of *CD8B* had a mean survival time of 103.58 months, compared to those with low expression of *CD8B* with a mean survival of 77.37 months (hazard ratio = 0.36, p = 0.05). 5-year survival for patients high for *CD8B* expression is 78% (61%, 100%), compared to 55% (44%, 68%) in the *CD8B* low group. This suggests that *CD8B* expression in the primary tumour has a favourable prognostic role.

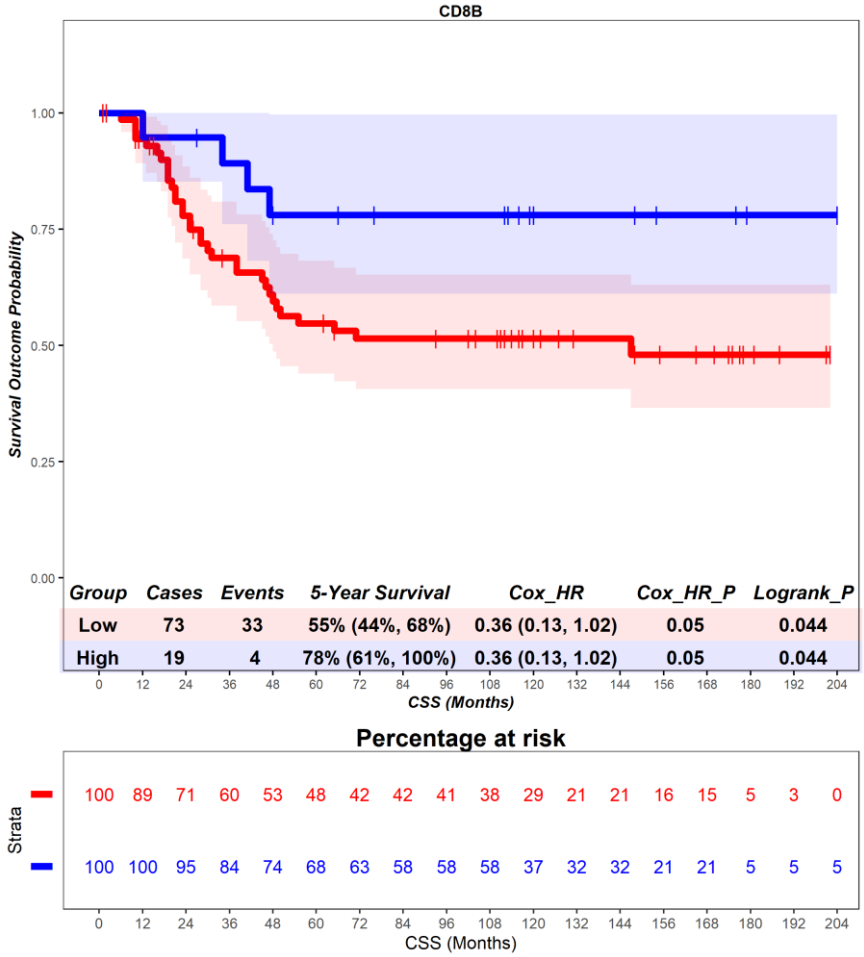

***Figure 6.68 – Time-to-event (cancer-specific survival) analysis for CD8B expression in the primary tumour**. Patients deemed 'High' or 'Low' for CD8B expression are shaded blue and red, respectively. Cox hazard ratio is univariate. The 'Low' group is used as the reference group on cox regression modelling.*

6.4.6 CD8 T cells - overall survival

OS was investigated in the context of transcriptional classification by *CD8A*, which encodes the CD8α chain. In the primary tumour, patients deemed high for *CD8A* expression are associated with a worse prognosis (Figure 6.69). Patients with a high expression of *CD8A* had a mean survival time of 66.20 months, compared to those with low expression of *CD8A* with a mean survival of 98.66 months (hazard ratio = 1.74, p = 0.03). 5-year survival for patients high for *CD8A* expression is 42% (30%, 59%), compared to 62% (49%, 77%) in the *CD8A* low group. This suggests that *CD8A* expression in the primary tumour has an unfavourable prognostic role.

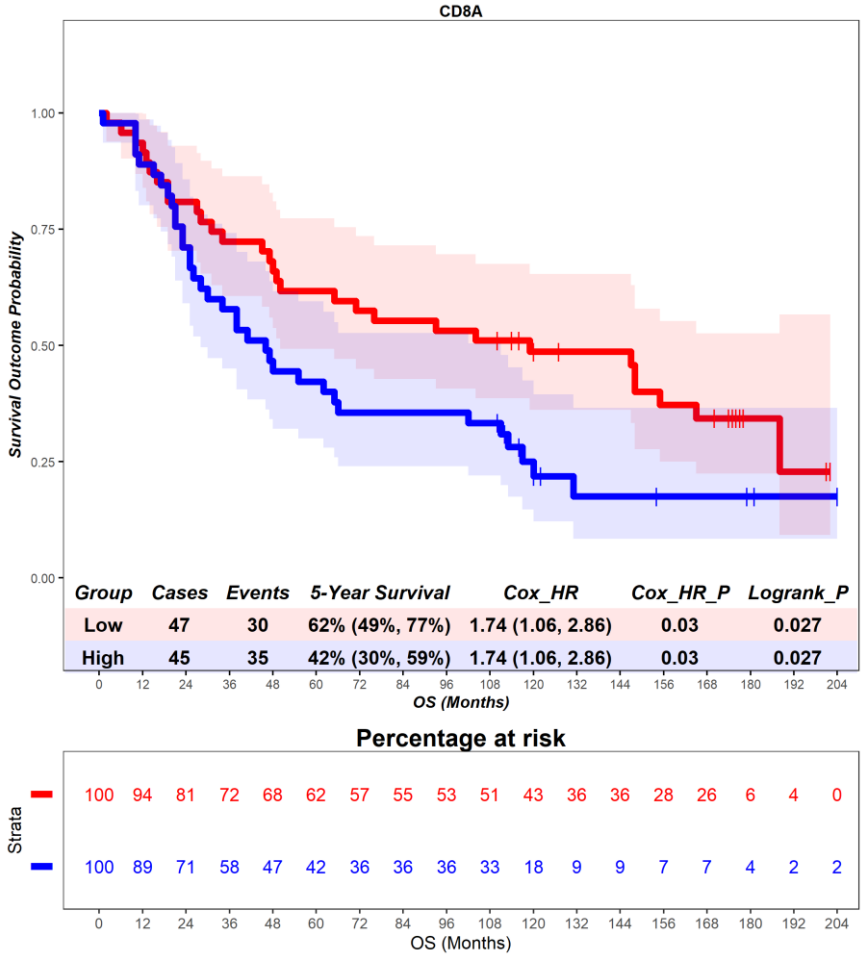

Figure 6.69 – Time-to-event (overall survival) analysis for CD8A expression in the primary tumour. *Patients deemed 'High' or 'Low' for CD8A expression are shaded blue and red, respectively. Cox hazard ratio is univariate. The 'Low' group is used as the reference group on cox regression modelling.*

OS was investigated in the context of transcriptional classification by *CD8B*, which encodes the CD8β chain. In the primary tumour, patients deemed high for *CD8B* expression are associated with a better prognosis (Figure 6.70). Patients with a high expression of *CD8B* had a mean survival time of 103.58 months, compared to those with low expression of *CD8B* with a mean survival of 77.37 months (hazard ratio = 0.59, p = 0.12). 5-year survival for patients high for *CD8B* expression is 68% (50%, 93%), compared to 48% (38%, 61%) in the *CD8B* low group. This suggests that *CD8B* expression in the primary tumour has a favourable prognostic role.

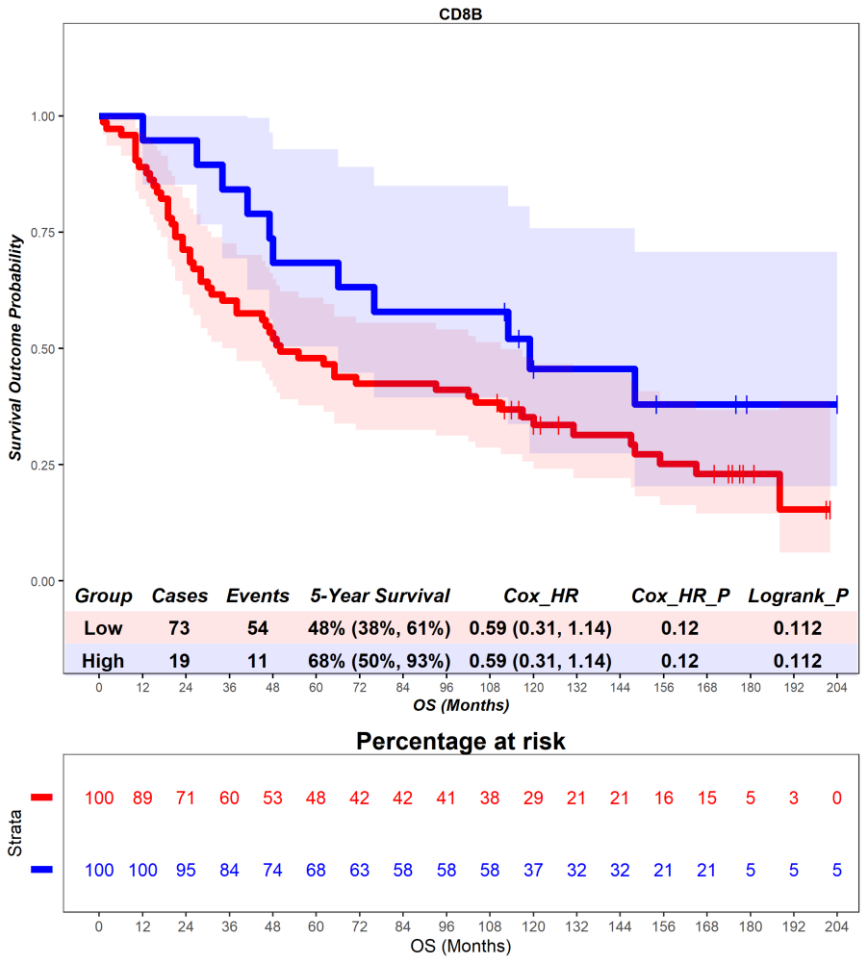

Figure 6.70 – Time-to-event (overall survival) analysis for CD8B expression in the primary tumour. *Patients deemed 'High' or 'Low' for CD8B expression are shaded blue and red, respectively. Cox hazard ratio is univariate. The 'Low' group is used as the reference group on cox regression modelling.*

6.4.7 CD8 T cells – disease-free survival

DFS was investigated in the context of transcriptional classification by *CD8A*, which encodes the CD8α chain. In the primary tumour, patients deemed high for *CD8A* expression are associated with a worse prognosis (Figure 6.71). Patients with a high expression of *CD8A* had a mean survival time of 57.85 months, compared to those with low expression of *CD8A* with a mean survival of 95.45 months (hazard ratio = 1.86, p = 0.01). 5-year survival for patients high for *CD8A* expression is 39% (27%, 56%), compared to 60% (47%, 75%) in the *CD8A* low group. This suggests that *CD8A* expression in the primary tumour has an unfavourable prognostic role.

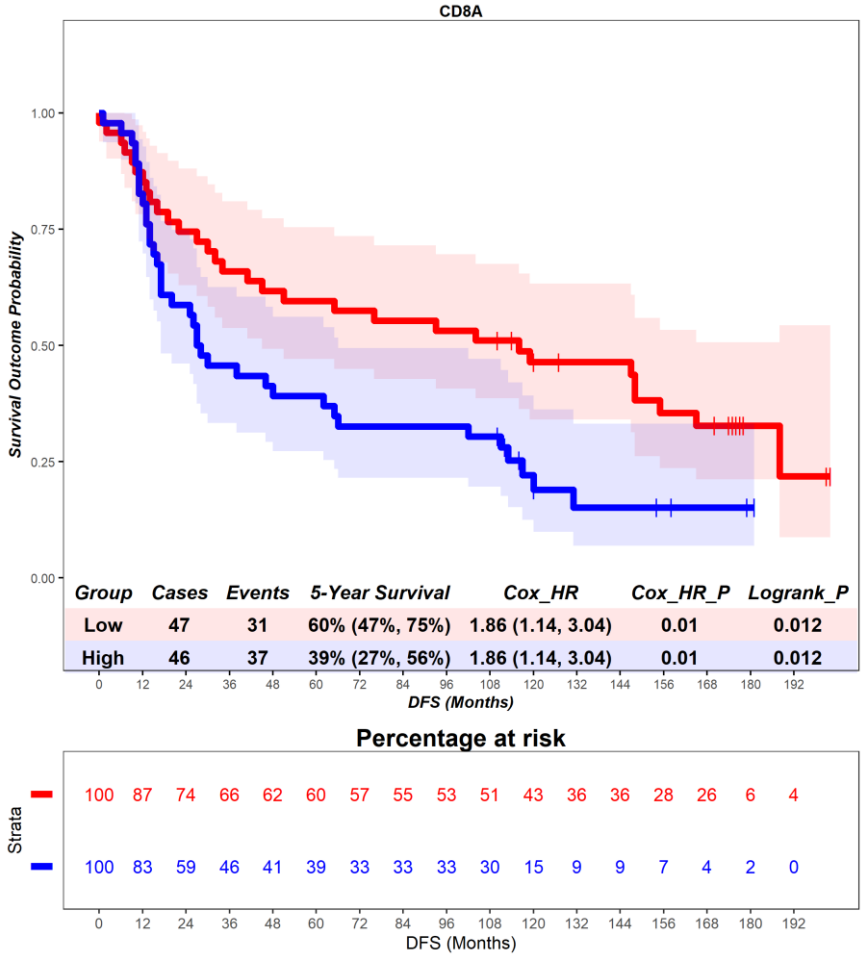

***Figure 6.71 – Time-to-event (disease-free survival) analysis for CD8A expression in the primary tumour**. Patients deemed 'High' or 'Low' for CD8A expression are shaded blue and red, respectively. Cox hazard ratio is univariate. The 'Low' group is used as the reference group on cox regression modelling.*

DFS was investigated in the context of transcriptional classification by *CD8B*, which encodes the CD8β chain. In the primary tumour, patients deemed high for *CD8B* expression are associated with a better prognosis (Figure 6.72). Patients with a high expression of *CD8B* had a mean survival time of 92.16 months, compared to those with low expression of *CD8B* with a mean survival of 72.92 months (hazard ratio = 0.67, p = 0.2). 5-year survival for patients high for *CD8B* expression is 63% (45%, 89%), compared to 46% (36%, 59%) in the *CD8B* low group. This suggests that *CD8B* expression in the primary tumour has a favourable prognostic role.

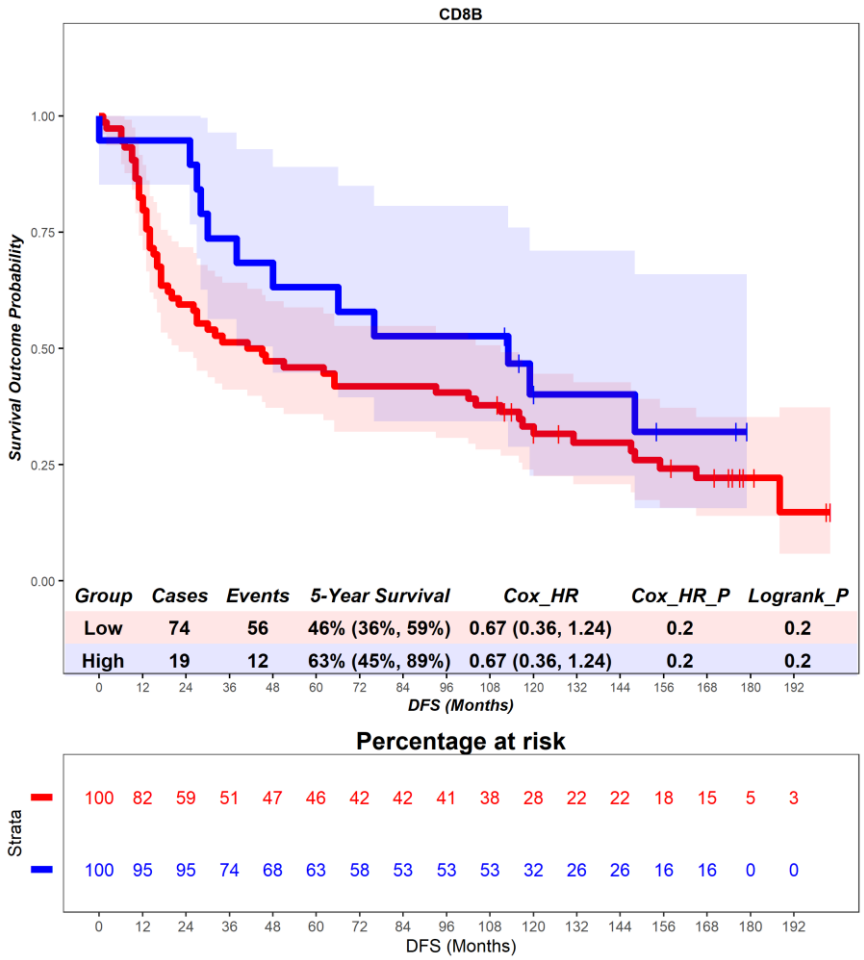

Figure 6.72 – Time-to-event (disease-free survival) analysis for CD8B expression in the primary tumour. *Patients deemed 'High' or 'Low' for CD8B expression are shaded blue and red, respectively. Cox hazard ratio is univariate. The 'Low' group is used as the reference group on cox regression modelling.*

6.4.8 CD8 T cells – recurrence-free survival

RFS was investigated in the context of transcriptional classification by *CD8A*, which encodes the CD8α chain. In the primary tumour, patients deemed high for *CD8A* expression are associated with a worse prognosis (Figure 6.73). Patients with a high expression of *CD8A* had a mean survival time of 57.85 months, compared to those with low expression of *CD8A* with a mean survival of 95.45 months (hazard ratio = 1.97, p = 0.05). 5-year survival for patients high for *CD8A* expression is 48% (35%, 66%), compared to 70% (57%, 85%) in the *CD8A* low group. This suggests that *CD8A* expression in the primary tumour has an unfavourable prognostic role.

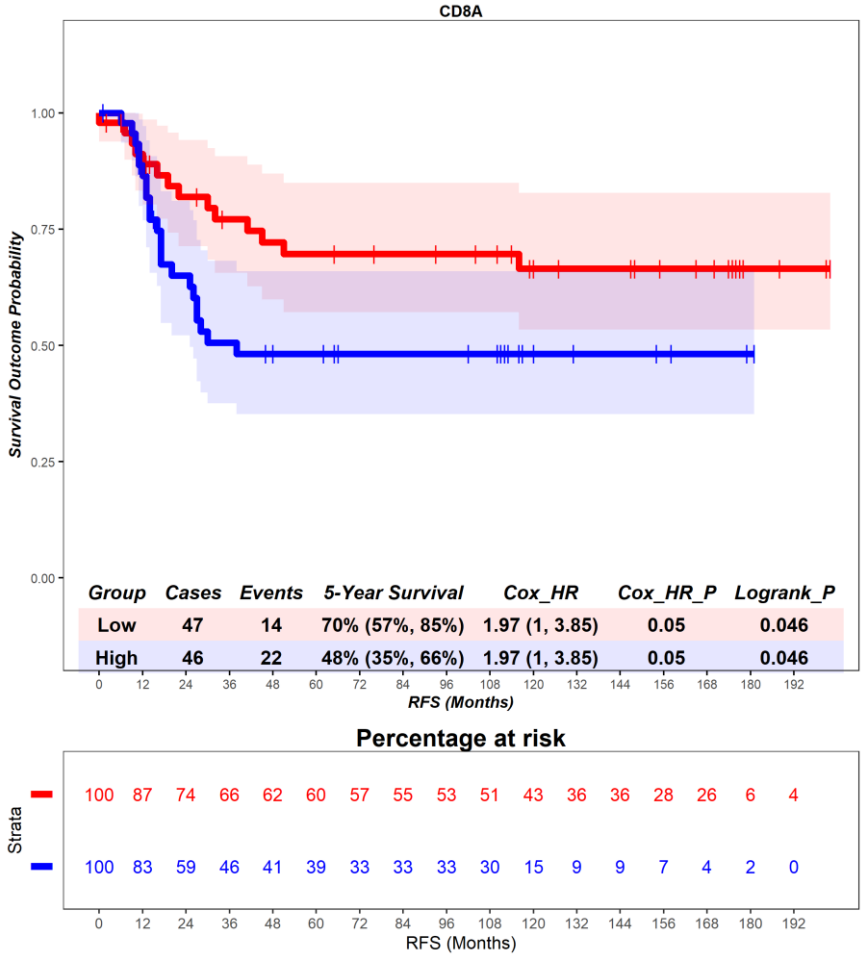

Figure 6.73 – Time-to-event (recurrence-free survival) analysis for CD8A expression in the primary tumour. *Patients deemed 'High' or 'Low' for CD8A expression are shaded blue and red, respectively. Cox hazard ratio is univariate. The 'Low' group is used as the reference group on cox regression modelling.*

RFS was investigated in the context of transcriptional classification by *CD8B*, which encodes the CD8β chain. In the primary tumour, patients deemed high for *CD8B* expression are associated with a better prognosis (Figure 6.74). Patients with a high expression of *CD8B* had a mean survival time of 92.16 months, compared to those with low expression of *CD8B* with a mean survival of 72.92 months (hazard ratio = 0.48, p = 0.13). 5-year survival for patients high for *CD8B* expression is 73% (55%, 96%), compared to 55% (44%, 69%) in the *CD8B* low group. This suggests that *CD8B* expression in the primary tumour has a favourable prognostic role.

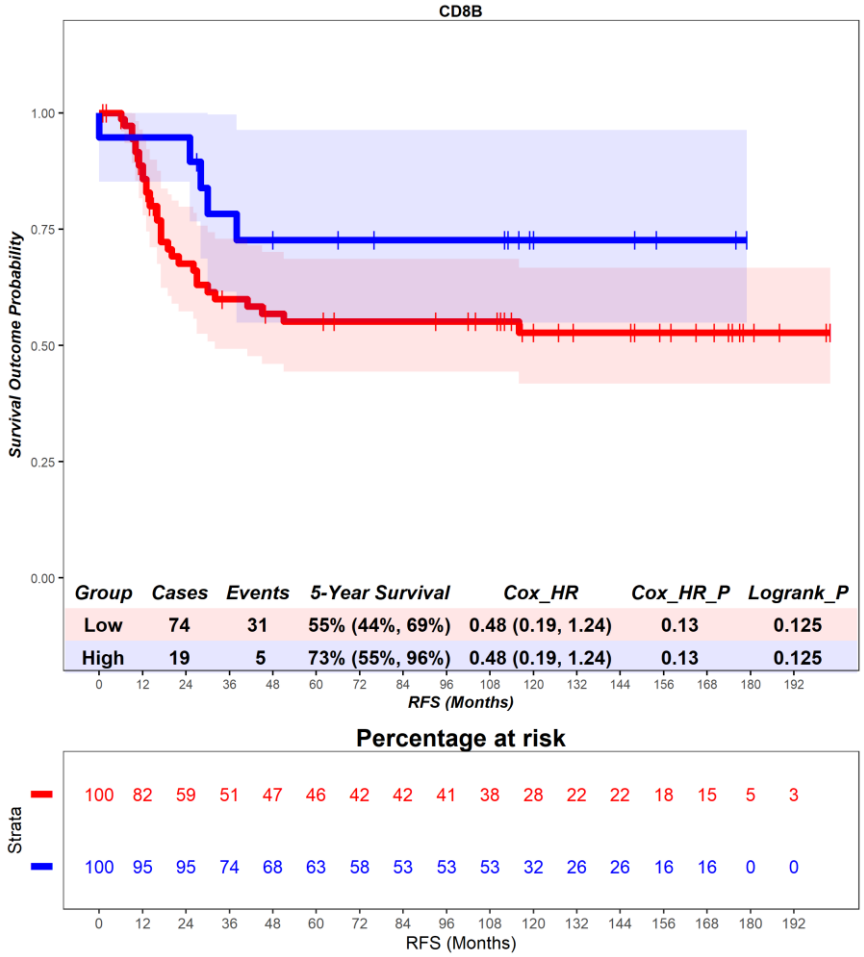

Figure 6.74 – Time-to-event (recurrence-free survival) analysis for CD8B expression in the primary tumour. *Patients deemed 'High' or 'Low' for CD8B expression are shaded blue and red, respectively. Cox hazard ratio is univariate. The 'Low' group is used as the reference group on cox regression modelling.*

6.5 Differential expression of genes by histological classification of T cell density

To understand if the transcriptional landscape can differentiate cases classified by histological analysis as ‘low’ or ‘high’ for γδ T cells or CD8 T cells, differential gene expression was analysed using volcano plots. Potentially, this analysis may reveal genes that can be investigated in future functional studies at the protein level to determine if their expression is causal for lymphocyte density.

6.5.1 γδ T cells – differentially expressed genes

In the primary tumour, cases classed as high for γδ T cells had a greater expression of; *HLA-DQB1* which forms part of a peptide presentation receptor [318]; *DUSP1*, a negative regulator of cell proliferation [319, 320]; *DOCK8*, a guanine nucleotide exchange factor associated with immune deficiency [321]; *TYROBP (DAP12)*, a mediator of signal transduction for immune cell receptors [322, 323]; *CLIP4*, a member of the microtubule organising CLIP-170 family of proteins [324]; *CD52*, a mature lymphocyte marker which is also present on sperm [325, 326]; *SLC38A5*, an amino acid transporter [327]; *CITED2*, a cell cycle mediator [328]; *BMP6*, an iron regulator [329, 330] and a *BMP* enhanced *KCP* [331]; *FMN1*, an actin regulator [332]; *MARCH1*, a negative regulator of MHC class II [333]; *EPB41L3*, *SCPEP1*, *C8orf82_33840*, *TMEM50B* and *SOWAHD*, whose functions remains unclear (Figure 6.75). Cases classed as low for γδ T cells had a greater expression of *SUMF2*, encoding a protein key to post-translational modification of sulphatases [334] (Figure 6.75).

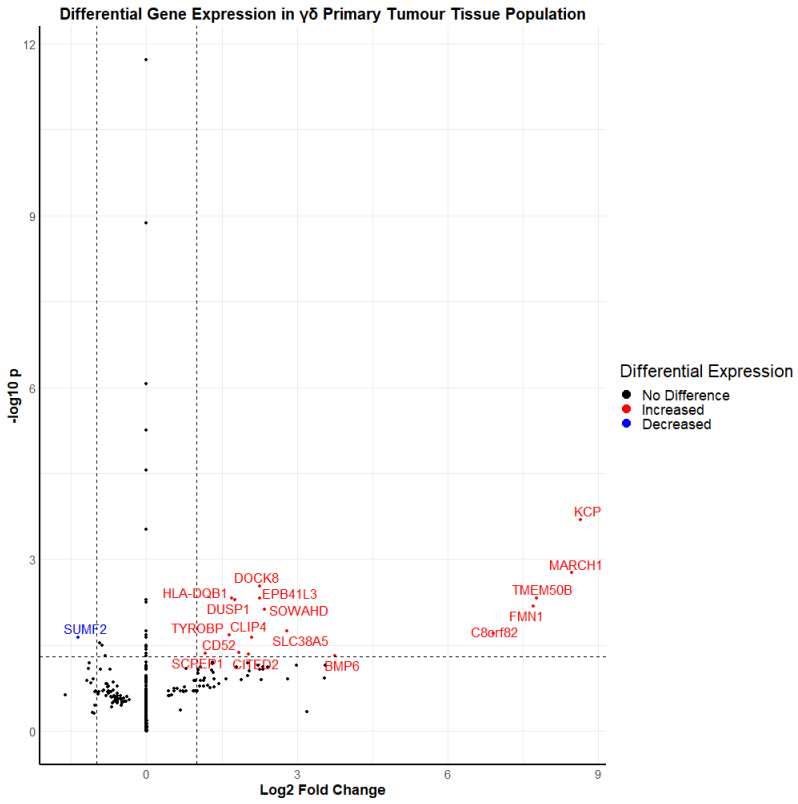

Figure 6.75 – Volcano plot highlighting genes differentially expressed by γδ T cell density in the primary tumour. *X axis denotes the log2 fold change. Y axis denotes the -log10 of the p value as determined via Wald's test. Vertical dashed lines mark a log2 fold change of 1 (fold change of 2) and a log2 fold change of -1 (fold change of 0.5). Horizontal dashed line marks -log10 of the significance threshold, 0.05.*

6.5.2 CD8 T cells – differentially expressed genes

In the primary tumour, cases classed as high for γδ T cells had a greater expression of; *CDCP1*, the homeostatic function of which is not understood; *DCBLD2*, a poorly understood gene which is associated with an unfavourable prognosis in CRC [335]; *IGHV1-46*, encoding the variable region of immunoglobulin heavy chains; *WARS*, an understudied component of the viral immune response [336]; *APOE*, which encodes a component of lipid transportation [337]; *BCAT1*, an enzyme for amino acid transamination [337] (Figure 6.76). Cases classed as low for CD8 T cells had a greater expression of *HSD1787*, a cholesterol synthase enzyme [338] (Figure 6.76).

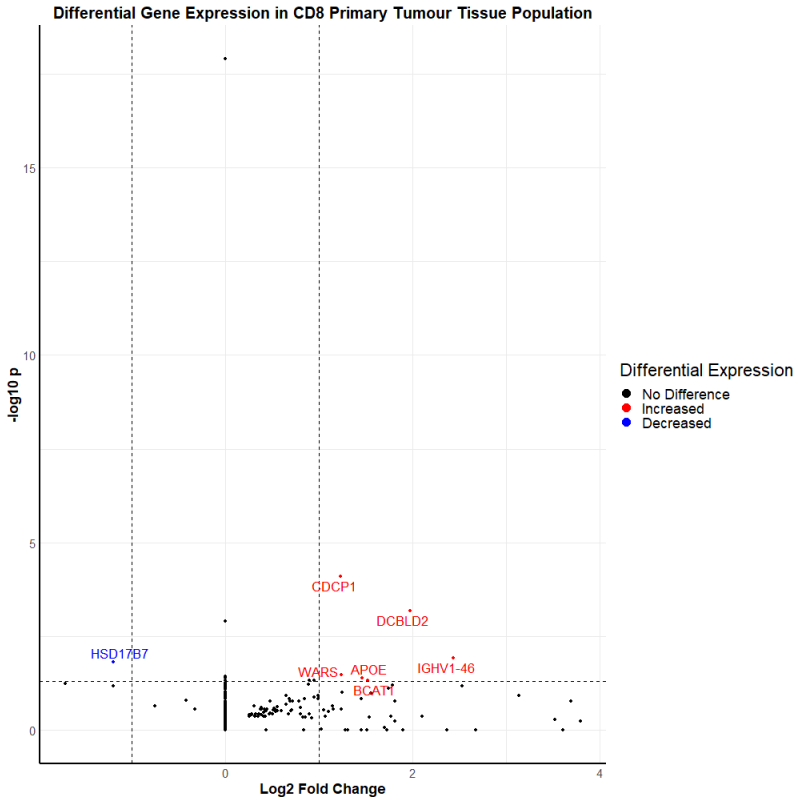

Figure 6.76 – Volcano plot highlighting genes differentially expressed by CD8 T cell density in the primary tumour. *X axis denotes the log2 fold change. Y axis denotes the -log10 of the p value as determined via Wald's test. Vertical dashed lines mark a log2 fold change of 1 (fold change of 2) and a log2 fold change of -1 (fold change of 0.5). Horizontal dashed line marks -log10 of the significance threshold, 0.05.*

6.6 Pathway analysis

6.6.1 γδ T cells – pathway analysis

To understand if specific pathways are upregulated or downregulated in γδ high cases compared to γδ low cases, gene set enrichment analysis was conducted using 'hallmark' gene sets which represent well defined biological processes. Some hallmark pathways demonstrated a strong enrichment score, however only 'KRAS signalling DN', which represents genes downregulated during *KRAS* activation, reached the standard adjusted significance threshold of an FDR value of 0.25 (Table 6.3). Only gene sets associated with inflammation, interferon α response, interferon γ response and TNF signalling via NF-κB showed any association with either group (Figure 6.77A-D). In the case of the inflammatory response, interferon γ response and TNFα signalling via NF-κB, there was the presence of gene set components along the length of gene ranks but with a greater density at the top of the rankings. In the case of interferon α response, gene set components were aggregated at the top of the gene rankings with a lesser aggregation at the bottom of the gene ranks. *DUSP1*, shown to be differentially expressed in cases high for γδ T cells (Figure 6.75), is a leading edge gene in the 'Hypoxia' and 'TNF signalling via NF-κB' hallmarks, which include genes upregulated in response to hypoxia and genes regulated by NF-κB in response to TNF signalling, respectively. *CITED2*, shown to be differentially expressed in cases high for γδ T cells (Figure 6.75), is a leading edge gene in the 'Hypoxia' and 'Glycolysis' hallmarks, which include genes upregulated in response to hypoxia and genes encoding proteins integral to glycolysis, respectively.

Table 6.3 – Gene set enrichment data for top 10 positively and negatively enriched gene sets in the context of histological classification of γδ T cell density. *Pathway size quantifies the number of individual genes present in the pathway that are also present in the input data. Leading edge genes are those that contribute most heavily to the enrichment score.*

Pathway	P Value	FDR	log2 Error	Enrichment Score	Normalised Enrichment Score	Pathway Size	Leading Edge
CHOLESTEROL HOMEOSTASIS	0.354	0.907	0.093	0.995	1.338	74	ATF5, ANTXR2
INTERFERON ALPHA RESPONSE	0.174	0.907	0.136	0.998	1.322	96	OASL, IRF9
BILE ACID METABOLISM	0.024	0.606	0.352	0.999	1.313	112	BMP6, BCAR3
SPERMATOGENESIS	0.306	0.907	0.094	0.996	1.304	133	PIAS2, PEBP1
HYPOXIA	0.134	0.907	0.148	0.998	1.253	199	CITED2, DUSP1, DDIT3
INFLAMMATORY RESPONSE	0.239	0.907	0.107	0.997	1.253	200	LCP2, CD69, STAB1, SPHK1
INTERFERON GAMMA RESPONSE	0.140	0.907	0.145	0.998	1.252	198	LCP2, SECTM1, OASL, CD69, IRF9
TNFA SIGNALING VIA NFKB	0.348	0.907	0.085	0.996	1.252	200	DUSP1, CD69, TNFAIP8, SPHK1, EIF1
GLYCOLYSIS	0.171	0.907	0.129	0.997	1.251	198	CITED2, ERO1A
HEME METABOLISM	0.208	0.907	0.117	0.997	1.247	194	UCP2, HDGF
MITOTIC SPINDLE	0.708	0.907	0.079	-0.571	-0.711	199	SEPTIN9, TAOK2, LRPPRC, KIF5B, RICTOR, CDC42BPA, CDK1, AKAP13, PALLD, RAB3GAP1, ARHGEF12, MYO1E, NUSAP1, NIN
HEDGEHOG SIGNALING	0.784	0.907	0.060	-0.496	-0.727	36	CDK6, PTCH1, CELSR1, TLE3, DPYSL2
MYC TARGETS V1	0.697	0.907	0.079	-0.587	-0.733	194	MCM7, HNRNPU
REACTIVE OXYGEN SPECIES PATHWAY	0.506	0.907	0.082	-0.653	-0.950	49	ABCC1, PRDX6, NDUFS2, GLRX, FTL, SOD1, PRDX4, FES, EGLN2
E2F TARGETS	0.522	0.907	0.095	-0.993	-1.239	196	MCM7
P53 PATHWAY	0.578	0.907	0.089	-0.990	-1.241	195	NUDT15
KRAS SIGNALING DN	<0.001	0.029	0.477	-0.999	-1.253	195	NR6A1
UV RESPONSE UP	0.468	0.907	0.098	-0.994	-1.270	156	HNRNPU
ANGIOGENESIS	0.221	0.907	0.135	-0.867	-1.271	36	VCAN, VAV2, TNFRSF21, APP, FSTL1
WNT BETA CATENIN SIGNALING	0.123	0.907	0.185	-0.997	-1.476	42	AXIN1

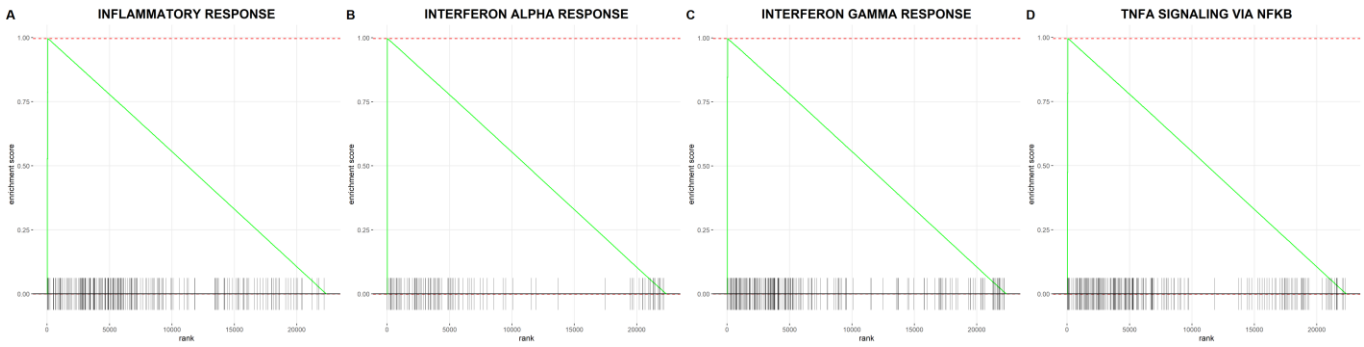

Figure 6.77 – Enrichment plots for pathways selected from the gene set enrichment analysis results in the context of histological classification of γδ T cell density. *A – Enrichment plot for angiogenesis. B – Enrichment plot for interferon alpha signalling. X axis denotes the continuous scale of gene ranks. Genes which are present in the gene set of interest are marked by a vertical bar at 0.0 on the y axis, at the X axis coordinate representing their gene rank. Y axis denotes the enrichment score. Green line reflects the unnormalised enrichment score. Red dashed lines are minimum and maximum enrichment scores values.*

6.6.2 CD8 T cells – pathway analysis

To understand if specific pathways are upregulated or downregulated in CD8 high cases compared to CD8 low cases, gene set enrichment analysis was conducted using 'hallmark' gene sets which represent well defined biological processes. Some hallmark pathways demonstrated a strong enrichment score, however none of these reached the standard adjusted significance threshold of an FDR value of 0.25 (Table 6.4). Only gene sets associated with angiogenesis and interferon α response showed any association with either group and this association is minimal (Figure 6.78A/B). In the case of angiogenesis, the spread of ranked genes although absent in the highest ranked genes was consistent across the remaining ranks (Figure 6.78A). In the case of interferon α response, the spread of gene set components amongst the ranked genes was inconsistent although there was an aggregation of ranked genes at the top of the rankings with a leading edge consisting of VCAN, VAV2, TNFRSF21, APP and FSTL1, indicating that interferon α signalling response genes are upregulated to a degree in cases that are high for CD8 T cells compared to those that are low for CD8 T cells (Figure 6.78B). *DCBLD2*, shown to be differentially expressed in cases high for CD8 T cells (Figure 6.76), is a leading edge gene in the 'Apical surface' hallmark which encompasses genes that are over represented on the apical surface of epithelial cells, and also in the KRAS signalling UP hallmark which includes genes upregulated during *KRAS* activation. *BCAT1*, shown to be differentially expressed in cases high for CD8 T cells (Figure 6.76), is a leading edge gene in the 'Allograft rejection' hallmark which is composed of genes up-regulated during transplant rejection.

Table 6.4 – Gene set enrichment data for top 10 positively and negatively enriched gene sets in the context of histological classification of CD8 T cell density. *Pathway size quantifies the number of individual genes present in the pathway that are also present in the input data. Leading edge genes are those that contribute most heavily to the enrichment score.*

Pathway	P Value	FDR	log2 Error	Enrichment Score	Normalised Enrichment Score	Pathway Size	Leading Edge
HEDGEHOG SIGNALING	0.230	0.710	0.113	0.995	1.440	36	PML, MYH9
APICAL SURFACE	0.040	0.667	0.288	0.999	1.428	44	DCBLD2, CROCC
COAGULATION	0.252	0.710	0.094	0.997	1.228	138	PLAU, ANXA1, GSN, GNG12
MYOGENESIS	0.025	0.617	0.352	0.999	1.165	199	TNNI2, GSN
KRAS SIGNALING DN	0.023	0.617	0.352	0.999	1.165	196	KLK7, SLC6A14, AKR1B10
ESTROGEN RESPONSE EARLY	0.122	0.710	0.138	0.998	1.164	199	CALB2, MYBL1, CA12
APICAL JUNCTION	0.123	0.710	0.137	0.998	1.164	199	CLDN6, CALB2, ITGA10, LAMA3, INSIG1
KRAS SIGNALING UP	0.227	0.710	0.096	0.997	1.162	199	DCBLD2, PLAU, BIRC3, ADAM17
ALLOGRAFT REJECTION	0.147	0.710	0.125	0.998	1.162	195	BCAT1, AKT1
P53 PATHWAY	0.280	0.710	0.085	0.997	1.161	195	TNFSF9, RAP2B, UPP1, TM4SF1, SAT1, VAMP8
BILE ACID METABOLISM	0.978	0.978	0.076	-0.335	-0.603	112	IDI1, PRDX5, IDH2, SOD1, SLC29A1, PEX13, CAT, ABCA1, ACSL5, PFKM, ALDH9A1, MLYCD, CH25H, PEX7, ABCA2, PEX11G
HEME METABOLISM	0.741	0.849	0.111	-0.433	-0.795	194	VEZF1, HAGH, RNF19A, PICALM, TOP1, SELENBP1, DMTN, CAT, KHNYN, TMEM9B, SLC11A2, MFHAS1, ARHGEF12, LAMP2, GAPVD1
INTERFERON ALPHA RESPONSE	0.438	0.710	0.115	-0.555	-1.003	96	LY6E, UBE2L6, PLSCR1, PSMB9, GBP2, RNF31, B2M, MX1, SLC25A28
SPERMATOGENESIS	0.386	0.710	0.140	-0.557	-1.028	133	PRKAR2A, VDAC3
MYC TARGETS V2	0.343	0.710	0.120	-0.612	-1.093	58	FARSA, WDR43, NOP2, NOC4L, EXOSC5, NOLC1, PRMT3, AIMP2, SLC29A2, MYBBP1A
UNFOLDED PROTEIN RESPONSE	0.301	0.710	0.152	-0.617	-1.111	110	FUS, PARN, DCP2, ALDH18A1, NFYA, ERN1, CEBPB, SPCS1, ATF6, KHSRP
ANGIOGENESIS	0.338	0.710	0.117	-0.659	-1.150	36	NRP1, TNFRSF21, ITGAV, S100A4, APP
FATTY ACID METABOLISM	0.197	0.710	0.207	-0.648	-1.204	156	HSD17B7
TGF BETA SIGNALING	0.115	0.710	0.217	-0.792	-1.417	54	SKI, TGFBR1, ACVR1, SLC20A1

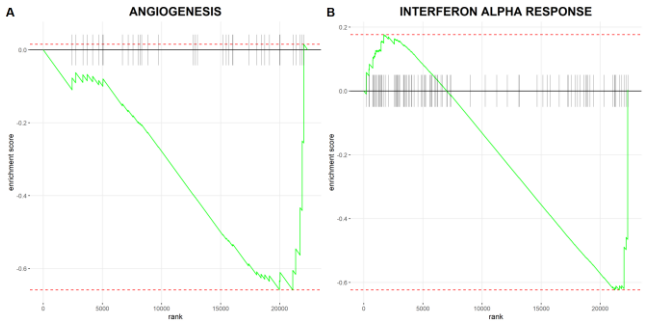

Figure 6.78 – Enrichment plots for pathways selected from the gene set enrichment analysis results in the context of histological classification of CD8 T cell density. *A – Enrichment plot for angiogenesis. B – Enrichment plot for interferon alpha signalling. X axis denotes the continuous scale of gene ranks. Genes which are present in the gene set of interest are marked by a vertical bar at 0.0 on the y axis, at the X axis coordinate representing their gene rank. Y axis denotes the enrichment score. Green line reflects the unnormalised enrichment score. Red dashed lines are minimum and maximum enrichment scores values.*

6.7 Discussion

Attempts at transcriptional lymphocyte deconvolution have so far produced accurate results in many lymphocyte subsets, but others including γδ T cells have been less successful. The most oft cited algorithm is that of CIBERSORT which does not accurately identify γδ T cells nor does it utilise the genes encoding the γδ T cell chains, and both its original development and attempts to refine it have relied on micro-array analysis of purified samples of circulating $V\gamma9V\delta2^{+}$ T cells which are not the resident population in the intestine [11, 187]. To transcriptionally validate the histological classification of γδ T cells, and with CIBERSORT not an appropriate choice, the expression of genes encoding γδ T cell and CD8 T cell chains were compared between cases histologically classed as low or high γδ T cells and CD8 T cells.

In the context of CD8 T cells, there was no difference in the expression of genes related to γδ T cells or CD8B (CD8β), but there was a difference in CD8A (CD8α) expression with CD8 high cases having a higher median expression, although there was significant overlap between low and high groups (Figure 6.1B). The intestine is populated by unconventional T cells expressing either the αβ or γδ TCR which are primarily either $CD4^{-}CD8^{-}$ or express a CD8αα homodimer [339-341], potentially accounting for the greater expression of CD8A but not CD8B. In contrast, cases high for γδ T cells had a much higher expression of both CD8A and CD8B with no difference in expression between CD8A and CD8B (Figure 6.1A), suggesting that the difference in CD8 expression is greater in the context of γδ T cells than in αβ T cells which will also be detected when cases are classed by CD8 expression. In the context of γδ T cells, there was no expression of the genes encoding for Vδ2 or Vδ3 chains, whilst there was expression of the gene encoding for the tissue associated Vδ1 chain (Figure 6.1A). In addition, cases for high for γδ T cells had a much greater expression of the gene encoding the intestine associated Vγ4 chain (Figure 6.1A). Vγ3 also was also expressed although with great variance. Interestingly, gene encoding for Vγ10, believed to be a pseudogene in humans but functional in other primates, was highly expressed in both γδ T cell low and high cases with no difference between the two. This may translate into a non-functional protein or not be translated at all, but further investigation would be of value given its comparable expression to that of the gene encoding the Vγ4 chain.

Further to unknown translational status of these RNA, genes encoding T cell chains are recombinant genes and so these measures of T cell chain gene expression are representative of disparate RNA sequences. In addition, although differential expression was found between groups histologically classified as low or high, correlation analysis showed no strong correlations between the raw % positive score and gene expression. In addition, Chi^2 analysis of the categorical low/high classification of both histological data and transcriptional data showed no associations. Together, these observations suggest that histological classification of γδ is transcriptionally validated although some unexpected observations occurred and warrant further investigation. However, it should be stressed that the group numbers are severely imbalanced with only three γδ low cases (of 79) and seven CD8 high cases (of 80).

To understand if regulatory molecules are key factors in lymphocyte density, associations were explored with the intestine restricted butyrophilin like molecules BTNL3 and BTNL8, which dimerise and bind the γ chain of γδ T cells to enable their development and maintenance within the intestine. Our current understanding of the relationship between γδ T cells and BTNL proteins would lead to the hypothesis that a reduced expression of BTNL3/8 would be associated with a lower density of γδ T cells but interestingly this data does not support that hypothesis as there was no difference in their expression (Figure 6.7). There is no known function for BTNL9, which was expressed at a slightly higher level than BTNL3/8, in the intestinal immune landscape but BTNL9 having a comparable expression profile to BTNL3 and BTNL8 may point to an active role that warrants further investigation. It would also be of value to histologically explore the status of BTNL proteins in this cohort. However, caution must again be exercised when drawing conclusions due to the numbers available in the groups.

Having compared histological and transcriptional lymphocyte density, analysis was conducted to determine if the prognostic value of these populations in the primary tumour is also reflected in the transcriptional data. Cases classed as high for expression of *TRDV1*, which encodes the Vδ1 chain associated with intestinal γδ T cells, were associated with an unfavourable cancer-specific prognosis (Figure 6.9) as in the case of those histologically classed as γδ high (Figure 4.6). There was no correlation between cancer-specific survival and expression of *TRDV2* or *TRDV3* (Figures 6.10 and 6.11), encoding the Vδ2 and Vδ3 chains respectively. In contrast, cases high for *TRGV1*, *TRGV3* and *TRGV9,* encoding the Vγ1, Vγ3 and Vγ9 chains respectively, had a favourable cancer-specific prognosis (Figures 6.12, Figure 6.14, and Figure 6.18). No other genes showed an association. However, it should be noted that the group number were severely imbalanced for all but the *TRDV1* analysis, which is also theoretically the most reflective of the intestinal γδ compartment. In the context of overall and disease-free survival, cases classed as high for *TRDV1* expression again reflected the unfavourable prognosis seen in cases histologically classed as high for γδ T cells (Figure 6.21 and Figure 6.33) whilst those classed as high for *TRGV4* expression had a favourable prognosis (Figure 6.27 and Figure 6.39). It is interesting that Vγ4 showed a favourable prognosis for overall survival, but again the group numbers are heavily imbalanced in this analysis. In the context of recurrence-free survival, histological analysis did not show a prognostic role for γδ T cells, but cases classed as high for *TRDV1* expression had an unfavourable recurrence-free prognosis (Figure 4.24 and Figure 6.45). In the context of cancer-specific, overall, disease-free, and recurrence-free survival, cases classed as high for expression of *CD8A* (CD8α) associated with an unfavourable prognosis (Figure 6.67, Figure 6.69, Figure 6.71, and Figure 6.73) whilst those classed as high for expression of *CD8B* (CD8β) associated with a favourable prognosis (Figure 6.68, Figure 6.70, Figure 6.72, and Figure 6.74). When classified as low or high for CD8 T cells using histological data, cases high for CD8 T cells had a favourable cancer-specific and recurrence-free prognosis with no difference in in overall or disease-free survival. It is interesting that *CD8B* expression reflects the histological findings but *CD8A* expression does not. It is possible that γδ T cells resident in this tissue are equipped with CD8αα homodimers and thus the two populations are connected and associating with a shared prognostic effect, but to understand this would require further analysis via multiplex staining. Thus, transcriptional classification of patients as low or high for γδ T cells and CD8 T cells in the primary tumour indicates a prognostic value reflective of that seen under histological classification.

Analysis of differentially expressed genes did not highlight any γδ T cell specific genes, but did highlight *DAP12* which is expressed on γδ T cells and mediates signal transduction for innate immune cell receptors [322, 323] (Figure 6.75). There was a weak association between histological classification of γδ T cells and some immune related hallmark gene sets (Figure 6.77A-D), but these associations were not convincing, and none reached significance. The Scotland cohort includes comprehensive data for the NF-κB pathways, so future work could explore this further. Of those genes differentially expressed in cases histologically classed as high for CD8 T cells, there was again no representation of relevant genes (Figure 6.76) and again even the most promising hallmark gene sets were unconvincing (Figure 6.78A-D). The most convincing hallmarks identified during pathway analysis relate to immune pathways, including both interferon α and interferon γ signalling. These pathways orchestrate all arms of the immune response. Interferon γ is a key activator of macrophages and induces MHC-II expression and expressed by multiple T cell populations.

These analyses suggest that there is concordance between the transcriptional landscape and histological data and that further refinement transcriptional methodologies for lymphocyte deconvolution may benefit not just from expanding the training samples to include tissue resident subsets, but the deliberate inclusion of genes specific to the TCR chains of γδ T cells. Unfortunately, differential gene expression was not insightful to explaining the results seen so far.

Chapter 7:
Summary Discussion

Chapter 7: Discussion

CRC is the third most common cancer in men and second most common in women worldwide, rising from fourth and third most common in 2002, respectively [1-3]. CRC is estimated to kill over 881 000 people worldwide [1-3]. The current gold standard prognostic tool employed in the clinic, TNM staging, is powerful but suffers from a lack of prognostic accuracy in some groups of patients [4, 66]. As our understanding of the role of the immune system in cancer has developed, efforts to utilise the immune landscape to improve prognostic tools has led to the development of Immunoscore®, which shows a level of improved prognostic power compared to TNM staging [8, 9]. In recent times, efforts have been made to utilise unconventional T cell subsets such as γδ T cells, but these efforts have relied on transcriptional studies which are based on a flawed methodology [11, 187]. To date, there has not been a comprehensive histological study investigating the prognostic role of γδ T cells, and this thesis seeks to resolve that gap in our understanding. To that end, this thesis sought to interrogate lymphocyte density within our cohorts and use this data to investigate the prognostic role of these lymphocyte populations. This is achieved by developing a digital image analysis workflow and applying this to images of full sections to histologically establish the density of γδ T cells and CD8 T cells and classify each case as 'low' or 'high' using the maximally selected rank statistic. These classifications are then used to stratify cases for in depth survival analysis (cancer-specific, overall, disease-free, and recurrence-free). These analyses are conducted across three geographically distinct cohorts and include density metrics for the whole primary tumour and if available the normal tissue adjacent to the primary tumour – these tissue regions are further broken down into epithelium and stroma/lamina propria. Thus, this thesis can comprehensively investigate - using varied study cohorts, histological staining, and advanced digital analysis methodologies – the relative density and prognostic role of γδ T cells and CD8 T cells and contextualise these data using extensive clinical data available in the study cohorts. This constitutes the first stage of this thesis and fills a significant gap in our understanding of γδ T cells in CRC and how this role compares to that of the CD8 T cells that have been the primary effector population investigated to date.

Having elucidated the density of lymphocyte populations and their prognostic role, the second stage of the project asked the question 'What underlies the histological classification of cases by lymphocyte density and do these same factors underly their prognostic role?'. Although functional assays are not utilised in this study, and thus causal links are outside of the scope of the thesis, this work seeks to determine the mutational and transcriptional landscapes associated with these histological classifications and their prognostic roles. Thus, candidates can be proposed for future studies with the aim of making causal connections. To achieve this, the mutational landscape associated with histological classifications was identified using the maftools package in R. Analysis revealed genes in which mutations are associated with histological classification, the degree of co-mutation between highlighted genes, the location and classification of mutations, associations between the highlighted mutations and relevant clinical factors and the prognostic role associated with these mutations. This approach was then expanded to transcriptomics data, revealing differentially expressed genes by histological classification of lymphocyte density and potentially relevant pathways. In addition, transcriptional data was used to validate histological findings and investigate genes encoding key regulatory proteins for γδ T cells.

Summary of Findings

Lymphocyte density

The intestinal tract, acting as a frontline defence against external factors, contains a dense and complex immune landscape, including T cells [262, 342, 343]. Immune cell exclusion is an established phenomenon in the cancer setting [344], but other studies have shown an increased density of leucocytes and differing phenotypes in CRC tumours compared to normal tissue [146, 345] and also in matched liver metastases [346]. This increased immune infiltrate is especially notable in MSI CRC cases [41, 44-46]. Interestingly, in this data both γδ T cells and CD8 T cells were reduced in the primary tumour compared to the adjacent normal tissue, across all cohorts (except for CD8 T cells in the Norway cohort). This would suggest that the exclusion of T cells in CRC is a consistent characteristic but that there is a differentiating factor in the Norway population. However, even if a large population of T cells is present, the TME can be immunosuppressive such that even present T cells may be dysfunctional or even hijacked for pro-tumourigenic purposes [347]. The phenotype of these lymphocyte populations cannot be investigated within this study and so it is important to keep the distinction between lymphocyte density and lymphocyte functionality in mind.

Lymphocytes within the intestinal tissue are typically housed within the epithelium where they can conduct their patrolling behaviour and so density was compared between the epithelium and the stroma/lamina propria. Interestingly, γδ T cells were present at a greater density in the stroma than the epithelium, whilst CD8 T cells were similarly distributed in the Scotland cohort but not the Norway cohort. One explanation for this unexpected result is that the localisation of these cells has been altered in the cancer setting. However, it is also possible that this is an analytical flaw as these cells are typically moving along the epithelium and not necessarily within the cellular layer, so they may be counted as stromal despite actively engaging with the epithelial cells. The key finding in terms of lymphocyte density was that both populations are present at a reduced density in the primary tumour compared to adjacent normal tissue.

Survival analysis

T cells, including CD8 T cells specifically, have a demonstrated favourable prognostic role in CRC [8, 79, 348, 349] and are a strong candidate to improve the current methods patient stratification. γδ T cells have been suggested to have a favourable prognostic role but these data are based on flawed methodology [10, 187]. Therefore, this work sought to determine the prognostic role of γδ T cells and CD8 T cells in these cohorts. Having determined the density of γδ T cells and CD8 T cells in these populations, patients underwent histological classification as 'low' or 'high' for γδ T cells or CD8 T cells using the maximally selected rank statistic. Survival analysis was conducted with these classifications as groups.

γδ T cells were found to be an unfavourable prognostic marker in the Scotland cohort. CD8 T cells were found to be a favourable prognostic marker in the Scotland cohort. Both γδ T cells and CD8 T cells failed to demonstrate prognostic value in the Norway cohort. This is likely because the cut point from the Scotland cohort is used to classify cases in the Norway cohort which is a distinct population. Indeed, when the cut points are generated using the Norway cohort, similar results are seen in the Norway cohort as were previously seen in the Scotland cohort and the Scotland cohort no longer demonstrates prognostic effect. This would suggest that the prognostic effect of the populations is consistent but the relative density of these populations in each cohort distorts this as the Scotland does have a higher inflammatory state. However, to be used clinically a candidate biomarker usually needs to have a widely applicable cut point, but in this case, it may not be possible to apply one cut point to all populations. The key finding from this analysis is that whilst CD8 T cells are favourably prognostic, γδ T cells are unfavourably prognostic, challenging the transcriptional data available to date.

Underlying Genomics and Transcriptomics

The first stage of this thesis determined the density of γδ T cells and CD8 T cells in three cohorts of CRC patients and elucidated the prognostic role that these lymphocyte populations play and how this differs between cases deem 'low' or 'high'. Next, we sought to understand what genomic landscape underlies these differences in lymphocyte density and prognostic effect. Genomic analysis showed that mutations in genes that are often mutated in the microsatellite regions in MSI cases (*ASTE1, TTK*), a context in which they associate with greater immune infiltrate, were more prevalent in cases histologically classed as high for γδ T cells or CD8 T cells. Interestingly, there was no histological difference in lymphocyte density between MMR deficient and MMR proficient cases. This leads to the hypothesis that MMR deficiency does not result in a greater immune infiltrate by itself, but rather when these mutations occur this combination leads to a greater immune infiltrate. Mutations in *BRAF*, which cooccur with mutations in *TTK* and *ASTE1*, were also associated with a high density of CD8 T cells. Mutations in *BRAF* are also associated with MSI and right sided disease. The key finding from mutational analysis is that there is a strong representation of MSI within cases classed as high for γδ T cells and CD8 T cells, and this may be a key factor in this lymphocyte density. Transcriptomic analysis identified a handful of differentially expressed genes, but of these only *DAP12* is T cell relevant, being expressed on γδ T cells and mediating signal transduction for innate receptors. There was a minor degree of association between lymphocyte density and some hallmark gene sets, primarily immune related. However, none of the pathway analysis was convincing and is unlikely to be relevant. Despite the lack of informative results from transcriptomic analysis, genomic analysis showed a strong association between lymphocyte density and mutations associated with MSI.

Transcriptomic Validation of Histological Data

Attempts at lymphocyte deconvolution using transcriptional methodologies have been found flawed due to their reliance on circulatory γδ T cells. In addition, the gene signatures for γδ T cells are not based on γδ T cell-specific genes. Thus, the degree of transcription of genes encoding the γδ TCR or CD8 coreceptor chains were compared between those classed as low and high for γδ T cells or CD8 T cells. This produced two results that support the need for transcriptional deconvolution to utilise these key genes. First, cases histologically classed as high for CD8 T cells had a greater transcription of CD8α, but not CD8β, suggesting that not only is this a good identifier for CD8 T cells, but that the CD8 T cells being detected are likely to have a dominant proportion of CD8αα T cells. Second, only the gene encoding Vδ1, the intestinal dominant δ chain, was expressed. Furthermore, the dominant γ chain (Vγ4) was transcribed at a higher level in γδ high cases compared to γδ low cases. Thus, the transcription of these key genes aligns with histological findings, strongly suggesting that future deconvolution methods should be supervised for inclusion of these genes. In addition, the expression of *BTNL3* and *BTNL8*, which encode regulatory genes integral to the formation and maintenance of the γδ T cell compartment, was compared between cases classed as low and high for γδ T cells. Surprisingly, there was no difference in expression between low and high cases. Regulatory molecules may have been an additional source of improvement to lymphocyte deconvolution, but this data suggests that this is not the case. Potentially, this is because the maintenance of the γδ compartment is reliant on the presence of Btnl proteins, but that a threshold of expression is sufficient and so does not correlate with γδ T cell density.

Validation was expanded to survival analysis. Histology based survival analysis showed very clear prognostic roles for both γδ T cells and CD8 T cells. There are significant flaws in current methodologies of lymphocyte deconvolution to date, making transcriptional survival analysis unreliable. Interestingly, when survival analysis was applied to the Scotland cohort with cases classed as low or high for γδ T cells or CD8 T cells based on the transcription of genes encoding the γδ TCR or CD8 coreceptor chains, comparable results were seen. This highlights a key issue with current methods of lymphocyte deconvolution for γδ T cells which do not include γδ T cell-specific genes in the signatures employed for deconvolution, whereas this analysis would suggest that this is the more appropriate approach. The key finding from this data is that despite flaws in current transcriptional methods of lymphocyte deconvolution, transcriptional data can be an accurate metric of γδ T cell density and could greatly improve these efforts within the field.

Future Perspectives

Future work stemming from this thesis should look to carry out more in-depth classification of the lymphocyte populations, explore their functional status and analyse the predictive role of these lymphocyte populations.

Multiplex Immunostaining

Singleplex immunohistochemistry was employed in this study to stain many full sections from patient samples. Thus, data is available for γδ T cells and CD8 T cells, but not in the same tissue. By applying multiplex immunostaining, the relative density (and relative localisation) of γδ T cells and CD8 T cells (and their proportion of total $CD3^+$ T cells) can be determined, including colocalization of γδ and CD8. This will a provide a more accurate relative density and account for the population of T cells that are both γδ and CD8 positive, which singleplex analysis cannot determine. In addition, if the appropriate antibodies could be developed, it would be beneficial to stain for specific γ and δ chains as γδ T cells subsets are distinct in their homeostatic localisation, functions, and ligands. This will also highlight whether there is an influx of circulating Vγ9Vδ2 T cells. Transcriptomic analysis suggests that the γδ compartment is dominated by the expected Vγ4Vδ1 population, but transcriptomics does not necessarily translate to proteomics and so having a histological stain to quantify would be invaluable. However, it is not financially feasible to apply this level of staining to this number of samples, so it would likely have to be applied to a sub-cohort. In some projects this could be approached using a tissue microarray (TMA) to stain a small portion of multiple cases in one section, however, due to the low density of γδ T cells this study found that TMA analysis was not feasible for this cell population.

Functional Assays

A notable limitation of this study is that the methodologies employed show the density of lymphocyte populations and their respective associations with survival outcomes. However, this study is unable to characterise the functional state of these lymphocyte populations. For example, it may be that a high density of γδ T cells associates with a poor survival outcome, but if specific interactions are not occurring in the TME then those cells lack a function that causes that poor outcome, and so that association is lost. Understanding the functionality of these cells would be an interesting additional context.

A potential experiment would be to extract lymphocytes from these cases and perform cytotoxicity assays against CRC cell lines and potentially against organoids grown from these same cases. This would provide some insight into how well these cells actively kill cancer cells and with alterations to their environment insight could also be gained into what other factors might be influencing their cytotoxicity. However, there are two key issues with this approach. These cohorts are pre-existing to this study and so these cell populations can no longer be obtained, requiring a new study cohort. In addition, even if experiments are conducted with organoids the true TME cannot be replicated and so such experiments would provide insight but not conclusive answers. Other cytokines of interest include IL-17, a key pro-tumourigenic cytokine.

Analysis of Predictive Value

It is hoped that integration of the immune landscape into stratification tools could allow for prediction of treatment response, particularly with an emphasis on immunotherapies that are currently being fiercely developed. Immunotherapies that target checkpoint receptors are of limited use in tumours without significant immune infiltrate, including CRC patients that do not have MSI. Thus, lymphocyte density may be a useful metric for determining if a positive treatment response is likely. In addition to this, the proportion of T cells belonging to various T cell subsets may also be a factor in predicting treatment response. For example, the effects of PD-1 blockage on γδ T cells have been explored in cancer types including CRC [350, 351]. Unfortunately, due to the age of these cohorts, this data is not available as treatment protocols have developed over time. It would be of great benefit to build a cohort with data available for current approaches to CRC treatment. This would likely mean a long wait for answers however and would constitute a long-term goal.

Additional Cohorts

This study utilises cohorts from three geographically distinct populations and includes stage I-III patients (stage IV excluded). It would be interesting to expand this work to two additional cohorts, a metastatic cohort, and an early development cohort, of comparable size to the cohorts used so far. This would extend the timeline of the study and reveal whether these findings are consistent as tumours initially develop and when they metastasise. This is of particular interest because γδ T cells have been previously implicated in metastatic development. It would also be of value to stain these cohorts for the Btnl proteins, key regulatory molecules for γδ T cells, as this study only investigates these molecules from a transcriptional perspective, but this does not necessarily reflect the proteomic reality.

Conclusion

The density of γδ T cells and CD8 T cells, determined histologically, is reduced in the primary tumour compared to the adjacent normal tissue of CRC patients, and is also reduced in the epithelium compared to the stroma/lamina propria, and this observation is consistent across three geographically distinct cohorts. When cases are classified by their histological density, γδ T cells and CD8 T cells have differential prognostic roles in CRC. γδ T cells are an unfavourable prognostic factor whilst CD8 T cells are a favourable prognostic factor. These data were transcriptionally validated within the Scotland cohort by reclassifying cases as low or high based on transcription of genes encoding the TCR γδ chain and CD8 coreceptor. These classifications showed results comparable to that of the histological data. Unfortunately, the specific subsets of γδ T cells would not be histologically determined due to a lack of appropriate antibodies and the use of singleplex analysis. This is a key limitation that future work could resolve using multiplex immunostaining. However, transcriptional analysis of genes encoding the TCR γδ chain and CD8 coreceptor would suggest that the dominant population of γδ T cells is the expected Vγ4Vδ1 population. Genomic analysis revealed a consistent theme of MSI related genes being mutated in cases histologically classed as high for γδ T cells or CD8 T cells. Specifically, mutations were more likely in *ASTE1* and *TTK*, which are frequently mutated in the microsatellite regions of MSI patients and associate with great immune infiltrate. In addition, these mutations often co-occurred with mutations in *BRAF*, which is likewise associated with MSI and a right sided pathology. Transcriptional analysis was not greatly informative in this study but of those genes found to be differentially expressed, one was *DAP12* which is involved in mediating signal transduction for innate receptors. Pathway analysis provided very weak suggestions of immune pathways being upregulated. The results of this study could be improved by a more in-depth histological analysis via multiplex staining, the use of functional assays in relation to lymphocytes harvested from patients, and extension of the selection of patient cohorts to include the early stages of disease progression and metastasis to the liver. These data, especially if the noted limitations can be resolved, form part of a continually growing evidence base suggesting that the immune infiltrate is a key factor in the progression, classification and treatment of CRC and that new methodologies of stratifying patients by utilising the immune landscape could be of great benefit to future generations of CRC patients.

Appendices

Chapter 3 - Lymphocyte Density

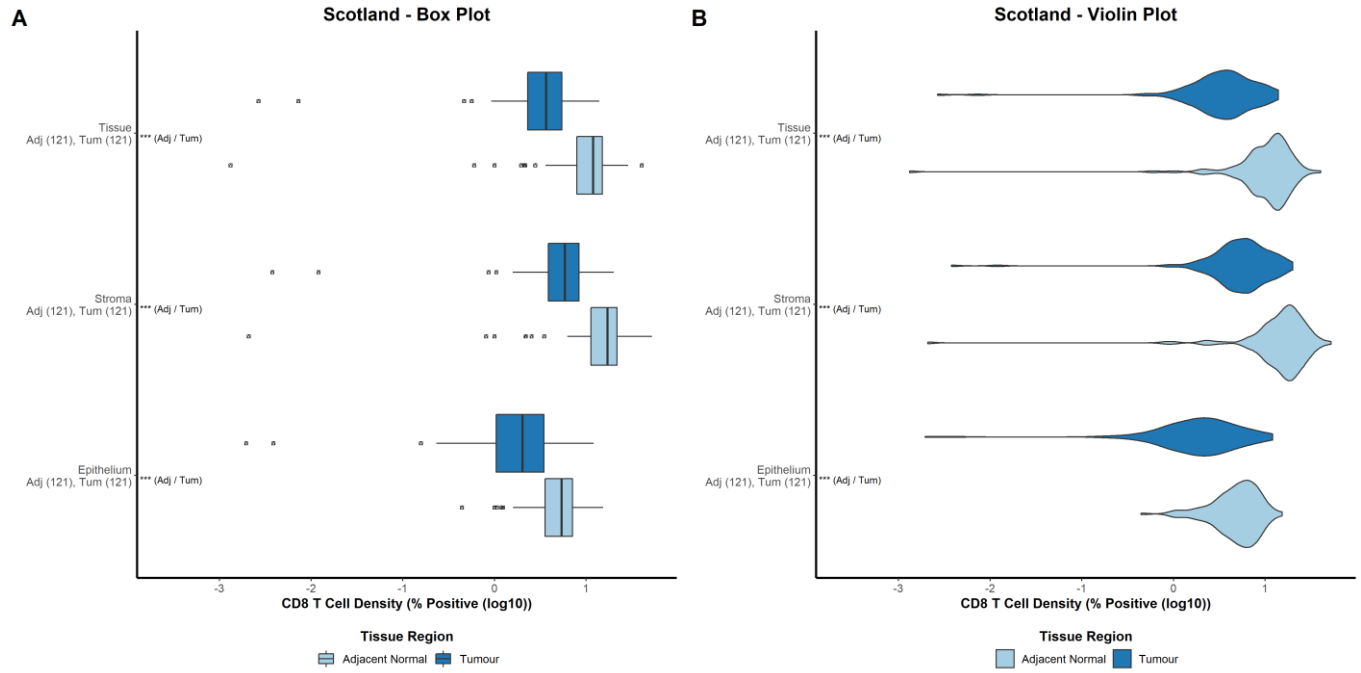

Figure S1 - Assessment of γδ T cell density in the primary tumour and adjacent normal tissue of the Scotland cohort without rectal cases. *Box plot presentation of γδ T cell density in the primary tumour (dark blue) and adjacent normal tissue (light blue). The box is representative of the interquartile range (middle 50% of data points), the vertical line denotes the median and the minimum and maximum are denoted by whiskers. Outliers are represented by an open triangle within an open square (A). Violin plot presentation of γδ T cell density in the primary tumour (dark blue) and adjacent normal tissue (light blue). The shape of the data reflects the distribution of the data points, which is not discernible in box plots (B). Y axis labels state the tissue compartment (epithelium, stroma and whole tissue) and below, the test groups with number of cases in brackets. X axis is log10 of the % of total cells within a region positive for the marker of interest. Inline labels denote the lowest standard statistical significance threshold reached (non-significant not shown) using a paired t-test, <0.05 (*), <0.01 (**) or <0.001 (***), with test groups in brackets.*

Chapter 4 - Survival

4.1 – Additional survival statistics

Table S1 – Median survival time for patients in the Glasgow cohort per analysis, stratified as low or high for a given lymphocyte population. *Median survival time represents the time taken to reach a state of 50% of patients having experienced an event. Median of survival time is the median value of the raw survival time.*

Group Descriptors			Median Values					
Cohort	Status	Variable	Median Survival Time (Low)	Median Survival Time (High)	Median of Survival Time (Low)	Median of Survival Time (High)	Mean of Survival Time (Low)	Mean of Survival Time (High)
Glasgow	CSS	GD_PercPositiveCellsinHealthyTissue	NA	130.00	112.00	79.50	97.46	82.68
Glasgow	CSS	GD_PercPositiveCellsinTumourTissue	NA	NA	128.00	67.00	105.61	79.61
Glasgow	CSS	GD_PercPositiveCellsinHealthyEpithelium	NA	130.00	112.00	78.00	97.53	81.08
Glasgow	CSS	GD_PercPositiveCellsinTumourEpithelium	NA	NA	122.00	66.50	100.71	79.90
Glasgow	CSS	GD_PercPositiveCellsinHealthyStroma	NA	105.00	112.00	78.50	96.82	81.02
Glasgow	CSS	GD_PercPositiveCellsinTumourStroma	NA	NA	128.00	66.00	111.04	79.02
Glasgow	CSS	CD8_PercPositiveCellsinHealthyTissue	NA	NA	102.00	119.50	90.13	99.29
Glasgow	CSS	CD8_PercPositiveCellsinTumourTissue	NA	NA	76.00	99.00	83.42	93.71
Glasgow	CSS	CD8_PercPositiveCellsinHealthyEpithelium	122.00	NA	62.00	114.00	78.68	94.12
Glasgow	CSS	CD8_PercPositiveCellsinTumourEpithelium	NA	NA	77.00	97.50	83.97	87.90
Glasgow	CSS	CD8_PercPositiveCellsinHealthyStroma	NA	NA	112.00	100.50	95.55	89.58
Glasgow	CSS	CD8_PercPositiveCellsinTumourStroma	122.00	NA	52.00	93.00	78.76	86.26
Glasgow	OS	GD_PercPositiveCellsinHealthyTissue	117.00	79.50	112.00	79.50	97.46	82.68
Glasgow	OS	GD_PercPositiveCellsinTumourTissue	152.00	67.00	128.00	67.00	105.61	79.61
Glasgow	OS	GD_PercPositiveCellsinHealthyEpithelium	117.00	78.00	112.00	78.00	97.53	81.08
Glasgow	OS	GD_PercPositiveCellsinTumourEpithelium	122.00	66.50	122.00	66.50	100.71	79.90
Glasgow	OS	GD_PercPositiveCellsinHealthyStroma	116.00	78.50	112.00	78.50	96.82	81.02
Glasgow	OS	GD_PercPositiveCellsinTumourStroma	152.00	66.00	128.00	66.00	111.04	79.02
Glasgow	OS	CD8_PercPositiveCellsinHealthyTissue	102.00	123.00	102.00	119.50	90.13	99.29
Glasgow	OS	CD8_PercPositiveCellsinTumourTissue	76.00	99.00	76.00	99.00	83.42	93.71
Glasgow	OS	CD8_PercPositiveCellsinHealthyEpithelium	62.00	117.00	62.00	114.00	78.68	94.12
Glasgow	OS	CD8_PercPositiveCellsinTumourEpithelium	77.00	97.50	77.00	97.50	83.97	87.90
Glasgow	OS	CD8_PercPositiveCellsinHealthyStroma	117.00	100.50	112.00	100.50	95.55	89.58
Glasgow	OS	CD8_PercPositiveCellsinTumourStroma	52.00	93.00	52.00	93.00	78.76	86.26
Glasgow	DFS	GD_PercPositiveCellsinHealthyTissue	116.00	55.00	112.00	55.00	94.03	70.98
Glasgow	DFS	GD_PercPositiveCellsinTumourTissue	152.00	53.50	128.00	53.50	104.50	73.65
Glasgow	DFS	GD_PercPositiveCellsinHealthyEpithelium	117.00	54.00	112.00	54.00	93.79	69.25
Glasgow	DFS	GD_PercPositiveCellsinTumourEpithelium	122.00	53.00	122.00	53.00	100.58	73.76
Glasgow	DFS	GD_PercPositiveCellsinHealthyStroma	116.00	53.00	111.50	53.00	93.40	67.57
Glasgow	DFS	GD_PercPositiveCellsinTumourStroma	152.00	52.00	128.00	52.00	109.75	73.08
Glasgow	DFS	CD8_PercPositiveCellsinHealthyTissue	83.00	123.00	83.00	119.50	82.73	98.33
Glasgow	DFS	CD8_PercPositiveCellsinTumourTissue	59.50	96.00	59.50	96.00	76.79	87.57
Glasgow	DFS	CD8_PercPositiveCellsinHealthyEpithelium	53.00	112.00	53.00	111.00	73.16	87.32
Glasgow	DFS	CD8_PercPositiveCellsinTumourEpithelium	58.00	92.50	58.00	92.50	76.91	83.52
Glasgow	DFS	CD8_PercPositiveCellsinHealthyStroma	112.00	89.00	111.00	89.00	92.17	81.63
Glasgow	DFS	CD8_PercPositiveCellsinTumourStroma	46.00	78.00	46.00	78.00	71.85	79.78
Glasgow	RFS	GD_PercPositiveCellsinHealthyTissue	NA	NA	102.00	55.00	85.80	70.06
Glasgow	RFS	GD_PercPositiveCellsinTumourTissue	NA	NA	120.00	45.00	90.43	70.20
Glasgow	RFS	GD_PercPositiveCellsinHealthyEpithelium	NA	NA	105.50	54.00	86.01	68.08
Glasgow	RFS	GD_PercPositiveCellsinTumourEpithelium	NA	NA	19.50	46.00	64.00	71.07
Glasgow	RFS	GD_PercPositiveCellsinHealthyStroma	NA	69.00	93.00	53.00	85.95	66.12
Glasgow	RFS	GD_PercPositiveCellsinTumourStroma	NA	NA	111.00	44.00	87.67	70.12
Glasgow	RFS	CD8_PercPositiveCellsinHealthyTissue	NA	NA	56.00	120.00	75.55	98.67
Glasgow	RFS	CD8_PercPositiveCellsinTumourTissue	NA	NA	42.50	111.00	70.52	96.22
Glasgow	RFS	CD8_PercPositiveCellsinHealthyEpithelium	NA	NA	46.00	91.00	62.72	82.75
Glasgow	RFS	CD8_PercPositiveCellsinTumourEpithelium	98.00	NA	39.50	89.00	70.62	86.03
Glasgow	RFS	CD8_PercPositiveCellsinHealthyStroma	NA	NA	109.00	59.50	88.26	74.90
Glasgow	RFS	CD8_PercPositiveCellsinTumourStroma	46.00	NA	38.00	55.00	65.22	75.33

Table S2 - Median survival time for patients in the Norway cohort per analysis, stratified as low or high for a given lymphocyte population. *Median survival time represents the time taken to reach a state of 50% of patients having experienced an event. Median of survival time is the median value of the raw survival time.*

Group Descriptors			Median Values					
Cohort	Status	Variable	Median Survival Time (Low)	Median Survival Time (High)	Median of Survival Time (Low)	Median of Survival Time (High)	Mean of Survival Time (Low)	Mean of Survival Time (High)
Norway	CSS	GD_PercPositiveCellsinHealthyTissue	NA	NA	72.00	78.00	77.24	74.00
Norway	CSS	GD_PercPositiveCellsinTumourTissue	NA	NA	65.00	72.00	70.91	77.07
Norway	CSS	GD_PercPositiveCellsinHealthyEpithelium	NA	NA	72.00	84.00	77.17	74.29
Norway	CSS	GD_PercPositiveCellsinTumourEpithelium	NA	NA	65.00	72.00	70.54	77.11
Norway	CSS	GD_PercPositiveCellsinHealthyStroma	NA	NA	72.50	72.00	77.46	71.00
Norway	CSS	GD_PercPositiveCellsinTumourStroma	NA	NA	67.00	71.50	71.85	75.58
Norway	CSS	CD8_PercPositiveCellsinHealthyTissue	NA	NA	76.00	72.00	81.54	83.89
Norway	CSS	CD8_PercPositiveCellsinTumourTissue	NA	NA	68.00	69.00	70.20	78.05
Norway	CSS	CD8_PercPositiveCellsinHealthyEpithelium	NA	NA	82.00	68.00	88.53	76.12
Norway	CSS	CD8_PercPositiveCellsinTumourEpithelium	NA	NA	68.00	70.00	69.41	75.26
Norway	CSS	CD8_PercPositiveCellsinHealthyStroma	NA	NA	80.00	60.00	86.42	66.41
Norway	CSS	CD8_PercPositiveCellsinTumourStroma	NA	NA	71.00	68.00	70.91	72.77
Norway	OS	GD_PercPositiveCellsinHealthyTissue	136.00	95.00	72.00	78.00	77.24	74.00
Norway	OS	GD_PercPositiveCellsinTumourTissue	113.00	NA	65.00	72.00	70.91	77.07
Norway	OS	GD_PercPositiveCellsinHealthyEpithelium	NA	95.00	72.00	84.00	77.17	74.29
Norway	OS	GD_PercPositiveCellsinTumourEpithelium	107.00	NA	65.00	72.00	70.54	77.11
Norway	OS	GD_PercPositiveCellsinHealthyStroma	136.00	105.00	72.50	72.00	77.46	71.00
Norway	OS	GD_PercPositiveCellsinTumourStroma	122.00	NA	67.00	71.50	71.85	75.58
Norway	OS	CD8_PercPositiveCellsinHealthyTissue	NA	NA	76.00	72.00	81.54	83.89
Norway	OS	CD8_PercPositiveCellsinTumourTissue	NA	105.00	68.00	69.00	70.20	78.05
Norway	OS	CD8_PercPositiveCellsinHealthyEpithelium	NA	126.00	82.00	68.00	88.53	76.12
Norway	OS	CD8_PercPositiveCellsinTumourEpithelium	NA	136.00	68.00	70.00	69.41	75.26
Norway	OS	CD8_PercPositiveCellsinHealthyStroma	NA	87.00	80.00	60.00	86.42	66.41
Norway	OS	CD8_PercPositiveCellsinTumourStroma	136.00	NA	71.00	68.00	70.91	72.77
Norway	DFS	GD_PercPositiveCellsinHealthyTissue	NA	NA	72.00	66.00	76.76	67.62
Norway	DFS	GD_PercPositiveCellsinTumourTissue	NA	NA	65.00	72.00	69.48	76.04
Norway	DFS	GD_PercPositiveCellsinHealthyEpithelium	NA	NA	72.00	60.00	76.70	67.00
Norway	DFS	GD_PercPositiveCellsinTumourEpithelium	NA	NA	65.00	72.00	69.02	76.18
Norway	DFS	GD_PercPositiveCellsinHealthyStroma	NA	NA	72.50	60.00	76.99	63.71
Norway	DFS	GD_PercPositiveCellsinTumourStroma	NA	NA	65.00	71.00	70.48	74.45
Norway	DFS	CD8_PercPositiveCellsinHealthyTissue	NA	NA	75.00	72.00	80.18	79.67
Norway	DFS	CD8_PercPositiveCellsinTumourTissue	NA	NA	65.00	69.00	67.75	78.05
Norway	DFS	CD8_PercPositiveCellsinHealthyEpithelium	NA	NA	80.00	68.00	87.03	74.25
Norway	DFS	CD8_PercPositiveCellsinTumourEpithelium	NA	NA	65.00	69.00	66.82	74.24
Norway	DFS	CD8_PercPositiveCellsinHealthyStroma	NA	NA	80.00	60.00	85.53	62.00
Norway	DFS	CD8_PercPositiveCellsinTumourStroma	NA	NA	68.00	68.00	68.41	71.38
Norway	RFS	GD_PercPositiveCellsinHealthyTissue	NA	NA	72.00	66.00	76.76	67.62
Norway	RFS	GD_PercPositiveCellsinTumourTissue	NA	NA	65.00	72.00	69.48	76.04
Norway	RFS	GD_PercPositiveCellsinHealthyEpithelium	NA	NA	72.00	60.00	76.70	67.00
Norway	RFS	GD_PercPositiveCellsinTumourEpithelium	NA	NA	65.00	72.00	69.02	76.18
Norway	RFS	GD_PercPositiveCellsinHealthyStroma	NA	NA	72.50	60.00	76.99	63.71
Norway	RFS	GD_PercPositiveCellsinTumourStroma	NA	NA	65.00	71.00	70.48	74.45
Norway	RFS	CD8_PercPositiveCellsinHealthyTissue	NA	NA	75.00	72.00	80.18	79.67
Norway	RFS	CD8_PercPositiveCellsinTumourTissue	NA	NA	65.00	69.00	67.75	78.05
Norway	RFS	CD8_PercPositiveCellsinHealthyEpithelium	NA	NA	80.00	68.00	87.03	74.25
Norway	RFS	CD8_PercPositiveCellsinTumourEpithelium	NA	NA	65.00	69.00	66.82	74.24
Norway	RFS	CD8_PercPositiveCellsinHealthyStroma	NA	NA	80.00	60.00	85.53	62.00
Norway	RFS	CD8_PercPositiveCellsinTumourStroma	NA	NA	68.00	68.00	68.41	71.38

Table S3 - Median survival time for patients in the Thailand cohort per analysis, stratified as low or high for a given lymphocyte population. *Median survival time represents the time taken to reach a state of 50% of patients having experienced an event. Median of survival time is the median value of the raw survival time.*

Group Descriptors			Median Values					
Cohort	Status	Variable	Median Survival Time (Low)	Median Survival Time (High)	Median of Survival Time (Low)	Median of Survival Time (High)	Mean of Survival Time (Low)	Mean of Survival Time (High)
Thailand	OS	GD_PercPositiveCellsinTumourTissue	52.32	53.45	52.32	53.45	48.78	51.75
Thailand	OS	GD_PercPositiveCellsinTumourEpithelium	51.27	54.72	51.27	54.72	48.11	53.66
Thailand	OS	GD_PercPositiveCellsinTumourStroma	52.24	53.85	52.24	53.85	48.79	51.78

Table S4 – Covariates used in multivariate analysis. *Covariates were selected by extracting univariate variables that were statistically significant in univariate models.*

Scotland.CSS	Scotland.OS	Scotland.DFS	Scotland.RFS	Norway.CSS	Norway.OS	Norway.DFS	Norway.RFS	Thailand.OS
Dukes	Dukes	Dukes	Dukes	Stage	T	Stage	Age65	N
tstage	tstage	tstage	tstage	T	Age65	T		M
nstage	nstage	nstage	nstage	N	TSP_Status	N		Sex
Diffcd	Age65	Age65	Age65	Age65		TSP_Status		Differentiation
vascinv	Diffcd	Diffcd	Diffcd	TSP_Status				Differentiation
Klintrup_code	vascinv	vascinv	vascinv					
TSP_2018	Klintrup_code	Klintrup_code	Klintrup_code					
		TSP_2018	TSP_2018					

4.2 – Time-to-event analysis by cutpoints generated from Norway data - Scotland

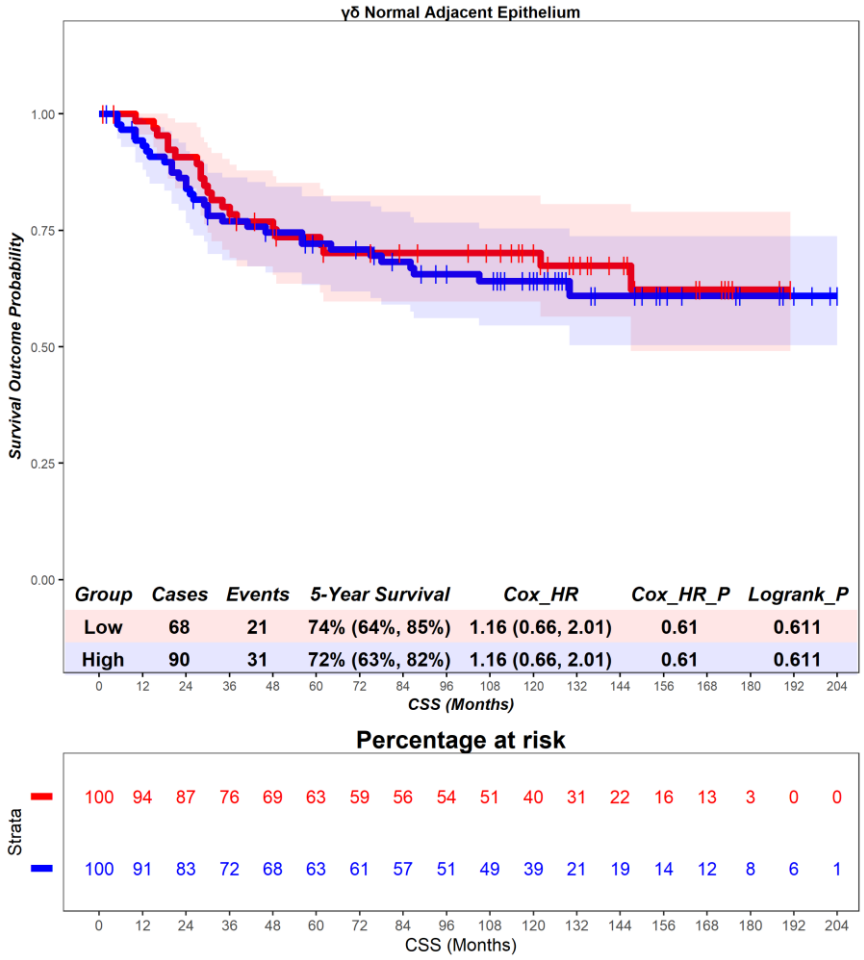

***Figure S2 – Time-to-event (cancer-specific survival) analysis for γδ T cells in the adjacent normal epithelium**. Patients deemed 'High' or 'Low' for γδ T cells are shaded blue and red, respectively. Cox hazard ratio is univariate. The 'Low' group is used as the reference group on cox regression modelling.*

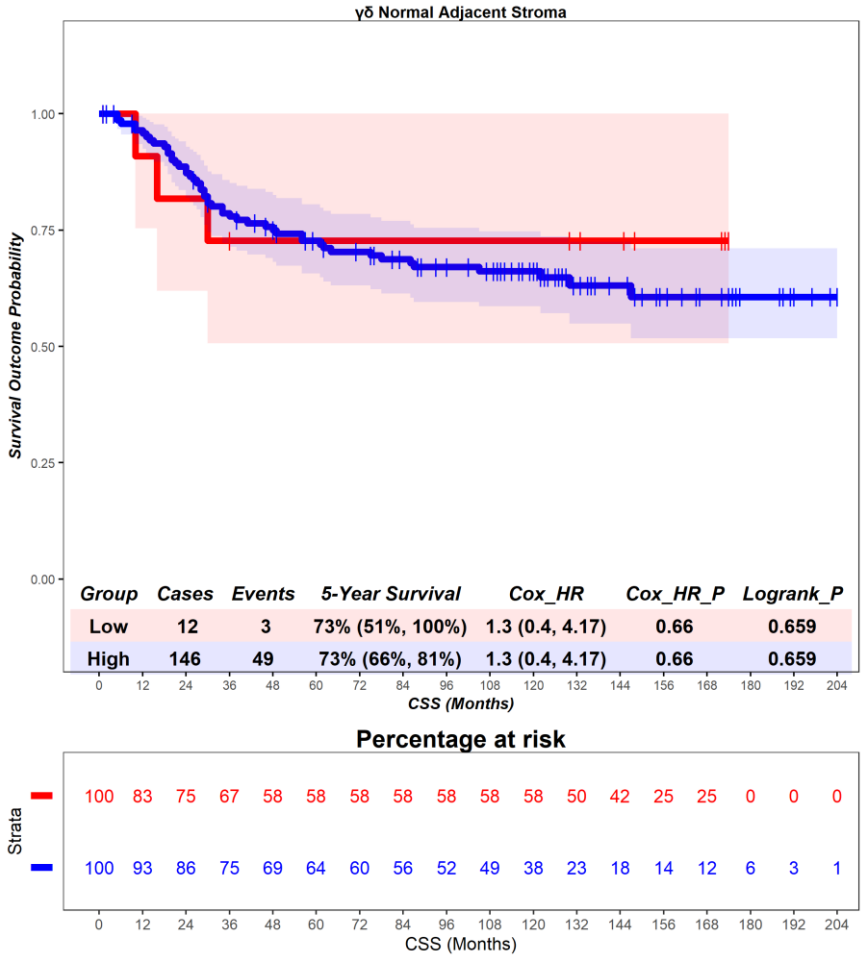

Figure S3 – Time-to-event (cancer-specific survival) analysis for γδ T cells in the adjacent normal stroma. *Patients deemed 'High' or 'Low' for γδ T cells are shaded blue and red, respectively. Cox hazard ratio is univariate. The 'Low' group is used as the reference group on cox regression modelling.*

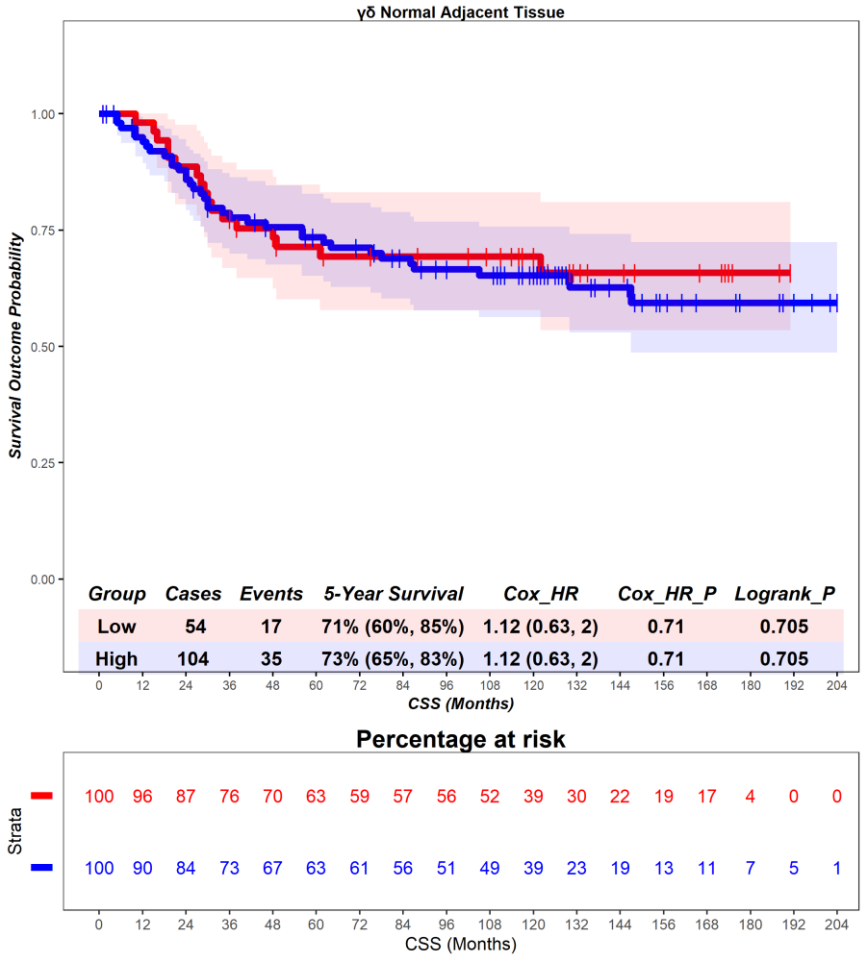

Figure S4 – Time-to-event (cancer-specific survival) analysis for γδ T cells in the adjacent normal tissue. *Patients deemed 'High' or 'Low' for γδ T cells are shaded blue and red, respectively. Cox hazard ratio is univariate. The 'Low' group is used as the reference group on cox regression modelling.*

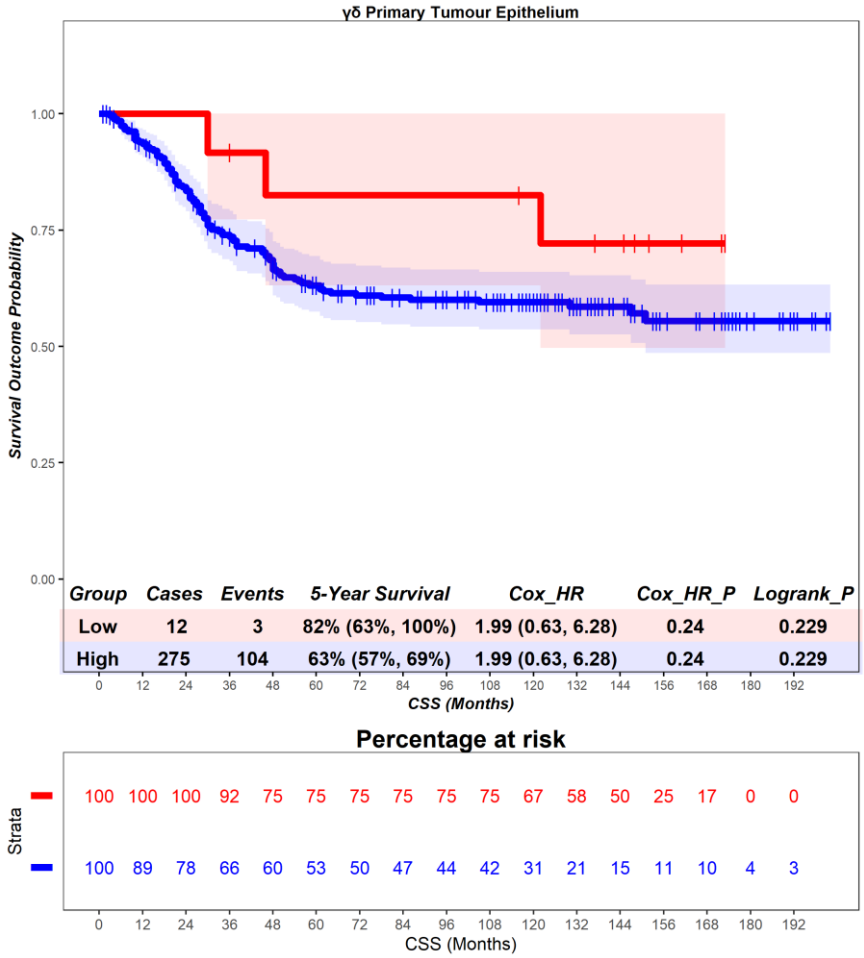

Figure S5 – Time-to-event (cancer-specific survival) analysis for γδ T cells in the primary tumour epithelium. *Patients deemed 'High' or 'Low' for γδ T cells are shaded blue and red, respectively. Cox hazard ratio is univariate. The 'Low' group is used as the reference group on cox regression modelling.*

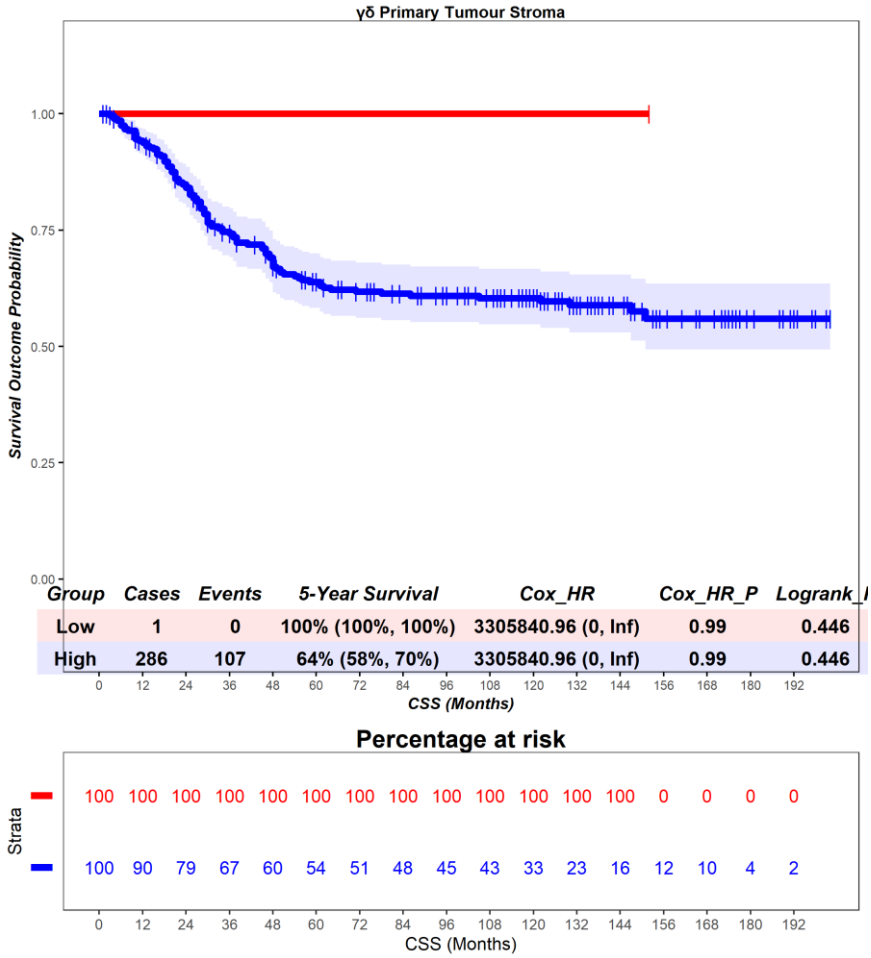

Figure S6 – Time-to-event (cancer-specific survival) analysis for γδ T cells in the primary tumour stroma. *Patients deemed 'High' or 'Low' for γδ T cells are shaded blue and red, respectively. Cox hazard ratio is univariate. The 'Low' group is used as the reference group on cox regression modelling.*

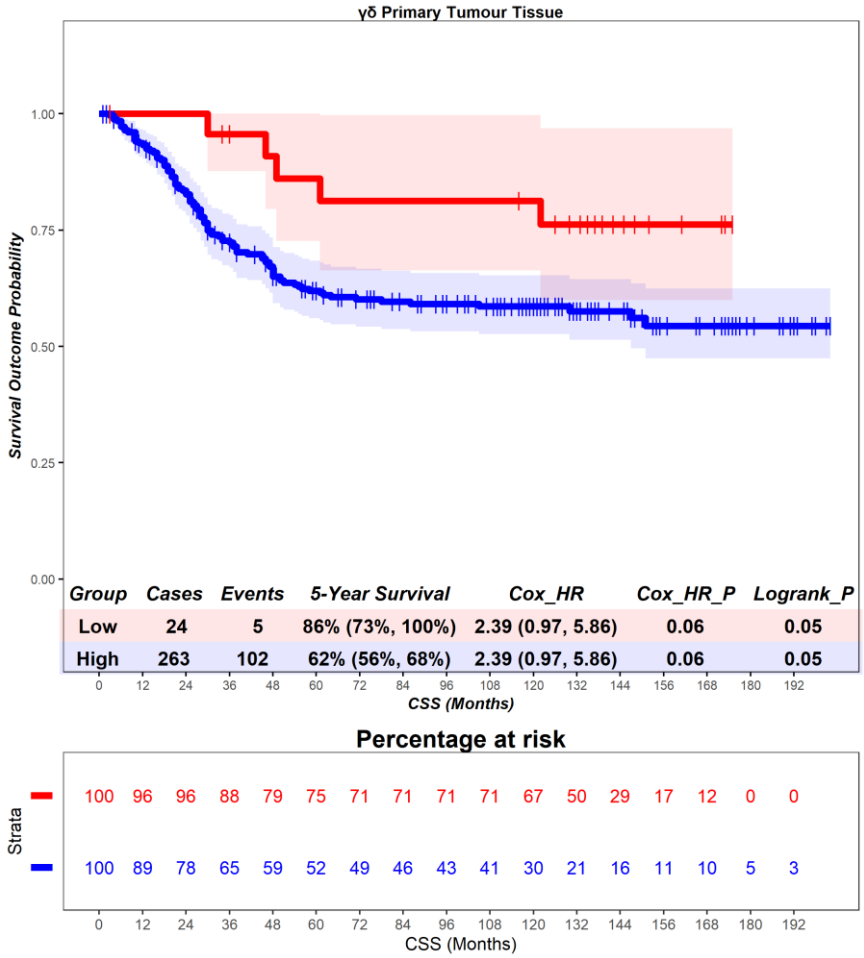

Figure S7 – Time-to-event (cancer-specific survival) analysis for γδ T cells in the primary tumour tissue. *Patients deemed 'High' or 'Low' for γδ T cells are shaded blue and red, respectively. Cox hazard ratio is univariate. The 'Low' group is used as the reference group on cox regression modelling.*

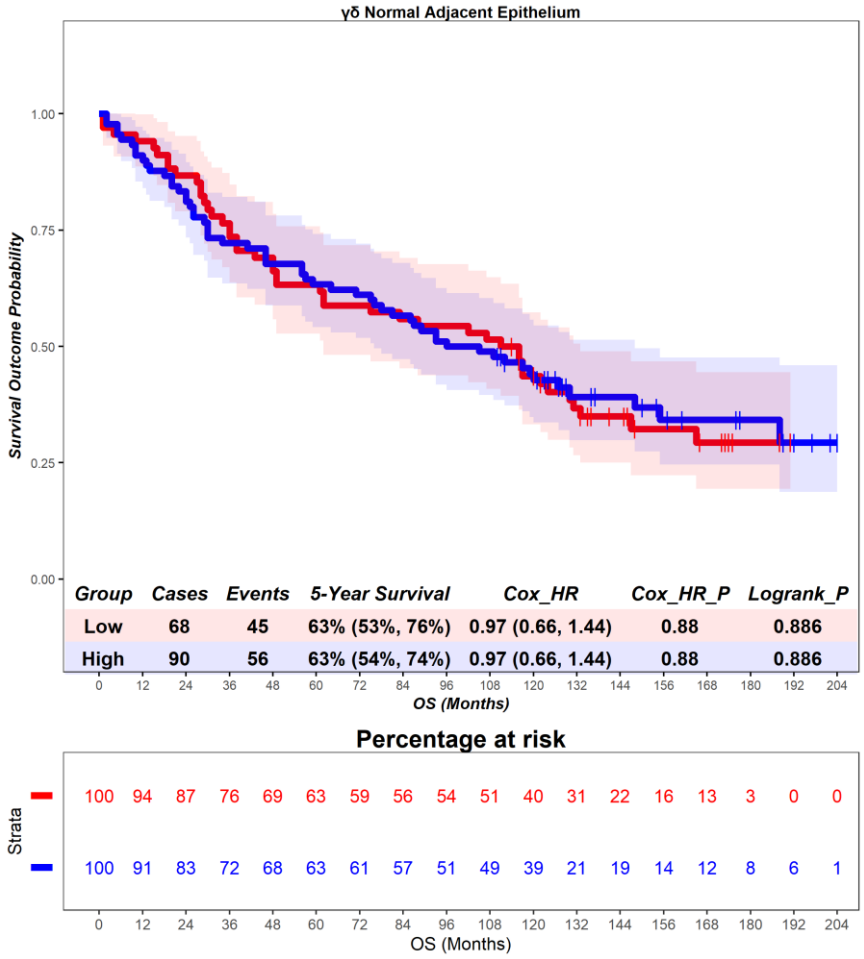

Figure S8 – Time-to-event (overall survival) analysis for γδ T cells in the adjacent normal epithelium. *Patients deemed 'High' or 'Low' for γδ T cells are shaded blue and red, respectively. Cox hazard ratio is univariate. The 'Low' group is used as the reference group on cox regression modelling.*

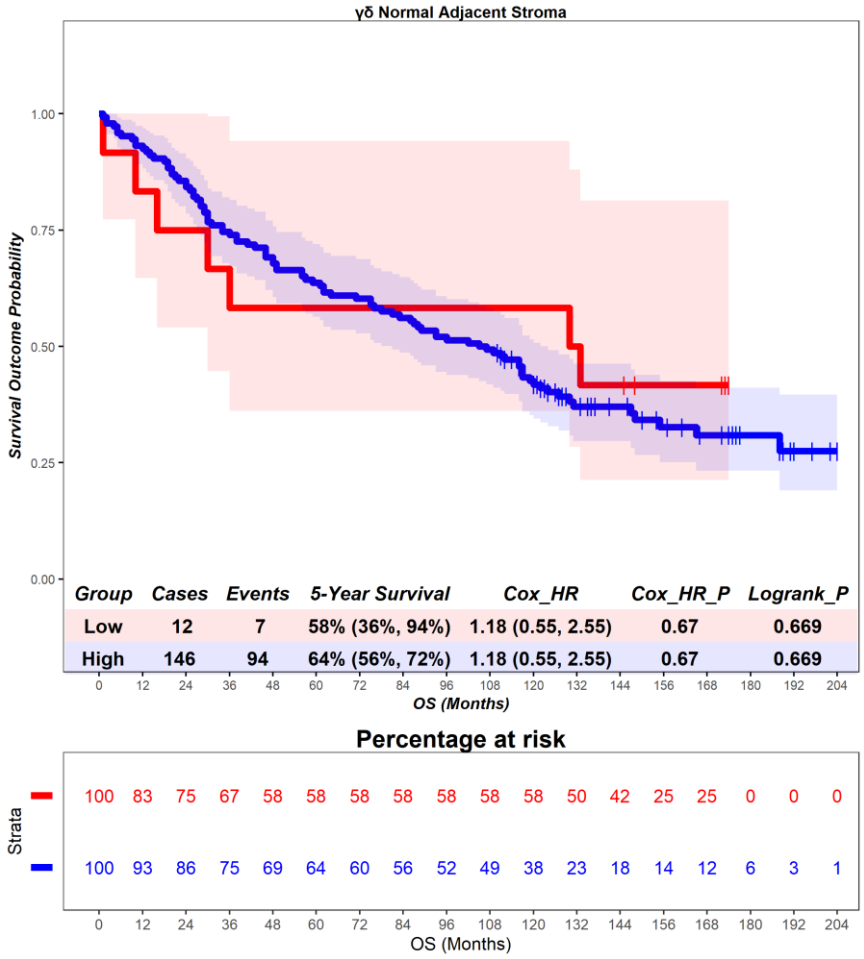

Figure S9 – Time-to-event (overall survival) analysis for γδ T cells in the adjacent normal stroma*. Patients deemed 'High' or 'Low' for γδ T cells are shaded blue and red, respectively. Cox hazard ratio is univariate. The 'Low' group is used as the reference group on cox regression modelling.*

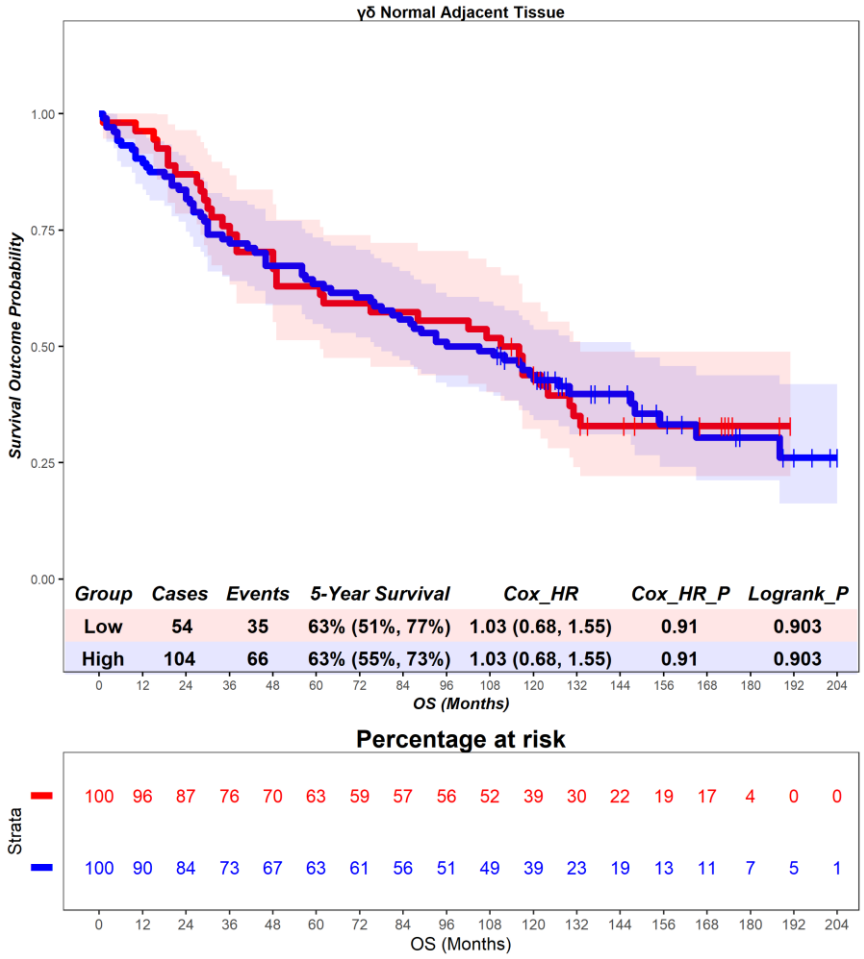

Figure S10 – Time-to-event (overall survival) analysis for γδ T cells in the adjacent normal tissue. *Patients deemed 'High' or 'Low' for γδ T cells are shaded blue and red, respectively. Cox hazard ratio is univariate. The 'Low' group is used as the reference group on cox regression modelling.*

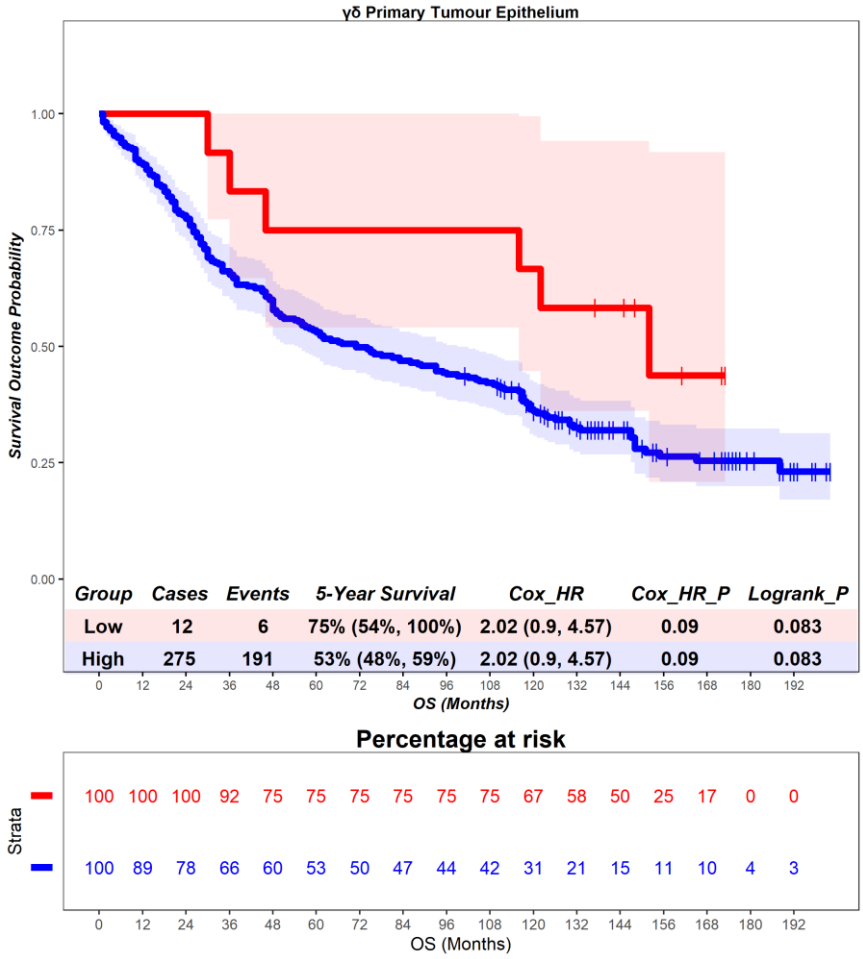

Figure S11 – Time-to-event (overall survival) analysis for γδ T cells in the primary tumour epithelium. *Patients deemed 'High' or 'Low' for γδ T cells are shaded blue and red, respectively. Cox hazard ratio is univariate. The 'Low' group is used as the reference group on cox regression modelling.*

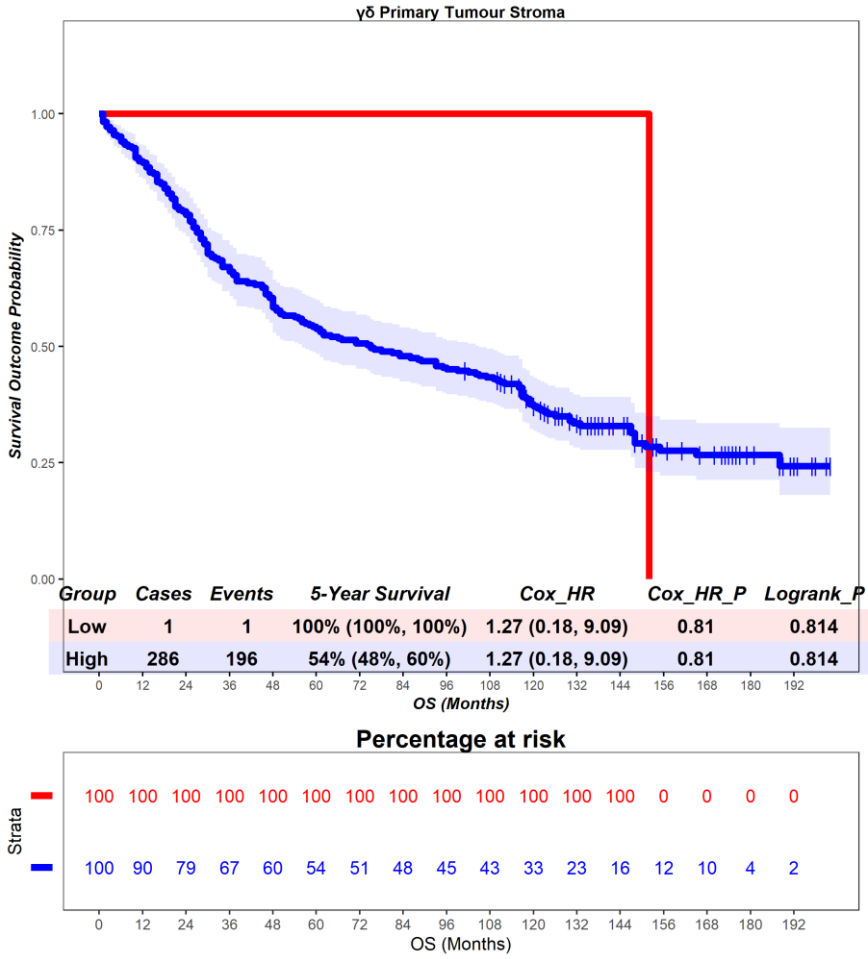

Figure S12 – Time-to-event (overall survival) analysis for γδ T cells in the primary tumour stroma. *Patients deemed 'High' or 'Low' for γδ T cells are shaded blue and red, respectively. Cox hazard ratio is univariate. The 'Low' group is used as the reference group on cox regression modelling.*

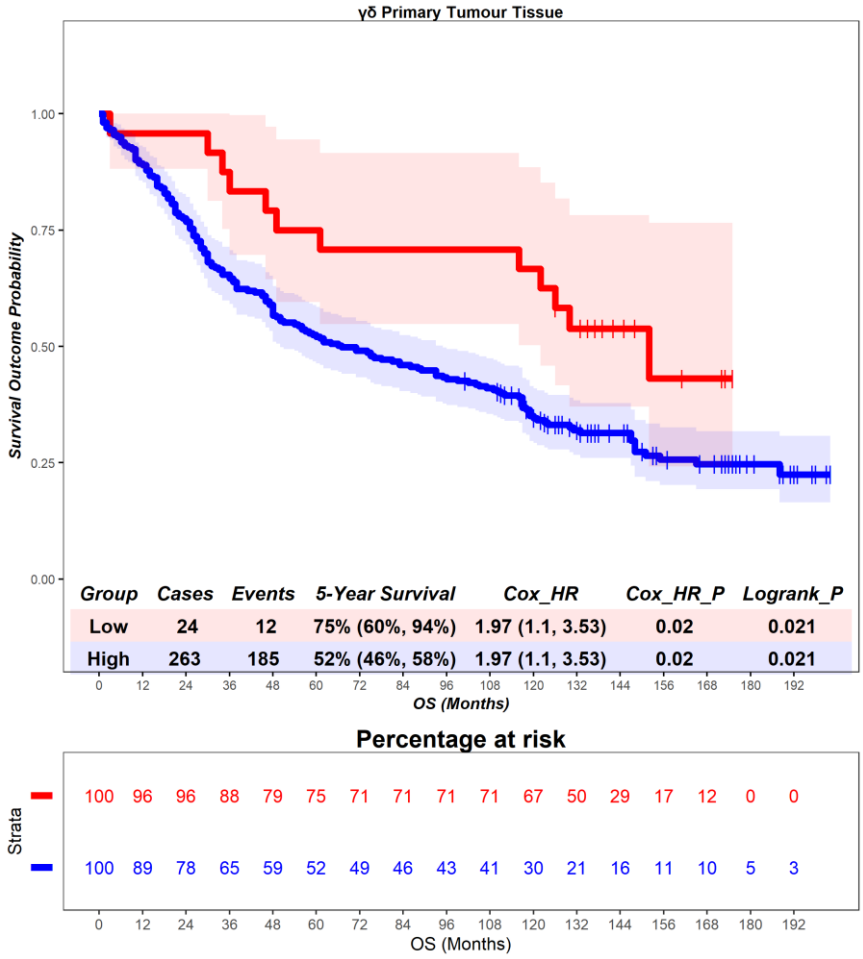

Figure S13 – Time-to-event (overall survival) analysis for γδ T cells in the primary tumour tissue. *Patients deemed 'High' or 'Low' for γδ T cells are shaded blue and red, respectively. Cox hazard ratio is univariate. The 'Low' group is used as the reference group on cox regression modelling.*

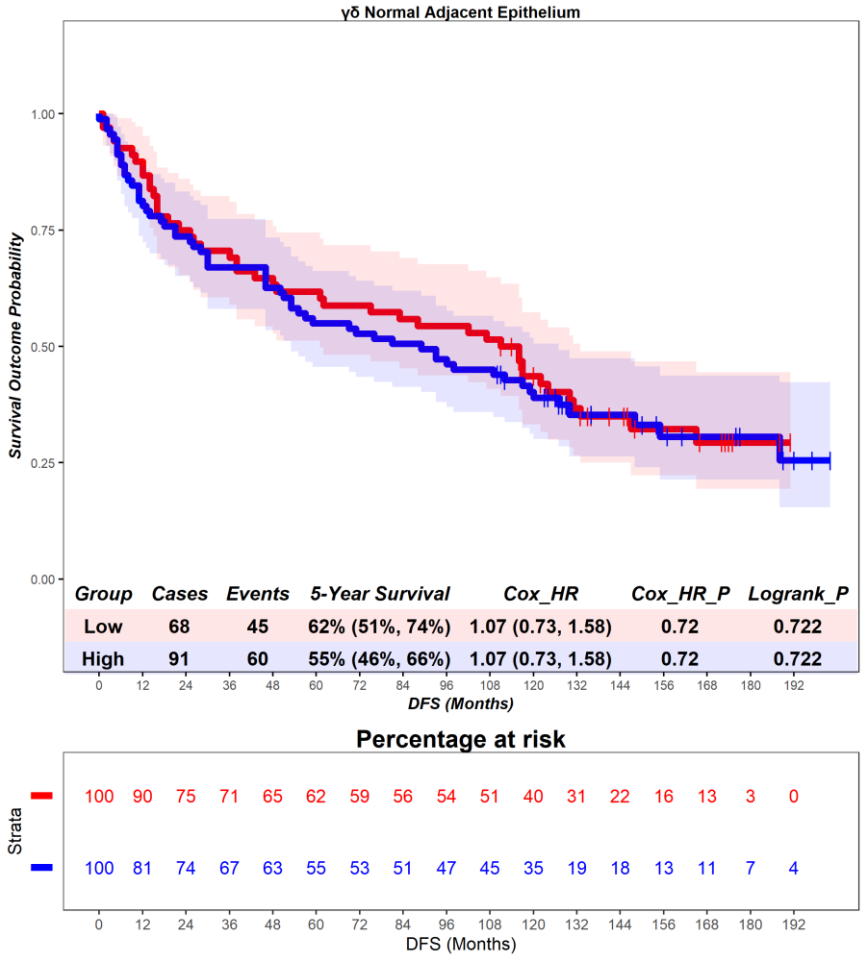

Figure S14 – Time-to-event (disease-free survival) analysis for γδ T cells in the normal adjacent epithelium. *Patients deemed 'High' or 'Low' for γδ T cells are shaded blue and red, respectively. Cox hazard ratio is univariate. The 'Low' group is used as the reference group on cox regression modelling.*

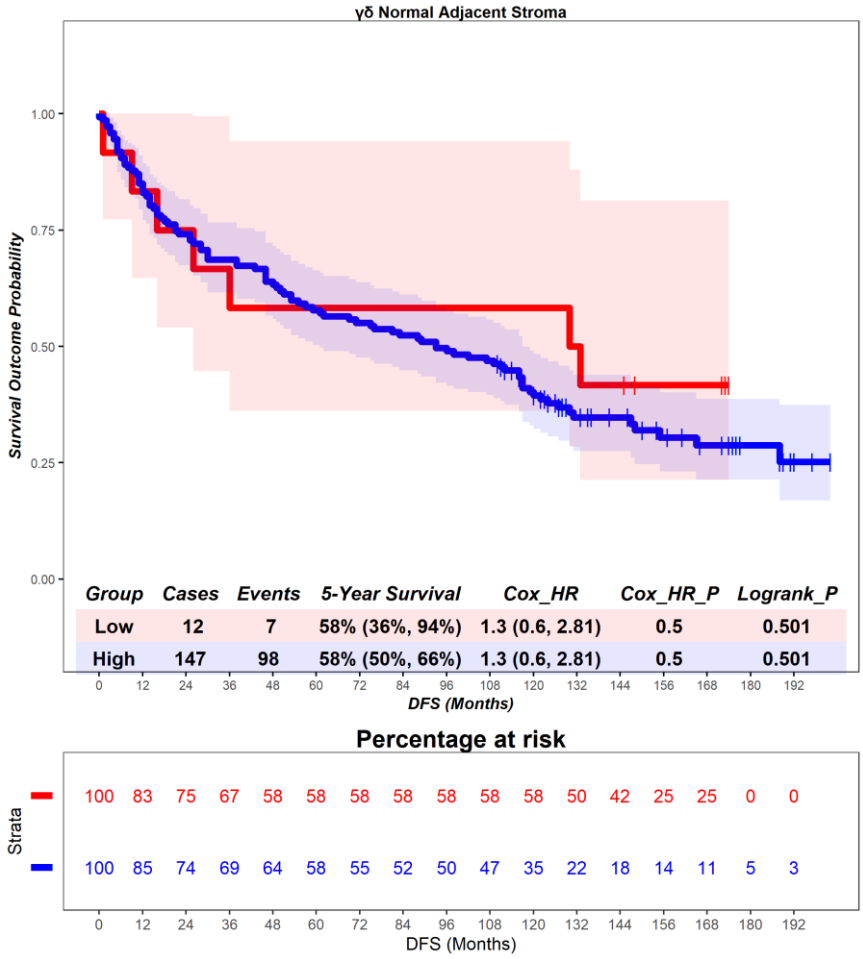

Figure S15 – Time-to-event (disease-free survival) analysis for γδ T cells in the normal adjacent stroma. *Patients deemed 'High' or 'Low' for γδ T cells are shaded blue and red, respectively. Cox hazard ratio is univariate. The 'Low' group is used as the reference group on cox regression modelling.*

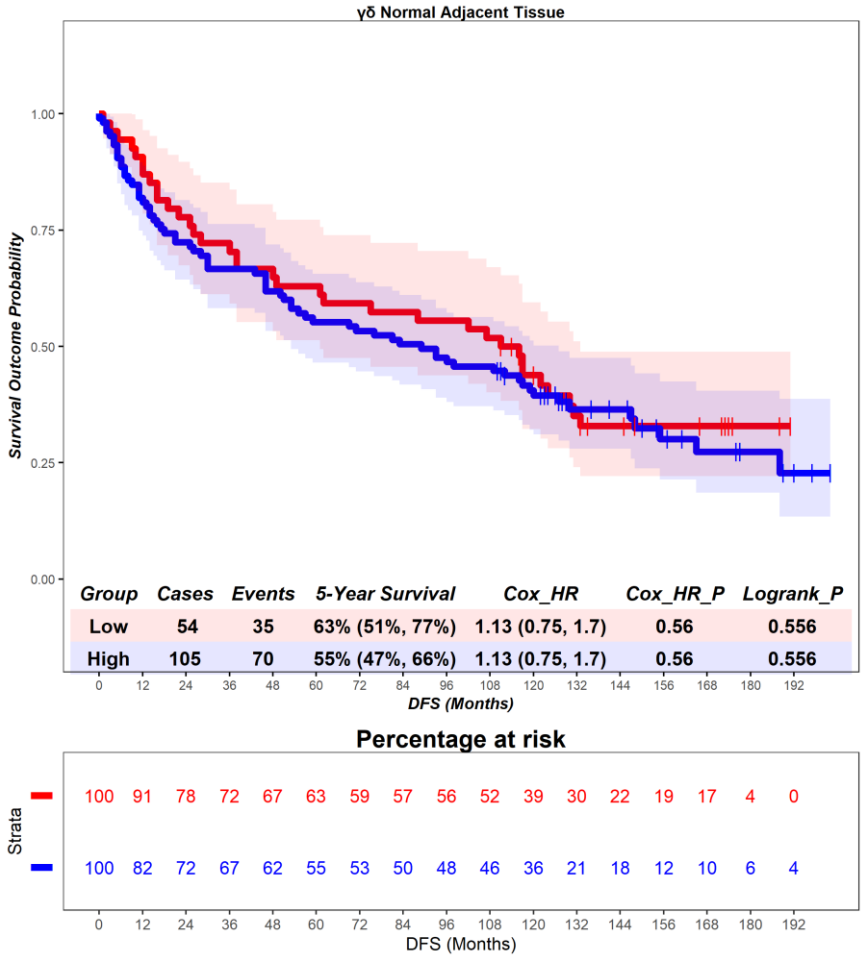

Figure S16 – Time-to-event (disease-free survival) analysis for γδ T cells in the normal adjacent epithelium. *Patients deemed 'High' or 'Low' for γδ T cells are shaded blue and red, respectively. Cox hazard ratio is univariate. The 'Low' group is used as the reference group on cox regression modelling.*

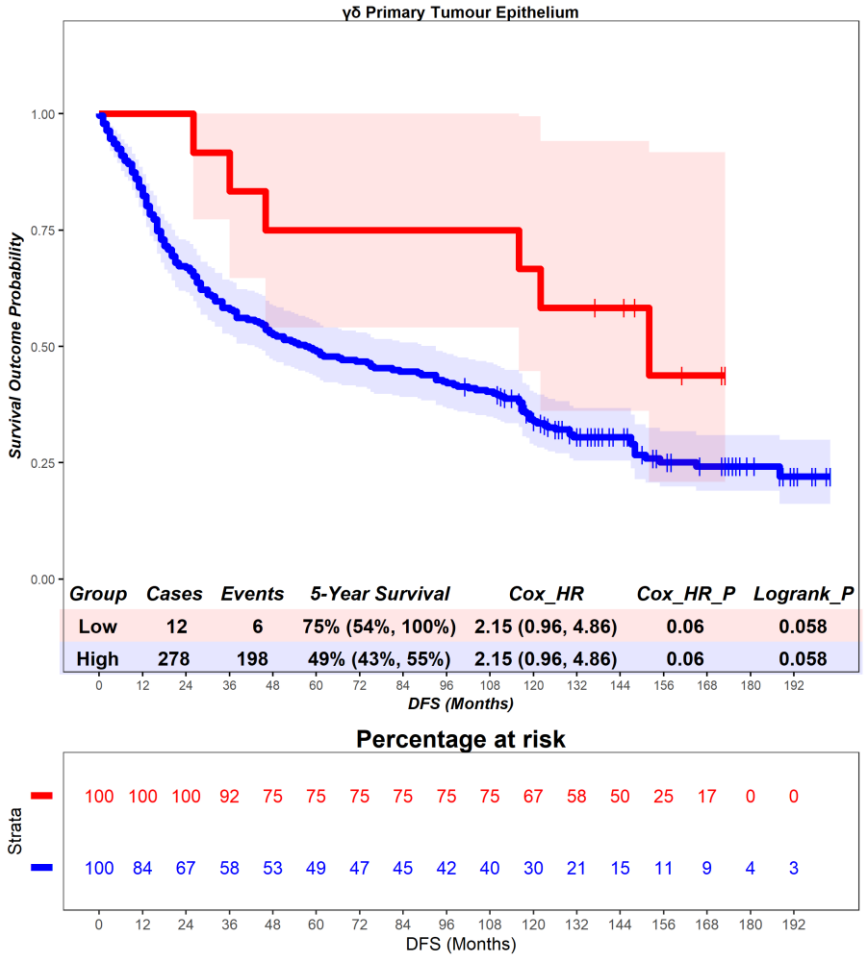

Figure S17 – Time-to-event (disease-free survival) analysis for γδ T cells in the primary tumour epithelium. Patients *deemed 'High' or 'Low' for γδ T cells are shaded blue and red, respectively. Cox hazard ratio is univariate. The 'Low' group is used as the reference group on cox regression modelling.*

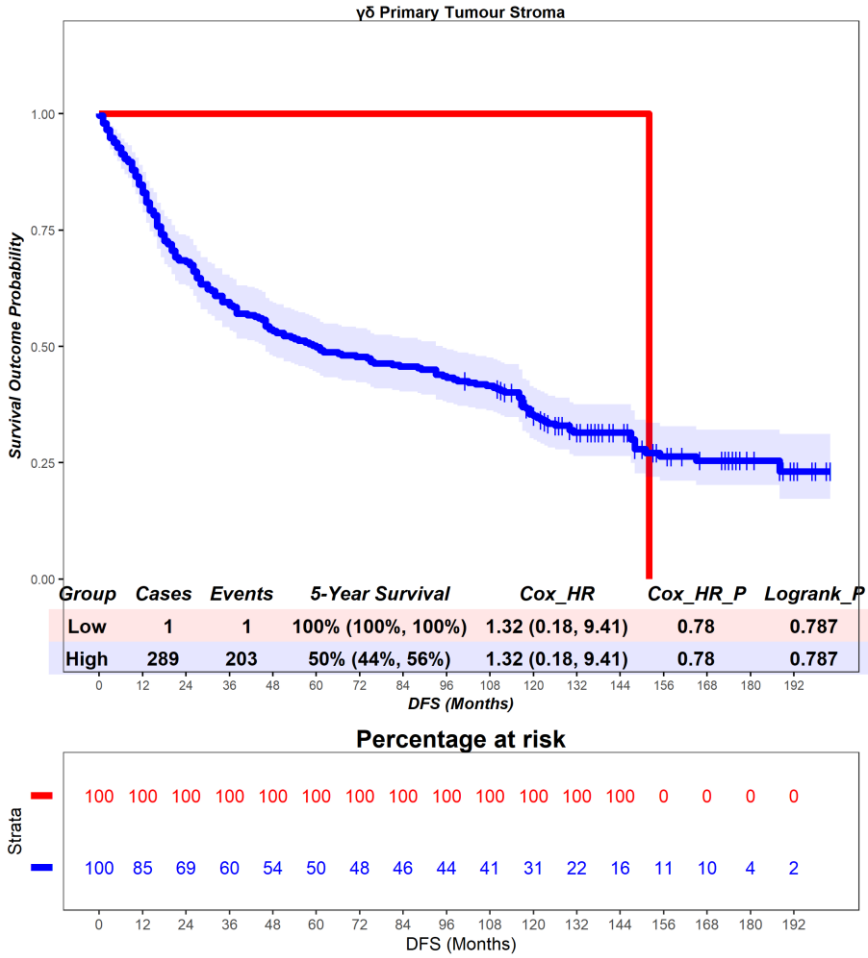

Figure S18 – Time-to-event (disease-free survival) analysis for γδ T cells in the primary tumour stroma. *Patients deemed 'High' or 'Low' for γδ T cells are shaded blue and red, respectively. Cox hazard ratio is univariate. The 'Low' group is used as the reference group on cox regression modelling.*

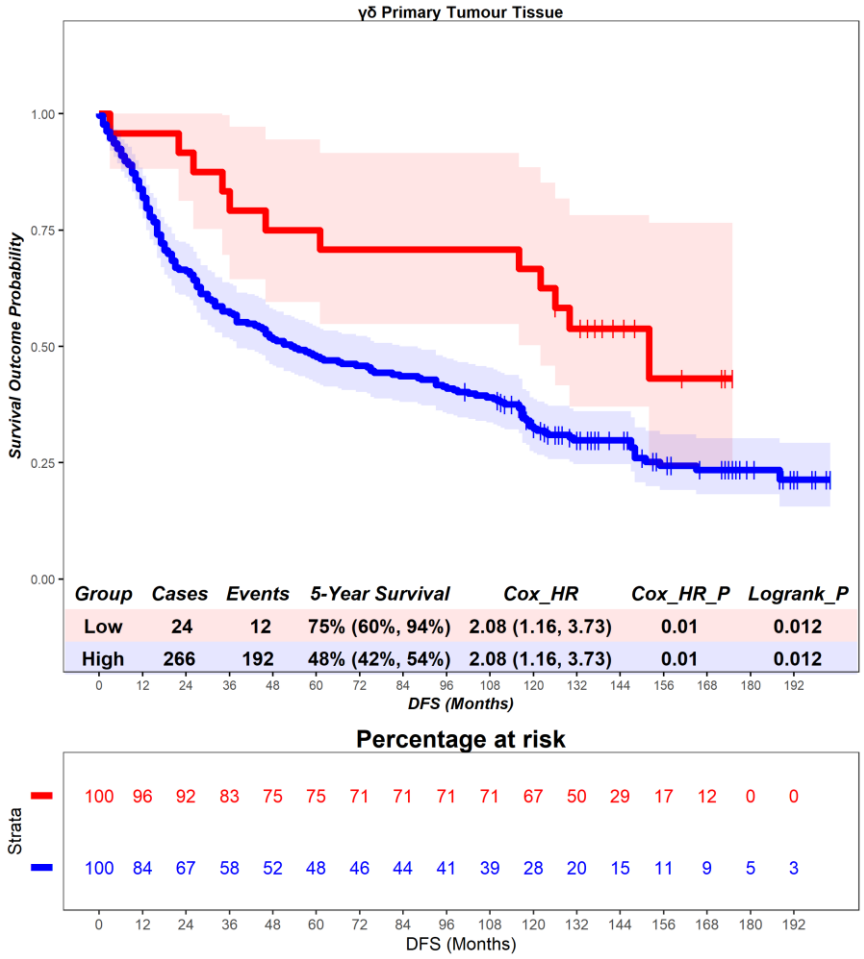

Figure S19 – Time-to-event (disease-free survival) analysis for γδ T cells in the primary tumour tissue. *Patients deemed 'High' or 'Low' for γδ T cells are shaded blue and red, respectively. Cox hazard ratio is univariate. The 'Low' group is used as the reference group on cox regression modelling.*

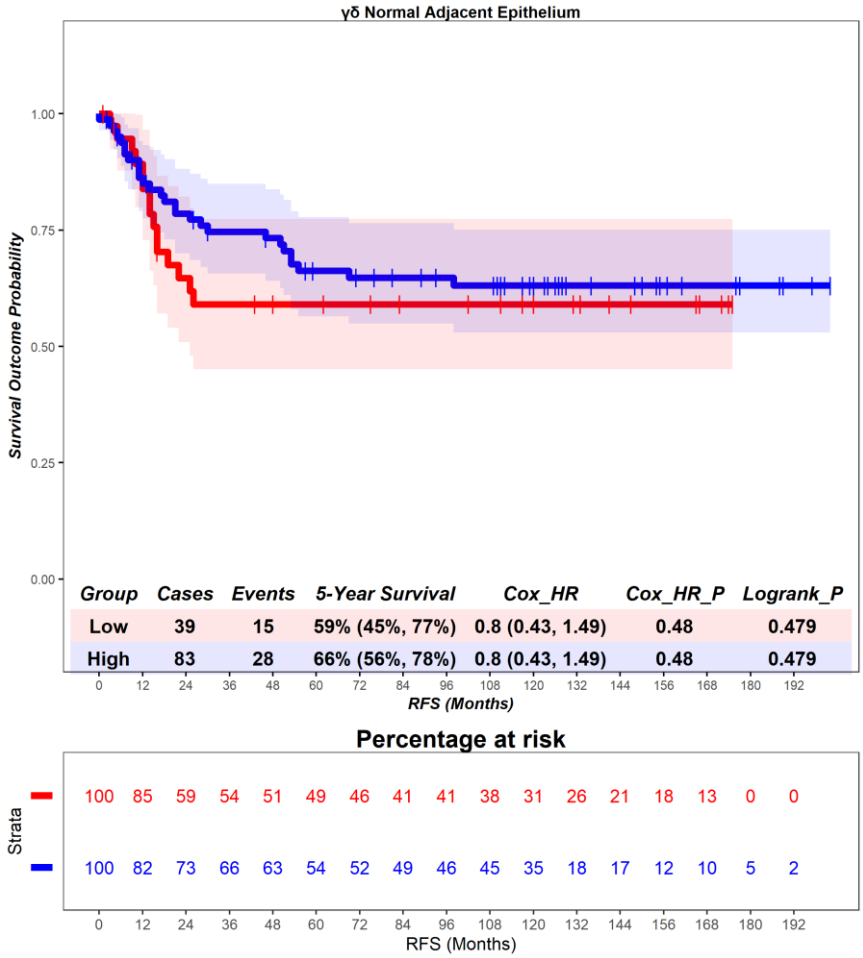

Figure S20 – Time-to-event (recurrence-free survival) analysis for γδ T cells in the adjacent normal epithelium. *Patients deemed 'High' or 'Low' for γδ T cells are shaded blue and red, respectively. Cox hazard ratio is univariate. The 'Low' group is used as the reference group on cox regression modelling.*

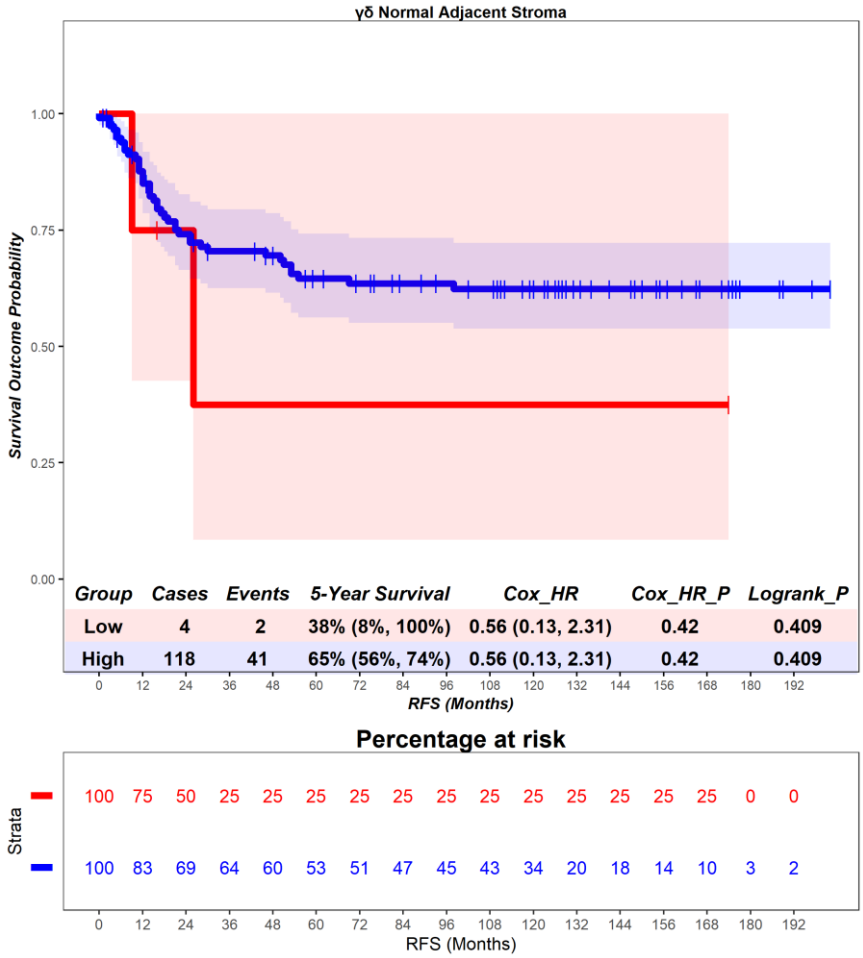

Figure S21 – Time-to-event (recurrence-free survival) analysis for γδ T cells in the adjacent normal stroma*. Patients deemed 'High' or 'Low' for γδ T cells are shaded blue and red, respectively. Cox hazard ratio is univariate. The 'Low' group is used as the reference group on cox regression modelling.*

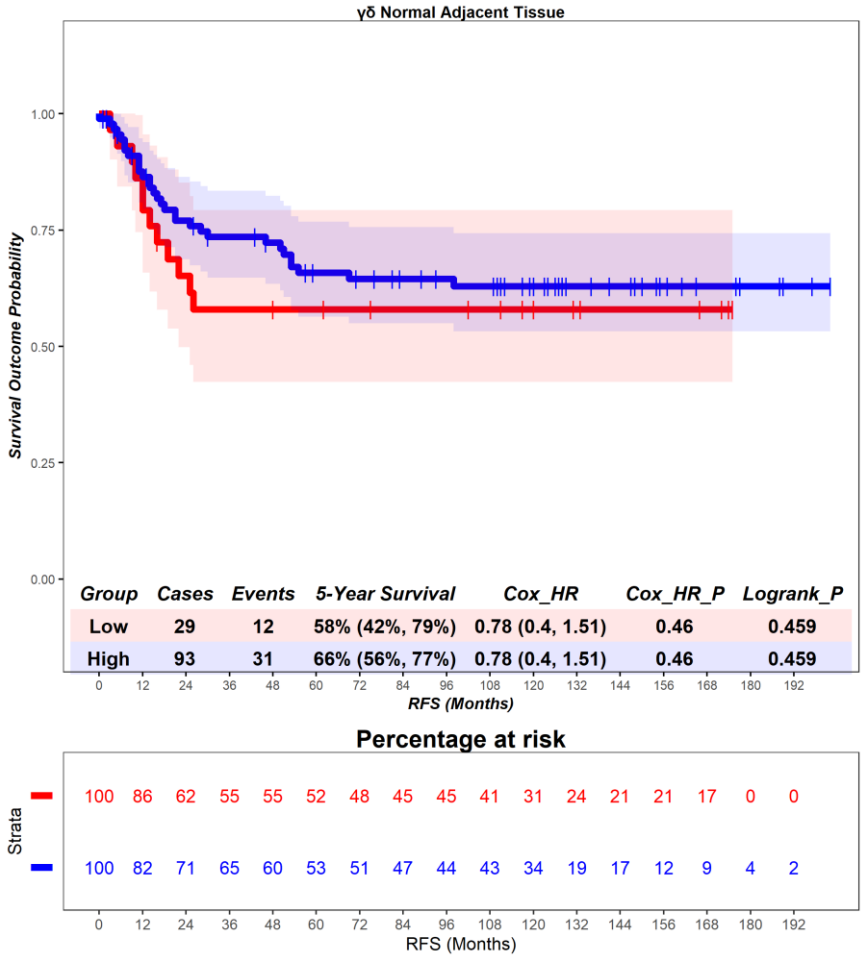

Figure S22 – Time-to-event (recurrence-free survival) analysis for γδ T cells in the adjacent normal tissue. *Patients deemed 'High' or 'Low' for γδ T cells are shaded blue and red, respectively. Cox hazard ratio is univariate. The 'Low' group is used as the reference group on cox regression modelling.*

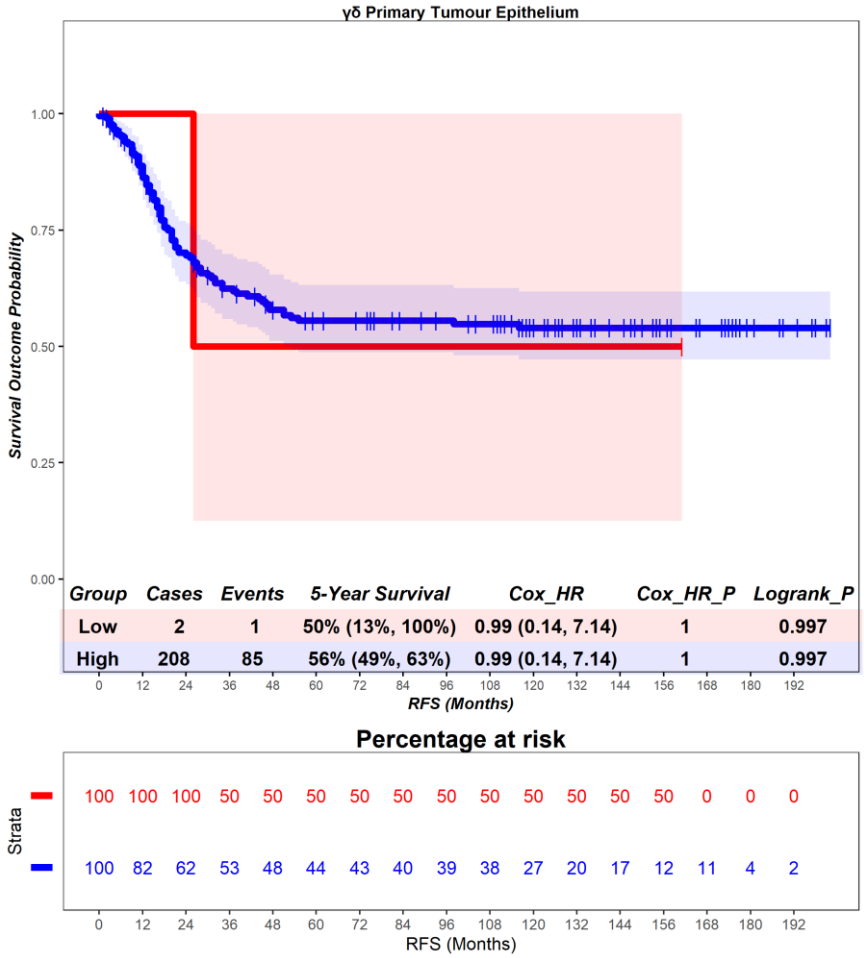

Figure S23 – Time-to-event (recurrence-free survival) analysis for γδ T cells in the primary tumour epithelium. *Patients deemed 'High' or 'Low' for γδ T cells are shaded blue and red, respectively. Cox hazard ratio is univariate. The 'Low' group is used as the reference group on cox regression modelling.*

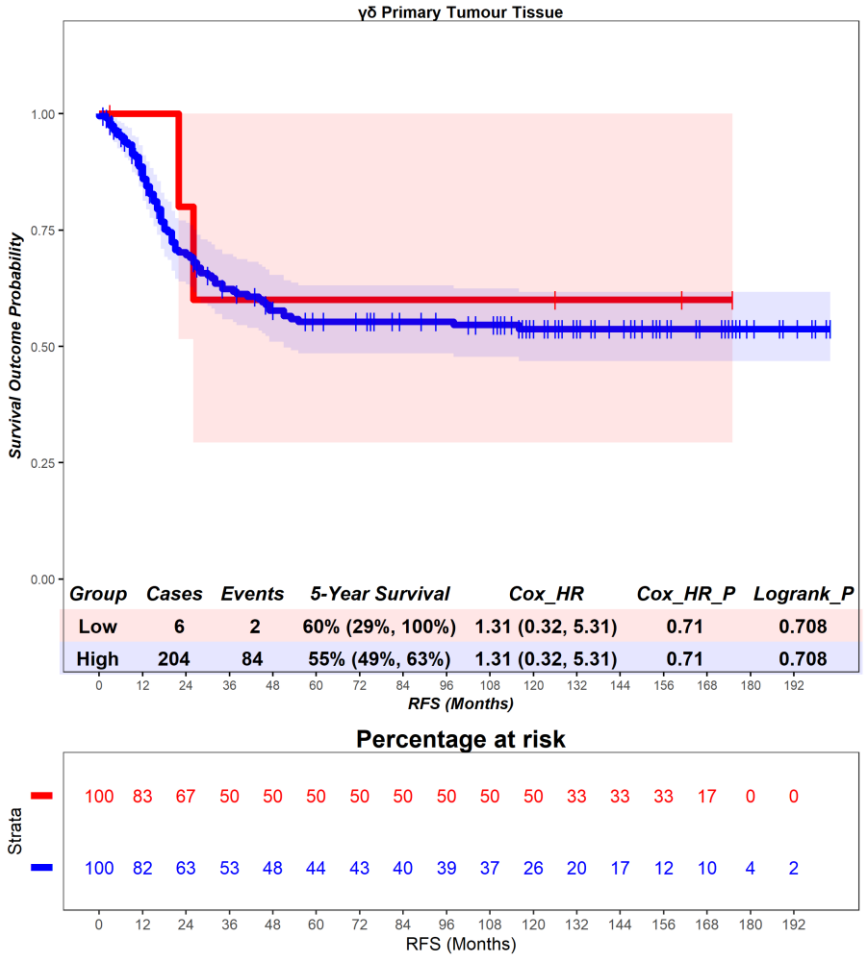

Figure S24 – Time-to-event (recurrence-free survival) analysis for γδ T cells in the primary tumour stroma. *Patients deemed 'High' or 'Low' for γδ T cells are shaded blue and red, respectively. Cox hazard ratio is univariate. The 'Low' group is used as the reference group on cox regression modelling.*

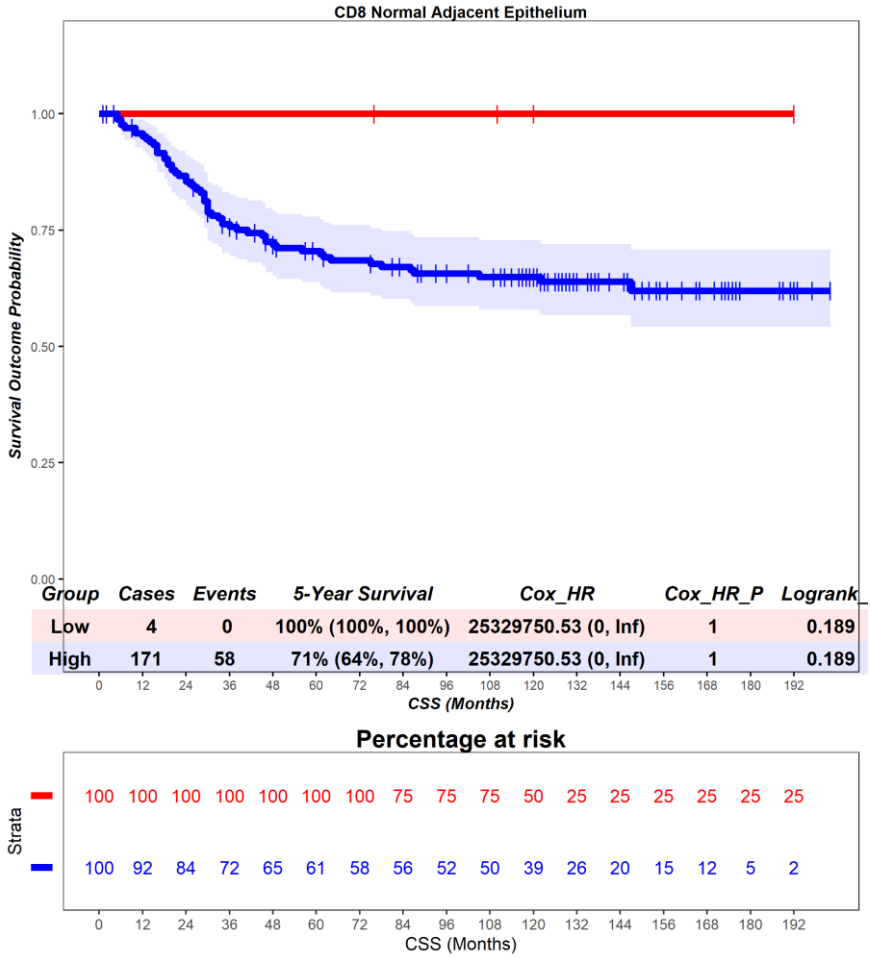

Figure S25 – Time-to-event (cancer-specific survival) analysis for CD8 T cells in the adjacent normal epithelium. *Patients deemed 'High' or 'Low' for CD8 T cells are shaded blue and red, respectively. Cox hazard ratio is univariate. The 'Low' group is used as the reference group on cox regression modelling.*

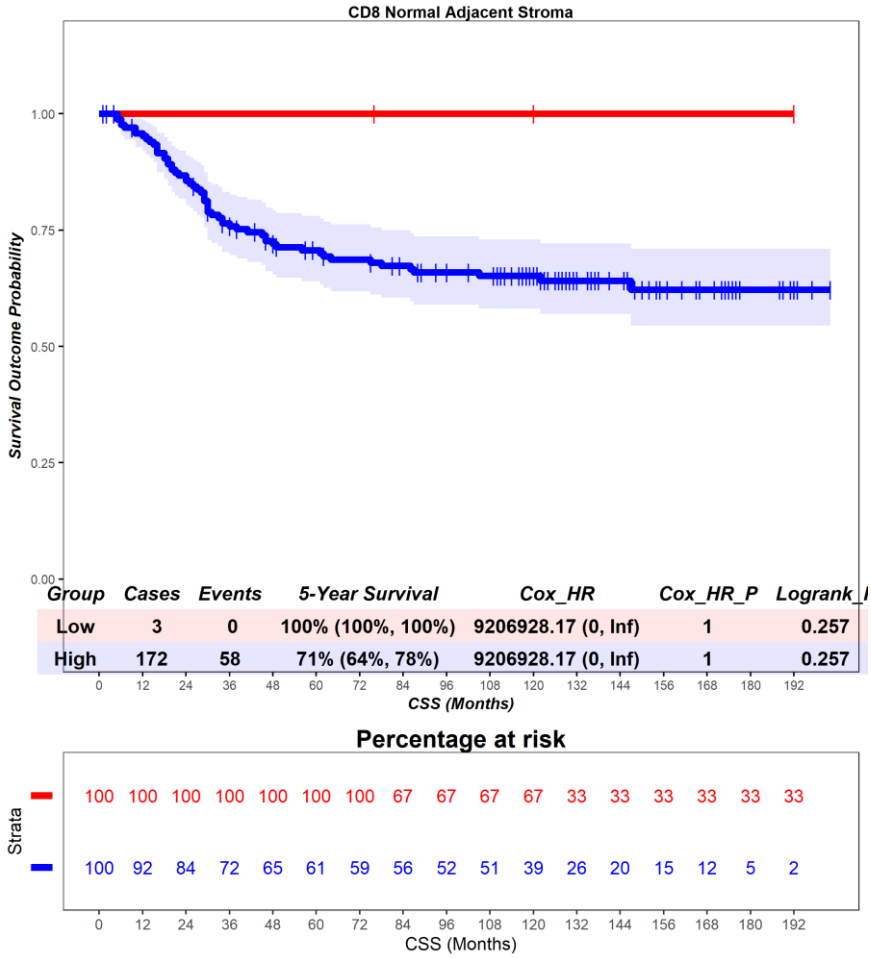

Figure S26 – Time-to-event (cancer-specific survival) analysis for CD8 T cells in the adjacent normal stroma. *Patients deemed 'High' or 'Low' for CD8 T cells are shaded blue and red, respectively. Cox hazard ratio is univariate. The 'Low' group is used as the reference group on cox regression modelling.*

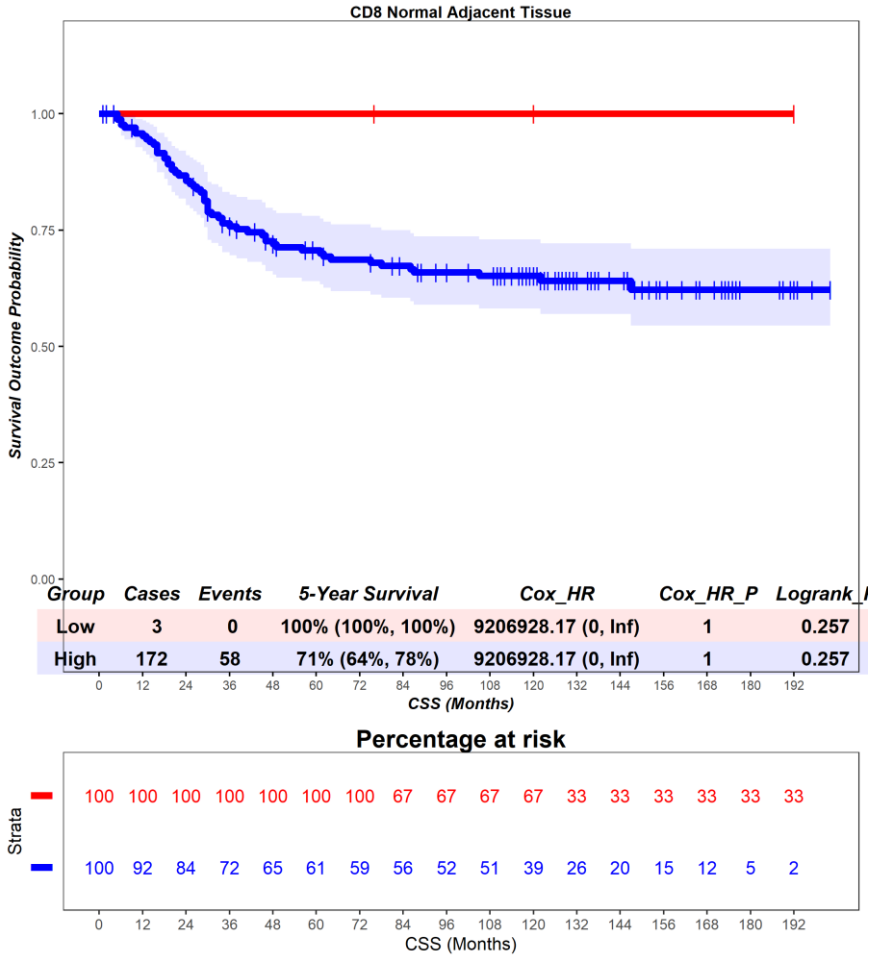

Figure S27 – Time-to-event (cancer-specific survival) analysis for CD8 T cells in the adjacent normal tissue. *Patients deemed 'High' or 'Low' for CD8 T cells are shaded blue and red, respectively. Cox hazard ratio is univariate. The 'Low' group is used as the reference group on cox regression modelling.*

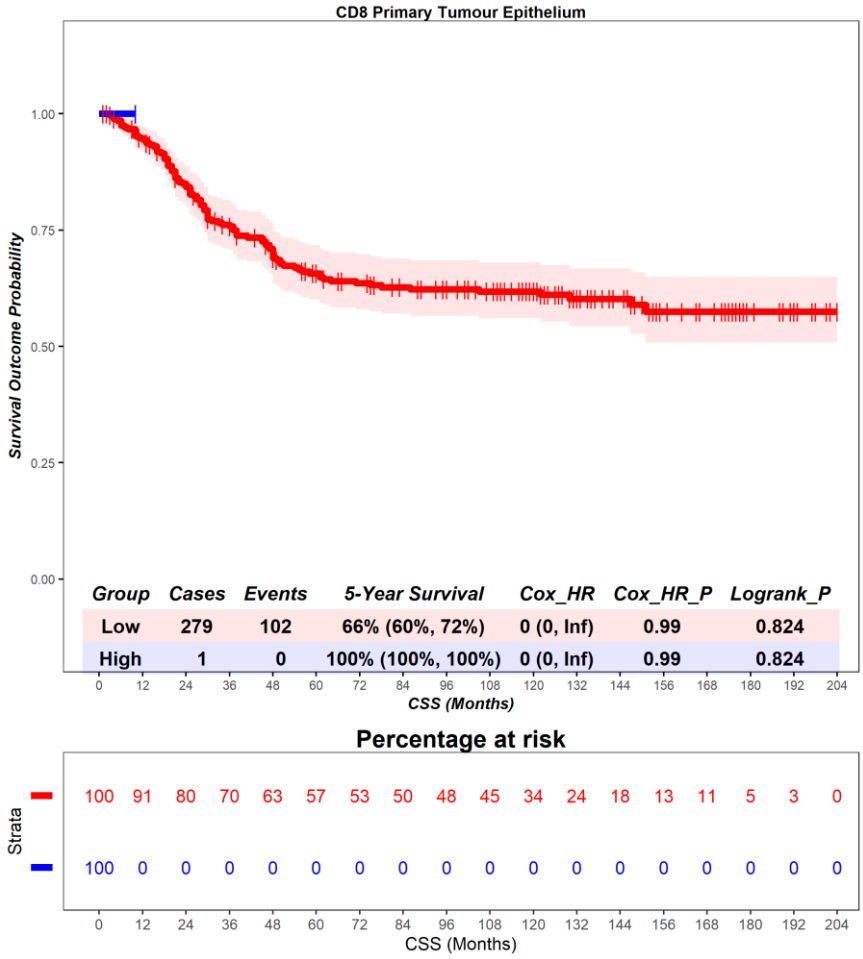

Figure S28 – Time-to-event (cancer-specific survival) analysis for CD8 T cells in the primary tumour epithelium. *Patients deemed 'High' or 'Low' for CD8 T cells are shaded blue and red, respectively. Cox hazard ratio is univariate. The 'Low' group is used as the reference group on cox regression modelling.*

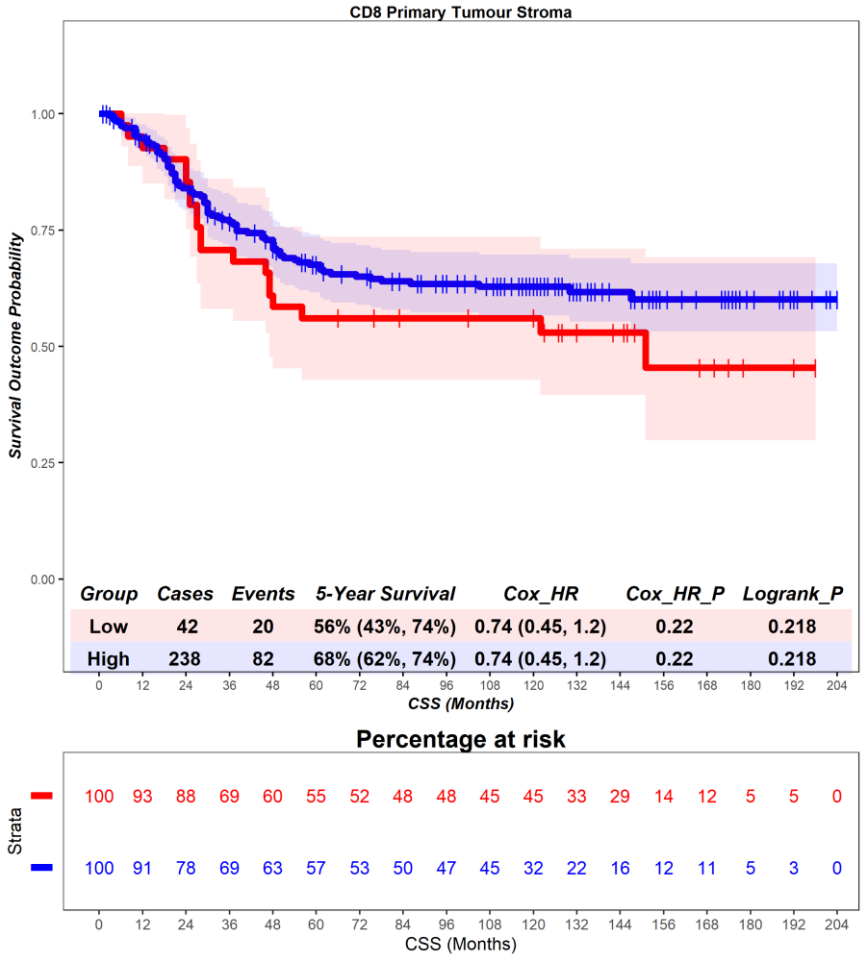

Figure S29 – Time-to-event (cancer-specific survival) analysis for CD8 T cells in the primary tumour stroma. *Patients deemed 'High' or 'Low' for CD8 T cells are shaded blue and red, respectively. Cox hazard ratio is univariate. The 'Low' group is used as the reference group on cox regression modelling.*

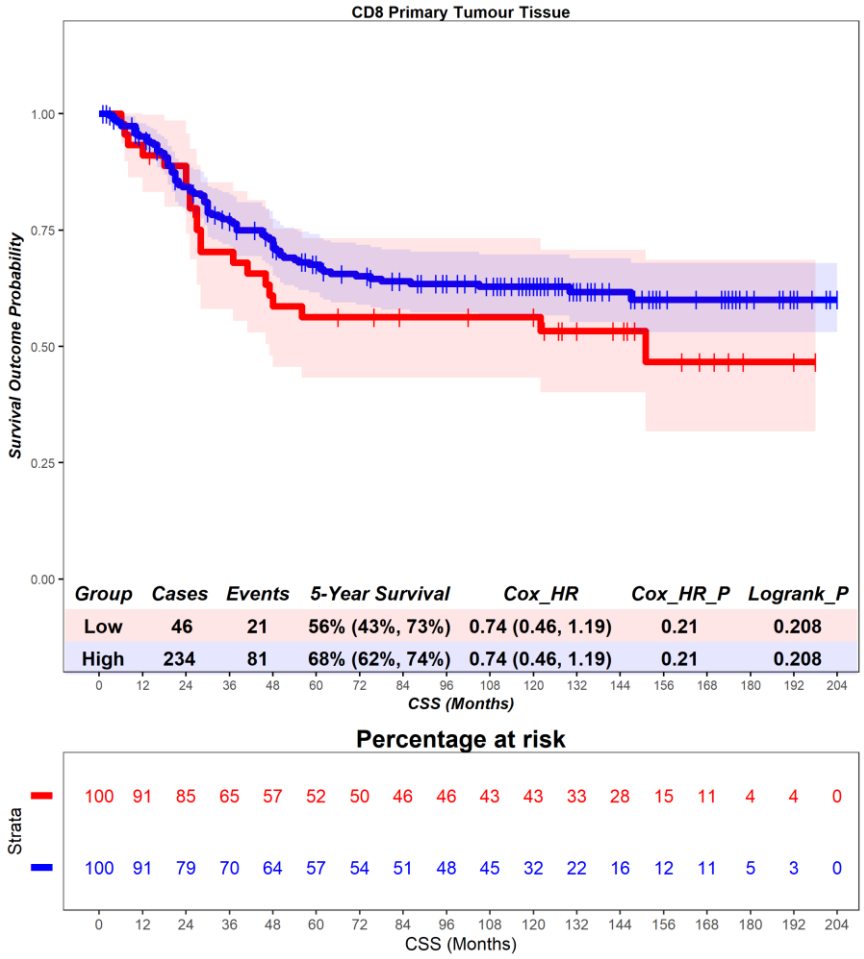

Figure S30 – Time-to-event (cancer-specific survival) analysis for CD8 T cells in the primary tumour tissue. Patients *deemed 'High' or 'Low' for CD8 T cells are shaded blue and red, respectively. Cox hazard ratio is univariate. The 'Low' group is used as the reference group on cox regression modelling.*

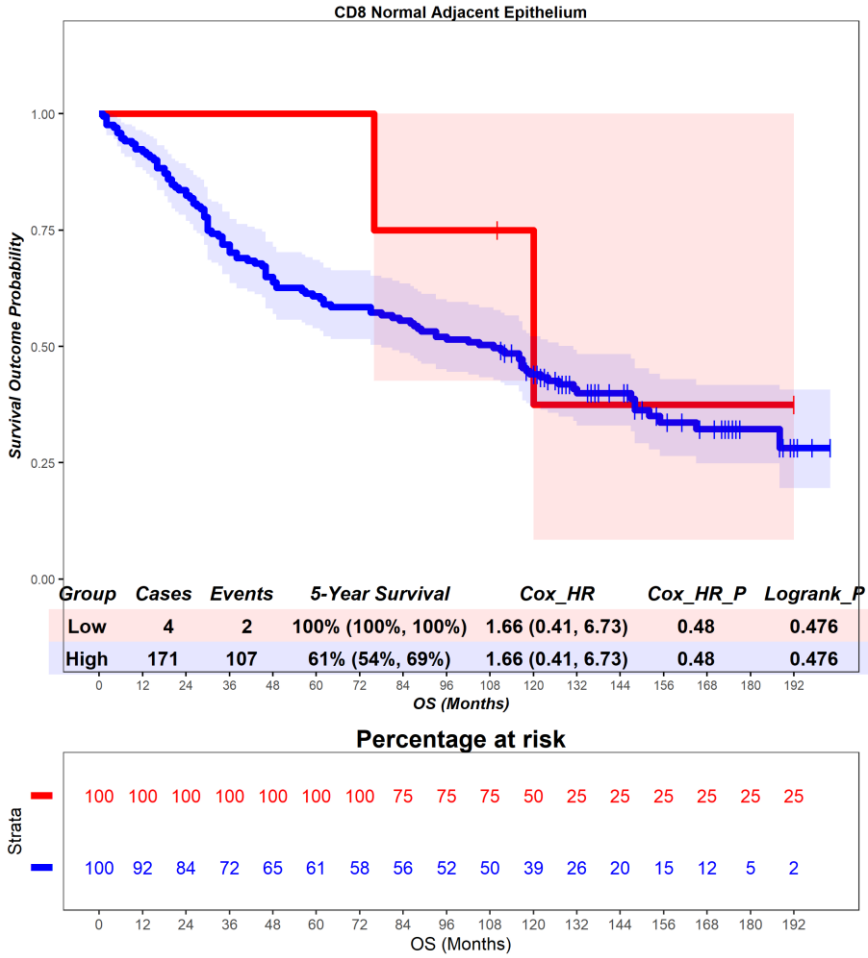

Figure S31 – Time-to-event (overall survival) analysis for CD8 T cells in the adjacent normal epithelium. *Patients deemed 'High' or 'Low' for CD8 T cells are shaded blue and red, respectively. Cox hazard ratio is univariate. The 'Low' group is used as the reference group on cox regression modelling.*

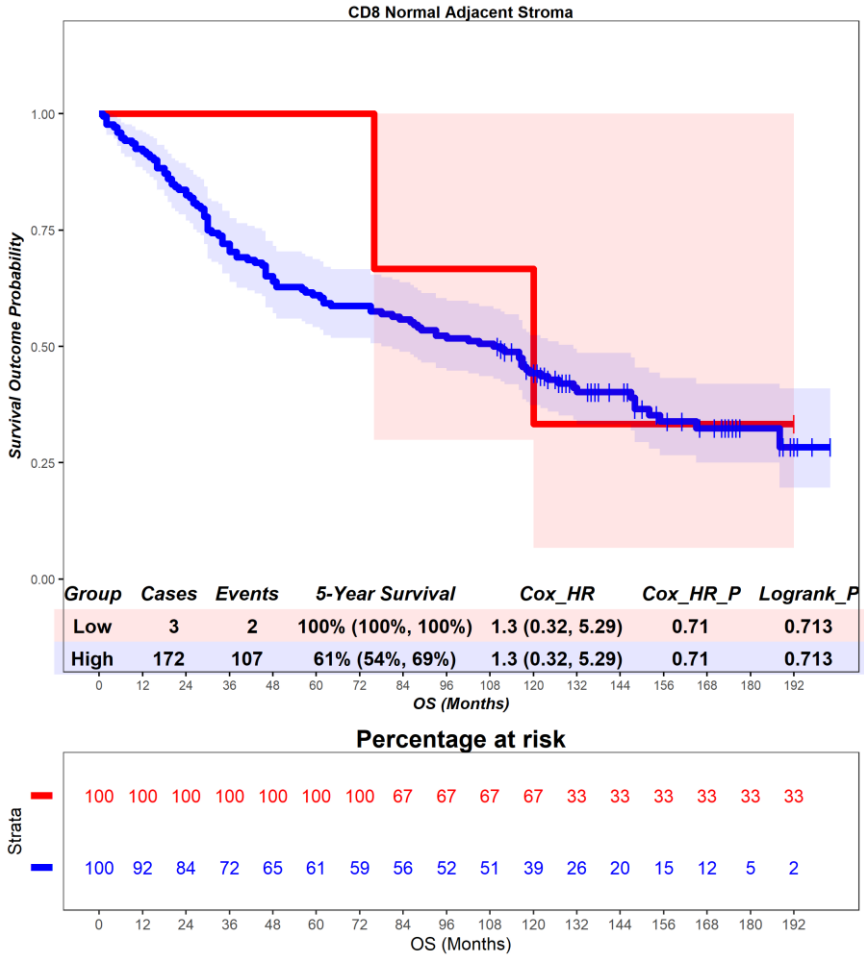

Figure S32 – Time-to-event (overall survival) analysis for CD8 T cells in the adjacent normal stroma. *Patients deemed 'High' or 'Low' for CD8 T cells are shaded blue and red, respectively. Cox hazard ratio is univariate. The 'Low' group is used as the reference group on cox regression modelling.*

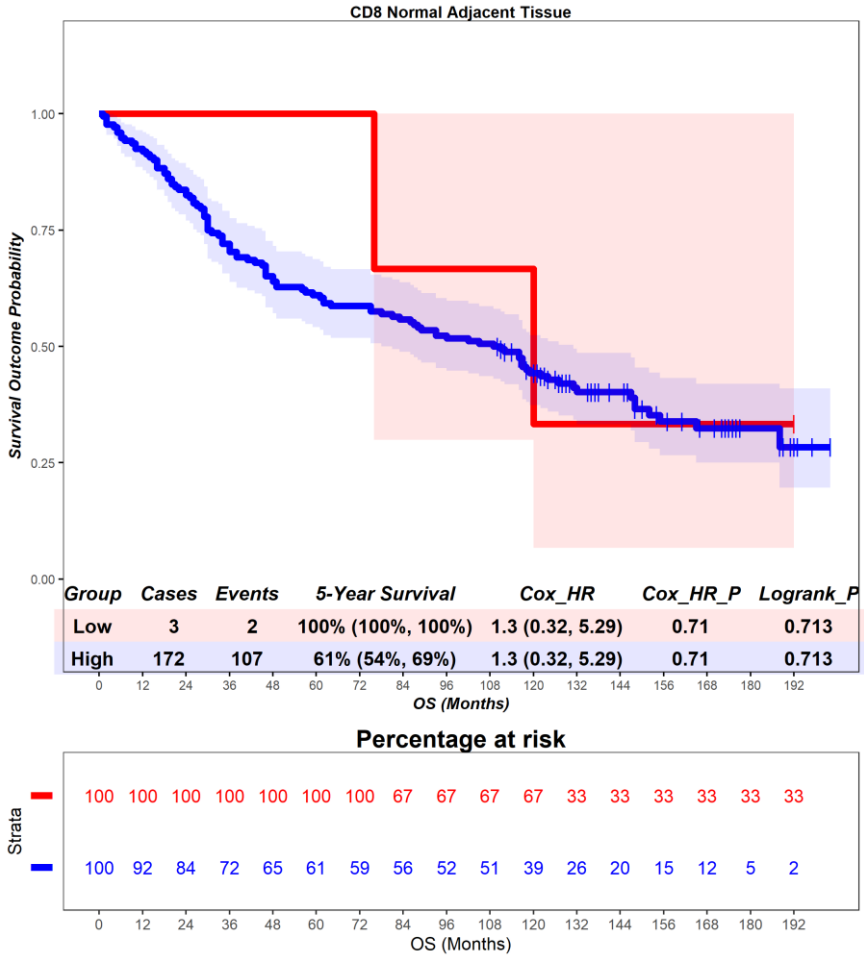

Figure S33 – Time-to-event (overall survival) analysis for CD8 T cells in the adjacent normal tissue. *Patients deemed 'High' or 'Low' for CD8 T cells are shaded blue and red, respectively. Cox hazard ratio is univariate. The 'Low' group is used as the reference group on cox regression modelling.*

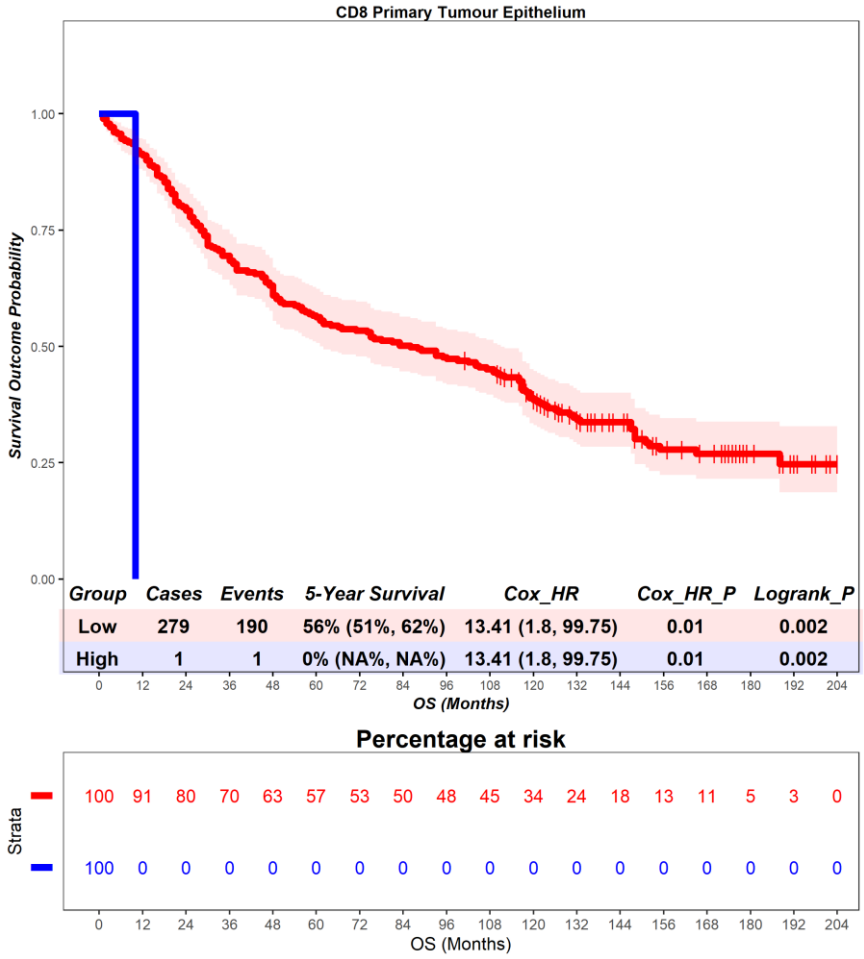

Figure S34 – Time-to-event (overall survival) analysis for CD8 T cells in the primary tumour epithelium. *Patients deemed 'High' or 'Low' for CD8 T cells are shaded blue and red, respectively. Cox hazard ratio is univariate. The 'Low' group is used as the reference group on cox regression modelling.*

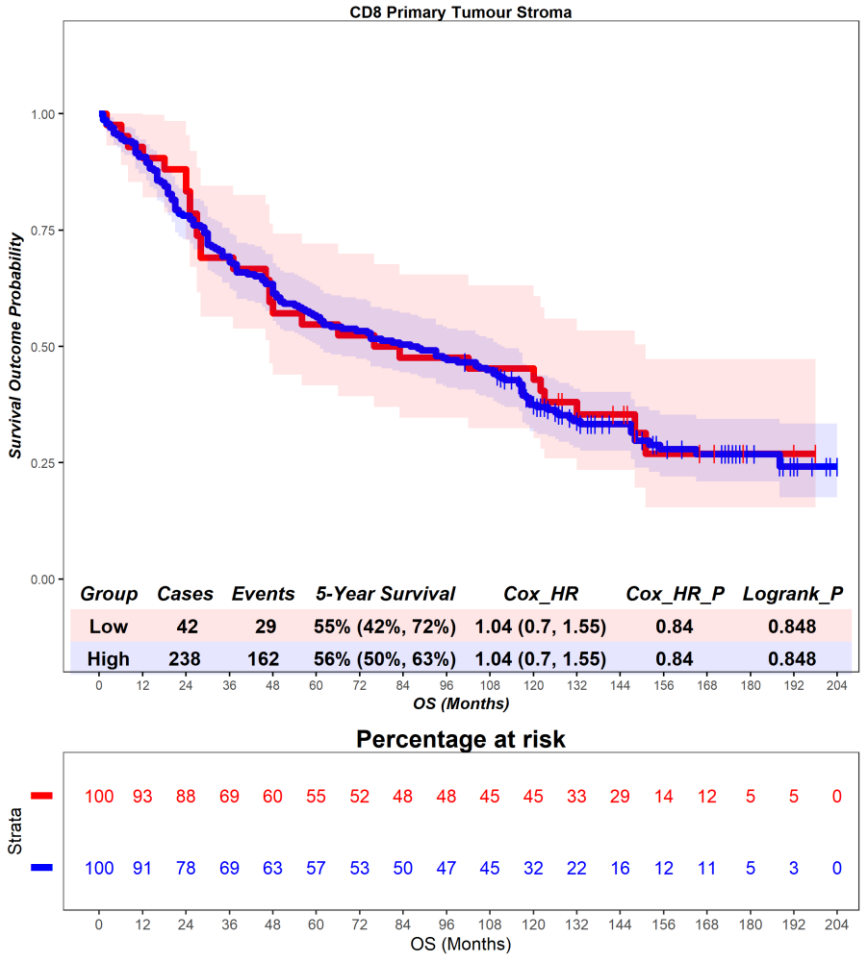

Figure S35 – Time-to-event (overall survival) analysis for CD8 T cells in the primary tumour stroma. *Patients deemed 'High' or 'Low' for CD8 T cells are shaded blue and red, respectively. Cox hazard ratio is univariate. The 'Low' group is used as the reference group on cox regression modelling.*

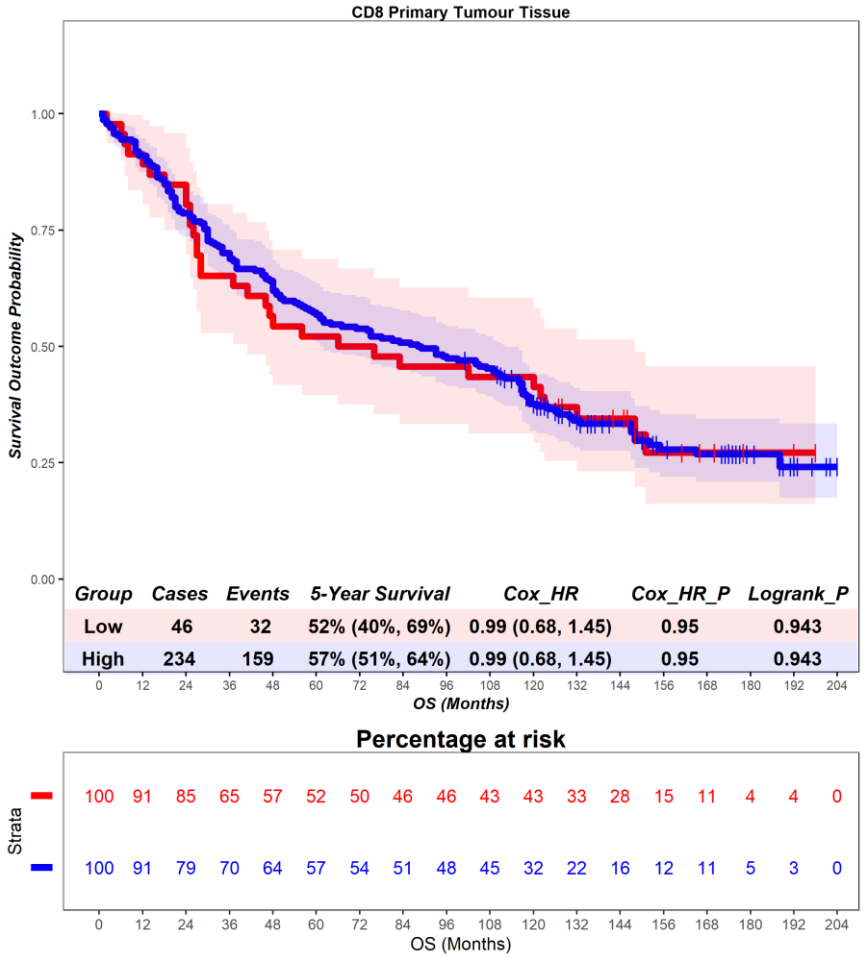

Figure S36 – Time-to-event (overall survival) analysis for CD8 T cells in the primary tumour tissue. *Patients deemed 'High' or 'Low' for CD8 T cells are shaded blue and red, respectively. Cox hazard ratio is univariate. The 'Low' group is used as the reference group on cox regression modelling.*

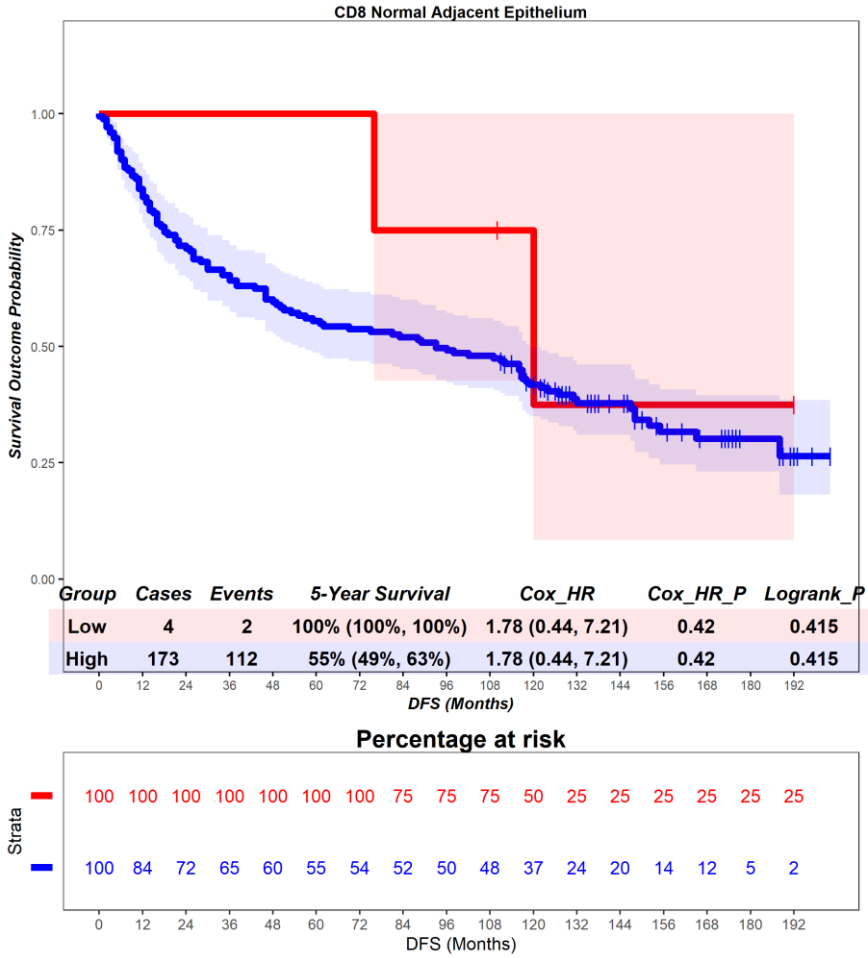

Figure S37 – Time-to-event (disease-free survival) analysis for CD8 T cells in the adjacent normal epithelium. *Patients deemed 'High' or 'Low' for CD8 T cells are shaded blue and red, respectively. Cox hazard ratio is univariate. The 'Low' group is used as the reference group on cox regression modelling.*

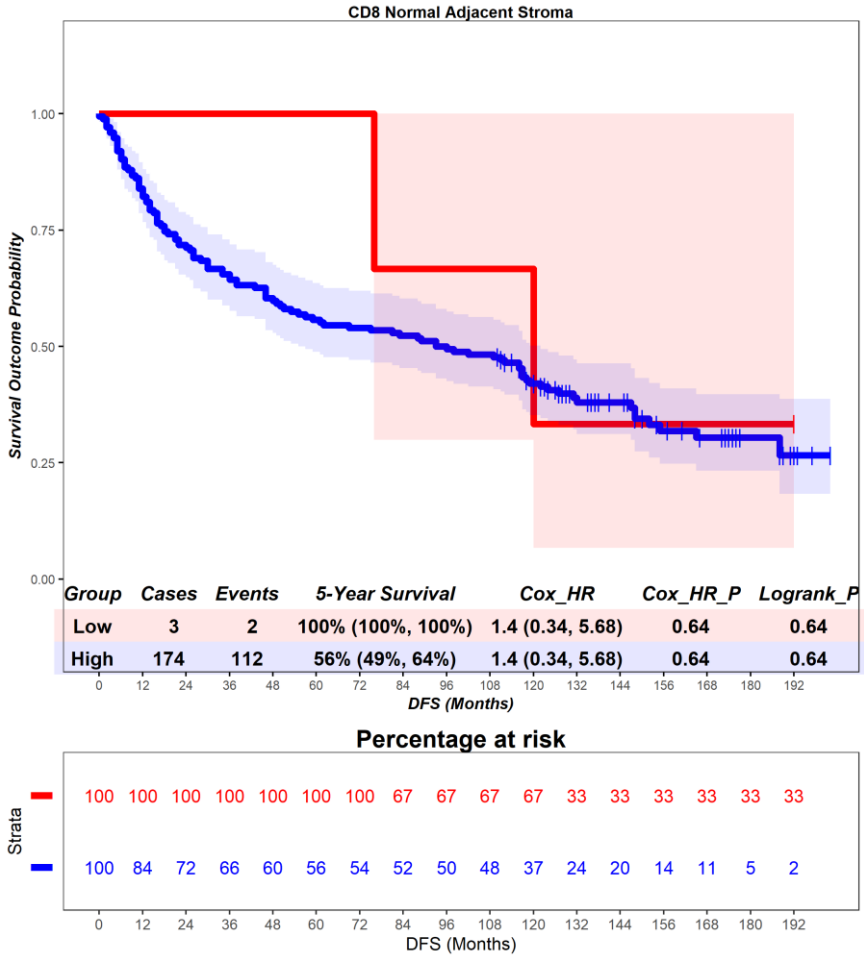

Figure S38 – Time-to-event (disease-free survival) analysis for CD8 T cells in the adjacent normal stroma. *Patients deemed 'High' or 'Low' for CD8 T cells are shaded blue and red, respectively. Cox hazard ratio is univariate. The 'Low' group is used as the reference group on cox regression modelling.*

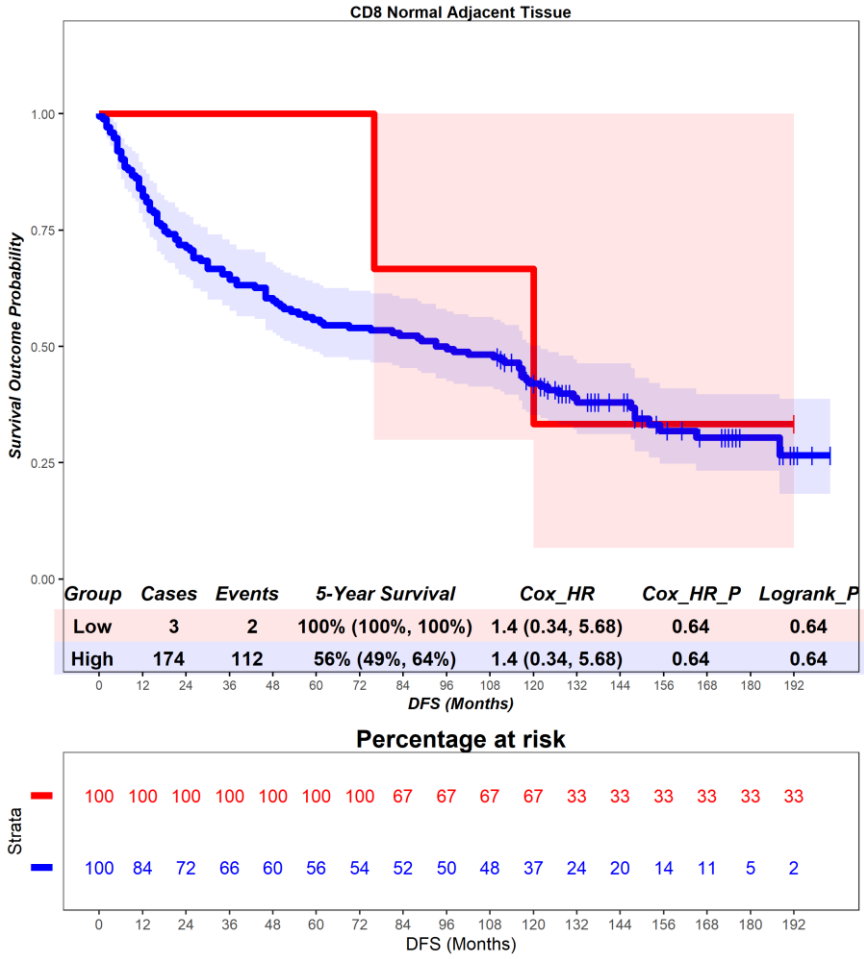

Figure S39 – Time-to-event (disease-free survival) analysis for CD8 T cells in the adjacent normal tissue. Patients *deemed 'High' or 'Low' for CD8 T cells are shaded blue and red, respectively. Cox hazard ratio is univariate. The 'Low' group is used as the reference group on cox regression modelling.*

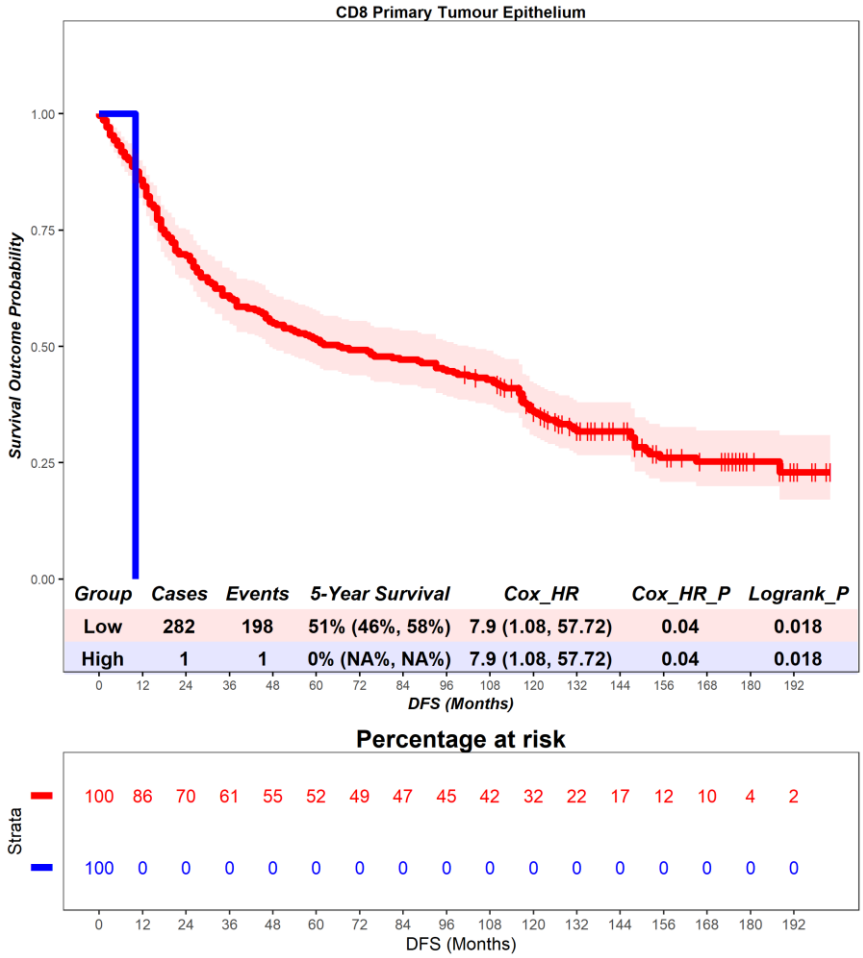

Figure S40 – Time-to-event (disease-free survival) analysis for CD8 T cells in the primary tumour epithelium. *Patients deemed 'High' or 'Low' for CD8 T cells are shaded blue and red, respectively. Cox hazard ratio is univariate. The 'Low' group is used as the reference group on cox regression modelling.*

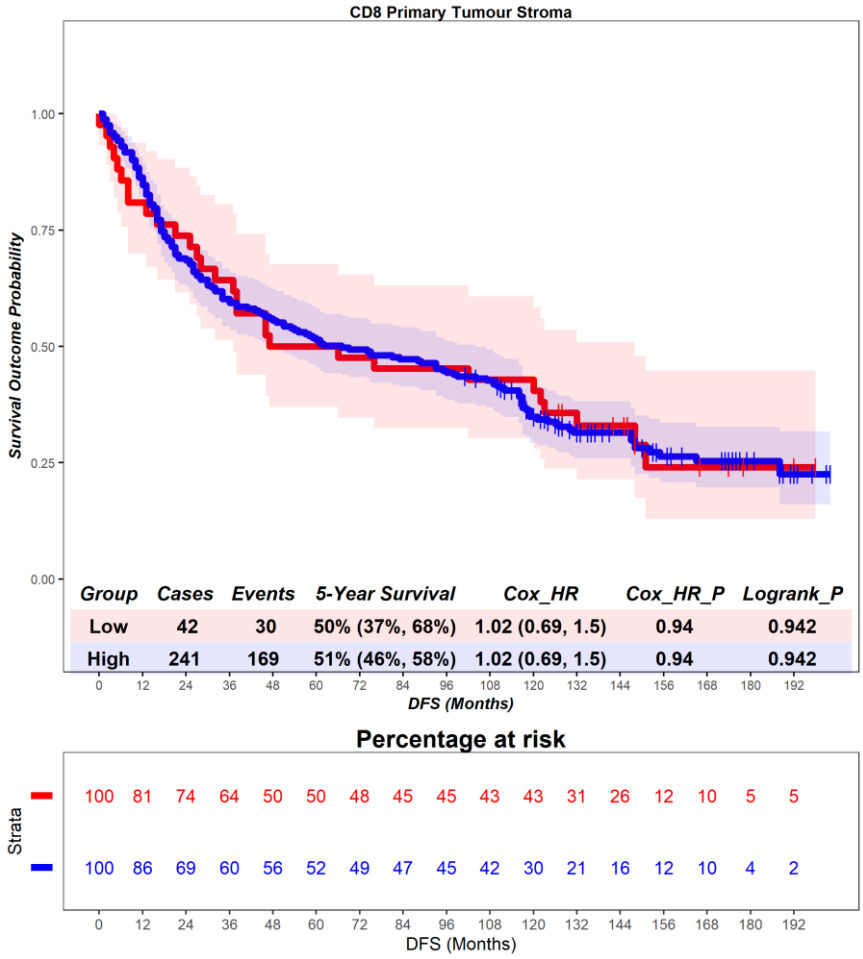

Figure S41 – Time-to-event (disease-free survival) analysis for CD8 T cells in the primary tumour stroma. *Patients deemed 'High' or 'Low' for CD8 T cells are shaded blue and red, respectively. Cox hazard ratio is univariate. The 'Low' group is used as the reference group on cox regression modelling.*

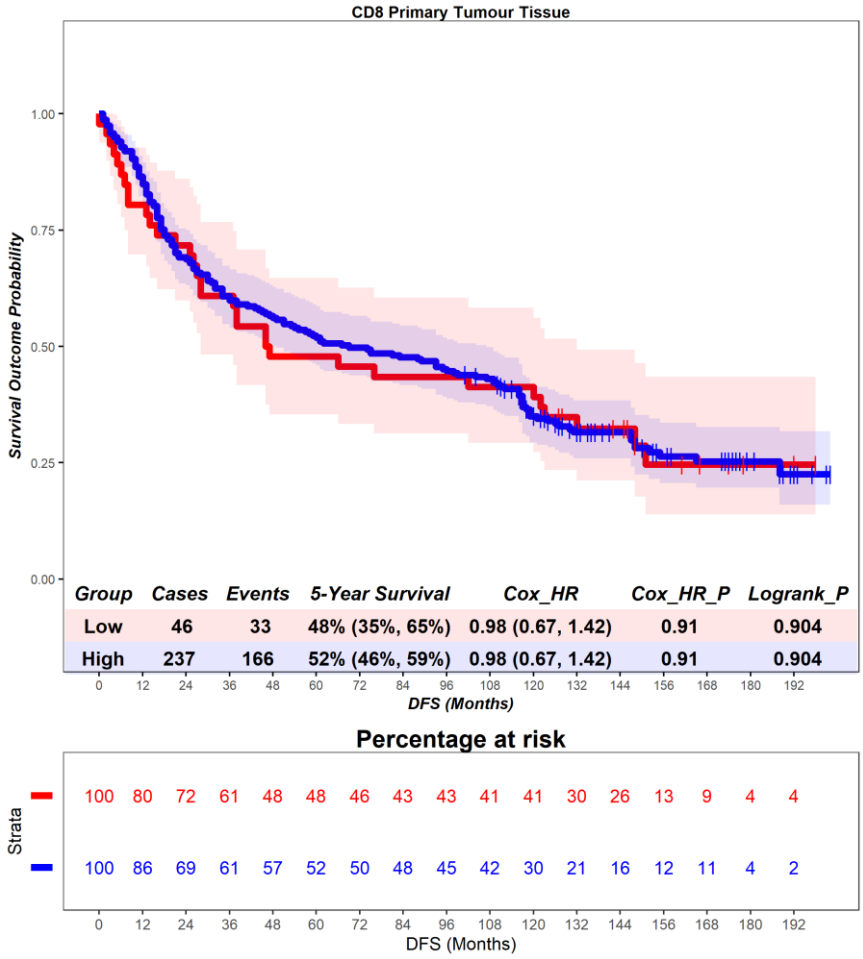

Figure S42 – Time-to-event (disease-free survival) analysis for CD8 T cells in the primary tumour tissue. *Patients deemed 'High' or 'Low' for CD8 T cells are shaded blue and red, respectively. Cox hazard ratio is univariate. The 'Low' group is used as the reference group on cox regression modelling.*

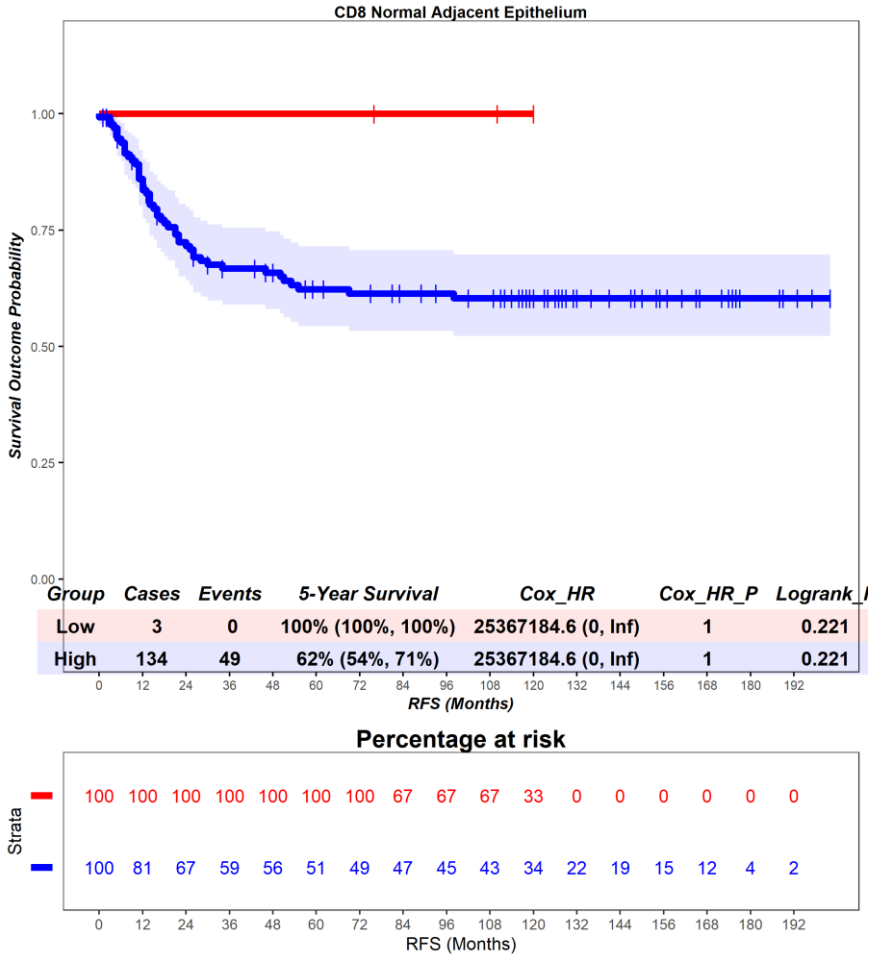

Figure S43 – Time-to-event (recurrence-free survival) analysis for CD8 T cells in the adjacent normal epithelium. *Patients deemed 'High' or 'Low' for CD8 T cells are shaded blue and red, respectively. Cox hazard ratio is univariate. The 'Low' group is used as the reference group on cox regression modelling.*

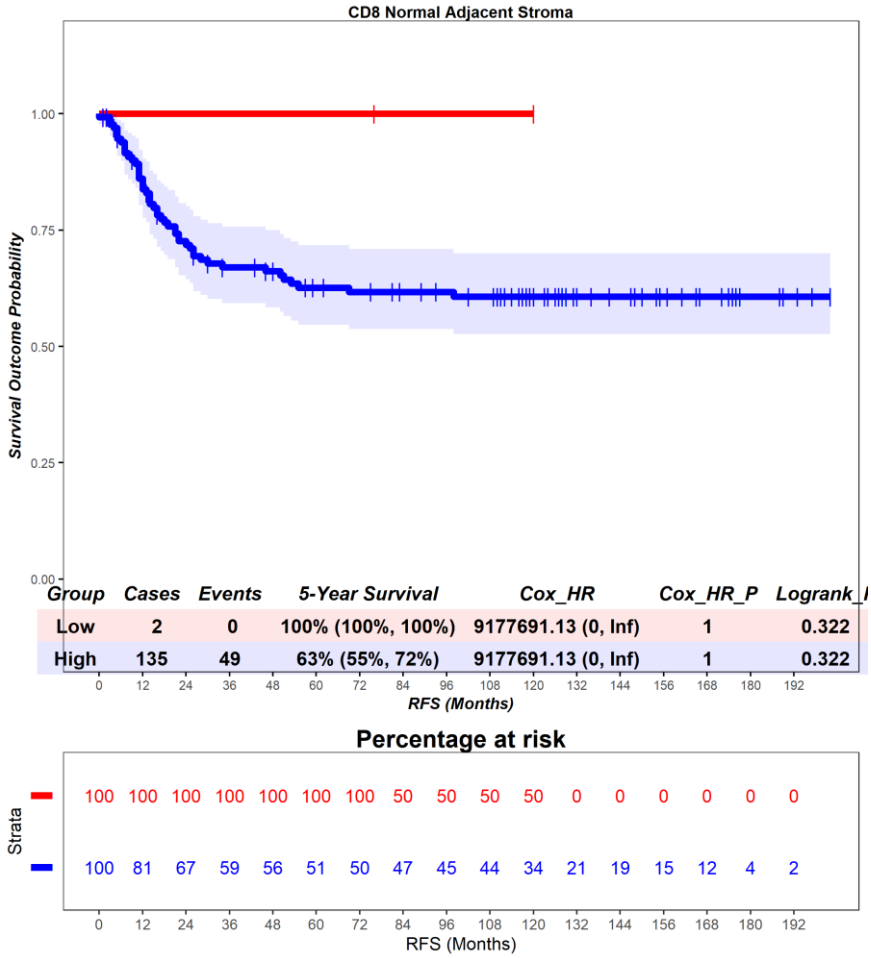

Figure S44 – Time-to-event (recurrence-free survival) analysis for CD8 T cells in the adjacent normal stroma. *Patients deemed 'High' or 'Low' for CD8 T cells are shaded blue and red, respectively. Cox hazard ratio is univariate. The 'Low' group is used as the reference group on cox regression modelling.*

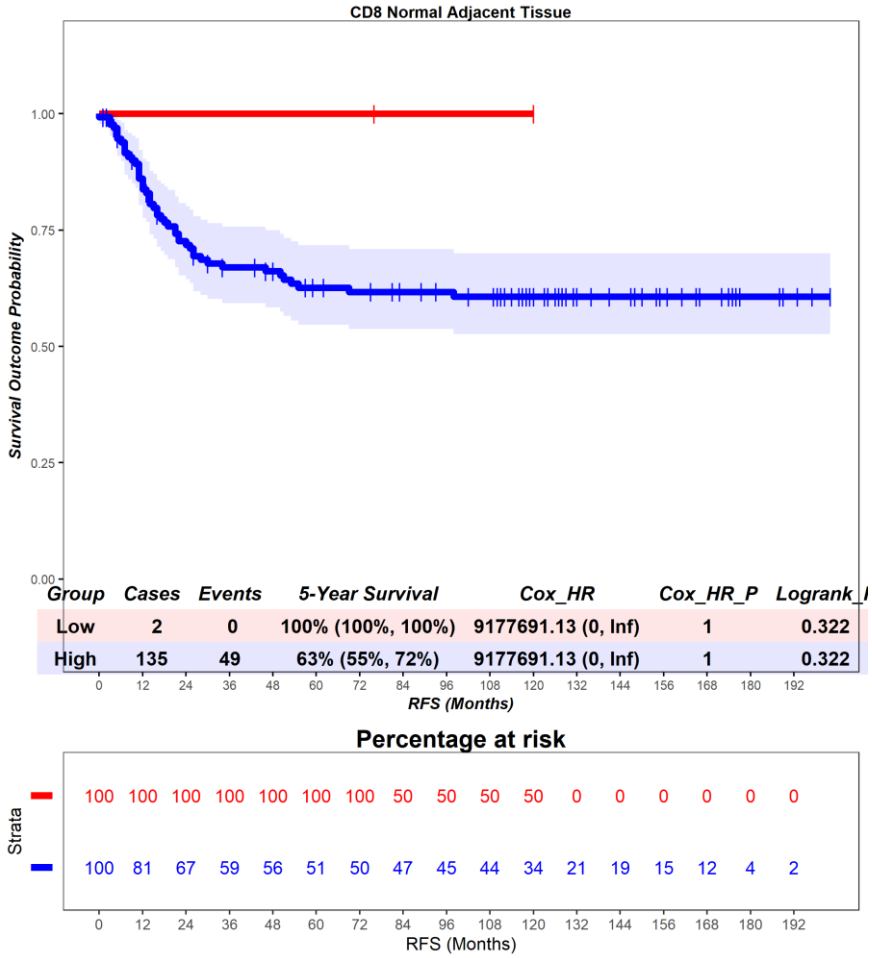

Figure S45 – Time-to-event (recurrence-free survival) analysis for CD8 T cells in the adjacent normal tissue. *Patients deemed 'High' or 'Low' for CD8 T cells are shaded blue and red, respectively. Cox hazard ratio is univariate. The 'Low' group is used as the reference group on cox regression modelling.*

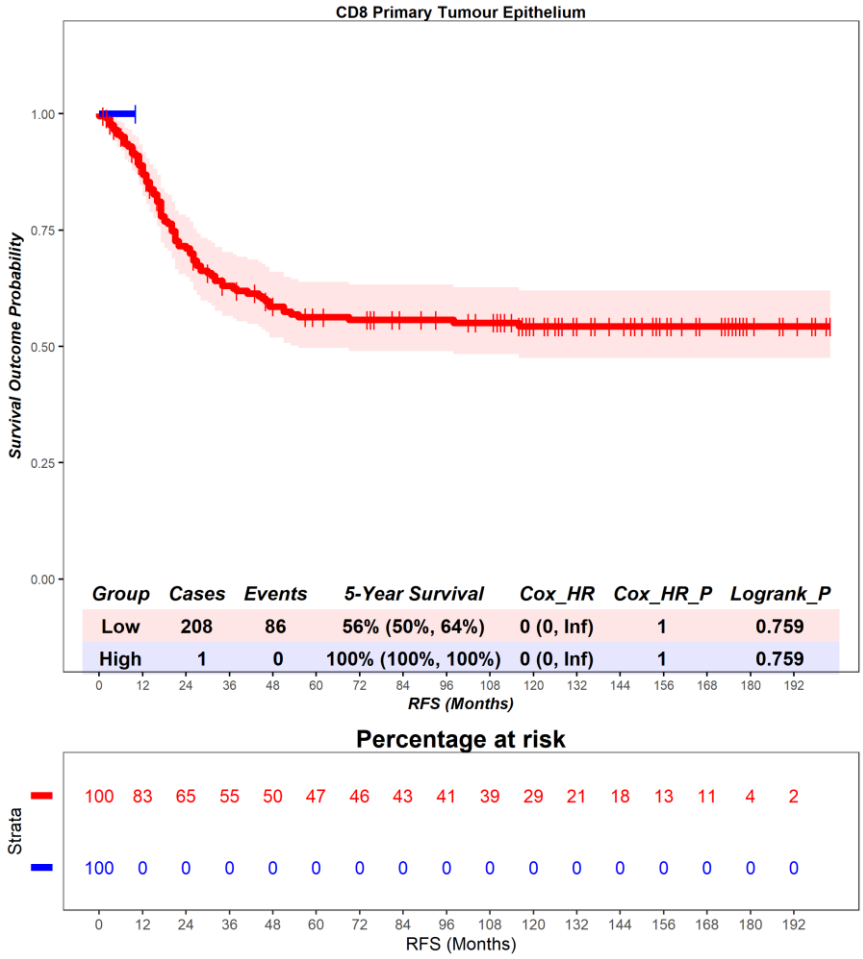

Figure S46 – Time-to-event (recurrence-free survival) analysis for CD8 T cells in the primary tumour epithelium. *Patients deemed 'High' or 'Low' for CD8 T cells are shaded blue and red, respectively. Cox hazard ratio is univariate. The 'Low' group is used as the reference group on cox regression modelling.*

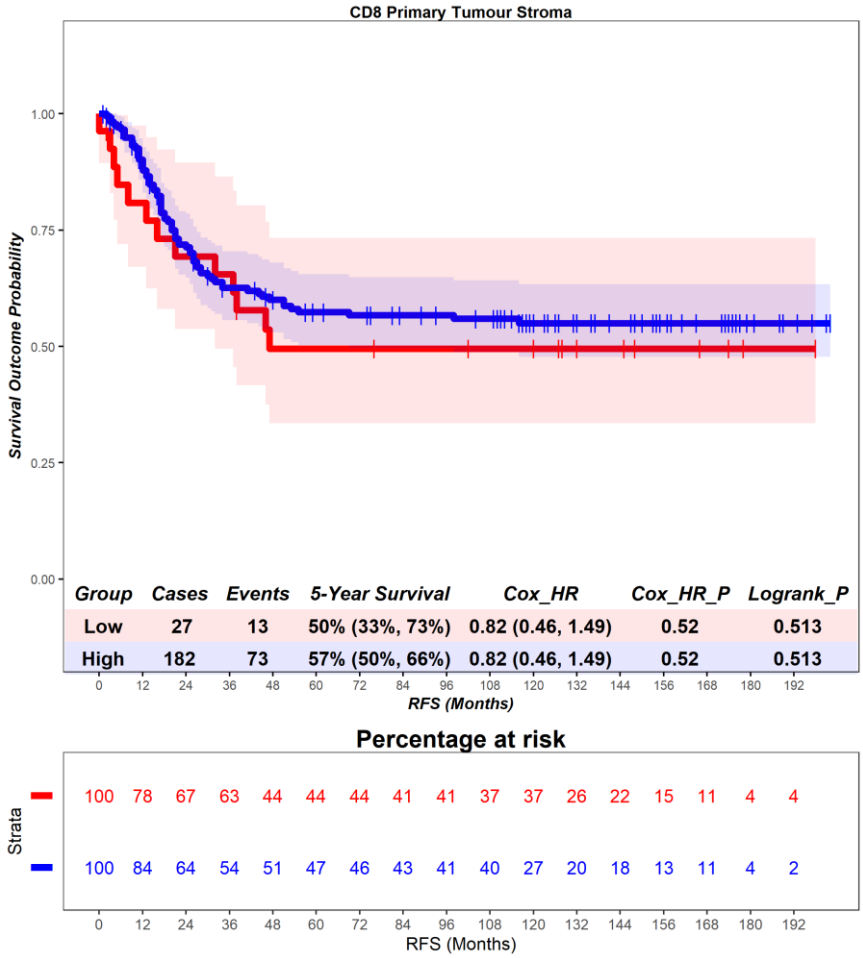

Figure S47 – Time-to-event (recurrence-free survival) analysis for CD8 T cells in the primary tumour stroma. *Patients deemed 'High' or 'Low' for CD8 T cells are shaded blue and red, respectively. Cox hazard ratio is univariate. The 'Low' group is used as the reference group on cox regression modelling.*

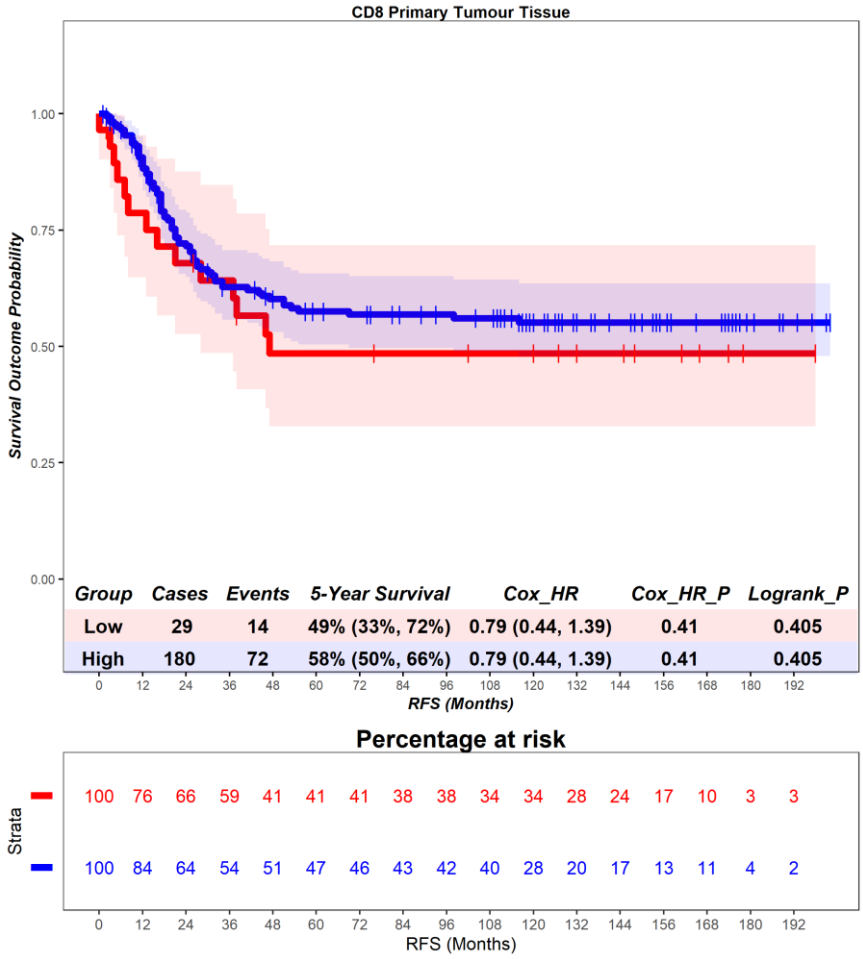

Figure S48 – Time-to-event (recurrence-free survival) analysis for CD8 T cells in the primary tumour tissue. *Patients deemed 'High' or 'Low' for CD8 T cells are shaded blue and red, respectively. Cox hazard ratio is univariate. The 'Low' group is used as the reference group on cox regression modelling.*

4.3 – Time-to-event analysis by cutpoints generated from Norway data – Norway

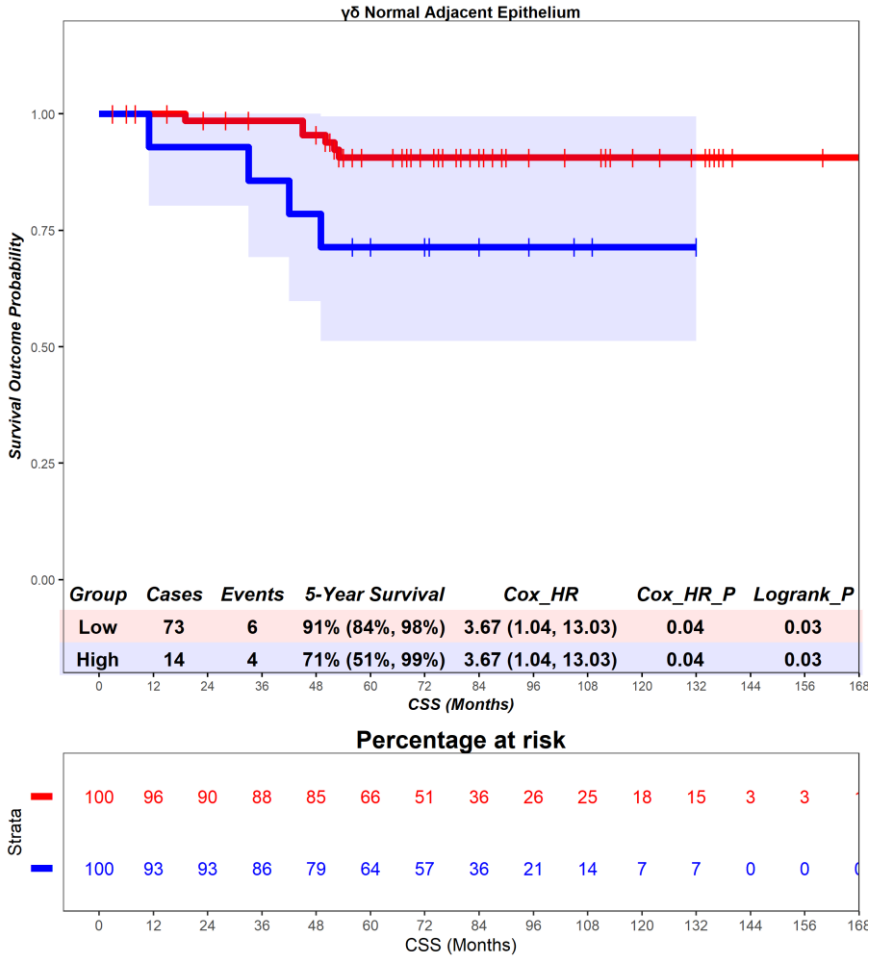

Figure S49 – Time-to-event (recurrence-free survival) analysis for γδ T cells in the adjacent normal epithelium. *Patients deemed 'High' or 'Low' for γδ T cells are shaded blue and red, respectively. Cox hazard ratio is univariate. The 'Low' group is used as the reference group on cox regression modelling.*

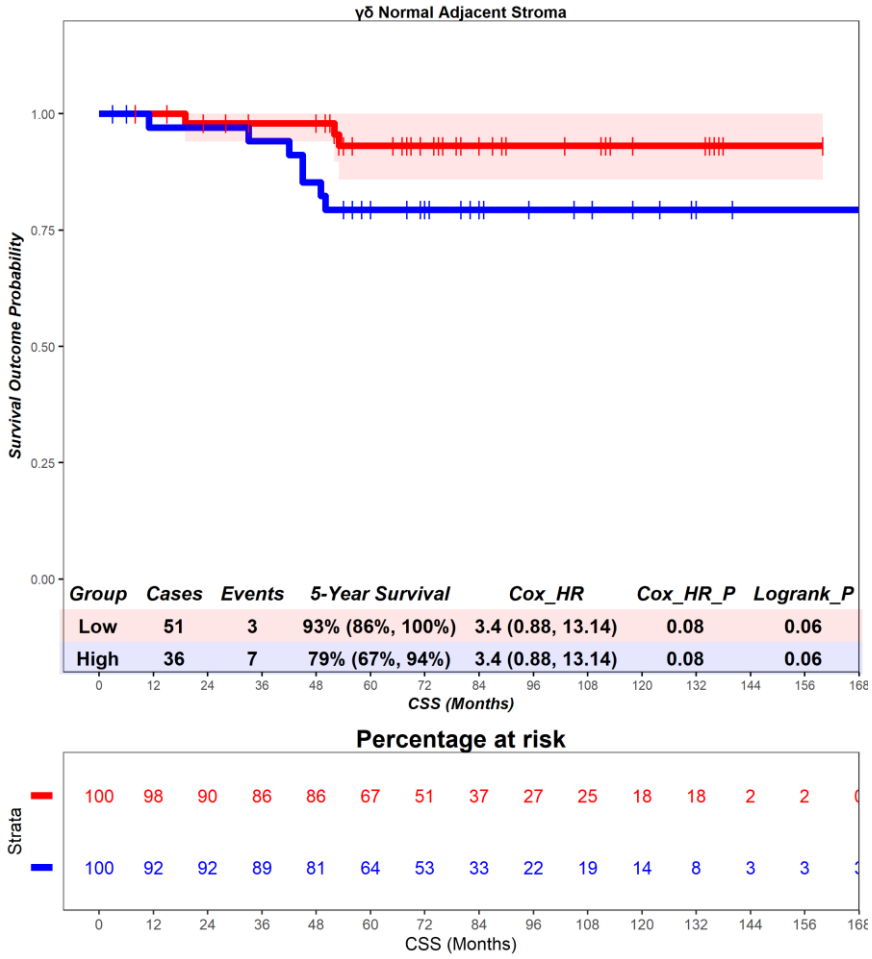

Figure S50 – Time-to-event (cancer-specific survival) analysis for γδ T cells in the adjacent normal stroma. *Patients deemed 'High' or 'Low' for γδ T cells are shaded blue and red, respectively. Cox hazard ratio is univariate. The 'Low' group is used as the reference group on cox regression modelling.*

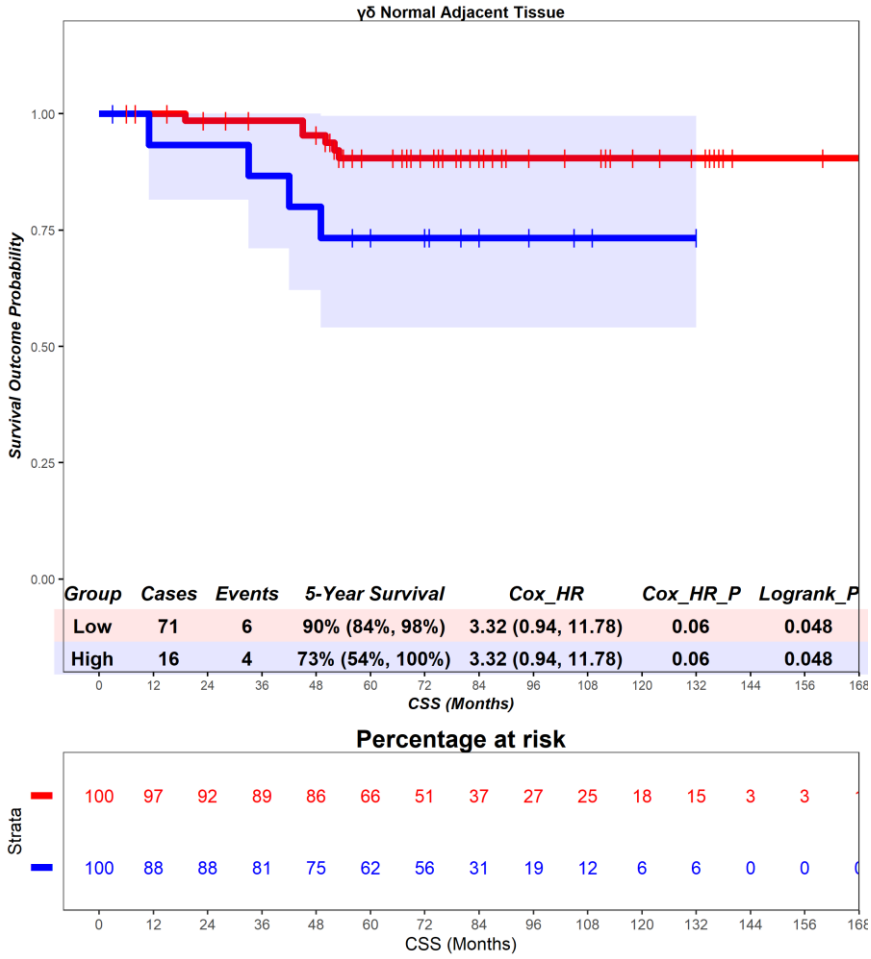

Figure S51 – Time-to-event (cancer-specific survival) analysis for γδ T cells in the adjacent normal tissue. *Patients deemed 'High' or 'Low' for γδ T cells are shaded blue and red, respectively. Cox hazard ratio is univariate. The 'Low' group is used as the reference group on cox regression modelling.*

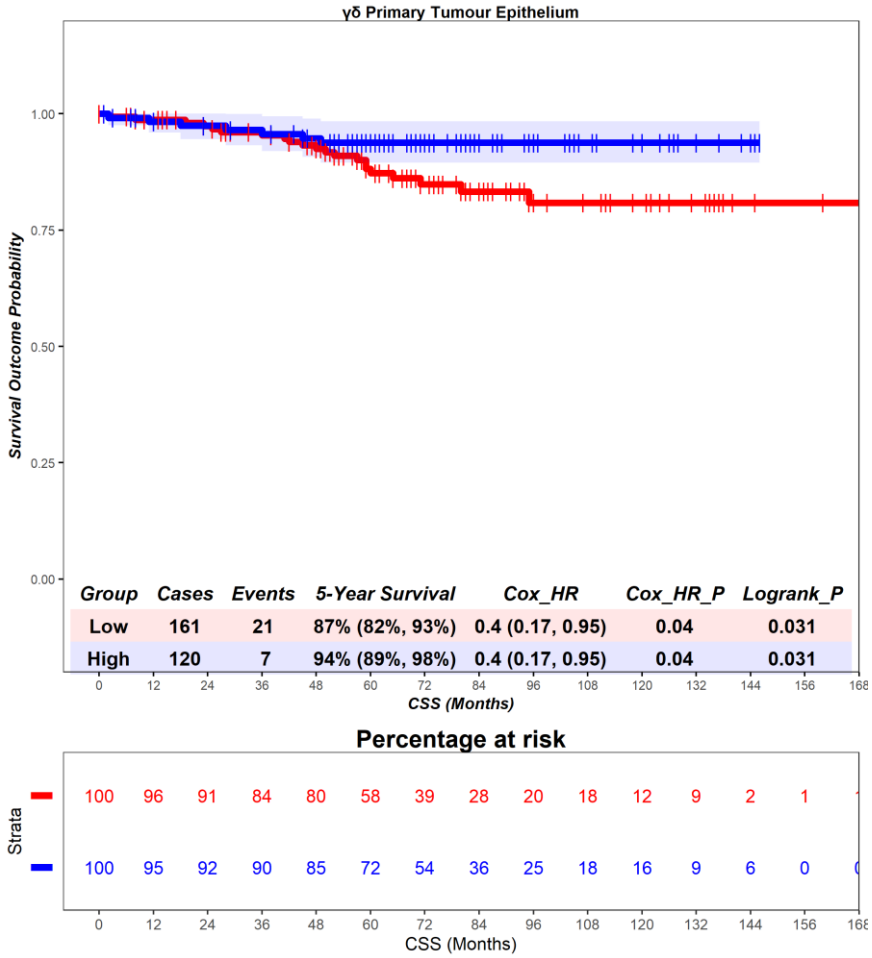

Figure S52 – Time-to-event (cancer-specific survival) analysis for γδ T cells in the primary tumour epithelium. *Patients deemed 'High' or 'Low' for γδ T cells are shaded blue and red, respectively. Cox hazard ratio is univariate. The 'Low' group is used as the reference group on cox regression modelling.*

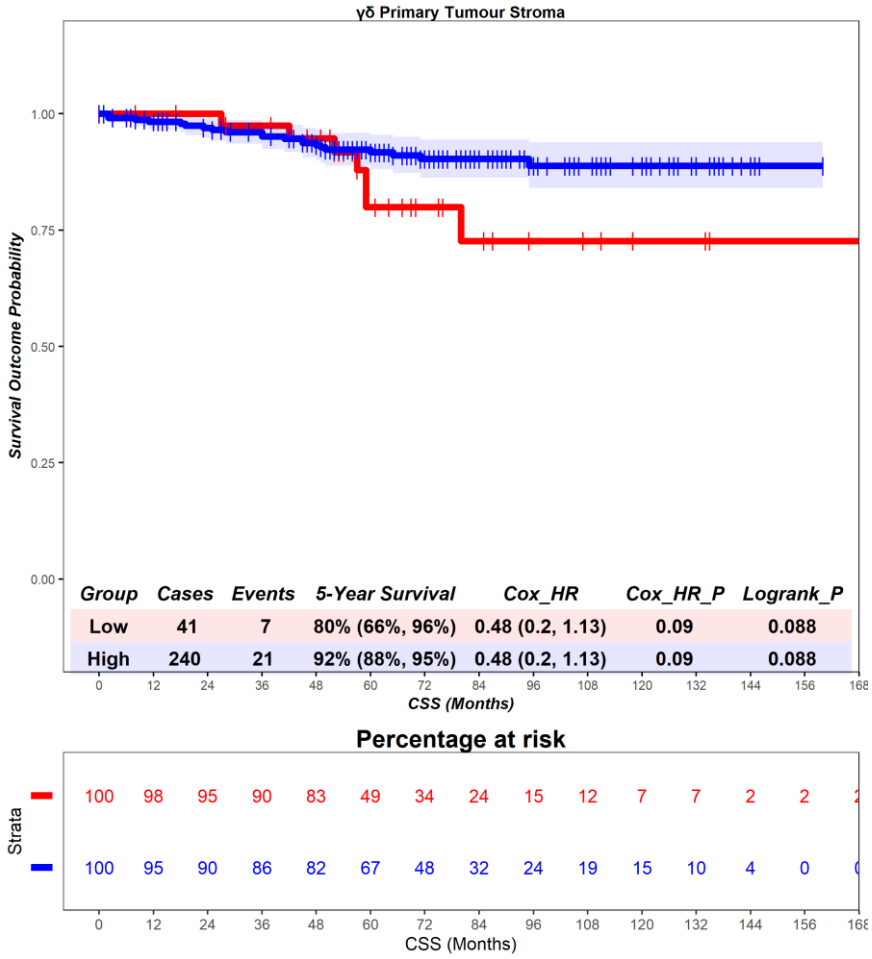

Figure S53 – Time-to-event (cancer-specific survival) analysis for γδ T cells in the primary tumour stroma. *Patients deemed 'High' or 'Low' for γδ T cells are shaded blue and red, respectively. Cox hazard ratio is univariate. The 'Low' group is used as the reference group on cox regression modelling.*

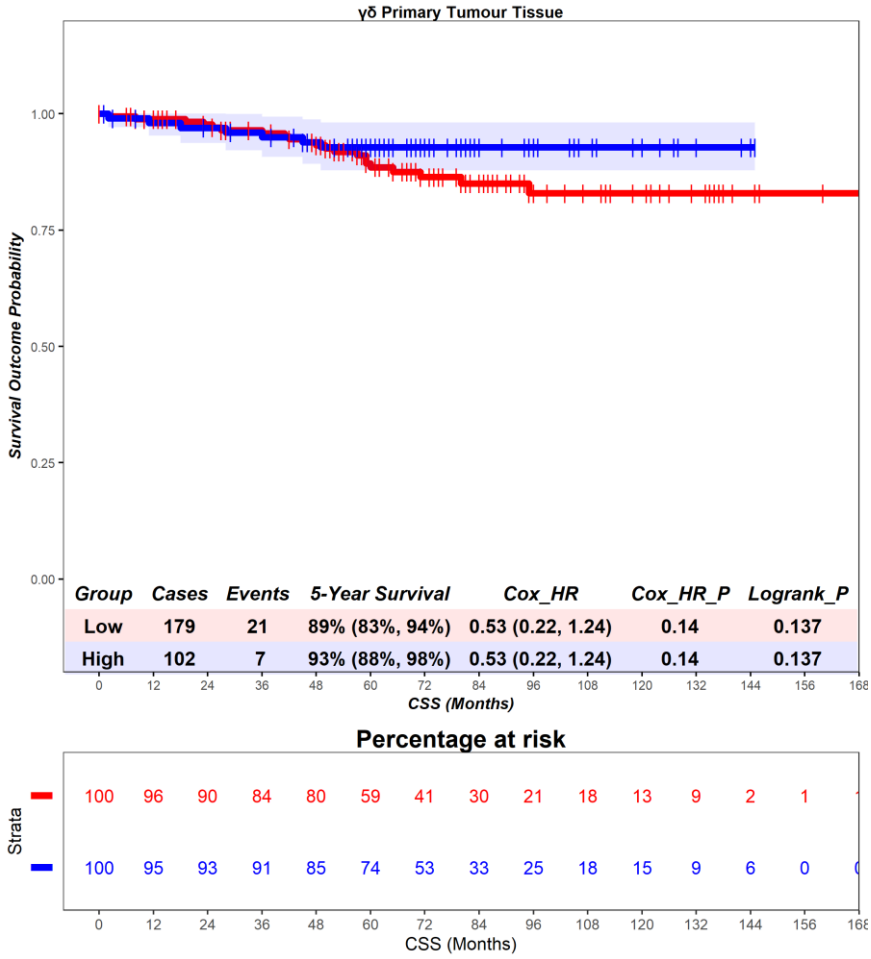

Figure S54 – Time-to-event (cancer-specific survival) analysis for γδ T cells in the primary tumour tissue. *Patients deemed 'High' or 'Low' for γδ T cells are shaded blue and red, respectively. Cox hazard ratio is univariate. The 'Low' group is used as the reference group on cox regression modelling.*

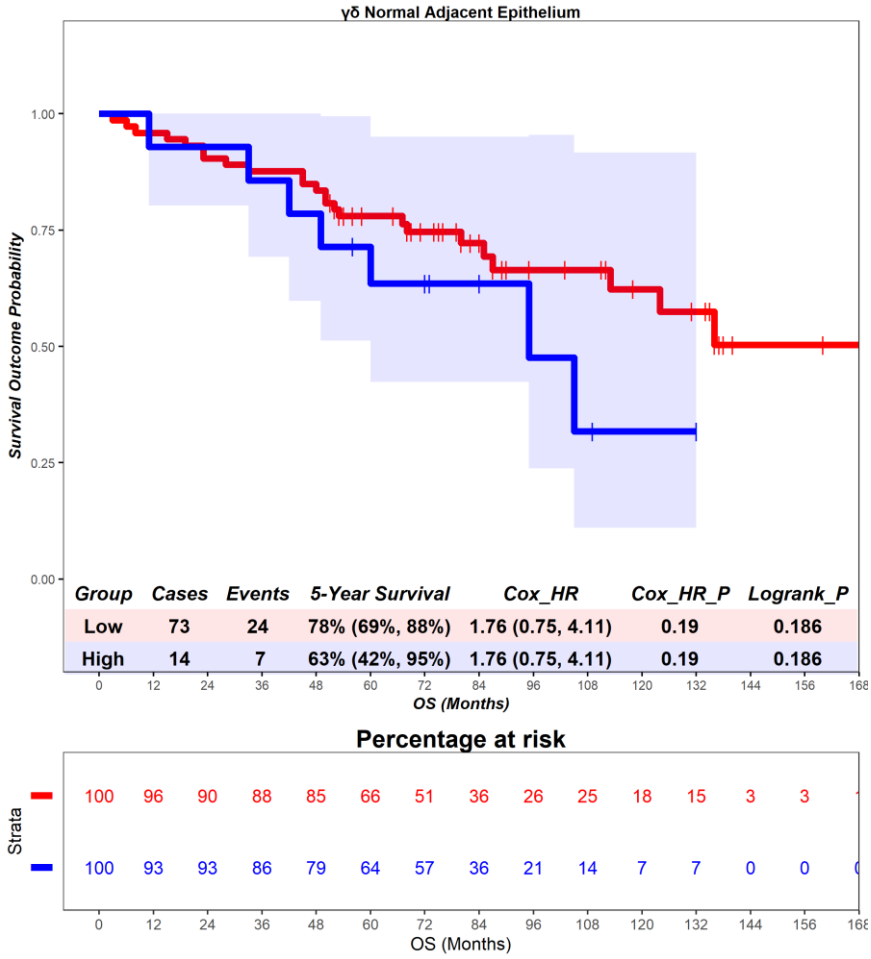

Figure S55 – Time-to-event (overall survival) analysis for γδ T cells in the adjacent normal epithelium. *Patients deemed 'High' or 'Low' for γδ T cells are shaded blue and red, respectively. Cox hazard ratio is univariate. The 'Low' group is used as the reference group on cox regression modelling.*

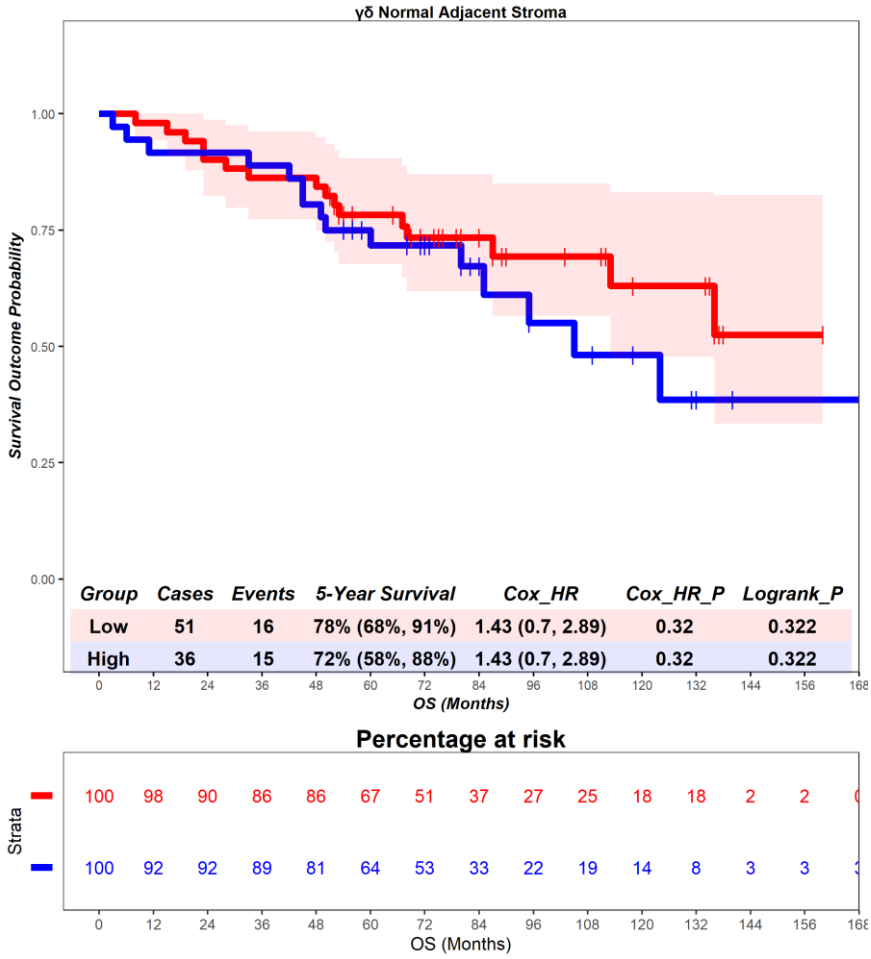

Figure S56 – Time-to-event (overall survival) analysis for γδ T cells in the adjacent normal stroma. *Patients deemed 'High' or 'Low' for γδ T cells are shaded blue and red, respectively. Cox hazard ratio is univariate. The 'Low' group is used as the reference group on cox regression modelling.*

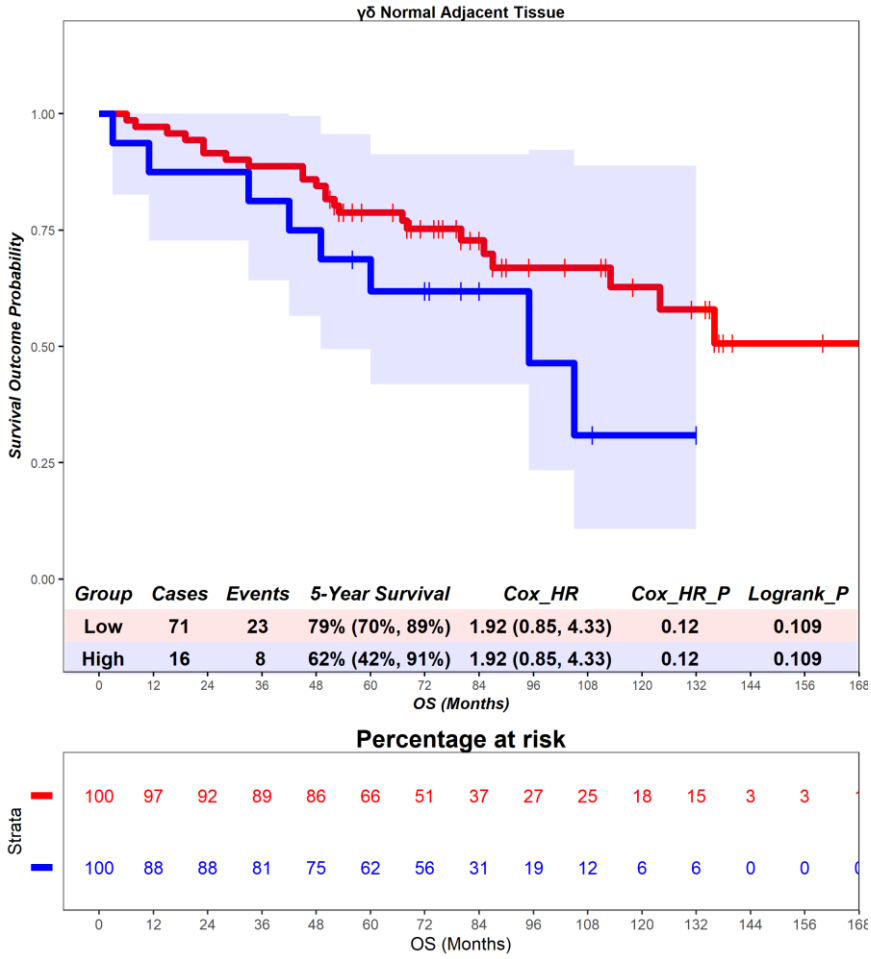

Figure S57 – Time-to-event (overall survival) analysis for γδ T cells in the adjacent normal tissue. *Patients deemed 'High' or 'Low' for γδ T cells are shaded blue and red, respectively. Cox hazard ratio is univariate. The 'Low' group is used as the reference group on cox regression modelling.*

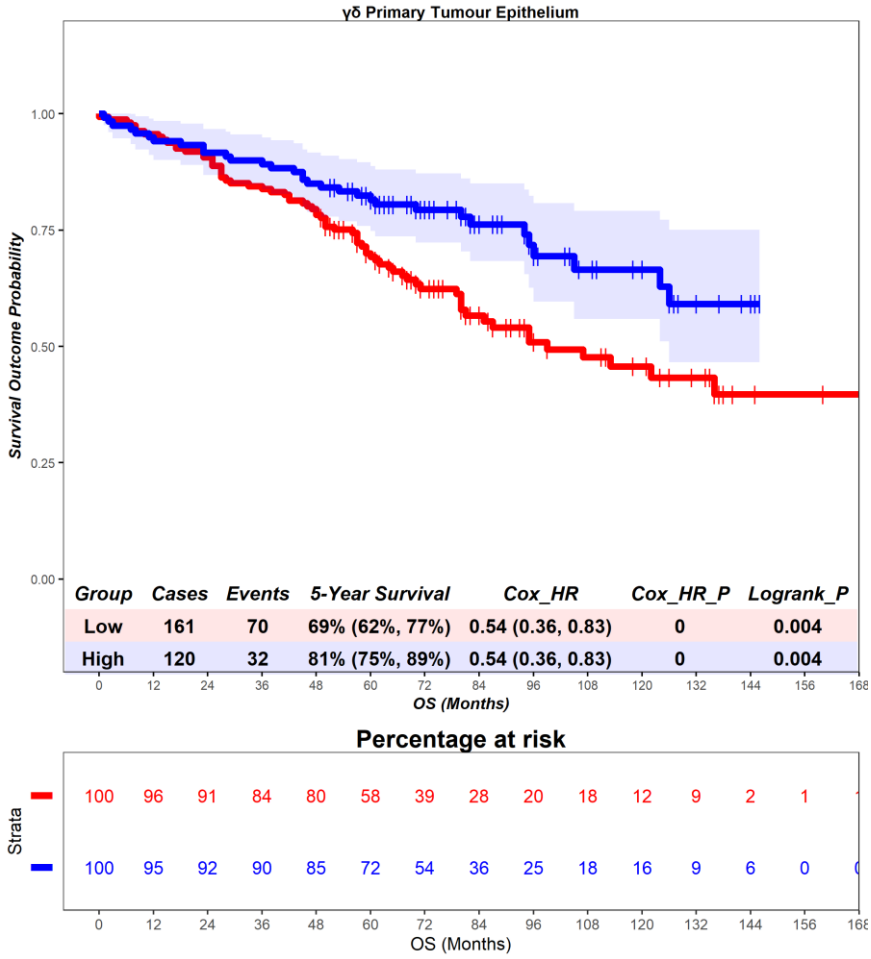

Figure S58 – Time-to-event (overall survival) analysis for γδ T cells in the primary tumour epithelium. *Patients deemed 'High' or 'Low' for γδ T cells are shaded blue and red, respectively. Cox hazard ratio is univariate. The 'Low' group is used as the reference group on cox regression modelling.*

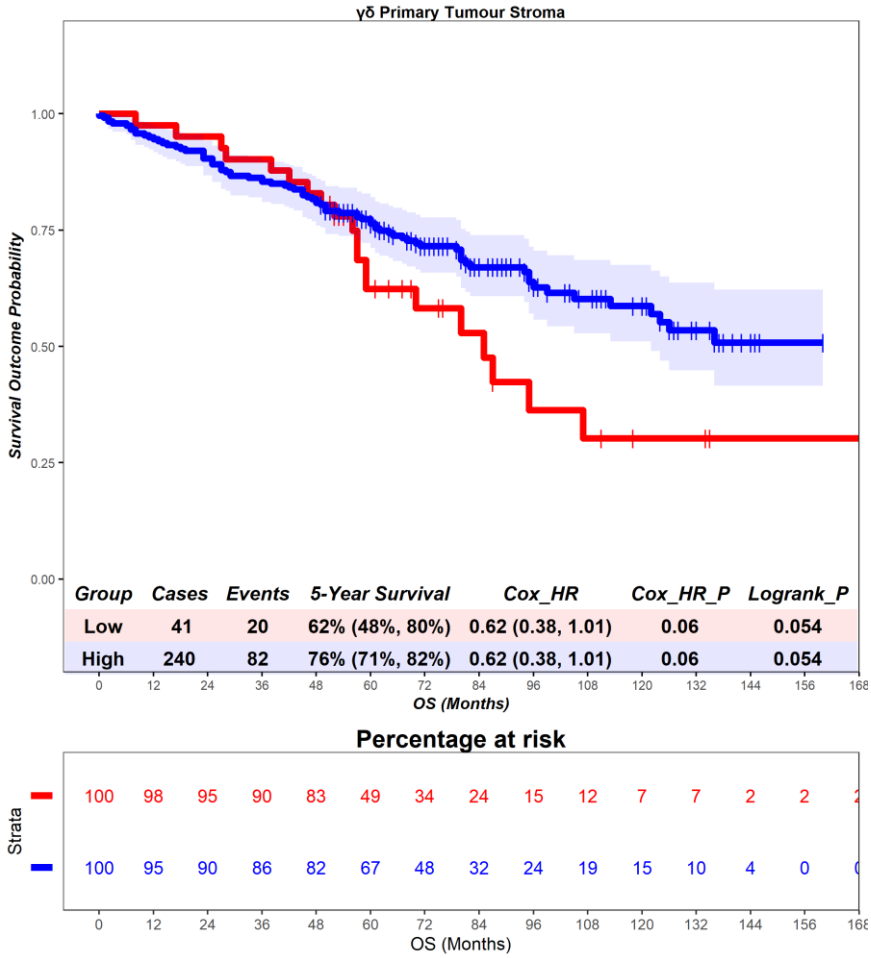

Figure S59 – Time-to-event (overall survival) analysis for γδ T cells in the primary tumour stroma. *Patients deemed 'High' or 'Low' for γδ T cells are shaded blue and red, respectively. Cox hazard ratio is univariate. The 'Low' group is used as the reference group on cox regression modelling.*

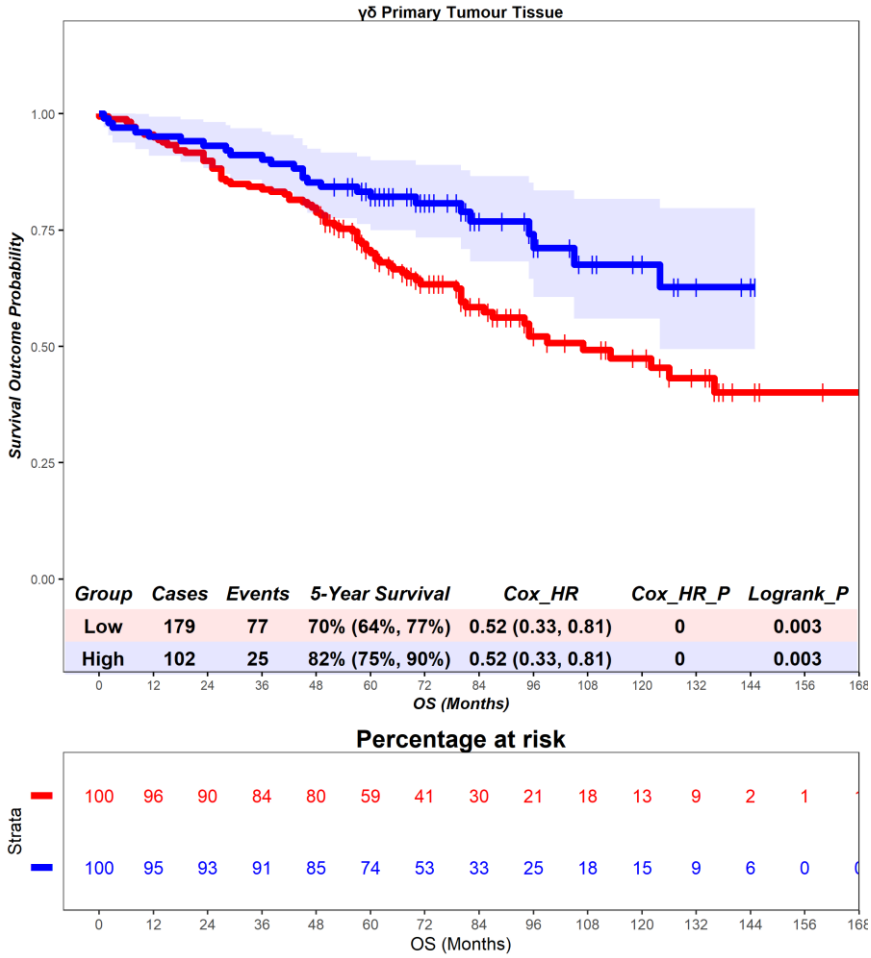

Figure S60 – Time-to-event (overall survival) analysis for γδ T cells in the primary tumour tissue. *Patients deemed 'High' or 'Low' for γδ T cells are shaded blue and red, respectively. Cox hazard ratio is univariate. The 'Low' group is used as the reference group on cox regression modelling.*

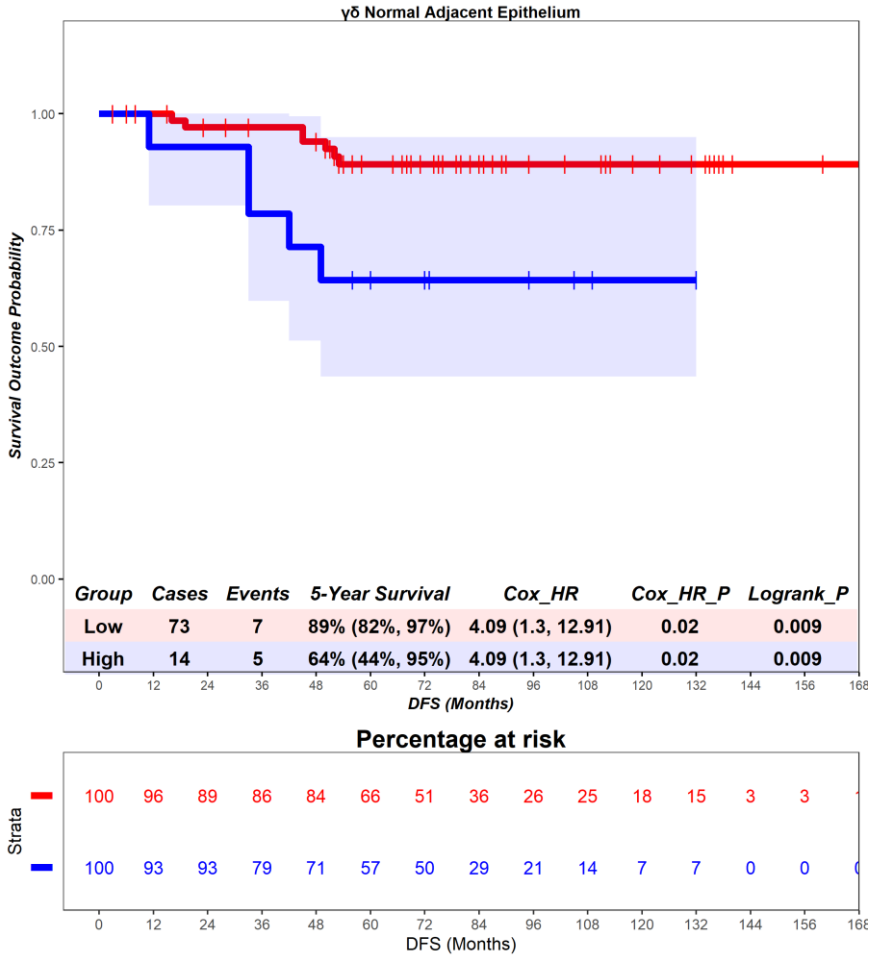

Figure S61 – Time-to-event (disease-free survival) analysis for γδ T cells in the normal adjacent epithelium. *Patients deemed 'High' or 'Low' for γδ T cells are shaded blue and red, respectively. Cox hazard ratio is univariate. The 'Low' group is used as the reference group on cox regression modelling.*

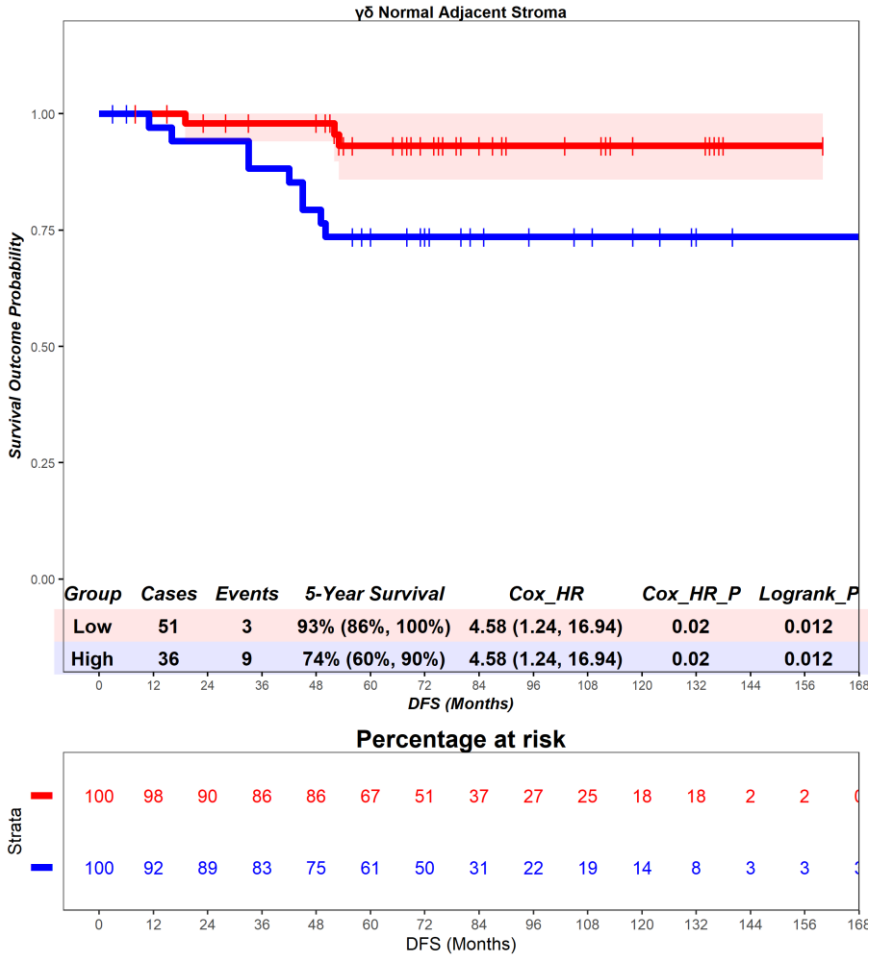

Figure S62 – Time-to-event (disease-free survival) analysis for γδ T cells in the normal adjacent stroma. *Patients deemed 'High' or 'Low' for γδ T cells are shaded blue and red, respectively. Cox hazard ratio is univariate. The 'Low' group is used as the reference group on cox regression modelling.*

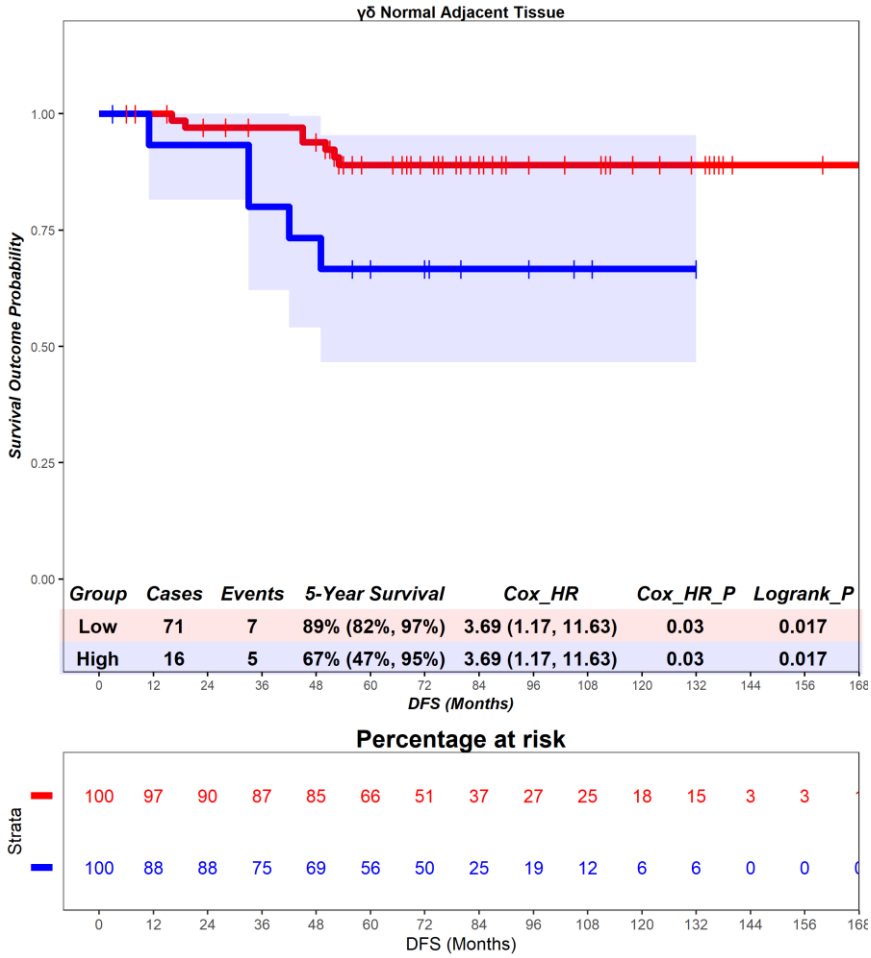

Figure S63 – Time-to-event (disease-free survival) analysis for γδ T cells in the normal adjacent tissue. *Patients deemed 'High' or 'Low' for γδ T cells are shaded blue and red, respectively. Cox hazard ratio is univariate. The 'Low' group is used as the reference group on cox regression modelling.*

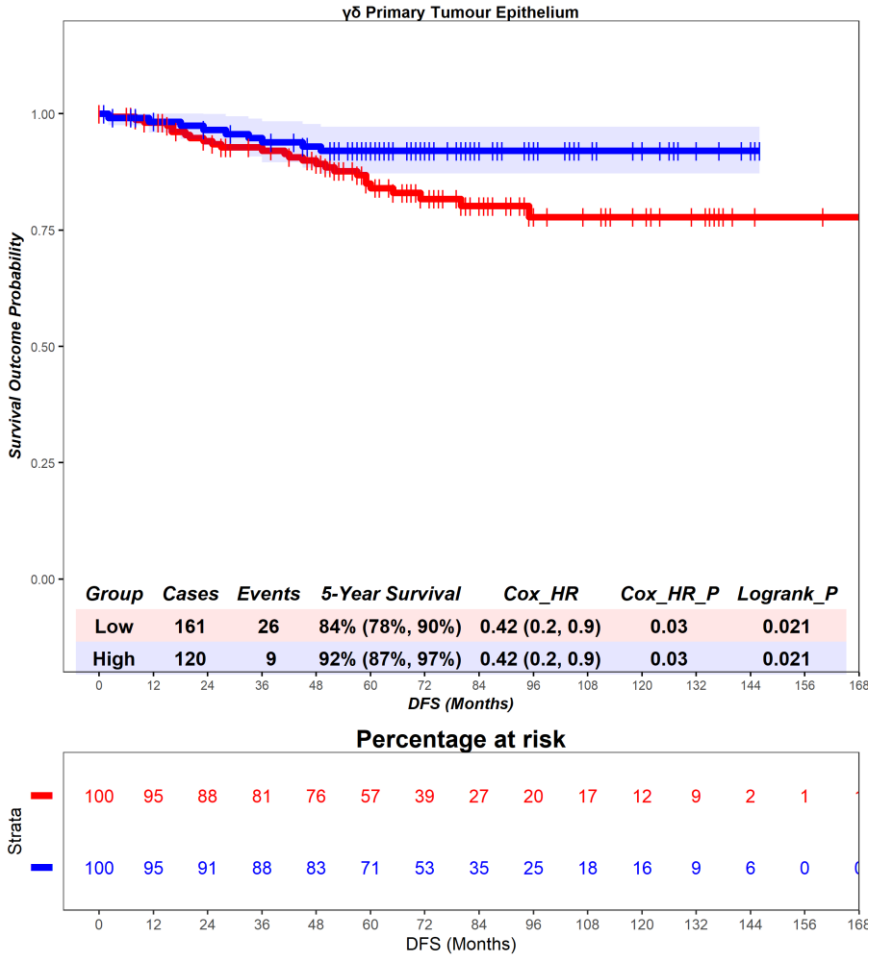

Figure S64 – Time-to-event (disease-free survival) analysis for γδ T cells in the primary tumour epithelium. *Patients deemed 'High' or 'Low' for γδ T cells are shaded blue and red, respectively. Cox hazard ratio is univariate. The 'Low' group is used as the reference group on cox regression modelling.*

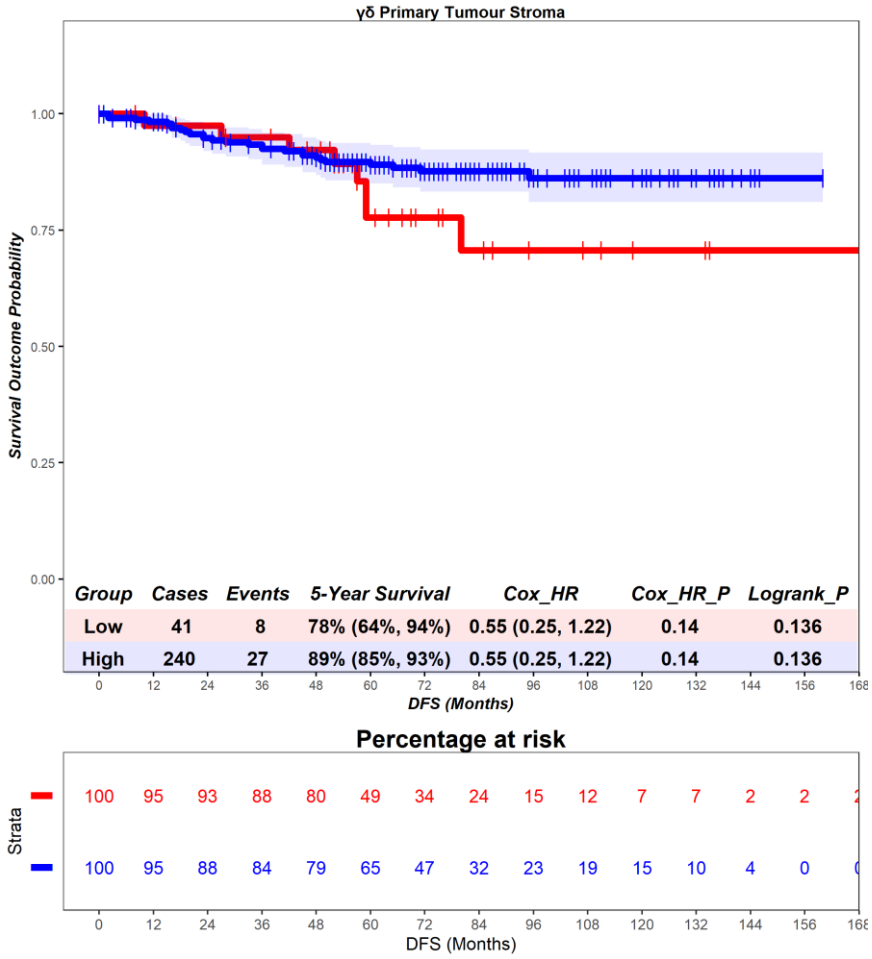

Figure S65 – Time-to-event (disease-free survival) analysis for γδ T cells in the primary tumour stroma. *Patients deemed 'High' or 'Low' for γδ T cells are shaded blue and red, respectively. Cox hazard ratio is univariate. The 'Low' group is used as the reference group on cox regression modelling.*

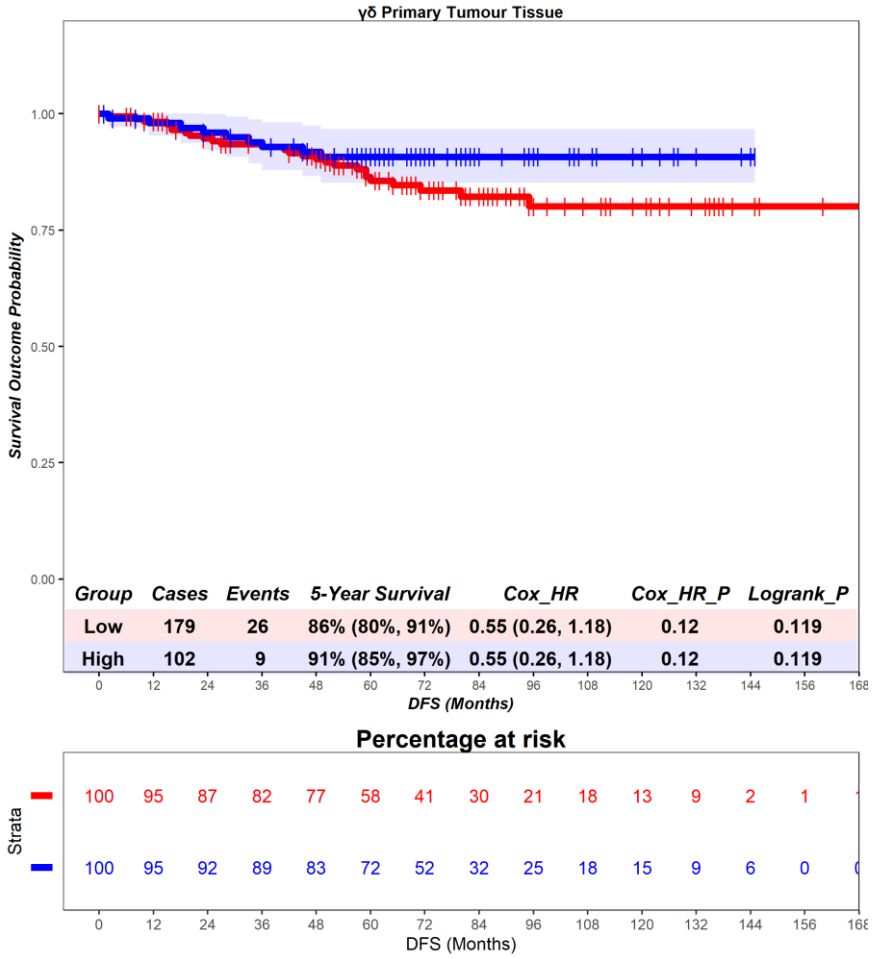

Figure S66 – Time-to-event (disease-free survival) analysis for γδ T cells in the primary tumour tissue. *Patients deemed 'High' or 'Low' for γδ T cells are shaded blue and red, respectively. Cox hazard ratio is univariate. The 'Low' group is used as the reference group on cox regression modelling.*

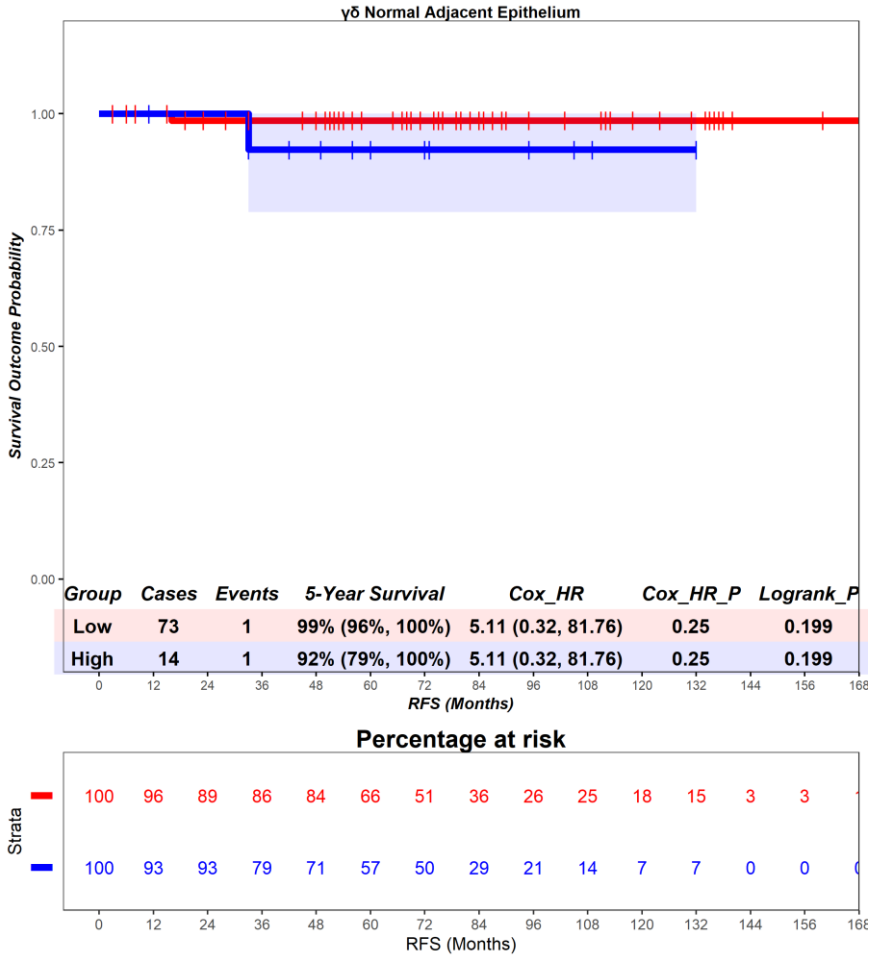

Figure S67 – Time-to-event (recurrence-free survival) analysis for γδ T cells in the normal adjacent epithelium. *Patients deemed 'High' or 'Low' for γδ T cells are shaded blue and red, respectively. Cox hazard ratio is univariate. The 'Low' group is used as the reference group on cox regression modelling.*

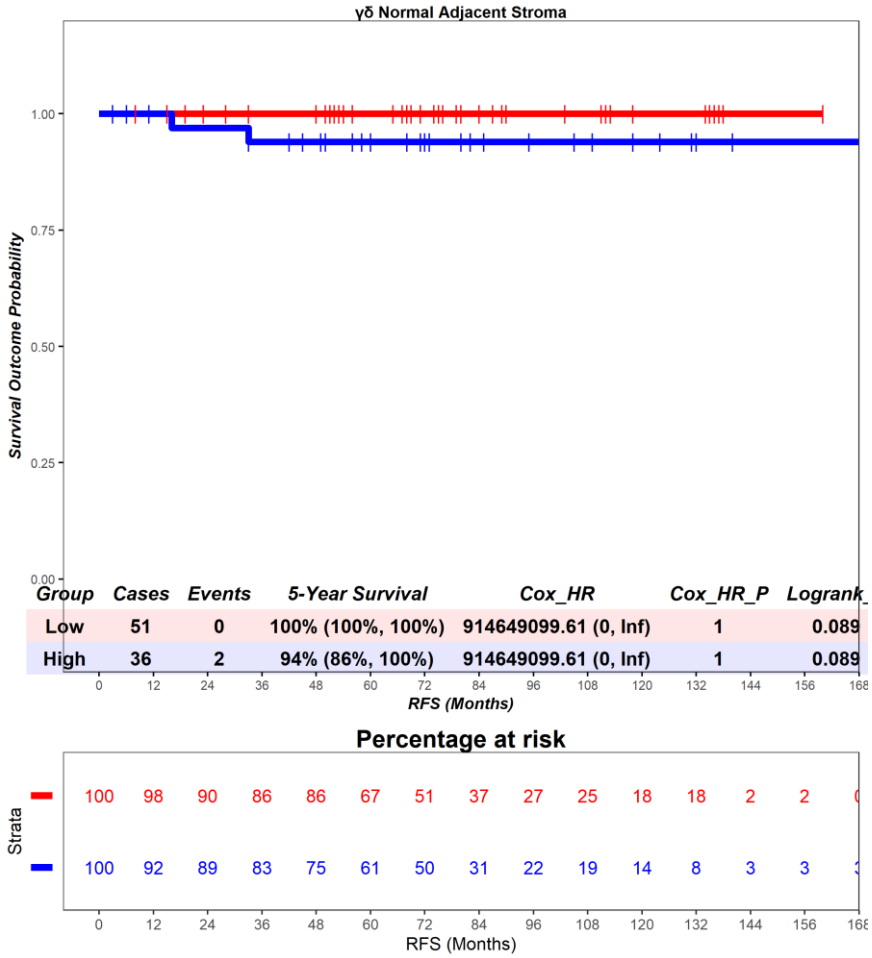

Figure S68 – Time-to-event (recurrence-free survival) analysis for γδ T cells in the normal adjacent stroma. *Patients deemed 'High' or 'Low' for γδ T cells are shaded blue and red, respectively. Cox hazard ratio is univariate. The 'Low' group is used as the reference group on cox regression modelling.*

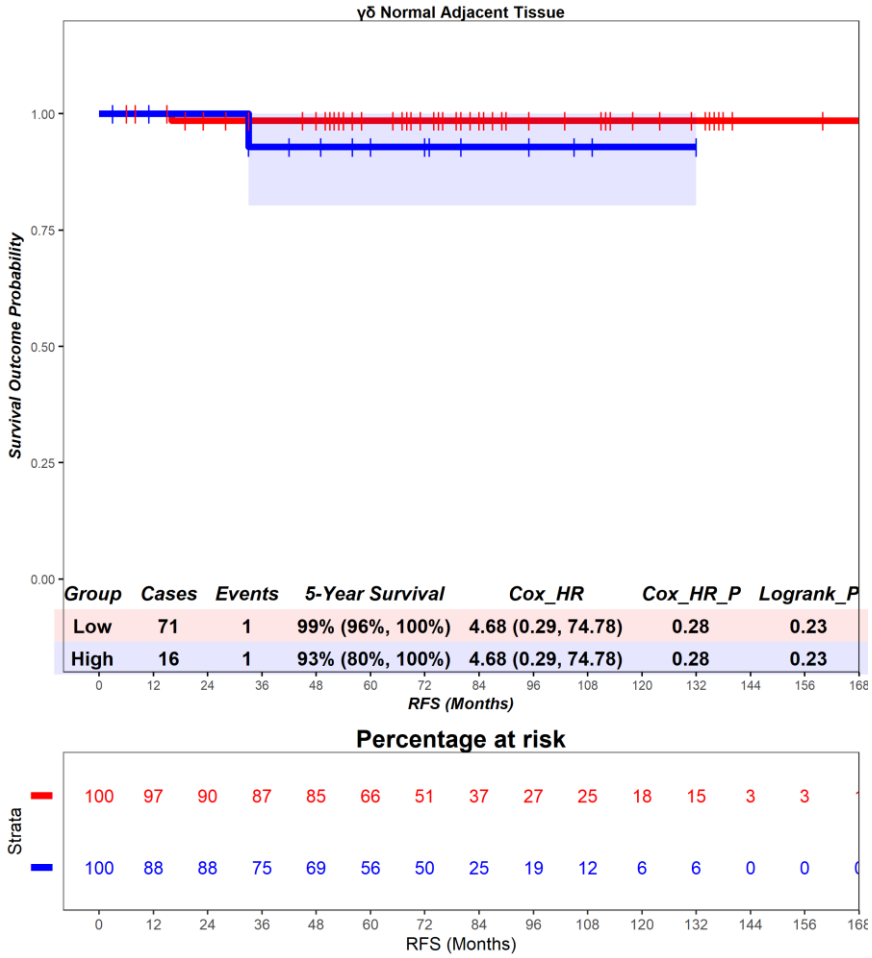

Figure S69 – Time-to-event (recurrence-free survival) analysis for γδ T cells in the normal adjacent tissue. *Patients deemed 'High' or 'Low' for γδ T cells are shaded blue and red, respectively. Cox hazard ratio is univariate. The 'Low' group is used as the reference group on cox regression modelling.*

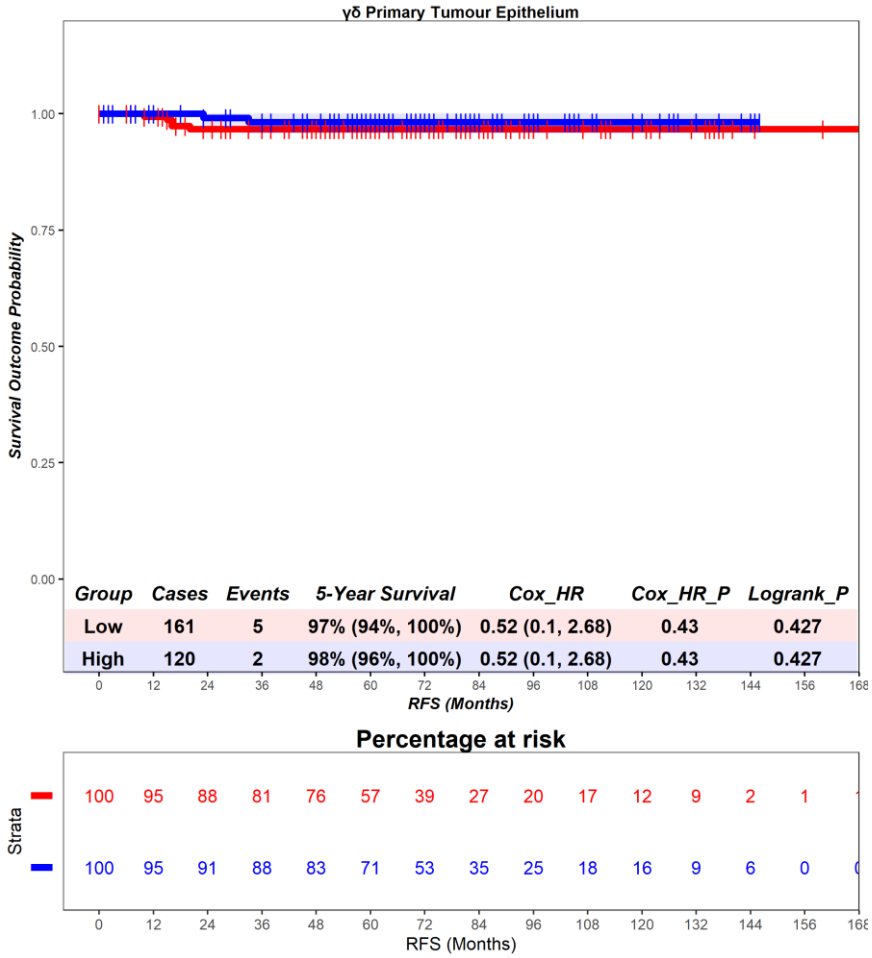

Figure S70 – Time-to-event (recurrence-free survival) analysis for γδ T cells in the primary tumour epithelium*. Patients deemed 'High' or 'Low' for γδ T cells are shaded blue and red, respectively. Cox hazard ratio is univariate. The 'Low' group is used as the reference group on cox regression modelling.*

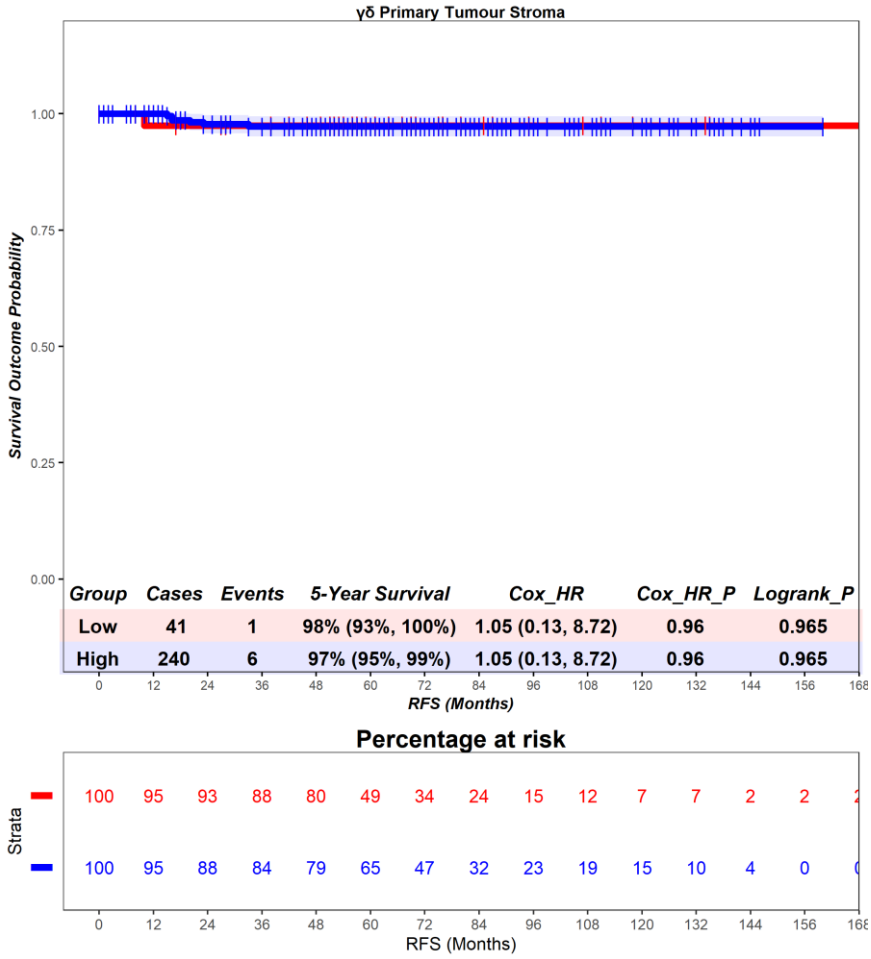

Figure S71 – Time-to-event (recurrence-free survival) analysis for γδ T cells in the primary tumour stroma. *Patients deemed 'High' or 'Low' for γδ T cells are shaded blue and red, respectively. Cox hazard ratio is univariate. The 'Low' group is used as the reference group on cox regression modelling.*

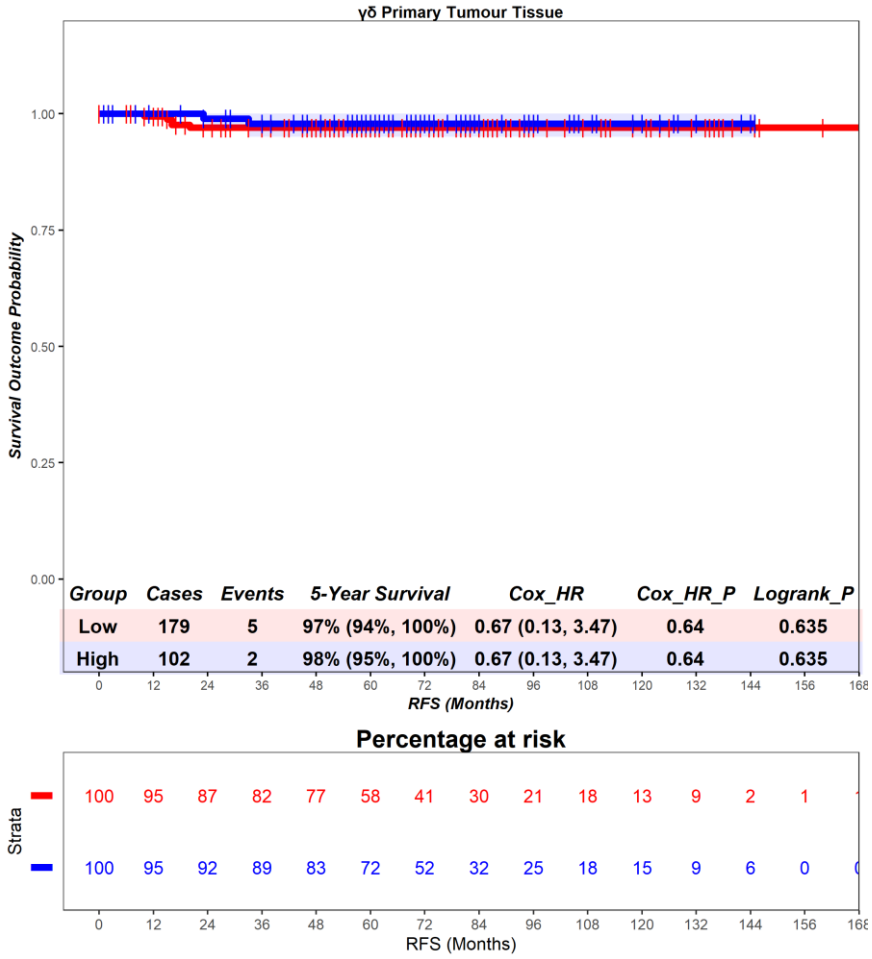

Figure S72 – Time-to-event (recurrence-free survival) analysis for γδ T cells in the primary tumour tissue. *Patients deemed 'High' or 'Low' for γδ T cells are shaded blue and red, respectively. Cox hazard ratio is univariate. The 'Low' group is used as the reference group on cox regression modelling.*

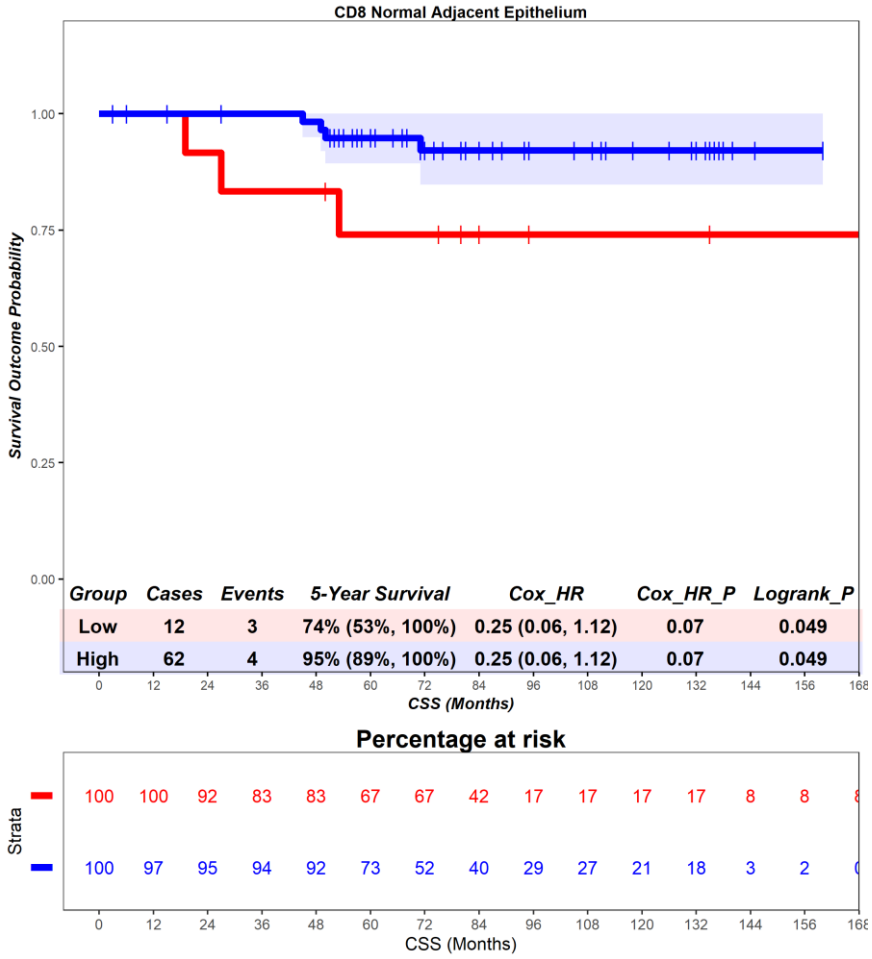

Figure S73 – Time-to-event (cancer-specific survival) analysis for CD8 T cells in the adjacent normal epithelium. *Patients deemed 'High' or 'Low' for CD8 T cells are shaded blue and red, respectively. Cox hazard ratio is univariate. The 'Low' group is used as the reference group on cox regression modelling.*

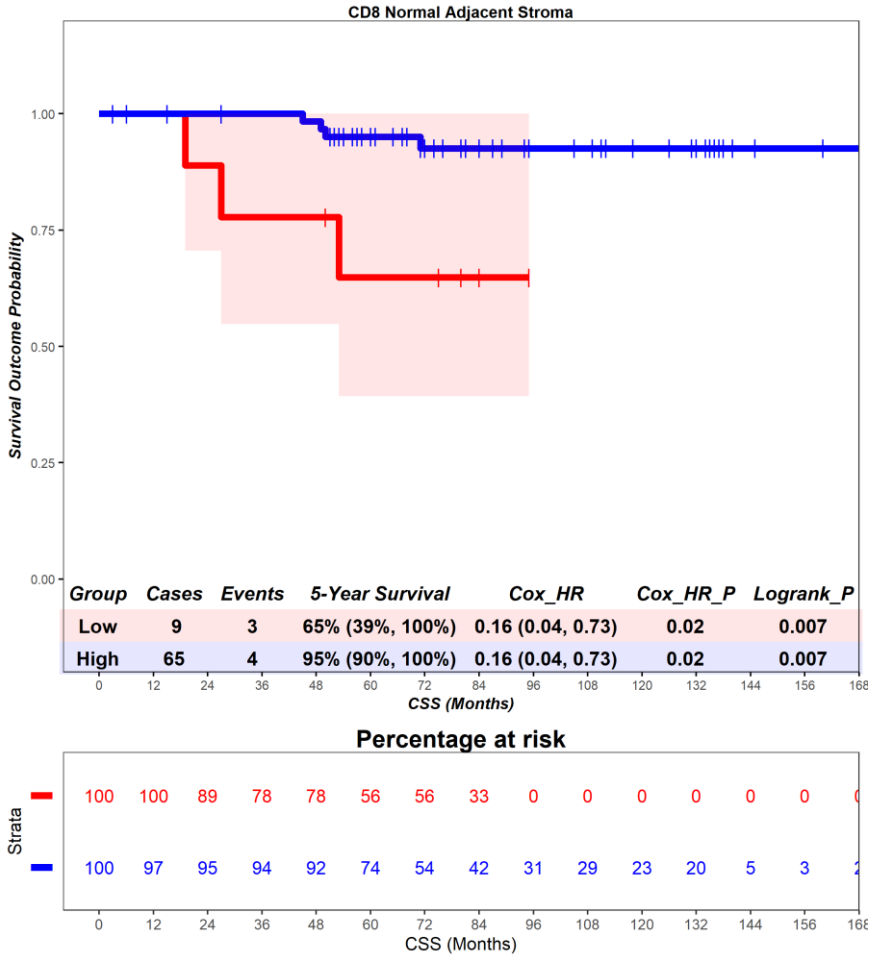

Figure S74 – Time-to-event (cancer-specific survival) analysis for CD8 T cells in the adjacent normal stroma. *Patients deemed 'High' or 'Low' for CD8 T cells are shaded blue and red, respectively. Cox hazard ratio is univariate. The 'Low' group is used as the reference group on cox regression modelling.*

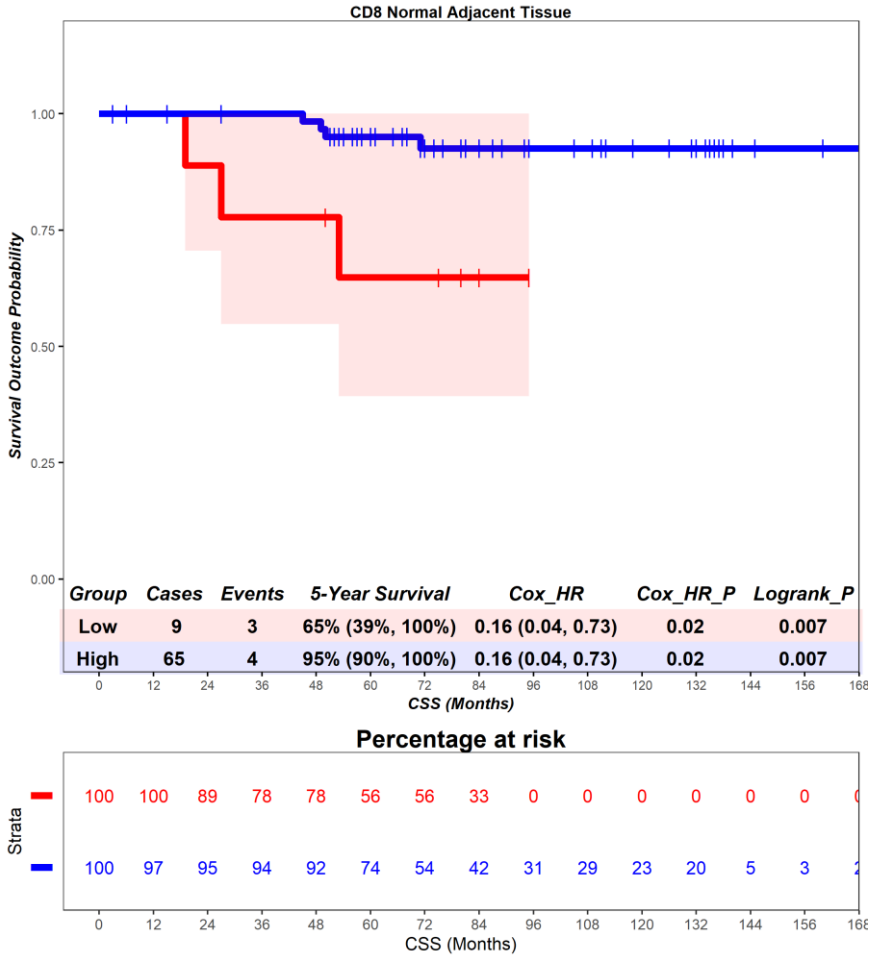

Figure S75 – Time-to-event (cancer-specific survival) analysis for CD8 T cells in the adjacent normal tissue. *Patients deemed 'High' or 'Low' for CD8 T cells are shaded blue and red, respectively. Cox hazard ratio is univariate. The 'Low' group is used as the reference group on cox regression modelling.*

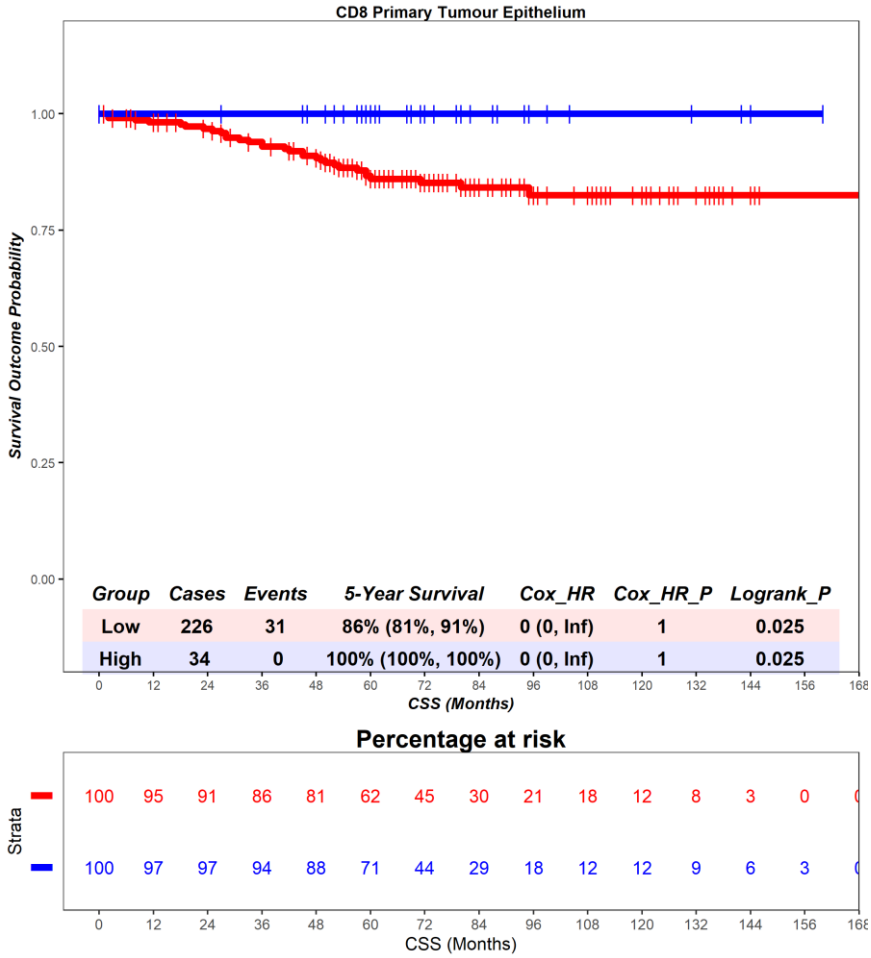

Figure S76 – Time-to-event (cancer-specific survival) analysis for CD8 T cells in the primary tumour epithelium. *Patients deemed 'High' or 'Low' for CD8 T cells are shaded blue and red, respectively. Cox hazard ratio is univariate. The 'Low' group is used as the reference group on cox regression modelling.*

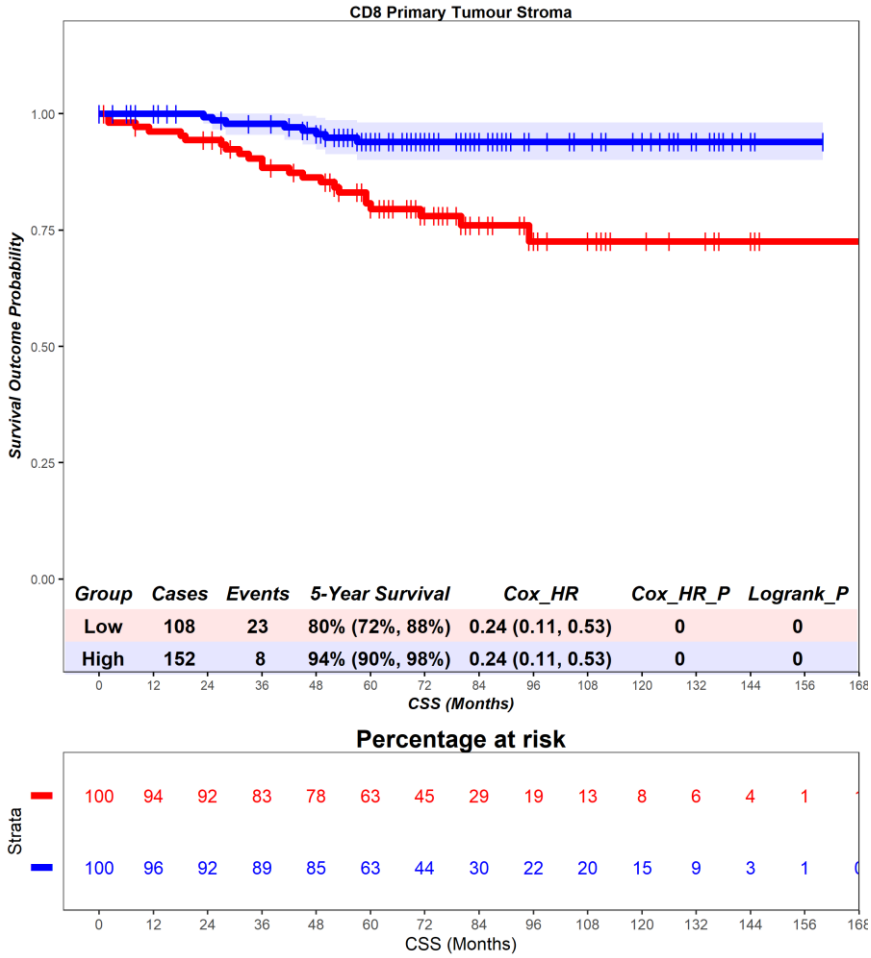

Figure S77 – Time-to-event (cancer-specific survival) analysis for CD8 T cells in the primary tumour stroma. *Patients deemed 'High' or 'Low' for CD8 T cells are shaded blue and red, respectively. Cox hazard ratio is univariate. The 'Low' group is used as the reference group on cox regression modelling.*

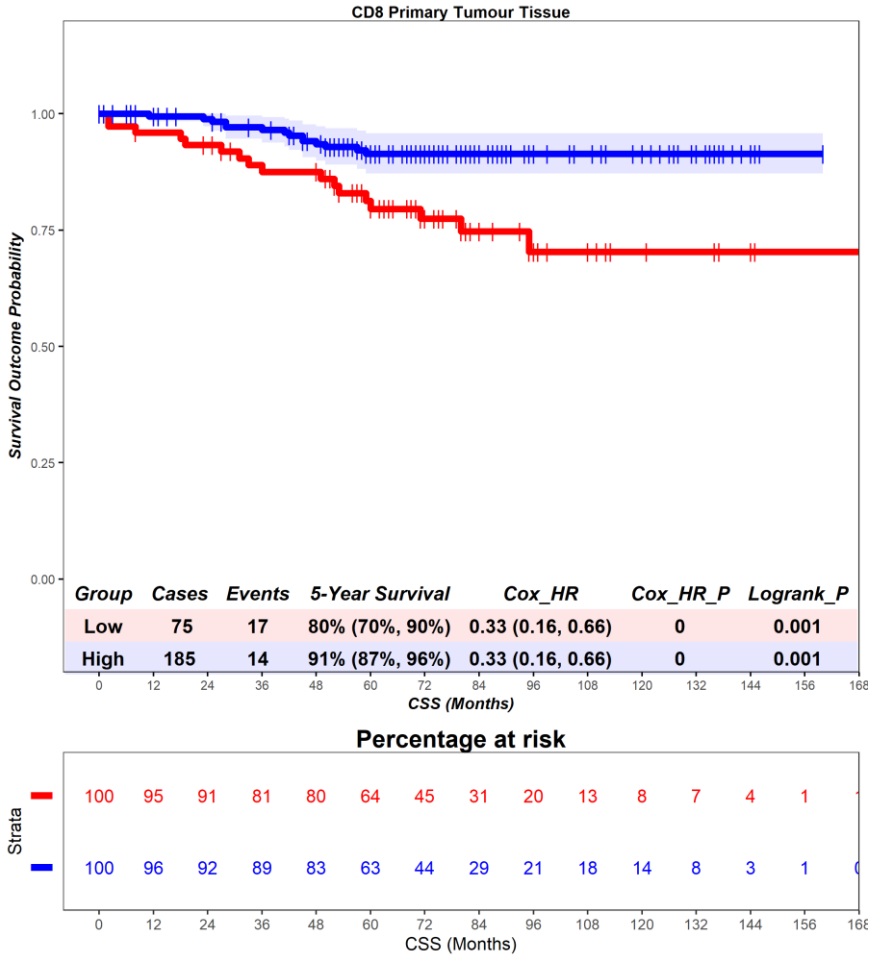

Figure S78 – Time-to-event (cancer-specific survival) analysis for CD8 T cells in the primary tumour tissue. *Patients deemed 'High' or 'Low' for CD8 T cells are shaded blue and red, respectively. Cox hazard ratio is univariate. The 'Low' group is used as the reference group on cox regression modelling.*

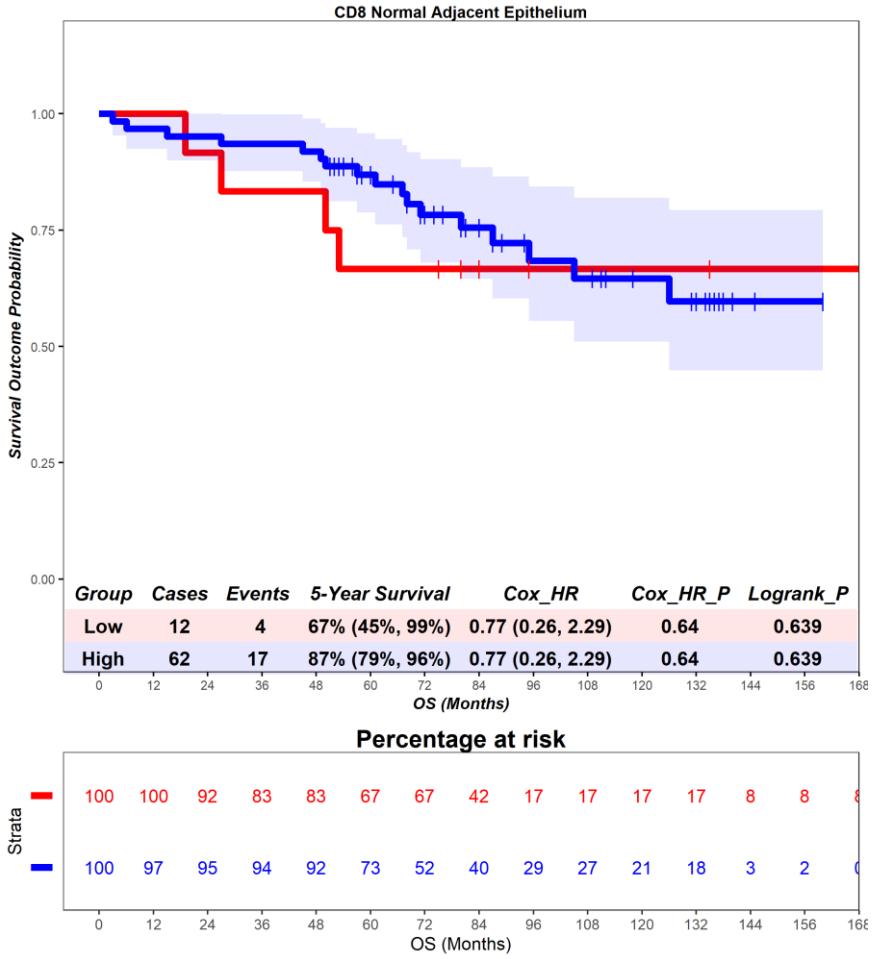

Figure S79 – Time-to-event (overall survival) analysis for CD8 T cells in the healthy tissue epithelium. *Patients deemed 'High' or 'Low' for CD8 T cells are shaded blue and red, respectively. Cox hazard ratio is univariate. The 'Low' group is used as the reference group on cox regression modelling.*

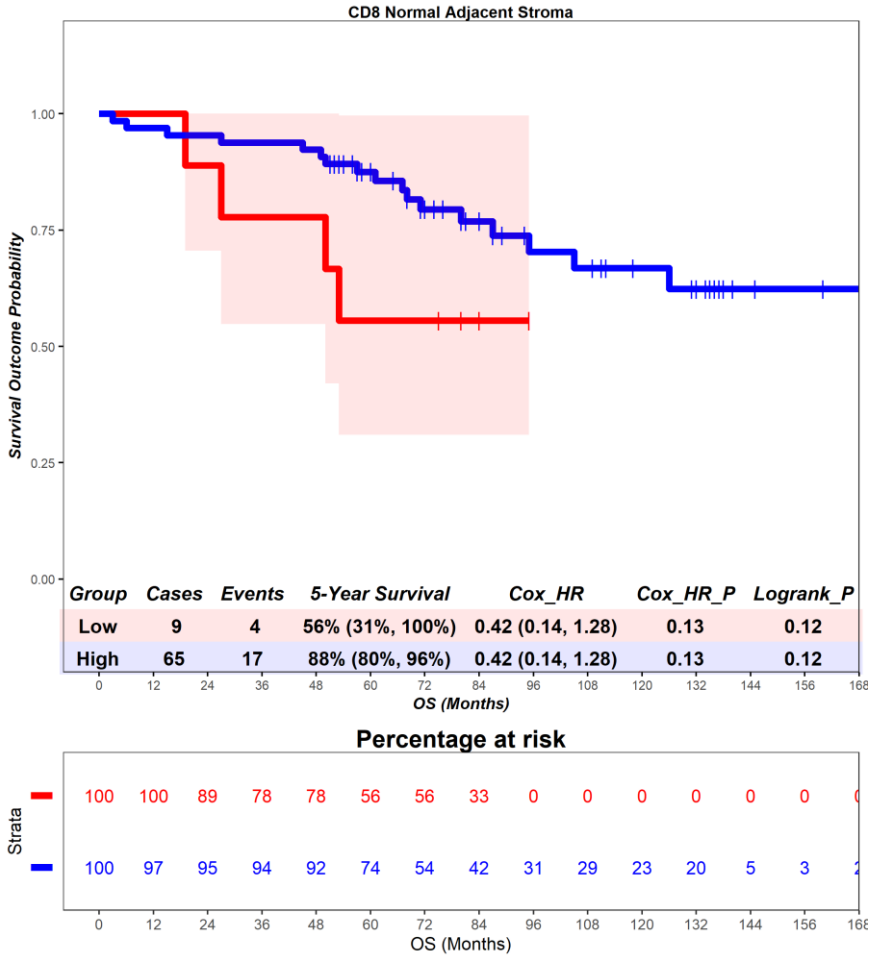

Figure S80 – Time-to-event (overall survival) analysis for CD8 T cells in the healthy tissue stroma. *Patients deemed 'High' or 'Low' for CD8 T cells are shaded blue and red, respectively. Cox hazard ratio is univariate. The 'Low' group is used as the reference group on cox regression modelling.*

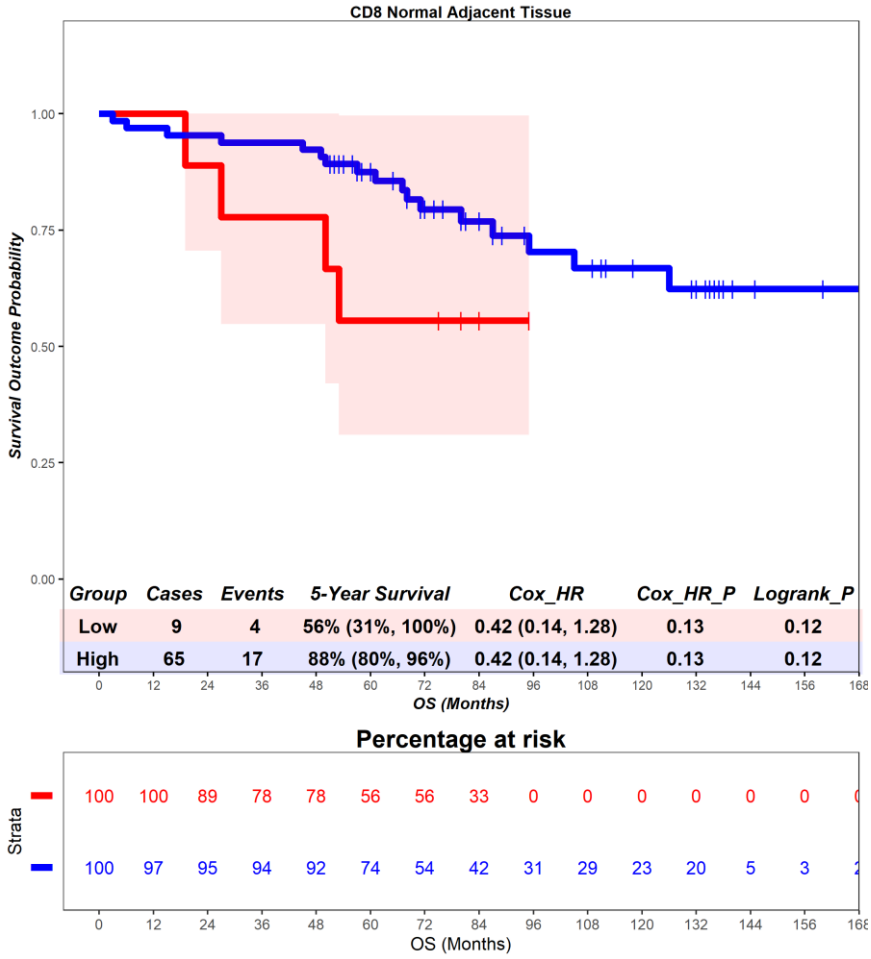

Figure S81 – Time-to-event (overall survival) analysis for CD8 T cells in the healthy tissue tissue. *Patients deemed 'High' or 'Low' for CD8 T cells are shaded blue and red, respectively. Cox hazard ratio is univariate. The 'Low' group is used as the reference group on cox regression modelling.*

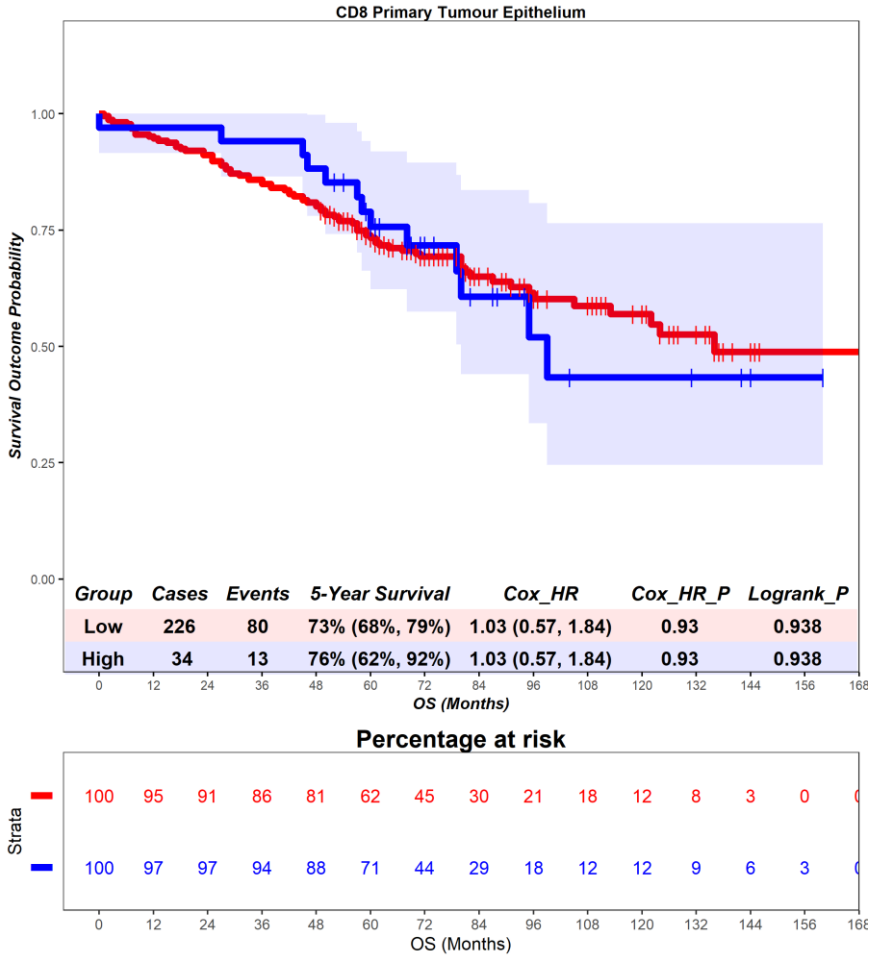

Figure S82 – Time-to-event (overall survival) analysis for CD8 T cells in the primary tumour epithelium. *Patients deemed 'High' or 'Low' for CD8 T cells are shaded blue and red, respectively. Cox hazard ratio is univariate. The 'Low' group is used as the reference group on cox regression modelling.*

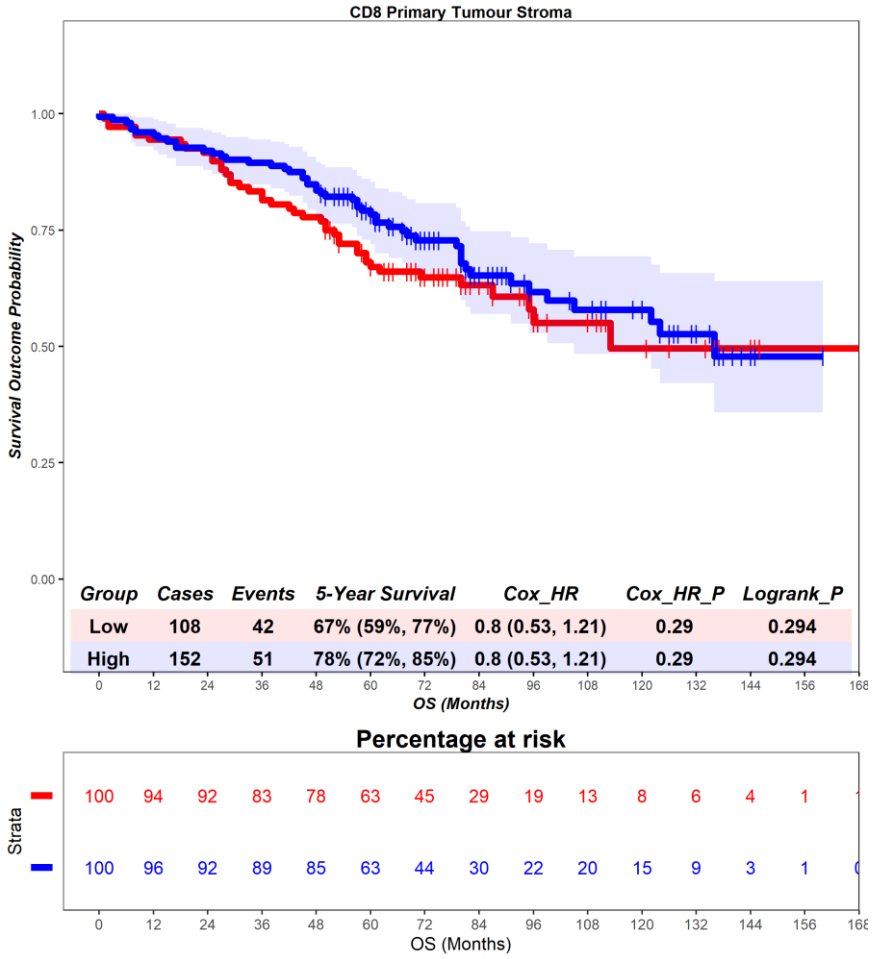

Figure S83 – Time-to-event (overall survival) analysis for CD8 T cells in the primary tumour stroma. *Patients deemed 'High' or 'Low' for CD8 T cells are shaded blue and red, respectively. Cox hazard ratio is univariate. The 'Low' group is used as the reference group on cox regression modelling.*

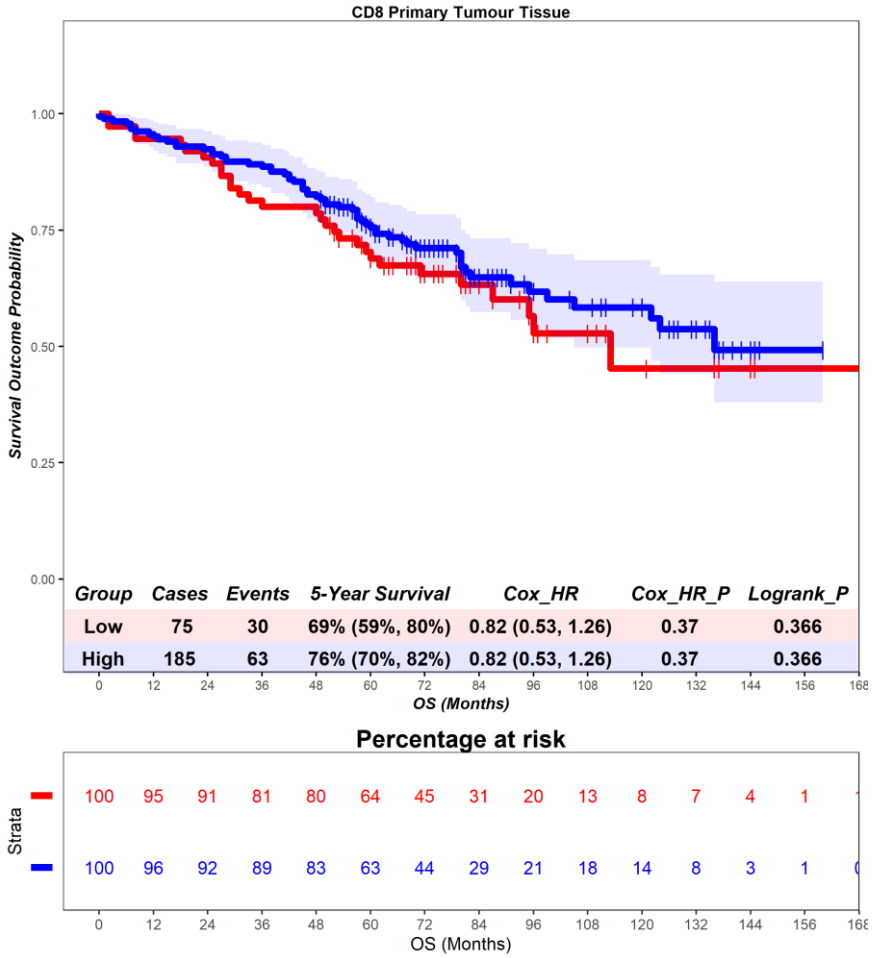

Figure S84 – Time-to-event (overall survival) analysis for CD8 T cells in the primary tumour tissue. *Patients deemed 'High' or 'Low' for CD8 T cells are shaded blue and red, respectively. Cox hazard ratio is univariate. The 'Low' group is used as the reference group on cox regression modelling.*

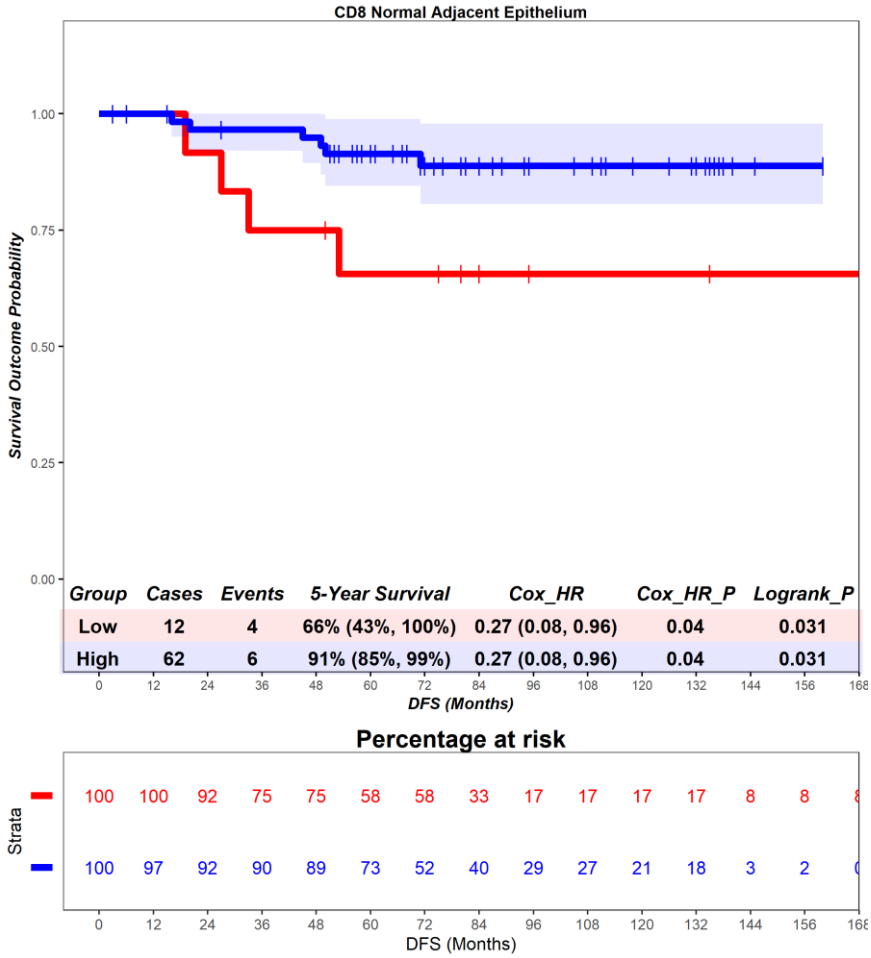

Figure S85 – Time-to-event (disease-free survival) analysis for CD8 T cells in the normal adjacent epithelium. *Patients deemed 'High' or 'Low' for CD8 T cells are shaded blue and red, respectively. Cox hazard ratio is univariate. The 'Low' group is used as the reference group on cox regression modelling.*

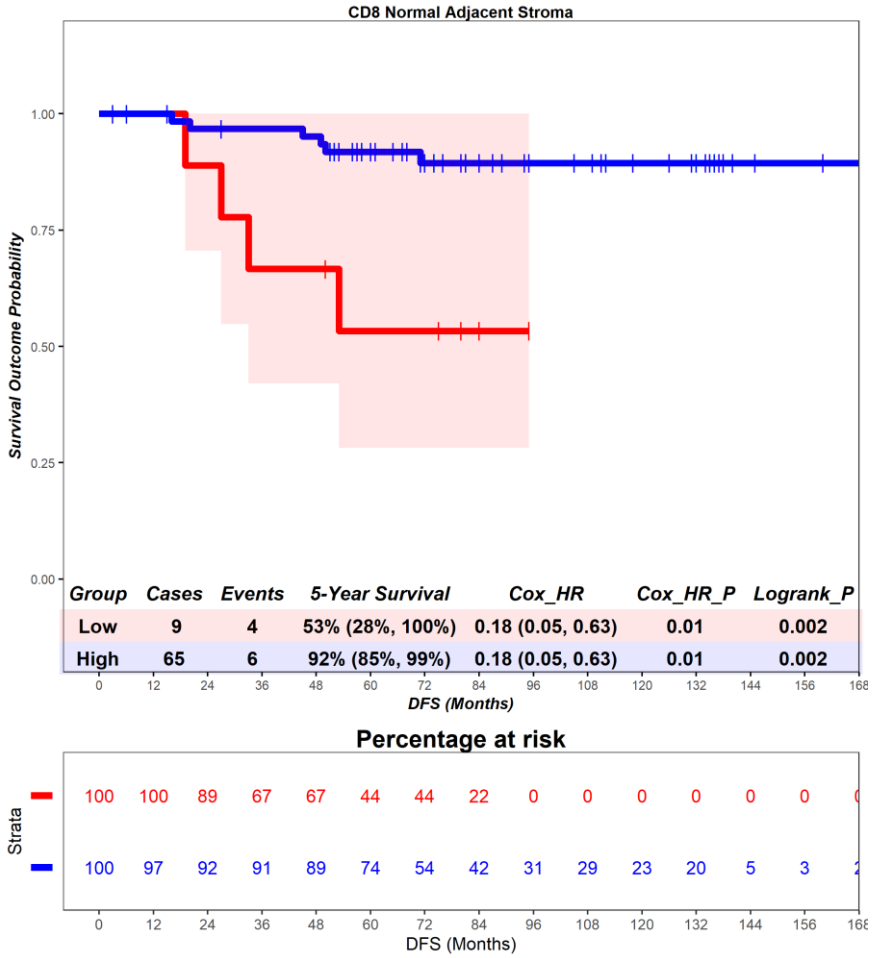

Figure S86 – Time-to-event (disease-free survival) analysis for CD8 T cells in the normal adjacent stroma. *Patients deemed 'High' or 'Low' for CD8 T cells are shaded blue and red, respectively. Cox hazard ratio is univariate. The 'Low' group is used as the reference group on cox regression modelling.*

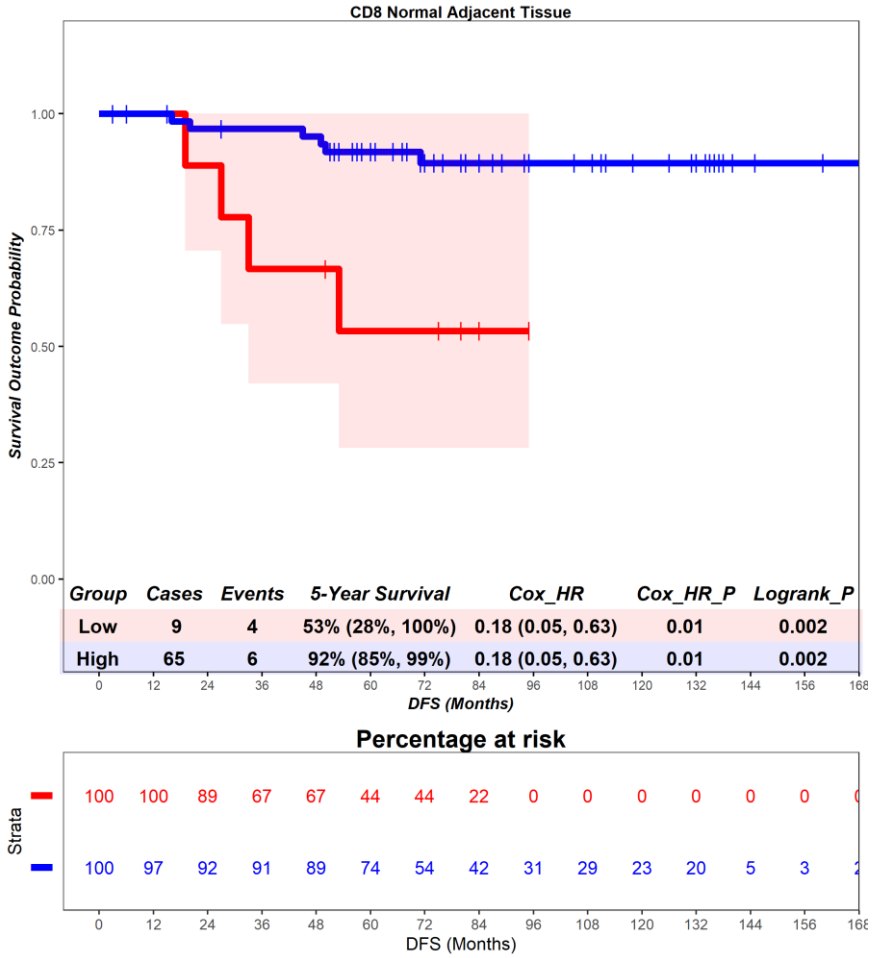

Figure S87 – Time-to-event (disease-free survival) analysis for CD8 T cells in the normal adjacent tissue. *Patients deemed 'High' or 'Low' for CD8 T cells are shaded blue and red, respectively. Cox hazard ratio is univariate. The 'Low' group is used as the reference group on cox regression modelling.*

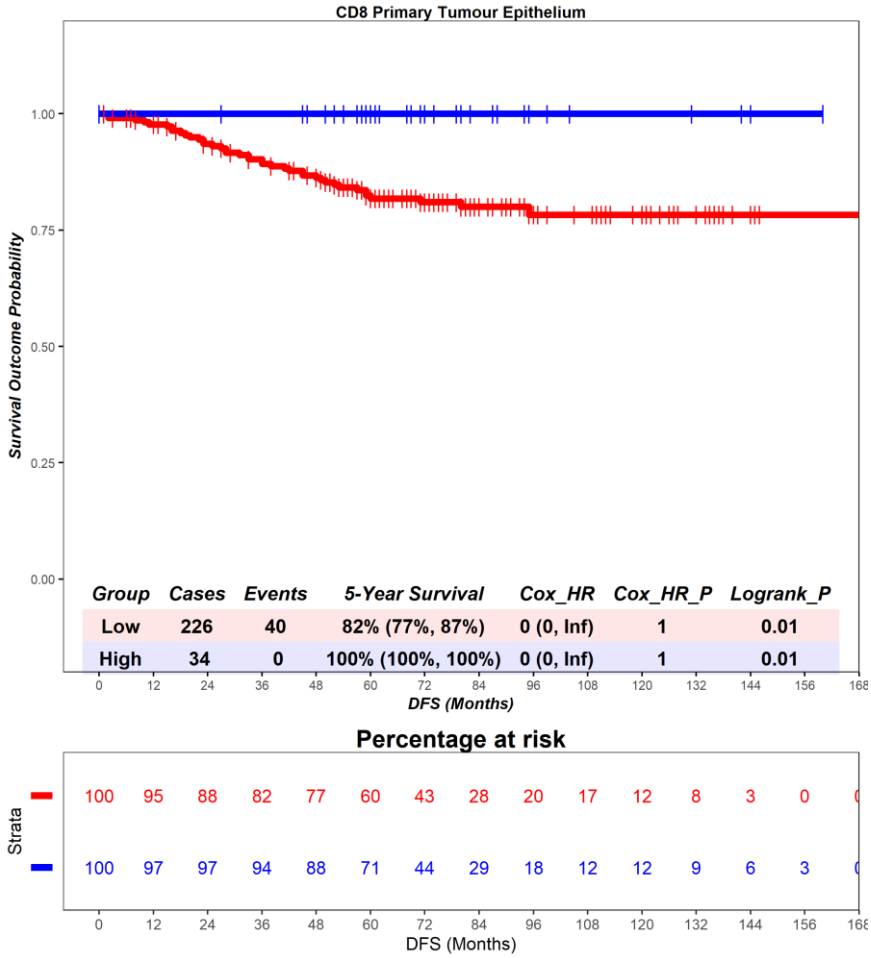

Figure S88 – Time-to-event (disease-free survival) analysis for CD8 T cells in the primary tumour epithelium*. Patients deemed 'High' or 'Low' for CD8 T cells are shaded blue and red, respectively. Cox hazard ratio is univariate. The 'Low' group is used as the reference group on cox regression modelling.*

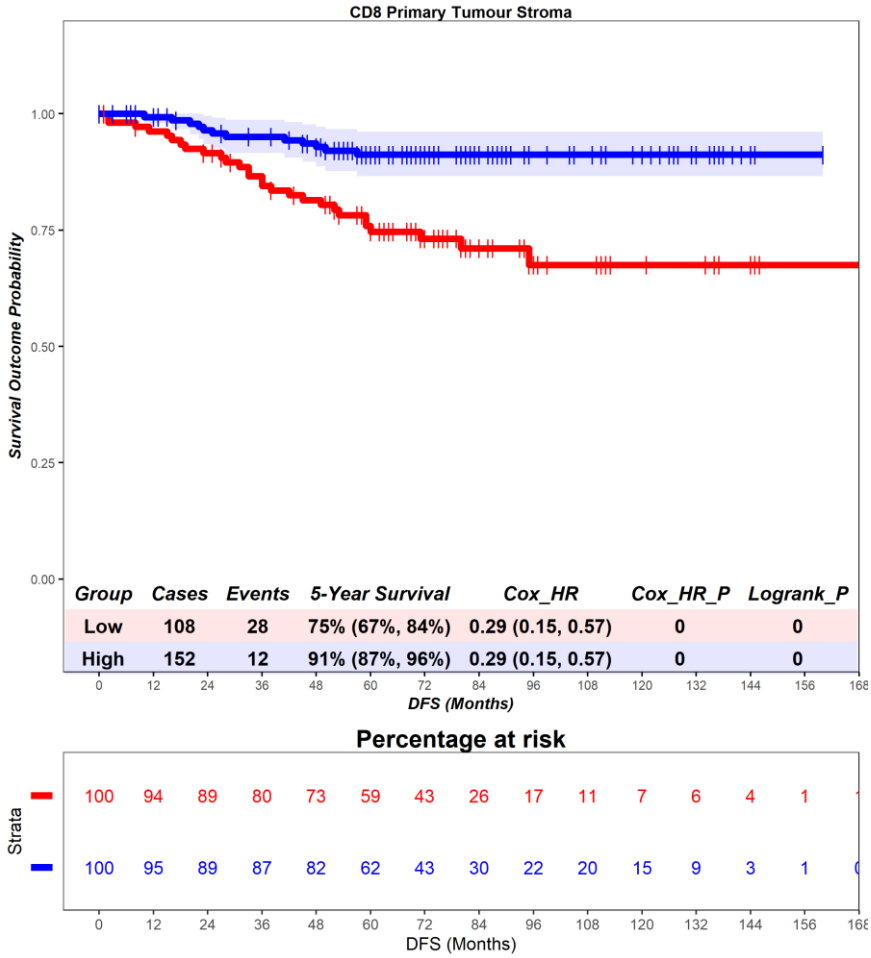

Figure S89 – Time-to-event (disease-free survival) analysis for CD8 T cells in the primary tumour stroma. *Patients deemed 'High' or 'Low' for CD8 T cells are shaded blue and red, respectively. Cox hazard ratio is univariate. The 'Low' group is used as the reference group on cox regression modelling.*

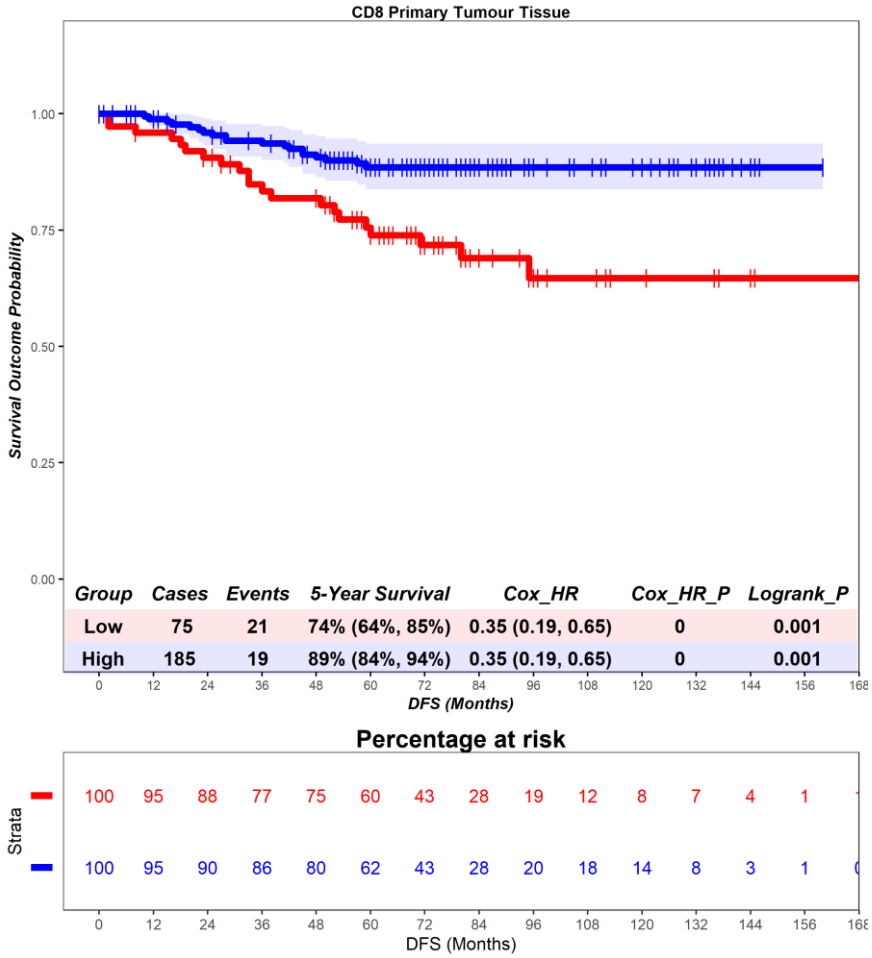

Figure S90 – Time-to-event (disease-free survival) analysis for CD8 T cells in the primary tumour tissue. *Patients deemed 'High' or 'Low' for CD8 T cells are shaded blue and red, respectively. Cox hazard ratio is univariate. The 'Low' group is used as the reference group on cox regression modelling.*

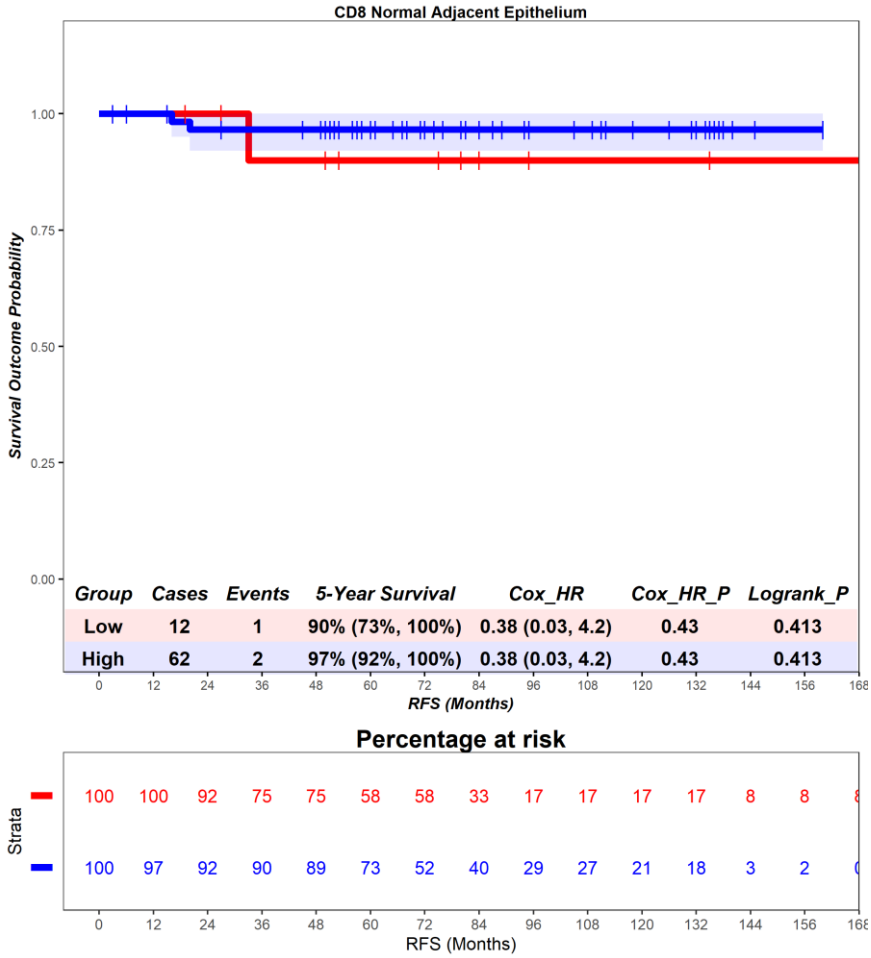

Figure S91 – Time-to-event (recurrence-free survival) analysis for CD8 T cells in the normal adjacent epithelium. *Patients deemed 'High' or 'Low' for CD8 T cells are shaded blue and red, respectively. Cox hazard ratio is univariate. The 'Low' group is used as the reference group on cox regression modelling.*

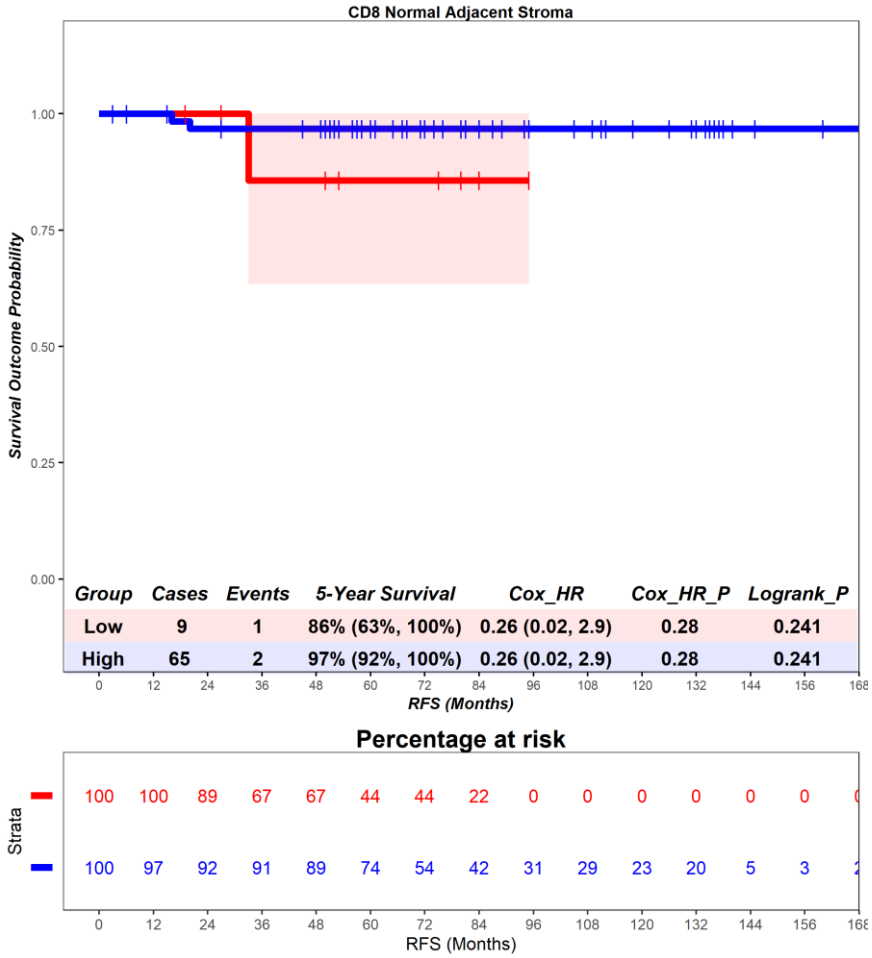

Figure S92 – Time-to-event (recurrence-free survival) analysis for CD8 T cells in the normal adjacent stroma. *Patients deemed 'High' or 'Low' for CD8 T cells are shaded blue and red, respectively. Cox hazard ratio is univariate. The 'Low' group is used as the reference group on cox regression modelling.*

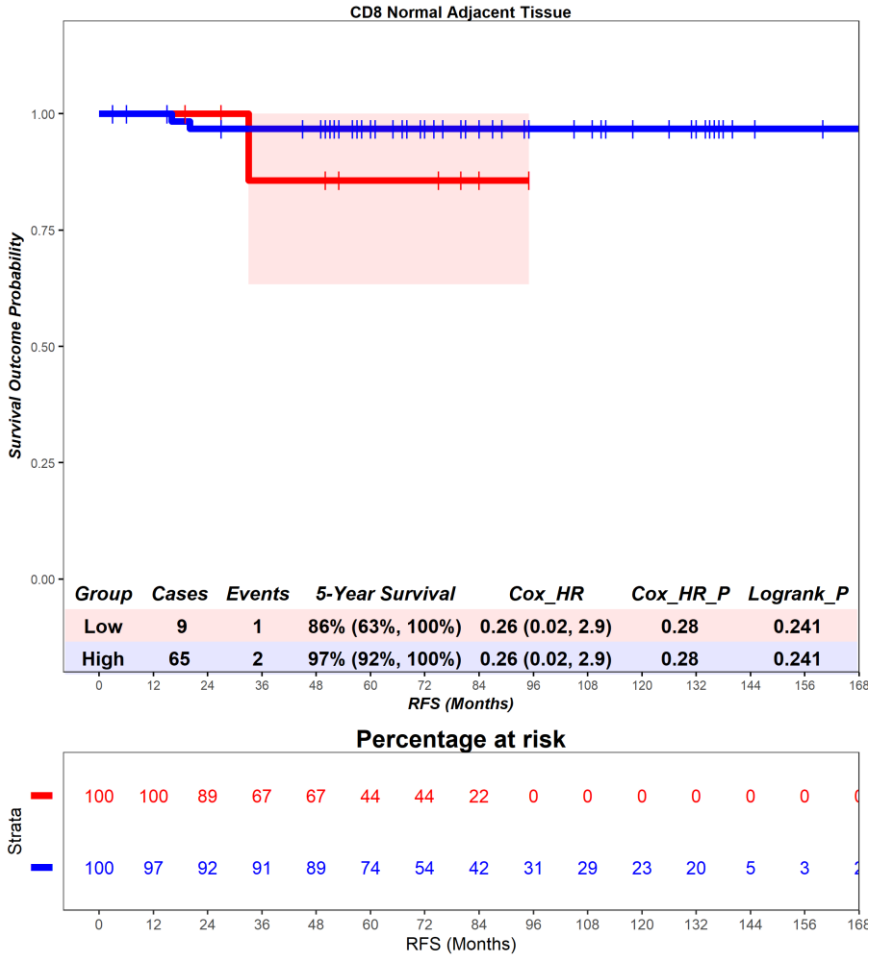

Figure S94 – Time-to-event (recurrence-free survival) analysis for CD8 T cells in the normal adjacent tissue. *Patients deemed 'High' or 'Low' for CD8 T cells are shaded blue and red, respectively. Cox hazard ratio is univariate. The 'Low' group is used as the reference group on cox regression modelling.*

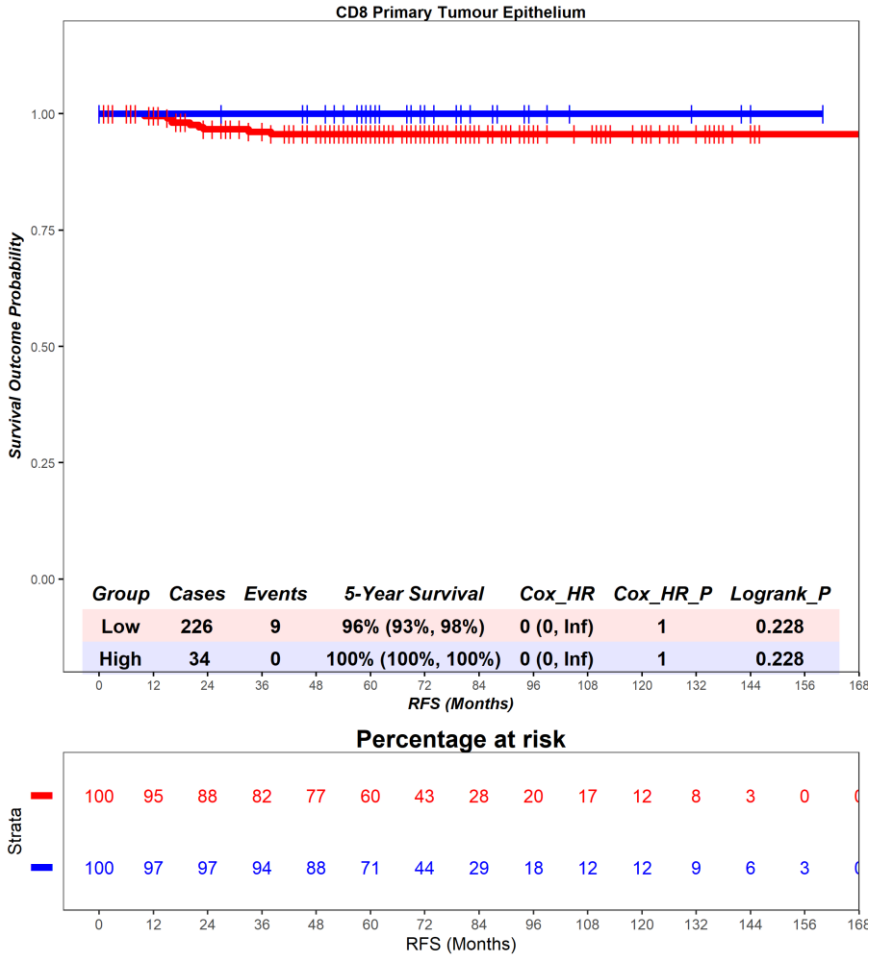

Figure S95 – Time-to-event (recurrence-free survival) analysis for CD8 T cells in the primary tumour epithelium. *Patients deemed 'High' or 'Low' for CD8 T cells are shaded blue and red, respectively. Cox hazard ratio is univariate. The 'Low' group is used as the reference group on cox regression modelling.*

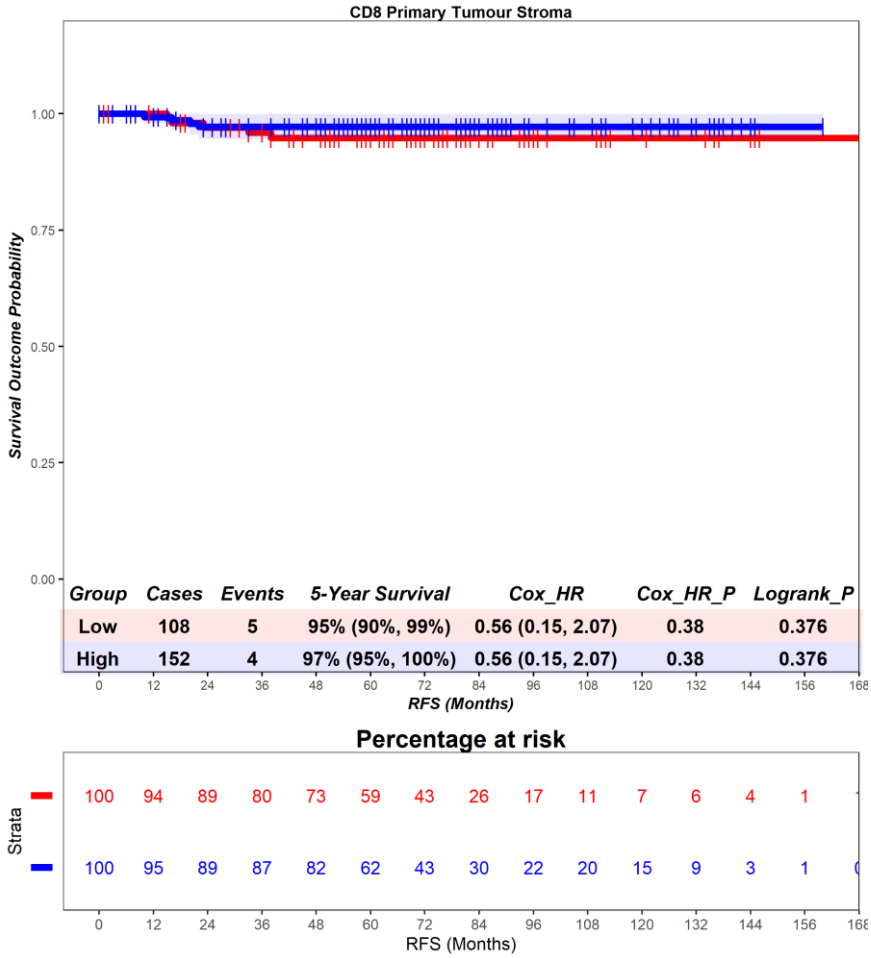

Figure S96 – Time-to-event (recurrence-free survival) analysis for CD8 T cells in the primary tumour stroma. *Patients deemed 'High' or 'Low' for CD8 T cells are shaded blue and red, respectively. Cox hazard ratio is univariate. The 'Low' group is used as the reference group on cox regression modelling.*

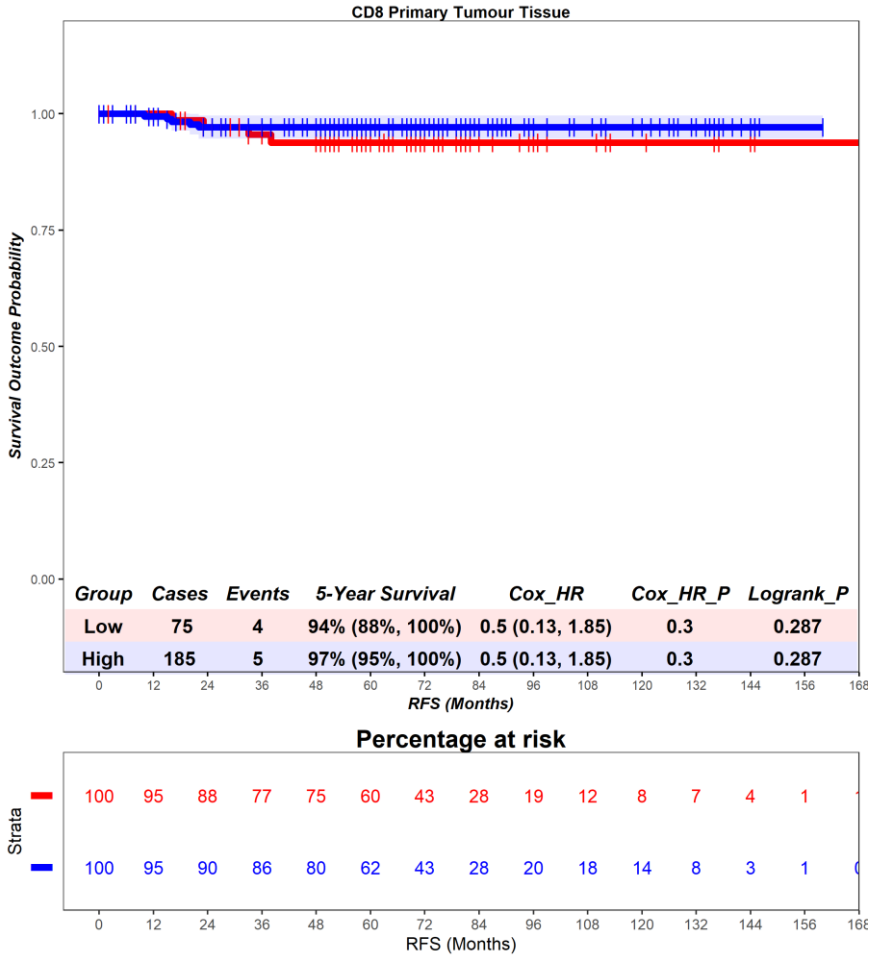

Figure S97 – Time-to-event (recurrence-free survival) analysis for CD8 T cells in the primary tumour tissue. *Patients deemed 'High' or 'Low' for CD8 T cells are shaded blue and red, respectively. Cox hazard ratio is univariate. The 'Low' group is used as the reference group on cox regression modelling.*

4.4 – Time-to-event analysis by cutpoints generated from Norway data – Thailand

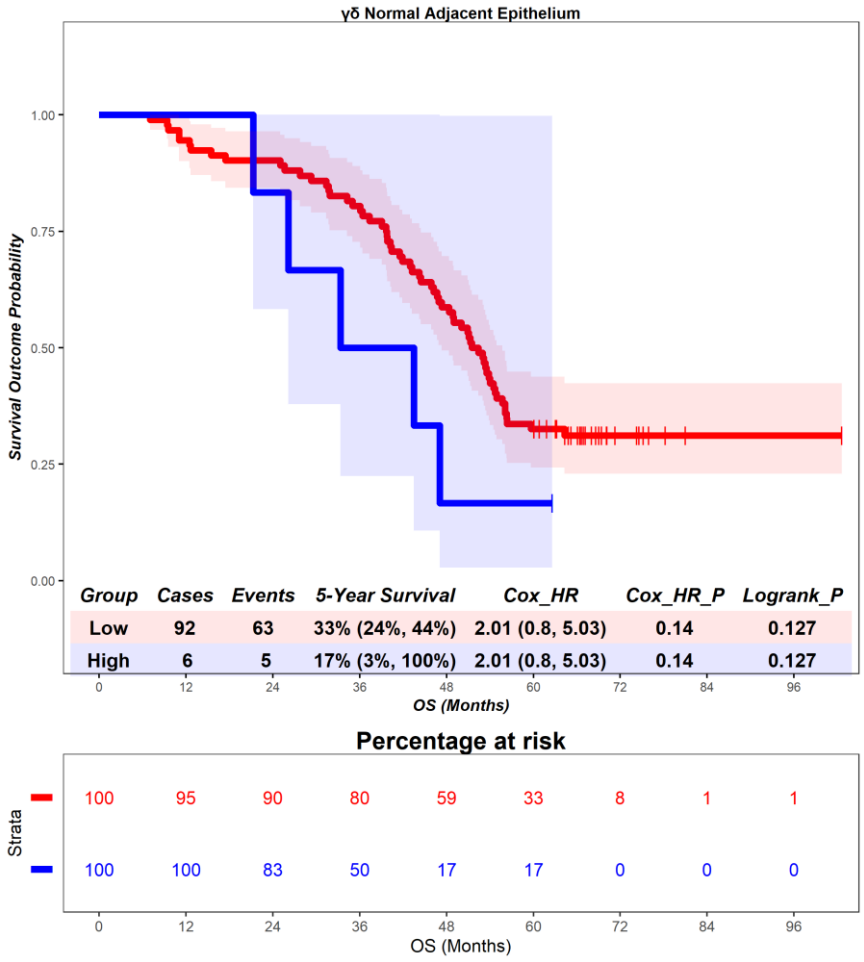

Figure S98 – Time-to-event (overall survival) analysis for γδ T cells in the normal adjacent epithelium. *Patients deemed 'High' or 'Low' for γδ T cells are shaded blue and red, respectively. Cox hazard ratio is univariate. The 'Low' group is used as the reference group on cox regression modelling.*

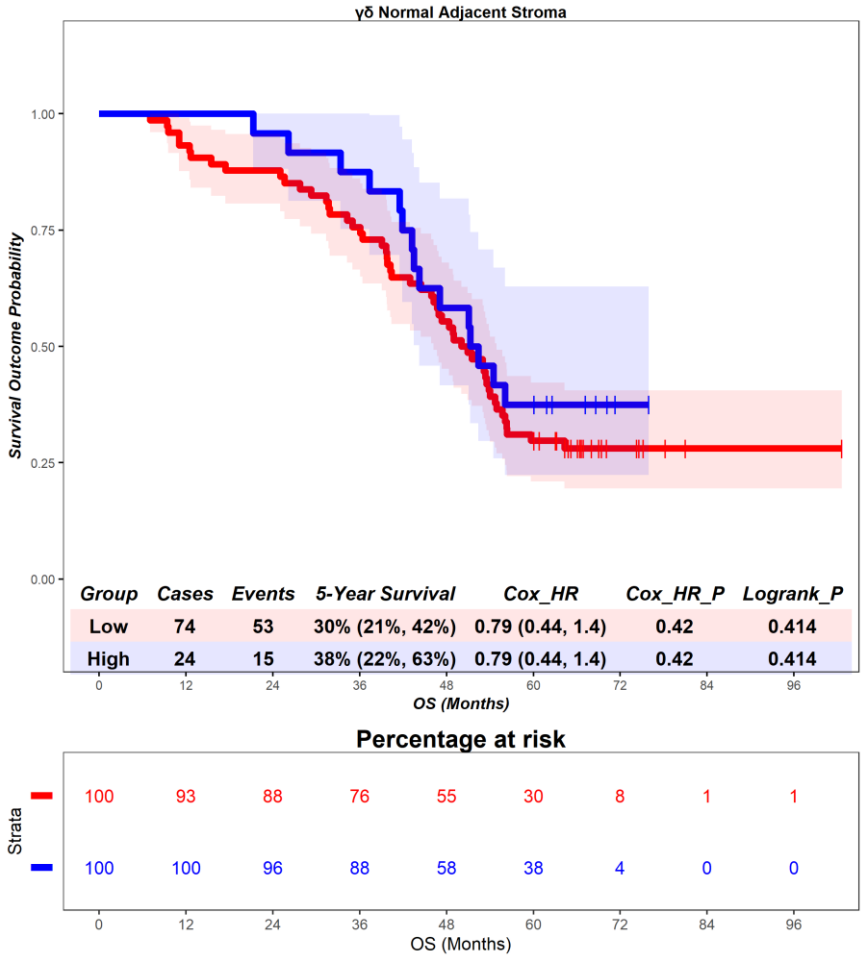

Figure S99 – Time-to-event (overall survival) analysis for γδ T cells in the normal adjacent stroma. *Patients deemed 'High' or 'Low' for γδ T cells are shaded blue and red, respectively. Cox hazard ratio is univariate. The 'Low' group is used as the reference group on cox regression modelling.*

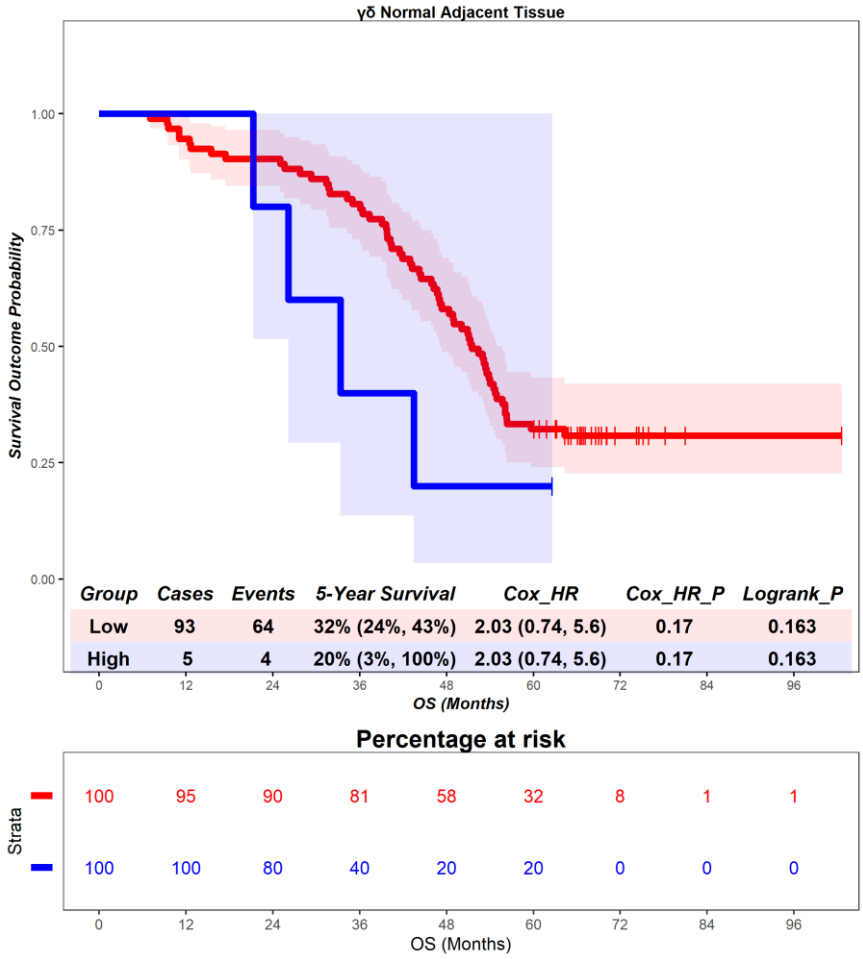

Figure S100 – Time-to-event (overall survival) analysis for γδ T cells in the normal adjacent tissue. *Patients deemed 'High' or 'Low' for γδ T cells are shaded blue and red, respectively. Cox hazard ratio is univariate. The 'Low' group is used as the reference group on cox regression modelling.*

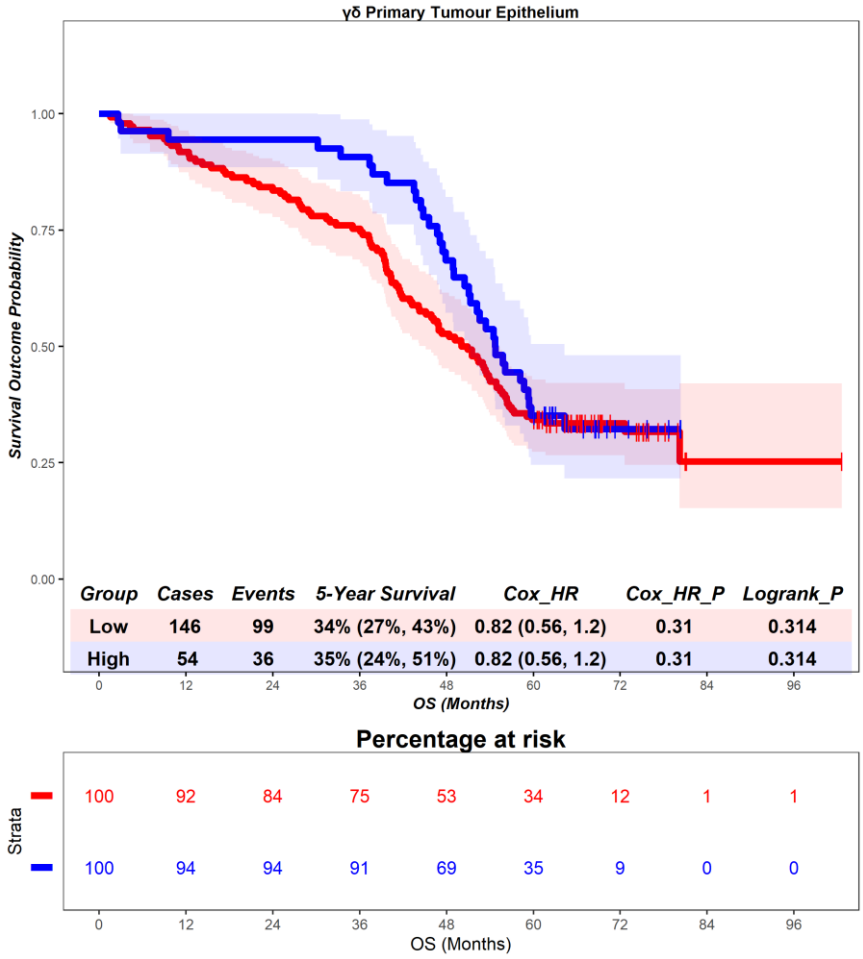

Figure S101 – Time-to-event (overall survival) analysis for γδ T cells in the primary tumour epithelium. *Patients deemed 'High' or 'Low' for γδ T cells are shaded blue and red, respectively. Cox hazard ratio is univariate. The 'Low' group is used as the reference group on cox regression modelling.*

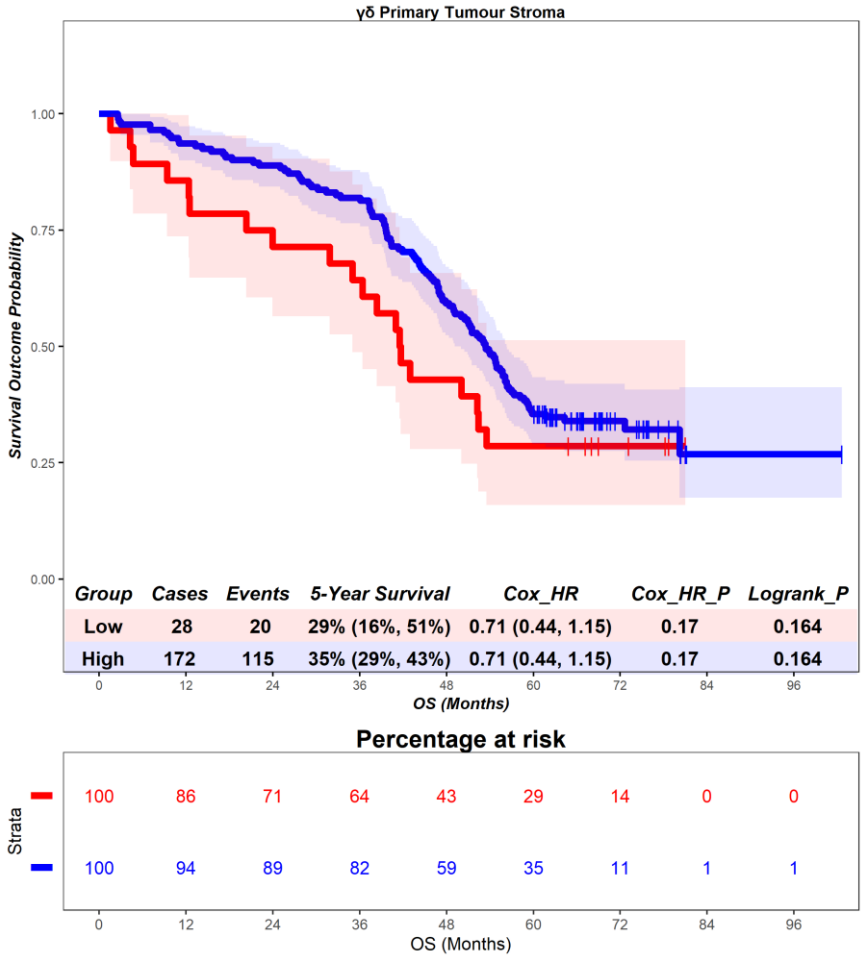

Figure S102 – Time-to-event (overall survival) analysis for γδ T cells in the primary tumour stroma. *Patients deemed 'High' or 'Low' for γδ T cells are shaded blue and red, respectively. Cox hazard ratio is univariate. The 'Low' group is used as the reference group on cox regression modelling.*

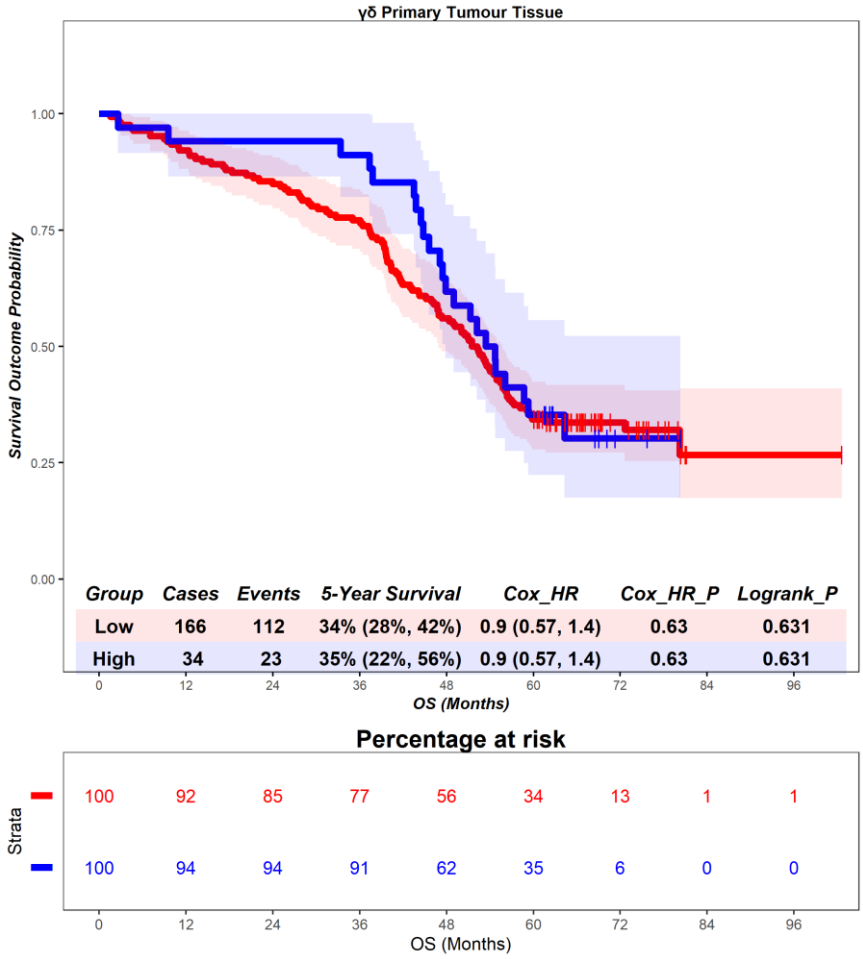

Figure S103 – Time-to-event (overall survival) analysis for γδ T cells in the primary tumour tissue. *Patients deemed 'High' or 'Low' for γδ T cells are shaded blue and red, respectively. Cox hazard ratio is univariate. The 'Low' group is used as the reference group on cox regression modelling.*

References

1. Parkin, D.M., et al., *Global cancer statistics, 2002.* CA Cancer J Clin, 2005. **55**(2): p. 74-108.
2. Sung, H., et al., *Global Cancer Statistics 2020: GLOBOCAN Estimates of Incidence and Mortality Worldwide for 36 Cancers in 185 Countries.* CA: A Cancer Journal for Clinicians, 2021. **71**(3): p. 209-249.
3. Bray, F., et al., *Global cancer statistics 2018: GLOBOCAN estimates of incidence and mortality worldwide for 36 cancers in 185 countries.* CA Cancer J Clin, 2018. **68**(6): p. 394-424.
4. Li, J., et al., *TNM Staging of Colorectal Cancer Should be Reconsidered According to Weighting of the T Stage: Verification Based on a 25-Year Follow-Up.* Medicine, 2016. **95**(6): p. e2711-e2711.
5. Tong, G.-J., et al., *Comparison of the eighth version of the American Joint Committee on Cancer manual to the seventh version for colorectal cancer: A retrospective review of our data.* World journal of clinical oncology, 2018. **9**(7): p. 148-161.
6. Guinney, J., et al., *The consensus molecular subtypes of colorectal cancer.* Nat Med, 2015. **21**(11): p. 1350-6.
7. Isella, C., et al., *Selective analysis of cancer-cell intrinsic transcriptional traits defines novel clinically relevant subtypes of colorectal cancer.* Nature Communications, 2017. **8**(1): p. 15107.
8. Galon, J., et al., *Type, Density, and Location of Immune Cells Within Human Colorectal Tumors Predict Clinical Outcome.* Science, 2006. **313**(5795): p. 1960-1964.
9. Galon, J., et al., *Towards the introduction of the 'Immunoscore' in the classification of malignant tumours.* The Journal of pathology, 2014. **232**(2): p. 199-209.
10. Gentles, A.J., et al., *The prognostic landscape of genes and infiltrating immune cells across human cancers.* Nature medicine, 2015. **21**(8): p. 938-945.
11. Newman, A.M., et al., *Robust enumeration of cell subsets from tissue expression profiles.* Nature methods, 2015. **12**(5): p. 453-457.
12. Fidler, M.M., I. Soerjomataram, and F. Bray, *A global view on cancer incidence and national levels of the human development index.* Int J Cancer, 2016. **139**(11): p. 2436-46.
13. Center, M.M., et al., *Worldwide variations in colorectal cancer.* CA Cancer J Clin, 2009. **59**(6): p. 366-78.
14. Johnson, C.M., et al., *Meta-analyses of colorectal cancer risk factors.* Cancer Causes Control, 2013. **24**(6): p. 1207-22.
15. Hawkins, N., et al., *CpG island methylation in sporadic colorectal cancers and its relationship to microsatellite instability.* Gastroenterology, 2002. **122**(5): p. 1376-87.
16. Park, S.J., et al., *Frequent CpG island methylation in serrated adenomas of the colorectum.* (0002-9440 (Print)).
17. Lichtenstein, P., et al., *Environmental and heritable factors in the causation of cancer--analyses of cohorts of twins from Sweden, Denmark, and Finland.* N Engl J Med, 2000. **343**(2): p. 78-85.
18. Salovaara, R., et al., *Population-based molecular detection of hereditary nonpolyposis colorectal cancer.* J Clin Oncol, 2000. **18**(11): p. 2193-200.
19. Lynch, H.T. and A. de la Chapelle, *Genetic susceptibility to non-polyposis colorectal cancer.* J Med Genet, 1999. **36**(11): p. 801-18.
20. Lynch, H.T., et al., *Hereditary factors in cancer. Study of two large midwestern kindreds.* Arch Intern Med, 1966. **117**(2): p. 206-12.
21. Boland, C.R. and F.J. Troncale, *Familial colonic cancer without antecedent polyposis.* Ann Intern Med, 1984. **100**(5): p. 700-1.
22. Ligtenberg, M.J., et al., *Heritable somatic methylation and inactivation of MSH2 in families with Lynch syndrome due to deletion of the 3' exons of TACSTD1.* Nat Genet, 2009. **41**(1): p. 112-7.
23. Fishel, R., et al., *The human mutator gene homolog MSH2 and its association with hereditary nonpolyposis colon cancer.* Cell, 1993. **75**(5): p. 1027-38.
24. Leach, F.S., et al., *Mutations of a mutS homolog in hereditary nonpolyposis colorectal cancer.* Cell, 1993. **75**(6): p. 1215-25.
25. Miyaki, M., et al., *Higher frequency of Smad4 gene mutation in human colorectal cancer with distant metastasis.* Oncogene, 1999. **18**(20): p. 3098-3103.
26. Akiyama, Y., et al., *Germ-line mutation of the hMSH6/GTBP gene in an atypical hereditary nonpolyposis colorectal cancer kindred.* Cancer Res, 1997. **57**(18): p. 3920-3.
27. Peltomäki, P. and H. Vasen, *Mutations associated with HNPCC predisposition -- Update of ICG-HNPCC/INSiGHT mutation database.* Dis Markers, 2004. **20**(4-5): p. 269-76.
28. Barnetson, R.A., et al., *Identification and survival of carriers of mutations in DNA mismatch-repair genes in colon cancer.* N Engl J Med, 2006. **354**(26): p. 2751-63.
29. Bronner, C.E., et al., *Mutation in the DNA mismatch repair gene homologue hMLH1 is associated with hereditary non-polyposis colon cancer.* Nature, 1994. **368**(6468): p. 258-61.
30. Ten Broeke, S.W., et al., *Cancer Risks for PMS2-Associated Lynch Syndrome.* J Clin Oncol, 2018. **36**(29): p. 2961-2968.

31. Beggs, A.D., et al., *Peutz-Jeghers syndrome: a systematic review and recommendations for management.* Gut, 2010. **59**(7): p. 975-86.
32. Talseth-Palmer, B.A., *The genetic basis of colonic adenomatous polyposis syndromes.* Hered Cancer Clin Pract, 2017. **15**: p. 5.
33. Sansom, O.J., et al., *Loss of Apc in vivo immediately perturbs Wnt signaling, differentiation, and migration.* (0890-9369 (Print)).
34. Morin, P.J., et al., *Activation of β-Catenin-Tcf Signaling in Colon Cancer by Mutations in β-Catenin or APC.* Science, 1997. **275**(5307): p. 1787-1790.
35. Bos, J.L., et al., *Prevalence of ras gene mutations in human colorectal cancers.* Nature, 1987. **327**(6120): p. 293-7.
36. Fearon, E.R., et al., *Identification of a chromosome 18q gene that is altered in colorectal cancers.* Science, 1990. **247**(4938): p. 49-56.
37. Naguib, A., et al., *Alterations in PTEN and PIK3CA in colorectal cancers in the EPIC Norfolk study: associations with clinicopathological and dietary factors.* BMC Cancer, 2011. **11**(1): p. 123.
38. Kandoth, C., et al., *Mutational landscape and significance across 12 major cancer types.* Nature, 2013. **502**(7471): p. 333-339.
39. Iino, H., et al., *DNA microsatellite instability and mismatch repair protein loss in adenomas presenting in hereditary non-polyposis colorectal cancer.* Gut, 2000. **47**(1): p. 37-42.
40. Fearon, E.R. and B. Vogelstein, *A genetic model for colorectal tumorigenesis.* Cell, 1990. **61**(5): p. 759-67.
41. Boland, C.R. and A. Goel, *Microsatellite instability in colorectal cancer.* Gastroenterology, 2010. **138**(6): p. 2073-2087.e3.
42. Zhang, L., et al., *Immune Landscape of Colorectal Cancer Tumor Microenvironment from Different Primary Tumor Location.* Frontiers in immunology, 2018. **9**: p. 1578-1578.
43. Glebov, O.K., et al., *Distinguishing Right from Left Colon by the Pattern of Gene Expression1.* Cancer Epidemiology, Biomarkers & Prevention, 2003. **12**(8): p. 755-762.
44. Tougeron, D., et al., *Tumor-infiltrating lymphocytes in colorectal cancers with microsatellite instability are correlated with the number and spectrum of frameshift mutations.* Modern Pathology, 2009. **22**(9): p. 1186-1195.
45. Maby, P., et al., *Correlation between Density of CD8+ T-cell Infiltrate in Microsatellite Unstable Colorectal Cancers and Frameshift Mutations: A Rationale for Personalized Immunotherapy.* Cancer Research, 2015. **75**(17): p. 3446-3455.
46. Ahn, C.H., et al., *Mutational analysis of TTK gene in gastric and colorectal cancers with microsatellite instability.* (2005-9256 (Electronic)).
47. Maby, P., et al., *License to kill: microsatellite instability and immune contexture.* Oncoimmunology, 2021. **10**(1): p. 1905935.
48. Kang, S., et al., *The significance of microsatellite instability in colorectal cancer after controlling for clinicopathological factors.* Medicine (Baltimore), 2018. **97**(9): p. e0019.
49. Taieb, J., et al., *Prognosis of microsatellite instability and/or mismatch repair deficiency stage III colon cancer patients after disease recurrence following adjuvant treatment: results of an ACCENT pooled analysis of seven studies.* Ann Oncol, 2019. **30**(9): p. 1466-1471.
50. South, C.D., et al., *Immunohistochemistry staining for the mismatch repair proteins in the clinical care of patients with colorectal cancer.* Genetics in Medicine, 2009. **11**(11): p. 812-817.
51. Murphy, K.M., et al., *Comparison of the microsatellite instability analysis system and the Bethesda panel for the determination of microsatellite instability in colorectal cancers.* J Mol Diagn, 2006. **8**(3): p. 305-11.
52. Nazemalhosseini Mojarad, E., et al., *The CpG island methylator phenotype (CIMP) in colorectal cancer.* Gastroenterol Hepatol Bed Bench, 2013. **6**(3): p. 120-8.
53. Deaton, A.M. and A. Bird, *CpG islands and the regulation of transcription.* Genes Dev, 2011. **25**(10): p. 1010-22.
54. Issa, J.-P., *CpG island methylator phenotype in cancer.* Nature Reviews Cancer, 2004. **4**(12): p. 988-993.
55. Nosho, K., et al., *Comprehensive biostatistical analysis of CpG island methylator phenotype in colorectal cancer using a large population-based sample.* PLoS One, 2008. **3**(11): p. e3698.
56. van Rijnsoever, M., et al., *Characterisation of colorectal cancers showing hypermethylation at multiple CpG islands.* Gut, 2002. **51**(6): p. 797-802.
57. Curtin, K., M.L. Slattery, and W.S. Samowitz, *CpG island methylation in colorectal cancer: past, present and future.* Patholog Res Int, 2011. **2011**: p. 902674.
58. Slattery, M.L., et al., *A comparison of colon and rectal somatic DNA alterations.* Dis Colon Rectum, 2009. **52**(7): p. 1304-11.
59. Carmichael, J.C. and S. Mills, *Anatomy and Embryology of the Colon, Rectum, and Anus*, in *The ASCRS Textbook of Colon and Rectal Surgery*, S.R. Steele, et al., Editors. 2016, Springer International Publishing: Cham. p. 3-26.
60. Lobo., P.K.P.M.C.J.W.S., *Anatomy, Abdomen and Pelvis, Large Intestine*. 2021, StatPearls Publishing.

61. Kalady, M.F., et al., *BRAF Mutations in Colorectal Cancer Are Associated With Distinct Clinical Characteristics and Worse Prognosis.* Diseases of the Colon & Rectum, 2012. **55**(2).
62. James, K.R., et al., *Distinct microbial and immune niches of the human colon.* Nature Immunology, 2020. **21**(3): p. 343-353.
63. Dukes, C.E., *The classification of cancer of the rectum.* The Journal of Pathology and Bacteriology, 1932. **35**(3): p. 323-332.
64. Haq, A.I., et al., *The Dukes staging system: a cornerstone in the clinical management of colorectal cancer.* The Lancet Oncology, 2009. **10**(11): p. 1128.
65. Brierley, J.D., M.K. Gospodarowicz, and C. Wittekind, *TNM Classification of Malignant Tumours*. 2017: Wiley.
66. Oh, H.S., et al., *Differences in overall survival when colorectal cancer patients are stratified into new TNM staging strategy.* Cancer Res Treat, 2007. **39**(2): p. 61-4.
67. Blank, A., et al., *Tumor Heterogeneity in Primary Colorectal Cancer and Corresponding Metastases. Does the Apple Fall Far From the Tree?* Front Med (Lausanne), 2018. **5**: p. 234.
68. Isella, C., et al., *Stromal contribution to the colorectal cancer transcriptome.* Nat Genet, 2015. **47**(4): p. 312-9.
69. Dunne, P.D., et al., *Cancer-cell intrinsic gene expression signatures overcome intratumoural heterogeneity bias in colorectal cancer patient classification.* Nature Communications, 2017. **8**(1): p. 15657.
70. Roseweir, A.K., et al., *Colorectal cancer subtypes: Translation to routine clinical pathology.* Cancer Treat Rev, 2017. **57**: p. 1-7.
71. Roseweir, A.K., et al., *Histological phenotypic subtypes predict recurrence risk and response to adjuvant chemotherapy in patients with stage III colorectal cancer.* J Pathol Clin Res, 2020. **6**(4): p. 283-296.
72. Nakayama, G., C. Tanaka, and Y. Kodera, *Current Options for the Diagnosis, Staging and Therapeutic Management of Colorectal Cancer.* Gastrointestinal Tumors, 2014. **1**(1): p. 25-32.
73. Iveson, T., et al., *3-month versus 6-month adjuvant chemotherapy for patients with high-risk stage II and III colorectal cancer: 3-year follow-up of the SCOT non-inferiority RCT.* Health Technol Assess, 2019. **23**(64): p. 1-88.
74. Feeney, G., et al., *Neoadjuvant radiotherapy for rectal cancer management.* World J Gastroenterol, 2019. **25**(33): p. 4850-4869.
75. Cedermark, B., et al., *Improved survival with preoperative radiotherapy in resectable rectal cancer.* N Engl J Med, 1997. **336**(14): p. 980-7.
76. Minsky, B.D., *Short-Course Radiation Versus Long-Course Chemoradiation for Rectal Cancer: Making Progress.* Journal of Clinical Oncology, 2012. **30**(31): p. 3777-3778.
77. Formenti, S.C. and S. Demaria, *Systemic effects of local radiotherapy.* Lancet Oncol, 2009. **10**(7): p. 718-26.
78. Pagès, F., et al., *In situ cytotoxic and memory T cells predict outcome in patients with early-stage colorectal cancer.* J Clin Oncol, 2009. **27**(35): p. 5944-51.
79. Mlecnik, B., et al., *Histopathologic-based prognostic factors of colorectal cancers are associated with the state of the local immune reaction.* J Clin Oncol, 2011. **29**(6): p. 610-8.
80. Jiang, Y., et al., *PD-1 and PD-L1 in cancer immunotherapy: clinical implications and future considerations.* Hum Vaccin Immunother, 2019. **15**(5): p. 1111-1122.
81. Buchbinder, E.I. and A. Desai, *CTLA-4 and PD-1 Pathways: Similarities, Differences, and Implications of Their Inhibition.* Am J Clin Oncol, 2016. **39**(1): p. 98-106.
82. Makaremi, S., et al., *Immune Checkpoint Inhibitors in Colorectal Cancer: Challenges and Future Prospects.* Biomedicines, 2021. **9**(9).
83. Overman, M.J., et al., *Nivolumab in patients with metastatic DNA mismatch repair-deficient or microsatellite instability-high colorectal cancer (CheckMate 142): an open-label, multicentre, phase 2 study.* Lancet Oncol, 2017. **18**(9): p. 1182-1191.
84. Overman, M.J., et al., *Durable Clinical Benefit With Nivolumab Plus Ipilimumab in DNA Mismatch Repair–Deficient/Microsatellite Instability–High Metastatic Colorectal Cancer.* Journal of Clinical Oncology, 2018. **36**(8): p. 773-779.
85. Chen, E.X., et al., *Effect of Combined Immune Checkpoint Inhibition vs Best Supportive Care Alone in Patients With Advanced Colorectal Cancer: The Canadian Cancer Trials Group CO.26 Study.* JAMA Oncol, 2020. **6**(6): p. 831-838.
86. Hanna, C.R., et al., *Durvalumab (MEDI 4736) in combination with extended neoadjuvant regimens in rectal cancer: a study protocol of a randomised phase II trial (PRIME-RT).* Radiation Oncology, 2021. **16**(1): p. 163.
87. Haslauer, T., et al., *CAR T-Cell Therapy in Hematological Malignancies.* Int J Mol Sci, 2021. **22**(16).
88. Newick, K., et al., *CAR T Cell Therapy for Solid Tumors.* Annu Rev Med, 2017. **68**: p. 139-152.
89. Li, H., et al., *CAR-T cells for Colorectal Cancer: Target-selection and strategies for improved activity and safety.* J Cancer, 2021. **12**(6): p. 1804-1814.
90. Saura-Esteller, J., et al., *Gamma Delta T-Cell Based Cancer Immunotherapy: Past-Present-Future.* Frontiers in Immunology, 2022. **13**.

91. Morath, A. and W.W. Schamel, *αβ and γδ T cell receptors: Similar but different.* Journal of Leukocyte Biology, 2020. **107**(6): p. 1045-1055.
92. Allison, T.J. and D.N. Garboczi, *Structure of γδ T cell receptors and their recognition of non-peptide antigens.* Molecular Immunology, 2002. **38**(14): p. 1051-1061.
93. Adams, E.J., S. Gu, and A.M. Luoma, *Human gamma delta T cells: Evolution and ligand recognition.* Cell Immunol, 2015. **296**(1): p. 31-40.
94. Fichtner, A.S., S. Ravens, and I. Prinz, *Human γδ TCR Repertoires in Health and Disease.* Cells, 2020. **9**(4): p. 800.
95. Bassing, C.H., et al., *T cell receptor (TCR) alpha/delta locus enhancer identity and position are critical for the assembly of TCR delta and alpha variable region genes.* Proc Natl Acad Sci U S A, 2003. **100**(5): p. 2598-603.
96. Deusch, K., et al., *A major fraction of human intraepithelial lymphocytes simultaneously expresses the gamma/delta T cell receptor, the CD8 accessory molecule and preferentially uses the V delta 1 gene segment.* Eur J Immunol, 1991. **21**(4): p. 1053-9.
97. Tieppo, P., et al., *The human fetal thymus generates invariant effector γδ T cells.* J Exp Med, 2020. **217**(3).
98. Ribot, J.C., et al., *Human γδ thymocytes are functionally immature and differentiate into cytotoxic type 1 effector T cells upon IL-2/IL-15 signaling.* J Immunol, 2014. **192**(5): p. 2237-43.
99. Dimova, T., et al., *Effector Vγ9Vδ2 T cells dominate the human fetal γδ T-cell repertoire.* Proc Natl Acad Sci U S A, 2015. **112**(6): p. E556-65.
100. Davey, M.S., et al., *Clonal selection in the human Vδ1 T cell repertoire indicates γδ TCR-dependent adaptive immune surveillance.* Nat Commun, 2017. **8**: p. 14760.
101. Kallemeijn, M.J., et al., *Next-Generation Sequencing Analysis of the Human TCRγδ+ T-Cell Repertoire Reveals Shifts in Vγ- and Vδ-Usage in Memory Populations upon Aging.* Front Immunol, 2018. **9**: p. 448.
102. Di Lorenzo, B., S. Ravens, and B. Silva-Santos, *High-throughput analysis of the human thymic Vδ1+ T cell receptor repertoire.* Scientific Data, 2019. **6**(1): p. 115.
103. Papadopoulou, M., et al., *TCR Sequencing Reveals the Distinct Development of Fetal and Adult Human Vγ9Vδ2 T Cells.* The Journal of Immunology, 2019. **203**(6): p. 1468.
104. Parker, C.M., et al., *Evidence for extrathymic changes in the T cell receptor gamma/delta repertoire.* J Exp Med, 1990. **171**(5): p. 1597-612.
105. Morita, C.T., et al., *TCR usage and functional capabilities of human gamma delta T cells at birth.* J Immunol, 1994. **153**(9): p. 3979-88.
106. Casorati, G., et al., *Molecular analysis of human gamma/delta+ clones from thymus and peripheral blood.* J Exp Med, 1989. **170**(5): p. 1521-35.
107. Bos, J.D., et al., *T-cell receptor gamma delta bearing cells in normal human skin.* J Invest Dermatol, 1990. **94**(1): p. 37-42.
108. McVay, L.D., et al., *Regulated expression and structure of T cell receptor gamma/delta transcripts in human thymic ontogeny.* Embo j, 1991. **10**(1): p. 83-91.
109. Tyler, C.J., et al., *Antigen-Presenting Human γδ T Cells Promote Intestinal CD4(+) T Cell Expression of IL-22 and Mucosal Release of Calprotectin.* J Immunol, 2017. **198**(9): p. 3417-3425.
110. Fusco, A., et al., *Molecular evidence for a thymus-independent partial T cell development in a FOXN1-/- athymic human fetus.* PLoS One, 2013. **8**(12): p. e81786.
111. Di Marco Barros, R., et al., *Epithelia Use Butyrophilin-like Molecules to Shape Organ-Specific γδ T Cell Compartments.* Cell, 2016. **167**(1): p. 203-218.e17.
112. Melandri, D., et al., *The γδTCR combines innate immunity with adaptive immunity by utilizing spatially distinct regions for agonist selection and antigen responsiveness.* Nat Immunol, 2018. **19**(12): p. 1352-1365.
113. Willcox, C.R., et al., *Butyrophilin-like 3 Directly Binds a Human Vγ4(+) T Cell Receptor Using a Modality Distinct from Clonally-Restricted Antigen.* Immunity, 2019. **51**(5): p. 813-825.e4.
114. Arnett, H.A., et al., *BTNL2, a Butyrophilin/B7-Like Molecule, Is a Negative Costimulatory Molecule Modulated in Intestinal Inflammation.* The Journal of Immunology, 2007. **178**(3): p. 1523.
115. Hunter, S., et al., *Human liver infiltrating γδ T cells are composed of clonally expanded circulating and tissue-resident populations.* J Hepatol, 2018. **69**(3): p. 654-665.
116. Barker, N., et al., *Identification of stem cells in small intestine and colon by marker gene Lgr5.* Nature, 2007. **449**(7165): p. 1003-1007.
117. Hu, M.D., et al., *Epithelial IL-15 Is a Critical Regulator of γδ Intraepithelial Lymphocyte Motility within the Intestinal Mucosa.* Journal of immunology (Baltimore, Md. : 1950), 2018. **201**(2): p. 747-756.
118. Edelblum, K.L., et al., *Dynamic migration of γδ intraepithelial lymphocytes requires occludin.* Proceedings of the National Academy of Sciences of the United States of America, 2012. **109**(18): p. 7097-7102.
119. Ismail, A.S., et al., *Gammadelta intraepithelial lymphocytes are essential mediators of host-microbial homeostasis at the intestinal mucosal surface.* Proc Natl Acad Sci U S A, 2011. **108**(21): p. 8743-8.

120. Groh, V., et al., *Recognition of stress-induced MHC molecules by intestinal epithelial gammadelta T cells.* Science, 1998. **279**(5357): p. 1737-40.
121. Groh, V., et al., *Cell stress-regulated human major histocompatibility complex class I gene expressed in gastrointestinal epithelium.* Proc Natl Acad Sci U S A, 1996. **93**(22): p. 12445-50.
122. Groh, V., et al., *Broad tumor-associated expression and recognition by tumor-derived gamma delta T cells of MICA and MICB.* Proc Natl Acad Sci U S A, 1999. **96**(12): p. 6879-84.
123. Brenner, M.B., et al., *Two forms of the T-cell receptor γ protein found on peripheral blood cytotoxic T lymphocytes.* Nature, 1987. **325**(6106): p. 689-694.
124. Borst, J., et al., *A T-cell receptor γ/CD3 complex found on cloned functional lymphocytes.* Nature, 1987. **325**(6106): p. 683-688.
125. Gao, G.F., *CD8αα and CD8αβ: truly different?* Trends in Immunology, 2002. **23**(4): p. 177.
126. Xu, B., et al., *Crystal structure of a gammadelta T-cell receptor specific for the human MHC class I homolog MICA.* Proc Natl Acad Sci U S A, 2011. **108**(6): p. 2414-9.
127. Ghadially, H., et al., *MHC class I chain-related protein A and B (MICA and MICB) are predominantly expressed intracellularly in tumour and normal tissue.* British Journal of Cancer, 2017. **116**(9): p. 1208-1217.
128. Marlin, R., et al., *Sensing of cell stress by human γδ TCR-dependent recognition of annexin A2.* Proc Natl Acad Sci U S A, 2017. **114**(12): p. 3163-3168.
129. Willcox, C.R., et al., *Cytomegalovirus and tumor stress surveillance by binding of a human γδ T cell antigen receptor to endothelial protein C receptor.* Nat Immunol, 2012. **13**(9): p. 872-9.
130. Zeng, X., et al., *γδ T cells recognize a microbial encoded B cell antigen to initiate a rapid antigen-specific interleukin-17 response.* Immunity, 2012. **37**(3): p. 524-34.
131. Russano, A.M., et al., *CD1-Restricted Recognition of Exogenous and Self-Lipid Antigens by Duodenal γδ⁺ T Lymphocytes.* The Journal of Immunology, 2007. **178**(6): p. 3620.
132. Van Rhijn, I. and J. Le Nours, *CD1 and MR1 recognition by human γδ T cells.* Mol Immunol, 2021. **133**: p. 95-100.
133. Le Nours, J., et al., *A class of γδ T cell receptors recognize the underside of the antigen-presenting molecule MR1.* Science, 2019. **366**(6472): p. 1522-1527.
134. Uldrich, A.P., et al., *CD1d-lipid antigen recognition by the γδ TCR.* Nat Immunol, 2013. **14**(11): p. 1137-45.
135. Luoma, A.M., et al., *Crystal structure of Vδ1 T cell receptor in complex with CD1d-sulfatide shows MHC-like recognition of a self-lipid by human γδ T cells.* Immunity, 2013. **39**(6): p. 1032-42.
136. Bai, L., et al., *The majority of CD1d-sulfatide-specific T cells in human blood use a semiinvariant Vδ1 TCR.* Eur J Immunol, 2012. **42**(9): p. 2505-10.
137. Roy, S., et al., *Molecular Analysis of Lipid-Reactive Vδ1 γδ T Cells Identified by CD1c Tetramers.* J Immunol, 2016. **196**(4): p. 1933-42.
138. Rice, M.T., et al., *Recognition of the antigen-presenting molecule MR1 by a Vδ3(+) γδ T cell receptor.* Proc Natl Acad Sci U S A, 2021. **118**(49).
139. Arnett, H.A. and J.L. Viney, *Immune modulation by butyrophilins.* Nat Rev Immunol, 2014. **14**(8): p. 559-69.
140. Karunakaran, M.M., et al., *Butyrophilin-2A1 Directly Binds Germline-Encoded Regions of the Vγ9Vδ2 TCR and Is Essential for Phosphoantigen Sensing.* Immunity, 2020. **52**(3): p. 487-498.e6.
141. Sandstrom, A., et al., *The intracellular B30.2 domain of butyrophilin 3A1 binds phosphoantigens to mediate activation of human Vγ9Vδ2 T cells.* Immunity, 2014. **40**(4): p. 490-500.
142. Nguyen, K., et al., *The butyrophilin 3A1 intracellular domain undergoes a conformational change involving the juxtamembrane region.* Faseb j, 2017. **31**(11): p. 4697-4706.
143. Salim, M., et al., *BTN3A1 Discriminates γδ T Cell Phosphoantigens from Nonantigenic Small Molecules via a Conformational Sensor in Its B30.2 Domain.* ACS Chem Biol, 2017. **12**(10): p. 2631-2643.
144. Gober, H.J., et al., *Human T cell receptor gammadelta cells recognize endogenous mevalonate metabolites in tumor cells.* J Exp Med, 2003. **197**(2): p. 163-8.
145. Corvaisier, M., et al., *V gamma 9V delta 2 T cell response to colon carcinoma cells.* J Immunol, 2005. **175**(8): p. 5481-8.
146. Meraviglia, S., et al., *Distinctive features of tumor-infiltrating γδ T lymphocytes in human colorectal cancer.* Oncoimmunology, 2017. **6**(10): p. e1347742.
147. Maeurer, M.J., et al., *Human intestinal Vdelta1+ lymphocytes recognize tumor cells of epithelial origin.* J Exp Med, 1996. **183**(4): p. 1681-96.
148. Devaud, C., et al., *Antitumor Activity of γδ T Cells Reactive against Cytomegalovirus-Infected Cells in a Mouse Xenograft Tumor Model.* Cancer Research, 2009. **69**(9): p. 3971-3978.
149. Halary, F., et al., *Shared reactivity of V{delta}2(neg) {gamma}{delta} T cells against cytomegalovirus-infected cells and tumor intestinal epithelial cells.* J Exp Med, 2005. **201**(10): p. 1567-78.
150. Wu, D., et al., *Ex vivo expanded human circulating Vδ1 γδT cells exhibit favorable therapeutic potential for colon cancer.* Oncoimmunology, 2015. **4**(3): p. e992749.

151. Wu, J., V. Groh, and T. Spies, *T cell antigen receptor engagement and specificity in the recognition of stress-inducible MHC class I-related chains by human epithelial gamma delta T cells.* J Immunol, 2002. **169**(3): p. 1236-40.
152. Rincon-Orozco, B., et al., *Activation of V gamma 9V delta 2 T cells by NKG2D.* J Immunol, 2005. **175**(4): p. 2144-51.
153. Mikulak, J., et al., *NKp46-expressing human gut-resident intraepithelial Vδ1 T cell subpopulation exhibits high antitumor activity against colorectal cancer.* JCI Insight, 2019. **4**(24).
154. Devaud, C., et al., *Anti-metastatic potential of human Vδ1(+) γδ T cells in an orthotopic mouse xenograft model of colon carcinoma.* Cancer immunology, immunotherapy : CII, 2013. **62**(7): p. 1199-1210.
155. Suzuki, T., et al., *Gut γδ T cells as guardians, disruptors, and instigators of cancer.* Immunological Reviews, 2020. **298**(1): p. 198-217.
156. Wakita, D., et al., *Tumor-infiltrating IL-17-producing gammadelta T cells support the progression of tumor by promoting angiogenesis.* Eur J Immunol, 2010. **40**(7): p. 1927-37.
157. Rei, M., et al., *Murine CD27(-) Vγ6(+) γδ T cells producing IL-17A promote ovarian cancer growth via mobilization of protumor small peritoneal macrophages.* Proc Natl Acad Sci U S A, 2014. **111**(34): p. E3562-70.
158. Ma, S., et al., *IL-17A produced by γδ T cells promotes tumor growth in hepatocellular carcinoma.* Cancer Res, 2014. **74**(7): p. 1969-82.
159. Coffelt, S.B., et al., *IL-17-producing γδ T cells and neutrophils conspire to promote breast cancer metastasis.* Nature, 2015. **522**(7556): p. 345-348.
160. Van hede, D., et al., *Human papillomavirus oncoproteins induce a reorganization of epithelial-associated γδ T cells promoting tumor formation.* Proceedings of the National Academy of Sciences, 2017. **114**(43): p. E9056-E9065.
161. Rakoff-Nahoum, S. and R. Medzhitov, *Regulation of spontaneous intestinal tumorigenesis through the adaptor protein MyD88.* Science, 2007. **317**(5834): p. 124-7.
162. Grivennikov, S.I., et al., *Adenoma-linked barrier defects and microbial products drive IL-23/IL-17-mediated tumour growth.* Nature, 2012. **491**(7423): p. 254-8.
163. Wang, K., et al., *Interleukin-17 receptor a signaling in transformed enterocytes promotes early colorectal tumorigenesis.* Immunity, 2014. **41**(6): p. 1052-63.
164. Chae, W.J., et al., *Ablation of IL-17A abrogates progression of spontaneous intestinal tumorigenesis.* Proc Natl Acad Sci U S A, 2010. **107**(12): p. 5540-4.
165. Marsh, L., et al., *Altered intestinal epithelium-associated lymphocyte repertoires and function in ApcMin/+ mice.* Int J Oncol, 2012. **40**(1): p. 243-50.
166. Wu, S., et al., *A human colonic commensal promotes colon tumorigenesis via activation of T helper type 17 T cell responses.* Nat Med, 2009. **15**(9): p. 1016-22.
167. Housseau, F., et al., *Redundant Innate and Adaptive Sources of IL17 Production Drive Colon Tumorigenesis.* Cancer Res, 2016. **76**(8): p. 2115-24.
168. Dejea, C.M., et al., *Patients with familial adenomatous polyposis harbor colonic biofilms containing tumorigenic bacteria.* Science, 2018. **359**(6375): p. 592-597.
169. Kathania, M., et al., *Itch inhibits IL-17-mediated colon inflammation and tumorigenesis by ROR-γt ubiquitination.* Nat Immunol, 2016. **17**(8): p. 997-1004.
170. Zhong, C. and J. Zhu, *Small-Molecule RORγt Antagonists: One Stone Kills Two Birds.* Trends Immunol, 2017. **38**(4): p. 229-231.
171. Caccamo, N., et al., *Differentiation, phenotype, and function of interleukin-17-producing human Vγ9Vδ2 T cells.* Blood, 2011. **118**(1): p. 129-38.
172. Ness-Schwickerath, K.J., C. Jin, and C.T. Morita, *Cytokine requirements for the differentiation and expansion of IL-17A- and IL-22-producing human Vgamma2Vdelta2 T cells.* J Immunol, 2010. **184**(12): p. 7268-80.
173. Michel, M.L., et al., *Interleukin 7 (IL-7) selectively promotes mouse and human IL-17-producing γδ cells.* Proc Natl Acad Sci U S A, 2012. **109**(43): p. 17549-54.
174. Wu, P., et al., *γδT17 cells promote the accumulation and expansion of myeloid-derived suppressor cells in human colorectal cancer.* Immunity, 2014. **40**(5): p. 785-800.
175. Hu, G., et al., *Tumor-infiltrating CD39(+)γδTregs are novel immunosuppressive T cells in human colorectal cancer.* Oncoimmunology, 2017. **6**(2): p. e1277305.
176. Amicarella, F., et al., *Dual role of tumour-infiltrating T helper 17 cells in human colorectal cancer.* Gut, 2017. **66**(4): p. 692-704.
177. Jackstadt, R. and O.J. Sansom, *Mouse models of intestinal cancer.* J Pathol, 2016. **238**(2): p. 141-51.
178. Tauriello, D.V.F., et al., *TGFβ drives immune evasion in genetically reconstituted colon cancer metastasis.* Nature, 2018. **554**(7693): p. 538-543.
179. Daley, D., et al., *γδ T Cells Support Pancreatic Oncogenesis by Restraining αβ T Cell Activation.* Cell, 2016. **166**(6): p. 1485-1499.e15.
180. Jackstadt, R., et al., *Epithelial NOTCH Signaling Rewires the Tumor Microenvironment of Colorectal Cancer to Drive Poor-Prognosis Subtypes and Metastasis.* Cancer Cell, 2019. **36**(3): p. 319-336.e7.

181. Rutkowski, M.R., et al., *Microbially driven TLR5-dependent signaling governs distal malignant progression through tumor-promoting inflammation.* Cancer Cell, 2015. **27**(1): p. 27-40.
182. Jin, C., et al., *Commensal Microbiota Promote Lung Cancer Development via γδ T Cells.* Cell, 2019. **176**(5): p. 998-1013.e16.
183. Nagtegaal, I.D., P. Quirke, and H.J. Schmoll, *Has the new TNM classification for colorectal cancer improved care?* Nat Rev Clin Oncol, 2011. **9**(2): p. 119-23.
184. Eugène, J., et al., *The inhibitory receptor CD94/NKG2A on CD8(+) tumor-infiltrating lymphocytes in colorectal cancer: a promising new druggable immune checkpoint in the context of HLAE/β2m overexpression.* Mod Pathol, 2020. **33**(3): p. 468-482.
185. Ma, C., et al., *Tumor-infiltrating γδ T lymphocytes predict clinical outcome in human breast cancer.* Journal of immunology (Baltimore, Md. : 1950), 2012. **189**(10): p. 5029-5036.
186. Patil, R.S., et al., *IL17 producing γδT cells induce angiogenesis and are associated with poor survival in gallbladder cancer patients.* International Journal of Cancer, 2016. **139**(4): p. 869-881.
187. Tosolini, M., et al., *Assessment of tumor-infiltrating TCRVγ9Vδ2 γδ lymphocyte abundance by deconvolution of human cancers microarrays.* Oncoimmunology, 2017. **6**(3): p. e1284723-e1284723.
188. Tosolini, M., et al., *Clinical Impact of Different Classes of Infiltrating T Cytotoxic and Helper Cells (Th1, Th2, Treg, Th17) in Patients with Colorectal Cancer.* Cancer Research, 2011. **71**(4): p. 1263-1271.
189. Rooney, M.S., et al., *Molecular and genetic properties of tumors associated with local immune cytolytic activity.* Cell, 2015. **160**(1-2): p. 48-61.
190. Narayanan, S., et al., *Cytolytic Activity Score to Assess Anticancer Immunity in Colorectal Cancer.* Ann Surg Oncol, 2018. **25**(8): p. 2323-2331.
191. Narayanan, S., et al., *Tumor Infiltrating Lymphocytes and Macrophages Improve Survival in Microsatellite Unstable Colorectal Cancer.* Sci Rep, 2019. **9**(1): p. 13455.
192. de Vries, N.L., et al., *High-dimensional cytometric analysis of colorectal cancer reveals novel mediators of antitumour immunity.* Gut, 2020. **69**(4): p. 691-703.
193. Wistuba-Hamprecht, K., et al., *Proportions of blood-borne Vδ1+ and Vδ2+ T-cells are associated with overall survival of melanoma patients treated with ipilimumab.* Eur J Cancer, 2016. **64**: p. 116-26.
194. Kobayashi, H., et al., *Complete remission of lung metastasis following adoptive immunotherapy using activated autologous gammadelta T-cells in a patient with renal cell carcinoma.* Anticancer Res, 2010. **30**(2): p. 575-9.
195. Kakimi, K., et al., *γδ T cell therapy for the treatment of non-small cell lung cancer.* Transl Lung Cancer Res, 2014. **3**(1): p. 23-33.
196. Nicol, A.J., et al., *Clinical evaluation of autologous gamma delta T cell-based immunotherapy for metastatic solid tumours.* Br J Cancer, 2011. **105**(6): p. 778-86.
197. Sakamoto, M., et al., *Adoptive immunotherapy for advanced non-small cell lung cancer using zoledronate-expanded γδTcells: a phase I clinical study.* J Immunother, 2011. **34**(2): p. 202-11.
198. Nakajima, J., et al., *A phase I study of adoptive immunotherapy for recurrent non-small-cell lung cancer patients with autologous gammadelta T cells.* Eur J Cardiothorac Surg, 2010. **37**(5): p. 1191-7.
199. Wang, H., et al., *Indirect stimulation of human Vγ2Vδ2 T cells through alterations in isoprenoid metabolism.* J Immunol, 2011. **187**(10): p. 5099-113.
200. Nada, M.H., et al., *Enhancing adoptive cancer immunotherapy with Vγ2Vδ2 T cells through pulse zoledronate stimulation.* J Immunother Cancer, 2017. **5**: p. 9.
201. Izumi, T., et al., *Ex vivo characterization of γδ T-cell repertoire in patients after adoptive transfer of Vγ9Vδ2 T cells expressing the interleukin-2 receptor β-chain and the common γ-chain.* Cytotherapy, 2013. **15**(4): p. 481-91.
202. Zocchi, M.R., et al., *Zoledronate can induce colorectal cancer microenvironment expressing BTN3A1 to stimulate effector γδ T cells with antitumor activity.* Oncoimmunology, 2017. **6**(3): p. e1278099.
203. Wragg, K.M., et al., *High CD26 and Low CD94 Expression Identifies an IL-23 Responsive Vδ2(+) T Cell Subset with a MAIT Cell-like Transcriptional Profile.* Cell Rep, 2020. **31**(11): p. 107773.
204. Espinosa, E., et al., *Chemical synthesis and biological activity of bromohydrin pyrophosphate, a potent stimulator of human gamma delta T cells.* J Biol Chem, 2001. **276**(21): p. 18337-44.
205. Chargui, J., et al., *Bromohydrin pyrophosphate-stimulated Vgamma9delta2 T cells expanded ex vivo from patients with poor-prognosis neuroblastoma lyse autologous primary tumor cells.* J Immunother, 2010. **33**(6): p. 591-8.
206. Bouet-Toussaint, F., et al., *Vgamma9Vdelta2 T cell-mediated recognition of human solid tumors. Potential for immunotherapy of hepatocellular and colorectal carcinomas.* Cancer Immunol Immunother, 2008. **57**(4): p. 531-9.
207. Lu, H., et al., *B7-H3 inhibits the IFN-γ-dependent cytotoxicity of Vγ9Vδ2 T cells against colon cancer cells.* Oncoimmunology, 2020. **9**(1): p. 1748991.
208. Harly, C., et al., *Key implication of CD277/butyrophilin-3 (BTN3A) in cellular stress sensing by a major human γδ T-cell subset.* Blood, 2012. **120**(11): p. 2269-79.

209. Todaro, M., et al., *Efficient killing of human colon cancer stem cells by gammadelta T lymphocytes.* J Immunol, 2009. **182**(11): p. 7287-96.
210. Alexander, A.A., et al., *Isopentenyl pyrophosphate-activated CD56+ {gamma}{delta} T lymphocytes display potent antitumor activity toward human squamous cell carcinoma.* Clin Cancer Res, 2008. **14**(13): p. 4232-40.
211. Bürk, M.R., L. Mori, and G. De Libero, *Human V gamma 9-V delta 2 cells are stimulated in a cross-reactive fashion by a variety of phosphorylated metabolites.* Eur J Immunol, 1995. **25**(7): p. 2052-8.
212. Tanaka, Y., et al., *Natural and synthetic non-peptide antigens recognized by human gamma delta T cells.* Nature, 1995. **375**(6527): p. 155-8.
213. Mattarollo, S.R., et al., *Chemotherapy and zoledronate sensitize solid tumour cells to Vgamma9Vdelta2 T cell cytotoxicity.* Cancer Immunol Immunother, 2007. **56**(8): p. 1285-97.
214. Kaymak, I., et al., *Mevalonate Pathway Provides Ubiquinone to Maintain Pyrimidine Synthesis and Survival in p53-Deficient Cancer Cells Exposed to Metabolic Stress.* Cancer Res, 2020. **80**(2): p. 189-203.
215. Freed-Pastor, W.A., et al., *Mutant p53 disrupts mammary tissue architecture via the mevalonate pathway.* Cell, 2012. **148**(1-2): p. 244-58.
216. Moon, S.H., et al., *p53 Represses the Mevalonate Pathway to Mediate Tumor Suppression.* Cell, 2019. **176**(3): p. 564-580.e19.
217. Sugai, T., et al., *Analysis of molecular alterations in left- and right-sided colorectal carcinomas reveals distinct pathways of carcinogenesis: proposal for new molecular profile of colorectal carcinomas.* J Mol Diagn, 2006. **8**(2): p. 193-201.
218. Marcu-Malina, V., et al., *Redirecting αβ T cells against cancer cells by transfer of a broadly tumor-reactive γδT-cell receptor.* Blood, 2011. **118**(1): p. 50-9.
219. Gründer, C., et al., *γ9 and δ2CDR3 domains regulate functional avidity of T cells harboring γ9δ2TCRs.* Blood, 2012. **120**(26): p. 5153-62.
220. Deniger, D.C., et al., *Bispecific T-cells expressing polyclonal repertoire of endogenous γδ T-cell receptors and introduced CD19-specific chimeric antigen receptor.* Mol Ther, 2013. **21**(3): p. 638-47.
221. Mirzaei, H.R., et al., *Prospects for chimeric antigen receptor (CAR) γδ T cells: A potential game changer for adoptive T cell cancer immunotherapy.* Cancer Lett, 2016. **380**(2): p. 413-423.
222. Almeida, A.R., et al., *Delta One T Cells for Immunotherapy of Chronic Lymphocytic Leukemia: Clinical-Grade Expansion/Differentiation and Preclinical Proof of Concept.* Clin Cancer Res, 2016. **22**(23): p. 5795-5804.
223. de Bruin, R.C.G., et al., *A bispecific nanobody approach to leverage the potent and widely applicable tumor cytolytic capacity of Vγ9Vδ2-T cells.* Oncoimmunology, 2017. **7**(1): p. e1375641.
224. Misale, S., et al., *Resistance to anti-EGFR therapy in colorectal cancer: from heterogeneity to convergent evolution.* Cancer Discov, 2014. **4**(11): p. 1269-80.
225. Lausen, B. and M. Schumacher, *Maximally Selected Rank Statistics.* Biometrics, 1992. **48**(1): p. 73-85.
226. Hothorn, T. and B. Lausen, *On the exact distribution of maximally selected rank statistics.* Computational Statistics & Data Analysis, 2003. **43**(2): p. 121-137.
227. Alboukadel Kassambara, M.K., Przemyslaw Biecek, *Survminer: Survival Analysis and Visualization*. 2016.
228. Hothorn, T., *Maxstat: Maximally selected rank statistics with*

several p-value approximations. 2019.
229. Therneau, T.M., *Survival: survival analysis*. 2022.
230. Wiesweg, M., *survivalAnalysis: High-Level Interface for Survival Analysis and Associated Plots*. 2022.
231. R Core Team, *R: A Language and Environment for Statistical Computing*. 2021, R Foundation for Statistical Computing: Vienna, Austria.
232. RStudio Team, *RStudio: Integrated Development Environment for R*. 2019, RStudio, Inc.: Boston, MA.
233. Mayakonda, A., et al., *Maftools: efficient and comprehensive analysis of somatic variants in cancer.* Genome Res, 2018. **28**(11): p. 1747-1756.
234. Mistry, J., et al., *Pfam: The protein families database in 2021.* Nucleic Acids Research, 2021. **49**(D1): p. D412-D419.
235. Meyer, D., A. Zeileis, and K. Hornik, *The Strucplot Framework: Visualizing Multi-way Contingency Tables with vcd.* Journal of Statistical Software, 2006. **17**(3): p. 1 - 48.
236. Korotkevich, G., et al., *Fast gene set enrichment analysis.* bioRxiv, 2021: p. 060012.
237. Subramanian, A., et al., *Gene set enrichment analysis: A knowledge-based approach for interpreting genome-wide expression profiles.* Proceedings of the National Academy of Sciences, 2005. **102**(43): p. 15545-15550.
238. Liberzon, A., et al., *The Molecular Signatures Database (MSigDB) hallmark gene set collection.* Cell Syst, 2015. **1**(6): p. 417-425.
239. Klintrup, K., et al., *Inflammation and prognosis in colorectal cancer.* European Journal of Cancer, 2005. **41**(17): p. 2645-2654.

240. Clarke, S.L., et al., *CD4+CD25+FOXP3+ regulatory T cells suppress anti-tumor immune responses in patients with colorectal cancer.* PloS one, 2006. **1**(1): p. e129-e129.
241. Groh, V., et al., *Human lymphocytes bearing T cell receptor gamma/delta are phenotypically diverse and evenly distributed throughout the lymphoid system.* The Journal of experimental medicine, 1989. **169**(4): p. 1277-1294.
242. Borst, J., et al., *Distinct molecular forms of human T cell receptor gamma/delta detected on viable T cells by a monoclonal antibody.* The Journal of experimental medicine, 1988. **167**(5): p. 1625-1644.
243. Ullrich, R., et al., *γδ T cells in the human intestine express surface markers of activation and are preferentially located in the epithelium.* Cellular Immunology, 1990. **128**(2): p. 619-627.
244. Chabab, G., et al., *Diversity of Tumor-Infiltrating, γδ T-Cell Abundance in Solid Cancers.* Cells, 2020. **9**(6): p. 1537.
245. Bankhead, P., et al., *QuPath: Open source software for digital pathology image analysis.* Scientific Reports, 2017. **7**(1): p. 16878.
246. Humphries, M.P., P. Maxwell, and M. Salto-Tellez, *QuPath: The global impact of an open source digital pathology system.* Computational and Structural Biotechnology, (2001-0370 (Print)).
247. A/S, V. *VisioPharm About Us*. 2021 [cited 2021 15/03/2021]; Available from: https://visiopharm.com/about-us/.
248. Mousavi, N., et al., *Application of digital image analysis on histological images of a murine embryoid body model for monitoring endothelial differentiation.* Pathology, research and practice, (1618-0631 (Electronic)).
249. Lea, D., et al., *A template to quantify the location and density of CD3 + and CD8 + tumor-infiltrating lymphocytes in colon cancer by digital pathology on whole slides for an objective, standardized immune score assessment. LID - 10.1007/s00262-020-02834-y [doi].* Cancer immunology, immunotherapy, (1432-0851 (Electronic)).
250. Rahman, M.A. and Y. Wang. *Optimizing Intersection-Over-Union in Deep Neural Networks for Image Segmentation*. in *Advances in Visual Computing*. 2016. Cham: Springer International Publishing.
251. Bland, J.M. and D.G. Altman, *STATISTICAL METHODS FOR ASSESSING AGREEMENT BETWEEN TWO METHODS OF CLINICAL MEASUREMENT.* The Lancet, 1986. **327**: p. 307-310.
252. Koo, T.K. and M.Y. Li, *A Guideline of Selecting and Reporting Intraclass Correlation Coefficients for Reliability Research.* Journal of chiropractic medicine, 2016. **15**(2): p. 155-163.
253. Shrout, P.E. and J.L. Fleiss, *Intraclass correlations: uses in assessing rater reliability.* Psychological Bulletin, (0033-2909 (Print)).
254. Hu, M.D., L. Jia, and K.L. Edelblum, *Policing the intestinal epithelial barrier: Innate immune functions of intraepithelial lymphocytes.* Current pathobiology reports, 2018. **6**(1): p. 35-46.
255. Vuik, F.E.R., et al., *Increasing incidence of colorectal cancer in young adults in Europe over the last 25 years.* Gut, 2019. **68**(10): p. 1820.
256. White, A., et al., *A review of sex-related differences in colorectal cancer incidence, screening uptake, routes to diagnosis, cancer stage and survival in the UK.* BMC Cancer, 2018. **18**(1): p. 906.
257. Abancens, M., et al., *Sexual Dimorphism in Colon Cancer.* Frontiers in Oncology, 2020. **10**.
258. Klingbiel, D., et al., *Prognosis of stage II and III colon cancer treated with adjuvant 5-fluorouracil or FOLFIRI in relation to microsatellite status: results of the PETACC-3 trial.* Ann Oncol, 2015. **26**(1): p. 126-132.
259. Nielsen, M.M., D.A. Witherden, and W.L. Havran, *γδ T cells in homeostasis and host defence of epithelial barrier tissues.* Nature reviews. Immunology, 2017. **17**(12): p. 733-745.
260. Chen, X., et al., *Distribution and functions of γδ T cells infiltrated in the ovarian cancer microenvironment.* Journal of Translational Medicine, 2019. **17**(1): p. 144.
261. Song, X., C. Wei, and X. Li, *Association between γδ T cells and clinicopathological features of breast cancer.* International Immunopharmacology, 2022. **103**: p. 108457.
262. McCarthy, N.E. and M. Eberl, *Human γδ T-Cell Control of Mucosal Immunity and Inflammation.* Frontiers in immunology, 2018. **9**: p. 985-985.
263. Siegel, R.L., et al., *Colorectal cancer statistics, 2020.* CA: A Cancer Journal for Clinicians, 2020. **70**(3): p. 145-164.
264. Nosho, K., et al., *Tumour-infiltrating T-cell subsets, molecular changes in colorectal cancer, and prognosis: cohort study and literature review.* The Journal of pathology, 2010. **222**(4): p. 350-366.
265. Tamas, K., et al., *Rectal and colon cancer: Not just a different anatomic site.* Cancer Treatment Reviews, 2015. **41**(8): p. 671-679.
266. Baran, B., et al., *Difference Between Left-Sided and Right-Sided Colorectal Cancer: A Focused Review of Literature.* Gastroenterology research, 2018. **11**(4): p. 264-273.
267. Mik, M., et al., *Right- and left-sided colon cancer - clinical and pathological differences of the disease entity in one organ.* (1734-1922 (Print)).
268. Missiaglia, E., et al., *Distal and proximal colon cancers differ in terms of molecular, pathological, and clinical features.* (1569-8041 (Electronic)).
269. Phillips, S.M., et al., *Tumour-infiltrating lymphocytes in colorectal cancer with microsatellite instability are activated and cytotoxic.* British Journal of Surgery, 2004. **91**(4): p. 469-475.
270. Bos Jl Fau - Fearon, E.R., et al., *Prevalence of ras gene mutations in human colorectal cancers.* (0028-0836 (Print)).

271. Zaidi, S.H., et al., *Landscape of somatic single nucleotide variants and indels in colorectal cancer and impact on survival.* Nature Communications, 2020. **11**(1): p. 3644.
272. Yaeger, R., et al., *Clinical Sequencing Defines the Genomic Landscape of Metastatic Colorectal Cancer.* (1878-3686 (Electronic)).
273. Picard, E., et al., *Relationships Between Immune Landscapes, Genetic Subtypes and Responses to Immunotherapy in Colorectal Cancer.* Frontiers in Immunology, 2020. **11**.
274. Albasri, A.M. and M.A. Elkablawy, *Clinicopathological and prognostic significance of androgen receptor overexpression in colorectal cancer. Experience from Al-Madinah Al-Munawarah, Saudi Arabia.* (0379-5284 (Print)).
275. Shaw, R.J. and L.C. Cantley, *Ras, PI(3)K and mTOR signalling controls tumour cell growth.* Nature, 2006. **441**(7092): p. 424-430.
276. Samuels, Y., et al., *Mutant PIK3CA promotes cell growth and invasion of human cancer cells.* Cancer Cell, 2005. **7**(6): p. 561-573.
277. Ogino, S., et al., *PIK3CA mutation is associated with poor prognosis among patients with curatively resected colon cancer.* (1527-7755 (Electronic)).
278. Gonsalves, W.I., et al., *Patient and tumor characteristics and BRAF and KRAS mutations in colon cancer, NCCTG/Alliance N0147.* J Natl Cancer Inst, 2014. **106**(7).
279. Barras, D., *BRAF Mutation in Colorectal Cancer: An Update.* Biomark Cancer, 2015. **7**(Suppl 1): p. 9-12.
280. Liu, C., et al., *BRAF inhibition increases tumor infiltration by T cells and enhances the antitumor activity of adoptive immunotherapy in mice.* (1557-3265 (Electronic)).
281. Wilmott, J.S., et al., *Selective BRAF Inhibitors Induce Marked T-cell Infiltration into Human Metastatic Melanoma.* Clinical Cancer Research, 2012. **18**(5): p. 1386-1394.
282. Mauri, G., et al., *The Evolutionary Landscape of Treatment for BRAF(V600E) Mutant Metastatic Colorectal Cancer. LID - 10.3390/cancers13010137 [doi] LID - 137.* (2072-6694 (Print)).
283. Benten, W.P., et al., *Functional testosterone receptors in plasma membranes of T cells.* (0892-6638 (Print)).
284. Guan, X., et al., *Androgen receptor activity in T cells limits checkpoint blockade efficacy.* Nature, 2022. **606**(7915): p. 791-796.
285. Chen, F., et al., *Computational analysis of androgen receptor (AR) variants to decipher the relationship between protein stability and related-diseases.*
286. Vellano, C.P., et al., *Androgen receptor blockade promotes response to BRAF/MEK-targeted therapy.* Nature, 2022. **606**(7915): p. 797-803.
287. Cantley, L.C., *The phosphoinositide 3-kinase pathway.* (1095-9203 (Electronic)).
288. Carver, B.S., et al., *Reciprocal feedback regulation of PI3K and androgen receptor signaling in PTEN-deficient prostate cancer.* (1878-3686 (Electronic)).
289. Nusrat, M., et al., *The immune impact of PI3K-AKT pathway inhibition in colorectal cancer.* Journal of Clinical Oncology, 2022. **40**(4_suppl): p. 154-154.
290. Maréchal, A. and L. Zou, *DNA damage sensing by the ATM and ATR kinases. LID - 10.1101/cshperspect.a012716 [doi] LID - a012716.* (1943-0264 (Electronic)).
291. Schrempf, A., J. Slyskova, and J.I. Loizou, *Targeting the DNA Repair Enzyme Polymerase ϑ in Cancer Therapy.* (2405-8025 (Electronic)).
292. Yuan, H., et al., *Histone methyltransferase SETD2 modulates alternative splicing to inhibit intestinal tumorigenesis.* (1558-8238 (Electronic)).
293. Cortes-Ciriano, I., et al., *A molecular portrait of microsatellite instability across multiple cancers.* Nature Communications, 2017. **8**(1): p. 15180.
294. Wright, C.M., et al.
295. Tsukiyama, T., et al., *A phospho-switch controls RNF43-mediated degradation of Wnt receptors to suppress tumorigenesis.* Nature Communications, 2020. **11**(1): p. 4586.
296. Reitman, Z.J. and H. Yan, *Isocitrate Dehydrogenase 1 and 2 Mutations in Cancer: Alterations at a Crossroads of Cellular Metabolism.* JNCI: Journal of the National Cancer Institute, 2010. **102**(13): p. 932-941.
297. Grassian, A.R., et al., *IDH1 mutations alter citric acid cycle metabolism and increase dependence on oxidative mitochondrial metabolism.* (1538-7445 (Electronic)).
298. Huang, J., et al., *IDH1 and IDH2 Mutations in Colorectal Cancers.* American Journal of Clinical Pathology, 2021. **156**(5): p. 777-786.
299. Zhou, Y., et al., *DNMT3A facilitates colorectal cancer progression via regulating DAB2IP mediated MEK/ERK activation.* Biochimica et Biophysica Acta (BBA) - Molecular Basis of Disease, 2022. **1868**(4): p. 166353.
300. Wu, K., et al., *The role of DAB2IP in androgen receptor activation during prostate cancer progression.* Oncogene, 2014. **33**(15): p. 1954-1963.
301. Saxton, R.A. and D.M. Sabatini, *mTOR Signaling in Growth, Metabolism, and Disease.* (1097-4172 (Electronic)).
302. Francipane, M.G. and E. Lagasse, *mTOR pathway in colorectal cancer: an update.* (1949-2553 (Electronic)).

303. Wang, C., et al., *Genomic signature of MTOR could be an immunogenicity marker in human colorectal cancer.* BMC Cancer, 2022. **22**(1): p. 818.
304. Di Fabio, F., et al., *Somatic mosaicism of androgen receptor CAG repeats in colorectal carcinoma epithelial cells from men.* J Surg Res, 2009. **154**(1): p. 38-44.
305. Xia, T., et al., *Androgen receptor gene methylation related to colorectal cancer risk.* Endocr Connect, 2019. **8**(7): p. 979-987.
306. Disciglio, V., et al., *Whole exome sequencing and single nucleotide polymorphism array analyses to identify germline alterations in genes associated with testosterone metabolism in a patient with androgen insensitivity syndrome and early-onset colorectal cancer.* Chin J Cancer, 2016. **35**(1): p. 51.
307. Korphaisarn, K., et al., *FBXW7 missense mutation: a novel negative prognostic factor in metastatic colorectal adenocarcinoma.* Oncotarget, 2017. **8**(24): p. 39268-39279.
308. Shang, W., et al., *Clinical significance of FBXW7 tumor suppressor gene mutations and expression in human colorectal cancer: a systemic review and meta-analysis.*
309. Kim, Y.S., et al., *Unique characteristics of ARID1A mutation and protein level in gastric and colorectal cancer: A meta-analysis.* Saudi J Gastroenterol, 2017. **23**(5): p. 268-274.
310. Kamori, T., et al.
311. Tokunaga, R., et al.
312. Fang, T., et al., *Prognostic role and clinicopathological features of SMAD4 gene mutation in colorectal cancer: a systematic review and meta-analysis.*
313. Wasserman, I., et al.
314. Woodford-Richens, K.L., et al., *SMAD4 mutations in colorectal cancer probably occur before chromosomal instability, but after divergence of the microsatellite instability pathway.* Proc Natl Acad Sci U S A, 2001. **98**(17): p. 9719-23.
315. Toh, J.W.T., et al., *Cytotoxic CD8+ T cells and tissue resident memory cells in colorectal cancer based on microsatellite instability and BRAF status.* World J Clin Oncol, 2021. **12**(4): p. 238-248.
316. Zhang, X.-M., et al., *The human T-cell receptor gamma variable pseudogeneV10 is a distinctive marker of human speciation.*
317. Lebrero-Fernández, C., et al., *Altered expression of Butyrophilin (BTN) and BTN-like (BTNL) genes in intestinal inflammation and colon cancer.* Immun Inflamm Dis, 2016. **4**(2): p. 191-200.
318. Choo, S.Y., *The HLA system: genetics, immunology, clinical testing, and clinical implications.* Yonsei Med J, 2007. **48**(1): p. 11-23.
319. Hammer, M., et al., *Dual specificity phosphatase 1 (DUSP1) regulates a subset of LPS-induced genes and protects mice from lethal endotoxin shock.* Journal of Experimental Medicine, 2005. **203**(1): p. 15-20.
320. Shah, S., et al., *Roles for the mitogen-activated protein kinase (MAPK) phosphatase, DUSP1, in feedback control of inflammatory gene expression and repression by dexamethasone.* J Biol Chem, 2014. **289**(19): p. 13667-79.
321. Kearney, C.J., K.L. Randall, and J. Oliaro, *DOCK8 regulates signal transduction events to control immunity.*
322. Lanier, L.L., et al., *Immunoreceptor DAP12 bearing a tyrosine-based activation motif is involved in activating NK cells.* Nature, 1998. **391**(6668): p. 703-707.
323. Turnbull, I.R. and M. Colonna, *Activating and inhibitory functions of DAP12.* Nature Reviews Immunology, 2007. **7**(2): p. 155-161.
324. Howard, J. and A.A. Hyman, *Dynamics and mechanics of the microtubule plus end.* Nature, 2003. **422**(6933): p. 753-758.
325. Samten, B., *CD52 as both a marker and an effector molecule of T cells with regulatory action: Identification of novel regulatory T cells.* Cellular & Molecular Immunology, 2013. **10**(6): p. 456-458.
326. Zhao, Y., et al., *The immunological function of CD52 and its targeting in organ transplantation.* Inflamm Res, 2017. **66**(7): p. 571-578.
327. Bröer, S., *The SLC38 family of sodium–amino acid co-transporters.* Pflügers Archiv - European Journal of Physiology, 2014. **466**(1): p. 155-172.
328. Chou, Y.T., et al., *CITED2 functions as a molecular switch of cytokine-induced proliferation and quiescence.* Cell Death & Differentiation, 2012. **19**(12): p. 2015-2028.
329. Rishi, G. and V.N. Subramaniam, *The liver in regulation of iron homeostasis.* Am J Physiol Gastrointest Liver Physiol, 2017. **313**(3): p. G157-g165.
330. Meynard, D., et al., *Lack of the bone morphogenetic protein BMP6 induces massive iron overload.* Nat Genet, 2009. **41**(4): p. 478-81.
331. Lin, J., et al., *Kielin/chordin-like protein, a novel enhancer of BMP signaling, attenuates renal fibrotic disease.* Nat Med, 2005. **11**(4): p. 387-93.
332. Katoh, M. and M. Katoh, *Identification and characterization of the human FMN1 gene in silico.* Int J Mol Med, 2004. **14**(1): p. 121-6.

333. Walseng, E., et al., *Ubiquitination regulates MHC class II-peptide complex retention and degradation in dendritic cells.* Proc Natl Acad Sci U S A, 2010. **107**(47): p. 20465-70.
334. Zito, E., et al., *Sulphatase activities are regulated by the interaction of sulphatase-modifying factor 1 with SUMF2.* EMBO reports, 2005. **6**(7): p. 655-660.
335. He, J., et al., *Association of DCBLD2 upregulation with tumor progression and poor survival in colorectal cancer.* Cellular Oncology, 2020. **43**(3): p. 409-420.
336. Lee, H.C., et al., *Released Tryptophanyl-tRNA Synthetase Stimulates Innate Immune Responses against Viral Infection.* J Virol, 2019. **93**(2).
337. Hauser, P.S., V. Narayanaswami, and R.O. Ryan, *Apolipoprotein E: from lipid transport to neurobiology.* Prog Lipid Res, 2011. **50**(1): p. 62-74.
338. Ershov, P., et al., *Enzymes in the Cholesterol Synthesis Pathway: Interactomics in the Cancer Context.* Biomedicines, 2021. **9**(8): p. 895.
339. Rocha, B., P. Vassalli, and D. Guy-Grand, *Thymic and extrathymic origins of gut intraepithelial lymphocyte populations in mice.* J Exp Med, 1994. **180**(2): p. 681-6.
340. Yamagata, T., D. Mathis, and C. Benoist, *Self-reactivity in thymic double-positive cells commits cells to a CD8αα lineage with characteristics of innate immune cells.* Nature Immunology, 2004. **5**(6): p. 597-605.
341. Kadivar, M., et al., *CD8αβ⁺ γδ T Cells: A Novel T Cell Subset with a Potential Role in Inflammatory Bowel Disease.* The Journal of Immunology, 2016. **197**(12): p. 4584.
342. Mowat, A.M. and W.W. Agace, *Regional specialization within the intestinal immune system.* Nature Reviews Immunology, 2014. **14**(10): p. 667-685.
343. Ma, H., W. Tao, and S. Zhu, *T lymphocytes in the intestinal mucosa: defense and tolerance.* Cellular & Molecular Immunology, 2019. **16**(3): p. 216-224.
344. Pai, S.I., A. Cesano, and F.M. Marincola, *The Paradox of Cancer Immune Exclusion: Immune Oncology Next Frontier.* Cancer Treat Res, 2020. **180**: p. 173-195.
345. Strasser, K., et al., *Immunological differences between colorectal cancer and normal mucosa uncover a prognostically relevant immune cell profile.* Oncoimmunology, 2019. **8**(2): p. e1537693.
346. Dagenborg, V.J., et al., *Low Concordance Between T-Cell Densities in Matched Primary Tumors and Liver Metastases in Microsatellite Stable Colorectal Cancer.* Front Oncol, 2021. **11**: p. 671629.
347. Balta, E., G.H. Wabnitz, and Y. Samstag, *Hijacked Immune Cells in the Tumor Microenvironment: Molecular Mechanisms of Immunosuppression and Cues to Improve T Cell-Based Immunotherapy of Solid Tumors.* Int J Mol Sci, 2021. **22**(11).
348. Lalos, A., et al., *Prognostic significance of CD8+ T-cells density in stage III colorectal cancer depends on SDF-1 expression.* Scientific Reports, 2021. **11**(1): p. 775.
349. Millen, R., et al., *CD8(+) tumor-infiltrating lymphocytes within the primary tumor of patients with synchronous de novo metastatic colorectal carcinoma do not track with survival.* Clin Transl Immunology, 2020. **9**(7): p. e1155.
350. Hoeres, T., et al., *PD-1 signaling modulates interferon-γ production by Gamma Delta (γδ) T-Cells in response to leukemia.* Oncoimmunology, 2019. **8**(3): p. 1550618.
351. de Vries, N.L., et al., *γδ T cells are effectors of immune checkpoint blockade in mismatch repair-deficient colon cancers with antigen presentation defects.* bioRxiv, 2021: p. 2021.10.14.464229.